ELEVENTH ANNUAL COAL PREPARATION, UTILIZATION, AND ENVIRONMENTAL CONTROL CONTRACTORS CONFERENCE

Westin William Penn Hotel
Pittsburgh, Pennsylvania

July 12-14, 1995

PROCEEDINGS

Sponsored by: U.S. Department of Energy
Pittsburgh Energy Technology Center

DISCLAIMER

TABLE OF CONTENTS

COMPLIANCE TECHNOLOGY SESSION

TECHNOLOGY BASE ACTIVITIES SESSION

HIGH EFFICIENCY PREPARATION SESSION

AIR TOXICS SESSION

AIR TOXICS AND CO_2 CONTROL SESSION

SUPERCLEAN EMISSIONS SESSION

COMBUSTION 2000 SESSION

ADVANCED RESEARCH SESSION

COMMERCIAL AND INDUSTRIAL COMBUSTION SYSTEMS SESSION

ALTERNATIVE FUELS SESSION

ENVIRONMENTAL CONTROL POSTER SESSION

COAL UTILIZATION POSTER SESSION

DISCLAIMER

EVALUATION, ENGINEERING AND DEVELOPMENT

OF ADVANCED CYCLONE PROCESSES

THOMAS E. DURNEY/C. ALLEN COOK
COAL TECHNOLOGY CORPORATION, BRISTOL, VIRGINIA 24201

DAVE D. FERRIS
ICF KAISER ENGINEERS, INC., PITTSBURGH, PENNSYLVANIA 15222

A. L. DEVERNOE
INTERMAGNETICS GENERAL CORPORATION, GUILDERLAND, NEW YORK 12084

CONTRACT NUMBER: DE-AC22-90PC90177

PERIOD OF PERFORMANCE: OCTOBER 1, 1990, TO APRIL 30, 1996

INTRODUCTION

This research and development project is one of three seeking to develop advanced, cost-effective, coal cleaning processes to help industry comply with 1990 Clean Air Act Regulations. The specific goal for this project is to develop a cycloning technology that will beneficiate coal to a level approaching 85% pyritic sulfur rejection while retaining 85% of the parent coal's heating value. A clean coal ash content of less than 6% and a moisture content, for both clean coal and reject, of less than 30% are targeted. The process under development is a physical, gravimetric-based cleaning system that removes ash bearing mineral matter and pyritic sulfur. Since a large portion of the Nation's coal reserves contain significant amounts of pyrite, physical beneficiation is viewed as a potential near-term, cost-effective means of producing an environmentally acceptable fuel.

The project agenda consists of three phases. Phase I included a characterization of the four potential feedstock coals, one of which is to be used throughout the project, and a media evaluation consisting of a paper study and laboratory testing. The coal seams selected for use in this project are Upper Freeport, Pittsburgh No. 8, Meigs No. 9, and Illinois No. 6. Phase II involved testing several selected media and separator combinations in a closed loop circuit, conceptual cost estimates, and final medium/process selection. Phase III involves the development of a process Component Test Circuit design, equipment selection, construction and operation of a 1,000 lb/hr closed loop component test system. Prior to medium/separator testing, the selected deliquoring device will be performance tested utilizing conventional froth flotation products to determine applicability to existing coal preparation technology. During the process optimization period, performance tests with one of the four test coals are planned. Finally, generation of a conceptual design and economic analyses for large scale integrated plants is planned.

Nearly 50 media candidates were considered including aqueous suspensions, aqueous solutions, organic solutions and a magnetically enhanced medium (MEM).

Separators that were considered included small diameter, high pressure cyclones, centrifuges, a hybrid separator combining flotation and cycloning in a single device, and a separator designed for MEM. In addition to gathering physical property data via a literature search, laboratory measurements and test separations were completed to eliminate the less desirable media candidates, i.e., viscosity, solubility, pH, and filter cake washing experiments.

COAL TOPSIZE, MEDIUM AND SEPARATOR SELECTION

At the conclusion of Phase I, calcium nitrate/water and the organic mixture of methylene chloride/perchloroethylene (mcl/perc) were selected as the best true heavy liquid candidates for further testing in Phase II. The MEM separator could not be readily scaled up and was dropped. The separators tested in PTI's closed loop facility during Phase II were a Krebs Cyclone, an Alfa-Laval (A-L) Model MOCL hydrocyclone (nested miniclones), and a DOE/PTI vertical centrifuge separator. Testing of decanter centrifuges and Hydro Processing & Mining's Centrifloat separator occurred off-site. All of the indicated separators were tested with both aqueous and organic media except the Centrifloat, which utilizes a water only medium, and the A-L centrifuge, which did not use the organic medium because the lab where it was tested was not equipped to handle organic liquids. HPM's Centrifloat did not achieve the targeted value for pyritic sulfur rejection and was dropped. The vertical centrifuge separator required modification beyond the budget and timing of this project and was eliminated.

Coal characterization and washability of the four test coals showed that grinding the Component Test System feed coal to 100 mesh topsize would theoretically achieve the project goals. Phase II tests were conducted utilizing 100 mesh as the top size; however, 200 mesh and 500 mesh feed coals were also tested to determine separation effectiveness at smaller topsizes.

The separating performances of the calcium nitrate medium in a decanter centrifuge and the organic medium in a two-inch diameter cyclone were nearly identical, making the final separator selection a difficult task. The organic medium circuit is less costly than the salt circuit, both from a capital and operating cost standpoint. However, the calcium nitrate medium has significantly less health, safety and environmental liabilities. If a spill with the organic medium were to occur, it would shut the operation down, cause serious delays, and have the potential for very large clean-up and containment related costs. The difference in cost of the two circuits is viewed as the price paid for safety. Calcium nitrate is more commonly used for its nitrate content as fertilizer and at saturation is able to make a 1.55 sg solution. Viscosity of a 1.35 sg solution is less than 5 centipoise.

Selection of the decanter centrifuge as separator is required to meet the project goals if calcium nitrate medium is used. The high g force generated by the centrifuge is required for the calcium nitrate medium to work as a parting liquid. The Project Team achieved excellent separations with a P-660 Sharples (A-L) decanter. Comparison of the optimum separation results achieved in Phase II to the feed washability (ash vs yield relationship) is shown in Figure 1. Partition curves for the calcium nitrate/decanter centrifuge separation and others are shown in Figure 2. After considering these results and the environmental and safety elements above, the Project Team selected the calcium

nitrate medium, decanter centrifuge combination. A decanter centrifuge diagram is shown in Figure 3.

MEDIUM RECOVERY/REGENERATION (FILTERING, WASHING, EVAPORATION)

Development of a medium recovery system is a technical and economic requirement. The filtering system serves two functions: to recover medium and to deliver a relatively salt-free product. This operation is critical to the success of the project. The cost of the medium requires that it be recovered for reuse. Water is used to rinse the filter cake, and the dilute filtrate is recovered for restoration to the original medium gravity. The operating cost of the aqueous process is dominated by the medium regeneration, i.e., water evaporation and calcium nitrate replacement costs.

Test work was performed with two filter vendors to determine filtering efficiencies, capacities, etc. A capillary-effect filtration system utilizing ceramic disks manufactured by Outokumpu of Finland was selected. A diagram of the Outomec filter is shown in Figure 4.

By utilizing a porous sintered alumina material to create a capillary effect, the separation of liquid and solids can take place. Capillary effect causes liquids in small tubes to stand at a greater height than the corresponding static head. Capillary rise is described by:

$$H = \frac{4t \cos \theta}{g\, D\, (\rho_1 - \rho_2)}$$

where H is in cm, t is the surface tension of the liquid in dynes/cm, D is the diameter in cm, θ is the contact angle, $g = 981$ cm/sec^2, and ρ_1 and ρ_2 are the densities of the liquid and surrounding gas in g/cc.

If the height of the column H is multiplied by the difference in density and the acceleration due to gravity, the differential in pressure is obtained.

$$\Delta P = \frac{4t \cos \theta}{D}$$

The above expression indicates that the smaller the pore diameter, the greater the pressure. Capillary force in pores can be greater than that applied by vacuum. Due to the surface tension between the liquid and the hydrophilic porous material, the pores fill with liquid. The pores in the ceramic filter are of such a diameter that they are not emptied of the liquid contained in them and no air is allowed to pass. A small pump is used to convey the collected liquid away. Energy consumption is extremely low.

With the use of ceramic filter media, filter cloths and associated problems are eliminated. The ceramic media is non-blinding, non-tearing and provides an uncontaminated filtrate.

Preliminary process investigation indicates the optimum water evaporation system is a seven-effect evaporator utilizing falling-film and forced circulation units.

The device removes water from the diluted medium, restoring the working medium to its proper density. A diagram of the evaporator components is shown in Figure 5.

Since the medium regeneration system utilizes well understood technologies involving thermal evaporation of water, an evaporator manufacturer will be selected to perform the studies necessary for selection of the optimum medium regeneration evaporator configuration.

DESCRIPTION OF PROCESS CIRCUIT

Detailed engineering design of a Bench Scale Circuit (BSC) capable of processing coals at a feed rate of 1,000 lb/hr was completed in late 1993 but cost constraints and limited available funds dictated a change in project scope. A flowsheet of the BSC is shown in Figure 6. After study of project goals vs. available funds, it was decided that rather than construct the complete integrated circuit, portions of the detailed engineering and the primary circuit components will be utilized to construct a Component Test System (CTS), which will test, in closed loop at 1,000 lb/hr, first the capillary-effect filtration system with a standard preparation plant flotation product and tailings, water slurry, then the separator circuit with aqueous medium and preground project coals, and finally the deliquoring circuit with separator products. In the first phase of testing, the Outomec capillary-effect filter will be tested to determine its potential effectiveness as a dewatering device in existing coal preparation plants. Next, preground samples (100 mesh topsize) of the project coals will be slurried in a sump with calcium nitrate/water medium and beneficiated through the Alfa-Laval P-3000 decanter separator where a gravimetric separation of high and low ash material will be made. The decanter products are either directed back to the feed sump and recirculated or stored/segregated in separate sumps. With the completion of processing/sampling of the project feed coal through the high g separator, the decanter test loop is shut down. The tube and ceramic disc filter circuit, is then started. The stored/segregated low ash (product) solids are pumped to the clean coal side of the deliquoring circuit, comprised of the tube filter and three discs of the ceramic disc filter. Simultaneously, the high ash (refuse) solids are pumped to the refuse side of the filter, comprised of a single disc. The solids are deliquored/sampled and directed either to the feed sumps for recirculation or to final disposal.

CURRENT STATUS AND PLANS

Though this process has great potential, additional work is needed to lower processing costs. This need and cost constraints of the project led to the decision to adopt a simple component test circuit strategy. Construction of the component test facility is expected to be complete in the Spring of 1995, and the test program and final report completed in April, 1996.

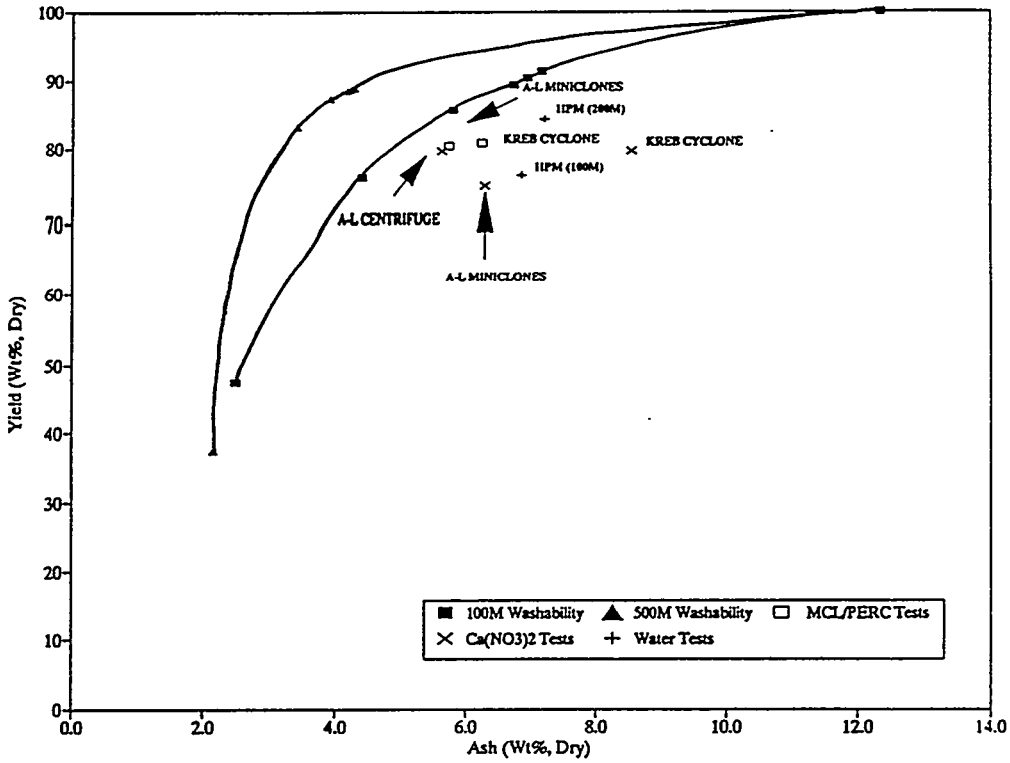

Figure 1. Comparison of Optimum Separation Results

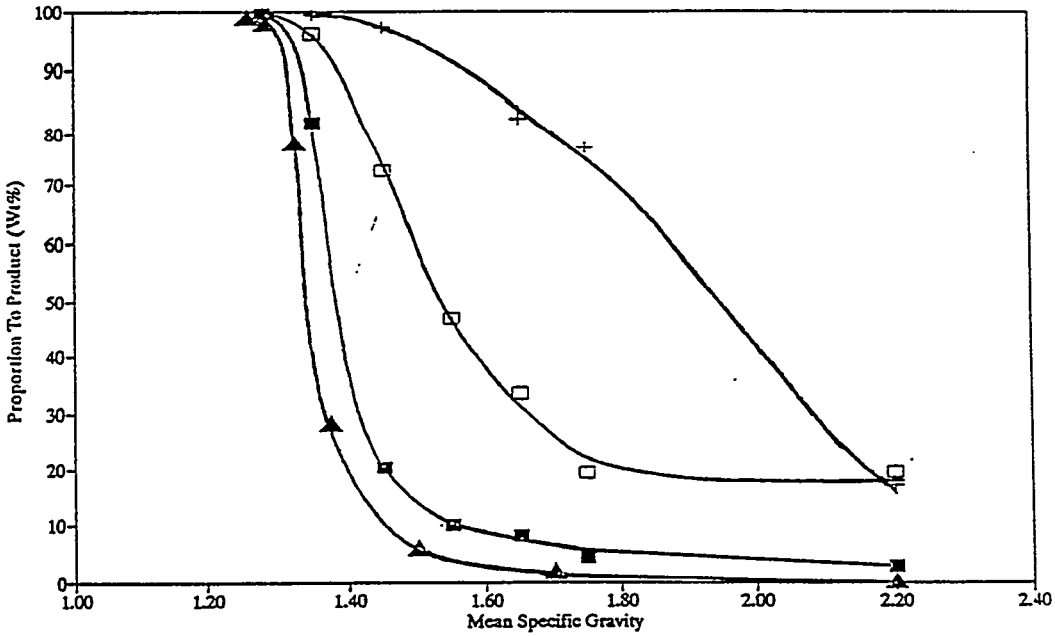

Legend	Media	Separator	Size	Media SG	Sep'n SG	Ep
▲	Micromag	3" Cyclone	28M x 400M	1.30	1.35	0.025
□	MCL/PERC	2" Cyclone	100M x 0	1.45	1.53	0.135
■	Ca(NO3)2	A-L Centrifuge	100M x 0	1.35	1.39	0.035
+	Ca(NO3)2	A-L Centrifuge	500M x 0	1.40	1.92	0.195

Figure 2. Partition Curves of Media/Separators

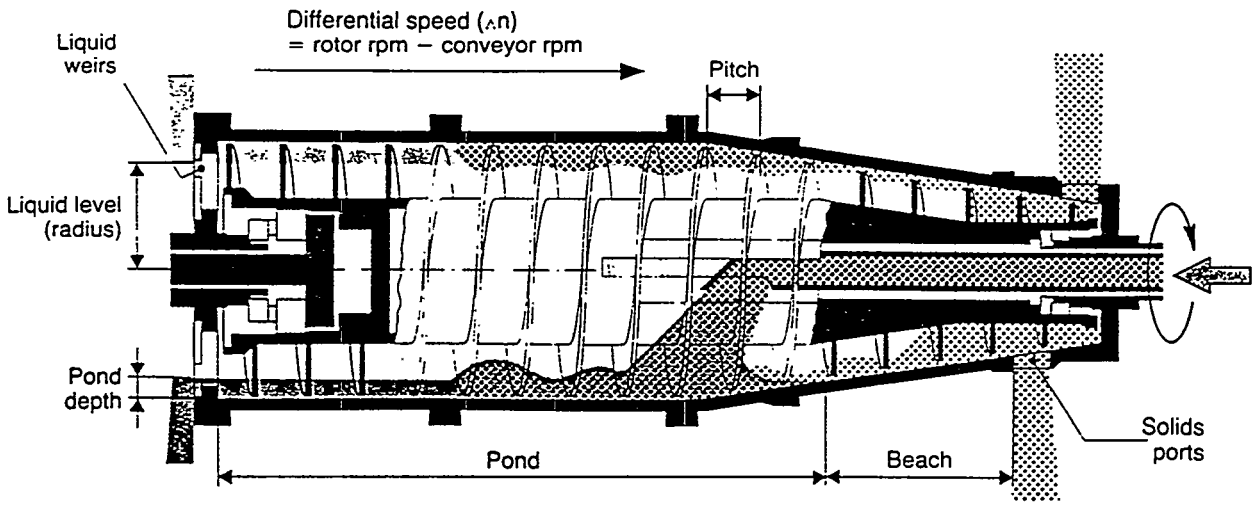

Figure 3. Decanter Centrifuge

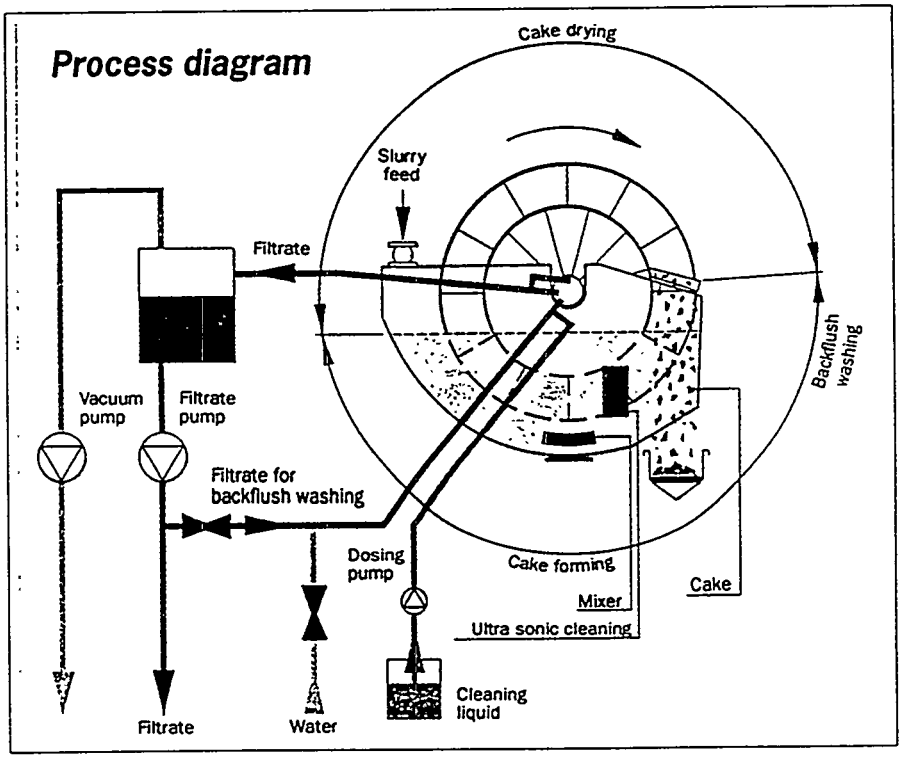

Figure 4. Capillary Effect Filter

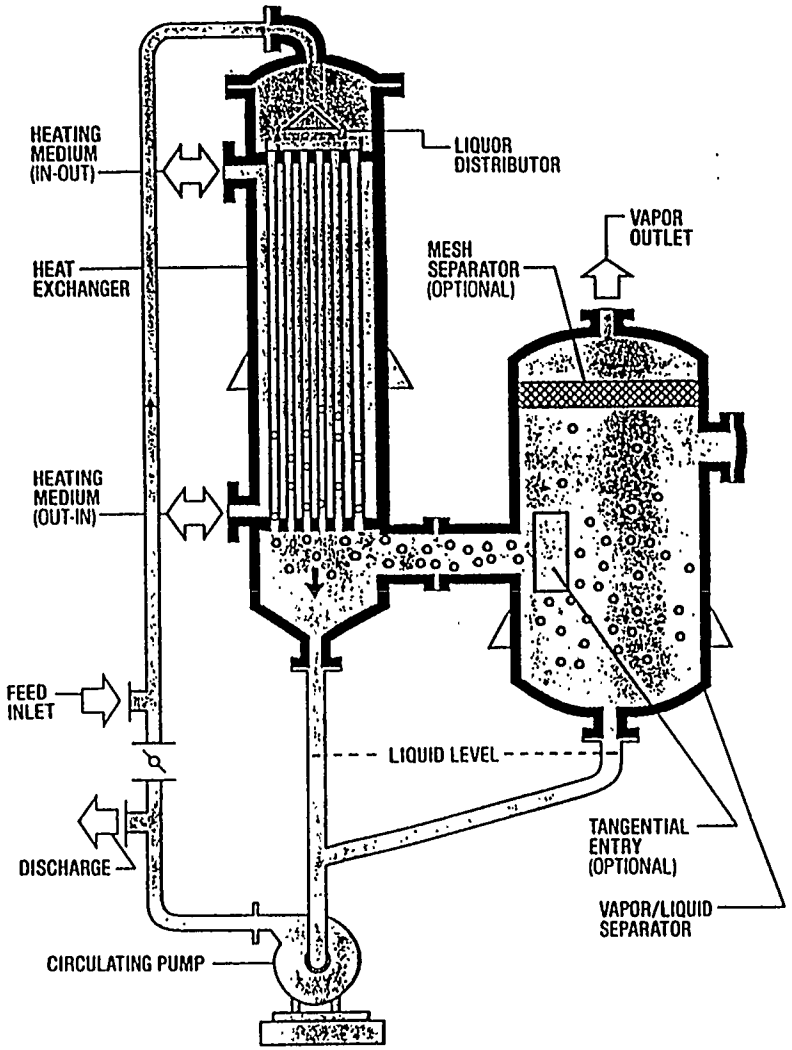

Falling Film Evaporator

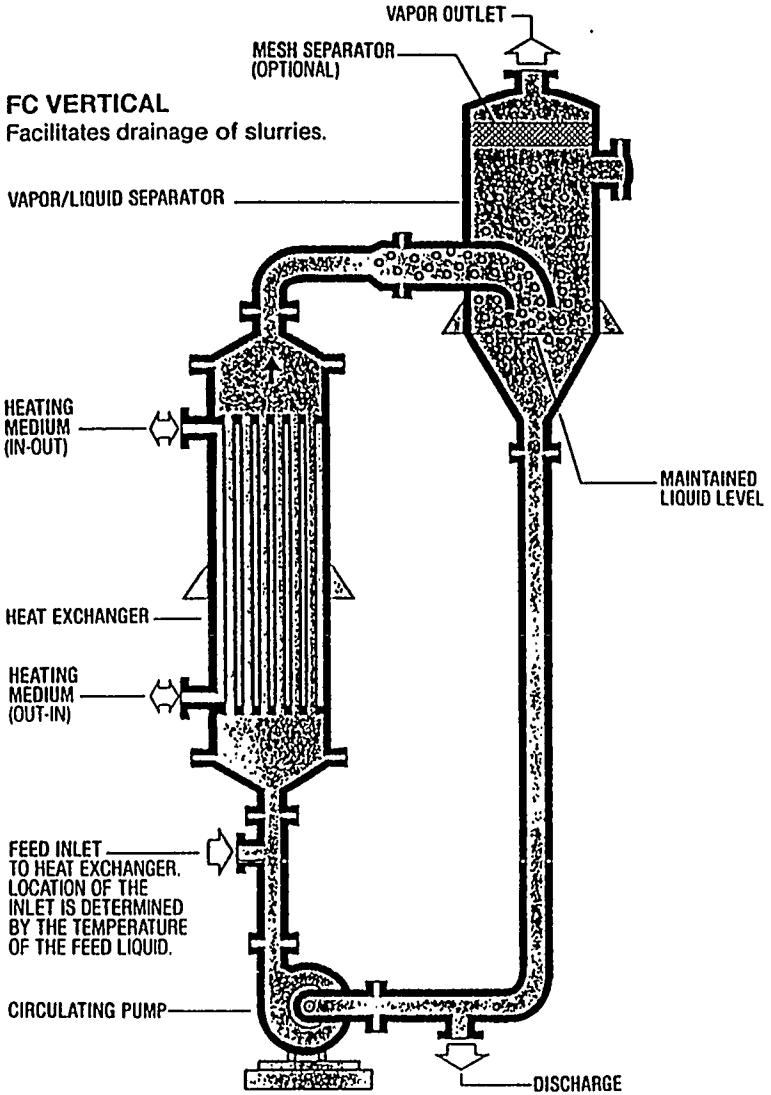

Forced Circulation Evaporator

Figure 5

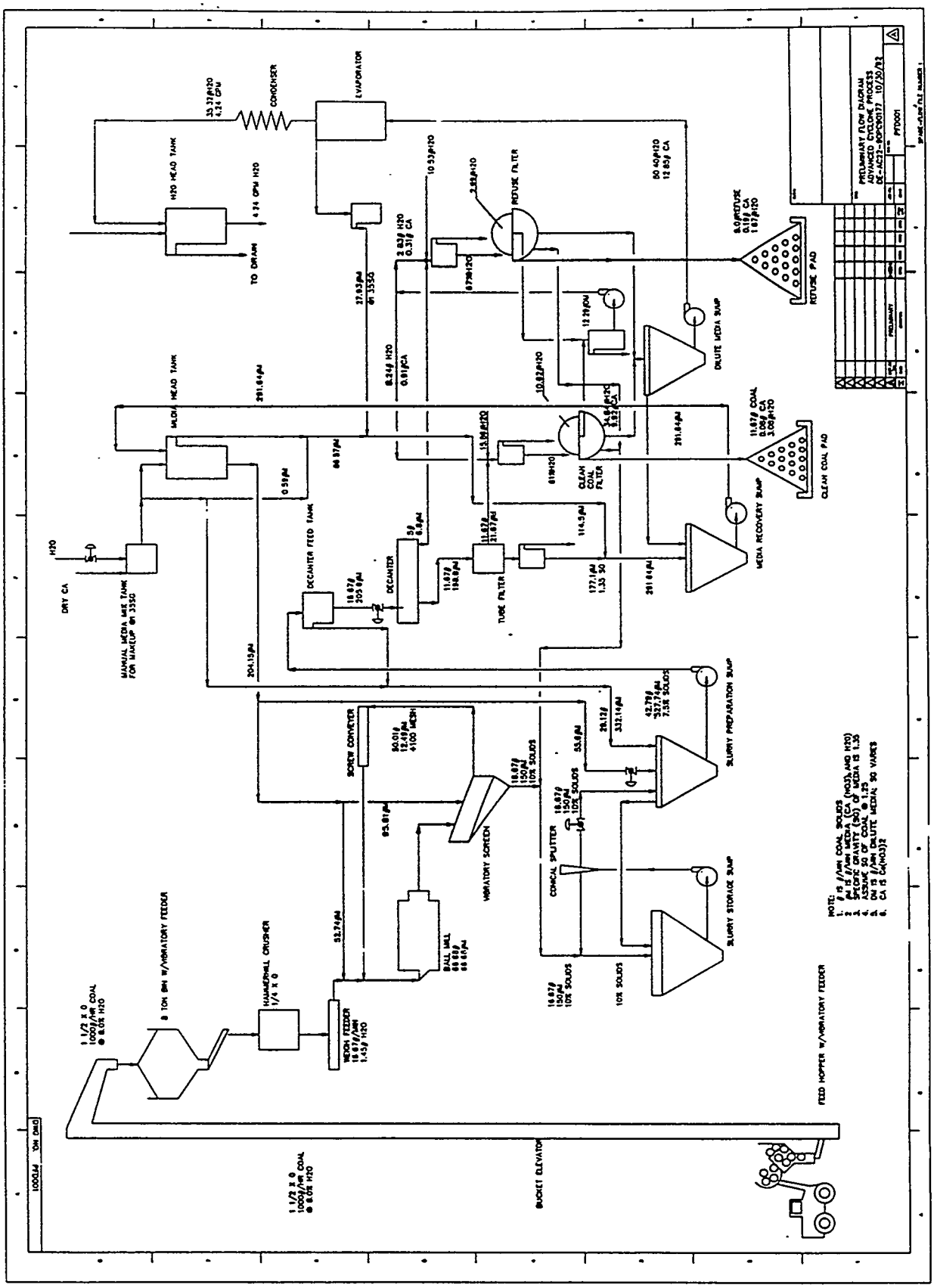

Figure 6. Bench Scale Circuit Flowsheet

ENGINEERING DEVELOPMENT OF ADVANCED PHYSICAL FINE COAL CLEANING TECHNOLOGIES - FROTH FLOTATION

DAVE D. FERRIS, PROJECT MANAGER
JOHN R. BENCHO, SENIOR PROCESS ENGINEER
ICF KAISER ENGINEERS, INC.
FOUR GATEWAY CENTER
PITTSBURGH, PA 15222

In 1988, ICF Kaiser Engineers was awarded DOE Contract No. DE-AC22-88PC88881 to research, develop, engineer and design a commercially acceptable advanced froth flotation coal cleaning technology. The DOE initiative is in support of the continued utilization of our most abundant energy resource. Besides the goal of commercialability, coal cleaning performance and product quality goals were established by the DOE for this and similar projects. Primary among these were the goals of 85 percent energy recovery and 85 percent pyrite rejection. Three nationally important coal resources were used for this project: the Pittsburgh No. 8 coal, the Upper Freeport coal, and the Illinois No. 6 coal. Following is a summary of the key findings of this project.

Proof-of-Concept (POC) Scale Test Results

The POC testing circuit was constructed as a addition to the John P. Apel Ohio Coal Testing and Development Center (OCTAD) located between Beverly and McConnellsville, Ohio. OCTAD is a state-of-the-art coal cleaning facility that contained much of the equipment needed to pre-clean the coal for the POC test program. A separate bay was added to the OCTAD facility to house the additional process equipment needed for the DOE POC test program. Many modifications were needed to the piping, electrical and process control systems to properly integrate the POC process into the OCTAD operation.

Figure 1 represents a simplified block flow diagram of the POC flowsheet. In the process, 1/4 inch x 48 mesh was cleaned using a heavy-media cyclone with the objective of removing coarse refuse from the coal matrix while at the same time maximizing the recovery of energy values. Clean coal from the heavy-media-cyclone overflow stream was crushed to minus 48 mesh using a cagepactor crusher and combined with the raw 48 mesh by zero and fed to a water-only cyclone. The water-only cyclone was used to remove liberated mineral matter and pyrite from the coal prior to grinding to finer sizes for additional liberation. Clean coal from the water-only cyclone reported to the ball-mill where it was ground to nominal 200 mesh by zero and fed to the column flotation cell for final cleaning. The microcel™ column flotation technology, developed at Virginia Polytechnic Institute and State University, was used in the POC flowsheet. Primary performance goals of the POC flowsheet were to achieve 85 percent energy recovery with 85 percent pyritic sulfur removal when compared to the raw coal feed of the plant.

Prior to the 24-hour demonstration runs for the three coal seams tested, each coal was subjected to a series of optimization runs to determine the effect of changing process variables and set-points on cleaning performance. Tests were completed to determine the optimum conditions to run the heavy-media cyclone and water-only cyclone operations. In addition, important variables were examined for their impact on the ability of the grinding mill to achieve fine grinding performance. To determine the best conditions for microcel™

column flotation cell, a fractional factorial experiment was completed to determine the best operating levels for frother type and amount, wash-water rate and aeration rate. Details of these results can be obtained in the reports filed for the project with DOE.

With the heavy-media cyclone and water-only cyclone maximized, and with the best conditions for aeration rate, wash-water rate, and frother type determined for the column flotation cell, investigators conducted a Box-Behnken test matrix on each of the three coals. Profiles were developed showing the energy recovery as a function of ash rejection, pyritic sulfur rejection, and total sulfur rejection for the overall POC circuit based upon Box-Behnken test matrices for the Pittsburgh No. 8, Upper Freeport, and Illinois No. 6 coal seams. As before, the results of these studies are available from DOE under separate cover.

To conduct the 24-hour demonstration runs, all process variables in the POC were pre-set at their optimum values as determined in the previous statistical studies. During the 24-hour tests, a complete set of samples were collected every eight hours for all of the pertinent circuits in the POC operation. Statistically adjusted material balances were constructed for each eight hour period using the Bilmat computer software. All of the eight hour periods were then averaged to obtain the condensed results for each of the three coals studied.

Results of the 24-hour demonstration runs for the Pittsburgh No. 8 seam are shown in Figure 2, which gives the material and attribute balance around the major unit operations within the POC process. Overall results indicated 48.2 percent yield, 89.5 percent energy recovery, and 73.6 percent pyrite rejection. Results for the Upper Freeport seam and Illinois No. 6 seam are summarized in Figures 3 and 4, respectively. Performance evaluations for the Upper Freeport seam indicated an overall energy recovery of 87.5 percent, while 76.2 percent of the raw pyritic sulfur was removed. For the Illinois No. 6 seam, the POC recovered 85.8 percent of the energy and removed 79.4 percent of the pyritic sulfur in the raw coal.

Table 1 presents the contributions of each coal-cleaning circuit to total energy loss and pyritic-sulfur removal for each of the three coals. These values are based on the average results obtained during the 24-hour demonstration runs. The heavy-media cyclone circuit for each coal removed the bulk of the pyritic sulfur while losing relatively low amounts of energy. Depending on the coal, the heavy-media cyclone circuit removed 60 to 70 percent of the total amount of pyrite that was removed. Meanwhile, the energy content in the heavy-media cyclone circuit refuse was only 32 to 36 percent of the total energy losses.

Since large amounts of pyrite have been removed prior to the water-only cyclone and the advanced froth flotation circuit, the ratio of pyrite rejection to energy loss is significantly lower for these circuits. For the Upper Freeport Seam, for example, the advanced froth flotation circuit removed 25 percent of the total amount of pyrite that was rejected, and the energy content in the flotation tailings accounted for 71 percent of the total energy losses. Contributing to the lower ratios is the more-difficult-to-clean nature of fine- and ultrafine-particle streams.

Cumulative plant availability during 24-hour demonstration runs for the three coals was 94.9 percent. Individually, plant availabilities for the Pittsburgh No. 8, the Upper Freeport and the Illinois No. 6 coals were 98.0, 97.4, and 89.9 percent, respectively. No downtime encountered during the demonstration runs was attributed to the advanced process equipment.

20 TPH Semi-Works and 200 TPH Commercial Plant Economic Analysis

As part of the DOE project, a 20 TPH Semi-Works facility was designed as a starting point to determine the economics of the advanced flotation process. Generally, the Semi-Works process flowsheet is identical to the block flow diagram as previously shown in Figure 1. To construct this facility, approximately $10.9 million will be required. Another $750K will be needed for the purchase of land and working capital.

Based on the capital cost of the Semi-Works plant, the cost for 200 and 500 TPH facilities were extrapolated. In addition, fixed and variable, first-year operating-and-maintenance costs were estimated for these commercial plants. Table 2 presents a summary of these costs for a 200 TPH facility operating 7,560 hours per year.

In order to compare these values to those of existing facilities and to evaluate them on an investment basis, these values were input into an economic model developed by EoS Technologies, Inc. for the U.S. Department of Energy. Based on the above costs and a set of economic assumptions, the model generates the clean coal price required for the investment to generate a user-established, after-tax rate of return. Also, the cost to remove sulfur, on a dollars per ton of SO_2 equivalent, is determined. Table 3 presents these values for 200 and 500 TPH commercial facilities as well as the economic assumptions on which the estimates are based.

As the table indicates, plant size and operating schedule both significantly affect the costs of coal production and thus, the desulfurization costs. For the Pittsburgh No. 8 coal, for example, desulfurization costs for a 200 TPH (product) plant operating 7,560 hours per year are estimated at $327 per ton of SO_2 equivalent. For a 500 TPH plant with the same operating schedule, desulfurization costs drop to $275 per ton. On an average, desulfurization costs decrease by 15 percent for the 500 TPH plants.

Due to the large capital requirements for these advanced plants, operating schedule affects costs to a greater extent than plant size. A typical coal preparation facility operates five days per week, two shifts per day. Maintenance is conducted on the third shift. This operating schedule results in 3,456 hours of operation per year and, as the cost estimates reveal, a gross under utilization of facilities. For the Illinois No. 6 coal, a 200 TPH plant operating 7,560 hours per year can remove sulfur for about $305 per ton of SO_2 equivalent. When the same size plant operates only 3,456 hours per year, the desulfurization cost climbs to $435 per ton.

Conclusions

(1) The proposed process technology is ready for commercialization. However, the product from the process may require reconstitution in order to be marketable.

(2) The proposed technology can recover 85 percent of the energy in each of the raw coals while removing 75 to 80 percent of the pyritic sulfur.

(3) Clean coal ash values of 7.2 to 10.3 percent were achieved with in the POC.

(4) Grinding to levels finer than 85 percent passing 200 mesh will be required to remove 85 percent of the pyrite while maintaining 85 percent energy recovery.

(5) Based on raw coal costs of $0.80 per million Btu, clean coal prices of $1.50 per million Btu will be needed to earn a 10 percent after-tax rate of return.

(6) Desulfurization costs, on a dollars per ton of SO_2 equivalent, of $255 to $275 are estimated for a 500 TPH commercial facility incorporating the proposed process.

Table 1
Contributions to Energy Loss and Pyritic Sulfur Removal*
During 24-Hour Demonstration Runs

Circuit (Size Cleaned)	Pittsburgh No. 8 Coal		Upper Freeport Coal		Illinois No. 6 Coal	
	Energy Loss	Pyrite Removal	Energy Loss	Pyrite Removal	Energy Loss	Pyrite Removal
Heavy-Media Cyclone (+48 mesh)	3.8	44.3	2.7	49.4	4.5	55.4
Water-Only Cyclone (48mesh x 0)	4.0	16.6	0.9	7.9	2.2	10.4
Adv. Froth Flotation (200 mesh x 0)	2.7	12.7	8.9	18.9	7.5	13.6

* Values represent the percentages of the raw coal energy content and pyritic sulfur content found in the refuse stream of each circuit.

Table 2
Capital Requirements and 1st Year Operating and Maintenance Costs
for a 200 TPH Advanced Froth Flotation Plant (7560 Hours)

Construction Capital Requirement	$59,624,735	$59,547,893	$59,669,206
Working Capital Requirement	$467,723	$449,603	$478,500
Fixed Operating and Maintenance Costs	$5,892,451	$5,892,451	$5,892,451
Variable Operating and Maintenance Costs	$12,080,238	$11,158,134	$12,613,895

Table 3
Advanced Froth Flotation Economics (Annualized Basis)

Cost Item	Pittsburgh No. 8	Upper Freeport	Illinois No. 6
200 TPH Commercial Plant Operating 7,560 Hours per Year			
Clean Coal Price ($/MMBtu)	1.49	1.50	1.55
Clean Coal Price ($/Ton)	40.65	40.27	41.96
Annualized Desulfurization Cost*	$326.82	$305.42	$304.60
200 TPH Commercial Plant Operating 3,456 Hours per Year			
Clean Coal Price ($/MMBtu)	1.81	1.81	1.87
Clean Coal Price ($/Ton)	49.32	48.68	50.63
Annualized Desulfurization Cost*	$477.08	$442.49	$435.09
500 TPH Commercial Plant Operating 7,560 Hours per Year			
Clean Coal Price ($/MMBtu)	1.38	1.39	1.44
Clean Coal Price ($/Ton)	37.68	37.30	38.99
Annualized Desulfurization Cost*	$275.27	$256.95	$259.84

ECONOMIC ASSUMPTIONS

Plant Life	20 Years	Inflation Rate	4.0 %
Royalties	None	Corporate Tax Rate	38.0 %
Financing	100% Equity	Rate of Return	10.0 %

* Annual Desulfurization Costs are per ton of SO_2 equivalent.

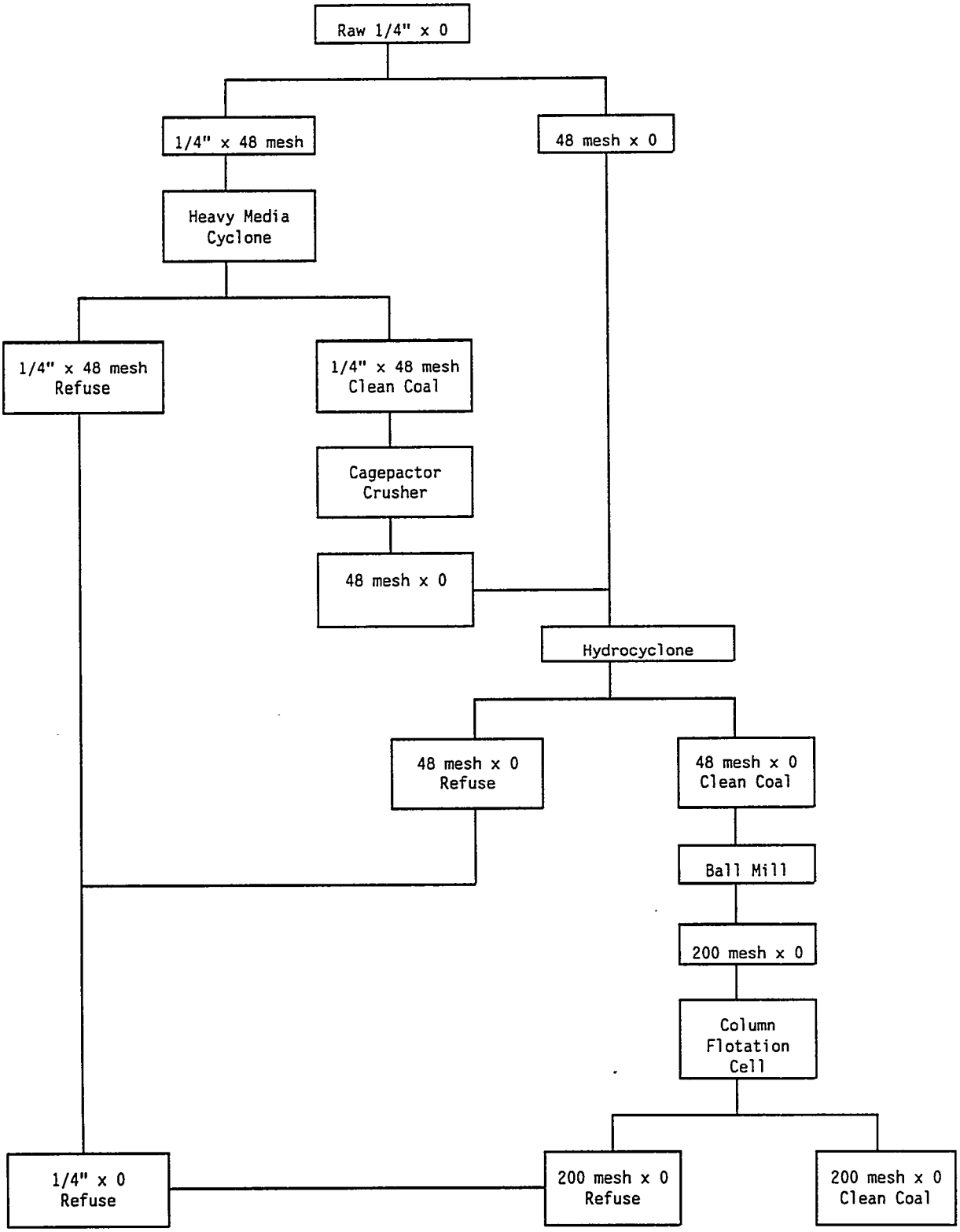

Figure 1. Simplified Block Diagram of the POC Process

Figure 2

Pittsburgh No. 8 Seam Coal Average Performance During 24-Hour Demonstration Run

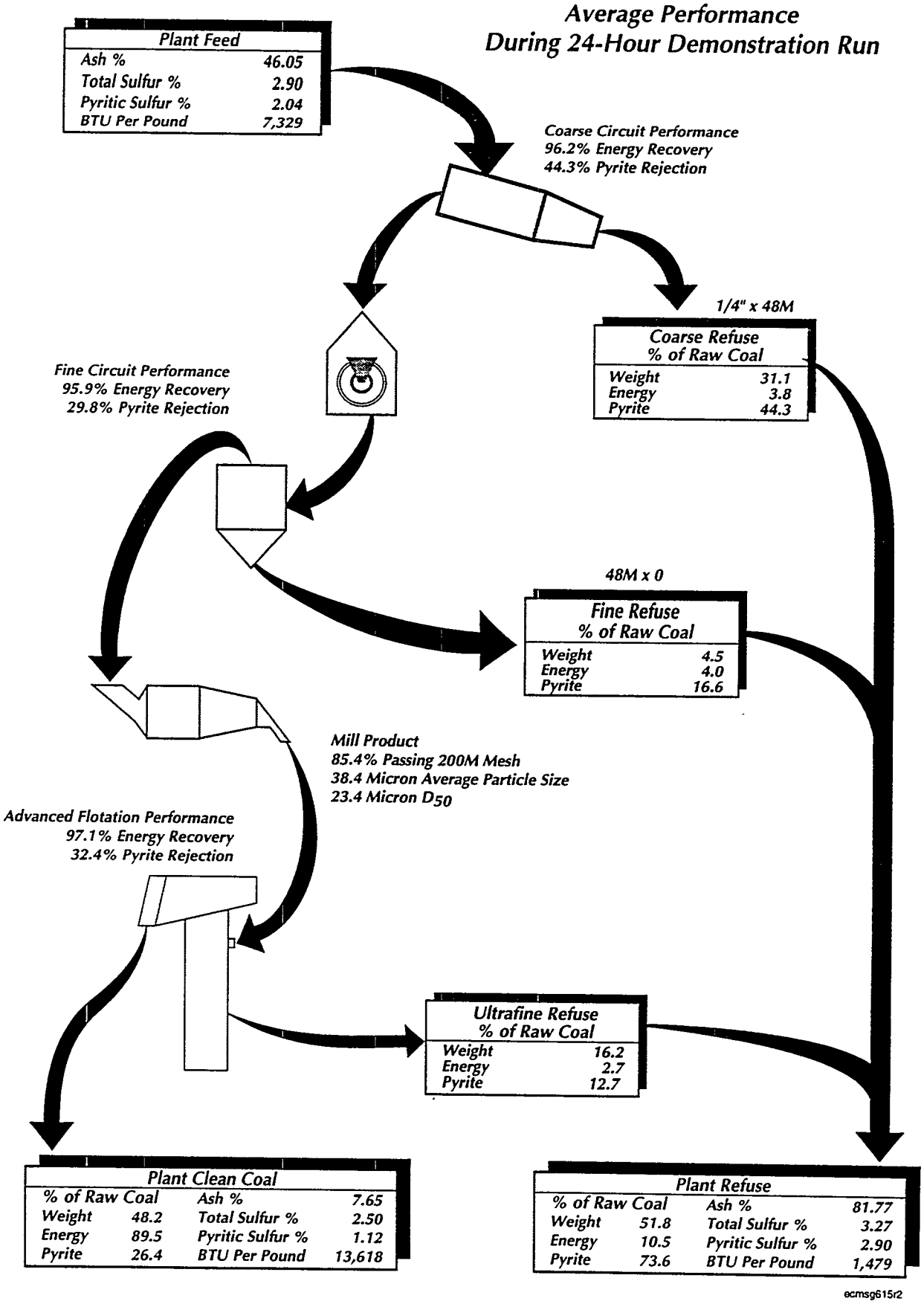

Figure 3
Upper Freeport Seam Coal Average Performance During 24-Hour Demonstration Run

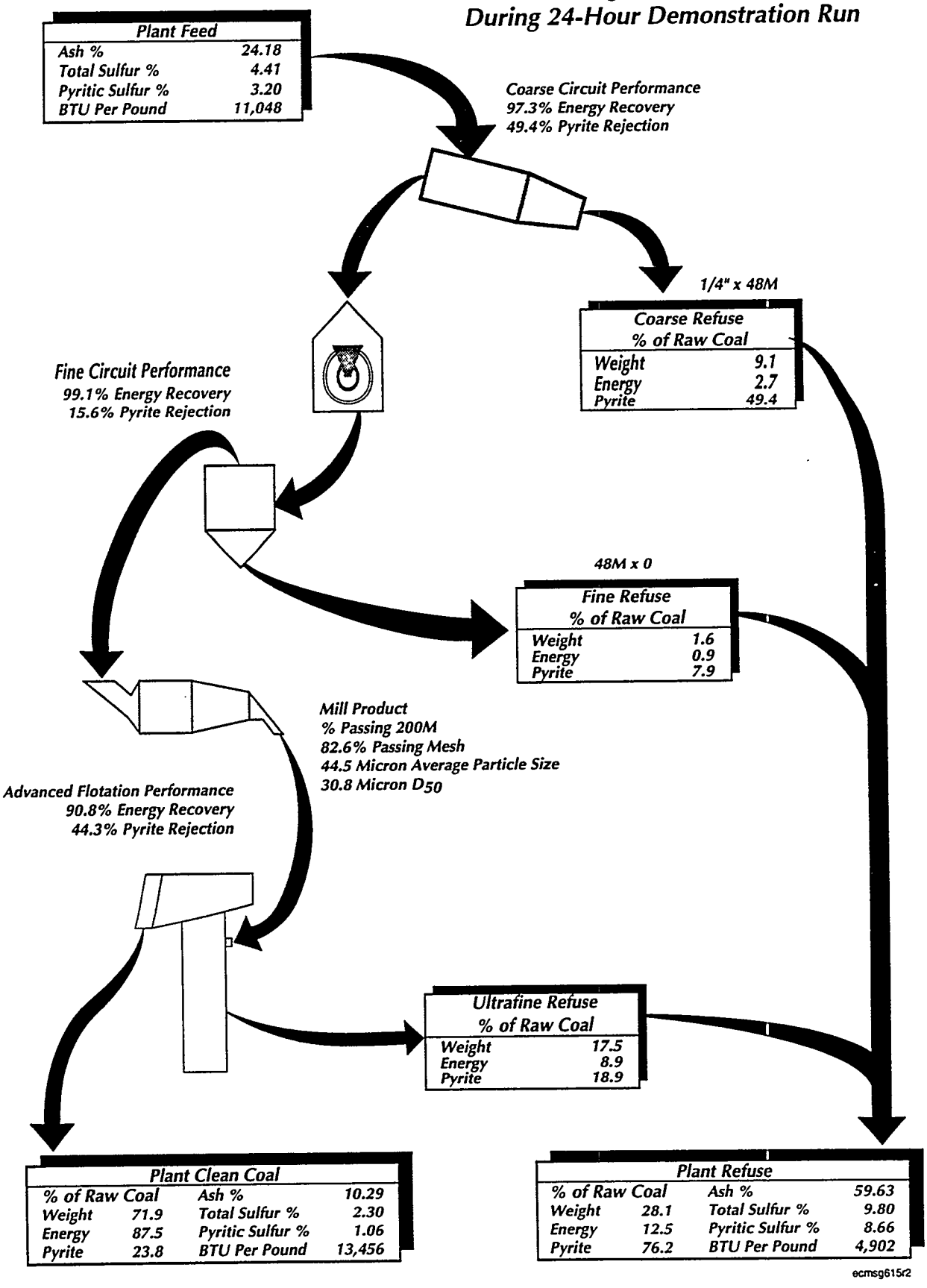

Figure 4

Illinois No. 6 Seam Coal Average Performance During 24-Hour Demonstration Run

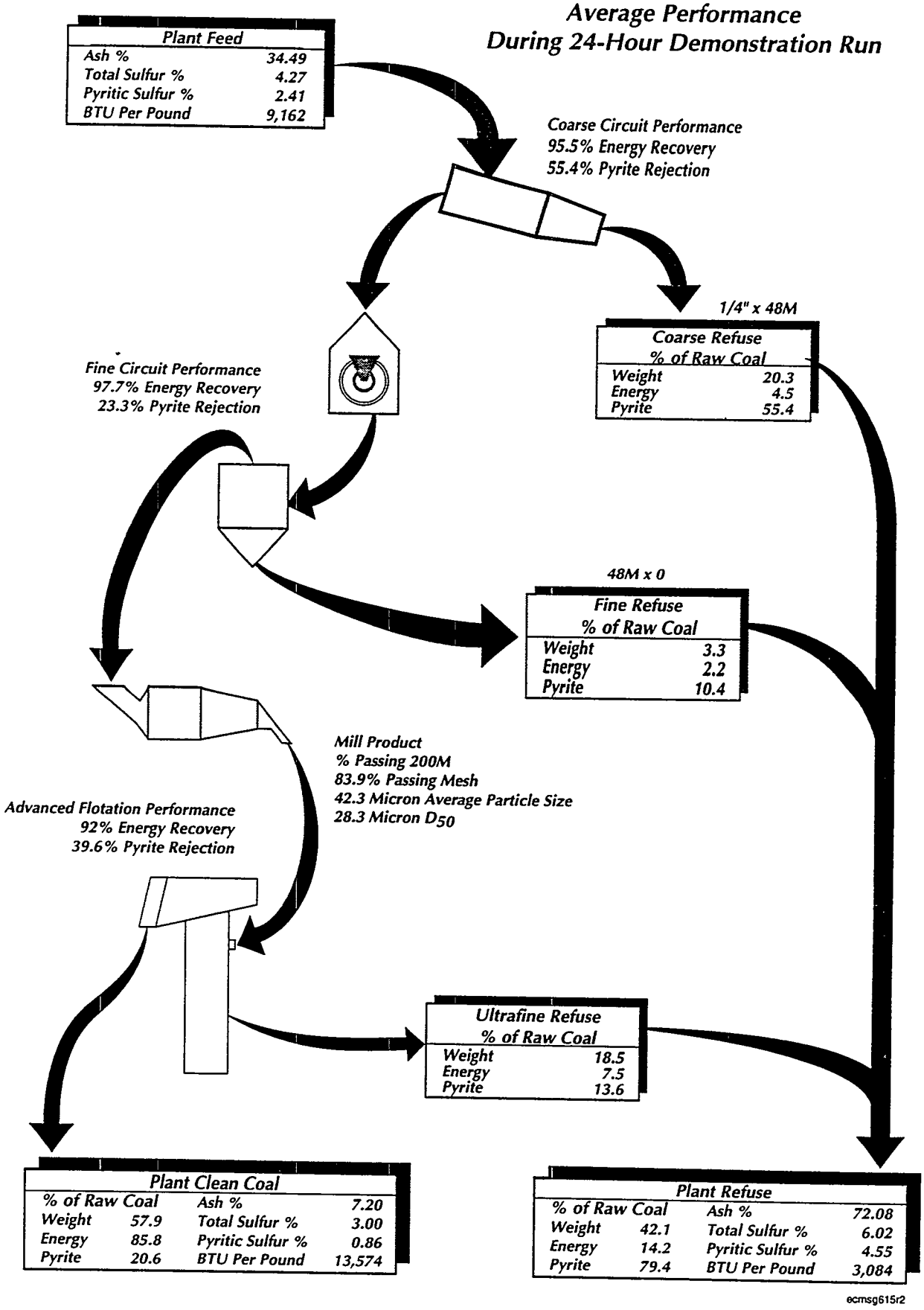

ENGINEERING DEVELOPMENT OF ADVANCED PHYSICAL FINE COAL CLEANING FOR PREMIUM FUEL APPLICATIONS

MAHESH C. JHA, FRANK J. SMIT, GENE L. SHIELDS, NICK MORO
AMAX R&D CENTER / ENTECH GLOBAL INC.
5950 MCINTYRE STREET, GOLDEN, COLORADO 80403

CONTRACT NO. DE-AC22-92PC92208

INTRODUCTION

The objective of this project is to develop the engineering design base for prototype fine coal cleaning plants based on Advanced Column Flotation and Selective Agglomeration processes for premium fuel and near-term applications. Removal of toxic trace elements is also being investigated. The scope of the project includes laboratory research and bench-scale testing of each process on six coals followed by design, construction, and operation of a 2 tons/hour process development unit (PDU). Three coals will be cleaned in tonnage quantity and provided to DOE and its contractors for combustion evaluation.

Amax R&D (now a subsidiary of Cyprus Amax Mineral Company) is the prime contractor. Entech Global is managing the project and performing most of the research and development work as an on-site subcontractor. Other participants in the project are Cyprus Amax Coal Company, Arcanum, Bechtel, TIC, University of Kentucky and Virginia Tech. Drs. Keller of Syracuse and Dooher of Adelphi University are consultants.

Additional details on the project can be found in two papers presented at the last two contractors conferences [1,. 2]. The selection of six feed coals (Taggart, Elkhorn No. 3, Winifrede, Indiana VII, Sunnyside and Dietz) is covered in a paper presented at the High Efficiency Coal Preparation Symposium [3]. The goal of this paper is to report on the progress made during the last twelve months in performing various tasks.

TASK 1. PROJECT PLAN REVISIONS

A revised Project Management Plan was prepared to reflect the organizational changes resulting from the Cyprus Amax merger. The project is now scheduled for completion by June 1997. The budget estimate remains the same. The Industrial Company of Steamboat Springs, Colorado, (TIC) was awarded a subcontract for the construction of the PDU. Dr. John Dooher was added as a consultant to assist in the coal water slurry fuel (CWF) formulation studies.

TASK 3. DEVELOPMENT OF NEAR-TERM APPLICATIONS

Cyprus Amax Coal Company, through its Cannelton division, has selected the Lady Dunn Coal Preparation Plant in West Virginia for evaluation of the advanced column flotation technology

to process minus 100 mesh coal fines. The plant is undergoing expansion which will increase the tonnage of fines.

Figure 1 shows typical results obtained in a laboratory column. It appears that a clean coal with 8 to 10 percent ash can be produced at about 80 to 90 percent energy recovery. These results are significantly better than those obtained in the past by conventional flotation process.

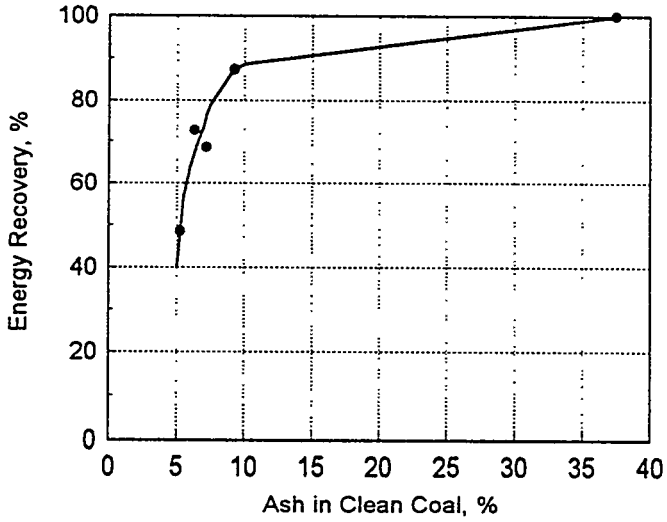

Figure 1. Laboratory Test Results on Lady Dunn Plant Coal Fines.

Based on the encouraging results and continued interest of the company in this technology, a 30-inch Microcel™ column is being installed at the Lady Dunn plant with help from Virginia Tech which will also assist in the operation of the column and evaluation of the results. This information will provide the design basis for the commercial plant - several columns of 10 or 12-ft diameter.

The clean coal slurry will be processed in a centrifuge or a filter press under a variety of conditions to determine the quality and quantity of product recovered and the anticipated cost for a commercial plant. Drying and briquetting of the clean coal fines will be investigated at vendor facilities to determine whether the product will be suitable for two niche markets - injection of dry coal fines in a blast furnace or use of briquettes as a stoker fuel.

In view of the importance of the dewatering of coal fines, a new subtask was added to the project for dewatering studies. Under Subtask 3.3, Virginia Tech will research and develop a hydrophobic dewatering process.

TASK 4. ADVANCED FLOTATION R & D FOR PREMIUM FUELS

This task consists of five subtasks which have all been completed. Results from Subtasks 4.1, Grinding, and 4.2, Process Optimization Research, were presented last year [2].

Subtask 4.3 covered coal water slurry fuel (CWF) formulation studies. Samples of clean coal produced in Subtasks 4.2 and 4.4 were used. It was found that the solids loading varied significantly based on the particle size of the coal and its inherent moisture content. Table 1

presents a summary of the results. The highest loading was attained with Taggart coal (about 70 percent). Elkhorn No. 3 and Sunnyside coals could be loaded to about 65 percent solids. The Indiana VII could be loaded to just above 50 percent solids. Attainment of a bimodal distribution by selective grinding of part of the cleaned coal was found to be the most important parameter. A small amount of A23 was used as dispersant. While the use of a stabilizer improved the stability of the slurries, it also increased the viscosity. A topical report presenting the detailed results has been submitted to DOE.

Table 1. CWF Slurry Comparison For Project Coals

	Taggart		Sunnyside	Elkhorn No. 3		Indiana VII	
	Regrind Blends	Selective Regrind	Regrind Blends	Regrind Blends	Coarsened Feedstock	Regrind Blends	Coarsened Feedstock
PSD MMD, microns	44	55	30	28	70	10	65
Coal Loading, wt%	64-68	68-70	63-65	61-64	64-66	47-51	50-53
Without Stabilizer							
Viscosity, cp	400-1400	800-1400	500-1200	500-1000	600-800	900-1600	600-1000
Stability Rating	1-3	1-3	1-3	1-3	1	1	1
With Stabilizer							
Viscosity, cp	800-2000	NA	NA	1600-3500	3500	NA	NA
Stability Rating	7-10	7-10	NA	7-10	3	NA	NA

Under Subtask 4.4, bench-scale (30-cm diameter) Ken-Flote™ and Microcel™ columns were installed and operated on the five bituminous coals. It was found that Taggart, Sunnyside, and Elkhorn No. 3 coals could be cleaned to meet the project specifications at design capacity (100 lb/hour or more). Indiana VII coal could be cleaned to the specifications but at a somewhat lower rate. Specifications could not be met with Winifrede coal. Better performance was obtained with the Microcel™ column. Based on the test results, greater confidence in scale up of the design, and commercial considerations, the Microcel™ column was selected for the PDU design. Samples of feed and product were analyzed to determine the removal of toxic trace elements. Samples were also provided to Combustion Engineering and Penn State for combustion evaluation. The results from this subtask are currently being compiled in the form of a topical report. Figure 2 shows a summary of results for Taggart, Sunnyside, and Indiana VII coals cleaned by the Microcel™ column under a variety of conditions.

The results from the above subtasks were used by Bechtel to prepare the conceptual design of the 2 tons/hour process development unit (PDU) and the advanced flotation module under Subtask 4.5. Taggart, Sunnyside, and Indiana VII coals were selected for the PDU design and operation. The plant will be able to process Sunnyside coal at design capacity, Taggart coal at a higher capacity, and Indiana VII coal at a lower capacity.

TASK 5. PDU AND FLOTATION MODULE DETAILED DESIGN

The detailed engineering design of the PDU and advanced flotation module was completed during the reporting period. The plant consists of four areas:

1. Area 100 Grinding
2. Area 200 Column Flotation
3. Area 300 Selective Agglomeration
4. Area 400 Dewatering

Detailed design of Area 300 will be performed under Task 7. Area 100 and 400 will serve both the column flotation and selective agglomeration modules as well as the utilities. A key feature of the design was the utilization of existing Amax R&D/DOE equipment and minimum alterations to the existing building structures.

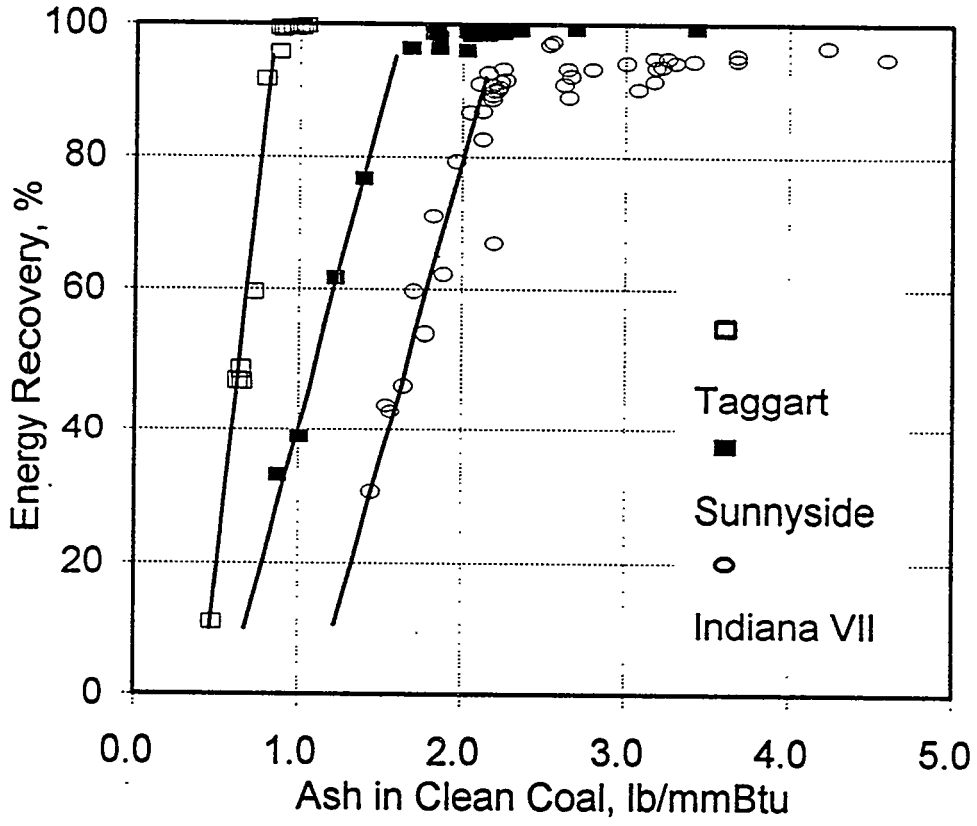

Figure 2. Performance of Taggart, Sunnyside, and Indiana VII coals in bench-scale column.

A 2-volume detailed engineering design package was prepared and submitted to DOE. The first volume contains Process Flow Diagrams (PFDs), Piping and Instrument Diagrams (P&IDs), Equipment Arrangement Drawings, Civil and Structural Design Drawings, Electrical Design Drawings, Equipment, Motor and Instrument List and Construction Specifications. The second volume contains Material Requisitions for various pieces of equipment and instruments.

Figure 3 shows a block flow diagram of the PDU and advanced flotation module. A closed grinding circuit will be used to assure efficient grinding of coals to required size. A Netzsch stirred ball mill will be used for fine grinding. Cyclones and Sizetec screens will be used for size classification. A 6-ft diameter Microcel™ column will be used for flotation. The concentrates will be dewatered by vacuum filtration and stored as filter cake. The tailings will be thickened, filtered, and disposed in a land fill. Normally, the PDU will be operated on a long day shift for parametric evaluation on each of the three coals. Once the optimum conditions have been established, 100-hour runs will be made to produce 200-ton lots of clean coal.

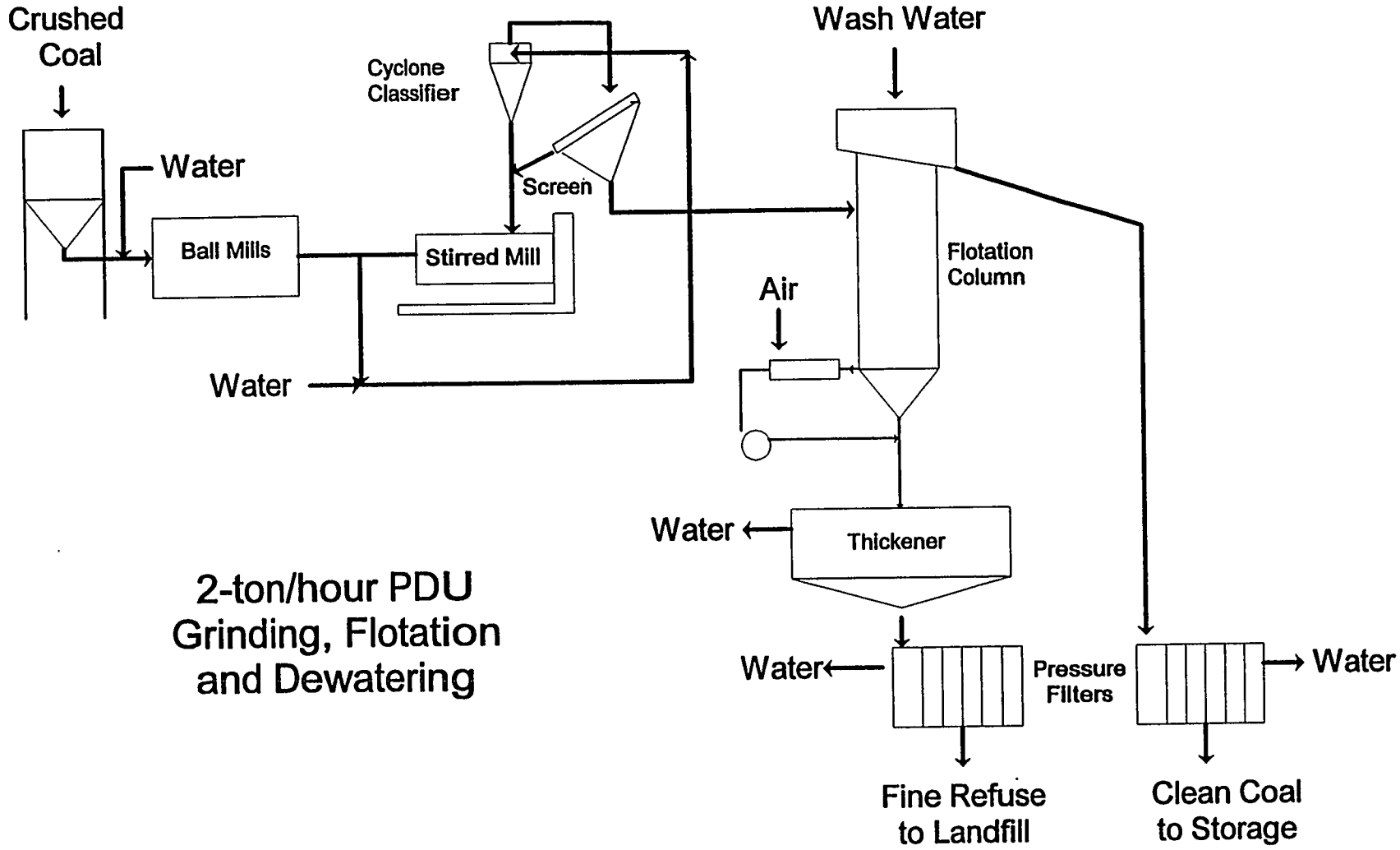

Figure 3. Block Flow Diagram for the PDU and Advanced Flotation Module.

TASK 6. SELECTIVE AGGLOMERATION R&D

This task is parallel to Task 4 for flotation. It is divided into six subtasks. Subtask 6.1, Agglomerating Agent Selection, and Subtask 6.2, Grinding, have been completed and the results have been presented in topical reports. They were covered in last year's presentation [2].

Subtask 6.3, Process Optimization Research, was completed during the reporting period and the topical report has been drafted. Two agglomerating agents (pentane and heptane) and two reactor design concepts (unitized reactor of a novel design and staged high and low shear reactors of a conventional design) were investigated in the test work performed at the Amax R&D Center and at Arcanum Corporation with Dr. Keller of Syracuse University providing guidance as a consultant.

Table 2 presents a summary of the results obtained with the unitized reactor using heptane as the agglomerating agent. It can be seen that ash specifications were met for all bituminous coals and the energy recoveries were significantly higher in comparison to the column flotation process. The low-rank coal could be cleaned, but it required acid pretreatment which will be costly. Simiiar results were obtained with pentane, but the feed slurry had to be cooled for steady operation. Arcanum evaluated the conventional two stage reactor design with heptane as the bridging liquid. Both ash specifications and energy recovery goals were met.

Table 2. Selective Agglomeration Process Optimization Results for Six Feed Coals

	Taggart	Indiana VII	Sunnyside	Elkhorn No. 3	Winifrede	Dietz
Clean Coal:						
Residual Ash, lb/mmBtu	0.99	1.62	1.80	1.83	1.75	1.9-2.5
Energy Recovery, %	99.8	98.6	99.4	99.4	94.2	93-98
Feed Slurry:						
Solids, %	10-13	10	7-10	7-13	7	7
Heptane/coal Ratio, g/g	0.21	0.28	0.22	0.25	0.35	0.5
Asphalt, lb/st	none	16	none	none	none	25-80
Acid	none	none	none	none	none	pH 3-4
High-Shear Mixing:						
Tip Speed, m/s	15.5	15.5	15.5	17.5	15.5	15.5
Retention, minutes	0.10	0.16	0.10	0.10	0.11	0.19
Low-Shear Mixing:						
Tip Speed, m/s	11.8	11.8	11.8	13.3	11.8	11.8
Retention, minutes	0.34	0.58	0.29	0.34	0.39	0.56
Estimated Mixing Energy:						
Unitized Reactor, kwhr/st	14-18	30	16-23	19-35	30	45

Subtask 6.4, CWF Formulation Studies, has been initiated. The test plan has been approved. For the most part, it will follow the approach used in Subtask 4.3. There will be greater emphasis on slurry stability and viscosity as they relate to atomization and combustion in commercial systems. Dr. John Dooher of Adelphi University has been retained as a consultant for this study.

Subtask 6.5, Bench-scale Testing and Process Scale-Up, is currently in progress. Based on the scale up considerations it was decided to use the conventional two stage design in the PDU and therefore in the 25 lb/hour bench-scale unit. Figure 4 shows a block flow diagram of the system. Besides the high and low-shear reactors and a vibrating screen for separation of clean coal agglomerates from ash laden tailings-slurry, the system includes a partially packed column for steam stripping of heptane, and a condenser for the recovery and recycling of heptane. Shake down testing has been completed and parametric testing is currently in progress.

A conceptual design of the selective agglomeration module was performed by Bechtel under Subtask 6.6. Based on the potential cost savings, the unitized reactor with pentane as the bridging liquid was selected for the preliminary design. However, a more thorough evaluation based on some of the measurements made in the laboratory reactor (Subtask 6.3 above), indicated that the cost savings may not be realized because of the expensive cooling (refrigeration) required for the pentane system. There was also concern for the scale up of the unitized reactor of the novel design. Thus, the detailed design to be performed under Task 7 will be based on the conventional two-stage system with heptane.

TASK 8. PDU CONSTRUCTION AND OPERATION

The Industrial Company (TIC) of Steamboat Springs, Colorado, has been selected as the construction subcontractor. The construction of the PDU started in March and is scheduled for completion by July with shakedown testing of equipment in August. Start up testing of the process will be performed in the September-October time frame followed by parametric testing on each of the three coals. It is planned to complete the testing of the advanced flotation module by August 1996.

ACKNOWLEDGMENTS

The authors would like to thank DOE/PETC and Cyprus Amax for sponsoring this project. We gratefully acknowledge the work performed by Entech Global and TIC personnel at the Amax R&D Center and other project team members at Arcanum, Bechtel, CAER, and Virginia Tech.

REFERENCES

1. Jha, M. C. and Smit, F. J., "Engineering Development of Advanced Physical Fine Coal Cleaning for Premium Fuel Applications", Proceedings of the Ninth Annual Coal Preparation , Utilization and Environmental Control Contractors Conference , Pittsburgh Energy Technology Center, Pittsburgh, 1993, PP 104 - 111.

2. Jha, M. C. and Smit, F. J., "Engineering Development of Advanced Physical Fine Coal Cleaning for Premium Fuel Applications", Proceedings of the Tenth Annual Coal Preparation , Utilization and Environmental Control Contractors Conference , Pittsburgh Energy Technology Center, Pittsburgh, 1994, PP 59 - 66.

3. Jha, M. C. and Smit, F. J., "Selection of Feed Coals for production of Premium Fuel Using Column Flotation and Selective Agglomeration Processes", in High Efficiency Coal Preparation: An International Symposium, S. K. Kawatra (editor), SME, Littleton, Colorado, 1995, PP 391-400.

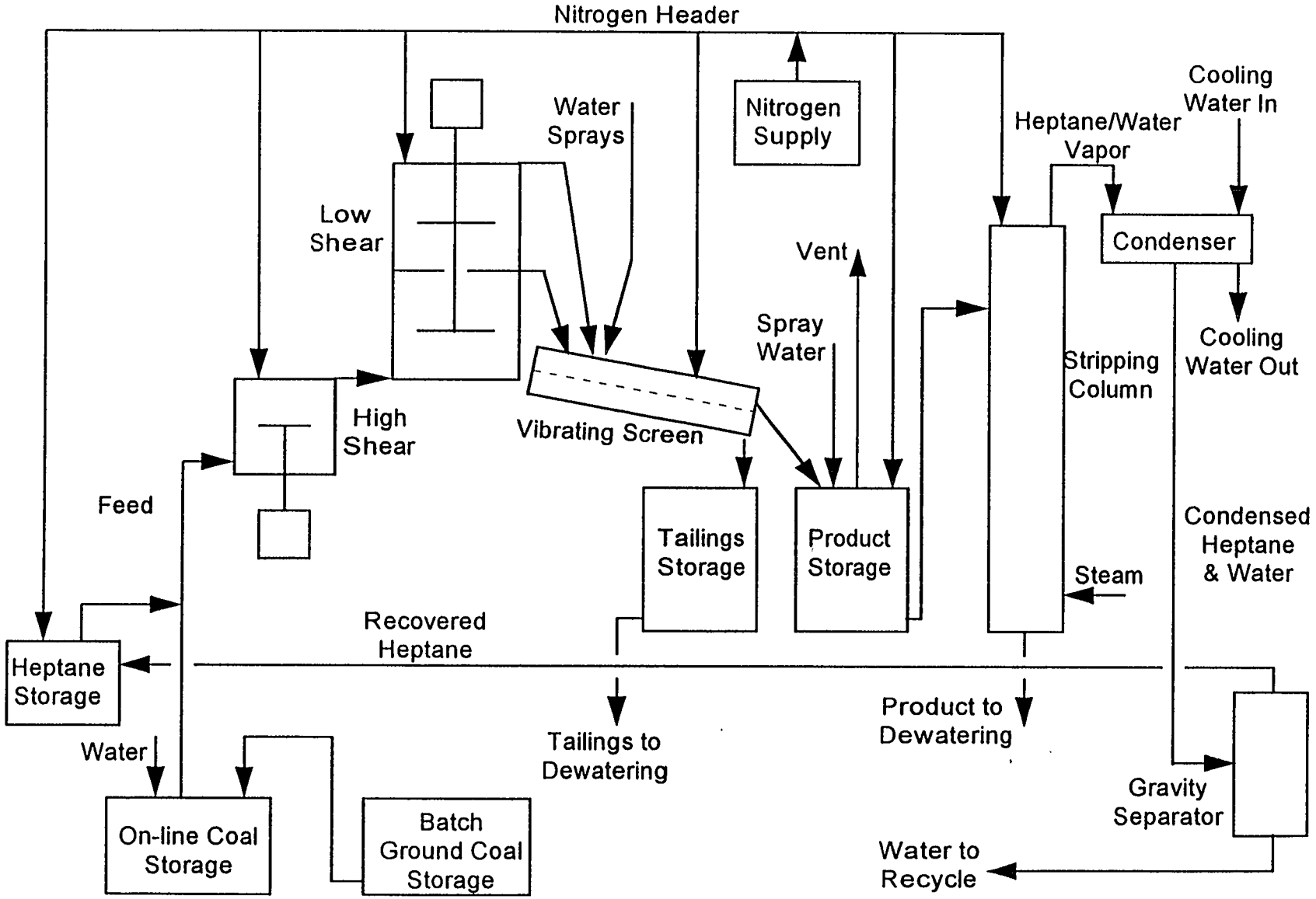

Figure 4. Schematic Block Flow Diagram of the Bench-scale Selective Agglomeration Unit.

CONTROLLING AIR TOXICS THROUGH ADVANCED COAL PREPARATION

W. E. STRASZHEIM, W. H. BUTTERMORE, AND J. L. POLLARD
FOSSIL ENERGY PROGRAM, AMES LABORATORY, USDOE
IOWA STATE UNIVERSITY, AMES IA

ABSTRACT

This project involves the assessment of advanced coal preparation methods for removing trace elements from coal to reduce the potential for air toxic emissions upon combustion. Scanning electron microscopy-based automated image analysis (SEM-AIA) and advanced washability analyses are being applied with state-of-the-art analytical procedures to predict the removal of elements of concern by advanced column flotation and to confirm the effectiveness of preparation on the quality and quantity of clean coal produced. Specific objectives are to maintain an acceptable recovery of combustible product, while improving the rejection of mineral-associated trace elements.

Current work has focused on determining conditions for controlling the column flotation system across its operating range and on selection and analysis of samples for determining trace element cleanability.

The column flotation system has traditionally yielded high recovery of coal, but with less than optimum rejection of ash and especially pyrite. Multiple factors were changed in order to gain greater mineral rejection while sacrificing a minimal amount of coal recovery. This was accomplished by raising the feed rate thus reducing the residence time, reducing the air addition rate thus reducing the air-to-coal ratio, and increasing the froth depth thus reducing entrained minerals. We were able to collect samples which well-defined the operating curve of this column for Pittsburgh No. 8 coal.

Samples of several column flotation runs, float-sink washability separations, and the head sample were analyzed for trace elements using state-of-the-art techniques. Those early results indicate that nearly all elements of concern show some affinity with mineral constituents. The elements arsenic, barium, cadmium, manganese, and lead show a strong affinity for the mineral constituents and can thus be greatly reduced through coal preparation. The other elements show more affinity for the organic components and so cannot be reduced as effectively; nevertheless, some reduction as a result of cleaning has been observed.

Seven pairs of froth and tails samples were selected from flotation runs along with three head samples representing a sampling of points over a wide range of ash and sulfur contents in the froth and tailings streams. Those samples have been submitted for trace element analysis to fill gaps along the operating curve and to verify the preliminary findings above. Those samples will also be examined by SEM-AIA for characterization of mineral components. Trace element and SEM-AIA mineral results will be combined to determine the association of trace elements with particular mineral phases. That, in turn, will be used with predictions of mineral removability to predict trace element cleanability.

PURPOSE

The purpose of this project is to determine the potential for reducing air toxics emissions from the conventional combustion of coal through the application of advanced coal preparation technologies. The major goal is to remove trace elements of concern such as arsenic, beryllium, mercury, lead, cadmium, chromium, manganese, cobalt, selenium, and zinc to the greatest extent possible while maintaining an acceptable recovery of heating value from the raw coal.

BACKGROUND

Increasing concern over potential environmental damage and risk to human health has led to efforts to minimize potential sources of air toxics. The sources of many air toxics resulting from the combustion of coal are trace elements that occur in coal at concentrations of less than one thousand parts per million (one-tenth of one percent). Because of the magnitude of coal use in this country, even low concentrations of toxic materials can lead to significant emissions when coal is burned and thus, may pose a threat to health and the environment. Potentially harmful trace elements may be associated with the mineral matter or organic (carbonaceous) portion of coal. Fortunately, most trace elements of environmental concern are associated with pyrite and accessory minerals in coal. For example, arsenic is commonly found in association with pyrite, as are cobalt, manganese, and selenium; lead is often found as galena or lead selenide, and zinc and cadmium are found with the mineral sphaelerite. The removal of minerals from coal through physical cleaning offers a simple and economical means for reducing air toxics resulting from the conventional combustion of coal.

APPROACH

The approach of this project is to predict the theoretical washability of trace elements in an economically significant coal, to perform advanced column flotation tests designed to remove trace elements from the froth product, and to compare the actual and predicted results for trace element partitioning.

PROGRESS

In early stages of this project, several items of fundamental significance were addressed. A quantity of Pittsburgh No. 8 coal was collected, divided, and stored under argon. A grinding protocol was established for repeatably producing a feed coal which approximates a typical power plant grind (i.e., 75% passing a 200-mesh sieve, herein referred to as "200-mesh"). The column flotation circuit was upgraded with several improvements made to the controlling algorithm to better handle fluctuation in conditions. Float-sink washability was determined for this coal by separating the feed coal in cesium chloride at densities of 1.3 g/cc and 1.6 g/cc. Samples of the feed coal were characterized by scanning electron microscopy-based automated image analysis (SEM-AIA) to determine the association of coal with mineral matter and to predict the cleanability of this sample of Pittsburgh No. 8 coal. The predicted cleanability of 200-mesh Pittsburgh No. 8 coal is shown in Figure 1 as determined from float-sink separation, as predicted by SEM-AIA, and as demonstrated by a column flotation run. The SEM-AIA predictions indicate that cleanability is greater for density-based (i.e., bulk) processes as compared to surface based processes. It indicates that better than 85% of the pyrite and other minerals should be removable while recovering more than 85% of the heating value. Both washability and column flotation data points fall below the cleanability curves indicated by

SEM-AIA. This is as expected since SEM-AIA tends to overestimate ideal cleanability by nature of its measurements while both actual separations are limited to less than ideal performance. The ideal cleanability curve would lie somewhere in the narrow band between these measurements.

The data points for column flotation plotted in Figure 1 are typical of many of our column flotation tests in that a high recovery of coal was achieved, but with less than optimum rejection of ash and especially pyrite. Therefore, multiple factors were changed in order to gain greater rejection while sacrificing a small amount of coal recovery. This was accomplished by raising the feed rate by a factor of two thus reducing the residence time, reducing the air addition rate thus reducing the air-to-coal ratio, and increasing the froth depth thus reducing entrained minerals. We were able to collect samples which well-defined the operating curve for this column for Pittsburgh No. 8 coal. That curve is shown in Figure 2 for a selection of runs to date. The conditions for these runs are shown in Table 1. Thus, the new runs have served to define the operating curve over a broad range. The most recent runs have been conducted in the region around the knee of the curve representing the greatest selectivity of separation.

Samples of several column flotation runs, density separations, and the head sample were analyzed for trace elements using state-of-the-art techniques. Samples selected for trace analysis are shown in Table 2. Data were checked for mass balance and generally good closure was obtained for all elements. Problems were noted for Cr and Ni results for two pairs of samples from flotation runs that had been performed with 5 μm coal according to earlier convention. The elevated levels of Cr and Ni in those samples was determined to be from the stainless steel grinding media and the extra grinding necessary to reduce the 200-mesh coal to 5 μm. Also, results for Sb and Hg showed levels of these elements in solution of less than the detection limit of 1 ppb which corresponds to about 0.1 ppm in the coal. Therefore, no conclusions can be reached regarding these elements for this coal.

A linear regression of trace element concentration versus ash content was performed to determine the association of trace elements with the coal and mineral components. Results are shown in Table 3 and in Figure 3 for the extreme cases of lead and beryllium. The concentrations of the elements in the organic fractions were determined assuming that an ideal, ash-free sample could be obtained. Good correlations of trace element concentration with ash content were generally found. This was mildly surprising in view of the fact that the composition of minerals which gave rise to the ash was not consistent across the range of ash contents. For example, pyrite generally accounted for large fraction of the ash in the low-ash float samples, while clays accounted for the bulk of the minerals in the high-ash samples. The correlations are summarized in Figure 4 showing the distribution of the elements between coal and mineral components in the feed sample. Since a large fraction of most elements are associated with the ash, substantial reductions should be achievable and were attained through column flotation.

The results were used to plot trace element rejection versus coal recovery for the actual data points in Figure 5. Similar curves can be prepared using the derived association of elements with the coal and ash. The elements arsenic, barium, cadmium, manganese, and lead show a strong affinity for the mineral constituents and can thus be greatly reduced through coal preparation. The elements beryllium, cobalt, and selenium show more affinity for the organic components and so cannot be reduced as effectively; nevertheless, some reduction as a result of cleaning has been observed.

Although the results shown above indicate a good correlation between most elements and ash content, there are several large gaps in the data. Therefore, additional samples have been selected for trace element analyses from recent column flotation runs. Seven pairs of froth and tails samples were selected from flotation runs along with three head samples representing a sampling of points over a wide range of ash and sulfur contents in both the froth and tailings streams. Those samples have been submitted for trace element analysis to verify the preliminary findings noted above.

Those samples will also be examined by SEM-AIA for characterization of mineral components. It is hoped that the composition of the mineral matter in these samples will vary from sample to sample so that it will be possible to determine the association of the trace elements with the various minerals. Assuming that will be the case, it should be possible to use the cleanability information from SEM-AIA for each of the minerals to predict the cleanability of the trace elements. Likewise, this information may help to focus the cleaning process for removal of the elements of most concern.

SUMMARY

Column flotation tests have been performed to define the grade-recovery curve for 200-mesh Pittsburgh No. 8 coal processed in our column flotation system. We found it necessary to increase feed rate (decrease residence time), to lower the air-to-coal ratio, and to increase the froth depth layer from our traditional settings in order to improve ash and pyrite rejection while sacrificing a minimal amount of coal recovery. Recovery of 80% of the heating value with rejection of nearly 80% the pyrite and mineral matter was attained for this sample of coal.

Trace element results were obtained for samples from float-sink washability and selected column flotation tests. Regression analyses of trace element concentration and ash contents of those samples showed a strong correlation between trace element concentration and ash content for many elements. Many of the trace elements showed a strong affinity for the ash-forming minerals. For others, there was only a slight dependence of elemental content on ash content. No cases were found where the trace element was associated only with the organic fraction. Therefore, significant reduction of the emission potential should be possible for most if not all elements.

Additional samples are currently undergoing trace element analysis to confirm the above findings. Samples are also being characterized by SEM-AIA in an effort to determine the association of trace elements with particular minerals.

ACKNOWLEDGEMENT

Ames Laboratory is operated for the U.S. Department of Energy by Iowa State University under Contract No. W-7405-ENG-82. This work was supported by the Assistant Secretary for Fossil Energy through the Pittsburgh Energy Technology Center.

Table 1. Conditions and results for selected column flotation tests for Pittsburgh No. 8 coal.

Conditions-feed rates (ml/min) Slurry/Reagent/Wash	MAF Rec. %	Froth T.S. %	Froth Ash %	Tails T.S. %	Tails Ash %	Mass Balance	Pyr Rej (Fd) %
400/40/400 bad MIBC	11.0	3.4	14.8	4.6	27.6	94	95
400/40/400	95.0	4.2	7.3	3.2	83.5	84	58
800/80/400 100% air	96.0	4.8	9.4	4.5	86.3	97	28
800/80/400 3/4 air	89.0	4.2	7.3	5.7	81.3	86	55
800/80/400 1/2 air	46.0	3.9	6.5	6.3	50.2	76	80
800/80/400 5/8 air	46.0	4.1	6.4	4.8	41.9	84	77
800/80/400 5/8 air	49.0	4.0	6.3	4.7	38.9	93	76
800/80/400 5/8 air Fuel oil 1 lb/ton	94.0	5.4	11.4	4.3	81.2	91	8
800/80/400 5/8 air Fuel oil .5 lb/ton	94.7	5.5	11.3	5.3	82.3	91	9
800/80/400 5/8 air Fuel oil .5 lb/ton (deep froth)	74.8	4.2	6.7	6.5	54.0	95	64
800/80/400 5/8 air Fuel oil .5 lb/ton (deep froth)	86.8	4.3	6.9	5.0	65.4	97	54

Table 2. Samples of Pittsburgh No. 8 coal selected for trace element analysis.

Sample	Wt. Frac.	Tot. S.	Ash%
Pitt #8 head sample	100.00	4.60	27.30
Pitt #8 1.30 float	40.20	2.85	2.83
Pitt #8 1.30-1.60	31.10	3.05	12.23
Pitt #8 1.60 sink	28.60	7.67	75.64
Pitt #8 04-14 F-1	62.70	3.29	3.51
Pitt #8 04-14 T-1	37.30	5.55	70.49
Pitt #8 05-03 F-2	71.90	3.99	6.01
Pitt #8 05-03 T-2	28.10	5.53	90.83
Pitt #8 06-23 F-4	81.30	4.35	7.76
Pitt #8 06-23 T-4	18.70	4.07	85.05

Table 3. Regression analysis of the association of trace elements with coal and ash-forming fractions of Pittsburgh No. 8 coal.

(conc. in ppm)	Ba	Mn	Zn	Cr	As	Pb	Ni	Co	Se	Be	Cd
Conc - org.	1.18	1.44	9.35	7.80	1.71	1.37	1.85	2.11	1.22	1.02	0.08
Conc - ash	352.60	267.30	100.53	134.00	43.45	27.77	6.35	9.60	3.92	2.21	0.25
R-squared	0.99	0.99	0.98	0.48	0.95	0.98	0.47	0.81	0.71	0.96	0.27
Feed - meas.	92.50	76.17	30.80	30.30	18.00	8.60	3.74	2.81	2.50	1.34	0.40
Feed - calc.	97.12	74.02	34.24	42.25	13.11	8.58	3.08	4.15	1.96	1.34	0.13
Org. contrib.	0.86	1.05	6.80	5.67	1.24	1.00	1.34	1.53	0.89	0.74	0.06
Ash contrib.	96.26	72.97	27.44	36.58	11.86	7.58	1.73	2.62	1.07	0.60	0.07
Org. fraction	0.01	0.01	0.20	0.13	0.09	0.12	0.44	0.37	0.45	0.55	0.46

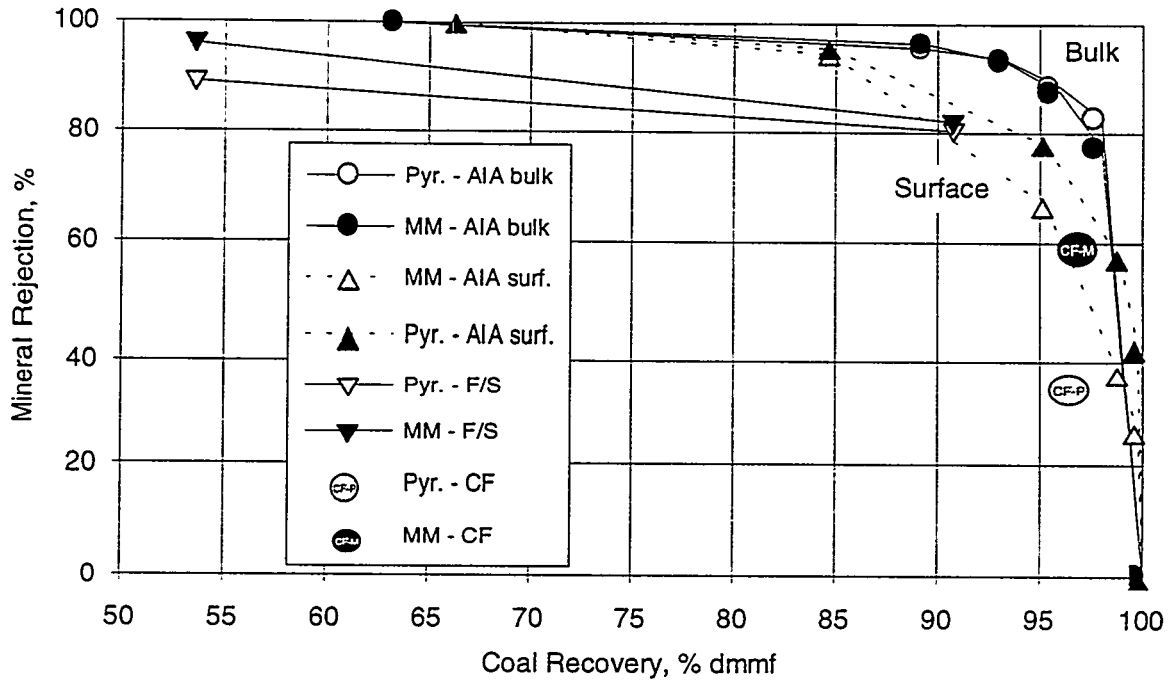

Figure 1. Rejection of minerals as a function of coal recovery for 200-mesh Pittsburgh No. 8 coal as predicted by SEM-AIA and as found by column flotation (CF) and centrifugal float sink (F/S).

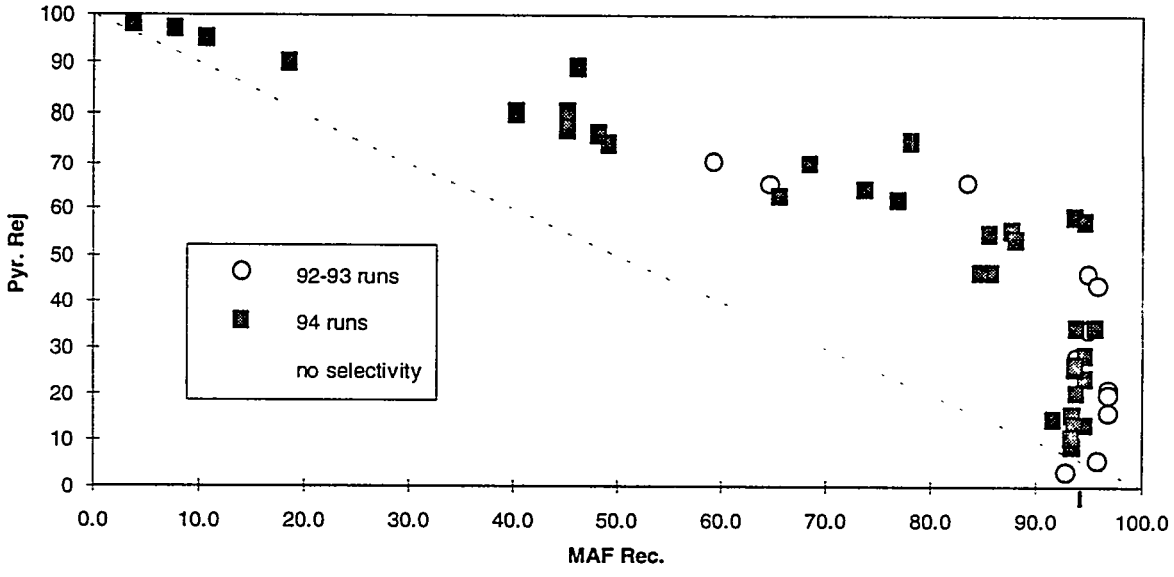

Figure 2. Pyrite rejection as a function of coal recovery for selected column flotation tests for 200-mesh Pittsburgh No. 8 coal.

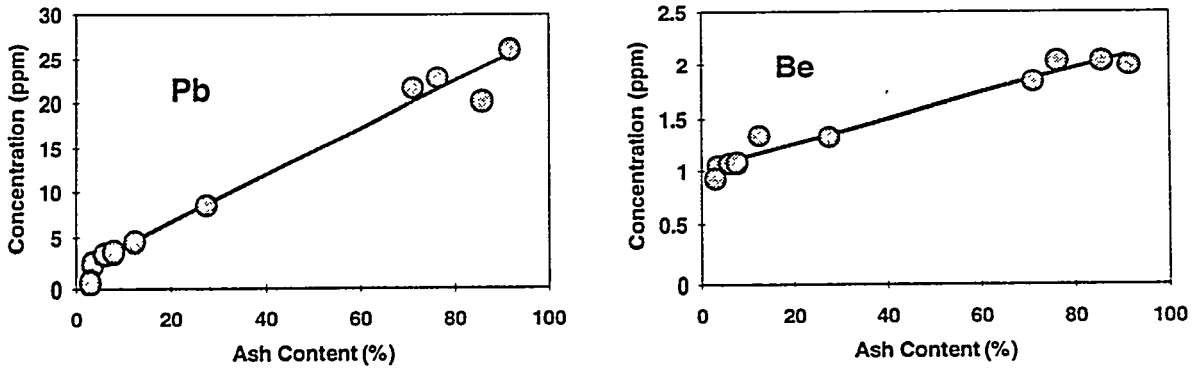

Figure 3. Concentration of Pb and Be as a function of ash content in samples of Pittsburgh No. 8 coal.

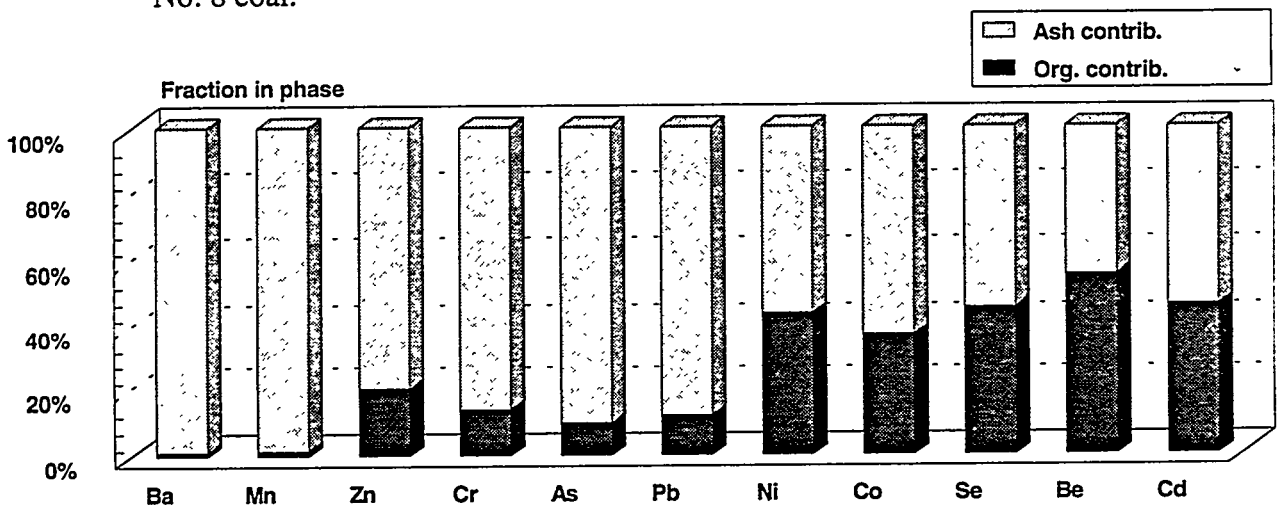

Figure 4. Distribution of trace elements between organic and ash-forming fractions in head sample of Pittsburgh No. 8 coal (27% ash content).

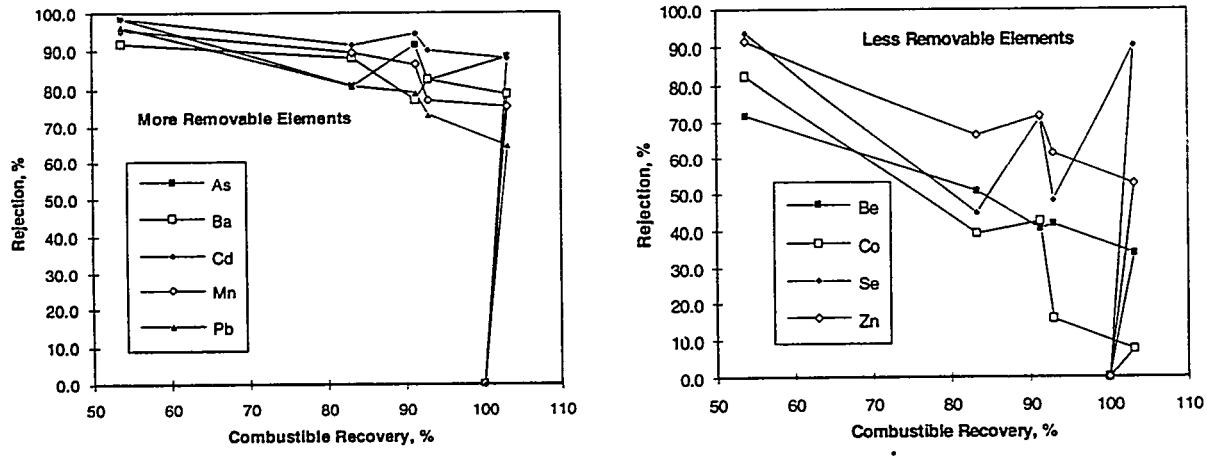

Figure 5. Rejection of trace elements as a function of recovery of 200-mesh Pittsburgh No. 8 coal using both column flotation and centrifugal float-sink data.

APPALACHIAN CLEAN COAL TECHNOLOGY CONSORTIUM

Keith Kutz and Roe-Hoan Yoon[1]
Virginia Polytechnic Institute and State University
Center for Coal and Minerals Processing
146 Holden Hall
Blacksburg, Virginia 24061-0258

INTRODUCTION

General

The Appalachian Clean Coal Technology Consortium (ACCTC) has been established to help U.S. coal producers, particularly those in the Appalachian region, increase the production of lower-sulfur coal. The cooperative research conducted as part of the consortium activities will help utilities meet the emissions standards established by the 1990 Clean Air Act Amendments, enhance the competitiveness of U.S. coals in the world market, create jobs in economically-depressed coal producing regions, and reduce U.S. dependence on foreign energy supplies.

The research activities will be conducted in cooperation with coal companies, equipment manufacturers, and A&E firms working in the Appalachian coal fields. This approach is consistent with President Clinton's initiative in establishing Regional Technology Alliances to meet regional needs through technology development in cooperation with industry. The consortium activities are complementary to the High-Efficiency Preparation program of the Pittsburgh Energy Technology Center, but are broader in scope as they are inclusive of technology developments for both near-term and long-term applications, technology transfer, and training a highly-skilled work force.

The consortium has three charter members, including Virginia Polytechnic Institute and State University, West Virginia University, and the University of Kentucky. Three other universities, namely, Pennsylvania State University, Ohio University, and Southern Illinois University, have been invited to join the consortium. The consortium also includes eight affiliate members[2] composed of coal companies, A&E firms, and equipment manufacturers.

Organization

The consortium is governed by a Council, which consists of representatives of the charter members, the Chairman of the Advisory Board, and the Director. The Advisory Board is made up

[1] Current Director of the Appalachian Clean Coal Technology Consortium
[2] AMVEST Minerals; Arch Minerals Corp.; A.T. Massey Coal Co.; Carpco, Inc.; CONSOL Inc.; Cyprus Amax Coal Co.; Pittston Coal Management Co.; and Roberts & Schaefer Co.

of representatives from participating industrial affiliate members. The board identifies the areas of research priorities and the member universities submit proposals to the Advisory Board. The results of the Board's review are submitted to the Council, which makes the final selection of the proposals.

First-Year Objectives

Because of the limitations in the funding available during the first year, the R&D activities have been limited to only two areas of research: fine coal dewatering and modeling of spirals. Participating industrial companies identified fine coal dewatering as the most needed area of technology development. They also suggested that there is a need for developing new spirals that can have lower specific gravity cuts. The dewatering studies are to be conducted by the University of Kentucky's Center for Applied Energy Research (CAER) and Virginia Tech's Center for Coal and Minerals Processing (CCMP). A spiral model is to be developed by West Virginia University.

DESCRIPTION OF INDIVIDUAL PROJECTS

At the time of preparing this communication, the Advisory Board has not competed the review process. Therefore, the project descriptions given below are based on the proposals submitted rather than approved by the Council. It should also be noted that the proprietary information contained in the proposals are not presented in this communication.

Virginia Tech - Innovative Approaches to Fine Coal Dewatering

Background

The coal industry has been discarding coal fines due to difficulties in cleaning and moisture removal. Recent developments in advanced column flotation technologies have largely solved the first problem; however, there are currently no practicable solutions to the problems associated with fine coal dewatering. The mechanical dewatering methods commonly used today are not capable of reducing the moisture to levels acceptable to electrical utilities and other coal users. Thermal drying can reduce the moisture to acceptable levels; however, conventional thermal dryers are capital-intensive and costly to operate. Therefore, there is an impending need for innovative approaches to solving problems in dewatering fine coal.

For this reason, a novel dewatering process has been developed at CCMP. In this process, a wet coal is contacted with liquid butane, which displaces water from the surface of coal. The spent butane is recovered and recycled. This process is capable of reducing the moisture to levels comparable to thermal drying. Since the process of displacing water with butane is spontaneous, no energy is consumed during this step. The majority of the energy consumption occurs during the recycling stage.

Objectives

The objectives of this work are i) to test the novel dewatering process developed at CCMP on a variety on coals from the Appalachian coal fields, and ii) to determine its economic feasibility.

Scope of Work

Batch dewatering tests will be conducted on fine coal products from different coal preparation plants in the Appalachian coal fields. The tests will be conducted to study the effects of various process variables on the efficiency of the process. After establishing the optimum operating conditions with one coal, other coal samples will be tested. The test results will be used for economic analysis.

University of Kentucky - Improving Dewatering of Fine Clean Coal Using High-Pressure Filters

Background

Pressure filtration of fine coal is capable of producing a product containing as little as 20% moisture which is lower than is typically possible with other mechanical dewatering processes. Unfortunately, the operating costs for pressure filters are higher than for other conventional dewatering devices, i.e., vacuum filters and screen-bowl centrifuges. The major factor contributing to the high operating cost of high-pressure filters is air consumption. High air consumption usually occurs when the filter cake develops cracks through which air escapes. Once cracks develop, the effectiveness of the pressure or vacuum filter diminishes significantly.

In preliminary work conducted at the CAER, paper pulp was added to a coal slurry prior to filtration. During filtration, it was observed that no cracks developed in the filter cake and that the final wet cake moisture was lowered by four percent over the same coal slurry filtered without the addition of paper pulp. The wet filter cake also exhibited exceptionally high compressive strength. This suggests that the addition of inexpensive fibrous material may help minimize the consumption of air, thus making high-pressure filtration a more viable process for fine coal dewatering.

Objectives

The main objectives of this project are to i) identify the factors responsible for the formation of cracks within the filter cake during vacuum and high-pressure filtration, and ii) evaluate the addition of various types of fibers to the coal slurry to reduce or eliminate the formation of cracks. A second objective is to harden the filter cake in situ to improve the handling characteristics of the dewatered coal.

Scope of Work

Dewatering studies will be performed on froth flotation products from two coal preparation plants in the Appalachian region. Initially, dynamic filtration tests will be run to determine the effects of various operating parameters and reagent addition on the dewatering characteristics of the froth products. Variables to be studied include reagent quantity, pH, percent solids in suspension, particle size distribution, filtration kinetics, and final wet cake moisture content.

Fiber addition studies will be carried out using pulps produced from newspapers, computer/copier waste paper, carpet waste, and wood powder. Aqueous suspensions of each material will be prepared and added to the coal slurry. The slurry will then be filtered using both vacuum and high-pressure filters. Variables to be investigated include density of the pulp suspensions, percent of fibers added, and final wet cake moisture. All filter cakes will be checked for cracking during filtration. If cracks are observed, the cake will be dissected and examined via microscopy to determine the origin of the cracks. Selected filter cakes will also be examined using SEM and petrography to gain insights as to the effect of fiber arrangement on dewatering efficiency.

The wet and dried filter cakes will also be evaluated for their handling characteristics using four criteria: compressive strength, resistivity during drop tests, abrasion index, and dust reduction efficiency.

West Virginia University - Modeling of Spirals

Background

The most promising approach to improving spiral separation efficiency is through extensive computer modeling of fluid and solids flow in the various operating regions of the spiral. Previous efforts at accurate modeling have failed, primarily due to the use of incorrect physical models describing the flowing slurry stream.

As operated, the modern spiral has two functioning regions. These are the Grandy region, where the water flows, and a stable dense media section where the physical separation takes place. The Knoll line separates the Grandy from the dense media section. The Grandy is further divided into upper and lower regions. The dense media section is also divided into two regions. The radially outboard region is the low density region while the radially inboard region is the high density region. Energy and fluid in the Grandy forms and powers the dense media section of the spiral.

The addition of makeup water to the spiral greatly affects the size, location and behavior of each flow region. A detailed physical model has been developed that delineates the complex behavior of water and solids within the Grandy and dense media regions.

Several key issues must be resolved to improve the performance of spirals. Since movement of particles into the separation zone of the spiral is the key to improving efficiency, the most important issue is control of fluid and particle flow. Critical questions to be answered include determining the optimum location for makeup water addition, how to control the position of the Roberts and Knoll lines, and how to control the movement of particles from the upper Grandy into the lower Grandy. In addition, the effects of spiral diameter, pitch and height on fluid/particle behavior also need to be determined.

Objectives

The objective of this project is to use computer modeling to develop better, more efficient spiral designs for coal cleaning. The fully-developed model will predict spiral performance based on variations in spiral profile, flow rate, and pitch. Specific goals are to: i) design spirals capable of making separations at a specific gravity of 1.5, and ii) broaden the size range at which spirals make effective separations.

Scope of Work

Three models will be used in this work: i) a physical model that qualitatively describes the physics of the spiral, ii) a mathematical model that quantifies the physical model, and iii) a numerical model that permits the calculation of the mathematical model. All three models will be studied simultaneously; however, the primary focus of the first year's effort will be to fully develop the numerical model. Sufficient experimental data are available from the literature to provide a baseline against which the computer model can be checked.

In the initial stage of this project, a flow field computer program will be used to simulate pure water flow down a smooth, infinitely wide inclined plane. The results will be closely checked with experimental results reported in the literature. As the initial model is validated, the program will then be used to simulate more complex topographies and channels. Again, the simulator results will be compared with those from the literature.

Following the studies with pure water flow, two approaches will be followed. The first will be to numerically simulate curvilinear flow and the second will be to simulate slurry flow on linear surfaces. Once these models are working properly, they will be combined. The combined model will simulate flow in the upper and lower Grandy regions. Experimental data used to validate the combined numerical model will be provided by Carpco, Inc.

ACKNOWLEDGMENT

The Appalachian Clean Coal Technology Consortium gratefully acknowledges the support of the U.S. Department of Energy under Cooperative Agreement Number DE-FC22-94PC94152.

The following manuscript was unavailable at time of publication.

PRODUCTION OF COMPLIANCE COAL FROM ILLINOIS BASIN COALS

Dr. Steven Hadley
Praxis Engineers
852 N. Hillview Drive
Milpitas, CA 95035

Please contact author(s) for a copy of this paper.

The following manuscript was unavailable at time of publication.

EPRI UPGRADED-COAL INTEREST GROUP

William Weber
Electric Power Research Institute
516 Franklin
Chattanooga, Tennessee 37411

Please contact author(s) for a copy of this paper.

The following manuscript was unavailable at time of publication.

OXIDATIVE STABILIZATION OF A DRIED LOW-RANK COAL

Karl Schroeder
U.S. Department of Energy
Pittsburgh Energy Technology Center
P.O. Box 10940, M.S. 83-226
Pittsburgh, PA 15236

Please contact author(s) for a copy of this paper.

THE KINETICS OF FOSSIL RESIN EXTRACTION FROM A FLOTATION CONCENTRATE

DE-AC22-93PC92251

L. Li, Q. YU, AND J. D. MILLER
UNIVERSITY OF UTAH, SALT LAKE CITY, UT 84112

ABSTRACT

The kinetics of fossil resin extraction from a flotation concentrate by heptane were investigated as a function of process variables using monosize particles. Experimental results provide for a better understanding of the refining process and the basis for subsequent design and construction of a continuous resin refining circuit. Based on the effect of process variables (particle size, stirring speed, and temperature) the resin extraction rate appears to be controlled by surface solvation phenomena. The initial extraction rate was found to be inversely proportional to the initial particle size and a kinetic model is being developed to describe the experimental results.

INTRODUCTION

Certain bituminous coals of the western U.S. are known to contain appreciable quantities of macroscopic fossil resin. Such resinous coals are found in the states of Arizona, Colorado, New Mexico, Utah, Washington, and Wyoming, etc. The Wasatch Plateau coal field in Utah has a particularly high content of fossil resin. It has been reported that many seams in this field average as much as 5% resin.[1-2] Macroscopic fossil resins are friable and tend to concentrate into the fine sizes during coal preparation. Therefore it is not unusual to find that fine coal streams in such coal preparation plants contain more than 10% recoverable macroscopic resin, even when the run-of-mine coal contains only 3% resin.[5]

Fossil resins have been recovered intermittently from the Wasatch Plateau coal field in Utah since 1929 by gravity and/or flotation processes. The production, however, has been on a very small scale and the technologies used have limited the development of a viable fossil resin industry. Resin flotation concentrates can be refined by solvent extraction and evaporation of the solvent. Solvent-purified resins have a market value of at least $1.00/kg as a chemical commodity and can be used in the ink, adhesive, rubber, varnish, enamel, paint and coatings, and thermoplastics industries.[3-6] Unfortunately, process technology for the recovery and utilization of fossil resins from coal has not received sufficient attention. Because of the lack of technology and the competition from synthetic resins, the valuable fossil resin resource from western coal has been wasted, being burned together with coal for electric power generation. It is estimated that the fossil resin from the Wasatch Plateau coal field burned each year as fuel has a value of $100 million as a chemical commodity - equivalent to the value of the coal itself! In this regard, significant efforts have been made to develop technology for a fossil resin industry in the western coal fields. As a result, several new flotation technologies for the recovery of fossil resin from coals have been developed.[5-8] These flotation technologies provide a highly efficient means to selectively recover fossil resin from coal (more than 80% recovery at about 80% concentrate grade). However, little attention has been given to the refining of the fossil resin flotation concentrate although solvent refining is a critical step in order to increase the

market value of the fossil resin. The objective of this DOE sponsored research project was to study the details of the refining technology so that the process for fossil resin recovery can be optimized and the quality of refined fossil resin products can be controlled to meet market specifications.

In this paper, the resin extraction kinetics from a Wasatch Plateau fossil resin concentrate are discussed based on the physical/chemical properties of the resin. The effects of important extraction variables are examined and a kinetic model for batch resin extraction with heptane is under development.

CHARACTERIZATION OF RESIN CONCENTRATE

Fossil Resin Flotation Concentrate

The fossil resin flotation concentrate used in this study was obtained from Wasatch Plateau coal of south central Utah and generated by pilot-plant flotation tests under a previous DOE-funded program "Selective Flotation of Fossil Resin from Wasatch Plateau Coal." The fossil resin flotation concentrate has a heptane soluble resin content of approximately 75%. It was naturally dried, sampled and stored in plastic bags for future research use. The ash and moisture contents of the resin concentrate were found to be 1.23% and 1.03% respectively. The resin concentrate has a relatively fine particle size distribution with more than 80% (by weight) being less than 200 mesh (74 microns) and about 64% (by weight) less than 400 mesh (37 microns).

Heterogeneity of the Fossil Resin

Since fossil resin fluoresces under blue light, fluorescence microscopy can be used to examine its macroscopic composition. Under blue light, fossil resin grains can be distinguished and sorted into four resin types: yellow, amber, light-brown and dark-brown resin.[9] Polished briquettes (pellets), in which the particles of the resin concentrate were mounted, were examined using an Axioplan Universal Microscope manufactured by Carl Zeiss, West Germany. It was found from this petrographic analysis that the resin concentrate consists predominately of amber (29%) and light-brown resins (35%) with some yellow resin (12%) and dark-brown resin (11%). A significant amount of coal fines (13%) were also found in the resin flotation concentrate. It is clear that the fossil resin concentrate is a heterogeneous material and preliminary results indicate that different extraction rates are associated with the four different resin types.[10]

Even at the molecular level fossil resin is known to be a complicated organic polymer. Fossil resin from the Wasatch Plateau coal field was classified by Anderson[11] et al. to belong to the class II resinites, which are believed to be derived from diterpenoic acid rich precursors. Based on the results of Py-GC/MS analysis, the bulk component of the Utah resin appears to be a polymer consisting of sesquiterpenoid ($C_{15}H_{24}$) repeat units. It has been reported that approximately 10% of the resin consists of a mixture of cyclic terpenoids.[12] In view of the foregoing, it is evident that the composition and structure of the Utah resin are not uniform. However, based on present results an approximate description can be made. The average elemental composition of heptane extracted resin is as follows:

C	H	N	S	O
86.88%	10.85%	0.17%	0.30%	1.80%

Only small amounts (2.3%) of heteroatoms (N, S and O) are found in the heptane extracted resin, which implies that the polar functional groups are rare. By adsorption chromatography with silica gel as the static phase and heptane as the elution solvent, a distinct component (7.7%) was separated from the heptane extracted resin. The IR spectra of this component and the remaining

more-polar fraction are shown in Figures 1a and 1b, respectively. Figure 1a has typical alkane features. For the more-polar fraction in Figure 1b, the peaks of the CH stretching vibrations (2850 to 2960 cm^{-1}) and CH bending vibrations (1462 and 1382 cm^{-1}) obviously predominate. However, there is a signal which shows significant carbonyl (C=O bond) stretching vibrations at 1711 cm^{-1} for the more-polar fraction. In conclusion, the fossil resin from the Wasatch coal field is heterogenous and nonuniform in its chemical composition. It mainly consists of hydrocarbons with small amounts of functional groups containing heteroatoms.

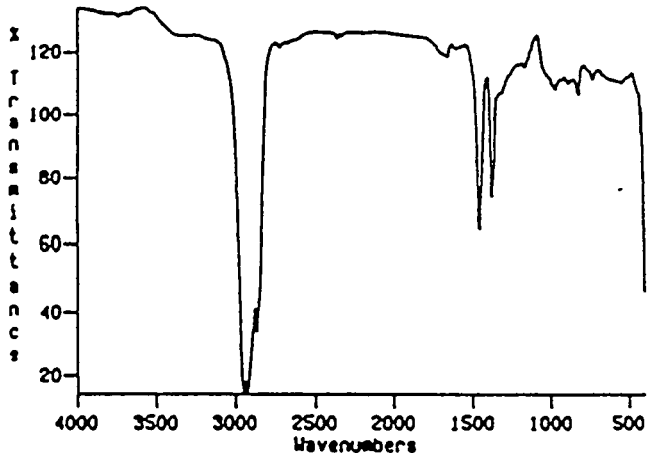

Figure 1a. IR spectrum of the component separated by elution chromatography from the heptane extracted resin.

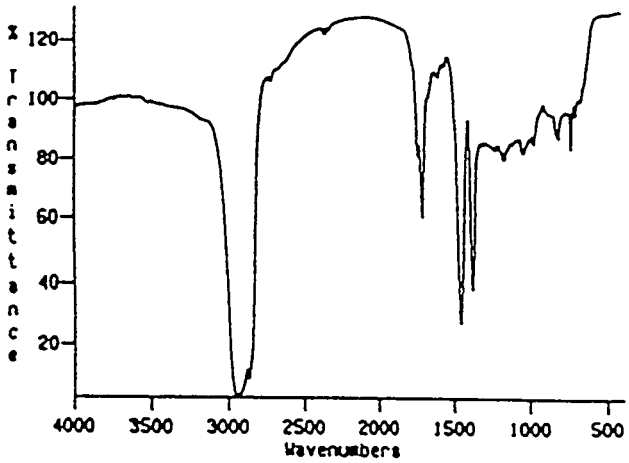

Figure 1b. IR spectrum of the remaining more-polar fraction separated by elution chromatography from the heptane extracted resin.

EXPERIMENTAL

A series of experiments for resin extraction by heptane were designed to study the effect of process variables on the rate of the resin extraction from monosize particles at a low solids concentration. Process variables studied included temperature, particle size and agitation intensity. The resin extraction kinetics were determined by analysis of the resin in heptane solutions taken at certain time intervals during extraction process.

Technical grade normal heptane (C_7H_{16}) was used as the solvent for the kinetics study. Heptane has a molecule weight of 100.21, density of 0.684 gram/cm^3 and boiling point of 98 ^{0}C. Four monosize samples (8×10, 28×35, 48×60, and 100×150 mesh) were prepared by wet screening from the flotation concentrate. The heptane-soluble resin content in all samples was determined to be between 88% to 95% with a TX-6 Soxhlet extraction unit at the boiling point of heptane (98 ^{0}C) for 6 hours.

The resin concentration in heptane was determined by a UV/Vis spectrophotometer (Beckman DU-7) at room temperature. It was found that a good linear relationship between UV absorbance at 300 nm and resin concentration in the heptane solution exists as long as the resin

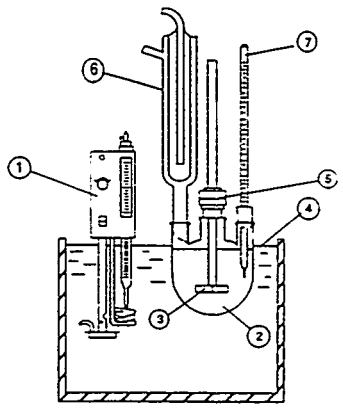

Figure 2. Schematic drawing of resin extraction apparatus.

concentration is below 500 ppm.

A schematic drawing of the experimental apparatus used for the kinetics study is presented in Figure 2. The reactor is a one liter round bottom 3-neck distillation flask. One liter of heptane was taken into the flask and heated to the desired temperature at which time 1.5 grams of resin sample was added to initiate the reaction. During the extraction process, about 3 ml of resin solution was taken from the suspension by a syringe with a prefilter at each desired time interval. The heptane solution was analyzed for resin concentration by UV/Vis spectroscopy. All the data presented in the following sections were normalized on the basis of the heptane-soluble resin content in the samples.

EXPERIMENTAL RESULTS AND DISCUSSION

Effect of Resin Particle Size

The effect of particle size on heptane extraction of resin at 20 °C and 500 RPM is presented in Figure 3. It is evident that the extraction rate decreases with an increase in extraction time, which is to be expected from geometric considerations and from the heterogeneity of the fossil resin. As shown in Figure 3, a strong dependence of resin extraction rate on particle size was found. The initial resin extraction rates ($d\alpha/dt$) are plotted against the inverse of the initial resin particle size in Figure 4 and the linear relationship suggests that the initial rate may be limited either by mass transfer or by surface reaction.

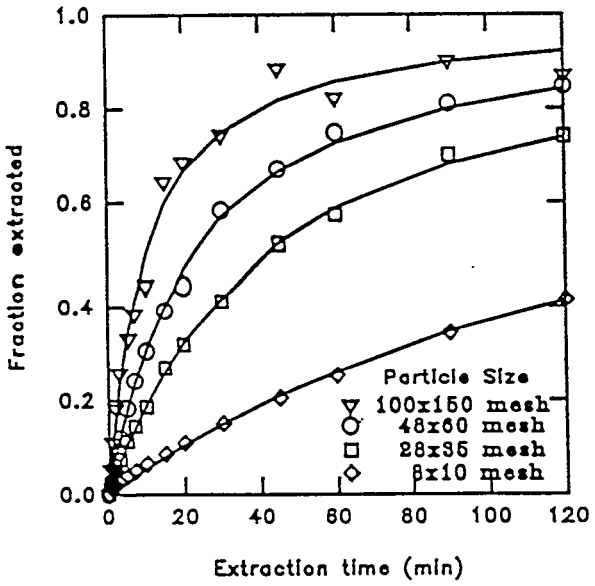

Figure 3. Effect of particle size on heptane extraction of resin at 25 °C and 500 rpm.

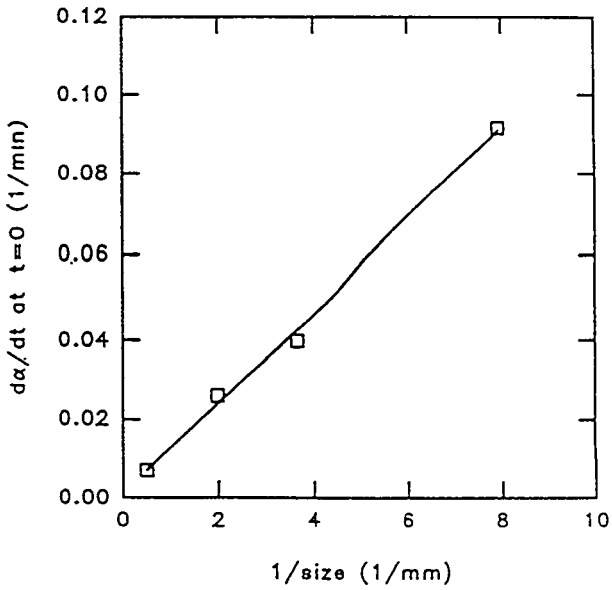

Figure 4. Initial extraction rates vs. the inverse of the particle size from data presented in Figure 3

Effect of Temperature

Several tests on heptane extraction of resin were performed at different temperatures in order to determine the effect of temperature on the extraction rate and the results are presented in Figure 5. As expected, the resin extraction rate was found to increase with an increase in extraction temperature. The effect of temperature is very significant. The initial extraction rates

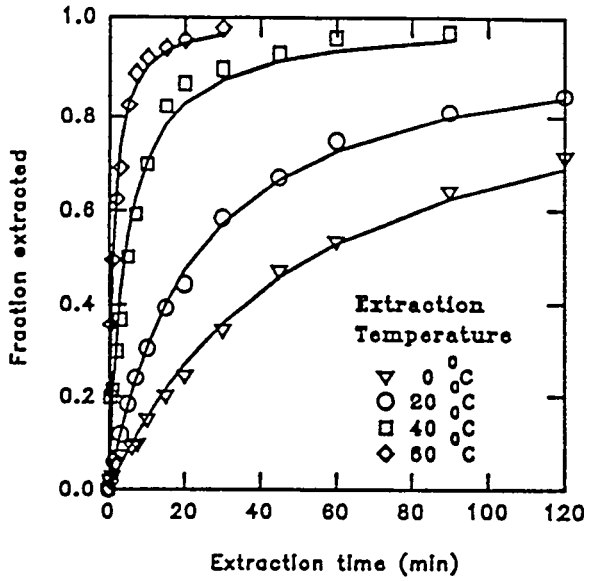

Figure 5. Effect of temperature on heptane extraction of 48×60 mesh resin particles and 500 rpm.

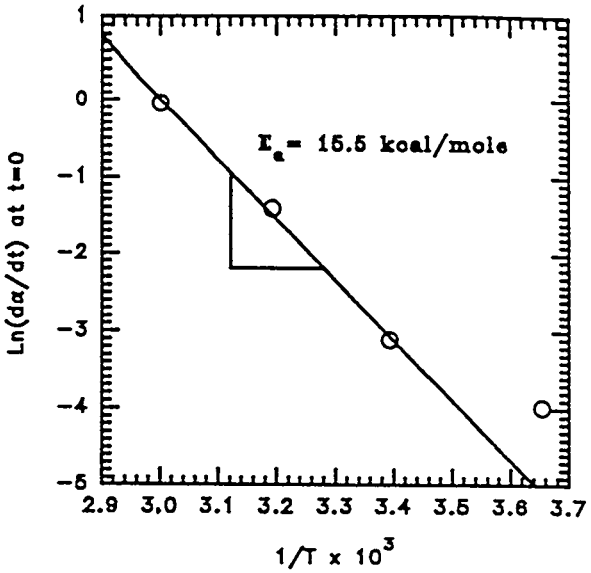

Figure 6. Arrhenius plot for heptane extraction of 48×60 mesh resin particles from data presented in Figure 5.

at different temperatures are plotted according to e Arrehenius equation in Figure 6 and a good linear relationship between the logarithm of the initial extraction rate and inverse temperature was found. From the slope of this linear relationship, an activation energy of 15.5 kcal/mole can be calculated. The magnitude of the activation energy indicates that the extraction process is controlled by a surface reaction mechanism involving the dissolution of resin molecules into the heptane solution. In this regard, the energetics of such solvation reactions are expected to be related to the observed activation energy.

Effect of Agitation Intensity

The effect of agitation intensity on heptane extraction of resin is presented in Figure 7 in terms of stirring speed (RPM). It was found that the agitation intensity has hardly any effect on the resin extraction rate, again providing evidence that the extraction process is not under diffusion or mass transfer control for these experimental conditions (room temperature, low solids concentration, and moderate stirring speed).

Solvent extraction and purification of fossil resin from a resin flotation concentrate is accomplished by dissolving the resin compounds into an organic solvent in which other coal macerals will not be dissolved. It should be possible to describe the resin extraction reaction

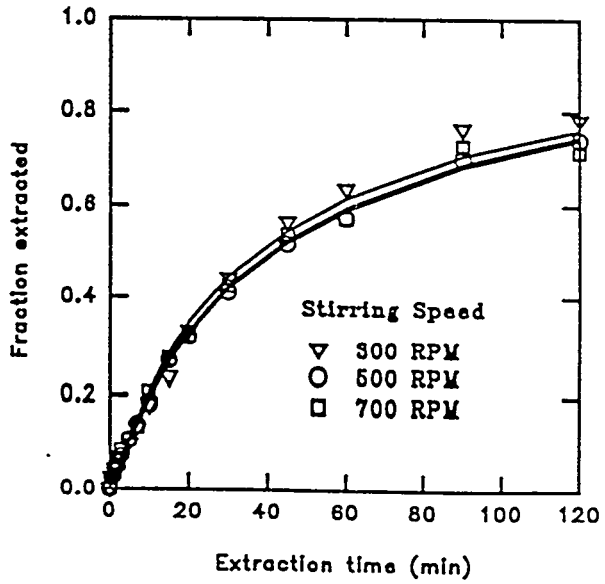

Figure 7. Effect of stirring speed on heptane extraction of 48×60 mesh resin particles at 25 °C and 500 rpm.

by a typical kinetic analysis for shrinking core geometry. However, it should be noted that the resin extraction reaction has special features. As mentioned before, the fossil resin particles are heterogeneous in terms of their structure (both macroscopic and molecular) and their chemical composition. And they are complex polymers and copolymers of varied molecular weight. Different components of the fossil resin, even components with the same structural characteristics but different in their molecular weight, are expected to have different dissolution rates in organic solvents such as heptane.

For nonporous uniform particles of spherical shape, the relationship between the extent of extraction (α) and the extraction time (t) for a batch reaction under surface reaction control can be described by the following equation,[13]

$$1 - (1 - \alpha)^{\frac{1}{3}} = kt \qquad (1)$$

where k is the overall rate constant which includes reactant concentration and many other factors such as surface area, intrinsic rate constant, initial particle size, shape factor, reactive sites on the particle surfaces et cetera. The constant, k, should be inversely proportional to the initial particle size. However, this traditional shrinking core model does not fit the data shown in Figure 3. It is expected that the rate constant varies with time and thus the kinetic analysis must be considered in more detail.

From characterization studies, it was found that the fossil resin particles are heterogeneous and not of uniform composition based on microscopic examination and chemical analysis. During extraction, it is expected that the resin components with high solubility will be extracted more rapidly than those with low solubility. Therefore, the composition of the extracted resin will change as a function of time and the rate will decrease more than might be expected as the extraction reaction proceeds. A sequential extraction test was conducted to examine this hypothesis. Sequential extraction of the concentrate was carried out for different time intervals and heptane extraction temperatures. One hundred and eighty grams of the concentrate and 1800 ml of heptane were taken into the reactor for the first stage of extraction. After the first extraction, the pregnant resin solution was filtered and the first resin product was obtained by evaporation. The residual resin concentrate was processed with fresh heptane using the same extraction procedure as the first extraction for desired times and temperatures. A stirring speed of 700 RPM was used throughout all experiments. Products from these sequential tests were recovered and the conditions with the analytical results are summarized in Table 2. A Klett-Summerson Photoelectric Colorimeter manufactured by Klett Manufacturing Co., Inc. was used to analyze the resin products obtained. The light beam of the colorimeter has a visible spectral range, from approximately 400 to 465 nm. Toluene was used as the solvent for these transmittance measurements, and the concentration of the resins in the toluene was fixed at 0.1 gram per 50 ml of toluene. The analytical results obtained from the transmittance measurements show that the extracted resin composition changes with an increase in extraction time.

Thus it can be imagined that the resin extraction kinetics must take into consideration the fact that the resin is nonuniform and should be characterized either by a distribution of rate constants or by taking into consideration the fact that the composition of the unreacted particle changes with time.

Table 2. Sequential extraction results and analysis of products

Extracted resin product	Extraction temperature (°C)	Extraction time (min)	Transmittance (%)	Extracted product	
				Wt. (%)	Cumulative Wt. (%)
Product 1	27	10	53.75	48.97	48.97
Product 2	27	20	46.78	12.76	61.73
Product 3	27	90	37.00	7.28	69.01
Product 4	60	20	23.44	3.67	72.68
Final residue			<1	27.32	100.00

CONCLUSIONS

Although fossil resin is heterogeneous in terms of its macroscopic and chemical composition, it is mainly composed of non-polar hydrocarbon compounds with a small number of functional groups containing heteroatoms. The solvent, heptane, is also a nonpolar aliphatic compound. It is expected that no chemical reactions occur in such an extraction process at low temperature (0-90 °C). The main interaction between resin and heptane is expected to be the van der Waals forces of interaction associated with solvation phenomena. In this regard, the resin extraction rate was found to be largely independent of agitation intensity at room temperature, low solids concentration and moderate agitation. Further the initial extraction rate was found to be inversely proportional to the initial particle diameter. Temperature has a significant effect on extraction rate and the activation energy for resin extraction by heptane was found to be 15.5 kcal/mole. On this basis it is expected that the extraction rate is controlled by surface solvation phenomena. Additional research is in progress to develop a kinetic model for the fossil resin extraction reaction.

ACKNOWLEDGMENTS

This research was performed in the Coal/Fossil Resin Surface Chemistry Laboratory established by the state of Utah. The financial support provided by the Department of Energy Contract No. 93PC92251, is gratefully recognized and appreciated by the authors.

REFERENCES

1. Crawford, A.L., and Buranek, A.M., 1952, Resinous Coals, No. 23 Utah Geological and Mineralogical Survey, p. 4.
2. Spieker, E.M., and Baker, A.A., 1928, Geology and Coal Resources of Salina Canyon Distict, Sevier Country, UT, Bulletin 796-C, US Geological Survey, p. 125.
3. Dawson, H.A., 1993, Bauer Resin Refinery, Dawson Metallurgical Laboratories, Inc.
4. Benemelis, R., 1990, Production and Utilization of Coal Resins, Preprint for the 1990 SME Annual Meeting, Salt Lake City, UT, February, 1990.
5. Miller, J.D., Ye, Y., Yu, Q., and Bukka, K., 1992, Fossil Resin, A Value-Added Product from Western Coal, Proceedings, Ninth Annual International Pittsburgh Coal Conference, Pittsburgh, PA., pp. 31-38.

6. Miller, J.D. and Ye, Y., 1989, Selective Flotation of Fossil Resin from Wasatch Plateau High-Volatile Bituminous Coal, Minerals & Metallurgical Processing, pp. 87-93.
7. Miller, J.D., Yu, Q., Bukka, K., and Ye, Y., 1993, Analysis of Selective Resinite Flotation for Wasatch Plateau Coal by pH Control, Coal Preparation, vol. 13, pp. 31-51.
8. Yu, Q., Bukka, K., and Miller, J.D., 1994, The Chemistry of Ozone Conditioning in the Selective Flotation of Macroscopic Fossil Resin from Utah Wasatch Plateau Coal, Coal Preparation, vol. 15, pp. 35-50.
9. Yu, Q., Bukka, K., Ye, Y., and Miller, J.D., 1991, Characterization of Resin Types from the Hiawatha Seam of the Wasatch Plateau Coal Field, Fuel Processing Technology, 28:105.
10. Yu, Q., Bukka, K., Ye, Y., and Miller, J.D., 1993, A Study of Hexane/Toluene Extraction of Fossil Resin Types from the Utah Wasatch Plateau Coal, Fuel, 73(8):1083-1092.
11. Anderson, K.B., and Winans, R.E., 1991, Structure and Structural Diversity in Resinites as Determined by Pyrolysis-Gas Chromatography-Mass Spectrometry, ACS Div. Fuel Chem. Prepr., vol. 36, pp. 765-773.
12. Meuzelaar, H.L.C., Huai, H., Lo, R., and Dworzanski, 1990, Chemical Composition and Origin of Fossil Resins from Utah Wasatch Plateau Coal, Prepr., S.M.E. Meeting, Salt Lake City, Utah, Feburary.
13. Eyring, H., Powell, R.E., Duffy, G.H., and Parlin, R.B., 1949, Chem. Rev., vol. 45, p.145.

BENCH-SCALE TESTING OF A MICRONIZED MAGNETITE, FINE-COAL CLEANING PROCESS

PETER J. SUARDINI

PROCESS ENGINEER
CUSTOM COALS, INTERNATIONAL
PITTSBURGH, PA

ABSTRACT

Custom Coals, International has installed and is presently testing a 500 lb/hr. micronized-magnetite, fine-coal cleaning circuit at PETC's Process Research Facility (PRF). The cost-shared project was awarded as part of the Coal Preparation Program's, High Efficiency Preparation Subprogram. The project includes design, construction, testing, and decommissioning of a fully-integrated, bench-scale circuit, complete with feed coal classification to remove the minus 30 micron slimes, dense medium cycloning of the 300 by 30 micron feed coal using a nominal minus 10 micron size magnetite medium, and medium recovery using drain and rinse screens and various stages and types of magnetic separators. This paper describes the project circuit and goals, including a description of the current project status and the sources of coal and magnetite which are being tested.

INTRODUCTION

A recent emphasis of the Department of Energy's (DOE's), Coal Preparation Program has been the development of high-efficiency technologies that offer near-term, low-cost improvements in the ability of coal preparation plants to address problems associated with coal fines. In 1992, three cost-shared contracts were awarded to industry, under the first High-Efficiency Preparation (HEP I) solicitation. All three projects involved bench-scale testing of various emerging technologies, at the Pittsburgh Energy Technology Center's (PETC's), Process Research Facility (PRF). The first project, completed in mid-1993, was conducted by Process Technology, Inc., with the objective of developing a computerized, on-line system for monitoring and controlling the operation of a column flotation circuit. The second project, completed in mid-1994, was conducted by a team led by Virginia Polytechnic Institute to test the Mozely Multi-Gravity Separator in combination with the Microcel Flotation Column, for improved removal of mineral matter and pyritic sulfur from fine coal. The third project, which is the subject of this paper, is presently being conducted by Custom Coals, International (CCI), to evaluate and advance the micronized magnetite-based, fine-coal cycloning technology through integrated circuit operation.

TECHNOLOGY DESCRIPTION

Over the last ten years, the use of micronized-magnetite cycloning for beneficiating fine coal has been researched by both the DOE and Genesis Research Corporation. Based on its work, the DOE received a patent in 1991 titled "Fine-Coal Cleaning via the Micro-Mag Process". Likewise, Genesis Research received patents in 1992 on more complicated processes (ie., Carefree and Self-Scrubbing Coal Processes), involving the micronized-magnetite cycloning technology. In 1993, Custom Coals brought together these technologies by purchasing the rights to the various DOE and Genesis Research patents, and is actively marketting and commercializing the technology both domestically and internationally. Custom Coals is currently constructing a 500 TPH commercial cleaning plant, in Somerset County, PA, employing these technologies, under the DOE's Clean Coal Technology Program. The DOE cofunded

demonstration project will occur through 1996, after which the plant will continue to operate commercially, producing compliance coal for local and regional utilities.

The micronized-magnetite coal cleaning technology is based on widely used conventional dense-medium cyclone applications, in that it utilizes a finely ground magnetite/water suspension as a separating medium for cleaning fine coal, by density, in a cyclone. However, the micronized-magnetite cleaning technology differs from conventional systems in several ways:

- It utilizes significantly finer magnetite (about 5 micron mean particle size), as compared to normal mean particle sizes of 10-20 microns.
- It can effectively beneficiate coal particles down to 30 microns in size, as compared to the most advanced, existing conventional systems that are limited to a particle bottom size of about 150 microns.
- Smaller diameter cyclones (ie., 4 to 10 inch) are used to provide the higher G-force required to separate the finer feed coal.
- Cyclone feed pressures 3 to 10 times greater that those used in conventional cleaning systems are employed to enhance the separating forces.
- More advanced magnetite recovery systems, including rare-earth drums or high-gradient magnetic separators, are required for recovery and reuse of the medium.

While the similarity of the micronized-magnetite technology to existing circuitry has contributed to its fairly rapid commercialization, only limited work has been done on the magnetite recovery aspects of the circuit, particularly in an integrated, continuous application. Custom Coals HEP-I project is being undertaken to evaluate and resolve some of these remaining issues, to better understand and improve the overall process economics.

PROJECT OBJECTIVES, DESCRIPTION, AND SCHEDULE

The general objective of the project is to design, construct, and operate a fully integrated, 500 lb/hr. continuous micronized-magnetite cycloning circuit for cleaning fine coal. The work will focus on the medium recovery circuit and the impact of recirculating medium quality on the separation performance of the cyclone. Past semi-continuous research has indicated that highly efficient separations can be achieved in the small diameter cyclone, for the entire 600 by 30 micron particle size range, with magnetite losses less than 10 pounds per ton of coal processed. The testing is designed test these conclusions in a fully-integrated continuous circuit.

In addition, the specific objectives of the project are:

- Establish classifying circuit operating conditions and efficiency for desliming at 30-40 microns.
- Verify past cyclone performance finding, relative to cyclone operating variable optimization.
- Quantify the amount and size of magnetite losses for various recovery circuit configurations.

- Determine the effects of magnetite particle size and medium purity changes on dense-medium cyclone performance.

- Assess the technical and economic feasibility of various magnetite recovery circuit options.

Technically, the testing and data evaluation will focus on establishing the least complicated, easiest to operate circuit, that will provide the proper recirculating medium and cyclone performance. Economically, the evaluation will focus on tradeoffs between circuit capital and operating costs versus overall system performance, including cost of magnetite losses.

To accomplish the various objectives, the project has been divided into 11 task series, which include:

- Task 100: Project Planning and Management
- Task 200: Final Circuit Design
- Task 300: Equipment and Supplies, Procurement and Fabrication
- Task 400: Magnetite and Coal Procurement
- Task 500: Circuit Installation
- Task 600: Circuit Commissioning
- Task 700: Circuit Testing
- Task 800: Analytical
- Task 900: Circuit Decommissioning
- Task 1000: Data Evaluation
- Task 1100: Final Reporting

Custom Coals is responsible for the performance of all the above-mentioned project tasks, in accordance with DOE's Environmental, Safety, and Health (ESH) regulations. They will also provide all personnel required for operation of the emerging technology circuit, including sampling and sample handling, and circuit maintenance.

The DOE staff at the PRF is responsible for (1) receiving and handling of raw coal, (2) preparation and delivery of 500 lb/hr. feed slurry to Custom Coals at the specified coal topsize and solids concentration, (3) receiving, handling, and disposing of all products and discharges from the Custom Coals circuit, and (4) providing all necessary air, water, and electrical utilities.

Table 1 shown below contains the original 16-month schedule for the project, broken down by the task series on the critical path. As of early May, 1995, when this paper is being written, the project has progressed in close proximity to the initial schedule. The circuit commissioning has been completed and the circuit testing is scheduled to begin on May 15th, once all the commissioning test data has been compiled and reported.

TABLE 1
ORIGINAL PROJECT 16-MONTH SCHEDULE
(Task Series on Critical Path)

Task	Task Description	Duration (Months)	Proposed Period
200	Final Circuit Design	4	September through December 1994
500	Circuit Installation	3	January through March 1995
600	Circuit Commissioning	1	April 1995
700	Circuit Testing	5	May through September 1995
900	Circuit Decommissioning	1	October 1995
1,100	Final Reporting	2	November through December 1995

PROJECT TEAM

The project team has been assembled to ensure that all the project objectives, and the specific task series can be completed in accordance with the preceding project schedule and the overall project budget ($1.2M). The project team members, include:

- Custom Coal's as project manager and also to provide site engineering for the installation, commissioning, testing, and decommissioning tasks.
- DOE/PETC staff for technical and financial project oversight.
- Gilbert Commonwealth staff at PETC to operate the existing PRF circuit, which provides feed and product handling for Custom Coals emerging technology (ET) circuit.
- CLI Corporation, which was subcontracted to design the ET circuit and assist with equipment selection.
- Rizzo & Sons Construction, which was subcontracted to install and decommission the ET circuit, and also assisted in the commissioning efforts.
- Commercial Testing & Engineering Co. (CT&E), which is providing the operating technicians for the testing task and conducting all routine coal sample analyses (proximate analyses, sulfur forms, screen analyses, and washabilities).
- MTU's Institute of Materials Processing (IMP), which has been subcontracted to perform the more complex magnetite-related analyses required in the project (ie., magnetic separations, magnetic moment measurements, fine particle size analyses, and magnetite rheology measurements).

The fineness of the micronized magnetite has made the sampling, sample preparation, and analytical requirements for this project more complex and challenging than in conventional coal cleaning applications.

CIRCUIT DESCRIPTION

Figure 1 contains the block flow diagram of the ET circuit that Custom Coals has installed in the PRF, and is presently testing. The circuit consists of three subcircuits:

- **Classification Circuit** - Which consists of a 2" Krebs Classifying Cyclone in combination with a Sizetec Inclined Desliming Screen. This equipment will be equipped with various cyclone orifices and screen panel sizes to make a separation at 30-40 microns, removing the ultrafine particles to the waste via the cyclone overflow. The classification circuit will receive feed slurry from the PRF at about 40Wt% solids, and will deliver a final product to the dense-medium cycloning circuit at about 50-60Wt% solids (ie., 500lb/hr of prinicipally 300 by 30 microns particles).

- **Dense-Medium Cycloning Circuit** - Which consists of two parallel Krebs Dense-Medium Cyclones (2" & 4" diameter). The 4" cyclone products will always be recirculated back to feed, and will be used for closed-loop testing. The 2" cyclone products will progress to the magnetite recovery circuit, and will be used for the open circuit testing. Magnetite will be added on a controlled basis from the Magnetite Bin to maintain the desired correct media specific gravity.

- **Magnetite Recovery Circuit** - Which consists of a Sizetec Inclined Desliming Screen (Drain Screen), and a Sizetec Horizontal Dewatering Screen (Rinse Screen). The circuit also consists of four Eriez Conventional, Wet-Drum Magnetic Separators configured as primary, secondary, tertiary, and cleaner separators, and an Eriez High Gauss, Rare-Earth Magnetic Separator to be used as a final scavenger. The final magnetic concentrates will report to the Correct Medium Sump and the scavenger tailings to the Waste Sump. The Waste Sump discharge will be dewatered using the PRF's existing Sharples Horizontal Centrifuge and Thickener, and all clarified water will be recirculated for reuse in the circuit.

In addition to the equipment shown in Figure 1, the ET circuit also contains a clarified water head tank and pump to provide all water additions to the circuit. A Motor Control Center (MCC) and Control Cabinet provide the power distribution and the required circuit control.

COAL AND MAGNETITE DESCRIPTION

Custom Coals has selected two coals for testing during the project. The two coals are a Pittsburgh No. 8 Seam Raw Coal from Belmont County, Ohio, and a Lower Kittanning "B" Seam Raw Coal from Somerset County, PA. Table 2 contains a description and raw coal analyses for both coals.

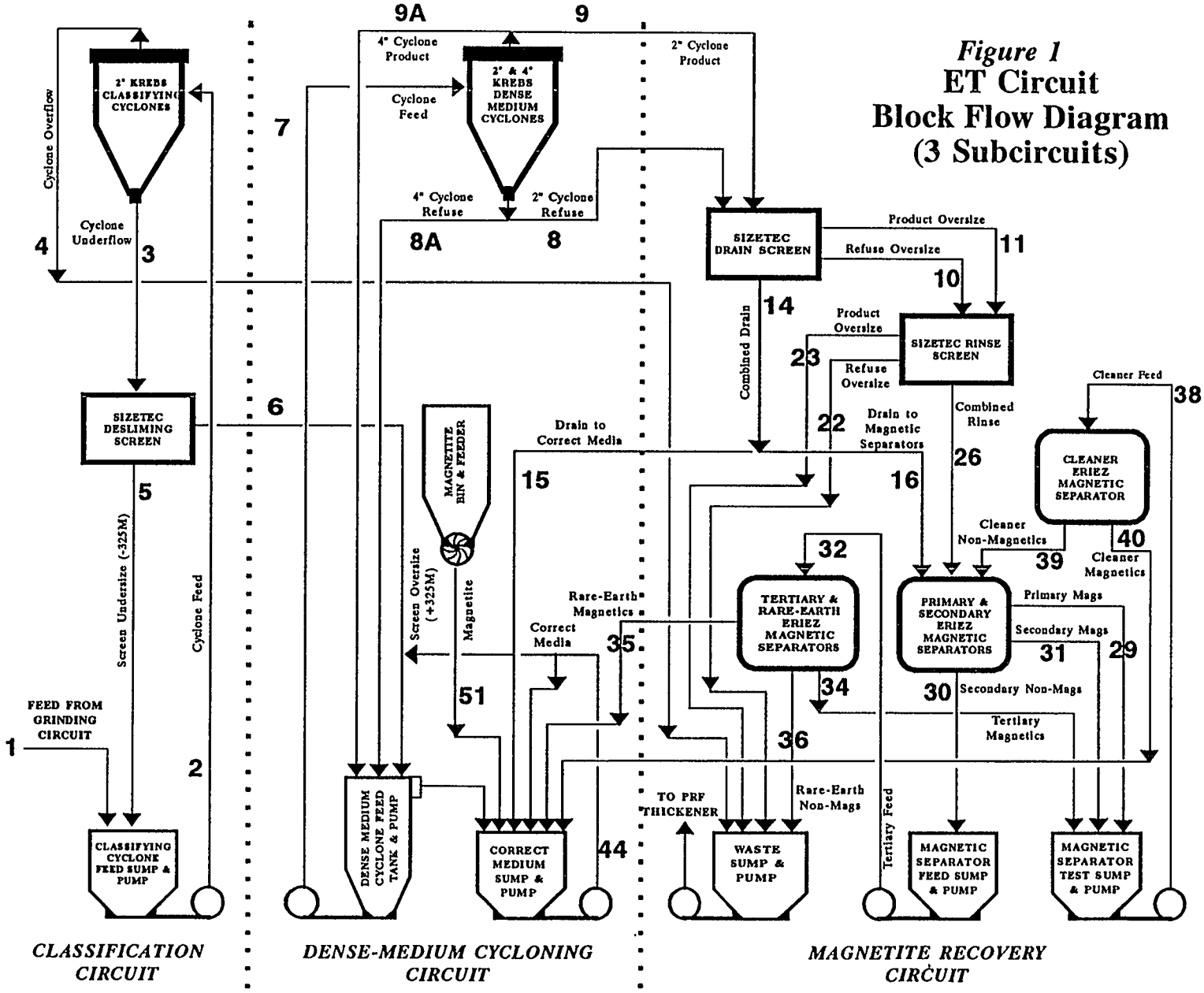

Figure 1
ET Circuit Block Flow Diagram (3 Subcircuits)

TABLE 2
TEST COAL CHARACTERISTICS

Description	Coal #1 (75-100 Tons)	Coal #2 (50-75 Tons)
Raw Coal Seam	Pittsburgh No. 8 Seam	Lower Kittanning "B" Seam
Company	Ohio Valley Coal Company	PB&S Coal Company
Mine	Powhatan #6 Mine	Longview Mine
County, State	Belmont County, OH	Somerset, PA

	Pittsburgh No. 8 Seam		Lower Kittanning "B" Seam	
Raw Coal Analyses	As Received	Dry Basis	As-Received	Dry Basis
Moisture (Wt%)	6.0	--	4.7	--
Ash (Wt%)	25.9	27.6	21.8	22.9
Sulfur (Wt%)	4.2	4.5	2.1	2.2
Pyritic Sulfur (Wt%)	2.1	2.2	1.3	1.4
Hardgrove Grind Index (HGI)		60-70		90-100

The two coals in Table 2 were selected for the testing because they both possess some common favorable characteristics, that include:

- they contain dry ash contents between 20 and 30 Wt%,
- that have over half of sulfur present in the pyritic form, and
- they have anticipated yields of 70-80Wt%, when cleaned at 1.60 SG.

These characteristics make them good candidates for aggressive cleaning studies. In addition, the large difference in the hardness of the two coals (see Table 2) will form an interesting comparison of how attrition affects fine-coal contamination of the recirculating medium, and subsequent medium recovery. Lastly, the Lower Kittanning "B" Seam raw coal is of specific interest, because it will be one of the major feed coals for eventual commercial operation, at the 500 TPH Cleaning Plant that Custom Coals is presently building in Somerset County, PA.

Initially, Custom Coals considered two potential sources of magnetite for this project and its commercial cleaning plant. They included:

- Synthetic Magnetite - Made from an iron chloride pickle liquor. Samples of this magnetite were previously provided by Hazen Research and tested in earlier research.

- Natural Magnetite - Made from dry grinding and classifying conventional Grade-B magnetite. Samples of this magnetite were provided by PennMag Inc.

Table 3 contains a comparison of the size consist of these two micronized magnetite options, and conventional Grade-B and Grade-E magnetite used by industry. It can be noted that the two micronized magnetites are considerably finer, and principally consist of 10 by 2 micron particles.

TABLE 3

Magnetite Types & Size Distribution

- MICRONIZED MAGNETITE OPTIONS
  - Penn Mag Grade-K: Natural Magnetite
  - Hazen High Temp: Synthetic Magnetite

Magnetite Type	Topsize (microns)	90% Passing Size (microns)	50% Passing Size (microns)	10% Passing Size (microns)
Commercial Grade-B *(1)*	100-150	40-50	15-20	5-10
Commercial Grade-E *(1)*	60-100	30-40	10-15	3-5
Hazen High Temp *(2)*	60	10	6.5	2.0
PennMag Grade-K *(2)*	20	11	4.8	2.0

(1) From Sieve Analyses
(2) From Microtrac Analyses

FIGURE 2

Davis Tube Recovery Profiles

Force = Mass * Magnetite Susceptibility * Field Strength * Field Gradient

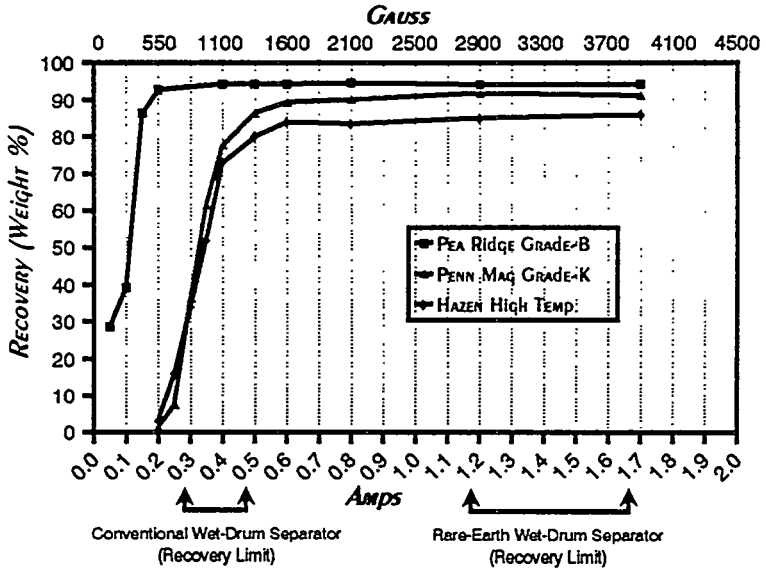

Figure 2 contains a comparison of the recoverability of the two micronized magnetites and a Grade-B magnetite, determined at various settings of a Davis-Tube. The lower magnetic susceptibility of the micronized magneitites is readily apparent, from the higher amperage/gauss levels required to recover the magnetite. Many of the particles are recovered at a Gauss Range (1000-1500 Gauss) that is near the limits of recoverability in conventional wet-drum magnetic separators. For this reason, Custom Coals and Eriez Magnetics have specified rare-earth drum magnetic separators as scavengers in the magnetite recovery circuits to ensure adequate micronized magnetite recovery.

At present, Custom Coals is planning to use natural magnetite provided by PennMag Inc., for the HEP-I project and the commercial plant. This natural magnetite was preferred over the synthetic magnetite, provided by Hazen Research, because:

- It can be provided at a lower cost ($160 per ton) than the synthetic magneitite,
- It can be made at high purity (95-98Wt% recovery at 1.70 amps on the Davis Tube) with little oversize (20 micron topsize), and
- The process for making it is not very complex or difficult to adapt for existing suppliers.

Custom Coals has obtained and plans to test two different sizes of micronized magnetite provided by PennMag during the HEP-I project. They include a Grade-J magnetite at 8-10 micron mean particle size, and the Grade-K magnetite at 4-6 micron mean particle size. A third, even finer grade of magnetite, will be tested, if these magnetites prove to make unstable mediums at high cyclone pressures.

TESTING PLAN

The circuit testing task is just beginning, and should occur over a 5-month period (May through September 1995). The circuit testing will be broken down into two phases for the two coal and two magnetite options, which include:

- Component Testing
- Integrated Testing

The Component Testing will focus on closed-loop testing of each subcircuit to optimize the individual unit operations and observe the impact of key process variables. The testing for each coal and magnetite will then culminate with the Integrated Testing, where the entire circuit is operated in longer duration, primarily to quantify magnetite losses, and determine the impacts of changing medium quality on cyclone performance. Several different feed coal topsizes and medium densities are planned for the Integrated Testing.

SUMMARY

This project is expected to provide significant insight into the effects of various medium recovery circuits on the recirculating medium quality and separation performance of a micronized-magnetite cycloning system for fine-coal cleaning. The technical and economic feasibility of the selected circuitry and operating conditions will be fully evaluated and translated into a practical assessment for the potential commercial application of the technology.

The following manuscript was unavailable at time of publication.

POC-TESTING OF OIL AGGLOMERATION TECHNIQUES AND EQUIPMENT FOR RECOVERY AND CLEANING OF FINE COAL FROM FINE COAL PROCESSING STREAMS

Leszek Ignasiak
Alberta Research Council
#1 Oil Patch Drive
Devon, Alberta
Canada TOC 1IO

Please contact author(s) for a copy of this paper.

POC-SCALE TESTING OF A DRY TRIBOELECTROSTATIC SEPARATOR FOR FINE COAL CLEANING

R.-H. Yoon, G. H. Luttrell and G.T. Adel
Center For Coal and Minerals Processing
Virginia Polytechnic Institute And State University
Blacksburg, Virginia 24061-0258

INTRODUCTION

Numerous advanced coal cleaning processes have been developed in recent years that are capable of substantially reducing both the ash and sulfur contents of run-of-mine coals. The extent of cleaning depends on the liberation characteristics of the coal, which generally improve with reducing particle size. However, since most of the advanced technologies are wet processes, the clean coal product must be dewatered before it can be transported and burned in conventional boilers. This additional treatment step significantly increases the processing cost and makes the industrial applicability of these advanced technologies much less attractive.

In order to avoid problems associated with fine coal dewatering, researchers at the Pittsburgh Energy Technology Center (PETC) developed a novel triboelectrostatic separation (TES) process that can remove mineral matter from dry coal. In this technique, finely pulverized coal is brought into contact with a material (such as copper) having a work function intermediate to that of the carbonaceous material and associated mineral matter. Carbonaceous particles having a relatively low work function become positively charged, while particles of mineral matter having significantly higher work functions become negatively charged. Once the particles become selectively charged, a separation can be achieved by passing the particle stream through an electrically charged field. Details related to the triboelectrostatic charging phenomenon have been discussed elsewhere (Inculet, 1984).

The TES process has been proven in bench-scale tests to be capable of better than 90% removal of pyritic sulfur and greater than 70% reduction of ash for several eastern U.S. coals (Link, 1987). The potential of this technique for achieving high separation efficiencies was demonstrated by its first place ranking in an interlaboratory round-robin test program conducted by DOE (see Figure 1). Since this technology is a dry process, it offers the advantages of lower ancillary costs and improved environmental acceptability as compared to wet processes. Furthermore, the TES process can be installed in-line at a power station, which allows existing pulverization equipment to be used for size reduction.

OBJECTIVE

The primary objective of this research and development project is to demonstrate the technical merits of a proof-of-concept (POC) triboelectrostatic separator at a continuous capacity of 200-250 kg/hr. The POC module will be constructed, installed and operated at the Coal Preparation Facility (CPF) at Virginia Tech. The test unit will combine the triboelectrostatic charging system developed at PETC with a novel triboelectrostatic separator developed by Carpco, Inc. The Carpo design has been

used successfully for the upgrading of triboelectrostatically charged particles of both minerals and plastics. The POC test unit will be totally self-contained and will include the necessary dry pulverization equipment for feed preparation and the gas-solid separation equipment for clean coal and refuse recovery. The continuous test unit is designed to be scaleable to larger pilot-plant and industrial sizes. Detailed test programs will be carried out to establish the performance capabilities of this process in terms of energy recovery, ash and sulfur rejection, and throughput capacity. Scale-up parameters will be identified and evaluated through testing at the POC and bench-scale. Independent technical and economic evaluations of the test system have been incorporated in the scope of work to provide critical information necessary to promote the future commercialization of TES technology.

PROPOSED WORK

The successful completion of the proposed work will require the active participation of several different research, engineering, manufacturing and industrial organizations. These will include the Center for Coal and Minerals Processing (CCMP), Carpco, Inc., Roberts & Schaefer Company (R&S) and Babcock & Wilcox (B&W). CCMP will serve as the prime contractor and will provide the contractual management, technical guidance, and overall supervision necessary to complete the proposed work in a timely and orderly fashion. Technical personnel from CCMP will also be primarily responsible for the design, installation, shakedown and testing of the proposed circuitry with assistance from the various participants. In addition, a variety of raw coal characterization studies and product sample analyses will be conducted in the coal analysis laboratories at CCMP. Carpco will design and fabricate the triboelectrostatic separator and will provide expertise related to the installation, shakedown and operation of the test unit. They will also assist in the analysis and interpretation of the experimental test data. R&S will provide basic engineering services, which will include such tasks as the layout of unit operations, specification of equipment and materials, detailing of miscellaneous contractual services, etc. Finally, B&W will provide services related to the technical and economic evaluation of the proposed technology.

The project is expected to begin in the third quarter of 1995 and continue for a period of 36 months. The proposed work has been broken down into ten individual tasks:

Task 1 - Project Planning
Task 2 - Sample Acquisition
Task 3 - Engineering Design
Task 4 - Procurement and Fabrication
Task 5 - Installation and Shakedown
Task 6 - Operation/Detailed Testing
Task 7 - Sample Analysis/Characterization
Task 8 - Process Evaluation
Task 9 - Decommissioning
Task 10 - Reporting

Tribocharger Design and Testing

In previous test work conducted by PETC, tribocharging was accomplished by passing finely pulverized coal through a helix formed from a long strand of copper tubing. More recently, tribocharger designs consisting of static in-line mixers constructed of various types of materials have been employed. For triboelectric charging, static mixers have the advantage that superb particle contact can be achieved in a very short distance. The enhanced rate of contact is a result of the tortuous path traveled by the particle suspension. Studies have shown that static mixers provide a large

degree of mixing in the radial direction. For the case of triboelectric charging, this characteristic provides a large number of particle-particle and particle-wall collisions over a very short period of time. The flow regime along the axial length of a static mixer is very close to plug-flow despite the fact that the flow through the static mixer is turbulent (Bor, 1971). As a result, particle charging along the length of a static mixer is relatively uniform, with the maximum degree of charging taking place at the exit of the static mixer. Both of these features are desirable characteristics of a triboelectric charger.

Numerous schemes have been presented in the literature for selecting static mixers for a given application. Unfortunately, nearly all of these guidelines apply to fluid blending or dispersion applications. The explicit use of static mixers for contacting particles in a gas stream is a relatively new area which has not been widely investigated. As a result, engineering criteria for establishing the number, type and size of static mixers required for triboelectrostatic charging must be developed and validated prior to the final commercialization of this technology.

In the present work, bench-scale test work will be carried out to establish scale-up criteria for the PETC tribocharger. Various static mixer geometries and element configurations will be examined over a wide range of operating conditions in order to establish the most effective system for triboelectric charging. The effectiveness of the charging process will be determined by passing finely pulverized coal dust and air through a given static mixer and monitoring the charging efficiency. Charging efficiency will be determined by passing the charged particle stream between two charged plates and measuring the capture efficiency.

Since it is likely that a wide range of static mixer configurations can be used for particle charging, the test data will need to be normalized before it can be used for scale-up. The normalization will be accomplished by converting each static mixer to an equivalent open-pipe length and diameter. Previous test work (Hartung and Hiby, 1972) indicates that complete gas homogenization occurs in an unrestricted pipe when the length-to-diameter (L/D) ratio of the pipe reaches 90. A static mixer having the same equivalent L/D ratio is capable of achieving the same degree of mixing at an actual L/D ratio of only 5. Although particle suspensions have not been studied, these results suggest that equivalent open-pipe L/D ratios may be used as the basis for triboelectrostatic charger scale-up. This procedure assumes that the efficiency of particle contact is maintained so long as the equivalent L/D ratio and superficial gas velocity is maintained through laboratory and full-scale test units. This assumption will be validated from the test data and modified accordingly. The test data will also be used to develop expressions for pressure drop across the various tribocharger designs. This information will be useful for determining the air flow rate and power requirements necessary for triboelectric charging.

Electrostatic Separator Design and Testing

Design deficiencies associated with the original PETC electrostatic separator will be corrected through the use of the Carpo's commercially successful triboelectrostatic separator. However, for the POC unit, it is planned to orient the rolls horizontally and feed the pulverized coal perpendicular to the rolls (see Figure 2). This design has been chosen because the separation of fine coal occurs very rapidly. This is due to the fact that the charge to mass ratio for individual particles is quite large, resulting in rapid movement of the charged particle in a turbulence-free atmosphere. In previous mineral and plastic systems tested by Carpco, the particles are much larger and the charge/mass ratio is

smaller. As a result, the separation occurs by deflecting the particle from a vertical "free-fall" path as opposed to having the particle become attached to the electrode.

The conceptual flowsheet for the proposed Carpco design is shown in Figure 3. As shown, pulverized coal from a gas-swept impact mill will be forced under pressure through the static mixer tribocharger system. The charged particles will enter at the top of the separator and will pass vertically through the electrostatic field. One important aspect of the separator design will be to provide baffles near the entrance of the separation chamber. This feature will provide laminar flow conditions between the electrodes, which is particularly important for separating fine particles. After passing through the separator, the clean coal and reject products will be discharged from the bottom of the separator through rotary air-lock valves. Secondary discharge of the fine clean coal and reject products will occur through gas discharge pipes connected directly to dust collectors. In addition, provisions have been made for the removal of "by-pass" material which passes through the electrostatic field without being separated. This material will be re-introduced into the coal pulverizer and recycled through the system until it becomes charged and/or separated. The entire triboelectrostatic test circuit will be operated under a net positive pressure by recirculating an inert gas via a blower system.

During the testing of the Carpco separator, several variables will be examined that have been previously determined to influence the efficiency of the triboelectrostatic separation process. These include, but are not limited to, particle size, solids concentration in the feed stream, velocity of the feed stream through the static mixer, static mixer design/configuration, and electrode potential. It is planned to investigate coarser feed sizes in the range of 50 to 100-mm top size. In addition, the effects of coal type will have to be examined. A statistical design of experiments will be used develop a test program for this phase of the work. The resultant test data will be evaluated using statistical techniques to establish clearly the significance of each variable and the degree to which it influences the performance of the triboelectrostatic separation of coal.

An important goal of the proposed work is to demonstrate the throughput capacity of the Carpco triboelectrostatic separator for coal applications. The unit proposed for the POC has a capacity that exceeds the stated feed rate of 200-250 kg/hr, and may in fact be capable of processing up to 1,000 kg/hr based on Carpco's experience with mineral separations. To establish the true design capacity, it is proposed to limit the width of the feed opening to the separator such that only a portion of the roll width is being utilized. This can be further refined by using vertical baffles which limit the separation width of the unit and confine the separation zone from top to bottom.

Scale-up of the triboelectrostatic separator is primarily a function of the separator width, i.e., mass rate of feed per unit of roller width. Thus, once the unit capacity (kg/cm) is established, the scale up to larger units is clearly established. The separation efficiency, on the other hand, will be a factor of other design features. One of the most important will be the path length for a particle in the separation zone (i.e., electrostatic field). In the proposed separator design, it will be possible to vary the length of the separation zone to optimize the separation efficiency. The initial design value for the separator length will be based on modeling predictions obtained from bench-scale test work. Another very important parameter, electrode voltage, will also be variable up to 50 kV on each electrode. This will yield a maximum total field intensity of 100 kV between the electrodes. Other operating parameters such as the solids loading in the gas stream, gas velocity, particle size, coal type, etc., will also be

evaluated in the POC test program. It is anticipated that at least three different levels for each operating parameter will be evaluated during the course of the investigation.

CIRCUIT LAYOUT

The entire POC test circuit will be installed in the high bay area at the Coal Preparation Facility (CPF) at Virginia Tech. Modular design concepts will be employed to speed installation of the required circuitry. This approach will limit the impact of construction on existing facilities and will minimize the amount of time required to fully assemble and shakedown the test circuit.

The conceptual flowsheet of the POC facility is shown in Figure 4. Raw coal will be brought into the coal receiving area by truck. As required, the raw coal will be fed to a 25 HP Jeffery hammer mill for primary size reduction. The coal obtained from the primary mill will have a top size of approximately 3 mm. A 12-ft long flight conveyor will transfer the hammer mill product to a secondary hammer mill (Holmes 451) which will further reduce the particle topsize to 28 mesh. The product from the secondary hammer mill will drop directly into a vibrating feed storage bin. Material from the bin will be fed at the desired production rate to the triboelectrostatic test circuit by means of a programmable weighbelt feeder and screw conveyor configuration. Since the capacity of the primary and secondary hammer mills far exceeds the design capacity of the triboelectrostatic separator, this portion of the POC circuit will be operated intermittently to keep the vibrating bin filled.

The -28 mesh coal will be fed from the vibrating feed bin to a gas-swept impact pulverizer equipped with a rotary valve feeder. The pulverizer will be operated under a positive nitrogen pressure in closed-loop with the rest of the circuit. A Mikro-ACM (Model 10) pulverizer has been selected for final stage of grinding because of its ability to provide a pulverized coal grind at the desired capacity, low heat rise during operation, and capability for on-line adjustment of grind size. Depending on the mill operating conditions, a pulverized coal product between 200 to 400 mesh can be prepared using this unit.

The newly installed triboelectrostatic test module will occupy most of the available high bay area on the left side of the test facility. The triboelectrostatic separator will be located on the top floor of the test facility, while the fine coal pulverizer and air blower will be located on the bottom floor. After passing through the tribocharger, the charged particles pass downward through the electrostatic separator where the positively-charged coal particles are attracted to the negative electrode and the negatively-charged ash-rich and pyritic sulfur particles are attracted to the positive electrode. Electrode voltage will be varied from 10,000 to 60,000 volts on each electrode (maximum 120,000 volts between the electrodes). The products will be collected and discharged through air-lock valves in the bottom of the separator and transferred via flexible screw conveyors into separate dust collectors. The dust collectors will be mounted on the bottom floor, but will pass up through the second floor because of their physical height. The clean coal and refuse products from the dust collectors will be continuously discharged through rotary valves into collection drums.

A blower system has been selected over a conventional air compressor to provide the circulating flow through the POC test circuit. Since high pressure heads are not required, the blower system is more practical for large-scale installations due to its high reliability and very low capital,

operating and maintenance costs. A centrifugal blower with radial blades is appropriate for this particular application. This type of blower is used in a variety of applications in both the mineral processing and coal preparation industries. The blower will be equipped with a variable speed drive so that on-line adjustments to the gas flow rate and pressure head can be made during operation. A total gas flow rate range between 0-1000 cfm can be studied using the proposed system. Appropriate duct work and valve control systems will be installed so that the gas flow rate through the pulverizer can be held constant with changes in the blower speed. This design will allow the ground coal to be passed through the static mixer tribocharger system at different pressures and gas/solids loadings without affecting the performance of the mill.

The entire POC circuit will be operated in an inert nitrogen atmosphere. The supply system for the nitrogen gas will be placed outside the main building for safety reasons. It will be necessary to recycle most of the gases in order to minimize the consumption of nitrogen gas. Gas recycling will be accomplished by connecting the dust collector air discharges to the blower that is connected to the manifold feeding the pulverizer and pulverizer by-pass to the static mixer. Provisions for adding fresh nitrogen directly to the separator will be provided as well as a bleed from the manifold feeding the system. Pressure relief valves and oxygen monitors will be provided as required to protect the equipment from over or under pressure situations. The nitrogen supply will also be connected to the dust collectors to operate the pulse cleaning required for the filter elements.

PROJECT PLANS

Future plans call for the completion of various subtasks related to the design, fabrication, installation and testing of the triboelectrostatic coal cleaning circuit. The most important of these tasks include (1) the design, fabrication and installation of all major unit process components and associated ductwork, electrical wiring, instrumentation, etc., as designated in the flowsheet approved by DOE/PETC, (2) the technical evaluation of the performance of the TES circuitry by conducting parametric studies as a function of key operating and design variables, (3) the validation of the steady-state performance of the optimized TES circuit by conducting long-duration test runs over a period of several days and by testing coals from other sources, and (4) the completion of economic feasibility studies to evaluate the commercialization potential of the TES technology for fine coal cleaning.

REFERENCES

Bor, T., 1971. "The Static Mixer as a Chemical Reactor," British Chemical Engineering, July, 1971, pp. 611-612.

Hartung, H.K. and Hiby, J.W., 1972. Chemical Engineering Technology, Volume 44 (18), pp. 1051-1060.

Inculet, I.I., 1984. Electrostatic Mineral Separation, John Wiley and Sons, Inc., New York, N.Y.

Jacobsen, P.E., Killmeyer, R.P. and Hucko, R.E., 1989. 'Evaluation of Advanced Surface-Modification, Gravity and Electrostatic Processes for Fine-Coal Beneficiation, Coal Prep '89, 6th International Coal Preparation Exhibition and Conference, May 2-4, 1989, Lexington, Kentucky.

Link, T.A., 1987. "Triboelectrostatic Separation," Quarterly Report, Coal Preparation Division, Pittsburgh Energy Technology Center, U.S. DOE, In-House Research and Development, Oct.1-Dec. 31, 1987.

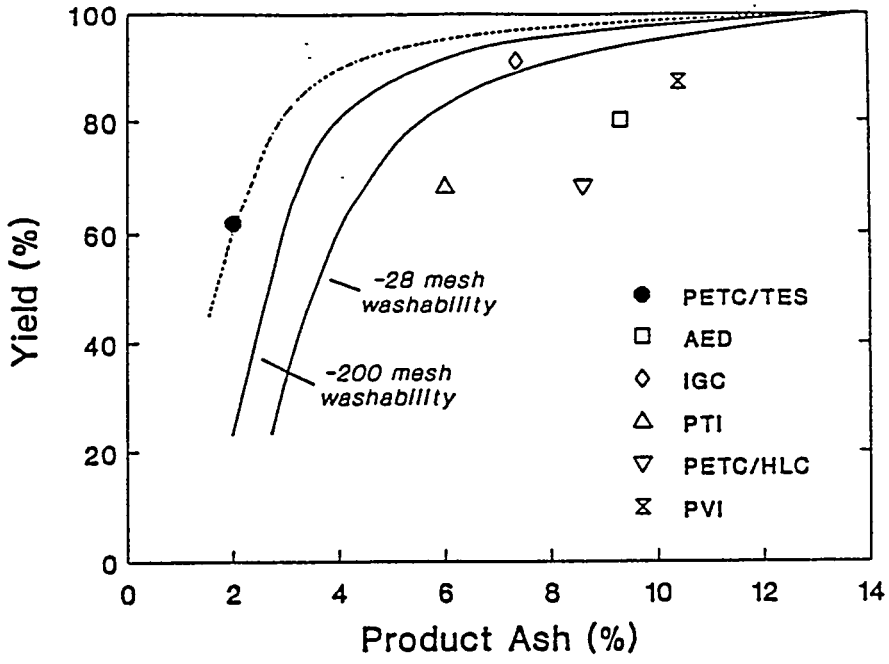

Figure 1. Results of round-robin tests conducted on an Illinois No. 6 coal comparing PETC's Triboelectrostatic Separator (PETC/TES), Advanced Energy Dynamics Electrostatic Separator (AED), Intermagnetics General Corporation Pseudo-Dense Media Separator (IGC), Process Tech's Heavy Liquid Cyclone (PTI), PETC's Heavy Liquid Cyclone (PETC/HLC) and Perfect View's Froth Flotation Chemical Pretreatment Process (PVI). (After Jacobsen *et al.*, 1989).

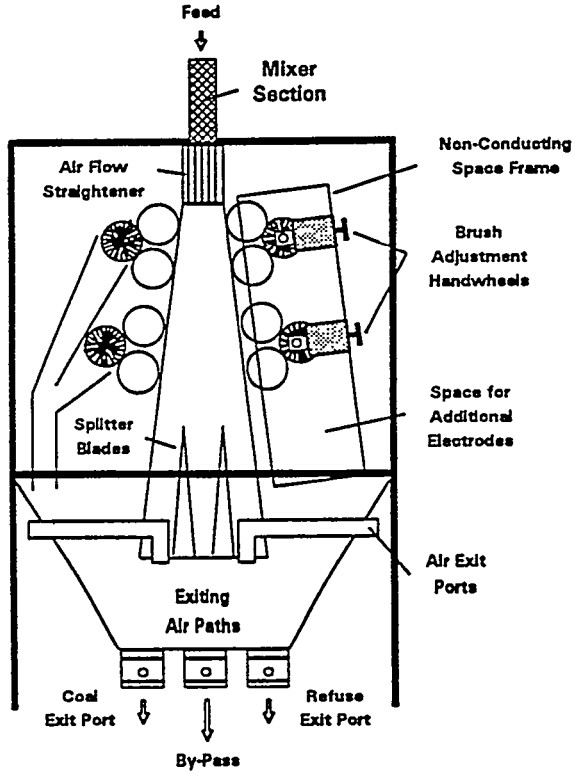

Figure 2. Schematic of Carpco's triboelectrostatic separator for fine coal cleaning.

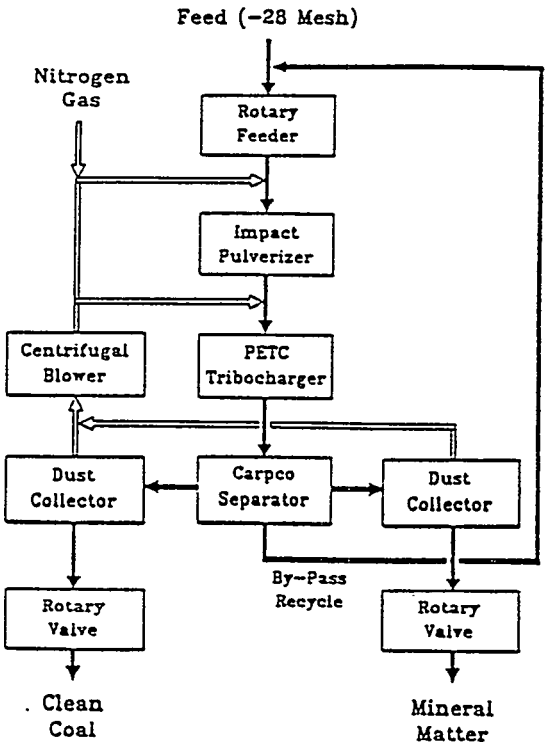

Figure 3. Conceptual block diagram for the triboelectrostatic separator test module.

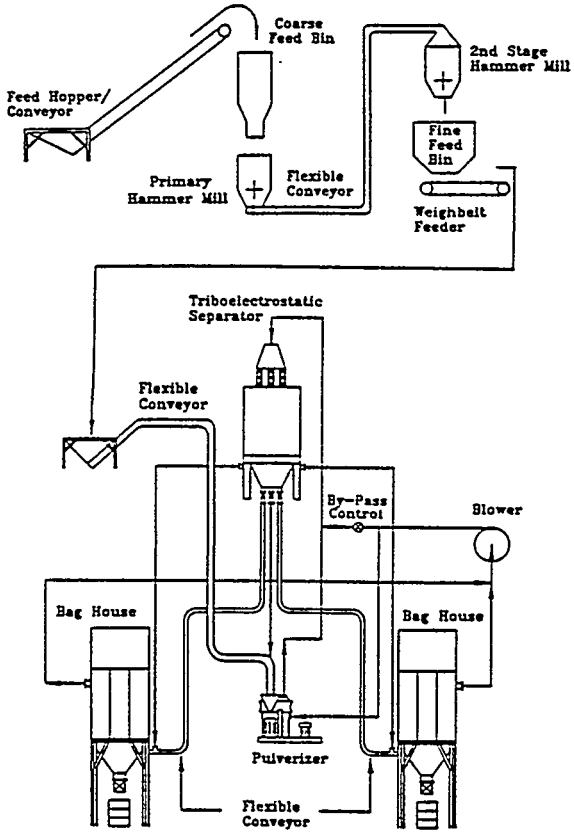

Figure 4. Process flowsheet for the proposed triboelectrostatic separator test circuit.

DEVELOPMENT, TESTING, AND DEMONSTRATION OF AN OPTIMAL FINE COAL CLEANING CIRCUIT

Mr. Mike Mishra
PROJECT MANAGER
CYPRUS EMERALD RESOURCES

Mr. Michael Placha
GENERAL MANAGER
ALLIED OPERATIONS

Mr. Peter Bethell
VICE PRESIDENT
ALLIED RESOURCES

Mr. Dennis Humphris and Mr. Steven Hadley
PROJECT MANAGER, PROJECT ENGINEER
PRAXIS ENGINEERS INC.

Introduction

The overall objective of this project is to improve the efficiency of fine coal cleaning. The project will be completed in two phases: bench-scale testing and demonstration of four advanced flotation cells and; in-plant proof-of-concept (POC) pilot plant testing of two flotation cells individually and in two-stage combinations. The goal is to ascertain if a two-stage circuit can result in reduced capital and operating costs while achieving improved separation efficiency.

The plant selected for this project, Cyprus Emerald Coal Preparation Plant, cleans 1200 tph of raw coal. The plant produces approximately 4 million tonnes of clean coal per year at an average as received energy content of 30.2 MJ/Kg (13,000 Btu/lb).

Project Objectives

This project will test flotation units with features which have shown promise in improving the grade/recovery relationship for fine coal. The objectives in completing this project can be summarized as:

- Evaluate emerging flotation equipment and practices
- Develop optimal flotation circuit designs
- Test single and two stage circuit designs
- Improve flotation selectivity at maximum cell capacities.

The project will systematically evaluate the use of four advanced flotation machines individually and in two-stage configurations in order to develop the best processes for 100 mesh x 0 fines. The advanced flotation equipment and circuit combinations to be evaluated in this project are:

- Outokumpu Mintec HG Tank cell
- Jameson cell
- Open Column (Pyramid Resources)
- Packed Column (G&LV)
- Two stage combinations of either a Jameson cell or Outokumpu cell and an open column or a packed column.

The objective is to operate the column flotation equipment at its froth-limited capacity and to use the mechanical cells (Outokumpu and Jameson) to recover the remaining coal, either as a rougher or as a scavenger configuration. The selection of the optimal circuit configuration will depend on the particle size and flotation response of the coal fines and will be determined experimentally.

Project Methodology

The project work will be predominately experimental in nature. Coal samples from the preparation plant will be tested at bench and Proof-of-Concept (POC) scales to quantify flotation cell performance. Relevant aspects of the project approach include:

- Use of commercially available flotation equipment
- Develop an optimization function to help guide testing
- Optimize operation of each machine at bench scale
- Use a two step approach for bench scale tests
- Select two machines for POC testing
- Test single and two-stage circuits at POC-scale.

The optimization function will relate flotation cell(s) performance (grade and recovery) to economic benefit for the preparation plant. The existing plant configuration will be used as a basis for comparison. The optimization function consists of:

- Discounted cash flow analysis
- Flotation circuit variables
  - Yield
  - Ash, sulfur, and moisture
  - Btu recovery
- Plant variables
  - Yield
  - Ash, sulfur, and moisture
  - Btu recovery
- Costs
  - Capital costs
  - Operating costs

The existing preparation plant has been modeled with respect to coal quality and yield by circuit. Any changes in the fine coal circuit product quality will be compensated for by

appropriate adjustments to the coarse coal heavy media circuit separation gravity such that the same overall plant clean coal energy content (as received basis) is achieved. This approach will insure that proper credit is given for flotation circuits that lower the fine clean coal ash content and/or increase the circuit Btu recovery. The evaluation will include costs related to increases in clarified water usage and plant space requirements. Preliminary analysis indicates that a net increase in plant Btu recovery of 0.5% to 1.0% can be achieved by improved fine coal cleaning.

Sample Characterization

Prior to the start of the bench scale test work, the coal fines were characterized. The proximate analysis and size consist are given in Table 1.

Table 1. Raw Coal Fines Sample Characterization Data

Size Consist, microns	Coal Analysis
d_{80} = 120	19.99% ash
d_{50} = 40	1.1% sulfur
d_{20} = 9	0.49% pyritic sulfur
	0.61% organic sulfur
	27.7 MJ/Kg (11,911 Btu/lb)

Conventional single-stage and two-stage (rougher-cleaner) batch flotation tests were also completed as part of this work as shown in Figure 1. The two-stage tests were completed to illustrate the improvement in clean coal ash by a reduction of entrained ash in the product via re-cleaning the first stage froth. These results suggest that a 5% ash product can be expected from the advanced flotation cells with high Btu recovery.

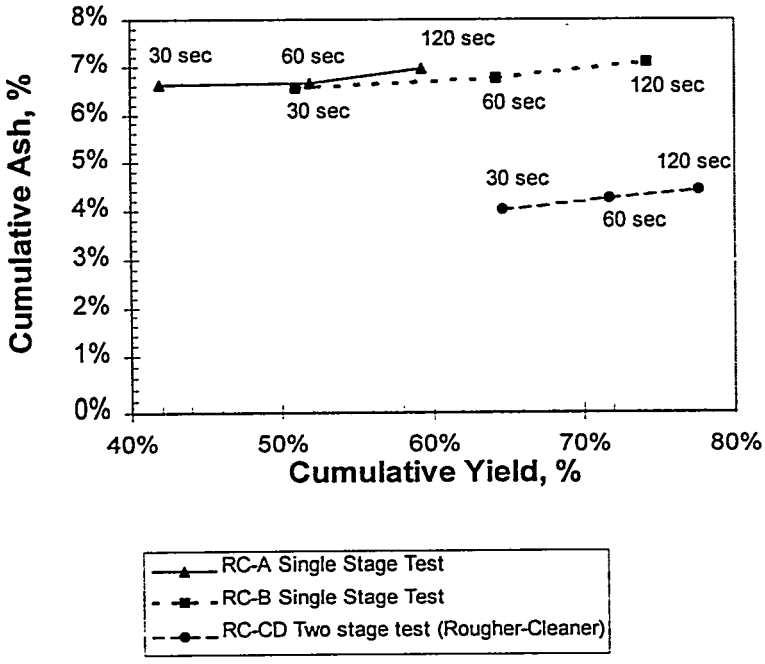

Figure 1. Conventional Batch Flotation Test Results

Bench Scale Test Work

A raw coal fines sample was collected from the preparation plant classifying cyclone overflow. A sample of the existing flotation circuit tailings was also collected after adjusting circuit operations to produce an ash content of approximately 40%. The tailings sample was collected to simulate a second stage feed stream.

Bench-scale work will first test each machine for single-stage operation using the raw coal fines sample. These tests will identify rate limiting conditions for high Btu recovery operation and low clean coal ash production. A series of tests will then be completed to establish a raw coal grade-recovery curve. Tailings samples (second-stage feed) will then be tested to determine conditions for efficient, high Btu recovery operations.

Bench Scale Test Analysis and Circuit Selection

Bench-scale test results will form the basis for selection of two flotation cells for in-plant POC testing. Analysis steps will include:

- Develop single and two-stage circuit material balances
- Use kinetic models to estimate second stage performance
- Extrapolate bench-scale results to full scale operation
- Determine full scale capital and operating costs
- Update economics.

The analysis will assume that the flotation circuit would be installed at the Cyprus Emerald preparation plant. The costs for consumables and utilities will be set to the average plant costs in the first quarter of 1995. Similarly, the value of additional raw coal recovery will be based on coal prices in the first quarter of 1995.

POC Design & Construction

A two-stage POC flotation circuit will be constructed at the Emerald coal preparation plant. Feed coal will be a taken as a slip stream from the classifying cyclone overflow at a nominal rate of 0.25 Kg/s (1.0 tph). The feed rate will be adjustable to facilitate determination of rate limiting conditions. The circuit design will incorporate features to measure mass flow rate and collect slurry samples for each process stream.

POC Operations

The POC test work will be completed in three phases:

- Single stage tests
- Two-stage tests
- Demonstration tests.

The POC tests will first replicate the optimal conditions determined during the bench-scale test program for verification of scale-up relationships. A series of parametric tests will then be run to optimize the process variables. Following the single stage optimization, two-stage tests will be run to determine the proper balance between first and second stage coal recovery for maximum capacity and separation efficiency. The demonstration phase will complete the two-stage optimization with regard to the following variables:

- System capacity and economics
- Product quality and yield
- Total reagent consumption and distribution between stages
- Process control
- Collection of data for system modeling and scale-up factors.

Final Technical and Economic Evaluation

The data collected during POC operations will be assimilated into process and economic models which will project the performance and costs of a commercial scale operation. Data reduction and process economics will be performed throughout the POC operation. Material balances will be calculated using raw and smoothed data as it becomes available. The final evaluation will encompass:

- Complete POC material balances as part of the test program
- Measurement of a grade/recovery relationship for each circuit
- Comparison of POC and Bench-scale test results
- Development of process models for scale-up
- Assessment of the controllability of the circuit
- Updated economics.

Project Status

The bench-scale test work is currently in progress. The results of these tests will be presented during the July 12-14, 1994 DOE contractors conference.

The following manuscript was unavailable at time of publication.

A FINE COAL CIRCUITRY STUDY USING COLUMN FLOTATION AND GRAVITY SEPARATION

Dr. Ricky Q. Honaker
Department of Mining Engineering
Southern Illinois University
Carbondale, IL 62901

Please contact author(s) for a copy of this paper.

IMPROVING THE PERFORMANCE OF CONVENTIONAL AND COLUMN FROTH FLOTATION CELLS

B. J. Arnold
CQ Inc.
Homer City, PA 15748

Introduction

Many existing mining operations hover on the brink of producing competitively priced fuel with marginally acceptable sulfur levels. To remain competitive, these operations need to improve the yield of their coal processing facilities, lower the sulfur content of their clean coal, or lower the ash content of their clean coal.

Fine coal cleaning processes offer the best opportunity for coal producers to increase their yield of high quality product. Over 200 coal processing plants in the U. S. already employ some type of conventional or column flotation device to clean fines. An increase in efficiency in these existing circuits could be the margin required to make these coal producers competitive.

To investigate potential improvements in existing froth flotation techniques, CQ Inc. engineers assessed the merits of high-speed, high-shear pre-treatment of conventional and column froth flotation feeds. This in-line device, which can be easily retrofit into existing circuitry, subjects the coal and flotation reagents to high-speed, high-shear mixing. While high-speed, high-shear mixing has been applied as part of oil agglomeration circuits, it has not been applied for improving conventional and column froth flotation. The purpose of this device is to totally disperse and coat the carbon particles in the froth cell feed with the collector chemicals. This assures better and more accurate bubble attachment for those carbon-bearing particles. With more accurate bubble attachment, the flotation process will reject more ash-forming and sulfur-bearing minerals while increasing clean coal yield and potentially reducing reagent consumption.

This project investigated the effect of high-speed, high-shear treatment of the feed to both conventional and column froth flotation cells at various collector rates using samples from two coal seams. The primary goal of the project was to determine the effects of high-speed, high-shear pre-treatment on flotation performance and reagent consumption. A secondary goal was to determine the effects of the pre-treatment on coal of different particle size ranges.

Fabrication of the High-Shear Mixer

CQ Inc. fabricated and tested a pilot/commercial model in-line, high-speed, high-shear mixing device, as shown in Figure 1 prior to installation. Slurry enters the bottom of the device and flows from the port near the top of the mixing chamber. Two blade types were tested. A Cowles-design C blade gives high shear, while a radial turbine blade gives more intense mixing. A variable speed drive allowed the testing of various levels of mixing. Conditions for the mixer were set based on a percentage of mixer speed. Values for rpm were measured at 50 and 100 percent:

Percent	Cowles C rpm	Radial rpm
50	584	615
100	1193	1178

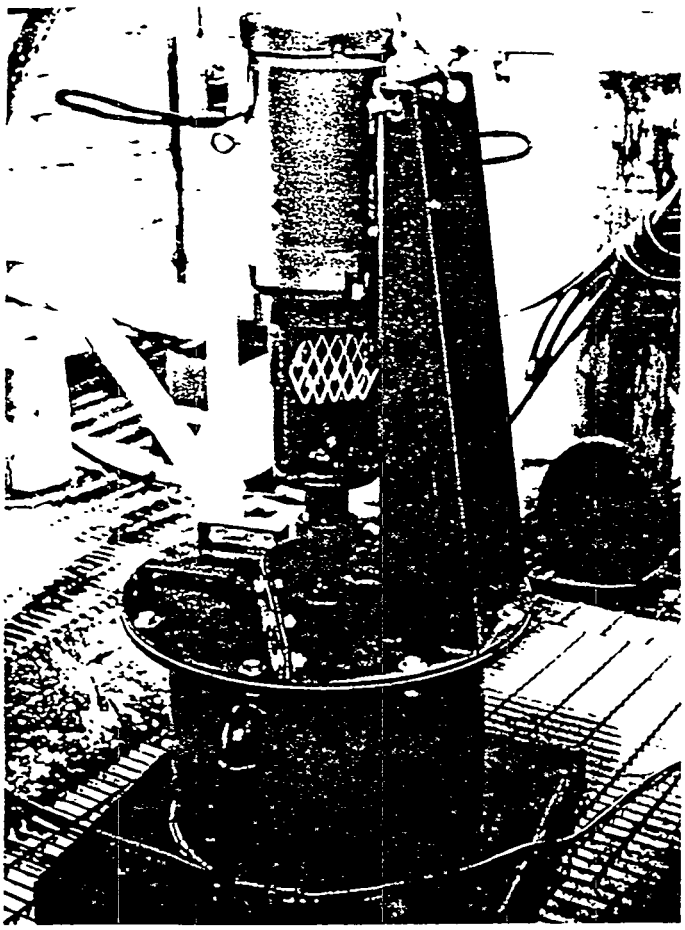

Figure 1. High-Shear Mixer

Testing Facilities

Tests were conducted at CQ Inc.'s Coal Quality Development Center (CQDC) in Homer City, Pennsylvania. The CQDC is a twenty ton per hour coal cleaning test facility, housing various fine coal cleaning devices and ancillary equipment for sizing, crushing, grinding, and dewatering coals. The facility houses the pilot-scale conventional and column continuous froth flotation circuits used in this project.

Coal Sources, Preparation Prior to Flotation Testing, and Test Matrix

Two coals were evaluated for this project. A Northern Appalachian coal from the Upper Freeport seam was obtained from the Rayne Mining Company in Indiana County, Pennsylvania. An Illinois Basin coal from the Illinois No. 6 seam was obtained from the Consolidation Coal Company's Rend Lake Mine near Sesser, Illinois. The Illinois No. 6 coal as-received at the CQDC was very wet and caused handling problems. The coal was first wet screened at 28 mesh to remove fine, clay material. The oversize was then prepared for flotation testing. The analyses of these coals are given in Table 1.

Table 1. Coal Characteristics

Analysis, Dry Basis	Upper Freeport As-Received	Illinois No. 6 As-Received	Illinois No. 6 Test Feed
Ash (Wt %)	22.47	40.41	21.99
Sulfur (Wt %)	1.10	0.93	1.22
Heating Value (Wt %)	11,925	7,780	11,092
lb SO_2/MBtu	1.84	2.30	2.20
Pyritic Sulfur (Wt %)	0.59	ND	0.56
Sulfatic Sulfur (Wt %)	0.01	ND	0.07
Organic Sulfur (Wt %)	0.50	ND	0.60

ND = Not determined

Prior to flotation testing, the coal--crushed to 1/4-in.--was conveyed to a 15-ton bin that discharged into a nominal one-tph ball mill. The coal was fed to the ball mill at a rate set to produce coal of the appropriate topsize, as measured by a Microtrac™ particle size analyzer. The slurry was then fed to a 15,000-gal agitated storage where percent solids was adjusted, if necessary.

In addition to adjustments in frother (methyl-isobutyl carbinol), collector (No. 2 fuel oil), and shear speed, tests were conducted with variations in cell type, particle size, and blade design as shown in Table 2.

Table 2. Test Matrix

Coal	Cell Type	Particle Size	Blade Design
Upper Freeport	Conventional	28 M x 0	Cowles Design C
		100 M x 0	Cowles Design C
		100 x 325 M	Cowles Design C
	Column	100 M x 0	Cowles Design C
			Radial Turbine
Illinois No. 6	Conventional	100 M x 0	Cowles Design C
			Radial Turbine

Note: Shear speed and reagent dosage were also varied during testing.

Results and Discussion

Upper Freeport Seam Coal. The Upper Freeport seam coal floated to good yields at low dosages of fuel oil collector. The results for the 28 mesh x 0 tests are given in Table 3. At the 0.15 lb/t dosage of fuel oil, a significant improvement in yield was noted with the addition of the high-speed, high-shear mixing. Yield increased from 50 without mixing to 81 percent with mixing in the high-speed, high-shear. However, at the higher dosage of fuel oil (0.26 lb/t), the increase in yield was relatively insignificant. This is probably because such a high energy recovery was already obtained without the high-speed, high-shear pre-treatment and there was little room for improvement.

Table 3. Upper Freeport Seam Conventional Flotation Results for 28 Mesh x 0 Feed

Conventional Flotation

MIBC 0.2 lb/t Cowles Design C Blade

Oil (lb/t)	Shear Speed (%)	Yield (Wt %)	Btu Rec (%)	Ash (Wt %)	Ash Rej (Wt %)	Sulfur (Wt %)	Sulf Rej (Wt %)
0.15	0	50	62	5.9	86	0.74	73
	50	68	82	6.4	79	0.77	59
	100	81	94	9.2	66	0.97	42
0.26	0	75	89	8.0	73	0.86	53
	0	81	95	9.2	66	0.95	44
	50	85	98	10.3	59	1.05	33
	50	84	97	10.4	60	1.04	36
	100	80	94	8.6	68	0.92	45

Ash and sulfur contents of the clean coal products all increased with increases in yields. It is interesting to compare the results of the 0.15 lb/t oil test with 100 percent mixing to the results of the 0.26 lb/t oil test with no mixing (second test). Both obtained an 81 percent yield with similar ash and sulfur results. The use of high-speed, high-shear mixing in this case would allow oil dosage to be reduced by half.

The results in Table 3 also show the reproducibility of the test results. At the 0.26 lb/t oil dosage and no mixing, the yield for the two tests differs by six percentage points. These tests were run on the same day but several hours apart. For the two tests with mixing at 50 percent, the yield only differs by one percentage point. These tests were run back-to-back.

Results for tests with the 100 mesh x 0 Upper Freeport seam coal are presented in Table 4. For both oil dosages presented, high-speed, high-shear mixing did not significantly improve the

flotation yield or ash or sulfur rejection. For this easy-to-float coal, it appears that little improvement can be made to energy recoveries that are already 98 percent.

Tests with the deslimed 100 M x 325M Upper Freeport seam coal showed little improvement with mixing as this size fraction also floated to good yields with minimal reagents.

Table 4. Upper Freeport Seam Conventional Flotation Results for 100 Mesh x 0 Feed

Conventional Flotation MIBC 0.25 lb/t Cowles Design C Blade

Oil (lb/t)	Shear Speed (%)	Yield (Wt %)	Btu Rec (%)	Ash (Wt %)	Ash Rej (Wt %)	Sulfur (Wt %)	Sulf Rej (Wt %)
0.25	0	80	96	9.6	68	0.82	41
	33	82	98	10.0	66	0.87	38
	67	81	98	9.8	68	0.86	42
	100	81	98	10.0	67	0.86	43
22	33	82	98	9.6	67	0.85	38
	67	80	98	9.9	69	0.87	39
	100	79	98	10.1	69	0.91	41
	100	81	98	11.1	64	0.95	30

The 100 mesh x 0 Upper Freeport seam coal was also tested in the pilot-scale column flotation circuit at the CQDC. Table 5 gives the results of these tests. As with the 100 mesh x 0 conventional flotation tests, no improvement was observed with the application of the high-speed, high-shear mixer between tests with similar reagent dosages. However, there is a noticeable difference in yield between the tests with the Cowles C blade (top of table) and the radial blade (bottom of table). A higher yield was obtained for the radial blade tests. However, these differences also appear in the tests without the high-speed, high-shear mixer, giving rise to concerns with the feedrate through the mixer and into the column cell.

There were also observable differences between the froth characteristics between the two blades. The radial turbine was noted to produce larger bubbles in the froth and appeared to give a larger air holdup in the column than did the Cowles C blade. Though there are noticeable differences in the test results and the observed behavior of the froth between tests with the two different blades, no definite conclusions can be drawn from the column flotation data as to the differences in the blades.

Table 5. Upper Freeport Seam Column Flotation Results for 100 Mesh x 0 Feed

Column Flotation

MIBC/Oil (lb/t)	Shear Speed (%)	Yield (Wt %)	Btu Rec (%)	Ash (Wt %)	Ash Rej (Wt %)	Sulfur (Wt %)	Sulf Rej (Wt %)
2.0/0.5	0 (C)	68	79	8.6	72	0.76	58
	50 (C)	65	77	8.9	73	0.87	54
	100 (C)	67	79	8.8	73	0.81	58
1.4/0.3	0 (R)	79	92	9.3	67	0.90	46
	50 (R)	78	90	9.7	66	0.98	43
	100 (R)	77	91	9.3	68	0.94	45
	100 (R)	77	92	9.2	69	0.94	47

Note: C = Cowles Design C Blade, R = Radial Turbine Blade

Illinois No. 6. Some preliminary tests were conducted with the Illinois No. 6 seam coal (100 mesh x 0) in the column flotation cell. The high oil dosages required to float the Illinois No. 6 seam coal to good yield prohibited testing in the column. This is thought to be due to the build up of an oil film at the froth/pulp interface that prohibits bubble/particle movement into the froth. No further testing in the column was conducted.

The conventional froth flotation tests required significant quantities of fuel oil collector to achieve good yield. Table 6 shows these results as well as results comparing the Cowles C and radial turbine blades.

For the 0.33 lb/t MIBC plus 3.25 lb/t fuel oil tests, the addition of high-speed, high-shear mixing greatly improved the flotation yield. Yield improved from 27 percent to 45 percent. However, at the higher reagent dosages, the improvement in yield was quite insignificant.

The first 100 percent shear test preceded the no shear test and the other followed it, so that reproducibility should be within a few points of yield. These results are similar to the results reported for the Upper Freeport seam 28 mesh x 0 tests, where the low yield tests showed great improvement and the high yield tests showed no improvement.

Table 6. Illinois No. 6 Seam Conventional Flotation Results for 100 Mesh x 0 Feed

Conventional Flotation

MIBC/Oil (lb/t)	Shear Speed (%)	Yield (Wt %)	Btu Rec (%)	Ash (Wt %)	Ash Rej (Wt %)	Sulfur (Wt %)	Sulf Rej (Wt %)
0.33/3.25	0	27	35	6.0	93	1.15	73
	100(C)	45	57	6.3	88	1.17	57
0.5/8.0	0	68	85	7.2	79	1.13	36
	100(C)	71	89	7.5	78	1.14	32
	100(C)	70	88	7.1	79	1.14	33
0.5/7.0	0	59	76	6.7	84	1.12	43
	100(C)	61	79	7.2	82	1.11	42
	100(R)	64	81	6.8	82	1.11	39

Note: C = Cowles Design C Blade, R = Radial Turbine Blade

A comparison between the Cowles C and radial turbine blades for the Illinois No. 6 conventional flotation tests shows that a small improvement in yield could be possible with the radial turbine blade over the Cowles C blade. Remember that the Cowles C gives more shear while the radial turbine gives more mixing. These tests were run back-to-back.

Residence Time Considerations. The results show that improvements in clean coal yield are possible with high-speed, high-shear pre-treatment showing reductions in collector dosage of almost half. However, all of these tests were conducted with a residence time of approximately two minutes in the high-speed, high-shear mixer. Residence time is an important consideration in the application of shear and is an important consideration for scale-up to commercial scale. A two-minute residence time applied commercially would result in a mixer that would be very large and not easily retrofitted into existing plant circuits. Conventional froth flotation circuits have approximately three to four minutes of residence time, so that the mixer would need to have a volume equal to that of one or two flotation cells. Commercial flotation cells range in volume from about 300 to 1000 cu ft. Minimizing residence time (or mixer volume) is an important consideration in the economic potential of high-speed, high-shear pre-treatment.

These tests were all conducted at solids concentrations believed to be best for flotation (approximately 8 percent for the 28 mesh tests and approximately 5 percent for the 100 mesh tests). However, solids content has implications for residence time. If the solids content is higher (water lower), then the overall flowrate is lower for the same solids feedrate. This gives an increase in residence time for a constant volume according to the relationship:

$\tau = V / Q$

where τ = mean residence time (min)
V = volume (cubic feet)
Q = volumetric flowrate (cubic feet per min)

Blade Design. As shown in tables 5 and 6, blade design affects the flotation results. Blade design is also an important feature of the commercial high-speed, high-shear mixer. High shear (Cowles Design C blade) versus more intense mixing (radial turbine blade) must be further investigated.

Conclusions and Recommendations

From the previous discussion, it can be concluded that high-speed, high-shear pre-treatment can improve flotation yield at reduced collector requirements. However, these results also pose several other questions that must be answered. Residence time in the mixer and, therefore, mixer size must be further evaluated. And percent solids in the mixer must also be investigated as it also relates to residence time.

Before a more costly Phase II commercialization effort can begin, these additional questions should be answered by a second Phase I effort so that CQ Inc. and its potential industry partners can be assured that an economically viable product will be available for more extensive commercial testing under Phase II. A proposal for an additional Phase I project has been submitted under the 1995 DOE SBIR solicitation.

The following manuscript was unavailable at time of publication.

INTEGRATION OF THICKNER UNDERFLOW INTO THERMAL DRYER CIRCUIT

Dr. Ronald W. Breault
TECOGEN, Inc.
45 First Avenue
Waltham, MA 02254-9046

Please contact author(s) for a copy of this paper.

POC-SCALE TESTING

OF AN ADVANCED FINE COAL DEWATERING EQUIPMENT/TECHNIQUE

J.G. GROPPO AND B.K. PAREKH
CENTER FOR APPLIED ENERGY RESEARCH
UNIVERSITY OF KENTUCKY
LEXINGTON, KY 40511

PATRICIA RAWLS
U.S. DEPARTMENT OF ENERGY
PITTSBURGH ENERGY TECHNOLOGY CENTER
PITTSBURGH, PA 15236

CONTRACT NO. DE-AC22-94PC94155

INTRODUCTION

Froth flotation technique is an effective and efficient process for recovering of ultra-fine (minus 74 μm) clean coal. Economical dewatering of an ultra-fine clean coal product to a 20 percent level moisture will be an important step in successful implementation of the advanced cleaning processes. This project is a step in the Department of Energy's program to show that ultra-clean coal could be effectively dewatered to 20 percent or lower moisture using either conventional or advanced dewatering techniques.

As the contract title suggests, the main focus of the program is on proof-of-concept testing of a dewatering technique for a fine clean coal product. The coal industry is reluctant to use the advanced fine coal recovery technology due to the non-availability of an economical dewatering process. In fact, in a recent survey conducted by U.S. DOE and Battelle, dewatering of fine clean coal was identified as the number one priority for the coal industry. This project will attempt to demonstrate an efficient and economic fine clean coal slurry dewatering process.

The cost-sharing program is for 36 months, which began October 1, 1994. The program will include laboratory, as well as pilot scale dewatering testing at a rate of 1 to 2 tons/hr of clean coal. The pilot scale studies will be conducted at the Powell Mountain Coal Company's Mayflower Preparation Plant located at St. Charles, VA.

This paper is the first public presentation on this program. It describes objectives and scope, and project plans of the program. Accomplishments of the first six months of the program are summarized.

OBJECTIVES AND SCOPE OF THE PROJECT

The main objective of the proposed program is to evaluate a novel surface modification technique, which utilizes the synergistic effect of metal ions-surfactant combination, for dewatering of ultra-fine clean coal on a proof-of-concept scale of 1 to 2 tph. The novel surface modification technique developed at the UKCAER will be evaluated using vacuum, centrifuge, and hyperbaric filtration equipment. Dewatering tests will be conducted using the fine clean coal froth produced by the column flotation units at the Powell Mountain Coal Company, Mayflower Preparation Plant in St. Charles, Virginia. The POC-scale studies will be conducted on two different types of clean coal, namely, high sulfur and low sulfur clean coal. The Mayflower Plant processes coals from five different seams, thus the dewatering studies results could be generalized for most of the bituminous coals.

PROJECT WORK AND MANAGEMENT PLANS

A highlight of the Project Work and Management Plans was prepared and submitted to DOE during the first quarter of the project. The plans will be revised annually.

Work Breakdown Structure

To accomplish the objectives, the project is divided into nine (9) tasks. As shown in Table 1, Work Breakdown Structure, many of the tasks are further divided into subtasks.

Project Organization

The University of Kentucky Center for Applied Energy Research (CAER) is the prime contractor for the project and most of the laboratory dewatering work will be performed at CAER. The Powell Mountain Coal Company is providing facilities and manpower at their Mayflower Preparation Plant for conducting pilot scale studies. Andritz Ruthner Inc. is providing their hyperbaric pilot unit and personnel to conduct high pressure dewatering tests. Each team member brings knowledge and experience in dewatering to accomplish the objectives of the program.

ACCOMPLISHMENTS

Currently in this program, Tasks 2, 3, 4, 5 and 6 are in progress.

Task 2. Sample Analysis and Laboratory Testing

The PMCC's Mayflower Preparation Plant processes high and low sulfur coal from five different seams. Samples of the column flotation products for the high and low sulfur coals were analyzed for particle size and ash distribution which are listed in Tables 2 and 3, respectively.

Table 1. Outline of Work Breakdown Structure

Task 1.	Project Work Planning	
	Subtask 1.1	Project Work Plan
	Subtask 1.2	Project Work Plan Revisions
Task 2.	Samples Analysis and Laboratory Testing	
	Subtask 2.1	Acquisition and Characterization of Samples
	Subtask 2.2	Laboratory Scale Testing
	Subtask 2.3	Optimization of Parameters
	Subtask 2.4	Analysis of Data
Task 3.	Engineering Design	
	Subtask 3.1	Conceptual Design Package
	Subtask 3.2	Final Design Package
	Subtask 3.3	Construction Schedule
Task 4.	Procurement and Fabrication	
	Subtask 4.1	Bid Packages
	Subtask 4.2	Fabricate/Assemble Components
	Subtask 4.3	Deliver POC-Scale Module and Install
	Subtask 4.4	Maintenance and Operating Manual
Task 5.	Installation and Shakedown	
	Subtask 5.1	Install and Tie-in Module
	Subtask 5.2	Startup Procedures/Shakedown
	Subtask 5.3	Operators Training
Task 6.	System Operation	
	Subtask 6.1	Test Coal No. 1
	Subtask 6.2	Test Coal No. 2
Task 7.	Process Evaluation	
Task 8.	Equipment Removal	
Task 9.	Reporting	
	Subtask 9.1	Monthly Reports
	Subtask 9.2	Project Final Report

Table 2. Particle size and ash distribution of high sulfur (non-compliance) clean coal froth slurry (% solids = 18.9)

Size (Mesh)	Weight (%)	% Ash	Ash Distribution
+100	8.96	6.30	6.65
-100+200	19.11	5.40	12.16
-200+325	16.91	6.20	12.36
-325+500	16.56	7.40	14.44
-500	38.46	12.00	54.39
Feed (Calc.)	100.00	8.49	100.00
Feed (Actual)		8.3	

Table 3. Particle size and ash distribution of low sulfur (compliance) clean coal froth slurry (% solids = 13.0)

Size (Mesh)	Weight (%)	% Ash	Ash Distribution
+100	7.77	3.00	3.06
-100+200	16.58	3.80	8.28
-200+325	16.39	4.80	10.34
-325+500	17.23	5.80	13.13
-500	42.04	11.80	65.19
Feed (Calc.)	100.00	7.61	100.00
Feed (Actual)		7.60	

Laboratory dewatering using the high pressure were conducted by Andritz using a 6.4 cm radius filter with a 125 sq. cm filter area. Tables 4 and 5 list the laboratory dewatering data for the high sulfur and low sulfur clean coal slurry, respectively. The dewatering efficiency index (DEI) for each test was calculated using the following formula

$$\textit{Dewatering Efficiency Index} = \frac{(\%\ \textit{dry solids recovery})\ (\%\ \textit{water in filtrate})}{\%\ \textit{moisture in product}}$$

For the high sulfur coal slurry filter cakes with moisture ranging from 21.3 to 24.5 percent and for low sulfur coal slurry filter cakes with moisture ranging from 20.7 to 22.5 percent were obtained. The DEI for high sulfur coal slurry was much higher than that of the low sulfur coal slurry.

Tasks 3, 4 and 5

The engineering and design of the POC-scale, procurement and fabrication task has been completed. The POC-scale unit for the hyperbaric filtration unit was successfully installed and tested at the Mayflower Preparation Plant.

Table 4. Laboratory hyperbaric filtration data for the high sulfur coal slurry.

Test No.	Filter Speed (rpm)	Pressure (bar)	Cake Formation Angle (degree)	Cake Thickness (mm)	% Moisture in Filter Cake	Dewatering Efficiency Index
HS-1	1.5	3	25	4.8	24.27	407.6
HS-2	0.5	3	25	14.3	21.31	466.7
HS-3	1.0	3	25	14.2	24.30	410.8
HS-4	1.0	3	85	17.3	23.57	422.8
HS-5	1.0	4	85	19.4	23.27	427.9
HS-6	1.0	5	85	21.4	22.89	435.2
HS-7	1.5	3	85	13.9	24.50	405.2
HS-8	1.5	4	85	15.2	22.60	440.7
HS-9	1.5	5	85	16.6	22.82	436.1
HS-10	2.0	3	85	13.0	24.43	406.5
HS-11	2.0	4	85	14.2	23.62	420.5
HS-12	2.0	5	85	15.6	23.72	419.8

Table 5. Laboratory hyperbaric filtration data for the low sulfur coal slurry.

Test No.	Filter Speed (rpm)	Pressure (bar)	Cake Formation Angle (degree)	Cake Thickness (mm)	% Moisture in Filter Cake	Dewatering Efficiency Index
LS-1	1.0	3	85	10.4	22.37	344.1
LS-2	1.0	4	85	11.4	21.55	361.9
LS-3	1.0	5	85	13.1	20.93	375.2
LS-4	1.5	3	85	8.7	22.70	337.5
LS-5	1.5	4	85	9.7	22.45	342.3
LS-6	1.5	5	85	10.6	21.38	365.1
LS-7	2.0	3	85	8.4	22.91	333.8
LS-8	2.0	4	85	9.5	22.51	341.3
LS-9	2.0	5	85	10.4	21.69	358.7

Task 6. System Operation

The first system tested for the program was the Andritz hyperbaric unit. The pilot hyperbaric unit has a disc of 1.4 meter (4.6 ft.) diameter with $2m^2$ (22 sq. ft.) filtration area which is enclosed in a 2.5 meter (8.2 ft.) diameter pressure vessel. The trailer-mounted unit is self-sufficient and has its own feed pumps and air compressor. The unit requires 440 volts power to run.

Baseline Testing. The primary operating variables that were evaluated in baseline testing were cake formation angle (CFA), filter speed and pressure. The CFA refers to the angle of rotation, measured from the horizontal position where the

rotating filter element enters the slurry, through which cake formation occurs and is analogous to the more common term 'cake formation time.' The filter speed simply refers to the rotation of the filter disc and is measured in revolutions per minute (rpm) while the pressure is the vessel pressure measured in bar (about 1 bar = 14.5 psi). Most of the tests were conducted at a feed rate of 50 gallons/minute (1.5 tons/hr dry solids) of slurry.

The effect of filter speed and cake thickness on cake moisture for the high sulfur clean coal froth product for 165° CFA is shown in Figure 1. The cake moisture increased with increasing filter speed as shown in Figure 1a. This was the case for both 1 and 2 bar pressures (1 bar = 14.5 psi). However, at 3 bar, cake moisture remained essentially constant at 23.5 percent moisture. Note, that increasing cake thickness from 10 to 20 mm, the filter cake moisture was lowered. This is very surprising, however, similar trends were observed in other tests conducted at different CFA. The lowest moisture of 23.2 percent was achieved using 2 and 3 bar pressures.

The effect of CFA on filter speed of 1.5 rpm is shown in Figure 2. As the CFA was increased from 85° to 165°, the cake moisture obtained at 1 bar pressure increased from 24.8% to 27% moisture. At higher pressure (3 bar), the cake moisture increased from 21% to 23.7% over the same range of CFA.

Air consumption and solids throughput are the two most important considerations in evaluating the performance of the hyperbaric filter. Figure 3 shows the air consumption requirements for tests conducted using various pressures and CFA. It shows that at a filter speed of 1.5 rpm and a CFA of 165°, the air consumption at 3 bar pressure was 460 scfm/ton. Figure 4 shows the dry solids throughput using the experimental conditions described above. The solids throughput at 1 bar pressure increased from 77 to 120 lb/ft^2/hr as the CFA was increased from 85° to 165°. At 3 bar pressure, the solids throughput increased significantly from 110 to 165 lb/ft^2/hr over the same range of CFA.

Before summarizing baseline testing results, it is important to recognize that while it is desirable to reduce cake moisture to the lowest levels possible, it is also desirable to obtain these results with minimum cost (i.e. minimize air consumption and maximize throughput). With these factors in mind, the baseline test conditions selected from these results to minimize moisture and air consumption while maximizing throughput were 3 bar pressure, 1.5 rpm filter speed and 165° CFA. These conditions produced a filter cake with 23.6% moisture and a cake thickness of 18 mm. These conditions resulted in a solids throughput of 165 lb/ft^2/hr and an air consumption of 460 scfm/ton.

ACKNOWLEDGEMENTS

The authors would like to thank Mr. Bill Peters, Larry Hall and Jim Mullins of the Powell Mountain Coal Company, and Mr. John Hugh and Mr. Garen Evans of Andritz Ruthner Inc. They would also like to acknowledge the assistance from CAER staff members John Stehn, X.H. Wang, John Wiseman and Darryl McLean.

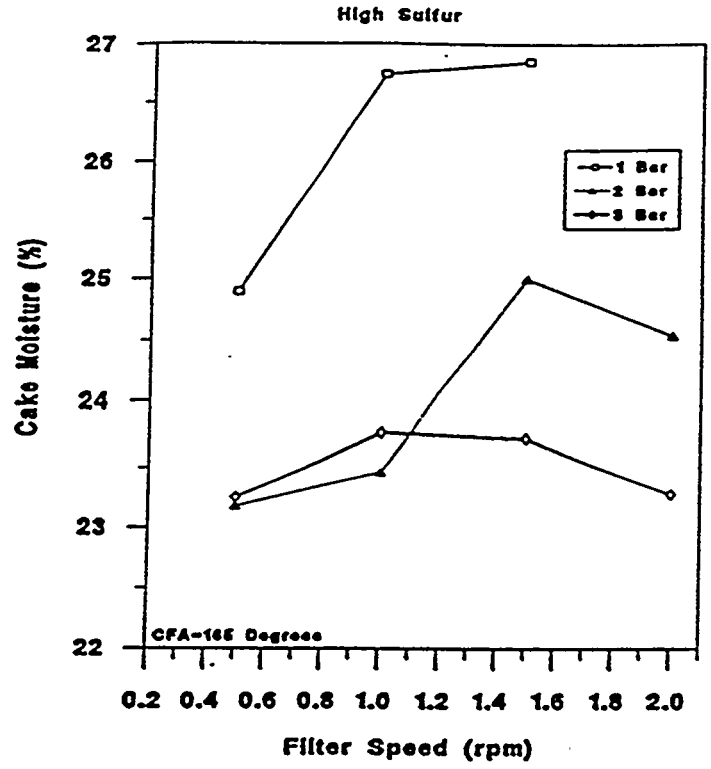

(a)

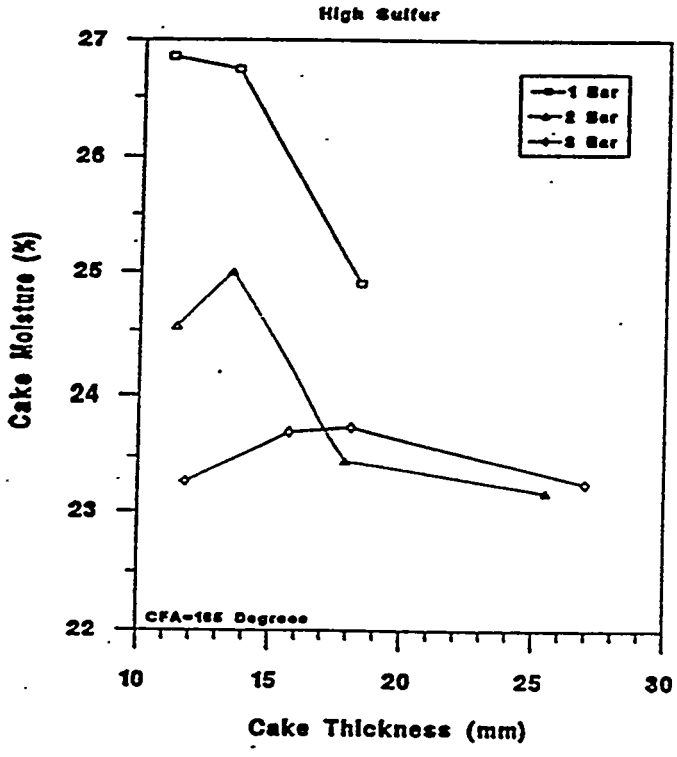

(b)

Figure 1. Effect of filter speed (a) and cake thickness (b) on filter cake moisture using 165° cake formation angle at various applied pressures

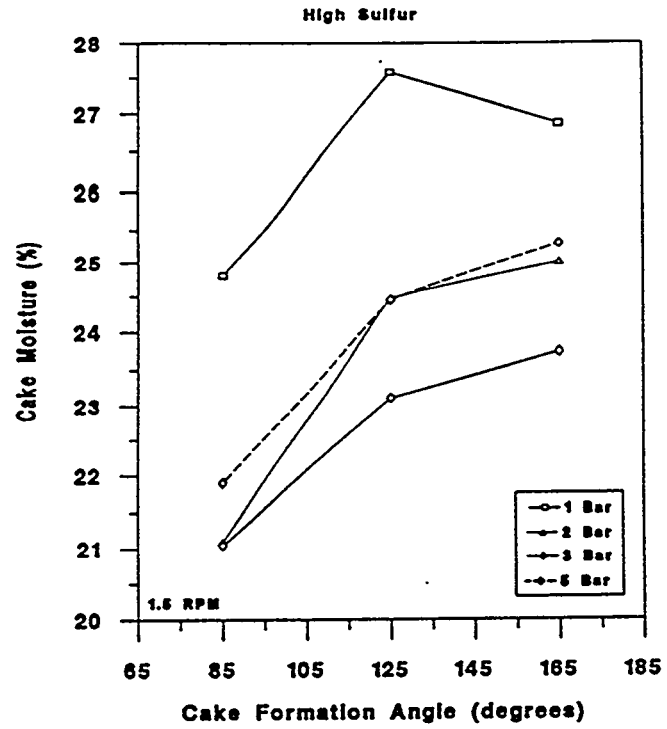

Figure 2. Effect of cake formation angle at various applied pressure on filter cake moisture obtained at 1.5 rpm filter speed

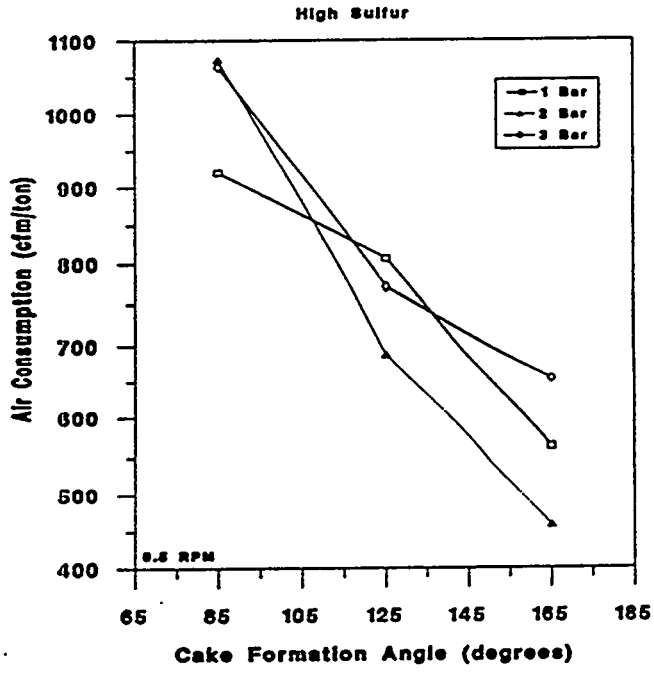

Figure 3. Effect of cake formation angle on air consumption for pressure filtration of high sulfur coal at 1.5 rpm filter speed and various vessel pressures

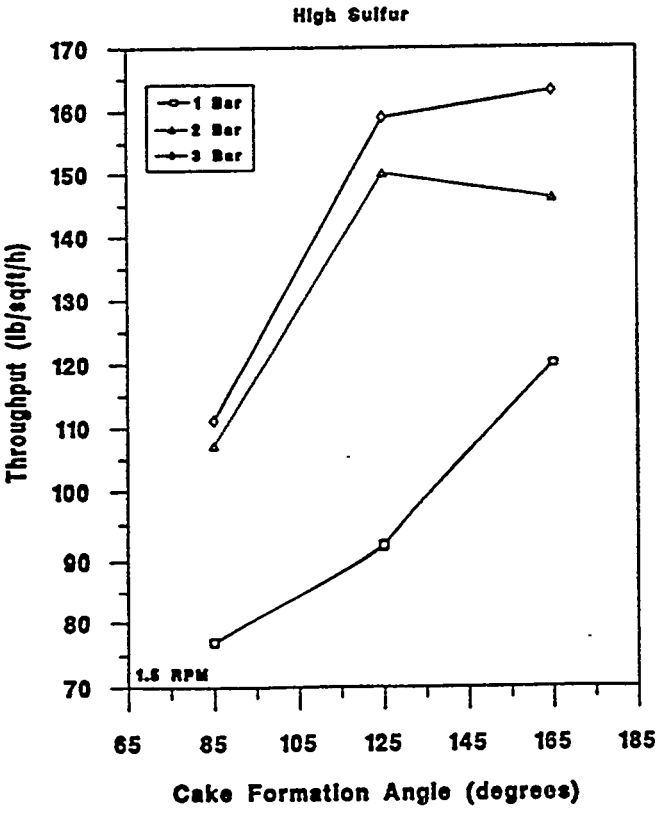

Figure 4. Effect of cake formation angle on throughput for pressure filtration of high sulfur coal at 1.5 rpm filter speed and various vessel pressures

The following manuscript was unavailable at time of publication.

IMPROVEMENT OF STORAGE, HANDLING, AND TRANSPORTABILITY OF FINE COAL

Russell C. Maxwell, Jr.
Energy International Corporation
135 William Pitt Way
Pittsburgh, PA 15238

Please contact author(s) for a copy of this paper.

The following manuscript was unavailable at time of publication.

BENCH-SCALE TESTING OF THE GRANUFLOW PROCESS FOR FINE COAL DEWATERING AND RECONSTITUTION: RESULTS USING A HIGH-G SOLID-BOWL CENTRIFUGE

George Wen
U.S. Department of Energy
Pittsburgh Energy Technology Center
P.O. Box 10940, M.S. 141L
Pittsburgh, PA 15236

Please contact author(s) for a copy of this paper.

The following manuscript was unavailable at time of publication.

CHARACTERIZATION OF AIR TOXICS FROM A LABORATORY COAL-FIRED COMBUSTOR AND UTILITY-SCALE POWER PLANTS

Dr. George Sverdrup
Battelle Columbus
505 King Avenue
Columbus, OH 43201

Please contact author(s) for a copy of this paper.

CHARACTERIZING MERCURY EMISSIONS FROM A COAL-FIRED POWER PLANT UTILIZING A VENTURI WET FGD SYSTEM

P. VANN BUSH
MANAGER, PARTICULATE SCIENCE & ENGINEERING
SOUTHERN RESEARCH INSTITUTE

EDWARD B. DISMUKES
CONSULTANT

WILLIAM K. FOWLER
SENIOR STAFF CHEMIST
SOUTHERN RESEARCH INSTITUTE

INTRODUCTION

Southern Research Institute (SRI) conducted a test program at a coal-fired utility plant from October 24 to October 29, 1994. The test schedule was chosen to permit us to collect samples during a period of consecutive days with a constant coal source. SRI collected the samples required to measured concentrations of anions and trace elements around two scrubber modules and in the stack. Anions of interest were Cl^-, F^-, and $SO_4^=$. We analyzed samples for five major elements (Al, Ca, Fe, Mg, and Ti) and 16 trace elements (As, B, Ba, Be, Cd, Co, Cr, Cu, Hg, Mn, Mo, Ni, Pb, Sb, Se, and V).

SRI made measurements across two scrubber modules, each treating nominally 20% of the total effluent from the boiler. Across one module we examined the effects of changes in the liquid-to-gas ratio (L/G) on the efficiency with which the scrubber removes trace elements and anions from the flue gas. Across another module we examined the effects of slurry pH on the removal of trace elements and anions from the flue gas. Measurements in the stack quantified emissions rates of anions and trace elements.

Special emphasis was placed on measurements of mercury concentrations. SRI sampled with two methods designed to measure mercury in flue gases -- EPA Method 29, and a proprietary modification to EPA Method 101A developed by Ontario Hydro Technologies.

Plant Features

Features of the plant that affect emissions of the chemical substances of interest are:

1) The coal is beneficiated by washing to remove a substantial fraction of mineral matter and sulfur.
2) The coal is burned in a cyclone furnace, with the attendant high temperature of combustion and the emission of a high concentration of nitrogen oxides, but the emission of a lower fraction of the ash than occurs with wall or tangential firing.
3) The fly ash evolved from the boiler is first subjected to collection in an ESP.

4) The residual fly ash at the outlet of the ESP and the SO_2 are subject to capture in a venturi scrubber with limestone as the basic reactant. Design specifications of the scrubber are particulate collection of 94% and SO_2 reduction of 84%.

The scrubber consists of six venturi modules. Normally, five scrubber modules are in service, and one is in maintenance. Customarily four of the active modules are operated at "high" pH and the fifth is operated at "low" pH. During this test the high pH was typically 5.7 and the low pH was typically 5.1. Scrubber sorbent is prepared at the plant by pulverizing limestone in a wet ball mill. Additional water is added to this slurry to maintain a solids concentration in the recycle tanks around 12%. The actual feed rate of limestone is governed by the pH of the recycle tanks. Fresh limestone slurry is supplied only to the high-pH modules; spent slurry from the high-pH modules performs the scrubbing in the low-pH module. Fresh limestone slurry is added at Ca/S mole ratio of about 1.05, or perhaps sometimes as high as 1.10. The scrubber is operated with forced oxidation to produce a waste product in which gypsum rather than calcium sulfite is dominant. Waste liquor and solids from the recycle tanks are pumped to an effluent tank and then to an ash pond.

The main constraint placed on the plant by our test program was the exclusive use of coal from one seam of one mine. Gross generation was kept within 0.5% of full load throughout our sampling periods. In addition to holding the load constant, soot blowing of air heaters was suspended during our sampling times to eliminate the effect of this erratic ash loading from our flue gas measurements.

Test Program

Our test program called for three operating conditions in the scrubber. We tested across a scrubber module at the normal liquid-to-gas ratio (L/G) and at a higher L/G each day of our test. The adjustment in L/G was made by reducing the flue gas flow through a scrubber module (identified as Module X) while maintaining the slurry feed rate. The flue gas flow was reduced by closing a louver-type damper at the inlet to the module. We also tested across another scrubber module operated at low and high pH levels on alternate days. The change in scrubber pH was made over night on another module (identified as Module Y). Module Y operated at low pH on the first and third days of our test, and high pH on the second and fourth test days.

Other than the operational changes in the scrubber modules and the restrictions on sootblowing, the boiler and scrubber systems operated during our test program as they would normally operate. The operators maintained very stable conditions during our test periods.

Samples taken during this program were comprised of both flue gas and process liquids and solids. Flue gas samples were taken at four locations over a four-day period:

1) Inlet to Scrubber Module X — 4 samples at normal L/G and 4 at high L/G
2) Outlet of Scrubber Module X — 4 samples at normal L/G and 4 at high L/G
3) Outlet of Scrubber Module Y — 2 samples at low pH and 2 at high pH
4) Stack — 4 samples.

The sampling methods we used for flue gases were as follows:

- Major metals and trace metals (including mercury) in both particulate and vapor forms were sampled using EPA Draft Method 29.
- Mercury was also collected as the single analyte by an impinger train developed by Dr. Keith Curtis of Ontario Hydro Technologies. The Ontario Hydro mercury train is a modification to the EPA Method 101A sampling train.
- Anions were sampled by use of the Method 5 train in which solids on the filter as well as sodium carbonate/bicarbonate impinger solutions were retained for analysis.
- Samples collected for metals analysis in three ranges of particle size were taken using teflon-coated cyclones I and II of the SRI/EPA Five Series Cyclone sampling system.

RESULTS

The emphasis in this paper is on the results of measurements of mercury concentrations, which was the main emphasis of the test program.

Mercury Concentrations in Coal

We determined mercury in the as-fired (washed) coal to assess the plausibility of the mercury concentrations measured in the flue gas. We had reason to believe the mercury value reported by analytical subcontractor Galbraith Laboratories (GL) for the cleaned coal was low. We had some samples of cleaned coal analyzed by Brooks Rand, Ltd. (BR). For the period October 25-28, the concentrations of mercury in the washed coal average 0.0837 µg/g in the analyses at BR, but only 0.0578 µg/g in the analyses at GL. We believe the reason for this difference is the use of different sample digestion procedures by the two labs. GL used a standard microwave digestion technique for sample preparation (based on Application Note MS-6 for coal digestion by CEM Corporation, manufacturer of the microwave oven). The BR sample preparation procedure employs perchloric acid to accomplish complete dissolution of the sample. Only the higher concentrations reported by BR could have produced the highly consistent flue-gas concentrations that were measured. The consistency of results of the BR analyses is shown below:

	µg/g
October 25	0.0781
October 26	0.0840
October 27	0.0883
October 28	0.0844
AVERAGE	**0.0837**
Std. Deviation.	0.0042

The average mercury concentration in the washed coal was 0.0837 μg/g, which for this coal would yield 9.7 μg/Nm^3 in the flue gas. (In our usage, Nm^3 is the dry flue gas volume in cubic meters corrected to 20°C, 1 atm pressure, and 3% O_2 content.) This concentration agrees very well with the measured concentrations of mercury in the flue gas, assuming that all mercury contributed by the coal was entrained in the flue gas.

Mercury Concentrations in Flue Gases

We used two different sampling methods to determine the concentration of mercury in flue gases. Both methods, Method 29 and the modified Method 101A (MM101A), ostensibly provide distinct measures of two ionic species of mercury — Hg(II) and Hg(0).

Analyses of filter solids were performed for SRI by Galbraith Laboratories, Inc. (GL). Both SRI and GL analyzed the impinger solutions. All impinger solutions were prepared for mercury determinations by EPA Method 7470. Mercury was determined primarily by CVAAS as per EPA Method 7470. But SRI's CVAAS instrument is also equipped for simultaneous determinations by atomic fluorescence spectrometry (AFS), which offers lower detection limits than CVAAS. Hence, those few samples in which the mercury levels were below the detection limit of the CVAAS technique were analyzed by CVAFS.

The Method 29 permanganate-containing impinger solutions and both types of MM101A impinger solutions were prepared and analyzed for mercury essentially in accordance with EPA Method 7470. At SRI, the Method 29 peroxide-containing impinger solutions were prepared for mercury determinations by a slightly modified version of EPA Method 7470. At the point where potassium permanganate was added to the solutions, we added solid potassium permanganate, after first adding the permanganate solution specified in the method, to minimize the increase in sample volume that is associated with this step. But GL encountered problems in their attempts to follow this protocol for peroxide-containing samples. Specifically, they found that their samples generated too much heat on addition of the solid permanganate. Indeed, the solution temperatures actually reached the boiling point on certain occasions, which raised concerns that certain volatile elements could be lost by evaporation.

It was later discovered that, in an attempt to attain the lowest possible detection limits for mercury, GL had used a lower sample-dilution ratio than we did. Thus, their samples had contained more of the original hydrogen peroxide than ours, and their peroxide-neutralization reactions were thus more intensely exothermic than ours. But in the absence of this knowledge, GL carried out a microwave digestion of these samples (i.e., the EPA Method 29 protocol for Method 29 impinger liquids) prior to any further preparation or analysis, in hopes of circumventing the problem altogether. Unfortunately, their mercury measurements on these samples correlated poorly with ours; their results were generally much lower and more variable. We can only speculate that they somehow experienced losses of mercury during their microwave sample-preparation step. Note that, if they had decomposed the hydrogen peroxide in the microwave oven, then portions of the ionic mercury could have been reduced to the neutral elemental form, leading to losses of elemental mercury vapor on opening the microwave vessels.

Although we did not attempt to speciate mercury in solid matter, it seems plausible that the mercury in this state is ionic (perhaps as the compound HgO), not elemental. The percentage of the total mercury found in the particulate state was 1% or less of the total, confirming the

expectation that mercury would occur mainly in the vapor state. At the scrubber inlet the solid phase mercury was 0.8% of the total. At the stack it was 0.5% of the total.

The average mercury concentrations in the vapor state are tabulated below for ready comparison. These averages were produced disregarding the scrubber L/G or pH, which was inconsequential as described later. Thus, there were eight individual measurements represented in the averages at Module X inlet for Method 29, seven individual measurements at Module X inlet for MM101A, eight measurements at Module X outlet for both sampling methods, and four measurements for each method at Module Y outlet and the stack. The concentrations are in the units $\mu g/Nm^3$; the percentages of the two forms of mercury are shown in parentheses:

	Method 29	Modified Method 101A
Inlet, Module X	$\mu g/Nm^3$	$\mu g/Nm^3$
Ionic	7.39 (74.3%)	4.74 (48.1%)
Elemental	2.56 (25.7%)	5.12 (51.9%)
Total	9.95	9.86
Outlet, Module X	$\mu g/Nm^3$	$\mu g/Nm^3$
Ionic	1.15 (20.8%)	0.56 (9.3%)
Elemental	4.37 (79.2%)	5.56 (90.7%)
Total	5.52	6.13
Outlet, Module Y	$\mu g/Nm^3$	$\mu g/Nm^3$
Ionic	-	0.51 (8.5%)
Elemental	-	5.54 (91.5%)
Total	-	6.06
Stack	$\mu g/Nm^3$	$\mu g/Nm^3$
Ionic	1.35 (22.6%)	0.52 (7.9%)
Elemental	4.63 (77.4%)	6.13 (92.1%)
Total	5.98	6.66

The more important observations from the above tabulation are as follows:

1. The two methods were in good agreement on the total concentration at each location where both methods were used. The differences range only from 0.1 to 0.6 $\mu g/Nm^3$.

2. Both methods indicate that the scrubber removed most of the ionic mercury. Either method shows good agreement between the outlet of Module X and the stack; MM101A also shows good agreement between the outlets of Modules X and Y.

3. The methods differ substantially on the proportions of mercury in the ionic and elemental states. At each sampling location Method 29 gave the higher percentage in the ionic state. Moreover, Method 29 seemed to show that part of the ionic mercury at the scrubber inlet was converted to the elemental form at the outlet.

The explanation for the difference in speciation cannot be explained unequivocally. It may have to do, however, with the lack of specificity of the peroxide impinger in Method 29 for capturing the ionic form of mercury. The combination of hydrogen peroxide and nitric acid in the so-called peroxide impinger surely has the oxidizing potential for converting part of the elemental mercury to the ionic state. The suggestion that ionic mercury shifts from the ionic state to the elemental state across the scrubber is contrary to the predictions of thermodynamics. Therefore, these data suggest Method 29 did not accurately differentiate the species of mercury.

Mercury Concentrations in Scrubber Solids and Liquids

Concentrations of mercury in streams associated with the scrubber are listed below:

	INPUT STREAMS		OUTPUT STREAMS	
Sampling Occasion	Make-up Water, ng/mL	Dry Limestone, µg/g	Recycle Slurry, µg/g	Discharge Slurry, µg/g
Oct. 25 AM	<0.010	0.0120	-	0.0248
PM	<0.010	<0.010	0.0295	0.0248
Oct. 26 AM	<0.010	<0.0087	0.0084	0.0248
PM	0.036	0.0150	0.0279	0.0248
Oct. 27 AM	<0.010	0.0100	0.0283	0.0240
PM	0.003	<0.00097	0.0289	0.0240
Oct. 28 AM	0.005	<0.0066	0.0303	0.0237
PM	<0.010	<0.010	0.0324	0.0237

It is to be noted that the concentrations in the liquid components of all slurries were in the units ng/mL, whereas those in the solids were in the units µg/g. Thus, there was a 1000-fold difference in the mercury concentrations in the two phases of the slurries.

The concentrations in the input water and limestone were often below the detection limits. The data can be conservatively summarized by the statements that in the water the value was always below 0.04 ppb and that in the limestone (where the detection limit was much higher) always below 0.02 ppm. The mercury entering the scrubber in the limestone slurry was far below that entering in the flue gas. In other words, the limestone slurry was responsible for only a small fraction of the total mercury.

The mercury in both liquid and solid phases leaving the scrubber as the recycle slurry or the discharge slurry was much enriched over the level entering in liquid and solid forms. As may be reasonably inferred, the increase was due to the uptake of mercury from the flue gas. There was some variability from sample to sample, but in either slurry composite the calculated mercury concentration was approximately 0.02-0.03 ppm. The composite analyses of the two slurries agree satisfactorily, in general.

Mass Balances

Coal vs. Scrubber Inlet

The plan of the investigation did not include collection of samples of bottom ash or ESP ash. Moreover, the plan did not include measurement of the proportions of ash leaving the boiler as bottom ash and fly ash or the measurement of ash removal in the ESP. The only task relevant to these general considerations that can be undertaken is a comparison of the concentrations of substances flowing in the duct leading to Module X against the concentrations that would have been observed if all of these substances originally in the coal had been entrained uniformly in the inlets to all five operating modules.

The average metal concentrations based on the coal analysis were compared with the averages found at the Module X inlet. For the major metals recoveries range approximately from 23-32%. For fly ash at the inlet of Module X, the recovery might be expected to fall somewhere within this range. It is consistent with what we know about this plant: 1) fly ash makes up about 30% of the total ash, and 2) the efficiency of the ESP is at most 40%.

The recovery of mercury was 105%. The result for this metal is highly gratifying. As we have said, over 99% of the total mercury was in the vapor phase. So we expected essentially all of the mercury in the coal to be present at the scrubber inlet.

Scrubber Module X Inlet vs. Outlet

We were able to calculate a mass balance around the scrubber Module X. Values fixed at the outset of calculations at 100% were recoveries for calcium, sulfate, and water. These assumptions were required in the absence of measured flow rates for scrubber slurries. We achieved a very gratifying balance of 99% for heat across the scrubber with these assumptions, which is to a degree independent of the assumed closure for water.

The percentage of mercury in the scrubber inlet streams that was accounted for in the scrubber outlet streams was 91% — an excellent mass balance. The inlet flue gas dominates input, and the outlet flue gas contains the majority of the output. All of the mercury data having to do with flue gas used in this calculated balance were based on Method 29.

Effects of Scrubber Operation

Measurements at the inlet and outlet of Module X provided data at two L/G ratios: the customary value around 85 gal/acf and an increased value of about 100 gal/acf. The data on mercury based on Method 29 or based on the modification of Method 101A lead to the same conclusion — that mercury removal in the scrubber is not altered by changing L/G.

Concentrations of mercury at the outlet of Module Y when scrubbing occurred at recycle pH values of 5.7 and 5.1 are not decisive enough to show any difference due to pH. A tabulation is given below for mercury concentrations in $\mu g/Nm^3$:

	Higher pH	Lower pH
Ionic	0.67, 0.50	0.37, 0.50
Elemental	4.75, 5.70	6.45, 5.26

Removal Efficiencies and Emissions Factors

The average reduction of mercury across scrubber Module X was 45% based on data from Method 29; the reduction was 38% based on data from modified Method 101A. As the data presented previously show, the removal of ionic mercury was very efficient across the scrubber. Method 29 results indicate 82% reduction of ionic mercury, and modified Method 101A indicates 89% reduction in ionic mercury. The speciation results from modified Method 101A data are more credible, for reasons discussed above.

The emissions factor for mercury was determined from the average concentration of mercury in the stack gas, gas volume per unit mass of coal, and coal calorific content. The emissions factor is 1.85 $g/10^{12}$ J , or 4.30 $lb/10^{12}$ Btu.

ACKNOWLEDGMENTS

This work was funded by DOE Contract No. DE-AC22-93PC93254. Dr. Michael J. Baird serves as the DOE Project Manager. We appreciate the cooperation of the host utility. Galbraith Laboratories, Inc. and Brooks Rand, Ltd. conducted some of the analyses reported in this paper. We appreciate the excellent work of Wynema Kimbrough of SRI in performing the mercury measurements at SRI.

A STUDY OF TOXIC EMISSIONS FROM A COAL-FIRED GASIFICATION PLANT

AL WILLIAMS AND GREG BEHRENS
RADIAN CORPORATION
8501 N. Mopac Boulevard
Austin, Texas 78759

Abstract

Toxic emissions were measured in the gaseous, solid and aqueous effluent streams in a coal-fired gasification plant. Several internal process streams were also characterized to assess pollution control device effectiveness. The program, consisted of three major phases. Phase I was the toxics emission characterization program described above. Phase II included the design, construction and shakedown testing of a high-temperature, high-pressure probe for collecting representative trace composition analysis of hot (1200°F) syngas. Phase III consisted of the collection of hot syngas samples utilizing the high-temperature probe. Preliminary results are presented which show the emission factors and removal efficiencies for several metals that are on the list of compounds defined by the Clean Air Act Amendments of 1990.

Background

The Louisiana Gasification Technology, Inc. (LGTI) project was selected by the U.S. Department of Energy (DOE) to demonstrate the Dow gasification process as part of the DOE Innovative Clean Coal Technology (ICCT) program. The primary goal of the DOE ICCT program is to demonstrate the technical readiness of clean coal technologies and to provide design and operating data that can be used in commercially developing these processes. The environmental performance of each of the demonstrated clean coal technologies is a critically important factor in determining their commercial readiness and endorsement.

During the LGTI demonstration program, the environmental characteristics of some streams, particularly the discharge streams, have been regularly monitored. However, with the passage of the Clean Air Act Amendments (CAAA) in 1990, it has become very important to define the fate of currently unregulated hazardous air pollutants (HAPs) within and from the LGTI process. Most of the HAPs have not yet been measured at the demonstration facility. For that reason, the DOE and the Electric Power Research Institute (EPRI) retained Radian Corporation to measure selected HAPs in the discharge streams and in most of the major internal process streams of the LGTI demonstration plant.

Within the last few years, EPRI and DOE have both implemented programs to measure HAPs in the process and discharge streams of conventional fossil-fueled power plants. Sampling and analytical methods for measuring HAPs in these streams have been identified and/or developed as a part of these programs. However, many of these methods are not be applicable for coal gasification systems, which differ considerably in both process conditions and process complexity from those of conventional systems. The gas matrix found at the turbine exhaust stacks (and to a lessor extent at the incinerator stack) is comparable to that found at most

conventional coal-fired power plants. Internal streams in a gasifier are typically reducing environments, with major gas components being hydrogen, carbon monoxide and carbon dioxide. Sulfur is present as primarily hydrogen sulfide and lessor amounts of other reduced sulfur species. Nitrogen is present, not as NO_x, but as ammonia and hydrogen cyanide. Trace elements may not be oxides, but rather hydrides or carbonyls.

It is not surprising then, that EPA Reference Methods often do not yield accurate results when applied to internal gasification streams. Unfortunately, reference methods do not exist for testing gasification process streams and any test methods that are used are subject to interpretation. During this test program, Radian used alternate test methods to augment analytical data from the EPA Method 29 multi-metals sampling train. The approach to the test program and results from alternative method testing are described in the following section.

The Process

LGTI (Louisiana Gasification Technology Inc.), a subsidiary of DESTEC Energy Inc., operates the coal gasification plant at the Dow Louisiana Division chemical complex in Plaquemine, Louisiana. The syngas project began operations in 1987 as the Dow Syngas Project. The gasification unit produces medium Btu synthesis gas (syngas) for consumption by gas turbine power generating units at the Louisiana site.

At full capacity, the LGTI Plant produces 30,000 MM Btu of equivalent syngas per day from approximately 2,200 tons per day of western subbituminous coal from the Rochelle mine in the Powder River Basin in Wyoming. The power unit produces the equivalent of 160 MW of net power considering both electricity and steam production.

Figure 1 is a block flow diagram of the LGTI gasification facility at Plaquemine. The block diagram includes the coal preparation, gas production, particulate removal, moisture removal, acid gas cleanup, power production, wastewater stripping, acid gas treatment, sulfur production, and tail gas incineration.

The coal is ground and slurried with water recycled from the process and pumped to the gasifier where it is mixed with oxygen and steam. The oxygen feed rate is carefully controlled to maintain the reactor temperature within a narrow range. Sulfur in the coal is almost totally converted to H_2S and small amounts of COS, while nitrogen is efficiently converted to NH_3 and trace amounts of cyanide and thiocyanate.

The raw gas passes through the heat recovery train where steam is produced. The partially cooled gas then passes through a venturi scrubber where particulate matter is removed. The gas is further cooled before it passes through sulfur (acid gas) removal in the Selectamine™ unit. Water, condensed from the gas during cooling, is sent to the sour water stripper and then to the water treatment unit. Over 97% of the sulfur species are captured in the sulfur removal process. The concentrated acid gases (primarily H_2S and CO_2) are sent to sulfur recovery.

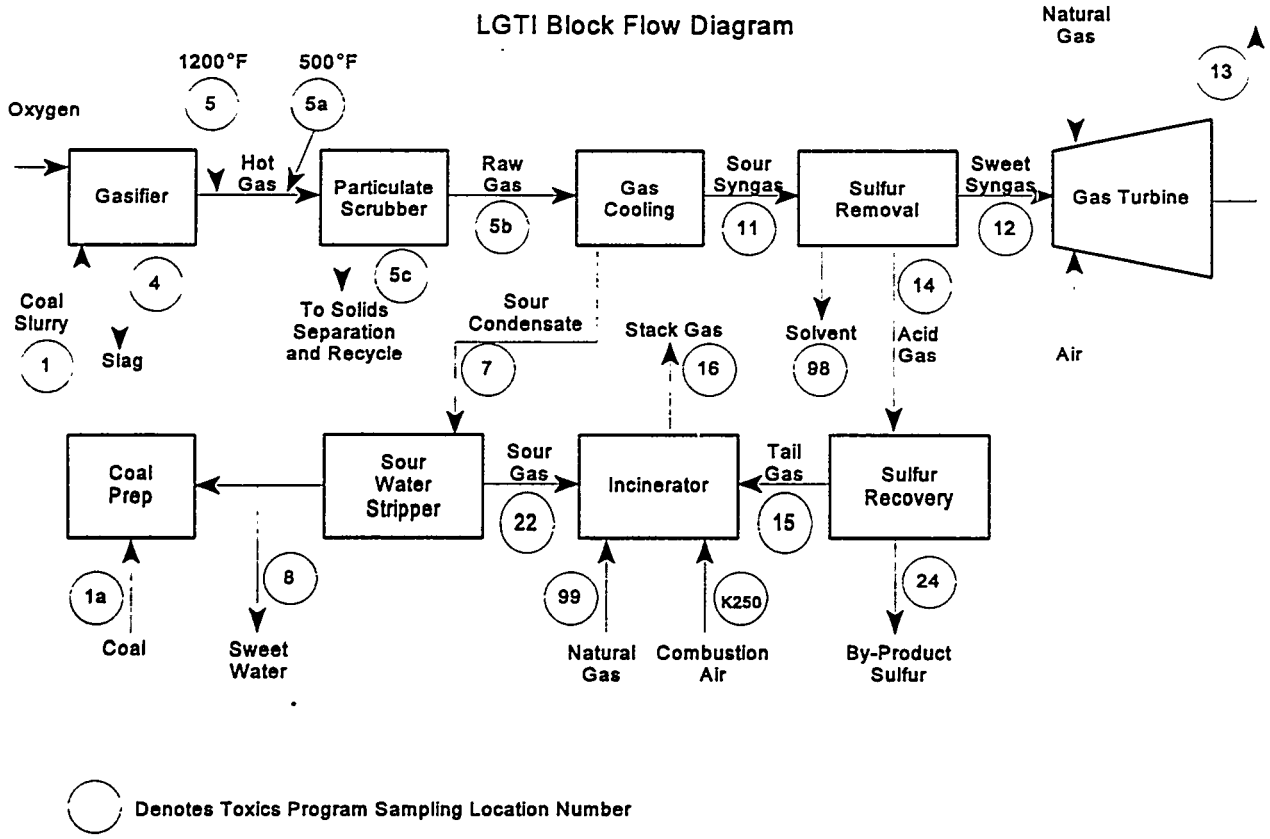

Figure 1. LGTI Block Flow Diagram

The Selectox™ process is used to recover sulfur from the acid gas produced in the Selectamine™ unit. This process is identical to the Claus process reactions, but the combustion furnace of the Claus process is replaced by a fixed bed of Selectox™ catalyst. Liquid sulfur produced from the process is sold as by-product. The sweetened syngas is sent by pipeline to Dow's Power II facility where it is mixed with natural gas and fired in two large combustion turbines. During the HAP's test program, approximately 60% of the fuel to the turbine tested was from syngas.

The sour water condensed from the product gas as it cools is directed to the wastewater treatment system which includes filtration and stripping. Stripped sour water (sweet water) from the treatment system is recycled to the coal preparation area. Excess sweet water is discharged to the Dow plant water system for further treatment. The Dow plant-wide water treatment system includes activated sludge and clarification. The gas which is stripped from the sour condensate is referred to as sour gas, and it is routed to the tail gas incinerator.

The incinerator receives tail gas from the Selectox™ unit, sour gas from the sour water stripper, and combustion air (including vapors from the tank vents). All are combusted in the natural gas-

fueled incinerator for efficient destruction of combustibles. The incinerator stack discharges its exhaust at a height of approximately 200 feet.

Testing

The measurement of HAPs at the LGTI plant was one of the most comprehensive ever performed at a coal gasification facility, and was conducted in three phases. Phase I included the majority of the toxics characterization. Phase II involved the design, manufacture and shakedown testing, of a probe for collecting gas samples from high-temperature, high-pressure process locations. During Phase III, the hot (1200°F) syngas was characterized for trace metal composition of the particulate and vapor phase syngas utilizing the high temperature probe.

As stated earlier, the majority of the program was performed as part of Phase I. The actual test effort required approximately two weeks to complete with a field crew of as many as 20 scientists and engineers. The two week test effort was conducted as three test periods. Each test period focused on the characterization of the process streams associated with a specific control device(s). The first test period encompassed the Selectamine™, gas turbine, and Selectox™ units. The sour water stripper and incinerator stack were testing during Period II, and the gasifier, venturi scrubber, and gas cooling sections were part of Period III testing. In all, samples were collected from 20 locations throughout the gasification and turbine blocks.

In previous test efforts conducted by Radian on gasification systems, results have indicated that EPA Reference Method 29 for trace elements did not yield accurate results. In general, the sampling and analytical methodologies that were used on this program were consistent with those used by EPRI during the Field Chemical Emissions Monitoring (FCEM) program[1]. However, Method 29 (for the internal process streams) was modified to try to compensate for the reducing gas matrix. The nitric/peroxide impingers were boosted to 10% nitric/30% peroxide and the potassium permanganate impingers were not used as the $KMnO_4$ is rapidly consumed by the H_2S in the syngas. In addition to Method 29, syngas was passed through quartz tubes containing specially prepared coconut-based charcoal. These tubes were subsequently digested in nitric acid and analyzed by either ICP-AES, GFAAS, or CVAAS for trace elements. Detection limits for elements determined by the charcoal adsorption technique are nominally in the range of 1 $\mu g/Nm^3$.

The sour syngas and the sweet syngas were also sampled for trace elements using an on-line vapor-phase atomic absorption spectrophotometer (VPAAS), developed by Radian. The AAS was modified to accept a syngas sample stream as part of the fuel supply going to the nebulizer mixing chamber and flame. In the flame, vapor-phase trace elements are atomized and absorb light energy from an element-specific light source just like aqueous samples in conventional AAS. The sample gas, fuel gas, and air supplies are regulated and monitored to determine the syngas component going to the flame, and ultimately the elemental concentration in the gas sample stream. Absorbance and concentration are related by Beer's law and gas concentration are determined by comparison with standard curves generated from aqueous standards. A simplified schematic of the VPAAS setup is shown in Figure 2.

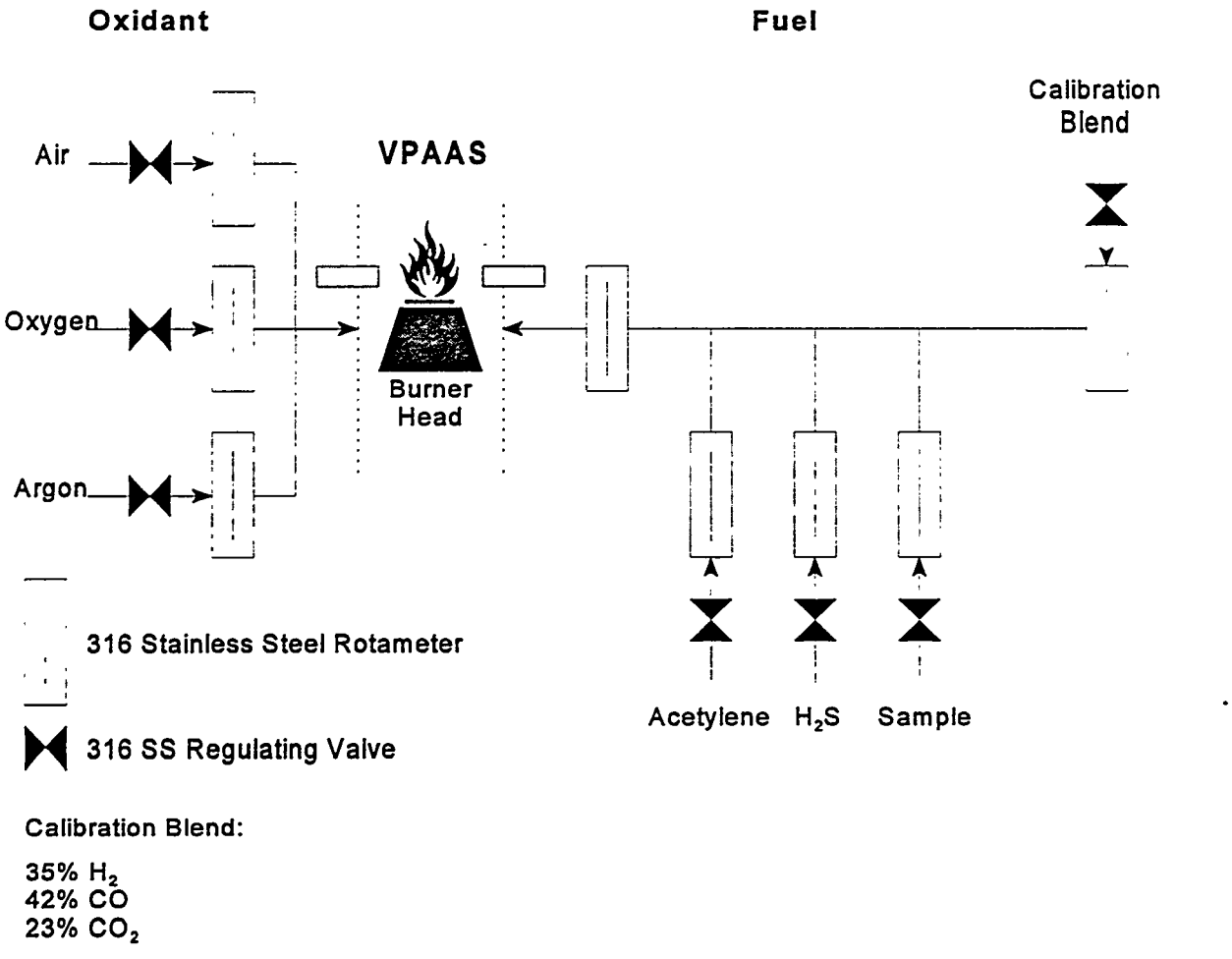

Figure 2. VPAAS Schematic

The second part (Phase II) of this program was done in parallel with Phase I. Design and manufacture of the hot gas probe was completed in December 1994. Performance and safety audits with LGTI engineers were done in the early spring of 1995 and the shakedown test was completed in May. The shakedown test was performed at a low temperature location (500°F) and was directed at operation (insertion and extraction) of the probe.

The probe was designed to operate at a maximum gas temperature of 1200°F, and a pressure of nominally 400 psig. Gas/particle separation takes place "in stack" at process conditions. The probe and filter assembly are inserted into the process gas stream via a double ball valve and packing gland arrangement. A constant nitrogen purge is maintained in the area of the packing gland so that any gas leakage during insertion or removal of the probe will be nitrogen and not syngas. Vapor phase samples can be collected from a slipstream of the sampled gas. Nitrogen can also be mixed with the sampled syngas as needed to either quench the gas temperature or to

dilute the overall gaseous sample and effectively lower the gas dew point. At the completion of testing, the probe is withdrawn from the process and collected solids are allowed to cool (in a nitrogen atmosphere) before being exposed to the air. Following the successful shakedown test, the probe was moved to the 8th level of the gasifier structure for testing of the hot syngas.

Hot syngas testing represents Phase III of the toxics program. This testing is scheduled to occur during the final week in May 1995. Gas phase samples will be collected for the analysis of trace elements, cyanide, ammonia, chloride and fluoride. In addition, collected particulate will be analyzed for trace elements.

Results

Preliminary results from the toxics emission testing program indicate the emissions are extremely low for most metals. Volatile metals which were present in the syngas as vapor phase compounds such as hydrides or carbonyls are found in the turbine exhaust in about the same range as that of a conventional coal-fired power plant. The results are presented graphically in Figure 3. Only cadmium and mercury had elemental reductions that were less than 90 percent.

References

1. *Field Chemical Emissions Monitoring (FCEM) Generic Sampling and Analytical Plan.* Electric Power Research Institute, Palo Alto, CA. March 1995. TR-104869.

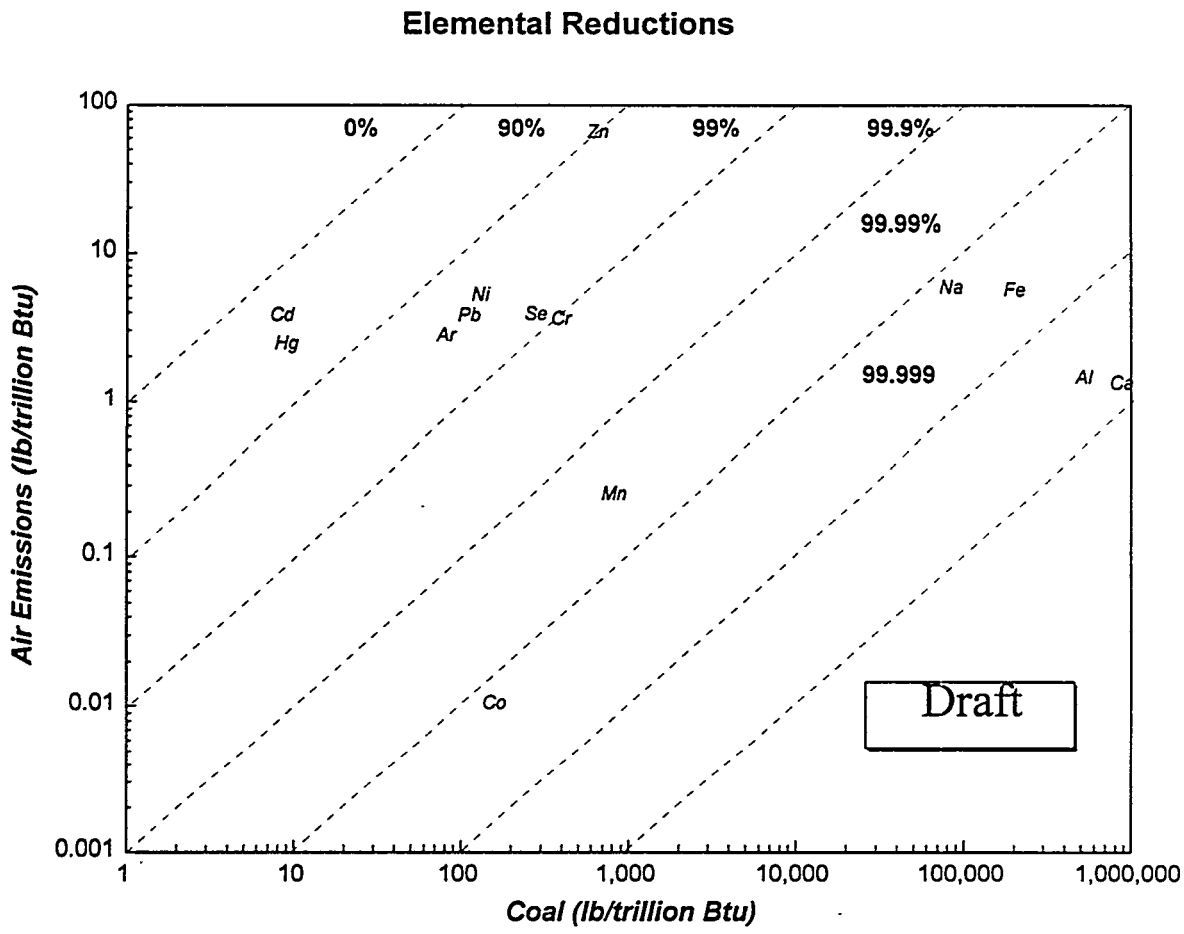

Figure 3. Elemental Emissions and Reductions

AUDITING OF SAMPLING METHODS FOR AIR TOXICS AT COAL-FIRED POWER PLANTS

R.O. AGBEDE, J.L. CLEMENTS, M.G. GRUNEBACH and R.P. KHOSAH
ADVANCED TECHNOLOGY SYSTEMS, INC.
3000 TECH CENTER DRIVE
MONROEVILLE, PA 15146

C. BRUFFEY, D.A. HERSHEY
INTERNATIONAL TECHNOLOGY CORPORATION
11499 CHESTER ROAD
CINCINNATI, OHIO 45246

Summary

Advanced Technology Systems, Inc. (ATS) with subcontract assistance from International Technology Corporation (IT) has provided external audit activities for Phase II of the Department of Energy-Pittsburgh Energy Technology Center's air emission test program. The objective of the audits is to help ensure that the data obtained from the emission tests are precise, accurate, representative, scientifically sound and legally defensible.

This paper presents the criteria that were used to perform the external audits of the emission test program. It also describes the approach used by ATS and IT in performing their audits.

Examples of findings of the audits along with the actions take to correct problems and the subsequent effect of those actions on the test data are presented. The results of audit spikes performed at the Plant 1 test site are also discussed.

Background

The U.S. Department of Energy is currently funding research to characterize hazardous air pollutants (HAPs) from coal-fired power plants. These studies, along with other current research being conducted by the U.S. Environmental Protection Agency (EPA), the Electric Power Research Institute (EPRI) and others, are required as part of the Clean Air Act Amendments (CAAA) of 1990.

In 1991, the Department of Energy's-Pittsburgh Energy Technology Center (DOE-PETC) commissioned five primary contractors to conduct emission studies at eight different coal-fired electric utilities. Prior to the initiation of this study, very little documented data on coal-fired utility HAPs emissions were available. In addition, the methods of sampling and analyzing the emissions required modifications and refinements in order to characterize HAPs emissions from coal-fired power plants. As a result, a critical concern to the sampling program was that

the collection and analysis of HAPs were accurate, precise, representative, scientifically sound and legally defensible.

To ensure that these data quality objectives were met, the DOE contracted independent Quality Assurance/Quality Control auditors to provide oversight for the air emission tests and other applicable test criteria for the emission testing program.

During Phase I of the testing program, Research Triangle Institute (RTI) was contracted as the independent auditor. Advanced Technology Systems, Inc. (ATS) with subcontract assistance from IT Corporation (IT) has been contracted to provide audit oversight for Phase II of the program.

Evaluation of the sampling and analytical methodologies requires both internal and external Quality Assurance/Quality Control. Suggested Quality Assurance/Quality Control criteria can include the following items: 1) Evaluation of the efficiency of the sampling procedures; 2) Performance evaluations of sampling and analytical equipment; 3) Determination of the robustness of the calibration procedures and practices and 4) The use of outside intervention (auditors) to pick out the non-obvious errors and problems.

The efficiency of the sampling procedures depends on two factors: 1) the ability of the sampling and subsequent analytical methods to collect and analyze the desired analyte and 2) the ability of the sampling and analytical crew to perform their assigned tasks. The sampling and analytical methodology can be evaluated by examining the precision and accuracy of the sample test results and by examining the precision and accuracy of the audit spikes. Data precision can be evaluated through the use of duplicate samples, duplicate spike samples and standard deviations or relative standard deviations for multiple sets of samples. Data accuracy can be evaluated using the recovery of matrix spikes, surrogate spikes, duplicate matrix spikes and internal audit spikes using certified standards. The closure of material balances is another tool often employed.

An evaluation of the performance of the sampling and analytical personnel is, of course, more subjective. The sampling and analytical personnel should be carefully observed, by both internal and external auditors, during the performance of their sampling or analytical activities. The auditor should evaluate the sampling teams on their organization and apparent knowledge of the sampling procedures and experience. Sampling train preparation, operation and recovery should be observed to determine if the correct protocol for the sampling method is followed. In addition the auditor should note if the sampling equipment was handled carefully and properly. Changes from the normal procedures for the sampling method being observed should be recorded so that its effect on the resulting data, if any, can be verified. In addition any deviations in the sampling procedures from the final sampling plan should be discussed with the sampling coordinator.

Furthermore, the auditor should check to see if the sampling data sheets are properly completed and if the appropriate chain-of-custody procedures are followed.

The performance of the sampling and analytical equipment also can be evaluated using the precision and accuracy of the sampling data and audit spikes. As with the sampling procedure evaluation, duplicate samples and matrix spikes, duplicate matrix spikes and audit samples can be used to evaluate sampling and analytical equipment performance.

Calibration check audits using critical orifices of known diameter and electronic signal generators can be performed on the sampling control boxes to evaluate their performance. EPA approved calibration quality objectives should be used in evaluating the control box performance. Failure to meet these objectives should be discussed with the sampling coordinator.

The analysis of certified standards can also be used to evaluate the performance of analytical equipment. As with the sampling control boxes, EPA approved data quality objectives for precision and accuracy should be used to evaluate the performance of analytical instruments. Failure to meet these objectives should be discussed with the analytical supervisor and may require the recalibration and/or repair of the instrument.

The quality of laboratory instrument calibrations can be checked by reviewing laboratory records. Calibration curves which do not meet laboratory or DOE data quality objective criteria should be rejected and new calibration curves should be generated.

Introduction

ATS, with subcontract assistance from IT Corporation, was contracted to provide external audit activity for Phase II of the DOE-funded test program. ATS audited the sampling activities of Southern Research Institute who were conducting a multi-pollutant field study to characterize toxic emissions from a coal-fired power plant burning pre-combustion cleaned bituminous coal (Plant 1). SRI performed sampling for multi-metals, acid gases, particulates and mercury . Sampling for mercury was performed using both EPA Method 29 and the Ontario Hydro Method. SRI's sampling program was coordinated with stack and helicopter plume sampling for mercury using the Bloom Method.

IT assisted with the auditing of two other sampling programs. One program was a multi-pollutant field study conducted by Battelle to collect and characterize toxic emissions from coal-fired utility boilers operating at different combustion intensities. The sampling site was the Sammis power plant near East Liverpool, Ohio. Battelle sampled for particulates, multi-metals, acid gases and mercury. The sampling program emphasized the relationship between the particle size range and pollutant concentration and the effect of dilution and cooling on pollutant composition.

The other sampling program audited by IT was the validation of EPA Method 29, by the Energy and Environmental Research Center (EERC) located at the University of North Dakota, for the assay of mercury from a pilot-scale combustor.

IT's efforts included review of the experimental plans, on-site observation of the testing activities, the preparation of performance audit samples and laboratory performance review. ATS also performed the above activities and oversaw IT's audit.

Audit Program Approach

The audit program employed consists of the following key elements:

- Pre-audit site visit and/or conference calls
- Review of sampling, analytical and QA/QC plans and problem resolution/recommendations
- Field and laboratory audits
- Final test report review

Within each key element, the evaluation criteria include:

1. Pre-audit site visit and/or conference calls
   - Gain knowledge of the plant layout and the condition of the sampling sites.
   - Observe plant operating conditions.
   - Obtain input on QA/QC matters.
   - Learn safety and security concerns and operating constrains at the site.
   - Determine the needed logistics such as the route to the site, nearest airport, lodging, rental car availability, FedEx and UPS locations, etc.

2. Review of sampling, analytical and QA/QC plans (project specific)
   - Determine the intended data use and the applicability of the selected test methods to that use.
   - Evaluate the experimental design for flaws or deficiencies.
   - Learn Quality Assurance/Quality Control objectives, the internal QA/QC activities planned and the corrective measures that will be implemented if needed.

3. Field and Laboratory Audits
   - Follow EPA audit guidelines.
   - Technical system audits - Review, observe and document the sampling and analytical practices, scrutinize the data reduction and review and the reporting activities. Also, examine the contractor facilities and equipment.
   - Performance evaluation audit - Spikes and performance evaluation audit samples are used to evaluate compliance.

4. Final test report review
   - Examine data validity.
   - Determine the credibility of the conclusions.
   - Evaluate data comparability

ATS visited the Plant 1 site one month prior to the start of sampling activities to establish the logistics previously discussed. No pre-audit site visits were made for the EERC and Sammis sites but the necessary logistical information was obtained from conference calls.

Experienced ATS and IT personnel reviewed each sampling plan. For each plan review, a document was prepared describing all questions, concerns and perceived plan deficiencies. These issues were discussed with the contractors until all parties were satisfied with the quality of the plan.

ATS and IT used a field check list to review each sampling procedure. The list was used to document the type of equipment used, the materials of construction, equipment and personnel performance and specific handling problems. The sample recovery and handling procedures were observed to ensure that the test samples were handled in a clean environment, with complete documentation of sample identity and chain-of-custody.

Equipment audits were performed using a critical orifice to verify the calibration of the dry gas meter and an Omega Instruments millivolt signal generator to check the accuracy of the digital temperature readouts. EPA data quality objectives were used to determine the ability of the sampling control boxes to meet calibration specifics. The thermocouples were audited using ASTM grade thermometers. The field barometers were evaluated by comparison to an independently calibrated field barometer supplied by the auditor. Spot checks of selected nozzle diameters were made using calipers supplied by the auditors.

Laboratory performance audits were also performed. The auditors observed sample receiving, handling and analytical procedures and reviewed laboratory practices for chain-of-custody, data review and documentation, sample numbering, and report procedures. Instrument calibration procedures and maintenance practices were also examined.

Spiked samples, including field spikes and laboratory audit samples were also a part of the audit program. Spiked samples or audit samples were left at the sampling site or sent to the analytical laboratory on return from the sampling activity. All spike samples were NIST materials or NIST-certified materials.

Results and Discussion

Field audit reports were prepared to document all findings. Battelle, EERC and SRI sampling programs were performed in accordance with the approved test plans. All studies are expected to yield acceptable data.

However, minor problems occurred with all of the sampling programs Many of these problems were corrected on site. The other problems should have only negligible affect on the data quality. Examples of these problems are presented below.

- At the Plant 1 tests, the initial samples for the recycle slurry process stream were taken at the wrong scrubber module. The problem was rectified after the first afternoon sample and all subsequent samples were taken from the correct module stream. The effect of the error on the data should be negligible because the metals concentrations in the scrubber recycle slurry should be sufficiently constant such that the two correct samples can represent the entire sampling effort.

- Sampling of the course refuse stream at the Plant 1 coal preparation plant originally included only the refuse screen oversize and not both the screen oversize and undersize. Upon recommendation, the sampling point was moved to a location where the entire refuse stream could be sampled. This change in the sampling location made the subsequent samples more representative of the course refuse stream. Only the samples obtained after the change in sampling location were used as refuse stream samples. The effect of this problem on the data should be minimal because the concentration of metals in the coal refuse stream should be consistent throughout the sampling period. As such the samples obtained after the sampling location change should represent the entire sampling period.

- The original process stream samples for magnetite, frother and anionic polymer at the Plant 1 Coal Preparation Plant were obtained in dirty mason jars with metallic lids. These samples were rejected by ATS because of possible contamination from the jars or lids. A second set of samples was obtained one day later using clean sterile sample jars. The second set of samples was accepted. This action improved the quality of the samples for these process streams by removing obvious sources of contamination that compromised the integrity of the first set of samples.

- The February 28, 1995 HEST test at the Sammis plant failed to pass the final leak test. As a result the test was voided by Battelle and their subcontractor, TRC Environmental Corporation, resulting in no effect on the data.

Blank spikes were performed at the Plant 1 site by ATS and IT sent laboratory check standards to EERC and Battelle to verify the accuracy of laboratory calibration materials. The results (triplicate averages) of the Plant 1 spikes are shown in Table 1.

Mercury spike results for the Ontario Hydro Method (modified Method 101A) were very good. The spike recoveries ranged from 87.74% to 102.69% with an average recovery of 94.79 $\pm$ 7.51%.

The filter and recovery solutions for the front-half acid wash and peroxide impingers of an EPA Method 29 train were spiked with a metals mixture. The permanganate impinger

recovery solution of the same train was spiked for mercury. The analytical results for these spiked samples were examined for arsenic, cadmium, lead, selenium and mercury ($KMnO_4$ impingers) and the percent recoveries of these analytes were calculated. Average spike recoveries for arsenic, cadmium, lead and selenium in all EPA Method 29 train samples were within $\pm$ 25% of the spiked values.

Lead had an average recovery of 88.50 $\pm$ 15.40% and cadmium had an average recovery of 76.77 $\pm$ 13.58%. Average recoveries for arsenic and selenium were 79.88 $\pm$ 13.75% and 76.94 $\pm$ 13.38% respectively. The average percent recovery of these four analytes from the filter was 80.69 $\pm$ 12.40%. Average recoveries from the front-half acid wash and H_2O_2 impingers were 69.33 $\pm$ 4.53% and 91.55 $\pm$ 10.67% respectively. The average recovery of mercury from the $KMnO_4$ impingers was 98.74 $\pm$ 1.80%.

No recovery data was obtained for the anion spikes because the blank values were larger than those obtained for the spiked samples. The results of the EERC and Sammis audit samples were not available when this paper was written.

Conclusions

The programs observed were well planned and executed research projects conducted by experienced field sampling and laboratory personnel. In spite of this, numerous questions and concerns with the test plans arose and were discussed in advance of the program. In addition, internal and external audits resulted in corrective actions to improve and/or enhance data quality.

The results from the spiked sample analyses (Plant 1) are testimony to the high quality of both the sampling and analytical expertise employed in these emission studies.

The value of the ongoing audit program is its ability to identify problems in the sampling program while corrective action can still be made. The continuation of this audit and report review program will ensure that the results of the air toxic studies under the direction of the DOE are legally and technically defensible and usable in a standards-setting process.

Acknowledgements

ATS and IT Corporation wish to acknowledge DOE Grant No. DE-AC22-93PC92583 which provided funding for this project.

doepaper

Table 1 Results for the Audit Spikes at the Plant 1 Test Site.

Test Method	Absorbent	Spike Conc.	Observed Conc.*	Percent Recovery
Ontario Hydro	Front-half Wash	501.5 ug Hg	471.3 ug Hg	93.98
	Back-half Wash	1003 ug Hg	1030 ug Hg	102.69
	KCl Imp.	1003 ug Hg	880 ug Hg	87.74
	$KMnO_4$ Imp.	1003 ug Hg	1010 ug Hg	100.70
EPA Method 29	Filter	40 ug As	30.6 ug As	76.50
		20 ug Cd	13.0 ug Cd	65.00
		10 ug Pb	9.1 ug Pb	91.0
		40 ug Se	36.1 ug Se	90.25
	Front-half Wash	80 ug As	54.5 ug As	68.13
		40 ug Cd	29.5 ug Cd	73.68
		20 ug Pb	14.4 ug Pb	72.00
		80 ug Se	50.8 ug Se	63.50
	H_2O_2 Imp.	160 ug As	152 ug As	95.00
		80 ug Cd	73.3 ug Cd	91.63
		40 ug Pb	41.0 ug Pb	102.50
		160 ug Se	123.3 ug Se	77.06
	$KMnO_4$ Imp.	501 ug Hg	494.6 ug Hg	98.74

* Average of triplicate analyses

doepaper

EVALUATION OF ACTIVATED CARBON FOR CONTROL OF MERCURY FROM COAL-FIRED BOILERS

STANLEY MILLER, DENNIS LAUDAL, AND GRANT DUNHAM
ENERGY & ENVIRONMENTAL RESEARCH CENTER
UNIVERSITY OF NORTH DAKOTA
PO BOX 9018
GRAND FORKS, ND 58202-9018

INTRODUCTION

The ability to remove mercury from power plant flue gas may become important because of the Clean Air Act Amendments' requirement that the U.S. Environmental Protection Agency (EPA) assess the health risks associated with these emissions. One approach for mercury removal, which may be relatively simple to retrofit, is the injection of sorbents, such as activated carbon, upstream of existing particulate control devices. Activated carbon has been reported to capture mercury when injected into flue gas upstream of a spray dryer baghouse system applied to waste incinerators or coal-fired boilers.[1,2] However, the mercury capture ability of activated carbon injected upstream of an electrostatic precipitator (ESP) or baghouse operated at temperatures between 200° and 400°F is not well known.

A study sponsored by the U.S. Department of Energy and the Electric Power Research Institute is being conducted at the University of North Dakota Energy & Environmental Research Center (EERC) to evaluate whether mercury control with sorbents can be a cost-effective approach for large power plants. Initial results from the study were reported last year.[3] This paper presents some of the recent project results. Variables of interest include coal type, sorbent type, sorbent addition rate, collection media, and temperature.

EXPERIMENTAL APPROACH

Baseline and sorbent injection tests were conducted at the EERC with a pulverized coal (pc)-fired combustor known as the particulate test combustor (PTC) and a pulse-jet baghouse. A complete description of the PTC and baghouse was given in a previous report.[4]

The tests were conducted with three coals: Powder River Basin subbituminous coals from the Absaloka mine, a similar coal from the Belle Ayr mine (Comanche), and a bituminous coal from the Pittsburgh No. 8 seam, Blacksville mine. Since the level of mercury in the coals ranged from 59 to 85 ppb, and the coal feed rate to the combustor is about 60 lb/hr, the required sorbent add rate is only about 2–20 g/hr to achieve sorbent-to-mercury ratios of 1000–10,000. Steady sorbent injection at the required low feed rate was accomplished by using a Model 3410 Dry Powder Disperser (DPD), manufactured by TSI Inc. This instrument is designed to disperse dry bulk powders into their original particle-size distribution in a carrier gas, with precise control over the feed rate. For all sorbent tests, the additive was injected with the DPD into the flue gas duct just upstream of a pulse-jet baghouse operated at an air-to-cloth ratio of 4 ft/min. The two primary carbon-based sorbents used in this study included a lignite-based activated carbon (LAC), commercially available from American Norit Co, Inc., and an activated carbon impregnated with an iodine compound (IAC) obtained from Barnebey & Sutcliffe Corp.

Simultaneous inlet and outlet mercury sampling was conducted according to EPA (Draft) Method 29, also known as a multimetal sampling train method. Method 29 does not claim to speciate between oxidized and elemental mercury, but bench- and pilot-scale results indicate that oxidized mercury will be trapped in the peroxide impingers and elemental mercury in the permanganate impingers.[3,5,6,7] However, further research is being conducted at the EERC to

evaluate the mercury speciation ability of Method 29.[8] In this paper, the fraction of mercury collected in the peroxide impingers is referred to as "oxidized" mercury, and the fraction collected in the permanganate impingers is called "elemental" mercury. Mercury analyses were completed with a Leeman PS200 cold-vapor atomic absorption analyzer.

RESULTS AND DISCUSSION

The inlet sampling location was upstream from the sorbent injection port, which allowed combining the inlet data for each coal. Average inlet mercury data for the Comanche coal are shown in Figure 1. Inlet data for the other coals were previously reported.[3] The total mercury measured by Method 29 includes mercury retained on the filter, mercury collected in the peroxide impingers, and the mercury collected in the permanganate impingers. Total inlet mercury concentrations were fairly constant from test to test as indicated by the error bars which represent plus or minus one standard deviation. A significant amount of mercury was retained on the filter, ranging from about 10% at 400°F to 60% at 200°F. The filter temperature of the Method 29 train was adjusted to the same temperature as the baghouse for each test.

Baseline tests without sorbent addition and tests in which activated carbon was injected just upstream of the baghouse were conducted with the pilot combustion system. Baghouse temperature ranged from 200°–400°F. Sorbent type included mainly LAC and IAC, but two tests were conducted with a mixture of LAC and IAC, and one test was run with a bituminous-based activated carbon (PC-100). Fabric type included Ryton and GORE-TEX® Membrane on GORE-TEX Felt. Most tests were completed over a continuous 2-day period and included 4 pairs of simultaneous inlet–outlet Method 29 measurements. The mercury removal results for the Comanche coal tests are shown in Figure 2. Values reported are based on the total inlet and total outlet mercury concentrations. Total mercury for both inlet and outlet included filter, oxidized, and elemental mercury. However, the baghouse particulate collection efficiency was typically about 99.99%, so very little fly ash was collected on the outlet sampling filter. In all cases, any mercury collected on the outlet filter was below detection limits, so the total measured outlet mercury consisted only of vapor-phase oxidized and elemental mercury. From Figure 2, a general trend is seen toward better mercury control at 200°F compared to 300°F. However, at 300°F a wide range in mercury removal was observed depending on the sorbent type and concentration. Perhaps the most surprising result for the Comanche coal tests was the ineffectiveness of the IAC, which showed no improvement in mercury removal over the baseline tests. Previous tests with Absaloka coal showed that IAC was highly effective at total mercury removal, removing essentially all of the elemental mercury. The mercury speciation data for the Comanche coal tests also indicate very little elemental mercury at the outlet. However for these tests, an equivalent increase in oxidized mercury was evident at the outlet with no improvement in total mercury removal. Examination of all of the pulse-jet baghouse tests with IAC shows that it removes much more elemental than oxidized mercury, but some of the elemental mercury is apparently converted to oxidized mercury by the IAC. This effect was especially significant for the Comanche coal tests at 300° and 400°F, but was also noticeable with Blacksville and Absaloka coals at temperatures of 350°F and greater. The Comanche coal test with IAC using the GORE-TEX fabric at 300°F also shows this conversion effect, which indicates it is a direct result of the IAC and not the result of an interaction among the fabric, sorbent, and mercury. The exact mechanism by which this occurs is not clear but could involve initial collection of the elemental mercury, the forming of mercury(II) iodide in the iodine-impregnated activated carbon, and then subsequent desorbing of mercury(II) iodide. Any mercury(II) iodide would most likely be collected in the hydrogen peroxide impingers and, therefore, be measured as oxidized mercury. The reason this effect appears to be much more significant for the Comanche coal than for the Absaloka coal is unknown, but could be related to the lower sulfur content of the Comanche coal or differences in ash composition. A comparison of the effectiveness of IAC for the three coals is shown in Figures 3 and 4. While the total mercury removal data (Figure 3) should be considered the most reliable, there is additional confidence in the conclusions if the vapor-phase data (Figure 4) show the same results. Since varying amounts of

mercury were captured on the inlet sampling filters, mainly because of temperature differences, the mercury vapor concentration at the baghouse inlet was more variable than the total inlet mercury concentration. Nevertheless, both the total and vapor-phase mercury data show that IAC was much more effective at mercury removal for the Absaloka coal than for the other two coals. The ineffectiveness of IAC with Blacksville coal is not surprising, since it had very little elemental mercury.

The effectiveness of the LAC also appears to be somewhat coal dependent as shown in Figures 5 and 6. Data on the total mercury removal indicate that the LAC works well for all three coals at temperatures lower than 250°F; however these data may be somewhat misleading, since they don't account for the amount of mercury that might be removed naturally at lower temperatures. The highest baseline mercury removal was observed with Absaloka coal, which explains why the total mercury removal with LAC was highest for Absaloka coal, while the highest vapor-phase mercury removal was observed with the Comanche coal. From the vapor-phase data, the conclusion is that the LAC is most effective with the Comanche coal. However, caution should be used when interpreting these data because of the low inlet vapor-phase mercury concentrations if a significant amount of mercury is retained on the sampling filter, and subsequent greater uncertainty in calculating the vapor-phase removal.

Another surprising effect observed in bench-scale tests with simulated flue gas was an interaction between the mercury and Ryton fabric. Results showed that mercury(II) chloride is absorbed by Ryton fabric and may be converted to elemental mercury and then to offgas at a later time. Initially, this effect was thought to be caused by exposed stainless steel surfaces; however, after coating surfaces with Teflon, the effect remained unchanged. When similar bench-scale tests were conducted with an all-PTFE (polytetrafluoroethylene) fabric, no evidence of this absorption and conversion was observed. Because of this observation, additional pilot-scale tests were conducted with an all-PTFE fabric (GORE-TEX Membrane on GORE-TEX Felt). The comparative results with the GORE-TEX fabric are shown in Figure 7. With the LAC, the mercury removal using the GORE-TEX fabric was somewhat higher than with Ryton fabric, but this is most likely the result of a higher sorbent add rate. For the baseline tests, the mercury removal was better with the GORE-TEX fabric at 300°F and slightly poorer at 200°F. Whether this difference lies within experimental variability is not clear. The more significant fabric effect with the IAC, however, suggests a possible interaction between the Ryton fabric and IAC. This result needs to be confirmed before a conclusion can be drawn. Whether the fabric effect is a short-term phenomenon that would disappear in tests longer than the completed 100-hour tests is not known.

From these results, temperature, coal-type, sorbent type, and possibly fabric type all appear to affect mercury removal significantly, at least under some conditions. EPA bench-scale test results showed much better elemental mercury removal for PC-100-activated carbon compared to the LAC used in our tests. Subsequently, tests were conducted with the PC-100 sorbent to see if it was superior to the LAC. Our results, shown in Figure 8, indicate no significant difference in total mercury removal and only a small difference in vapor-phase mercury removal between the LAC and the PC-100 bituminous-based activated carbon. The EPA results are partially in agreement with ours, since both showed somewhat better elemental mercury removal for the PC-100 (71% compared to 61% for the LAC). Our results, however, showed significantly poorer oxidized mercury removal for the PC-100 (53% compared to 82% for the FGD LAC). The bench-scale tests were conducted in a stream of pure nitrogen with elemental mercury, and the results may not be good indicators of sorbent performance with real flue gas that includes both oxidized and elemental mercury.

SUMMARY

- Inlet mercury speciation for the three coals was significantly different and was highly dependent on the Method 29 filter temperature.
- Iodine-impregnated activated carbon provided effective mercury control at 300° and 400°F with one subbituminous coal but was ineffective for a second subbituminous coal.
- Iodine-impregnated activated carbon was highly effective at reducing the outlet elemental mercury concentration for all three coals; however in some cases, the elemental mercury was apparently converted to oxidized mercury and was not captured.
- Lignite-based activated carbon provided some mercury control at lower temperatures for all three coals but appeared to work best for the Comanche coal.
- Mercury may interact with the Ryton fabric under some conditions to affect mercury speciation and control effectiveness.
- Bench-scale screening tests may not be good indicators of sorbent effectiveness unless flue gas conditions are adequately simulated.

REFERENCES

1. Felsvang, K.; et al. "Air Toxics Control by Spray Dryer Absorption Systems," Presented at the 2nd International Conference on Managing Hazardous Air Pollutants, Washington, 1993.
2. White, D.M.; et al. "Parametric Evaluation of Powdered Activated Carbon Injection for Control of Mercury Emissions from a Municipal Waste Combustor," Presented at the 85th Annual Meeting of the Air & Waste Management Association, Kansas City, 1992; Paper No. 92-40.06.
3. Laudal, D.L.; Miller, S.J. "Evaluation of Sorbents for Enhanced Mercury Control," *In* Proceedings of the 10th Annual Coal Preparation, Utilization, and Environmental Control Contractors Conference; Pittsburgh, PA, July 1994.
4. Miller, S.J.; Laudal, D.L. "Pulse-Jet Baghouse Performance Improvement with Flue Gas Conditioning," final project report for Project No. RP-3083-9 for Electric Power Research Institute, U.S. Department of Energy, and Canadian Electric Association; October 1992.
5. Biscan, D.A.; Gebhard, R.S.; Matviya, T.M. "Impact of Process Conditions on Mercury Removal from Natural Gas Using Activated Carbon," *In* Proceedings of the 8th International Conference on Liquefied Natural Gas; 1986, pp 1–12.
6. Tumati, P.R.; DeVito, M.S. "Partitioning Behavior During Coal Combustion," Presented at the Joint ASME/IEEE Power Generation Conference; Kansas City, 1993; Paper No. 93-JPGC-EC-8.
7. Chang, R. et al. "Pilot-Scale Evaluation of Activated Carbon for the Removal of Mercury at Coal-fired Utility Power Plants," Presented at the 2nd International Conference on Managing Hazardous Air Pollutants, Washington, 1993.
8. Laudal, D.L.; Heidt, M.; Nott, B. "Evaluation of Mercury Speciation By EPA (Draft)," To be presented at the Eleventh Annual Coal Preparation, Utilization and Environmental Control Contractors Conference, Pittsburgh, PA, July 1995.
9. Kirshnan, S.V.; Gullett, B.K.; Jozewicz, W. "Sorption of Elemental Mercury by Activated Carbons," *Environ. Sci. & Technol.* ***1994,*** *28* (8), 1506.

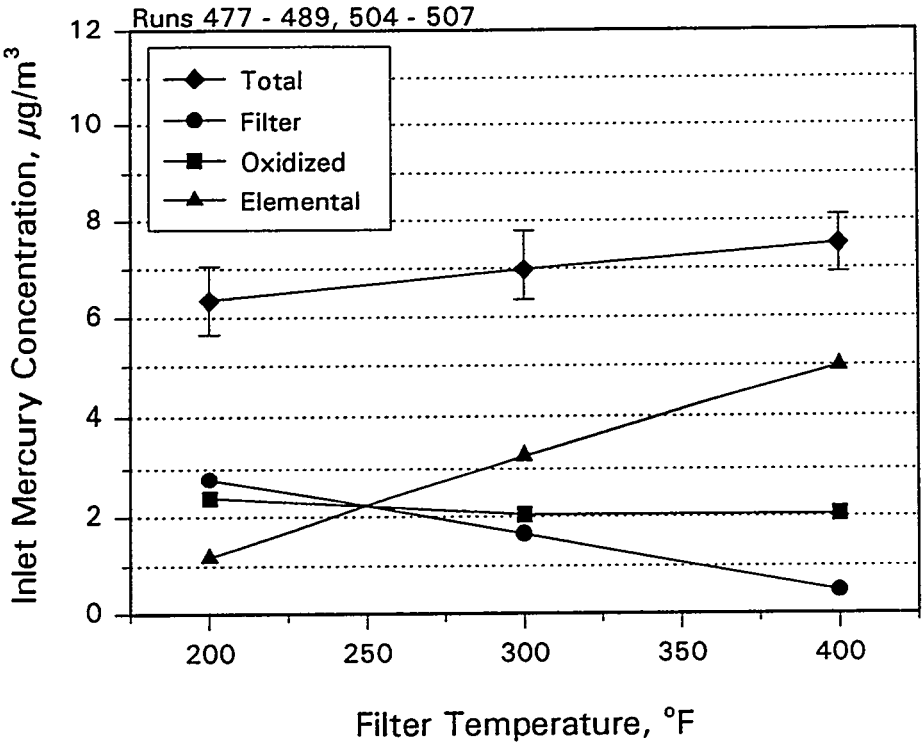

Figure 1. Average inlet mercury concentrations for Comanche subbituminous coal. Error bars represent plus or minus one standard deviation.

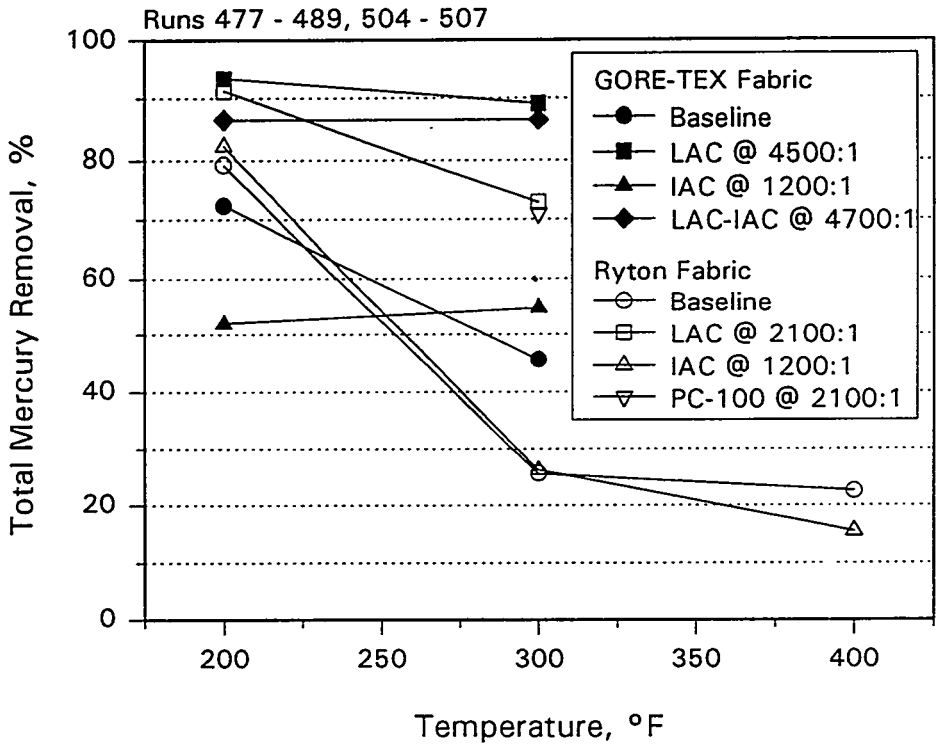

Figure 2. Total mercury removal across the baghouse for Comanche coal tests.

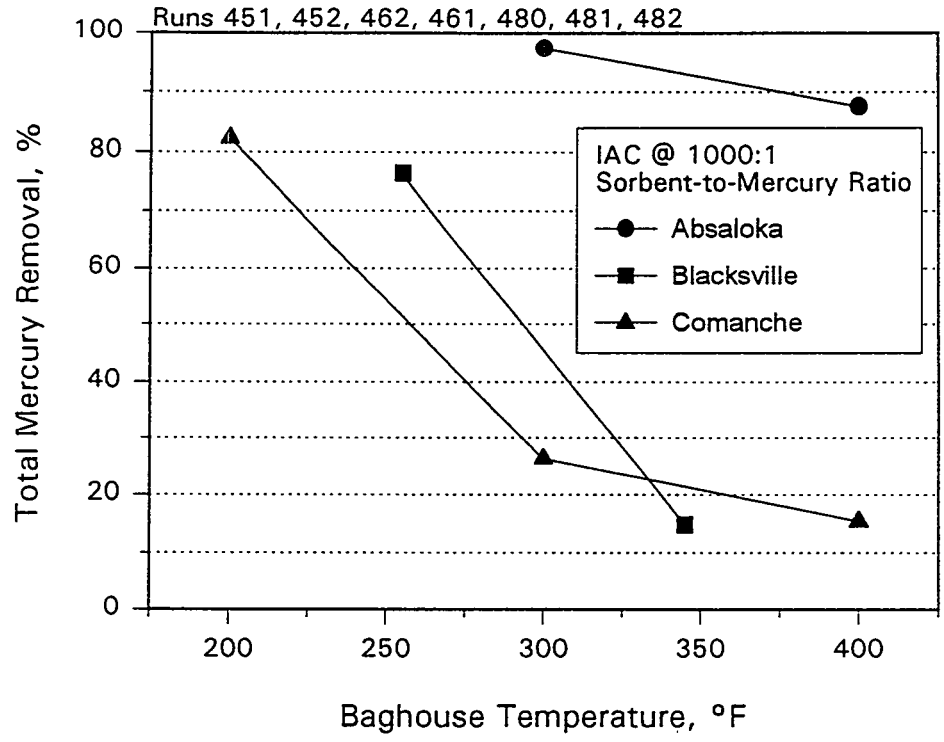

Figure 3. Effect of coal type on total mercury removal across the baghouse with iodine-impregnated activated carbon.

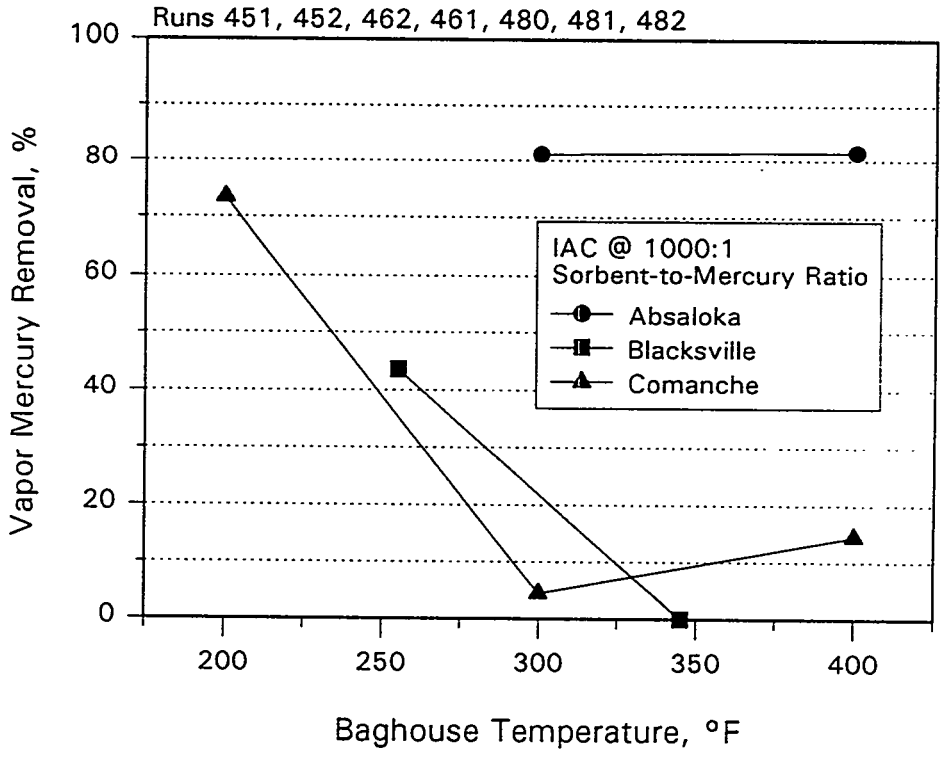

Figure 4. Effect of coal type on vapor-phase mercury removal across the baghouse with iodine-impregnated activated carbon.

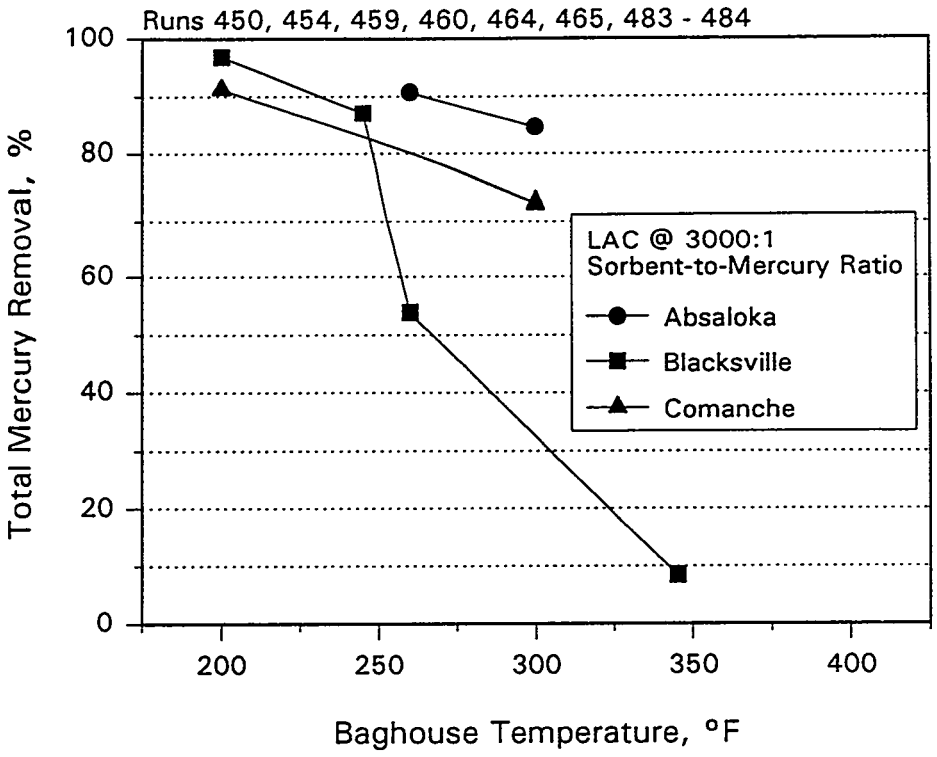

Figure 5. Effect of coal type on total mercury removal across the baghouse with lignite-based activated carbon.

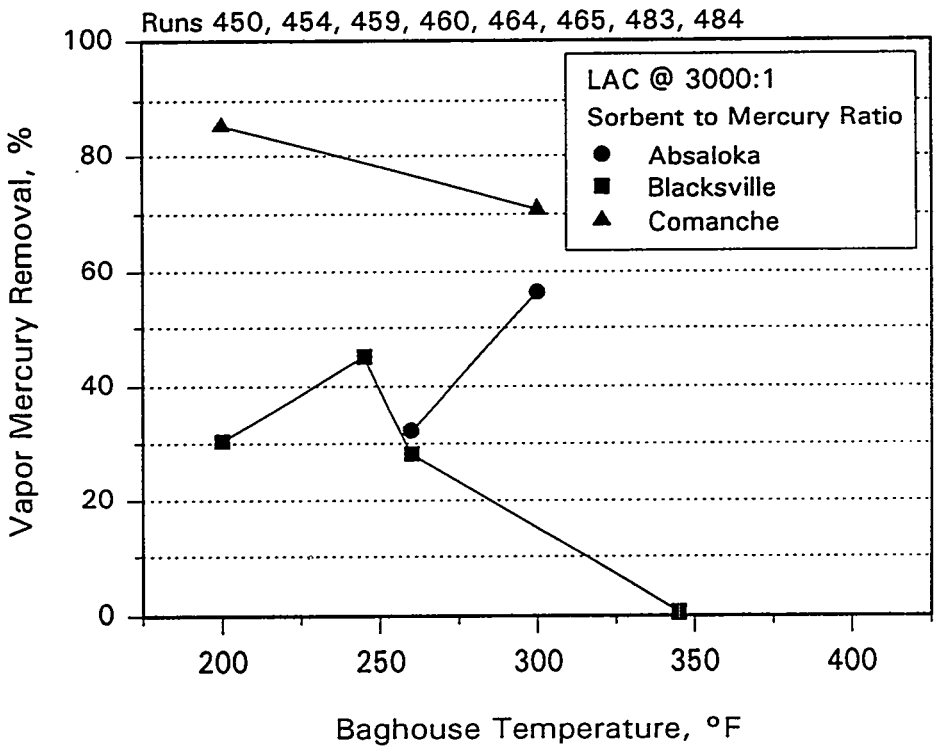

Figure 6. Effect of coal type on vapor-phase mercury removal across the baghouse with lignite-based activated carbon.

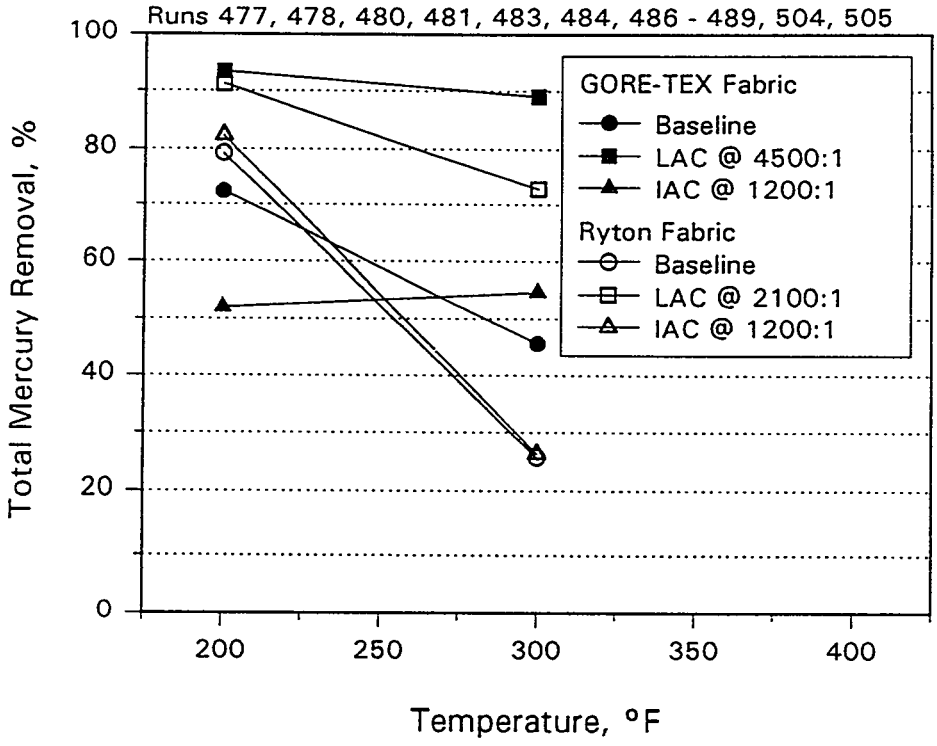

Figure 7. Effect of fabric type on total mercury removal for Comanche coal tests.

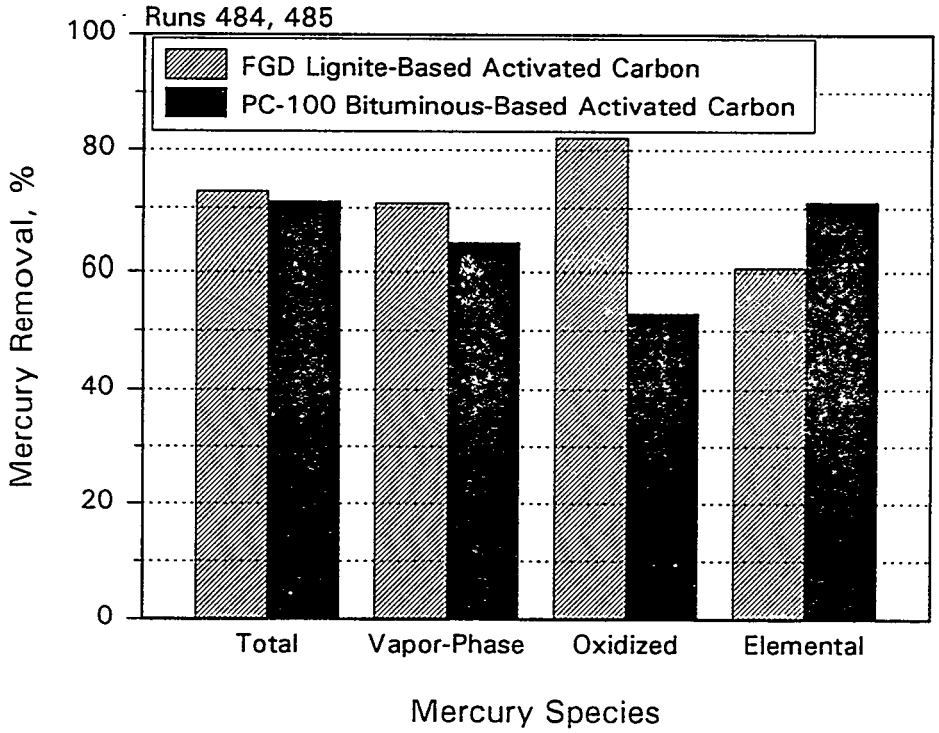

Figure 8. Effect of activated-carbon type on mercury species removal using Comanche coal.

REAL-TIME ANALYSIS OF

TOTAL, ELEMENTAL, AND TOTAL SPECIATED MERCURY

RICHARD J. SCHLAGER, SCIENTIST
KEVIN G. WILSON, SENIOR RESEARCH ENGINEER
ANDREW D. SAPPEY, SENIOR RESEARCH CHEMIST

ADA TECHNOLOGIES, INC.
304 INVERNESS WAY SOUTH, SUITE 110
ENGLEWOOD, CO 80112
(303) 792-5615

ABSTRACT

ADA Technologies, Inc., is developing a continuous emissions monitoring system that measures the concentrations of mercury in flue gas. Mercury is emitted as an air pollutant from a number of industrial processes. The largest contributors of these emissions are coal and oil combustion, municipal waste combustion, medical waste combustion, and the thermal treatment of hazardous materials. It is difficult, time consuming, and expensive to measure mercury emissions using current testing methods. Part of the difficulty lies in the fact that mercury is emitted from sources in several different forms, such as elemental mercury and mercuric chloride. The ADA analyzer measures these emissions in real time, thus providing a number of advantages over existing test methods: 1) it will provide a real-time measure of emission rates, 2) it will assure facility operators, regulators, and the public that emissions control systems are working at peak efficiency, and 3) it will provide information as to the nature of the emitted mercury (elemental mercury or speciated compounds). This update presents an overview of the CEM and describes features of key components of the monitoring system--the mercury detector, a mercury species converter, and the analyzer calibration system.

THE NEED FOR A MERCURY CEM

Future strategies for controlling hazardous air pollutants will involve the use of continuous emissions monitoring systems. These systems provide a real-time measure of pollutants being emitted from sources and are needed in terms of assuring compliance with emissions regulations. They can also be used to help facilities operate pollution control equipment at peak efficiencies.

Mercury is a pollutant that has been receiving much attention in terms of monitoring and control strategies. The toxicity of mercury has prompted industry and regulators

alike to develop means to control its release to the environment. Emissions monitoring systems will play a key role in assuring that emissions of this hazardous material are minimized.

Mercury is emitted from industrial sources in a variety of chemical forms depending on the specific process and flue gas conditions. For example, mercury is known to exist as elemental mercury [Hg^{o}] and as mercuric chloride [$HgCl_2$] in most industrial flue gases that contain mercury. A knowledge of the relative concentrations of mercury between its different forms will be required for air pollution control devices to operate effectively. An example of this principle is given in Table I for coal-fired power plants.

Table I. Mercury Removal Under Different Process Conditions

Plant	Ash Loading to Spray Dryer	Coal Cl	% Mercury Removed
A	High	Low	**14**
B	High	Low	**23**
C	High	Low	**6**
G	High	Low	**16**
E	Low	High	**55**
H	Low	High	**44**
F	Medium	High	**89**
D	High	High	**96**

Current standard testing techniques rely on manual "grab samples" where flue gas is drawn through filters and traps to collect mercury. The collected samples need to be analyzed in a chemistry laboratory using complex techniques and instrumentation. These field sampling and analytical techniques are cumbersome, labor intensive, and expensive. A 1-week comprehensive sampling program can cost in the range of $25,000-$50,000.

A continuous mercury monitoring system addresses the following needs:

- Since mercury control depends on the specific chemical form of the mercury, an analyzer that can distinguish between the chemical forms is needed to assure effective operation of the APCD.
- An analyzer will assure that the APCD is working properly.
- An analyzer can be used to control the feed rate of a process generating the mercury emission.
- An analyzer will help assure the public and regulatory agencies that emissions limitations are being complied with.

DESCRIPTION OF CEM

In response to the need for monitoring mercury emissions in real-time, ADA Technologies has developed a continuous emissions monitoring system that is capable of measuring total mercury, elemental mercury, and (by difference) total speciated mercury. The system features a sensitive mercury detector, a mercury species converter, and a calibration system. Figure 1 shows the components in a typical CEM arrangement.

The "converter" is used to change speciated mercury compounds to elemental mercury. When the sample gas is placed through the converter, a measure of the total mercury content of the flue gas is obtained. When the converter is bypassed, only elemental mercury is measured in the gas sample. The difference between the two measurements is the concentration of total speciated mercury content.

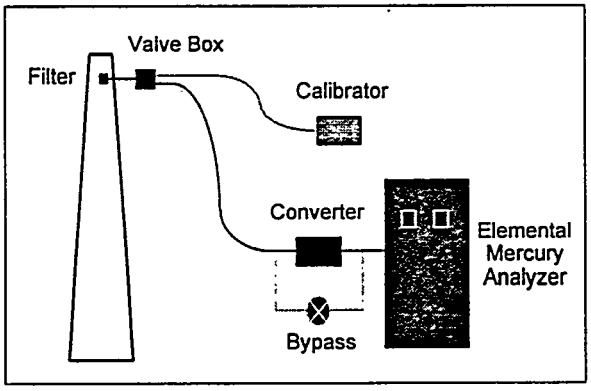

Figure 1. Mercury CEM arrangement.

A non-reactive sample transport line is used to convey the gas sample to the analyzer. Calibration gas is introduced to the end of the sample line in order to assure that the entire sampling system and the analyzer are calibrated as a single unit.

DESCRIPTION OF COMPONENTS

Mercury Detector

The analyzer uses a unique ultraviolet absorption spectrometer to measure the mercury. Proprietary optical components are incorporated that provide a measurement sensitivity below 1 $\mu g/m^3$ (less than approximately 0.1 ppb v/v). The analyzer has a linear response to a concentration of greater than 100$\mu g/m^3$. The optical design of the analyzer also eliminates the effects of interfering gases such as sulfur dioxide.

Figure 2 shows the analyzer response when elemental mercury was introduced at a concentration of 4.2 $\mu g/m^3$ (0.7 ppb v/v). Also shown in the figure is the signal when zero gas was introduced into the analyzer. Based on the peak-to-peak noise level observed, a minimum level of detection (defined as 2x noise level) of 0.2$\mu g/m^3$ (27 ppt v/v) is calculated.

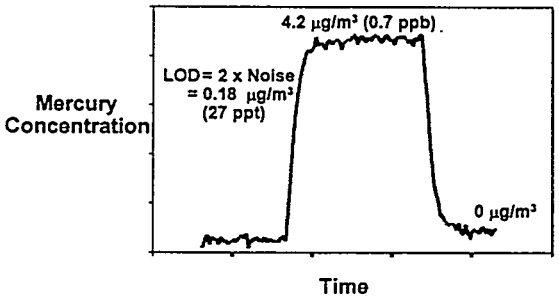

Figure 2. Response of the analyzer to 4.2 $\mu g/m^3$ of mercury.

The ADA analyzer incorporates a unique optical design that eliminates the effects of interfering gases such as sulfur dioxide. Figure 3 shows the response of the detection system when measuring mercury at a concentration of 10 $\mu g/m^3$ in the presence of sulfur dioxide at a concentration of 500 ppm.

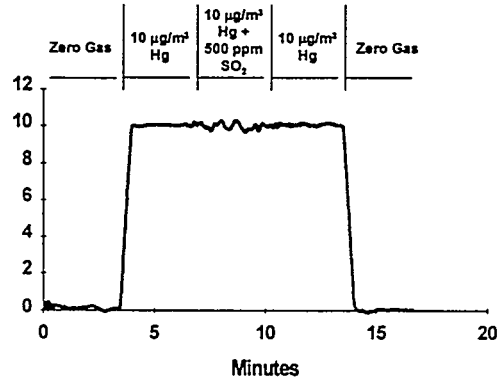

Figure 3. Mercury detector response when measuring mercury in the presence of sulfur dioxide.

Figure 4 shows the response of the analyzer over a concentration range of 0 to 6 ppb (v/v). This range is expected to cover most concentrations expected in coal-fired and municipal solid waste generated flue gases. A dilution probe is used on the analyzer

where high concentrations of mercury are expected, such as when monitoring uncontrolled emissions ahead of an APCD.

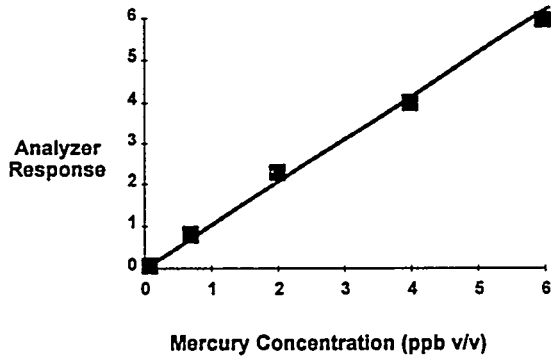

Figure 4. Linearity of the mercury detector.

Converter

A mercury species converter is another key component of the CEM system. The converter is used to distinguish between concentrations of elemental and"total" mercury found in the flue gas. Since the mercury detector measures elemental mercury alone, a converter is needed to change any speciated forms of mercury to elemental mercury for measurement. Total mercury is, therefore, measured by passing the flue gas sample through the converter. Elemental mercury concentrations are measured by the CEM when the flue gas sample bypasses the pre-conditioning converter. Total speciated mercury is then determined as the difference between the measured total mercury concentration and the elemental mercury concentration.

The converter uses unique design features that eliminate the need for wet chemicals or other expendable chemicals.

Figures 5 and 6 show the response of the analyzer when two surrogate speciated mercury compounds were input--mercuric chloride and dimethyl mercury. The test sequence followed the pattern of placing the mercury species through the converter, then the bypass valve was actuated to circumvent the converter. This sequence was followed for a number of cycles to establish the fact that the mercury compounds were being converted to elemental mercury.

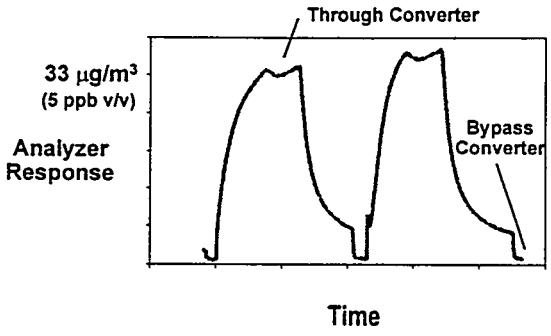

Figure 5. Mercuric chloride being converted to elemental mercury.

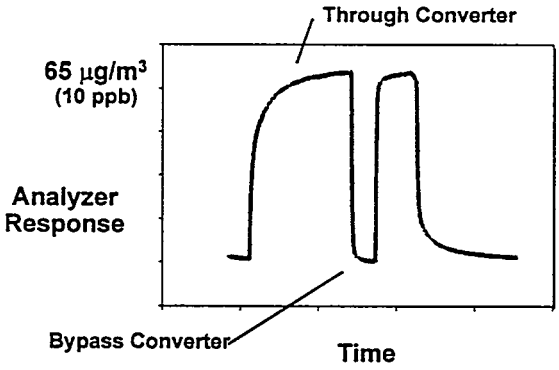

Figure 6. Dimethyl mercury being converted to elemental mercury.

Calibrator

ADA Technologies developed a calibrator for use with the mercury CEM. The calibrator is based on the use of permeation tubes to provide known and accurate concentrations of elemental mercury and mercuric chloride. These devices are considered primary standards for calibrating continuous monitors and they are used to calibrate ambient air analyzers. ADA developed a two-channel calibrator--one channel is used to calibrate the elemental mercury detector and the other is used to calibrate the converter.

EVALUATION OF MERCURY SPECIATION BY EPA (DRAFT) METHOD 29

DENNIS L. LAUDAL AND MARLYS K. HEIDT
ENERGY & ENVIRONMENTAL RESEARCH CENTER
15 NORTH 23RD STREET
GRAND FORKS, ND 58203

BABU NOTT
ELECTRIC POWER RESEARCH INSTITUTE
3412 HILLVIEW AVE
PALO ALTO, CA 94304

INTRODUCTION

The 1990 Clean Air Act Amendments require that the U.S. Environmental Protection Agency (EPA) assess the health risks associated with mercury emissions. Also, the law requires a separate assessment of health risks posed by the emission of 189 trace chemicals (including mercury) for electric utility steam-generating units. In order to conduct a meaningful assessment of health and environmental effects, we must have, among other things, a reliable and accurate method to measure mercury emissions. In addition, the rate of mercury deposition and the type of control strategies used may depend upon the type of mercury emitted (i.e., whether it is in the oxidized or elemental form).

It has been speculated that EPA (Draft) Method 29 can speciate mercury by selective absorption; however, this claim has yet to be proven. The Electric Power Research Institute (EPRI) and the U.S. Department of Energy (DOE) have contracted with the Energy & Environmental Research Center (EERC) at the University of North Dakota to evaluate EPA (Draft) Method 29 at the pilot-scale level. The objective of the work is to determine whether EPA (Draft) Method 29 can reliably quantify and speciate mercury in the flue gas from coal-fired boilers.

SCOPE OF WORK

Pilot- and bench-scale tests are being performed to statistically evaluate the ability of EPA (Draft) Method 29 to speciate mercury emissions. The bench-scale tests are designed to initially establish parameters that may affect mercury speciation, while the pilot-scale tests are designed to follow the verification criteria established in EPA Method 301. The pilot-scale tests are being completed using the particulate test combustor (PTC) which is a 550,000-Btu/hr pulverized coal (pc)-fired boiler designed to generate flue gas and fly ash representative of that produced in a full-scale utility boiler.

In accordance with EPA Method 301, quadtrain sampling with six quadtrain replicates was conducted. Since the EPA (Draft) Method 29 and the Method 301 criteria were designed for large ducts, some modifications were necessary to adapt the procedure to the EERC pilot-scale PTC. The most important modification is the probe location for the quadtrains. Since the pipe internal diameter is only 5.25 in. at the sampling locations, the system could not meet the 5% area criterion of Method 301. The alternate sample probe configuration used for this project (discussed with the EPA) has the nozzles 90° from each other and 1 in. apart, as shown in the photograph in Figure 1.

For EPA (Draft) Method 29, a total of seven impingers are included in the sampling train. Impinger 1 is empty and is intended to remove most of the moisture. Impingers 2 and 3 contain acidified hydrogen peroxide solution. It is in these impingers, it is speculated, that the oxidized mercury will collect. Impinger 4 is empty to prevent any mixing of the two types of trapping solutions. The mercury that passes the two peroxide impingers is thought to be elemental mercury and is subsequently captured in a solution of acidified permanganate in Impingers 5 and 6. Finally, Impinger 7 contains silica gel to ensure the flue gas is thoroughly dried before it leaves the impinger train. After the sampling is completed, the solutions are prepared and then analyzed for mercury using cold-vapor atomic absorption spectroscopy.

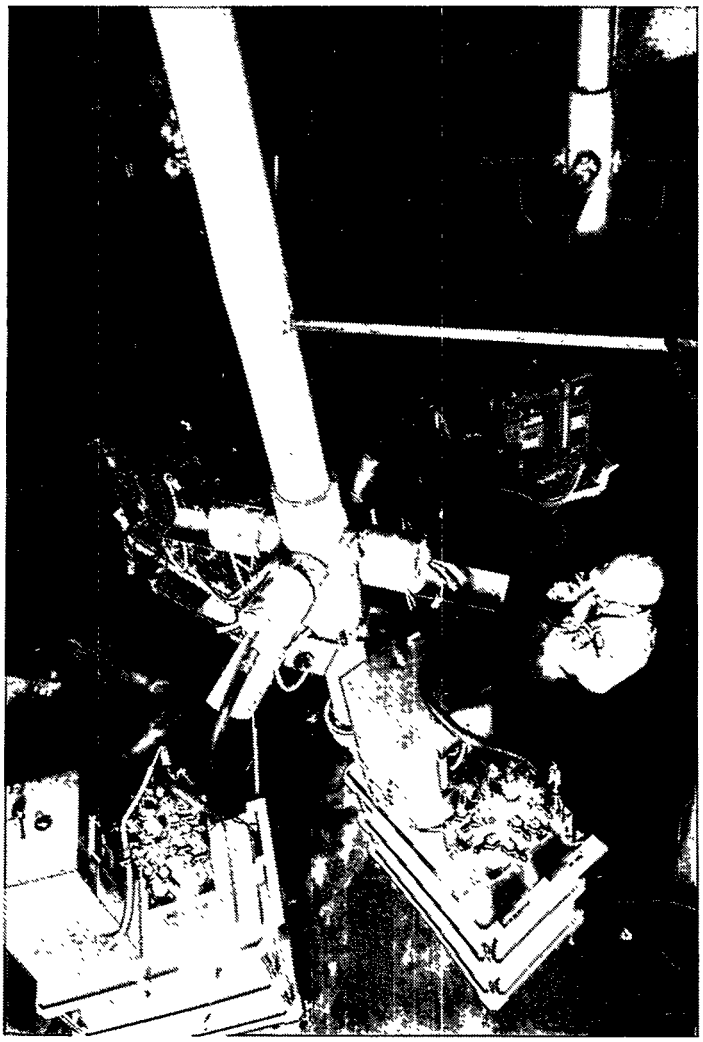

Figure 1. Photograph of EPA (Draft) Method 29 quadtrain setup.

A bench-scale test unit, shown in Figure 2, was designed and built to simulate flue gas conditions. Known quantities of elemental mercury vapor and mercury(II) chloride ($HgCl_2$) vapor were introduced into the system by flushing nitrogen around calibrated permeation tubes. The quantity of mercury vapor released into the gas stream was determined by its vapor pressure at a specific temperature. The temperature of the permeation tubes was maintained and controlled using a straight-tube condenser and water bath. The simulated flue gas consisted of 5% O_2, 10% water vapor, 15% CO_2, and 1000 ppm SO_2, with N_2 as the balance. For several of the tests, hydrogen chloride (HCl) was also added as a process variable.

Four pilot-scale tests have been completed to date. Details of the pilot-scale test combustor have been described in a previous report.[1] The conditions for each of these tests are shown in Table 1. Three of the four completed tests included six replicate quadtrains (four EPA [Draft] Method 29 sampling trains operated simultaneously at essentially the same point), resulting in a total of 24 EPA (Draft) Method 29 samples per test in accordance with EPA Method 301. The other test was designed to compare EPA (Draft) Method 29 results directly to those of Method 101A (total mercury measurement); this test was to help act as a quality control check.

Although direct spiking of the impinger solutions and filter is needed to determine the analytical uncertainty, it was also necessary to determine the uncertainty of the entire sampling train. Therefore, an important part of the overall test program was to spike the flue gas stream with mercury. A schematic of the mercury injection system is shown in Figure 3. The quantity of elemental mercury injected into the flue gas stream is controlled by changing the nitrogen flow rate through the condensers.

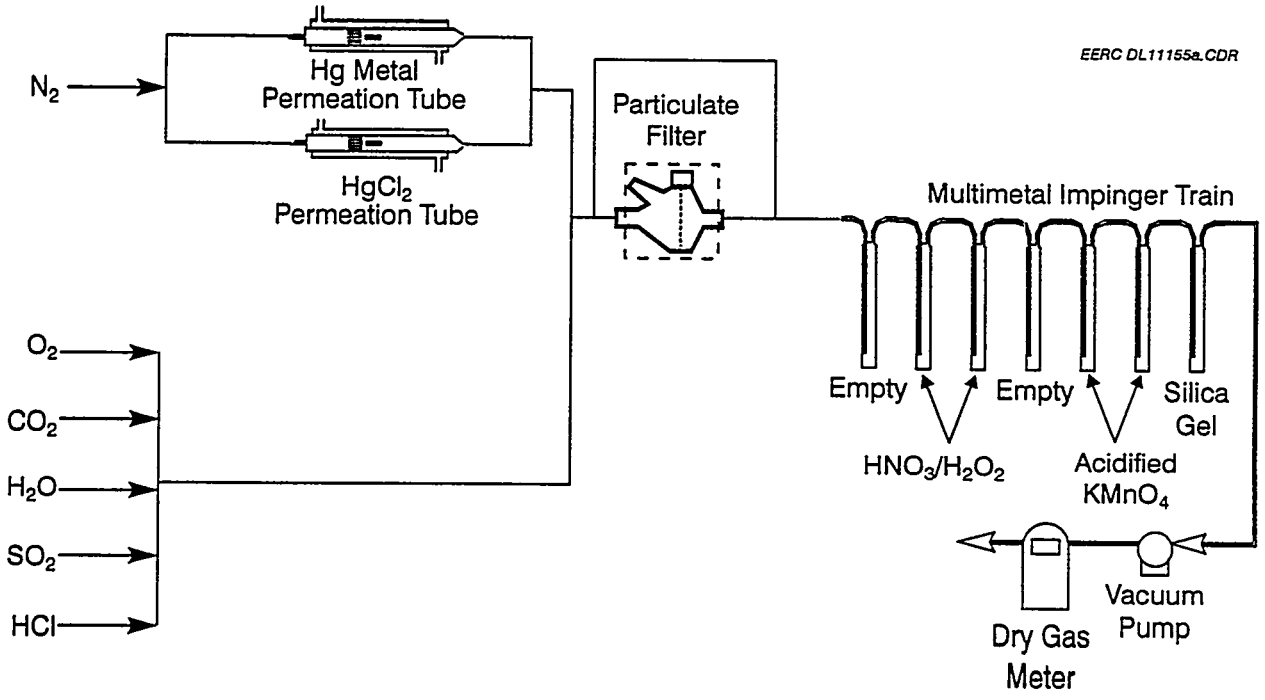

Figure 2. Schematic of bench-scale test system.

TABLE 1

Completed Pilot-Scale Test Matrix

Test No.	Fuel	Sampling Method	Sample Location (relative to the baghouse)	Spike Location[1]
1	Blacksville[2]	All Method 29	Inlet + outlet	None
2	Blacksville	All Method 29	Inlet	Inlet
3	Blacksville	All Method 29	Outlet	Outlet
4	Blacksville	Method 29 + Method 101A	Inlet + outlet	None

[1] Spike sample is the inlet Hg concentration plus enough mercury vapor to bring the flue gas concentration to 20 $\mu g/m^3$.

[2] Pittsburgh No. 8 bituminous coal.

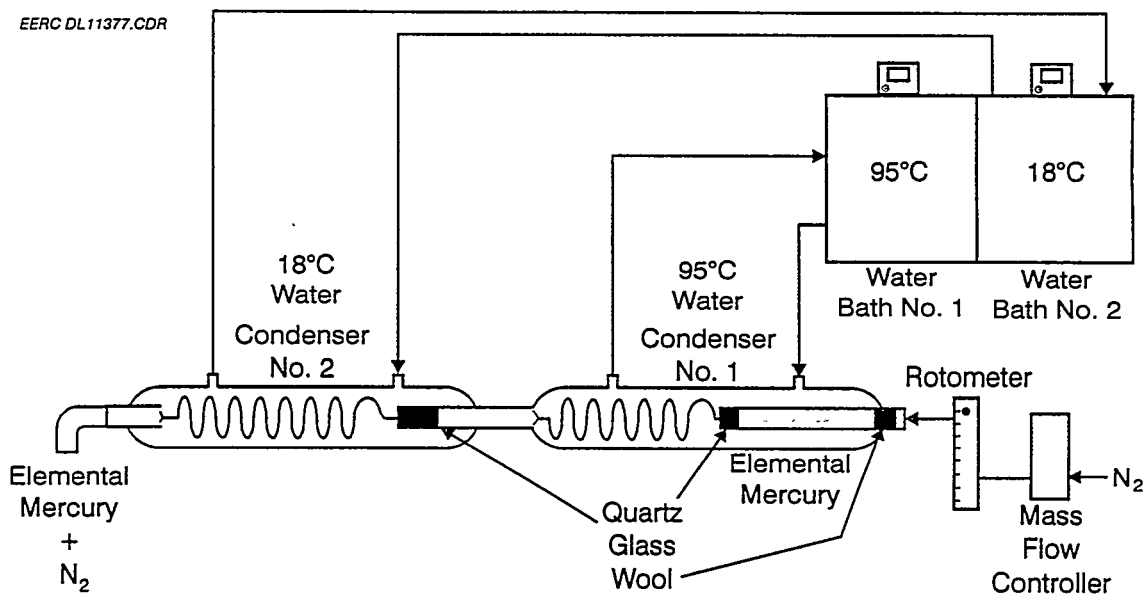

Figure 3. Schematic of elemental mercury spiking system.

RESULTS

Bench-Scale Tests

The first bench-scale tests were completed with only nitrogen as a carrier gas to determine whether EPA (Draft) Method 29 had any chance of speciating mercury. When elemental mercury was injected, almost all of the mercury was captured in the permanganate solution (>99%), and when $HgCl_2$ was injected, almost all of it was captured in the peroxide solution (96%). Since these results were encouraging, the remaining tests were then completed with simulated flue gas.

When $HgCl_2$ was added to the simulated flue gas without HCl present, about 90% was captured in the peroxide. The 10% captured in the permanganate may have been a result of sampling variation, and/or elemental mercury contamination in the $HgCl_2$ used to make the permeation tube. The data indicates little or no effect of the HCl on $HgCl_2$ speciation.

When elemental mercury was added to the simulated flue gas, with or without HCl, 90% of the mercury was captured in the permanganate solutions, and 10% was captured in the peroxide solutions. The data indicated that there was no clear effect from HCl addition. The data for both speciation tests are shown in Figure 4. As described later, pilot-scale tests at EERC have shown that some type of conversion of elemental mercury may occur in the flue gas stream, and it appears that the conversion may be related to the SO_2 concentration in the flue gas. For the bench-scale test completed to date, the SO_2 concentration was maintained at 1000 ppm. This level is compared to 1500–2000 ppm SO_2 in the flue gas for the pilot-scale tests firing Blacksville bituminous coal. Future bench-scale tests are planned to help determine the effect of SO_2 concentration on mercury speciation using EPA (Draft) Method 29.

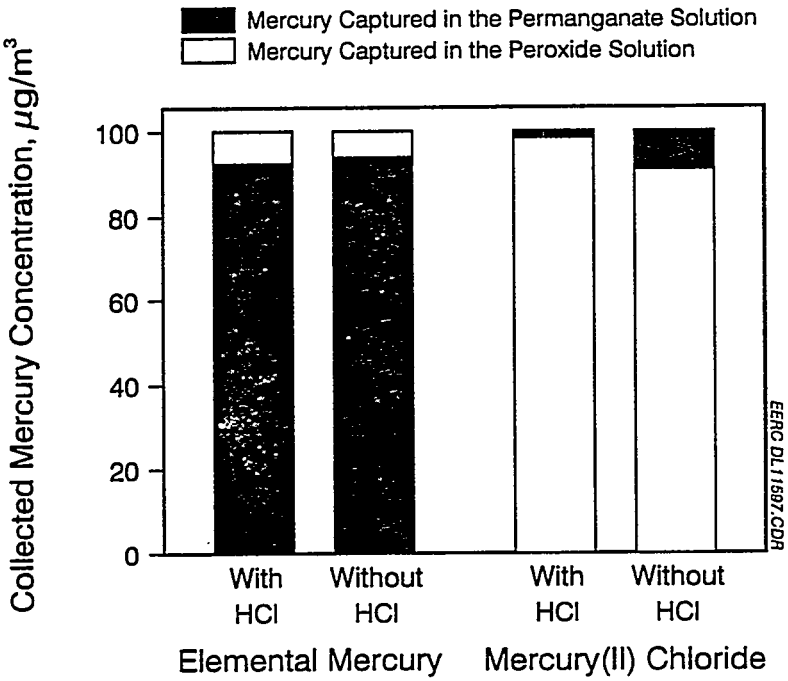

Figure 4. Mercury speciation by EPA (Draft) Method 29 as a function of HCl in bench-scale tests using a simulated flue gas.

Pilot-Scale Tests

During the shakedown testing, sampling was completed to determine if the flue gas flow rate and dust loading were the same at each of the ports of the quadtrain setup. A port analysis showed that the flue gas flow rate and dust loadings were within 10%. The most interesting result from the tests completed to date is that a substantial portion of the spiked elemental mercury collected in the peroxide solutions. When the baseline mercury concentrations, as determined from previous EPA (Draft) Method 29 tests, are compared to the tests with flue gas mercury spiking, approximately 60% of the spiked elemental mercury was collected in the peroxide solution, as is shown in Figure 5. The question, then, is whether EPA (Draft) Method 29 is speciating the mercury correctly, or some type of conversion of the elemental mercury is occurring in the flue gas stream prior to sampling. The original test matrix is being changed to allow future tests to be designed to help resolve this question.

The statistical analyses for the four tests are shown in Tables 2–5. From these tables, it can be seen that the data appear to be consistent and statistically valid. The spike recoveries are close to 90% in most cases, and the correction factors and relative standard deviations are low. The overall results show very good precision and low analytical bias.

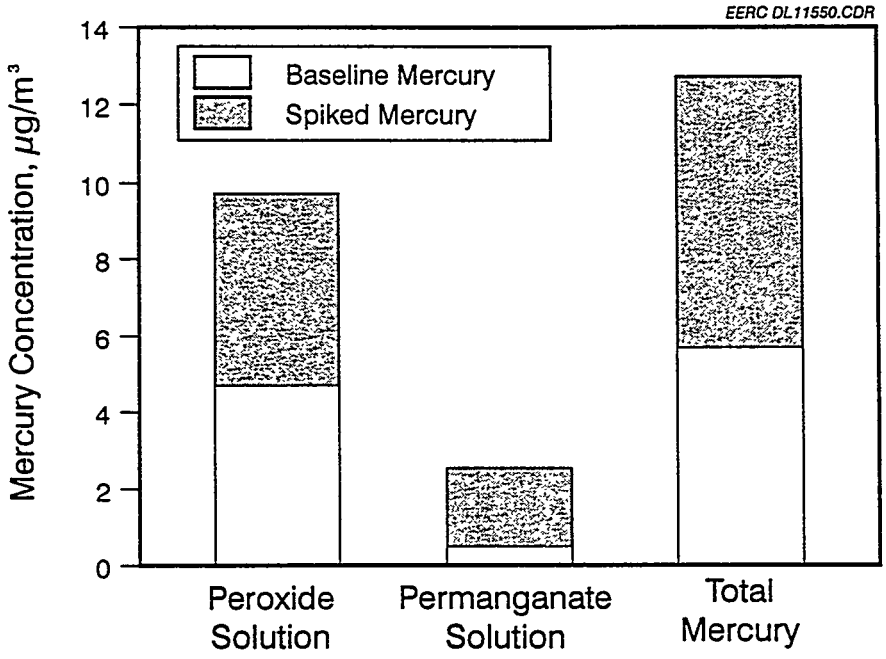

Figure 5. Speciation of the flue gas elemental mercury spike as determined by EPA (Draft) Method 29.

TABLE 2

Statistical Analysis for Test 1 of Pilot-Scale Test Matrix

	Corrected Values		
	Peroxide Solution, $\mu g/m^3$	Permanganate Solution, $\mu g/m^3$	Total Mercury, $\mu g/m^3$
Analyte Spike	0	0	----
Average	6.39	0.51	6.82
Analyte Spike	5.05	5.05	----
Average (with spike subtracted)	6.50	0.49	6.99
*Spike Recovery, %	93.9	96.1	---
Correction Factor	1.07	1.04	---
Relative Std. Dev., %	12.5	35.8	12.2

*Spike recoveries are based on the analytical data comparing the spiked and unspiked sample.

TABLE 3

Comparison of EPA (Draft) Method 29 to EPA Method 101A (Tests 1 and 5)

Test No.	Average, $\mu g/m^3$	Relative Standard Deviation, %
Test 1 (Method 29)	6.49	12.2
Test 4 (Method 29)	6.14	14.8
Test 4 (Method 101A)	5.79	9.6

TABLE 4

Statistical Analysis for Test 2 of Pilot-Scale Test Matrix

	Corrected Values			
	Filter Ash, $\mu g/m^3$	Peroxide Solution, $\mu g/m^3$	Permanganate Solution, $\mu g/m^3$	Total Mercury, $\mu g/m^3$
Analyte Spike	0	0	0	----
Average	0.37	12.43	3.14	15.94
Analyte Spike	----	6.45	6.45	----
Average (with spike subtracted)	0.41	12.44	3.14	15.98
*Spike Recovery, %	102.7	80.0	89.9	---
Correction Factor	1.00	1.25	1.11	---
Relative Std. Dev., %	53.7	4.4	12.5	3.1

*Spike recoveries are based on the analytical data comparing the spiked and unspiked sample.

TABLE 5

Statistical Analysis for Test 3 of Pilot-Scale Test Matrix

	Corrected Values		
	Peroxide Solution, $\mu g/m^3$	Permanganate Solution, $\mu g/m^3$	Total Mercury, $\mu g/m^3$
Analyte Spike	0	0	----
Average	10.17	4.00	14.17
Analyte Spike	6.81	6.81	----
Average (with spike subtracted)	10.29	4.04	14.32
*Spike Recovery, %	89.2	93.1	---
Correction Factor	1.12	1.07	---
Relative Std. Dev., %	9.4	13.9	4.8

*Spike recoveries are based on the analytical data comparing the spiked and unspiked samples.

PRELIMINARY OBSERVATIONS

- On the bench scale, HCl does not appear to influence mercury speciation by EPA (Draft) Method 29 when either injecting elemental or oxidized mercury.
- At the pilot-scale level, very precise mercury measurements with little bias can be obtained with EPA (Draft) Method 29.
- When elemental mercury is spiked into a flue gas stream while firing a medium-sulfur bituminous coal, a substantial portion is collected in the peroxide impingers.
- Additional tests are necessary to determine if a problem is associated with EPA (Draft) Method 29, and/or if some type of conversion of the elemental mercury is occurring in the flue gas stream.

FUTURE WORK

In addition to the completed pilot-scale test, three more tests are planned. The primary purpose of these tests is to compare other mercury sampling methods with EPA (Draft) Method 29 to try and establish whether elemental mercury is converted in the gas stream, or a problem exists with the premise of EPA (Draft) Method 29. The following four different mercury sampling methods will be tested.

- Mercury Speciation Absorption Method (Bloom Method)
- Conventional EPA Method 29
- The Keith Curtis Method which uses a solution of KCl instead of the peroxide solution of conventional EPA Draft Method 29
- Use of an acetate buffer as a first solution in EPA (Draft) Method 29

REFERENCE

1. Miller S.J.; Laudal D.L. "Pulse-Jet Baghouse Perfomance Improvement with Flue Gas Conditioning," EPRI Project No. RP-3083-9, October 1992.

The following manuscript was unavailable at time of publication.

MEASUREMENT OF MERCURY AND OTHER TRACE METALS IN COMBUSTION GASES

Dr. Lawrence Piper
Physical Sciences, Inc.
20 New England Business Center
Andover, MA 01810

Please contact author(s) for a copy of this paper.

LABORATORY-SCALE EVALUATION OF VARIOUS SAMPLING AND ANALYTICAL METHODS FOR DETERMINING MERCURY EMISSIONS FROM COAL-FIRED POWER PLANTS

R.O. AGBEDE, A.J. BOCHAN, J.L. CLEMENTS AND R.P. KHOSAH
ADVANCED TECHNOLOGY SYSTEMS, INC.
3000 TECH CENTER DRIVE
MONROEVILLE, PA 15146

Summary

Comparative bench-scale mercury sampling method tests were performed at the Advanced Technology Systems, Inc (ATS) laboratories for EPA Method 101A, EPA Method 29 and the Ontario Hydro Method. Both blank and impinger spiking experiments were performed.

The experimental results show that the ambient level of mercury in the ATS laboratory is at or below the detection limit (10 ng Hg) as measured by a cold vapor atomic absorption spectrophotometer (CVAAS) which was used to analyze the mercury samples. From the mercury spike studies, the following observations and findings were made.

a) The recovery of mercury spikes using EPA Method 101A was 104%.

b) The Ontario Hydro Method retains about 90% of mercury spikes in the first absorbing solution but has a total spike retention of 106%. As a result, the test data shows possible migration of spiked mercury from the first impinger solution (KCl) to the permanganate impingers.

c) For the EPA Method 29 solutions, when only the peroxide impingers were spiked, mercury recoveries were 65.6% for the peroxide impingers, 0.1% for the knockout impinger and 32.8% for the permanganate impingers with a average total mercury recovery of 98.4%. At press time, data was still being obtained for both the peroxide and permanganate impinger solution spikes. This and other data will be available at the presentation.

Background

Title III of the 1990 Clean Air Act Amendments requires the measurement and inventory of a possible 189 hazardous air pollutants (HAPs) from any stationary source producing more than 10 tons per year of any one pollutant or more than 25 tons per year of total pollutants. Coal-fired power plants are included on this list of potential emission sources requiring such inventories and possible regulation.

doeatspp

In 1991, the Department of Energy's-Pittsburgh Energy Technology Center (DOE-PETC) commissioned five primary contractors to conduct emission studies at eight different coal-fired electric utilities. The eight sites represented a cross section of feed coal type, boiler designs, and particulate and gaseous pollutant control technologies. The major goal of these studies was to determine the sampling and analytical methodologies that could be used to perform these emission tests while producing representative and reliable emission data. The successful methods could then be recommended to the EPA for use as compliance testing methods for the regulation of air toxic emissions from coal-fired power plants.

A secondary purpose of the testing was to determine the effectiveness of the control technologies in reducing target hazardous air pollutants.

The CAAA regulations did not identify the sampling and analytical methods that were to be used in performing the emission tests. As such, one of the challenges facing the primary contractors was to identify methods, previously used for other applications, that could be used for emission tests at coal-fired power plants to gather accurate HAPs emission data. A second challenge was to identify criteria that could be used to determine the efficacy of the selected sampling and analytical methods in performing their intended purpose.

The five primary contractors were Battelle, Energy and Environmental Research Corporation, Radian, Roy F. Weston, and Southern Research Institute. The eight locations at which the emission tests were performed were: Ohio Edison's Niles Station and Cooperative Power Association's Coal Creek Station (Battelle), Ohio Power Company's Cardinal Station (Energy and Environmental Research Corporation), Tucson Electric Power Company's Springerville Station and Northern Indiana Public Service Company's Bailly Station (Southern Research Institute), Illinois Power Company's Baldwin Station and Minnesota Power Company's Boswell Station (Roy F. Weston) and Georgia Power Company's Plant Yates (Radian Corporation).

The contractors tested for major and trace metals, mercury, total particulates, volatile organic compounds, semi-volatile organic compounds, aldehydes, acid gases (HF, HCl, HBr, F_2, Cl_2 and Br_2), ammonia, cyanide, phosphates, sulfates and radionuclides. Mercury testing was performed using EPA Method 29 and usually either the HEST or the Bloom methods. Most of the sampling and analytical methods employed were based on existing EPA-approved methodologies or modifications of methods that had previously been approved for other applications.

Advanced Technology Systems, Inc. (ATS) as a secondary DOE contractor on this project, has assessed the sampling and analytical plans and the emission reports of the five primary contractors to determine how successful the contractors were in satisfying their defined objectives. To accomplish this task ATS examined the precision and accuracy of the emission test results, the emission levels of the target hazardous air pollutants (HAPs), the precision and accuracy of the audit sample results and the closure of material balances for individual processing steps and for the overall combustion process.

doeatspp

As a result of these efforts, ATS identified several problem areas where the sampling and analytical methodologies applied were not able to adequately measure the concentration of the target analytes in the flue gas streams of coal-fired power plants. These areas included but were not limited to the measurement of mercury and other volatile metals such as arsenic and selenium, and the measurement of semi-volatile metals such as antimony, cadmium, lead, boron and molybdenum. Other areas of concern include the sampling and analysis of volatile organic compounds such as benzene and toluene and the sampling and analysis of acid gases such as HCl and Cl_2.

Introduction

As a result of the identification of deficiencies in the methods detailed above, ATS' assignment from DOE was to rectify the shortcomings in the sampling and analytical methodologies applied to flue gas sampling at coal-fired power plants by method improvement and/or method development. Consequently, ATS is presently involved in an intensive program of method development studies. These studies are being conducted in the laboratory with subsequent tests planned for selected pilot plant and power plant test sites.

ATS' approach to these method development studies has been to first test the existing methods under ideal laboratory conditions. The philosophy behind this approach is that if the methods cannot perform as designed under ideal laboratory conditions, there is little chance that they would produce desired performance results at a plant site environment.

The initial focus is on mercury. Five mercury sampling methods have been selected for testing at ATS laboratories. These methods are EPA Method 101A, EPA Draft Method 29, the Ontario Hydro Method, The Hazardous Element Sampling Train (HEST) Method and the Bloom Method. This paper will discuss the experimental results from tests with the first three methods. The findings from tests with the HEST and Bloom Methods will be discussed in later presentations.

Experimental

A. Design of Experiments.

Sampling performance evaluation tests were conducted for each method under investigation. These tests consisted of both blank and mercury spiking tests. The blank runs were performed to determine if the sampling method was collecting any mercury contamination that might be present in the laboratory environment. Once blank baseline mercury concentrations were established, mercury was introduced into the sampling train by spiking directly into the impinger solutions with a known concentration of mercury in the form of mercuric chloride. To provide for statistical evaluation of the data obtained, five spiked mercury replicates were performed for each test.

The sampling tests were performed using Nutech 2010 Stack Samplers. The sampling trains were assembled in accordance with the EPA methodology guidelines. Filter weights, and the weights

and volumes of the impingers and their contents were recorded before and after a sampling run. A sampling run consisted of collecting 108 cubic feet volume of ambient laboratory air. The time required to collect the required volume was approximately 3 hours. In addition, temperatures and vacuum pressures were carefully monitored and recorded every 30 minutes.

Upon completion of the sampling run, the train was disassembled, and the filter and impinger solutions were recovered as per appropriate EPA methodology. The impinger solutions were analyzed for mercury as per EPA Method 7470. Briefly, this method involves reducing the mercury collected (in the mercuric form) to elemental mercury, which is then aerated from the solution into an optical cell and measured by atomic absorption spectrophotometry. Mercury analysis was performed using a Bacharach Model MAS-50B CVAAS Mercury Analyzer System. Calibration of this unit was based on a five point calibration curve.

i) Blank Runs.

Blank tests were performed for each sampling method evaluated. Initially, five blank tests were performed for EPA Draft Method 29. The analytical results for these tests showed that the ambient level of mercury in the laboratory was below the detection limits of the analytical instrument. As a result only spot check blank tests were performed for the other two methods.

ii) Spiked Runs.

Mercury spiking experiments were performed for each method tested. These tests were performed by introducing known volumes of a mercuric chloride standard solution directly into the impingers using a repeater pipette. The mercury spike concentrations were based on the volumes of the recovery samples and the optimum working range of the CVAAS. After the impingers were spiked, the train was assembled, leak-checked and 108 cubic feet of laboratory air was drawn through the train. When the desired volume of air had been collected, the filter and impinger solutions were recovered as per EPA methodology for the method being tested and the impinger solutions were analyzed for mercury following EPA Method 7470 procedures.

The EPA Method 101A spiking tests were performed by spiking 5,000 ng of mercuric chloride into the second and third permanganate impingers then assembling the sampling train, performing the test and recovering the train as described above. This would theoretically produce a Hg level of 10,000 ng/L in the recovered samples.

The spiking scheme for the Ontario Hydro impinger mercury spiking tests was as follows. The first KCl impinger was spiked with 5000 ng of mercury and the first $KMnO_4$ impinger was spiked with 5000 ng of mercury. The filter was not spiked for this series of tests. A Hg level of 10,000 ng/L would be expected in the recovered samples.

Two series of spiking tests were performed for EPA Draft Method 29. In the first series of impinger spiking tests only the peroxide impingers were spiked. In these tests, the first peroxide impinger was spiked with 3,000 ng of mercuric chloride. In the second series of tests, the first

peroxide impinger was spiked with 3,000 ng of mercuric chloride and the first permanganate impinger was spiked with 4,000 ng of mercuric chloride. For all of these experiments the expected level of mercury in the recovery samples was 10,000 ng Hg/L.

Results and Discussion

The analytical results from the blank and mercury impinger spiking tests are presented in Tables 1 and 2. The results are shown in total ug for the blank tests and in both total ug and percent recovery for the impinger spiking tests. Both individual test results and average results are shown. Where appropriate, standard deviations are also presented.

The blank test results shown in Table 1 indicate that the level of mercury present in the laboratory is at or below the detection limit of the analytical instrument. These results demonstrate that only nominal amounts of mercury are present in the air sampled for the series of mercury spiking tests. As a result, all of the mercury present in the recovery samples from the mercury spiking tests can be considered to originate from the mercury spikes.

Previously, analysis of the Method 101A blank runs had yielded detectable mercury in concentrations ranging from 17.2 ng to 388 ng. It was presumed that the procedure for cleaning the glassware was insufficient in removing residual mercury from the sampling train glassware. Laboratory glassware was scrupulously cleaned between each sampling run in accordance with the EPA Method 29 guidelines. Cleaning the glassware consisted of a soapy (Citranox) wash and rinse followed by a 10% nitric acid soak for a minimum of 4 hours. The glassware was then triple-rinsed with deionized water and oven dried. As a precaution to prevent further contamination of blank runs, separate impingers and glassware were purchased to be used exclusively for the blank analysis of sampling methods. The current blank data was obtained with such glassware.

Table 2 shows that the EPA Method 101A mercury spike test results range from 103.24% recovery (tests 1, 3 and 5) to 107.88% recovery (test 2). The average recovery was 104.23% with a standard deviation of 2.04%. The precision and accuracy of these results are very good. As such, these results indicate that EPA Method 101A can serve as a standard against which the recovery results of all the other mercury spiking tests in this study can be compared.

Table 2 also shows that the experimental results for the Ontario Hydro Method ranged from 84.09% to 91.64% recovery of mercury for the first absorbing solution and 110.51% to 131.26% recovery for the permanganate absorbing solution. Total mercury recovery for the Ontario Hydro Method ranged from 98.24% to 111.45% The average percent recoveries of mercury were 88.11 $\pm$ 3.23 for the first absorbing solution, 124.47 $\pm$ 8.5 for the permanganate solution and 106.49 $\pm$ 4.88 for total recovery. These results show that the precision of mercury recovery for each impinger solution type and for total recovery are good. However, there is a reproducible portion of the mercuric chloride that appears to migrate from the first absorbing solution impingers to

the $KMnO_4$ impingers where it is retained. To investigate this migration effect, the experiment will be repeated with mercury spiking into only the first absorbing solution impingers.

The bottom half of Table 2 shows the experimental results for the peroxide impinger spiking tests performed using EPA Draft Method 29. The results from this series of tests indicate that the average recovery of mercuric chloride spikes into the peroxide impingers was only 65.6%. Recovery of mercury from the knockout impinger and from the permanganate impingers, which were not spiked, were 0.1% and 32.8% respectively. Total spiked mercury recovery was 98.4%. These results seem to indicate that the peroxide impinger solutions did not totally retain mercuric chloride species under the conditions of the test and that migration of the spiked mercuric chloride to the permanganate solutions occurred. A second series of tests is currently underway with spiking into both the peroxide and permanganate impingers. Results from this study will be available at the conference presentation.

Conclusions

The experimental results show that the ambient level of mercury in the ATS laboratory is at or below the detection limit for the cold vapor atomic absorption spectrophotometer used to analyze the mercury samples. The results also showed that, under the test conditions, the recovery of the mercury spikes using EPA Method 101A is complete within experimental error. This implies that Method 101A can serve as a control or standard for comparison with all of the other methods tested and those that will be tested in the future.

The results also showed that the Ontario Hydro Method retains about 90% of mercury spikes in the first absorbing solution and has a total spike retention of around 100%. As a result, migration of mercury spikes from the first impinger solution into the permanganate impingers is suspected. Further tests will be performed to verify if migration actually occurs.

In addition, the experimental results showed that the peroxide impingers were not able to totally retain oxidized mercury species spiked directly into them under ideal laboratory conditions. These results cast doubts on the ability of the method to perform correctly under more rigorous field conditions. Further tests are in progress to confirm this finding along with determining recoveries from both peroxide and permanganate impingers each spiked with equivalent amounts of mercury species.

Acknowledgements

ATS wishes to acknowledge DOE Grant No. DE-AC22-93PC92583 which provided funding for this project. ATS also wishes to acknowledge Mr. Chuck Schmidt, Mr. Tom Brown and Dr. Mike Baird of PETC for their helpful input.

doeatspp

Table 1. Concentration of Mercury in the Recovery Samples for the Blank and Mercury Spiking Tests.

Sample	Mercury Level (ug)					
	Test 1	Test 2	Test 3	Test 4	Test 5	Ave/*SD*
EPA Method 101A						
• Blank Test	0.053	-	-	-	-	0.053
• Spiking Tests	10.320	10.790	10.320	10.360	10.320	10.420/*0.206*
Ontario Hydro Method						
• Blank Test	ND	-	-	-	-	-
• Spiking Tests						
• KCl Impingers	4.393	4.299	4.581	4.204	4.550	4.405/*0.161*
• $KMnO_4$ Impingers	6.132	5.525	6.563	6.405	6.500	6.225/*0.424*
• Total Mercury	10.525	9.824	11.144	10.609	11.050	10.630/*0.525*
EPA Method 29						
Blank Tests						
• Front-half	ND	0.011	ND	ND	ND	0.011
• H_2O_2 Impingers	ND	0.011	ND	ND	0.018	0.015
• Knockout	ND	ND	ND	0.018	ND	0.018
• $KMnO_4$ Impingers	0.030	ND	ND	ND	0.030	0.030
• $KMnO_4$ Wash	ND	ND	ND	ND	ND	
H_2O_2 Spiking Tests						
• H_2O_2 Impingers	1.988	2.259	1.956	2.041	1.591	1.967/*0.241*
• Knockout	ND	ND	ND	ND	ND	ND
• $KMnO_4$ Impingers	0.977	1.092	0.820	1.012	1.013	0.983/*0.100*
• Total	2.965	3.351	2.776	3.053	2.604	2.950/*0.284*

ND - Non-detected at a detection limit of 0.010 ug.
- Not determined.

doeatspp

Table 2. Percent Recovery of Mercury from Mercury Spiking Tests.

Sample	Percent Recovery					
	Test 1	Test 2	Test 3	Test 4	Test 5	Ave/*SD*
EPA Method 101A	103.2	107.9	103.2	103.6	103.2	104.2/*2.0*
Ontario Hydro Method						
• KCl Impingers	87.7	86.0	91.6	84.1	91.0	88.1/*3.2*
• $KMnO_4$ Impingers	122.4	110.5	131.3	128.1	130.0	124.5/*8.5*
• Total Mercury	105.2	98.2	111.4	106.1	110.5	106.5/*4.9*
EPA Method 29						
H_2O_2 Spiking Tests						
• H_2O_2 Impingers	66.6	75.3	65.2	68.0	53.0	65.6/*8.1*
• Knockout	0.0	0.1	0.1	0.1	0.1	0.1/*0.0*
• $KMnO_4$ Impingers	32.6	36.4	27.4	33.7	33.8	32.8/*3.3*
• Total	98.8	111.8	92.6	101.8	86.9	98.4/*9.4*

doeatspp

COMPARING AND ASSESSING DIFFERENT MEASUREMENT TECHNIQUES FOR MERCURY IN COAL SYNTHESIS GAS

DAVID P. MAXWELL AND CARL F. RICHARDSON, Ph.D.
RADIAN CORPORATION
8501 N. Mopac Boulevard
Austin, Texas 78759

ABSTRACT

Three mercury measurement techniques were performed on synthesis gas streams before and after an amine-based sulfur removal system. The syngas was sampled using 1) gas impingers containing a nitric acid-hydrogen peroxide solution, 2) coconut-based charcoal sorbent, and 3) an on-line atomic absorption spectrophotometer equipped with a gold amalgamation trap and cold vapor cell. Various impinger solutions were applied upstream of the gold amalgamation trap to remove hydrogen sulfide and isolate oxidized and elemental species of mercury. The results from these three techniques are compared to provide an assessment of these measurement techniques in reducing gas atmospheres.

INTRODUCTION

The U.S. Department of Energy (DOE), the Electric Power Research Institute (EPRI), and Louisiana Gasification Technology, Inc. have sponsored a comprehensive assessment of toxic emissions from the integrated gasification combined cycle (IGCC) process located at Dow Chemical-Louisiana Division's facility in Plaquemine, Louisiana. Radian Corporation performed this assessment which included the measurement of vapor phase trace elements from various syngas streams and other reducing gas matrices in addition to the emission sources.

Reducing gas matrices containing reactive substances such as hydrogen sulfide adversely affect the ability of conventional gas sampling techniques (e.g., EPA Draft Method 29) to collect some vapor phase metal species. In this paper, vapor phase substances are defined as those elements collected in traps or impingers after particulate removal. For example, acidic potassium permanganate solutions typically used to oxidize and collect mercury in flue gas are quickly reduced by hydrogen sulfide, rendering the solution ineffective. In addition, metal carbonyls, hydride-forming compounds like arsenic, mercury, and other uncharacterized metal species are not efficiently collected in the nitric acid impinger solutions used for oxidized gas streams.

EXPERIMENTAL

Radian Corporation used three different sampling approaches to overcome the limited application of Method 29 on two internal process streams sampled during this test. First, the EPA Draft Method 29 impinger technique was modified by increasing the strength of the hydrogen peroxide component from 10% to 30% and the permanganate solutions were not used. Parallel with Method 29 sampling, sample tubes containing coconut-based charcoal were used to collect mercury and other vapor phase metals. In addition, direct analysis of the gas with an

atomic absorption spectrophotometer (AAS) was performed for mercury and a selected set of trace elements. The sour and sweet syngas streams were sampled to characterize the product gas before and after the sulfur removal system. The concentration of hydrogen sulfide is the primary difference between these two process streams.

Nitric Acid/Hydrogen Peroxide Impinger Sampling

EPA Draft Method 29 (M-29) consists of a filter media, which removes particulate matter, and a series of impingers. It is often assumed that substances collected in the impinger exist in the vapor state. This method uses two impingers containing a 5% HNO_3/10% H_2O_2 solution, followed by two impingers containing a 4% $KMnO_4$/10% H_2SO_4 solution for total mercury collection. Current research is attempting to determine the speciation capabilities of M-29. It is commonly believed that oxidized forms of mercury preferentially report to the nitric/peroxide impingers and elemental mercury can only be trapped in the permanganate impingers. When this method is applied to syngas or other reducing gas matrices containing hydrogen sulfide (H_2S), the permanganate impinger solution is quickly reduced so it is ineffective at collecting mercury. The standard nitric acid solution (5% nitric/10% peroxide) has also been shown to be ineffective in syngas applications for the collection of mercury and other trace elements.

In an effort to enhance the collection efficiency of the nitric acid impingers for other vapor phase metals in syngas, the concentrations of nitric acid and hydrogen peroxide were increased to 10% and 30%, respectively. Although the oxidation potential of this solution is enhanced, it does not effectively trap H_2S. The low pH of the impinger solution keeps the H_2S equilibrium shifted towards the gas phase. As such, H_2S does not dissociate and, therefore, oxidation and removal do not occur. Consequently, permanganate impingers were not used in the sampling trains for the sweet and sour syngas. Therefore, the potential to collect elemental mercury in this M-29 configuration is minimal.

To measure the analytical bias of the mercury measurements in this matrix, duplicate syngas samples were spiked with aqueous mercury standards before sample digestion and analysis. These spikes were recovered at 99 and 104 percent. The analytical results for the enhanced nitric acid/hydrogen peroxide matrix are considered acceptable and accurate.

Adsorption on Charcoal Sorbent

Some industrial processes utilize charcoal sorbents in guard beds to protect catalysts from metal poisoning. Using the same principle, charcoal has also been demonstrated as a suitable sorbent for the collection of mercury in flue gas.[1,2] Coconut-based charcoal was aggressively cleaned using concentrated nitric acid followed by an ultra-pure deionized water rinse then dried over night. The cleaning procedure required five days to complete. The charcoal was then loaded into precleaned quartz tubes.

Two charcoal tubes were placed in series for sample collection using Teflon® tubing and plastic connectors. A total of 100 L of syngas was sampled through the tubes at ambient temperature at a maximum flowrate of 1 L/min. After sample collection, the charcoal tubes were sealed with plastic caps and sent to the laboratory for analysis. The charcoal sorbent was digested with nitric

acid in a closed microwave digestion vessel to minimize losses of volatile elements. This digestate was analyzed for mercury by cold vapor atomic absorption spectrophotometry (CVAAS).

To assess the quality of mercury recovery from the charcoal, blank charcoal media was spiked before digestion with a commercially-prepared aqueous standard solution. Duplicate spikes (1 μg) were recovered at 52 and 62 percent. Duplicate analytical spikes introduced in the sweet syngas sample digestates were recovered at 77 and 81 percent. Blank media was analyzed to provide a measure of background concentrations for correction of the sample results. Three blanks were analyzed with concentrations ranging from 0.08-0.10 μg mercury per tube. Based on these quality control results, mercury data from the charcoal tube sampling method may be biased low.

Direct Analysis by Cold Vapor Atomic Absorption Spectrophotometry

Mercury analyses of the process stream were carried out on a semi-continuous basis using a cold vapor atomic absorption method.[3] The field apparatus, depicted in Figure 1, consisted of an impinger sampling train, a gold amalgamation unit, the CVAAS instrument, and units to clean and measure the volume of the sampled gas.

The gas stream temperature was controlled to avoid water condensation within the lines. A continual gas flow was maintained by by-passing the gas upstream of the impinger train when sampling was not being performed.

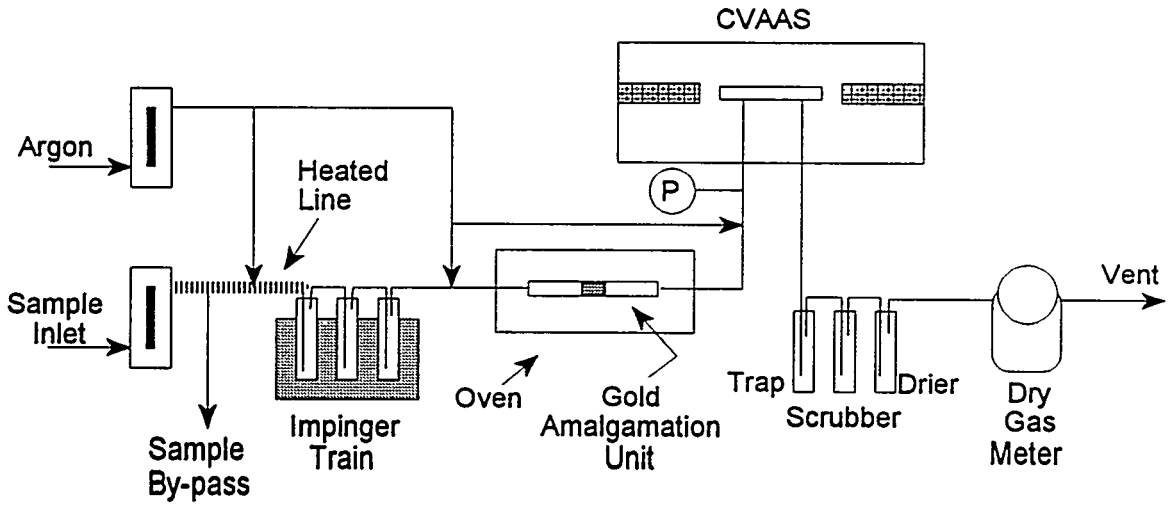

Figure 1. Schematic of CVAAS Sample Analysis System

The sample gas flowrate was 0.75 - 1.5 L/min through a series of ice-chilled impingers containing solutions designed to either pass or trap elemental and oxidized forms of mercury. The flow was controlled using calibrated flow meters and the volume was measured using a dry gas meter. The impingers consisted of 70 mL deep-well bottles with fritted tips. In most cases, solution volumes of 35 mL were used. The impinger solutions evaluated will be discussed below. Following the sample-gas purge, the impingers were flushed with argon to remove residual sample vapor.

Mercury from the gas stream was adsorbed onto the surface of cooled gold mesh, located in a half-inch quartz tube, to concentrate the mercury prior to analysis. The gold was then heated to 950°F, using a temperature-controlled tubular oven, to thermally desorb the mercury. A continuous flow of argon carried the desorbed mercury to the CVAAS cell for analysis. The CVAAS unit consisted of an ARL Model 93 atomic absorption spectrometer containing a 20 mL quartz analysis cell. The mercury absorbance at 253.3 nm was measured and results were recorded on a HP3390A integrator. The instrumental detection limit was determined to be 10 ng of mercury during this testing.

Impinger Solutions. The direct analysis in the field provided the opportunity to try several techniques for measuring total or speciated mercury. The impinger solutions used during this testing were chosen for their potential to either capture or pass different forms of mercury. Various combinations were used in attempts to overcome interferences associated with the syngas matrix. Various impingers, such as water, NaOH, and cold "knockouts," were evaluated for their ability to protect the mercury absorption and reduction solutions from these interferences.

Reductant solutions, such as 0.1M sodium borohydride ($NaBH_4$) and saturated stannous chloride ($SnCl_2$) in 10% H_2SO_4, were used to convert the mercury in the sample to the elemental form, Hg^o. The Hg^o, with a very low aqueous solubility, would be expected to remain in the gas stream and thus flow to the amalgamation unit where it would be adsorbed by the gold. These solutions were used exclusively to determine the total mercury in the gas stream. They were also used downstream of scrubbing impinger solutions designed to eliminate either the oxidized mercury or the matrix interferences.

Several solutions, including 4% hydrogen peroxide (H_2O_2), 80% isopropyl alcohol (IPA), and water, were tested for their abilities to capture oxidized mercury from the gas stream while enabling the Hg^o to pass. These solutions were located either in the first impinger, or in the second behind a knockout impinger. The H_2O_2 solution was acidified with 5% HNO_3 to increase both the relative oxidation strength and metal solubility within the solution. Elemental mercury, with its low solubility, would be expected to pass through the H_2O_2 solution. The H_2S adsorption into the IPA should be low, thus reducing the possibility of reactions with the solubilized mercury. Such reactions may result in the reduction of the captured mercury and its subsequent release from the solution. Diethyldithiocarbamic acid (DEDTCA) was added to the IPA impingers to chelate the adsorbed mercury, thus preventing its release back to the gas stream.

The ability of 5% potassium permanganate ($KMnO_4$) (+10% H_2SO_4) to capture mercury from the gas stream was evaluated. The high oxidation potential of this solution enables it to absorb both

elemental and oxidized forms of mercury. Initial tests verified previous results which showed that $KMnO_4$ is rapidly reduced by the H_2S present in the coal syngas. Therefore, these solutions were placed downstream of other impingers, such as NaOH, designed to remove the H_2S from the gas.

Gas Analysis. Gas samples were flowed through the impinger train as described above; sample volumes ranged from 20-60 L. The amount of mercury that passed through the impingers was determined by analyzing the quantity that adsorbed to the gold during sampling. Each impinger solution was analyzed individually by reducing it with $NaBH_4$ and purging the Hg^0 with argon to the amalgamation unit for subsequent analysis. The pH of the H_2O_2 impingers was adjusted to 7 with NaOH prior to the reduction step. The $KMnO_4$ solutions were neutralized with hydroxylamine hydrochloride prior to the $NaBH_4$ addition. Each reagent solution was analyzed for mercury and blank subtraction was carried out for each analysis. The mercury captured in the H_2O_2 and IPA impingers was presumed to be oxidized. The total mercury was calculated as the sum of all the individual analyses for a given sample. Chemical spikes using Hg^0 vapor and $HgCl_2$ standards were used to verify the recovery of elemental and oxidized mercury, respectively, from the impinger solutions.

RESULTS

The three mercury techniques were applied to the sour and sweet syngas. These two syngas streams are virtually identical in composition except for the H_2S and moisture content. Hydrogen sulfide in the sour syngas measured about 900 ppmv compared to about 30 ppmv in the sweet syngas. The sweet syngas is virtually dry while the sour syngas, although sampled downstream of a moisture knock-out, still contained a significant amount of water. Unfortunately, both H_2S and water can have an effect on some of the methods that were used. The results [and 95% confidence intervals (95% CI)] obtained from the charcoal and CVAAS methods are compared in Tables 1 and 2.

Table 1. Mercury Measured in Sour Syngas

Method	Impingers	Hg, µg/Nm³	95% CI
Charcoal	None	11	13
CVAAS	(1) 2N NaOH/$NaBH_4$	6.1	2.1
	(2) IPA/2N NaOH/$KMnO_4$	3.2	5.2

The following observations were made during this method comparison:

- Although highly variable, the charcoal tube method reported the higher total mercury value. These values are the average of three daily measurements and do not coincide with the test period using the CVAAS technique.

- The presence of H_2S appears to have an effect on the impinger capture (or measurement) of total mercury. Case 2 results by CVAAS is lower than Case 1. During sample collection in Case 2, there was H_2S breakthrough from the NaOH scrubbing solution, which may have biased the results low for Case 2.

Table 2. Mercury Measured in Sweet Syngas

Method	Impingers	Hg, µg/Nm³	95% CI
Charcoal	None	0.1	0.02
CVAAS	(1) 0.1N NaOH/$NaBH_4$	3.8	3.6
	(2) IPA/0.1N NaOH/$KMnO_4$	3.0	3.2
	(3) H_2O_2/0.1N NaOH/$KMnO_4$	3.6	2.3
	(4) IPA/0.1N NaOH/$NaBH_4$	3.1	1.5

The following observations were made regarding this data set for sweet syngas:

- Mercury collected on charcoal, with respect to the other collection/measurement methods, is significantly lower in the sweet syngas matrix. The reason for this is unknown.
- All of the impinger combinations used in the CVAAS study produced very similar results. Comparison with the charcoal or $NaBH_4$ results in Table 1 indicates 40-70% mercury removal across the Selectamine™ process.
- Results indicated the need for an H_2S scrubber upstream of the $KMnO_4$ or $NaBH_4$ impinger.

Mercury Speciation

Test results for oxidized mercury in the syngas are presented in Table 3. Due to schedule restraints, only a limited number of speciation runs were made at the sour syngas location. Hydrogen peroxide and isopropyl alcohol solutions were used to capture oxidized mercury in the CVAAS tests while 10% HNO_3/30% H_2O_2 was used in the M-29 testing.

Table 3. Mercury Speciation in Syngas

Absorbing Solution	Sweet Syngas		Sour Syngas	
	Oxidized Hg, µg/Nm³	95% CI	Oxidized Hg, µg/Nm³	95% CI
CVAAS: H_2O_2	1.01	1.04		
CVAAS: IPA	0.52	1.5	0.97	1.12
M-29: Nitric/Peroxide	0.23	0.22	0.81	0.93

The results in Table 3 show that measurable quantities of oxidized, or ionic mercury, species are present in the syngas.

- Despite relatively high variability, all three impingers measured the presence of oxidized mercury in the syngas streams.

- The numbers listed in Table 3 represent nominally 25% of the total mercury measured in the sweet syngas.

Elemental mercury spiked to these impingers was not retained. However, it is not known which forms of oxidized mercury are effectively retained or pass through these impinger solutions.

CONCLUSIONS AND RECOMMENDATIONS

Direct CVAAS analyses performed on-site identified promising alternatives or modifications to the Method 29 approach. Future efforts at quantifying mercury in synthesis gas should consider incorporating the following recommendations and assessing the results through a comprehensive quality control program.

- An H_2S scrubbing impinger (NaOH, etc) is required upstream of any reductant impingers to eliminate matrix effects with both the impinger solution and the gold amalgam trap. Sodium hydroxide appeared to work well for this purpose without absorbing any measurable quantities of mercury.

- The Method 29 HNO_3 /H_2O_2 impinger showed the ability to absorb mercury, presumably in the oxidized form, from the syngas. The results of this testing indicate that the addition of H_2S scrubbing impingers, upstream of the $KMnO_4$ impinger, may be a suitable modification to this method to enable the collection of mercury.

- Testing of charcoal sorbents in conjunction with the direct CVAAS system could a) determine breakthrough potential of charcoal; and b) indicate if charcoal adsorption of mercury is quantitative or species dependent.

- For measuring the effectiveness of sample collection methods and providing an alternate method for quantifying total mercury in syngas, the CVAAS experimental apparatus offers several advantages: 1) near real-time analysis of mercury for immediate feedback on the effectiveness of the measurement method; and 2) the ability to measure breakthrough of mercury through impingers by using the gold trap downstream of the impinger train.

ACKNOWLEDGMENTS

This work was sponsored by the U.S. Department of Energy, Pittsburgh Energy Technology Center and co-funded by the Electric Power Research Institute and LGTI under DOE Contract No. DE-AC22-93PC93253, Dr. Lori Gould, Project Manager.

REFERENCES

1. Germani, M.S. and W. H. Zoller. "Vapor-Phase Concentrations of Arsenic, Selenium, Bromine, Iodine, and Mercury in the Stack of a Coal-Fired Power Plant," Environ. Sci. Technol., 1988, 22, 1079-1085.

2. Meij, R., H. Spoelstra, and F.J. de Waard. "The Determination of Gaseous Inorganic Trace Compounds in Flue Gases From Coal-Fired Power Plants," Proceeding of the 8th World Clean Air Congress 1989, The Hague, The Netherlands, 11-15 September 1989. Elsevier Science Publishers B.V., Amsterdam.

3. "Method 303F—Determination of Mercury by the Cold Vapor Technique," Standard Methods for the Examination of Water and Wastewater, 16th Ed., APHA, AWWA, WPCF, 1985, American Public Health Association, Washington, D.C.

The following manuscript was unavailable at time of publication.

IEA - FULL FUEL CYCLE STUDY

Dr. Perry Bergman
U.S. Department of Energy
Pittsburgh Energy Technology Center
P.O. Box 10940, M.S. 922-247A
Pittsburgh, PA 15236

Please contact author(s) for a copy of this paper.

THE USE OF FLUE GAS FOR THE GROWTH OF MICROALGAL BIOMASS

KATHRYN G. ZEILER
KIRAN L. KADAM
DANA A. HEACOX
DAVID W. KERBAUGH
JOHN J. SHEEHAN

NATIONAL RENEWABLE ENERGY LABORATORY
1617 COLE BLVD., GOLDEN, CO 80401

ABSTRACT - Capture and utilization of carbon dioxide (CO_2) by microalgae is a promising technology to help reduce emissions from fossil fuel-fired power plants. Microalgae are of particular interest because of their rapid growth rates and tolerance to varying environmental conditions. Laboratory work is directed toward investigating the effects of simulated flue gas on microalgae, while engineering studies have focused on the economics of the technology. One strain of a green algae, *Monoraphidium minutum* , has shown excellent tolerance and growth when exposed to simulated flue gas which meets the requirements of the 1990 Clean Air Act Amendments (1990 CAAA). Biomass concentrations of ~2g/L have been measured in batch culture. Several other microalgae have also shown tolerance to simulated flue gas; however, the growth of these strains is not equivalent to that observed for *M. minutum*. Coupling the production of biodiesel or other microalgae-derived commodity chemicals with the use of flue gas carbon dioxide is potentially a zero-cost method of reducing the amount of carbon dioxide contributed to the atmosphere by fossil fuel-fired power plants. We have identified two major biological performance parameters which can provide sufficient improvement in this technology to render it cost-competitive with other existing CO_2 mitigation technologies. These are algal growth rate and lipid content. An updated economic analysis shows that growth rate is the more important of the two, and should be the focus of near term research activities. The long term goal of achieving zero cost will require other, non-biological, improvements in the process.

INTRODUCTION - Anthropogenic emissions of CO_2 are estimated to be 2×10^{10} metric tons/y, primarily from combustion of fossil fuels. In addition, the increasing global population pushes the demand for economical energy sources higher every year. Contrasted with its potential for harm is the value of CO_2. It is the source of carbon for photosynthesis, without which there would not be life on earth as we know it today. Carbon dioxide is a valuable resource for many of man's activities including enhanced oil and gas recovery, urea production, and food processing and beverage carbonation[1]. These activities and others of similar nature, however, can use only a very small percentage of the total CO_2 emissions from fossil fuel combustion.

Using CO_2 from fossil fuel combustion as a feedstock for photosynthetic microorganisms can provide a large sink for carbon assimilation. Microalgae are the most productive CO_2 users, with yields of biomass per acre threefold to fivefold greater than those from typical crop plant acreage[2]. Earlier studies[3-5] have discussed the potential applications of power plant flue gas to microalgal farming. Experimental data are needed to determine the feasibility of this technology. The work presented here discusses the current efforts at the National Renewable Energy Laboratory (NREL) toward deployment of this technology.

Research at NREL on microalgal technology has two major focuses. The culture studies described in this paper represent the work we are doing to develop technology for CO_2 trapping from power plant flue gas. The second, and related work, involves the development of genetically engineered algae capable of producing high levels of lipids for use in the production of biodiesel. The success of this technology depends on good coordination between these two efforts. This work is a good example of leveraged research between the Fossil Energy side of DOE and its Renewable Energy counterpart.

CULTURE STUDIES - Initial studies were carried out using a green alga, *Monoraphidium minutum* (NREL Strain Monor02). Particular emphasis was placed on the gas delivery apparatus, as efficient dosing of the flue gas is crucial to successful growth. Mass culture facilities typically provide CO_2 "on demand" as determined by pH of the culture. Appropriate dosing allows efficient utilization of the introduced carbon; which is important because the efficiency of CO_2 utilization will have a significant impact on process economics. Previous studies showed that exposing cultures to continuous dosing with simulated flue gas resulted in no evidence of growth or viability of the culture[6]. The experiments described here examine the effect of simulated flue gas containing 1990 CAAA levels of sulfur and nitrogen oxides on culture growth and biomass accumulation as a measure of carbon assimilation. The simulated flue gas contained 0.015% NO, 0.02% SO_2, 5% O_2, 13.6% CO_2, with the balance N_2. The control gas contained 13.6% CO_2, 5% O_2, with the balance N_2. Cultures were inoculated at $\geq 10^5$ cells/mL into a final culture volume of 300 mL (10% artificial sea water[7]). Light was provided continuously by Cool White® fluorescent bulbs at an intensity of ~200 uE $m^{-2}s^{-1}$. The cultures were continuously stirred with a magnetic stirrer at 150 rpm and the temperature was maintained at 25°C.

In the initial experiments, the cultures were exposed to either simulated flue gas or control gas delivered in three equal doses during an 8-h period each day. The flow rate in these studies was 60 mL/min at STP. Rate of growth, biomass accumulation, chlorophyll concentration, and pH were measured. In subsequent work the dosing rate was changed to determine if the carbon delivery scheme was limiting culture growth. The same total amount of carbon was delivered; however, the flow rate was decreased to 15 mL/min (at STP) in 2-min intervals 55 times during the 24-h period. Unlike the continuous sparging results, the two schemes for intermittent dosing of flue gas result in reasonable (and equivalent) growth. Figure 1 illustrates that there was no significant change in the rate of growth or total number of cells compared to the initial delivery schedule, suggesting that, over this range of flow rates, instantaneous carbon delivery rate is not limiting.

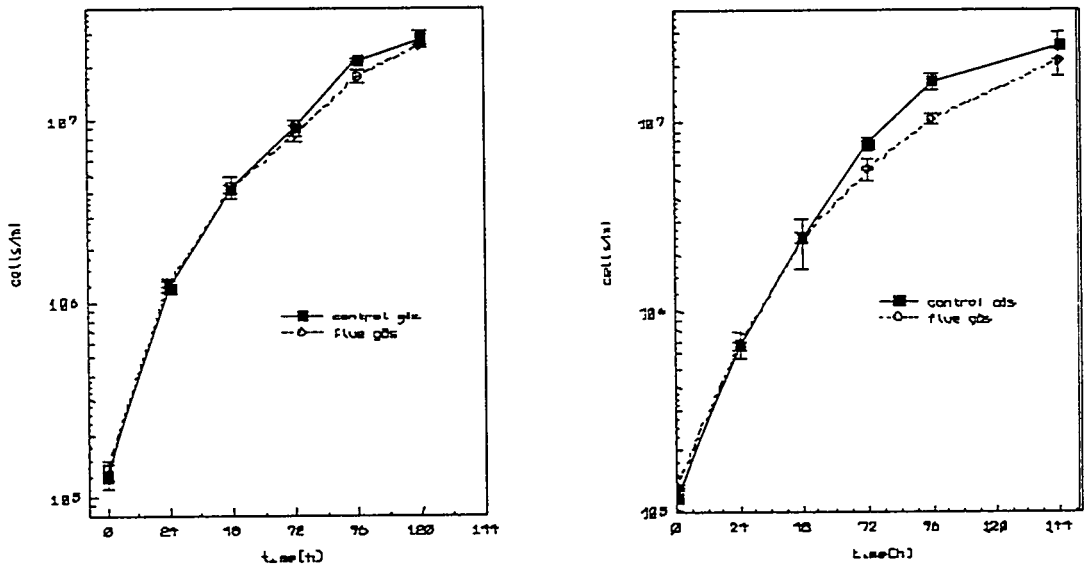

Figure 1. Comparison of cultures exposed to either 1990 CAAA simulated flue gas or control gas at 60 mL/min (at STP) three times per 24 h (left panel) or at 15 mL/min (at STP) 55 times per 24 h (right panel).

There is no significant difference in the rate of growth between cultures exposed to simulated flue gas and those exposed to control gas. These data indicate that 150 ppm NO and 200 ppm SO_2 do not inhibit culture growth under these conditions. Many of these experiments were carried out for as long as two weeks without evidence of inhibition. This is particularly encouraging because an accumulation of acidic sulfur species in the media could inhibit growth. Measurements of pH during the course of the experiment indicate that pH rises as biomass increases (data not shown). Early in the experiments, when biomass is low, the pH-lowering effect of the exposure to the gases is more significant even though the medium is buffered. The pH profile of media (that does not contain biomass) sparged with simulated flue gas or control gas does not exhibit this increase in pH in later time points (data not shown).

In the next series of experiments, the gas delivery and all other experimental conditions were as described above (using the 55 dose-per-day delivery scheme) except that the nitrogen concentration was increased threefold and the phosphorus concentration sixfold. Cell number, biomass and chlorophyll concentration increased dramatically at these higher nutrient levels (see Table 1).

	Low Nutrients 1.76 mM nitrate 36 μM phosphate		**High Nutrients** 5.28 mM nitrate 217 μM phosphate	
Measured Parameter	**Control Gas**	**Flue Gas**	**Control Gas**	**Flue Gas**
Ash-free Dry Weight (g/L)	1.32 ±0.0006	1.25 ±0.031	1.88 ±0.031	1.70 ±0.0474
chlorophyll (ug/mL)	7.40 ±0.087	9.08 ±0.308	39.17 ±0.662	41.39 ±0.345
cell number (x 10^7)	3	3	10	9

Table 1. Comparison of the effect of increased nitrogen and phosphorus on growth, biomass and chlorophyll concentrations for cultures exposed to either simulated flue gas or control gas (sparging was at 15 mL/min for 2 min., 55 times per 24 h).

The impact of these findings is that changes in the culture medium result in highly significant increases in the amount of carbon assimilated as reflected by fixation into biomass. Elemental analysis has shown these cells are approximately 50% C (data not shown). Based on the amount of carbon the cells were exposed to, we can estimate that at least 50% of the carbon supplied to the cultures has been fixed into biomass (data not shown). This is a high efficiency of utilization for a system which has not been optimized for maximum assimilation.

ECONOMIC MODEL - A spreadsheet-based (Microsoft Excel 5.0) economic model was developed for biological trapping of CO_2 from flue gases using microalgae. The rationale behind this approach was that a spreadsheet-based model is compliant and easy to manipulate. Information from the report by Neenan *et al.*[2] was used to develop a design basis for a "base case" process.

The model's consistency was judged to be satisfactory as the $400./t base-case algae cost is within 2% of that reported by Neenan *et al.* for the same "base case.".

The base-case process represents only the current state of technology; the "improved process" illustrates the potential that can be reached with some efforts devoted to research and development. An improved-case design basis was developed based on improvements potentially achievable in the near term. Table 2 provides a comparison of the two cases in terms of process parameters and cost performance in 1994 dollars. Table 3 summarizes the design parameters characterizing the improved process.

Table 2. Comparison of the Base Case Process and Improved Process (1994 $)

	Base Case Process	Improved process
Cell concentration, g/L	0.8	1.2
Lipid content, % wt	30	50
Residence time, d	7	4
Operating season, d/yr	250	300
Productivity, $g/m^2/d$	17.1	45
Photosynthetic efficiency, %	4.9	14.6
Algae cost, $/t	441.6	259.5
Lipid cost, $/bbl, $/gal (unextracted)	205.8 / 4.90	72.5 / 1.73
Lipid cost, $/bbl, $/gal w/ CO_2 credit[1] (unextracted)	170.4 / 4.06	45.2 / 1.08
CO_2 cost, % of annual cost	22.8	49.8
CO_2 mitigation cost[2], $/t CO_2	216.8	45.6

[1]CO_2 credit = $50/t CO_2
[2]Based on credit at the following rate: lipid = $240/t, protein = $120/t, carbohydrate = $120/t

Model Predictions - The updated model allows us to make some observations about the process. This model demonstrates in quantitative terms that our targeted improvements for productivity and lipid content more than double the relative impact of CO_2 collection cost on total annualized cost of the technology (see Table 2). Thus, cost-effective CO_2 collection and efficient delivery and utilization of CO_2 is even more important for the improved process. Accurate estimates for the cost of CO_2 collection are now being developed in order to provide a clearer understanding of this major cost component.

Model predictions were also used to compare the microalgal technology with alternative technologies for CO_2 mitigation costs. For an assumed cost of $66/t for CO_2 collection, the overall CO_2 mitigation cost for microalgal technology is $45.6/t for a targeted lipid content of 50% and a cell productivity of 45 $g/m^2/d$. This cost is competitive with other CO_2 remediation methods being proposed such as absorption with MEA (monoethanolamine).[8] Hence, deployment of this technology for CO_2 mitigation looks attractive if the parameters of the improved process are met. This assumes that there will be a market demand for CO_2 mitigation technology per se, which may not be generally true beyond limited niche situations. For this reason, our long term goal for the technology is to achieve zero cost for CO_2 mitigation. The current model will be used (and expanded) to assess the most effective engineering research directions to pursue towards this goal.

Table 3. Design Parameters for the Improved Process

			Source of Value
Facility Parameters			
Facility size	ha	1000	Neenan, p. 43
Module size	ha	20	Neenan, p. 53
Number of modules		43	Calculated
Total CO_2 processed	mt/yr	178284	Calculated from mass balance
Effective culture area fraction		0.86	Neenan, p. 53
Resource Parameters			
Land cost	$/ha	1420	Adjusted to 1994 (Neenan, p. 53)
Energy cost	$/kwh	0.065	Neenan, p. 53, assumed unchanged
Water cost	$/m^3	0.067	Neenan, p. 53, assumed unchanged
CO_2 cost	$/m^3	0.13	Adjusted to 1994 (Neenan model)
Evaporation rate	m/d	0.0035	Neenan, p. 53
Salinity of source water	g TDS/L	25	Neenan, p. 53
Biological Parameters			
Lipid content	wt. fr. dsb	0.5	Assumed
Protein content	wt. fr. dsb	0.2	Assumed
Carbohydrate content	wt. fr. dsb	0.12	Assumed
Ash content	wt. fr. dsb	0.08	Neenan, p. 54
Intermediate content	wt. fr. dsb	0.10	Neenan, p. 54
Solar radiation	kcal/m^2/d	5000	Neenan model, ref.dat
Photosynthetic efficiency	%	14.6	Calculated, Neenan p. 107
Salinity tolerance	g TDS/L	35	Neenan, p. 54
Operating Parameters			
Operating season	d/yr	300	Assumed
Cell concentration	g dcw/L	1.2	Assumed
Residence time	d	4	Assumed
Productivity	g/m^2/d	45.0	Calculated
Algal production, gross	mt/y	94041	Calculated
Lipid production, gross	mt/y	47021	Calculated
Downstream Processing Parameters			
Concentration factor, 1st stage, microstrainers		10	Neenan, p. 49
Concentration factor, 2nd stage, centrifuges		15	Neenan, p. 49
Concentration factor, overall		150	Calculated
Harvest efficiency, overall		0.95	Neenan model, ref.dat

Sensitivity Analysis - The economic model was used to study the effects of some key parameters on the process. CO_2 collection cost, lipid content, and residence time were selected for the sensitivity analysis due to their potential impact on process economics. Figure 2 shows the sensitivity of CO_2 mitigation cost to lipid content and CO_2 collection costs for the improved process. Utilization of algal biomass determines the economics of algal technology for CO_2 remediation. Algal biomass can be burned with coal or algal lipids can be extracted and converted to biodiesel. The higher specific energy of lipids is a benefit in co-burning. The desirability of higher lipid content is obvious if the algal biomass is to be used as a biodiesel feedstock. Thus, high lipid content confers a significant economic benefit to the process. In this model, credits are assumed for the value of lipids used for biodiesel manufacture and for the value of remaining carbohydrate and protein byproducts.

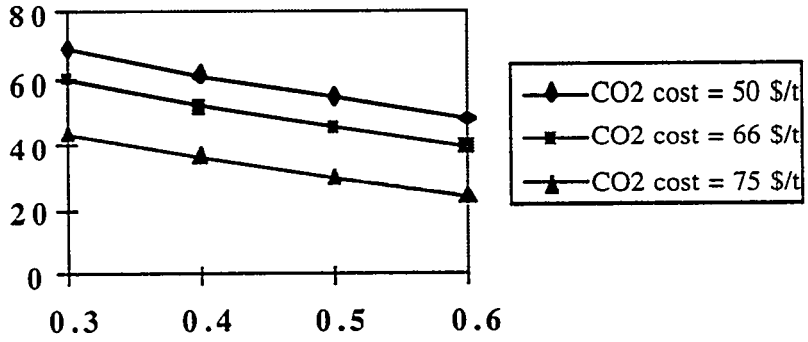

Figure 2. CO_2 mitigation costs ($/mt CO_2) at different lipid fractions and CO_2 Collection Costs.

Figure 3 shows the effect of dilution rate on CO_2 mitigation costs at different lipid fractions. The dilution rate, which is an inverse of the residence time and is directly related to biomass growth rate, determines the throughput at a given pond volume. As is evident from Figure 2, CO_2 mitigation costs rise precipitously at lower dilution rates. Hence, operating at a relatively high growth rate is important for an economical process. While there is an ability to trade off increases in growth rate for increases in lipid content, it is clear that increasing growth rate should be a research priority because of its strong impact on overall cost.

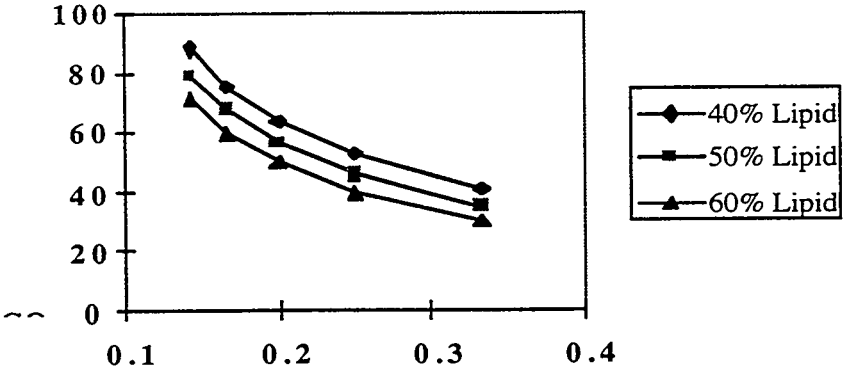

Figure 3. CO_2 mitigation costs ($/mt of CO_2) at different dilution rates and lipid fractions.

FUTURE TECHNICAL WORK - To date, we have identified one strain of green algae with relatively good growth rates, even in the presence of pollutants found in a simulated flue gas. Nutrient levels are also an issue. The two sets of experiments run at different levels of nitrogen and phosphorus demonstrate the effect of nutrient levels on CO_2 assimilation and cell growth. Further studies are needed to optimize nutrient levels based on a balance between nutrient supply costs and improved performance. The combined results of our experimental and economic analysis point toward an immediate need to develop high growth rate algae. We need to expand the range of organisms available for this application, and develop a clearer understanding of how to optimize growth rates of these organisms in order to achieve the goals identified in the economic analysis. In the mean time, efforts to develop genetically engineered strains capable of high lipid production also need to continue. Finally, as part of our effort to reach a long term goal of zero cost, we need to develop new process options beyond those used in the current economic model.

A STRATEGIC PERSPECTIVE - In addition to understanding the steps required for technology improvement, we are continually reassessing the broader, strategic perspective for microalgal technology which considers both internal and external factors that can influence our progress. For the purposes of this discussion, internal factors are the kind of technology-related issues discussed in the first paragraph. External factors are often overlooked in planning research strategies. They run the gamut from political issues to environmental and economic concerns. External factors which present obstacles for the development of microalgal trapping of CO_2 include:

- a utility industry focused almost exclusively on cost competitiveness in light of future increased deregulation
- continued uncertainty about the effects of greenhouse gases
- political pressure against "unfunded federal mandates" and general downsizing of government

On the positive side, opportunities include:

- a long term need for domestic transportation fuels and an increased use of coal
- a developing market for biodiesel in the U.S. as an outlet for microalgal products
- niche opportunities with more forward-thinking companies already exploring options for CO_2 mitigation
- spin-off opportunities in the growing plant biotechnology industry

Our approach, based on this strategic analysis, represents a balance between near term and long term concerns. In the past year, we have initiated R&D support to develop near term higher value niche opportunities for biodiesel, and for possible high value spin-offs from our algal technology development program. We are seeking out strategic partnerships in industry (including utilities, plant biotech companies, biodiesel start-up companies and others) to accelerate research progress and to leverage limited government funds. In the end, we need to balance these activities with our long term goal of providing a "no regrets" option for CO_2 mitigation and for meeting the needs of the transportation sector for domestic, renewable sources of fuels.

ACKNOWLEDGMENTS

The culture studies and economic analysis presented are being funded by the Department of Energy's Pittsburgh Energy Technology Center. Biodiesel and lipid genetics work are being supported by the Department of Energy's Biofuels Systems Division in the Office of

Transportation Technologies. We would like to acknowledge the contributions of Dr. Lewis Brown, formerly of NREL.

REFERENCES

1. C. R. Pauley, The Dow Chemical Co., *Chem. Eng. Prog.* (May 1984).
2. B. Neenan, D. Feinberg, A. Hill, R. McIntosh and K. Terry, **SERI/SP-231-2550**, Solar Energy Research Institute, Golden, CO, 149 (1986).
3. L. M. Brown and K. G. Zeiler, *Energy Convers. Mgmt* Vol. 34, No. 9-11, 1005-1013 (1993).
4. P. L. Chelf, L. M. Brown and C. E. Wyman, *Biomass and Bioenergy* Vol. 4, No. 3, 175-183 (1993).
5. E. A. Laws and J. L. Berning, *Biotech. and Bioengineering*, Vol. 37, 936-947 (1991).
6. J. T. Hauck, G. J. Olson and M. B. Perry, *Proceedings* from Ninth Annual Coal Preparation, Utilization and Environmental Control Contractors Conference, **U.S. DOE**, (1993).
7. L. M. Brown, *Phycologia*, **21**:408-410 (1982).
8. H. J. Herzog, Paper no. 94-RA113.02, Proc. 87th Air & Waste Manage. Assoc. Ann. Mtg. & Exhibit., Cincinnati, Ohio, 1994.

Observations of CO_2 Clathrate Hydrate Formation and Dissolution Under Deep-Ocean Disposal Conditions[1]

Robert P. Warzinski and Anthony V. Cugini
U.S. Department of Energy
Pittsburgh Energy Technology Center
Pittsburgh, PA 15236

Gerald D. Holder
Department of Chemical Engineering
University of Pittsburgh
Pittsburgh, PA 15261

1. INTRODUCTION

Disposal of anthropogenic emissions of CO_2 may be required to mitigate rises in atmospheric levels of this greenhouse gas if other measures are ineffective and the worst global warming scenarios begin to occur. Long-term storage of large quantities of CO_2 has been proposed, but the feasibility of large land and ocean disposal options remains to be established [1].

Determining the fate of liquid CO_2 injected into the ocean at depths greater than 500 m is complicated by uncertainties associated with the physical behavior of CO_2 under these conditions, in particular the possible formation of the ice-like CO_2 clathrate hydrate [1]. Resolving this issue is key to establishing the technical feasibility of this option. Experimental and theoretical work in this area is reported.

2. EXPERIMENTAL

Observations of the CO_2/water system were conducted in a high-pressure, variable-volume view cell. A description of the view-cell system as used in other work at temperatures above ambient has been published [2]. Modifications were made to permit the system to operate at temperatures in the hydrate forming region of interest (0°C to 10°C). The modifications included the incorporation of a cooling coil in the chamber containing the view cell, a small fan for improved air circulation in the chamber, and additional insulation.

Either potable water or water treated by reverse osmosis and deionization was used. CO_2 was obtained as a liquefied gas (99.5%) and used as received. In most experiments, water was first added to the cell then CO_2 was added either directly from the cylinder or from a high-pressure ISCO 260D syringe pump system. The cell was then chilled to the desired temperature and observations initiated. The pressure in the cell was varied during an experiment either by adding or venting CO_2 or by changing the position of a movable piston in the cell. Four phases are possible in this system: liquid water, gaseous CO_2, liquid CO_2, and solid CO_2 clathrate hydrate.

---

[1]This paper has been submitted and accepted for publication by Elsevier Science as part of the Proceedings of the 8th International Conference on Coal Science which is being held in Oviedo, Spain on September 10-15, 1995. Editors are J.A. Pajares and J.M.D. Tascón.

3. RESULTS AND DISCUSSION

Obtaining kinetic data applicable to the formation and decomposition of CO_2 hydrates under conditions that exactly simulate the deep ocean is not possible in the view cell or any similar device owing to contact of the CO_2 with metallic and glass surfaces. These surfaces promote nucleation and conduct heat differently than water and would therefore affect hydrate formation and dissolution. We are in the process of developing a system that precludes these problems. Described below are results obtained from experiments in the view cell that focused primarily on obtaining information that would provide important insights into the general behavior of the CO_2/water system under conditions anticipated for ocean disposal.

3.1 Phase behavior

The phase behavior of the CO_2/water system and the thermodynamic conditions for hydrate equilibrium have been determined [3]. The operation of the view cell was verified with this system by comparing the observed temperatures and pressures associated with hydrate formation and decomposition with the literature values. In these experiments, the conditions in the view cell were adjusted to obtain a lower water phase containing solid hydrates and an upper gaseous CO_2 phase. The presence of hydrates in the water phase provided nucleation sites for further hydrate growth. The amount of CO_2 in the cell and the position of the internal piston were adjusted to place the gas/liquid interface at a position convenient for observation. The pressure in the view cell was brought close to the value at which hydrate formation was anticipated. The pressure was then varied by small movements of the piston to cause additional hydrate to begin to either form or decompose at the CO_2/water interface. Phase changes could be detected with a pressure change of only 7.0 KPa, which was essentially the readability of the Heise gauge in use at this time. The pressures observed at the phase transition were near the literature values. For example, the phase transition occurred in the view cell at 3.06 MPa at 7.4°C to 7.5°C. The literature value was 3.08 MPa at 7.45°C [3].

3.2 Hydrate density

Pure CO_2 hydrates are denser than water or sea water and should sink [4]. Apart from any adverse ecological effects, this would be viewed as a benefit since it could result in very long CO_2 residence times in the ocean. However, some experimental accounts report that CO_2 hydrates float on the surface of water or seawater [5,6]. To help resolve this issue, observations were made of the relative densities of hydrates formed under various conditions in the view cell.

Observations were made on hydrates formed either (1) at the CO_2/water interface with gaseous CO_2, (2) at the CO_2/water interface with liquid CO_2 above the water, (3) in the CO_2 vapor space above a water phase, or (4) in a completely hydrostatic system from liquid CO_2 droplets. In all cases, once hydrate formation started, the hydrates grew rapidly and were snow-like in appearance. The hydrate masses were then broken apart using a magnetic stirring bar in the view cell. The snow-like hydrates were positively buoyant in the water phase. However, with extended time, the hydrates became more ice-like (transparent) in appearance and tended to sink in the view cell. Trapped, unconverted CO_2 may have caused the bulk density of the initially formed hydrates to be less than that of water. With time, this trapped CO_2 could be converted to hydrate, causing the density to increase and the appearance to change. It is interesting to note, that the hydrates sometimes formed a semi-solid mass which occupied the entire water phase. This mass did not impede the movement of the stirring bar but showed no evidence of rising or settling in the cell.

To study hydrate formation from one homogeneous phase, 1.75 g of CO_2 was dissolved in 30.0 g of water in the view cell at 18°C and 14 MPa. This solution would be about 80% saturated at 12°C and 12.662 MPa [7]. The cell was gradually cooled without stirring. Hydrates formed from solution near 5.0°C and 12.40 MPa. At the time of formation, the hydrates were ice-like in appearance and rapidly sank when disturbed by moving the stirring bar. The hydrates were observed for 16 hours under these conditions and appeared to be stable. Later in the experiment, they began to decompose without stirring when the view cell reached 5.4°C. Forming the hydrates from dissolved CO_2 appears to avoid the problem of entrapped CO_2 and results in hydrates that are denser than water.

3.3 Fate of hydrate-coated droplets

The last experiment described above was continued by introducing a liquid CO_2 droplet into the hydrate-containing water phase while the hydrate was still present. It immediately formed a hydrate coating but then exhibited no further change over a period of several hours in a non-agitated system. We have made similar observations in other experiments at different conditions.

When the hydrate coating formed on a CO_2 droplet in water relatively unsaturated with CO_2, the droplet shrank in size as it dissolved. For example, at 6.5°C and 11.1 MPa, a 2.6-mm diameter droplet decreased in radius at a rate of 0.0045 cm/h with slow agitation in the view cell. In the absence of a hydrate coating, a droplet of similar size at 6.1°C and 12.6 MPa decreased in radius at 0.10 cm/h. In comparison, Shindo et al. [8] measured dissolution rates of hydrate-covered CO_2 droplets at 28 MPa to 32 MPa (no temperature given) and found that they decreased in radius at a rate of 0.09 cm/h. The difference in rates may be due to dissimilarities in the experimental procedures and apparatus; however, differences in the thicknesses of the hydrate coating may also have been a factor.

The importance of understanding the kinetics of hydrate formation and dissolution may be illustrated using an earlier model we developed to determine the fate of liquid CO_2 droplets injected into the ocean [4]. At the time, the best kinetic data available for estimating the growth rate for CO_2 hydrates was that obtained from recent vapor phase studies. The above observations indicate these values may not be the most appropriate. Instead of growing in thickness as originally assumed, the hydrate layer on a droplet may remain relatively thin and serve to slow the dissolution rate of the CO_2 into the ocean.

The following illustrates the consequences of both scenarios on ocean disposal of CO_2. The original model predicted that a 1-cm droplet would need to be injected at 1900-m depth to insure effective sequestration if the hydrate shell thickness grew at a steady rate of 0.02 cm/h. In this case, the particle would begin to sink after rising to approximately 500 m owing to the thickening hydrate shell being denser than sea water. If instead of forming more hydrate, the particle dissolved at a rate of 0.09 cm/h, a 1-cm hydrate-coated droplet would still have to be injected at great depth. In this case, a depth of 1500 m would be required for the droplet to be completely dissolved by the time it reached 500 m. For the slower dissolution rate of 0.0045 cm/h, complete dissolution of the rising droplet would not be achieved before 500 m, even if injected at depths approaching those where liquid CO_2 becomes denser than seawater (approximately 2700 m). If injected at depths greater than 2700 m, the CO_2 would sink regardless of hydrate formation. Injection depths greater than 1500 m are not practical at

present [1]; thus understanding and controlling hydrate formation are paramount to successful sequestration of CO_2 in the ocean.

4. CONCLUSION

The observations made in the view cell and the recent observations of others have implications for the effective disposal of CO_2 in the ocean. Simply discharging the CO_2 at great depths may be insufficient if hydrate coatings form on liquid droplets of CO_2. Observations of single droplets indicate that the coating may impede the dissolution and permit the CO_2 droplet to rise to unacceptably shallow depths. Also, the possibility of growth of the hydrate shell cannot be ruled out based on observations of single droplets. In the vicinity of the injection device, the ocean will likely be near saturation owing to the enormous amounts of carbon dioxide being injected. If CO_2 cannot dissolve, then the growth of the hydrate coatings becomes more likely, especially as droplets collide and fresh CO_2 is released.

A better strategy than direct discharge would be to mix the CO_2 and water prior to reaching hydrate-forming depths and then introduce the mixture into some type of confined region that either permits pure hydrates to form under controlled conditions or fosters the growth of the hydrate coatings on CO_2 droplets. Density observations in the view cell indicate that pure hydrates formed in the first case would be negatively buoyant and sink. In the second case, if the hydrate coating contains more than approximately 30% of the CO_2 in the particle, the particle will also sink. Problems with plugging in the event of a flow interruption in such systems may be avoided by operating at slightly undersaturated conditions with respect to CO_2. Observations in the view cell indicate that these conditions favor the formation of a semi-solid mass rather than a solid hydrate plug.

ACKNOWLEDGMENT

The authors would like to thank Richard Hlasnik and Jerry Foster for performing the view cell experiments.

DISCLAIMER

Reference in this report to any specific product, process, or service is to facilitate understanding and does not imply its endorsement or favoring by the United States Department of Energy.

REFERENCES

1. DOE Report DOE/ER-30194, A Research Needs Assessment for the Capture, Utilization and Disposal of Carbon Dioxide from Fossil Fuel-Fired Power Plants, July 1993 (available NTIS).
2. R.P. Warzinski, C.-H. Lee, and G.D. Holder, J. Supercrit. Fluids, 5 (1992) 60.
3. A.T. Bozzo, H.-S. Chen, J.R. Kass, and A.J. Barduhn, Desalination, 16 (1975) 303.
4. G.D. Holder, A.V. Cugini, and R.P. Warzinski, Environ. Sci. Tech., 29 (1995) 276.
5. C.H. Unruh and D.L. Katz, Petroleum Transactions, AIME, (April 1949) 83.
6. S.M. Masutani, C.M. Kinoshita, G.C. Nihous, T. Ho, and L.A. Vega, Energy Convers. Manage., 34 (1993) 865.
7. R. Weibb and V.L. Gaddy, J. Am. Chem. Soc., 60 (1940) 815.
8. Y. Shindo, T. Hakuta, Y. Fujioka, K. Takeuchi, and H. Komiyama, Abstracts Second International Conference on Carbon Dioxide Removal, Kyoto, Japan (1994), 44.

Environmental Impacts of Ocean Disposal of CO_2

Eric Adams
Senior Research Engineer
Department of Civil & Environmental Engineering
Massachusetts Institute of Technology

Howard Herzog
Principal Research Engineer
Energy Laboratory
Massachusetts Institute of Technology

David Auerbach
Graduate Student
Department of Civil & Environmental Engineering
Massachusetts Institute of Technology

Jennifer Caulfield
Graduate Student
Department of Civil & Environmental Engineering
Massachusetts Institute of Technology

Overview

One option to reduce atmospheric CO_2 levels is to capture and sequester power plant CO_2. Commercial CO_2 capture technology, though expensive, exists today. However, the ability to dispose of large quantities of CO_2 is highly uncertain. The deep ocean is one of only a few possible CO_2 disposal options (others are depleted oil and gas wells or deep, confined aquifers) and is a prime candidate because the deep ocean is vast and highly unsaturated in CO_2 . The term disposal is really a misnomer because the atmosphere and ocean eventually equilibrate on a timescale of 1000 years regardless of where the CO_2 is originally discharged. However, peak atmospheric CO_2 concentrations expected to occur in the next few centuries could be significantly reduced by ocean disposal. The magnitude of this reduction will depend upon the quantity of CO_2 injected in the ocean. as well as the depth and location of injection.

Ocean disposal of CO_2 will only make sense if the environmental impacts to the ocean are significantly less than the avoided impacts of atmospheric release. Our project has been examining these ocean impacts through a multi-disciplinary effort designed to summarize the current state of knowledge. The end-product will be a report issued during the summer of 1996 consisting of two volumes: an executive summary (Vol I) and a series of six, individually authored topical reports (Vol II). A workshop with invited participants from the U.S. and abroad will review the draft findings in January 1996.

The six topical reports cover the following subjects:

(1) CO_2 loadings/scenarios

(2) near field perturbations

(3) far field perturbations (performed under subcontract to SAIC, Inc.)

(4) impacts of CO_2 transport (performed under subcontract to UMass-Lowell)

(5) environmental impacts of CO_2 release

(6) policy and legal implications of CO_2 disposal

Each subject area is summarized briefly below with elaboration given to the near field perturbations and environmental impacts of a dry ice release.

CO_2 loadings/Scenarios

A 500 MW_e pulverized coal fired power plant is chosen as a reference. Without capture, this plant will emit CO_2 to the atmosphere at the rate of 115 kg/s (Herzog and Drake, 1993). With ocean disposal we assume 90% CO_2 capture efficiency and a 20% energy penalty. The energy penalty implies that net energy production with capture is reduced by 20% for a given energy input or, alternatively, that the required energy input for a given electrical output is increased by 25%. Considering a net electrical output of 500 MW_e, the effect of ocean disposal on a standard power plant is summarized below:

		Release of Carbon Dioxide	
	Net Power	To Atmosphere	To Ocean
Without Capture	500 MW_e	115 kg/s	0 kg/s
With Capture	500 MW_e	14.4 kg/s	130 kg/s

The emissions loadings are being studied as multiples of the standard power plant. The following matrix summarizes the scenarios that will be investigated:

	Number of 500 MW_e Power Plants (130 kg/s CO_2 per plant)		
Analysis	One	Ten	One Hundred
Near Field (<25 km)	Five injection scenarios with generic ambient conditions	Five injection scenarios with generic ambient conditions	–
Mesoscale (25 km-2500 km)		3-5 specific sites off eastern U.S. with a generic injection at depth of 1000 m.	
Far Field (300 km-global)	–	–	One scenario: 50% injected at 1000 m off Tokyo & 50% injected at 1000 m off New York

One power plant is essentially the lowest level of disposal anticipated while the emissions from ten power plants represent an upper limit on the amount of emissions that are expected to be disposed of at a single point for reasons of economy of transport. One

hundred plants represents a loading of about 1.6% of the world's total anthropogenic CO_2 emissions and, as such, is a lower bound on the global amount of ocean disposal which could "make a difference" to atmospheric CO_2 levels.

For the near field analysis, five injection scenarios are considered:

- a droplet plume injected at 1000 m
- a CO_2 lake on the ocean bottom below 3700 m
- a dense CO_2 seawater plume injected at or below 500 m
- dry ice cubes released from the ocean surface
- a CO_2 hydrate plume injected at or below 500 m

Near Field Perturbations

The five injection scenarios are evaluated using separate models to describe 3-D concentration distributions of excess CO_2 and trace gases such as SO_2 and NO_x. The principal impacts of each scenario - the decrease in pH - are quantified using two criteria. First the spatial distribution of pH change is calculated. Then the range of time-histories of passive organisms traveling through the plume is calculated. Absolute pH is used in order to correlate the experiences with appropriate mortality data.

Far Field Perturbations

Far field perturbations refer to the change in total CO_2 concentration and associated pH at mesoscale and global scale.

Mesoscale simulations are being run for various locations along the eastern U.S.. The mesoscale dispersion model is a stochastic particle model driven by an externally calculated, time-dependent 3-D velocity field. "Particles" of CO_2 are continuously released at an injection site of 1000 m and tracked as they are advected by ocean currents, which include a mean current and turbulent fluctuations. The concentration of CO_2 at any one time can be plotted at a resolution of $1/4 \times 1/4$ degrees latitude and longitude.

A global carbon cycle model is being used to predict far-field long-term pertubations associated with one hundred 500 MW_e powerplants: 50 off of Tokyo and 50 off of New York. Injection depths of 1000 m will be used and simulations will run through the year 2500. The global discharge of anthropogenic CO_2 will be modeled as a simple logistics function of time. The global cycle model is based on the non-biological ocean circulation model of Mairer-Riemer and Hasselmann (1987), with biological carbon cycle components described by Bacastow and Mairer-Riemer (1990).

Environmental Impacts of CO_2 Transport Systems

Enviromental impacts may occur at several stages of transport. The major impact of on-shore pipes occurs during construction when vegetation must be cleared and trenches dug. After construction, land and vegetation needs to be restored. In populated areas, it may be difficult to obtain rights-of-way. There is a remote chance of pipe rupture with the release of vaporized CO_2 . CO_2 is not toxic, but is an asphyxant. Models are being used to estimate the dispersal of this dense vapor and the risk to the surrounding environment.

The major impact of off-shore pipes will also occur during pipe-laying. The first few kilometers will be laid on the continental shelf which may include coral beds, sea vegetation and other marine habitats. Accidental rupture of the pipe would release CO_2

into the seawater, with partial dissolution. The rest of the released CO_2 would rapidly bubble up to the surface and reenter the atmosphere. The dissolved CO_2 will cause acidification of the seawater in the vicinity of the ruptured pipe.

The environmental impacts of tanker transport include (a) accidental releases with possible injury to the tanker crew; (b) release into the atmosphere of fuel combustion gases and particles. Both diesel and steam propelled tankers release into the atmosphere particles (flyash and soot), SO_2 and NO_x, and of course CO_2 .

For pipe transport, on-shore facilities include a pumping station and storage tanks. Construction may require coastal land acquisition and disruption of coastal habitat. There is also a remote risk of accidental release of pressurized, liquid CO_2 . For tanker transport, docking facilities will be required in existing harbors, or specially built ports.

If tanker transport is used for deep sea disposal, floating platforms must be used to unload CO_2 and pump it into a pipe extending from the platform. The floating platforms will cause minimal impact but may be a navigation hazard. The operating crew on the platform will be exposed to storms and other environmental hazards, as well as possible accidental release of pressurized, liquid CO_2 . The vertical pipe should not cause significant impact on the marine environment.

Environmental Impacts of Ocean Disposal of CO_2

Marine life can be classified into four groups: phytoplankton, zooplankton, nekton, and benthos. The groups that will be affected by a CO_2 plume depend on the injection scenario and many scenarios preclude certain types of organisms from harm. The dry ice scenario is discussed below, but the methods and considerations are applicable to other scenarios.

Policy and Legal Implications of CO_2 Disposal

Important considerations relate both to site-specific discharges within or near a country's Exclusive Economic Zone as well as large scale worldwide CO_2 disposal. The Law of the Sea and the United Nations Environment Programme Agenda 21 are tone-setting and establish our committment to curb CO_2 emissions. The London Dumping Convention, as well as other regional treaties, are more specific and classify materials. prohibiting the discharge of some to the ocean.

Worldwide CO_2 disposal would require international cooperation and funding. Presumably it would not be initiated without consensus that avoided impacts/risks of global change outweigh any impacts to the ocean. In opposition to this philosophy, international treaty language is moving toward a precautionary principle and frowns upon end of pipe solutions or solutions which transfer pollution from one medium (air) to another (water). Furthermore, the emotional response of non-governmental organizations (NGOs) can not be discounted.

Analysis for Dry Ice Disposal

The near field perturbations and associated environmental impacts for dry ice injection are considered as an example our methodology. Dry ice cubes must be as large as practical, to insure that only a small fraction of the dissolution occurs near the surface. Cubes with 3 meter sides released from a fixed point were chosen; one standard power plant requires the release of one cube every 320 seconds. CO_2 dissolution to the water column as a function of depth was based on Nakashiki *et al.* (1991).

To obtain a steady state solution the release was approximated as a continuous line source. Turbulence induced by the falling cube was added to a scale-dependent ambient

diffusivity (Okubo, 1973) to obtain the total diffusivity as a function of distance. The solution for the excess total CO_2 concentration is then given by

$$C(x,y,z) = \frac{\dot{M}/u}{\sqrt{2\pi}\sigma} \exp\left(\frac{-y^2}{2\sigma^2}\right)$$

where $\dot{M}(z)$ is the mass flux (kg/m-s) at depth z, u is the current speed (m/s), and $\sigma(x)$ is the lateral standard deviation (m) found from the total diffusivity.

Excess CO_2 concentrations due to the disposal of dry ice were calculated for the one and the ten plant scenarios for $u = 0.02$ and 0.10 m/s. Results for one plant with $u = 0.02$ m/s current are shown in Figure 1. The excess CO_2 was added to the ambient CO_2 to compute new pHs. A map of the change in pH can be seen in Figure 2.

The average ocean CO_2 concentration experienced by an organism passing through the region can be calculated by assuming that the organism is subject to the same diffusivity as the CO_2 . Thus

$$\bar{C}(x,y_o,z) = \frac{C_{max}}{\sqrt{2}} \exp\left(\frac{-y_o^2}{2\sigma^2}\right)$$

where $\bar{C}(x,y_z)$ is the average excess CO_2 concentration experienced at location x and z by an organism that passes through the plume at a lateral distance y_o from the source, and $C_{\max}(x)$ is the concentration at the centerline ($y = 0$) given above. $\bar{C}$ is used to calculate average pH as a function of time. At each depth, several lateral sections are selected and a representative experience is found based on the value of y_o at the middle of each section. Figure 3 shows the experiences at a depth of 900 m for ten power plants in a 0.02 m/s current.

The environmental impact assessment focuses on zooplankton and assumes conservatively that they have no CO_2 avoidance ability. Knowing the volume of water that will experience a given time history of pH, and knowing the population density of organisms in the water is sufficient to estimate the numbers of zooplankton affected by the CO_2 .

Most studies on the effects of pH have been on fish in acidified lakes in response to acid rain concerns. Still, several useful studies have been performed on marine zooplankton in which either the animals were exposed to a constant pH, and mortality assessed at different times, or the animals were exposed to various pHs for a given time and mortality assessed (Grice *et al.*, 1973, Calabrese *et al.*, 1966, Havas and Hutchinson 1982 and Bamber 1987). Results from these studies have been superimposed on Figure 4 to give an approximate map of expected mortality as a function of pH and exposure time. ('Isomortality' curves are drawn for 0%, 50%, and 90% mortality as guides.)

Near field output such as Figure 3 can be discritized to yield the number of hours over which various sections of the plume experience different values of pH. The cumulative impact of a time-varying exposure can be estimated by using the isomortalilty curves to convert exposures into a common metric. For example, on Figure 4, an exposure of 50 hours at pH 6.0 causes roughly the same 10% mortality as an exposure of 15 hours at pH 5.5. Hence we can approximate an exposure of 50 hours at 6.0 plus 10 hours at 5.5 as 25 hours at 5.5. For such an exposure, the graph gives a mortality of 50%. Equivalently, converting the exposures to a metric of hours at 6.0 instead of 5.5, gives a total exposure of 90 hours corresponding to about 40% mortality. The table below illustrates this procedure using data from Figure 3 and compares it with an alternative method (Schubel, 1978).

Section width (m)	hrs. at pH 5.5	hrs. at pH 6.0	hrs. at pH 6.5	hrs. at pH 7.0	mortality % 1	mortality % 2
0-20	.417	2.71	5.97	14.8	0%	2.2%
20-60	0	.90	7.71	15.0	0%	1.3%
60-120	0	0	6.39	16.0	0%	1.0%
120-240	0	0	0	19.4	0%	0.5%

mortality % 1 = mortality using method described above. % 2 = mortality following Schubel (1978).

The section in the first row above is closest to the plume centerline and would experience the greatest effect; these data are plotted in Figure 4. It is clear that even the most severely affected organisms would scarcely be affected (method 2 by design will give non-zero mortalities since it assumes no threshold but these small numbers should be considered artifacts). Thus, we can safely expect little or no harm to pelagic organisms from the scenario of falling dry ice cubes. It should be mentioned that yhe dry ice cube scenario is expected to have the least impact because of the large dilution. We are in the process of studying other injection scenarios using similar methodology.

References

Bacastow, R. and E. Maier-Reimer (1990). "Ocean-circulation model of the carbon cycle" *Clim. Dyn.* 4:95-125.

Bamber, R.N. (1987). "The effects of acidic seawater on young carpet-shell clams Venerupis decussata (ℓ) (Mollusca: Veneracea)" *Journal of Experimental Marine Biology and Ecology*, 108:241-260.

Calabrese, A., and H.C. David (1966). "The pH tolerance of embryos andlLarvae of Mercenaria mercenaria and Crassotrea virginica" *Biological Bulletin*, 131:427-436.

Grice, G.D., E. Hoagland and P.H. Wiebe (1973). "Acid-iron waste as a factor affecting the distribution and abundance of zooplankton in the New York Bight" *Estuarine and Coastal Marine Science* 1:45-50.

Havas, M. and T.C. Hutchinson (1982). "Effects of low pH on the chemical composition of aquatic invertebrates from tundra ponds at the Smoking Hills, N.W.T. Canada" *Canadian Journal of Zoology* 61:241-249.

Herzog, H.J. and E.M. Drake (1993). " Long-Term Advanced CO_2 Capture Options". IEA Greenhouse Gas R&D Programme Report, IEA/93/OE6.

Maier-Reimer, E. and K. Hasselmann (1987). "Transport and storage of CO_2 in the ocean – an inorganic ocean-circulation carbon cycle model" *Clim. Dyn.* 2:63-90.

Nakashiki,N., T. Ohsumi, and K. Shitashima (1991). "Sequestering of CO_2 in the deep-ocean: Fall velocity and dissolution rate of solid CO_2 in the ocean" Central Research Institute of Electric Power Industry, Technical Report EU91003.

Okubo, A. (1971). "Oceanic diffusion diagrams" *Deep-Sea Research* 18:789-802.

Schubel, J. R., C.C. Coutant, and P.M.J. Woodhead (1978). "Thermal effects of entrainment" in *Power Plant Entrainment, A Biological Assessment* (Schubel, J.R. Marcy. B.C. Jr. eds) Academic Press Inc., New York.

Figure 1: Additional CO_2 concentrations due to the addition of the emissions of one standard power plant as 3 meter blocks of dry ice

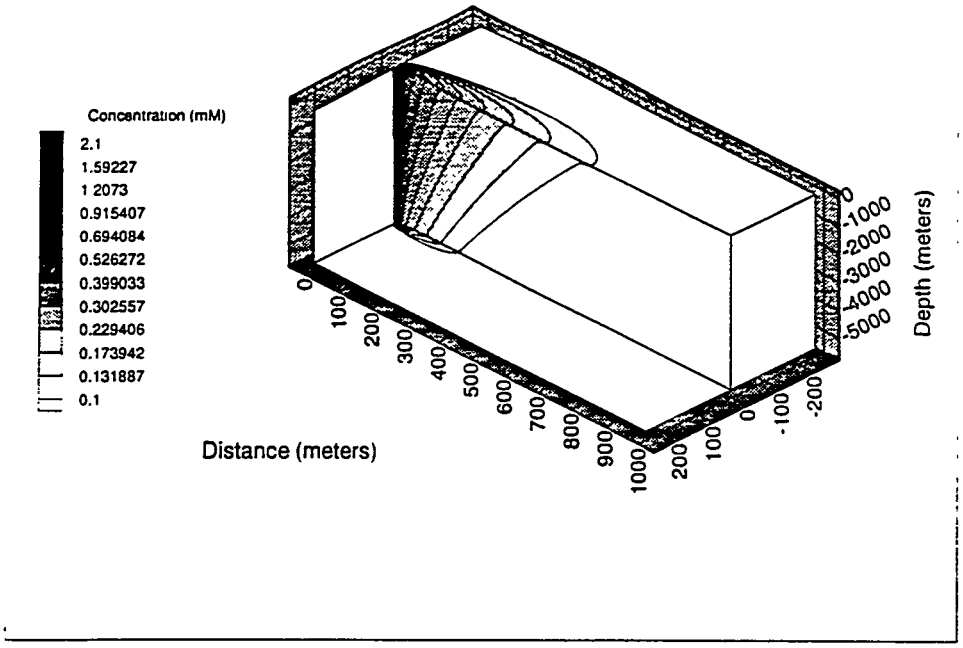

Figure 2: Change in pH resulting from dry ice addition

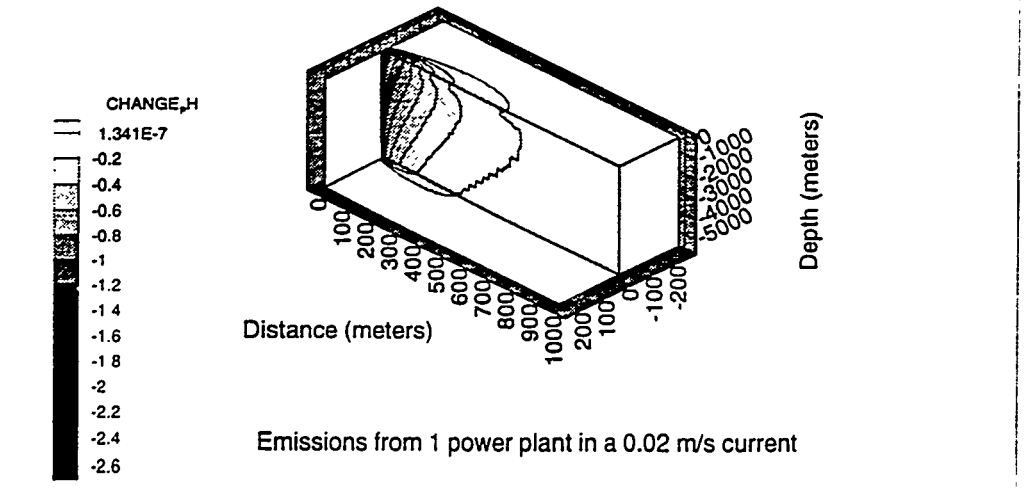

Figure 3: pH-Time experience for organisms at different distances from the plume centerline (conditions at a depth of 900 meters)

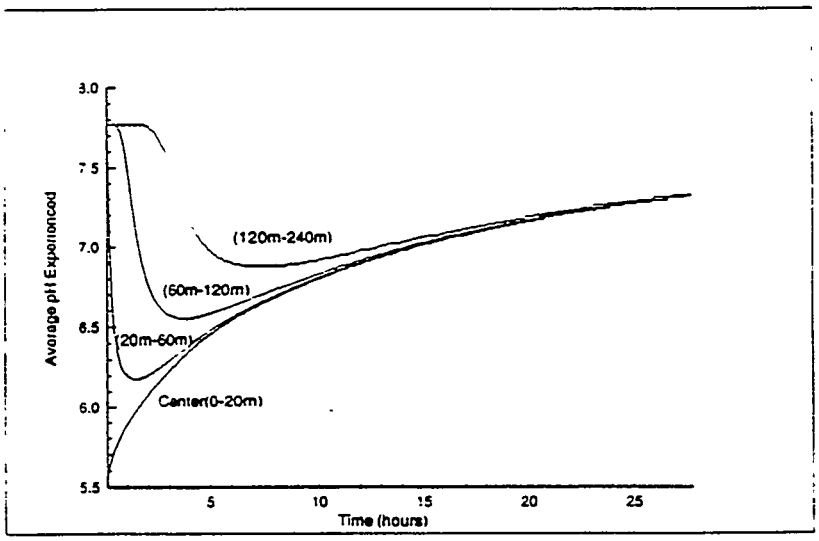

Figure 4: Mortality of zooplankton

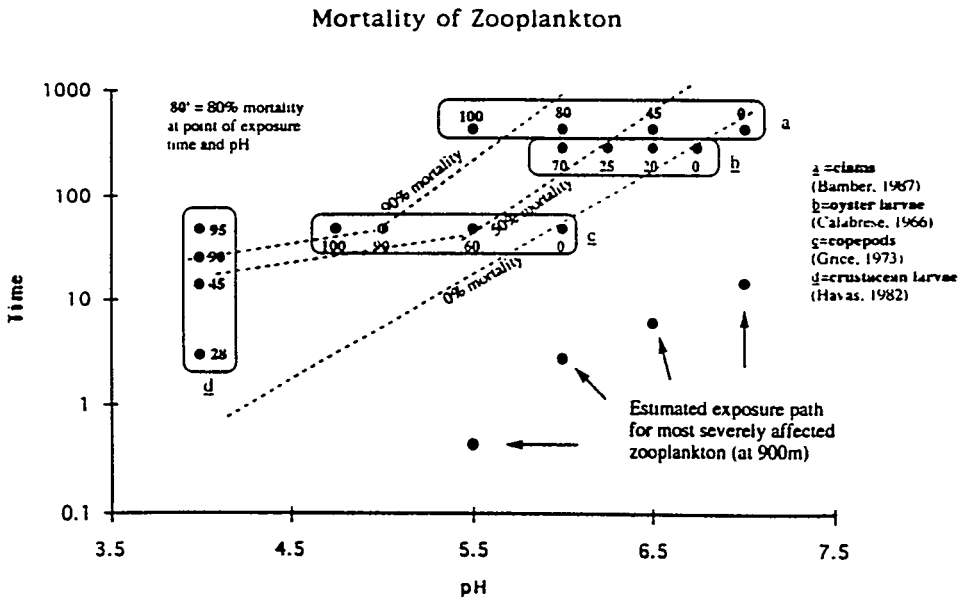

DISPOSAL OF CARBON DIOXIDE IN AQUIFERS IN THE U. S.

EDWARD M. WINTER
BURNS AND ROE SERVICES CORPORATION

PERRY D. BERGMAN
U.S. DEPARTMENT OF ENERGY
PITTSBURGH ENERGY TECHNOLOGY CENTER

ABSTRACT

Deep saline aquifers were investigated as potential disposal sites for CO_2. The capacity of deep aquifers for CO_2 disposal in the U.S. is highly uncertain. A rough estimate, derived from global estimates, is 5-500 Gt of CO_2. Saline aquifers underlie the regions in the U.S. where most utility power plants are situated. Therefore, approximately 65 percent of CO_2 from power plants could possibly be injected directly into deep saline aquifers below these plants, without the need for long pipelines.

INTRODUCTION

One of the options proposed for reducing the buildup of greenhouse gases in the atmosphere is to collect CO_2 from point sources, such as utility power plants, and dispose of the CO_2 by injection into underground structures, such as, abandoned oil and natural gas reservoirs or deep aquifers. This paper describes the the problems associated with locating and evaluating aquifers which are suitable for CO_2 storage in relation to utility power plant emission sources.

The locations of utility power plants and CO_2 emissions from each were taken from a Utility Data Institute (UDI) database. An estimate of aquifer disposal capacity was taken from recent International Energy Agency (IEA) reports. [1,2,3]

POWER PLANT SOURCES OF CO_2

CO_2 emissions from utility power plant CO_2 sources in the United States were calculated by using data on fuel type and annual consumption at each power plant. An average carbon content was used for each fuel type. The CO_2 emissions for 1990 are shown by state in Figure 1. The states with the highest CO_2 emissions are Texas (the largest emitter), Alabama, Georgia, Florida, and a belt of states extending across the upper Midwest from Missouri to New York. These 13 states generate almost 60 percent of U.S. power plant CO_2 emissions. The total CO_2 emissions from all power plants in 1990 was 2.0 Gt (giga tonnes). This estimate compares well with Energy Information Administration (EIA) calculations yielding 1.8 Gt CO_2. [4]

DISPOSAL OF CO_2 IN AQUIFERS

The aquifers most suitable for disposal of CO_2 are the deeper saline aquifers. Figure 2 shows the location of saline aquifers in the U.S. Approximately 65 percent of CO_2 power plant emissions comes from power plants which are situated directly above the aquifers shown in Figure 2. The capacity of saline aquifers for disposal is difficult to estimate because of a dearth of published data.

Figure 3 shows the effect of variations in underground pressure and temperature on storage efficiency. Some formations, mainly at shallow depths, will not be suitable for economical storage simply because low pressures will require much larger volumes of storage capacity per unit mass of CO_2.

The potential aquifer volume available for disposal of CO_2 has been estimated by a number of authors, the range of global totals corresponding to 100-10,000 Gt of CO_2. A recent IEA report discusses these estimates in detail [1] and also gives results of studies in three geographical areas, namely, 1) the Alberta Basin in Western Canada, 2) Senegal in Western Africa, and 3) East Midlands in the UK. The wide range of estimates shows the huge uncertainties involved. Many aquifers in the world are not close to power plants or other sources of CO_2 and cannot be used for storage. The IEA study team concluded that extrapolation of the limited data available to predict global potential was not reasonable at this time.

Prorating the range of capacities above, using relative land areas, gives an estimated disposal capacity in the U.S. of 5-500 Gt of CO_2. Further studies to determine aquifer capacity are obviously required.

By way of comparison, hazardous and nonhazardous industrial wastes in the U.S. are currently being disposed of by underground injection at the rate of approximately 75 million cubic meters per year (20 billion gallons per year). This volume corresponds to about 0.05 Gt of CO_2 or 1/40 the rate of CO_2 emissions from utility power plants.

Unfavorable CO_2 Flow Patterns

Super-critical CO_2, with a density of approximately 0.6 the density of typical brines, would be expected to rise to the top of a formation because of buoyancy. Also, since CO_2 at prevailing underground pressures and temperatures often has a lower viscosity than water, fingering would occur, that is, channeling and accelerated flow of the CO_2 phase relative to the native fluid. The CO_2 would tend to travel along the upper surface of the formation, moving rapidly in a geometry resembling fingers of flow out from the injection well and leaving behind pockets of the brine phase. Only a fraction of the native fluid in the aquifer would be displaced, and only a fraction of the aquifer volume would be filled by CO_2. The CO_2 would be expected to fill any trap (a stagnant pocket above the normal flow path) it might encounter, since the CO_2 is lighter than the formation water. Eventually, the CO_2 would continue on and reach the edge of the formation and escape earlier than the time calculated for the native fluid. It has been

estimated that possibly only 2-4 percent of the total volume of an aquifer would be filled with CO_2 because of these unfavorable properties. [5]

Limitations on Injection Pressure

The permissible injection flow rate depends on the rock permeability in the aquifer. If the permeability is low, the injection rate must be kept low to avoid excessive pressure. A pressure that is too high can cause either fracture of the cap rock and loss of containment or leakage around the injection well, or other wells nearby, within what is termed the cone of influence. The cone of influence is the region surrounding a waste injection well where injection pressure might cause damage to other wells, either operating or plugged and abandoned wells. The radius of this zone is at the discretion of each state but must be at least a quarter mile (0.8 km). In Texas, the cone of influence is taken as 2.5 miles (4 km). Regulations require that modeling of pressure-flow characteristics extend throughout this region when a permit is applied for. Monitoring of well pressure is required after a permit is issued and the well is in operation.

Multiple injection wells will undoubtedly be required. The CO_2 emitted from one moderately sized power plant is too much to be injected into underground storage sites through a single well. Several injection wells might be required, depending on power plant size and the permeability of the rock formation. These wells would have to be spaced a safe distance apart to avoid overpressuring. A network of connecting pipelines could be required, extending outside the boundaries of the power plant property. Or multiple non-vertical wells could be drilled from the same point at the surface at different angles.

Other Limiting Factors

Some authors have stated that geologic traps will be required for CO_2 disposal [1]. If this is the case, only a fraction of the aquifer volume would be available for disposal. Aquifers would be filled much sooner than if the whole aquifer could be used. Traps have not been identified in aquifers to the extent that they have in oil and natural gas containing structures. If traps are required, extensive drilling of test wells could be required to locate them. However, current practice in underground disposal of hazardous and nonhazardous industrial waste in the U.S. does not require injecting into a trap. Obtaining a permit can be based on modeling studies which show that the injected waste will not escape from the confining formation for at least 10,000 years. Very slow movement of the connate fluid in the formation, sometimes as low as a few centimeters per year, would give a retention time long enough to provide confinement for the required period.

The chemistry of some aquifer formations may not allow any disposal of CO_2 in them. Chemical reactions between the injected fluid and the reservoir rock can take place. For example, acid wastes have been known to react with limestone or dolomitic formations, liberating CO_2, which overpressured the formation and caused blowout of the well. If CO_2 is found to react unfavorably with certain types of rock structures, then these formations would not be suitable. The fluid can also chemically combine with the rock material, increasing the

storage capacity of the formation. Disposal capacity could be either reduced or increased depending on circumstances.

Different procedures and policies among various states can affect usable storage capacity. Title 40 of the Code of Federal Regulations, Parts 144-149, contains the regulations for underground injection control (UIC). It establishes minimum requirements for states to set up a UIC program and to obtain primary enforcement authority. Each state can adhere to the federal regulations or impose more stringent rules. Pennsylvania, for example, does not issue permits for underground injection at this time. Other states may have taken this position as well, either because their procedures have not yet been approved by the U.S. Environmental Protection Agency, or because of their policy position. A particular state may allow disposal of wastes in an aquifer, while an adjacent state does not issue permits for the same aquifer. Therefore, the presence of a suitable aquifer may not necessarily lead to approval for CO_2 disposal.

The agency issuing disposal permits is concerned about the fate of the waste material and the time required for the material to travel to the edge of the disposal zone and a number of other issues. What happens to the native brine is also important. The injected waste will displace the brine and may increase its flow velocity, resulting, for example, in increased rate of discharge into a lake or stream, which could handle the previous lower flow safely. Or the higher velocity may cause the brine to discharge along new paths into different zones, for example, mixing into drinking water aquifers that it previously bypassed. If modeling shows that CO_2 injection would accelerate the movement of hazardous and nonhazardous wastes injected in the past, states might limit or prohibit CO_2 injection into these aquifers, further reducing available capacity.

Several state agencies have reported growing resistance from the public to underground disposal of wastes. Permits are becoming harder to obtain. Acceptance of large-scale disposal of CO_2 by underground injection will require much more intensive research to minimize the technical uncertainties and risks.

CONCLUSIONS

The potential for CO_2 disposal in aquifers is very difficult to estimate from the information available. Disposal capacity is probably as great or greater than the capacity in oil and gas reservoirs. Many power plant CO_2 sources are closer to potential aquifer disposal sites than to large oil and gas reservoirs.

Based on this work, additional effort should be directed toward

- Locating and characterizing candidate aquifers to determine their potential for CO_2 disposal.
- Looking at possible chemical reactions between CO_2 and the formation rock.

- Modeling of CO_2 injection and movement into an aquifer to determine its capacity for storage.

REFERENCES

1. Stanley Ind Consultants, Aquifer Disposal of Carbon Dioxide, IEA/93/OE14, Chap. 10, pp. 1,2

2. Hendriks, C.A., Blok, K., "Underground Storage of Carbon Dioxide," Energy Convers. Mgmt. Vol. 34, 1993, pp 949-957.

3. Van der Meer, L.G.H., "The Conditions Limiting CO_2 Storage in Aquifers," Energy Convers. Mgmt., Vol 34, 1993; pp 959-966.

4. Emissions of Greenhouse Gases in the United States, 1985-1990, DOE/EIA-0573, 1993, p 13.

5. Van der Meer, L.G.H., Straaten, R.; Carbon Dioxide Disposal in Depleted Oil & Gas Wells, IEA/93/OE15, 1993; pp 7,66.

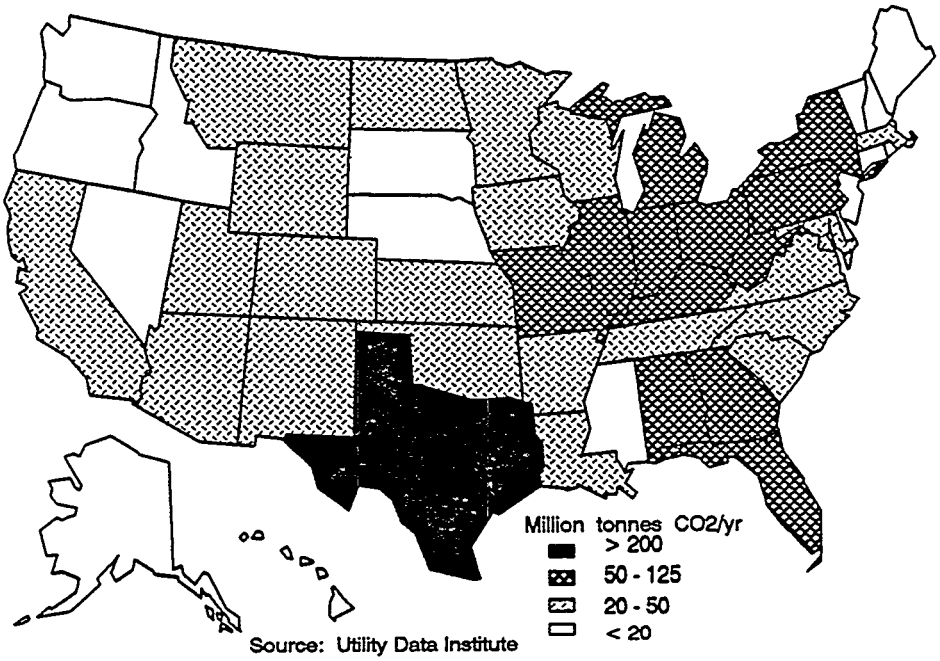

Figure 1. CO2 Emissions from Fossil-Fuel Fired Power Plants

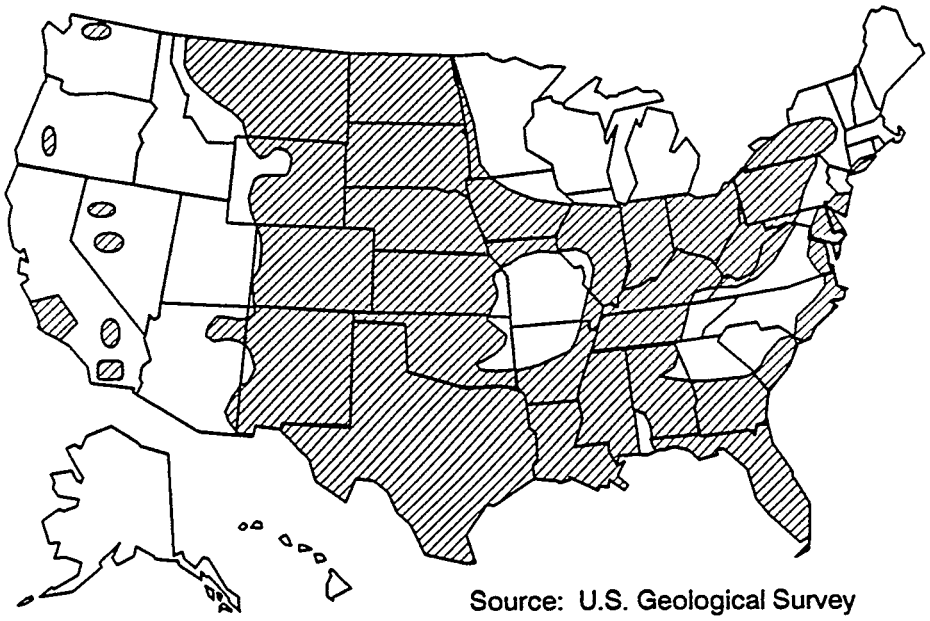

Figure 2. Saline Aquifers in the U. S.

Figure 3. Calculated CO2 Specific Volume at Various Depths
From Texas Natural Gas Reservoirs Atlas

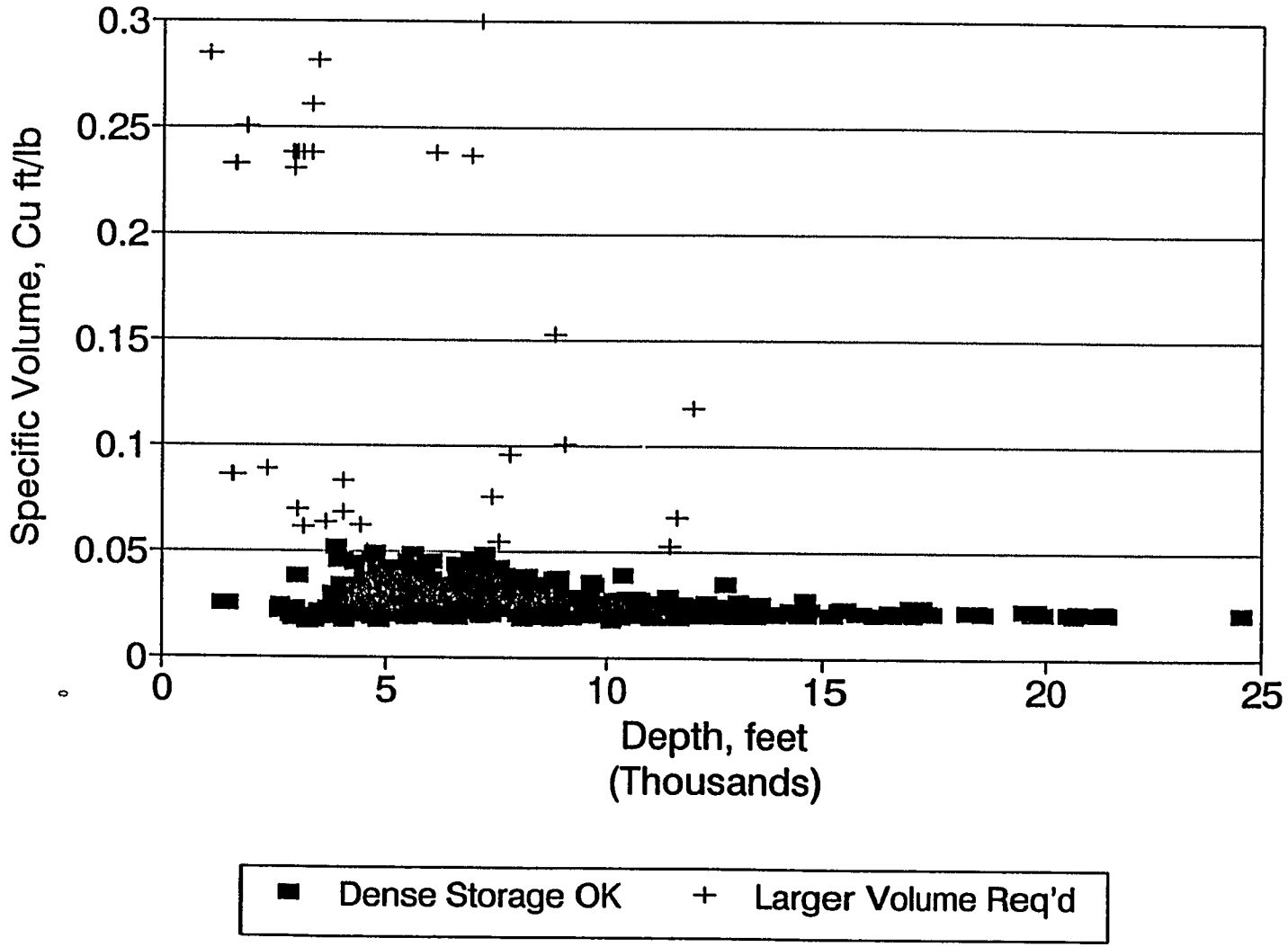

CO_2 CAPTURE AND BIOFUELS PRODUCTION WITH MICROALGAE

John R. Benemann
Department of Civil Engineering
University of California Berkeley
Berkeley, California, 94720

ABSTRACT

Microalgae cultivation in large open ponds is the only biological process capable of directly utilizing power plant flue gas CO_2 for production of renewable fuels, such as biodiesel, thus mitigating the potential for global warming. Past and recent systems studies have concluded that in principle this concept could be economically feasible, but that this technology still requires both fundamental and applied long-term R&D.

INTRODUCTION

The concept of the mass culture of microalgae, for foods, feeds and even renewable fuels production and CO_2 utilization for greenhouse gas mitigation, dates back about half a century (Burlew, 1953; Oswald and Golueke, 1960, see Benemann and Oswald, 1995). Since then the technology for microalgae cultivation has developed from an idea, studied in the laboratory and in very small outdoor systems ($< 10\ m^2$), to large-scale practical applications in wastewater treatment and the production of specialty human foods ("nutriceuticals") and animal feeds.

In wastewater treatment, the first practical application of microalgae culture, no specific algal species are cultivated, and, indeed, even recovery of the biomass is rare. In nutriceuticals production three specific genera of microalgae are being cultivated: Chlorella, Spirulina, and Dunaliella. The latter two are produced commercially in the U.S. (in California and Hawaii), and are also used in animal feeds, along with two recently introduced commercial microalgae being produced fermentatively: Schizochytrium and Spongiococcus. Small photobioreactors ($> 10\ m^2$) of various designs, are being used in the production of specialty aquaculture feeds and diagnostic reagents. Microalgae biotechnology is providing the basis for a growing industry in the U.S. and around the world (Benemann, 1990).

The production of commodities, feeds and fuels, with microalgae cultures has not yet been achieved. Currently microalgae biomass sells for roughly $25,000/ton (dry organic weight basis), while agricultural commodities cost less than $500/ton, and biomass fuels less than half that. The question arises if a two order of magnitude cost reduction could be achieved with current technology, or whether radically new production techniques and fundamental research breakthroughs are required.

The proposition argued herein is that for microalgal fuels production and CO_2 utilization both alternatives apply: Current technology for algal mass culture appears inherently capable of low-cost microalgal production, although only at very favorable sites. However, major technological advances will be required in many aspect of algal culture, in particular the ability to cultivate specific strains, at very high productivities, long-term culture stability, easy harvesting, and a high content of vegetable oils or other desirable compounds.

First the different large-scale microalgae production systems are described, followed by a review of the current state-of-the-art in microalgae culture, and concluding with a discussions of the research and development goals and needs in this field.

MICROALGAE MASS CULTURE SYSTEM DESIGNS

Three major types of systems are used for large-scale practical microalgae cultivation: extensive, intensive, and fermentative.

Extensive microalgae cultivation systems are typically large ponds (from under 1 hectare to up to 100 ha each), relatively deep (>50 cm), without mechanical mixing, or supply of CO_2. Such systems are used for the production of both Spirulina and Dunaliella, and, more widely, in municipal and industrial wastewater treatment. Extensive systems are inexpensive, consisting of simple earthworks with inlet/outlet structures. In extensive wastewater treatment systems no specific algal species are cultivated, and, indeed, may not be feasible to do so. Spirulina and Dunaliella are cultivated in highly alkaline (carbonate) or saline media, respectively, which allows the maintenance of these species as practically unialgal cultures, even in the in the uncontrolled environments of such extensive ponds.

Intensive systems use shallower (<30 cm) ponds, mechanical mixing, CO_2 supply, and hydraulic dilution rates that maintain the algal culture near optimal conditions. Much greater control over the pond environment is possible, and such systems achieve several fold higher productivities than extensive systems and, perhaps most important, can, at least in principle, maintain desired algal species. Of the large-scale intensive system designs, the most prevalent is a raceway ponds design, with ponds up to about 0.5 ha, and mixing typically by paddle wheels. Indeed, this is the basic design used for both Spirulina and one Dunaliella commercial operations in the U.S. Only three municipal wastewater treatment systems in the U.S. (in California) use intensive raceway ponds (mixed by pumps rather than paddle wheels). However, they do not use supplemental CO_2 to maximize algal production, or are specific algal strains cultivated, nor is the algal biomass harvested.

Recently algal production in dark fermenters (using sugars rather than sunlight and CO_2 as energy and C sources) has been developed commercially in the U.S., with two algae being produced: Spongiococcus, high in pigments useful in chicken feed, and Schizochytrium, high in omega-3 fatty acids, similar to fish oils, and useful as an

aquaculture feeds and, potentially, for human food. The price of these products is similar, or even lower, than outdoor pond cultivation costs. In conclusion, currently, microalgae production technology is only feasible for high cost specialty products.

LARGE-SCALE MICROALGAE PRODUCTION

For over three decades engineering cost analysis of increasing sophistication have concluded that it would be possible to produce microalgae at a large scale for the fuel production and utilization of power plant CO_2 (Oswald and Golueke, 1960, Benemann et al., 1982; Reagan and Gartside 1983, Neenan et al., 1986; Weissman and Goebel, 1987; Benemann and Oswald, 1995; see also Benemann, 1994 for a brief review). All these studies were based on similar intensive raceway pond designs, typically paddle wheel mixed. However, these designs also include some characteristics from the extensive systems: large individual growth ponds (10 ha or even larger), no plastic liners (used in most intensive algal production systems) and maximum economics of scale with production systems of 1,000 ha or more. Further, quite favorable assumptions are made about the site, from the cost of land (often negligible), to the low cost availability of water and a nearby power plant for a CO_2 supply. Even with such favorable assumptions and extrapolations, the economics of microalgae culture are still too high for fuel production, by an order of magnitude.

Low cost projections for microalgae production require additional assumptions:

1. The cultivation of genetically selected and improved algal strains in outdoor ponds for long periods with only, occasional, small, inoculations.
2. Achieving very high productivities, near the limits of photosynthetic efficiencies.
3. Production of biomass high in vegetable oils, hydrocarbons, or starches.
4. Harvesting the algal cells by simple sedimentation or other low cost processes.
5. Low cost processing the algal biomass to yield biodiesel and other fuels.

These assumptions represent the major R&D issues, and goals, in the development of a low cost process for fuels production and CO_2 mitigation, and are the main focus of this presentation. However, first some other issues are briefly addressed.

One is the potential of this technology for achieving significant reductions in power plant CO_2 emissions. The joint requirements for favorable climate, land, water, and CO_2 availability, limits this process to a small fraction ($< 5\%$, and probably only 1 - 2%) of U.S. power plant CO_2 emissions. However, even such modest reductions represents tens of millions of tons of CO_2 mitigation. Also, other arguments favor development of this technology, compared to the alternatives (see Conclusions).

Another issue is the technical feasibility of cultivating microalgae using power plant flue gases directly. Recent research in Japan (Hamasaki et al., 1995) and the U.S. (Brown et al., 1994), demonstrated that flue gas is a suitable CO_2 source for algal culture, with NOx, SOx, and other contaminants having little effect on algal growth and productivity. Thus, this is no longer a major uncertainty, and R&D can concentrate on the other, more important, issues, addressed next.

R&D ISSUES IN LARGE-SCALE MICROALGAE PRODUCTION.

Here a brief overview is presented of the issues that must be addressed in any R&D program for developing low-cost algal biomass production technologies. It should be recognized that these problems have, to various degrees, been the subject of much research over the past decades. Thus, one question is why they have, to a large part, not yet been resolved. The answer is that great progress has been made, much more is required. More importantly is the question of how likely they are to be solved in the foreseeable future, and what level of R&D funding would be required.

Cultivation of Selected Microalgal Strains

As stated above, only three algal genera are being commercially cultivated at a large-scale in outdoor ponds. Of these two (Spirulina and Dunaliella) require highly selective media (high bicarbonate and salinity respectively), which allows the maintenance of essentially unialgal cultures, even in extensive systems. However, even in intensive cultures these algal cultures also exhibit low productivities, about 20 to 30 t/ha/y (tons/hectare/year), a third to half of what is achieved by other algae, growing in less restrictive environments. The third microalga grown commercially (only in the Far East), Chlorella, is cultivated with great difficulty, as it has not been possible to maintain the culture for any length (more than a few days to a couple of weeks) in open ponds. Thus, large amounts of inoculum must be produced under highly controlled conditions, at high costs, and the cultures frequently restarted.

This commercial experience might suggest that it is not possible to grow microalgae in outdoor ponds, except for a few species that require unusual conditions and at relatively low productivities, or without inordinate efforts and costs for inoculum production. However, other experience contradict such a conclusion. A green alga, Scenedesmus, was successfully cultivated in simple inorganic freshwater media both in Germany (where this alga first was isolated from growth ponds) and several other countries (Egypt, Peru, Thailand), where commercialization of this technology was attempted. (The commercial failure of these projects, discussed in Benemann and Oswald, 1995, was related in large part to the high costs of harvesting and processing of the algal biomass, compared to its low value as a food and feed).

In intensive wastewater ponds unialgal Microactinium cultures were observed to dominate for many months, even years, over rather large ranges in weather and operating conditions (see review in Benemann and Oswald, 1995). Recently, in Japan, a single strain of Tetraselmis was successfully cultivated in small seawater-fed ponds with actual power plant flue gas for an entire year, under rather unfavorable climatic conditions. And work in New Mexico, sponsored by NREL (National Renewable Energy Laboratory), demonstrated the maintenance of some diatoms in large (1,000 m_2) outdoor ponds (Weissman and Tillett, 1989, 1992), experience that has been successfully applied in commercial bivalve aquaculture production (Weissman, personal communication, 1995).

One common thread in these, and other similar examples, is that the algal strains that successfully dominated such ponds are invading species, that take over from inoculated strains. Thus, making a virtue of necessity, it appears that it is, indeed, possible to cultivate selected strains in open pond cultures even in the absence of strong selective factors, such as high salinity or alkalinity. However, it is also clear that most strains favored by laboratory researchers, are not suitable for outdoor cultures. Thus, the approach to strain improvement should be to move from the outdoor ponds back to the laboratory, not, as has been singularly unsuccessful, to attempt to mass culture strains selected in the laboratory for some particular desired property (e.g. high lipid content, or availability of a genetic system, for example).

Of course, a strain that is relatively well adapted to the pond culture environment, and able to exclude or dominate other algal strains that contaminate the culture, is only a beginning. Successful algal mass culture also requires the control of grazers and other pests. Indeed, this is probably an even greater problem than avoiding the take-over by invading algal strains. Little information is available on this point either in the literature or from commercial operations (where grazer and infestation control generally is held as proprietary information). However, overall, although this is an important practical issue, it does not appear to be a fundamental limitation.

Maximizing Microalgal Biomass Productivities

In microalgae production for fuels and CO_2 mitigation, roughly half of the costs are productivity related. That is, doubling productivity would decrease costs of the final product (e.g. biodiesel) by a quarter. High productivities would also reduce land and water requirements and reduce transportation distances for flue gas, which would make this technology more widely applicable. Maximizing productivities must, thus, be a, if not the, major R&D objective in this field.

Although microalgae cultures have a reputation of very high productivities, this is not correct in actual practice: commercial, intensive, Spirulina production systems have productivities of perhaps only about 25 t/ha/y, which is similar to the gross biomass productivities of many agricultural crops. Of course, as noted above, the chemical environment in these ponds, is not conducive to high productivities. Productivities of algae in wastewater treatment, or of diatoms in brackish and seawater, are over 50 mt/ha/y, and it is likely that 100 mt/ha/y can be achieved at favorable climatic conditions with current technology. This would be similar to record, total biomass yields for the most highly productive higher plants, such as sugar cane, under ideal conditions.

Even higher productivities, 200 mt/ha/y or more should be achievable if the algal cultures are operated near the generally accepted limits of photosynthetic light energy conversion efficiencies, about 10% of solar energy. Indeed, such high conversion efficiencies are routinely obtained in the laboratory, but only at low light intensities. At full sunlight intensities, efficiencies are dramatically reduced,

typically by 50 to 80%, due to the light saturation effect. Essentially, algal cells in a typical culture have more light harvesting pigments (chlorophylls and others) than needed at high light intensities. This results in the algal cells near the surface absorbing more photons than they can readily use, with the excess being lost as heat and fluorescence, rather than being used for CO_2 fixation. The cells a bit further down the water column are shaded, and thus do not get enough light to grow. In theory, it would be relatively simple to use algal strains that have fewer light harvesting pigments. However, such strains are not found in nature (as they would have a competitive disadvantage) and must, thus, be developed by genetic selection and engineering techniques. Of course, such research should, after proof of concept, be carried out with algal strains known to be able to compete in outdoor ponds.

Production of Microalgal Biomass with High Oil Content.

The objective of microalgae cultures for CO_2 utilization is to produce substitutes for fossil fuels, thereby cutting overall CO_2 emissions. Due to the higher value of liquid fuels, compared to solid or even gaseous fuels, these have been the major objective in the microalgae field in recent years. Three types of liquid fuels could be produced from microalgae: ethanol, biodiesel, and liquid hydrocarbons. Ethanol could be fermented from the starch that is accumulated by many types of microalgae. However, the option of producing large quantities of ethanol from lignocellulosic biomass, has focused greater attention on the production of biodiesel from algae. Biodiesel, are the methanol or ethanol esters of fatty acids derived from vegetable oils and animal fats. Considerable work has been carried out on the genetics (Brown, et al., 1994) and physiology of microalgae oils production. In the laboratory biomass with a high (> 50%) lipid content can be produced without reducing productivity (Benemann and Tillett, 1986). Translating such findings to the field is required.

The direct production of hydrocarbon fuels is also possible with microalgae: one species, Botryococcus braunii, is known in the field and laboratory to produce high quantities of relatively large (> C30) hydrocarbons, that could be rather easily cracked to gasoline (see Regan and Gartside, 1983). Relatively little practical culture work has been done with this organism.

Harvesting and Processing of Microalgal Biomass.

Even assuming that culture stability, productivity, and product formation are feasible, there remains the challenge of harvesting (concentrating) the algal biomass, and converting it into a valuable fuel. Harvesting has been the subject of much research over the years, in particular for removal of microalgae from wastewater treatment ponds, a particular challenge due to the heterogeneous, and variable, algal populations present. However, when an essentially unialgal culture are maintained, harvesting is easier. In particular, low cost harvesting based on the settling characteristics of the algae could be used. The conversion of the freshly harvested algal biomass to liquid fuels requires attention, but presents no major challenges.

R&D NEEDS AND RECOMMENDATIONS

The prior feasibility analysis in this field, including the recently completed study sponsored by PETC (Benemann and Oswald, 1995), concluded that it is possible, in principle, to project microalgae derived biofuels costs that are within the range of energy prices forecast for early next century (a moving target, admittedly). This is particularly true if externalities, specifically CO_2 mitigation credits, are considered. Of course, such analysis and projections are, as in related fields (e.g. ethanol production from lignocellulosics), based on a multiplicity of favorable assumptions and extrapolations, whose individual validity appears plausible, at least to the researchers involved, but that have yet to be verified or integrated. Indeed, such feasibility analysis better establish the current state-of-the-art and, most importantly, the required R,D&D (research, development and demonstration), than they project actual costs for systems that still require many years for development and perfection.

It can, however, be projected with some confidence that biomass production costs for microalgae will be on the high side, and could not be justified with current fossil fuel economics without a substantial credit for CO_2 mitigation, much higher than similar projections for alternative biomass fuels, such as wood. Indeed, wood co-firing in coal-fired power plants may have the least cost for direct CO_2 mitigation in the utility industry. Furthermore, as already indicated above, overall impacts from microalgae fuels production will be a small fraction (1-2%) of power plant CO_2 emissions. Other biomass fuels, such as short rotation tree farms, are projected as being able to mitigate well over 10 to 20% of total U.S. CO_2 fossil fuel emissions.

This raises the question of why should such a minor, expensive, and long-range technology as CO_2 utilization with microalgae be developed, when there are other, more promising alternatives. However, there are several arguments that favor microalgae R&D over alternative concepts, specifically wood fuel production:

- **Microalgae R&D is much faster**, over an order of magnitude faster than R&D required to increase wood fuel supplies by means of short rotation forestry.
- **Microalgae R&D is much cheaper**. Most scale-up issues (e.g. culture stability, productivity, harvestability, etc.) can be addressed with appx. 100 to 1,000 m^2 ponds, at a couple of locations. Short rotation tree R&D will require dozens of locations, with hundred of hectares each, studied over several decades.
- **Microalgae R&D is easier to apply** at new sites as there are only two major, uncontrolled, factors: sunlight and temperature. (For trees soil and rainfall are complex additional factors that greatly complicates such extrapolations).
- **Microalgae R&D is specific** to the needs of the "end-of-pipe" CO_2 mitigation program, of particular interest to electric utilities.
- **Microalgae R&D can lead to breakthroughs** both in fundamental and applied fields. For example, increases in productivities achieved with microalgae cultures could potentially find applications in agriculture and forestry.
- **Microalgae R&D will increase U.S. competitiveness** and lead to technology transfer to the private sector, benefiting U.S. industry and export markets.

Of course, these pro arguments must be balanced with con: the undeveloped nature of this technology, the few sites where land/water/sun/CO_2 resources coincide, and the relatively high costs. Overall, the balance favors of a modest, though significant, microalgae R&D effort, that could generate continuing practical applications while proceeding to the long-term goal of a CO_2 mitigation and biofuels capture process. For example, wastewater treatment systems provide a unique opportunity as a sink for CO_2, while also treating and beneficially converting wastewaters to fuels. Seawater is probably the major available water resource for such algal production systems, which can also be used for bivalve aquaculture and other applications. Although eventually such R&D projects should be coupled directly to power plant flue gas utilization, the demonstrated ability of microalgae to grow on actual and simulated flue gases makes makes this a less immediate issue. Demonstration of culture stability, high productivities, easy harvesting and high contents of lipids are more pressing R&D needs. Such an R&D program should closely integrate outdoor pond research (at the 100 to 1,000 m^2 scale) with laboratory studies, including genetic engineering for strain improvement, to achieve rapid progress towards the goal of CO_2 mitigation and biofuels production.

REFERENCES

Benemann, J.R. 1990. "The Future of Microalgae Biotechnology". In R.C. Cresswell, et al., eds., Algal and Cyanobacterial Biotechnology, 317-337 Longman, London.

Benemann, J.R. 1994. "Systems and Economic Analysis of Microalgae Ponds for Conversion of CO_2 to Biomass". In 10th Annual Coal Preparation, Utilization, and Environmental Control Contractors Conf. Proceed. Vol I. pg. 255 (1994).

Benemann, J.R., and D.M. Tillett. 1987. "Microalgae Lipid Production". In D. Klass, ed., Symp. Proc. Energy Biomass Wastes XI, Inst. Gas Tech. Chicago, IL.

Benemann, J.R., R.P. Goebel, J.C. Weissman, D.C. Augenstein. 1982. Microalgae as a Source of Liquid Fuels, Final Report U.S. Department of Energy, pp. 202.

Benemann, J.R. and W.J. Oswald. Systems and Economic Analysis of Microalgae Ponds for Conversion of CO_2 to Biomass. Final Report to PETC (June 1995).

Burlew, J., ed. 1953. Algae Culture: From Laboratory to Pilot Plant, Carnegie Institute, Washington D.C.

Brown, L.M., S. Sprague, E.E. Jarvis, T.G. Dunahay, P.G. Roessler, and K.G. Zeiler, Biodiesel from Aquatic Species Project Report: FY 1993, NREL/TP -442-5726, Golden CO (1994).

Hamasaki, A., et.al., Carbon Dioxide Fixation by Microalgal Photosynthesis Using Actual Flue Gas from a Power Plant", App. Biochem. Biotech. in press (1995)

Neenan, B., et al. 1986. Fuels from Microalgae: Technology Status, Potential, and Research Requirements. Solar Energy Res. Inst, Golden CO,

Oswald, W.J., and C.G. Golueke. Adv. Appl. Microbiol., 11: 223 - 242 (1960).

Regan, D.L., and G. Gartside, Liquid Fuels from Microalgae in Australia, (1983).

Weissman, J. C. and R. P. Goebel. 1987. Design and Analysis of Pond Systems for the Purpose of Producing Fuels, Solar Energy Res. Inst., Golden CO.

Weissman, J.C. and D.T. Tillett, 1989, 1992. "Design and Operation of an Outdoor Microalgae Test Facility". In Aquatic Species Program, Annnual Reports, Solar Energy Res. Inst. (1989) and Natl. Ren. Energy Lab. (1990), Golden, CO.

BIOLOGICAL HYDROGEN PRODUCTION

J. R. Benemann
Department of Civil Engineering
University of California Berkeley
Berkeley, CA 94720

ABSTRACT

Biological hydrogen production can be accomplished by either thermochemical (gasification) conversion of woody biomass and agricultural residues or by microbiological processes that yield hydrogen gas from organic wastes or water.

Biomass gasification is a well established technology; however the synthesis gas produced, a mixture of CO and H_2, requires a shift reaction to convert the CO to H_2. Microbiological processes can carry out this reaction more efficiently than conventional catalysts, and may be more appropriate for the relatively small-scale of biomass gasification processes. Development of a microbial shift reaction may be a near-term practical application of microbial hydrogen production.

Microbial processes for producing hydrogen directly can be classified as fermentations, which require substrates such as organic wastes, and biophotolysis, the production of hydrogen (and oxygen) from water with microalgae. Microbial dark fermentations of organic wastes produce relatively little hydrogen, when compared to microbial methane yields under similar conditions. Development of dark anaerobic fermentations that produce higher yields of H_2 from organic wastes must be a major goal of R&D in this field. Photosynthetic bacteria have been used to boost yields in such waste fermentations, but low solar conversion efficiencies and the complexities of the required photobioreactors limit their potential.

Biophotolysis can result in direct, simultaneous, sustained, and highly efficient, H_2 and O_2 production from water. However, this has been only demonstrated under rather restrictive laboratory conditions. One problem is O_2 inhibition of H_2 evolution. Some microalgae system can overcome such O_2 inhibition by separating the H_2 and O_2 production reactions and coupling them through CO_2 fixation and metabolism. The nitrogen-fixing cyanobacteria (blue-green algae) can be used in such processes, but suffer from low efficiencies. A promising system is a two stage process in which green microalgae are grown in open ponds and then transferred to separate anaerobic reactors for hydrogen evolution, both in the dark and light. A preliminary feasibility analysis suggests that such a process could be competitive with photovoltaic hydrogen production. In the longer-term, the goal should be to overcome the O_2 inhibition in direct biophotolysis to allow the simultaneous production of H_2 and O_2 from water and sunlight. Recent research, supported by PETC, in photosynthesis and H_2 production suggest that the efficiency of photosynthesis in such a reaction can be much higher than previously thought.

INTRODUCTION

Biological processes can be used to produce a variety of biofuels: solid fuels (wood, straw, residues, etc.), alcohols, biodiesel, biogas, synthesis gas, and H_2 (Benemann, 1980). The two major routes for biological H_2 production are:

1. Gasification of woody and other lignocellulosic biomass, followed by the shift reaction to convert the CO in the synthesis gas to H_2, and
2. Microbiological H_2 production from organic wastes and directly from water.

Here these processes are briefly reviewed, with an emphasis on the development of processes for the production of hydrogen from water and sunlight - biophotolysis. A report on this subject was recently completed for PETC (Benemann, 1995).

THE MICROBIAL SHIFT REACTION

The technologies for biomass gasification to produce H_2 (Larson and Katofsky, 1992; Ogden and Nitsch, 1992) are much more advanced than microbial processes, which are mostly still at the laboratory, or even conceptual stage. Biomass gasification is currently the only technologically available process for hydrogen production from biomass, and is being developed with DOE funding. However, the relatively small scale of biomass gasification, imposed by availability and high costs of transportation of biomass, makes even this process relatively uneconomical, at least with current fossil fuel prices and conventional gasification-shift reaction technologies. The use of microbial catalysts to carry out the shift reaction could lower the costs and improve the overall prospects of this technology.

The shift reaction involves the conversion of CO and H_2O to H_2 and CO_2. The fundamental advantage of the microbial shift reaction is that it is carried out at room temperature, where the thermodynamic equilibrium favors H_2 formation. At higher temperatures only a partial conversion takes place and the CO and H_2 have to be separated, and the CO recycled. The microbial shift reaction, first discovered about 20 years ago (Uffen, 1976), is carried out by a number of photosynthetic bacteria that can catalyze this reaction in the dark (where they do not grow). This reaction has most recently been studied by two groups in the U.S. (Klasson et al., 1993; Weaver et al., 1993). The latter isolated over 400 strains of such bacteria and demonstrated rates of H_2 formation of 1.5 mmole H_2/min/gram cell dry weight, about ten times higher than the rates reported from the former study.

A microbial shift reaction process has been demonstrated at the bench-scale, in which the bacteria are grown in a separate reactor, immobilized on a support, and operated as a gas-phase microbial biofilter (Weaver, 1995). Stable operations for several weeks were noted. Large-scale microbial biofilters are used in industry for a variety of air decontamination and gas clean-up applications. Thus, scale-up of this process appears possible. A feasibility analysis would be of interest.

DARK FERMENTATIONS

Hydrogen evolution from organics can be accomplished in the dark by a variety of microbes, through action of well studied anaerobic metabolic pathways and hydrogenase enzymes. In most such systems the H_2 is derived from rather easily metabolizable substrates, such as starches and glucose, in a relatively rapid process. Microbial cultures can even metabolize the more difficult to convert cellulose and hemicelluloses in woody and herbaceous biomass (lignocelullosics), and produce some H_2, although at a much slower rate an with very low yields. Indeed, dark fermentations have generally low yields, only about 10% of stoichiometric, and the H_2 is evolved at typically only relatively low partial pressure (>0.1 atmospheres).

This discouraging state of affairs is due to the thermodynamic limitations of H_2 production: although the anaerobic conversion of glucose (and other substrates) to H_2 is slightly favored thermodynamically, microbes can not obtain sufficient energy for growth from such a process unless the partial pressure of hydrogen is kept very low. Also, in nature, and the laboratory, such fermentation systems can be quickly colonized by methane producing bacteria, that can convert even traces of hydrogen to methane gas. Therefore, fermentative hydrogen evolution is rather rare in nature, being limited to a few restricted microbial populations, for example in termite guts and occasionally even human intestines.

In principle, the thermodynamic limitations to dark, anaerobic, fermentative hydrogen production should not be an insurmountable obstacle to such a process: the energy yielding (catabolic) reactions in cells might be decoupled (chemically, metabolically, or genetically) from the hydrogen producing (anabolic) ones, by decoupling growth from hydrogen evolution, as in the case of the CO shift reaction.

In practice, such a process faces several difficulties. As it must be carried out in "open" systems, as sterilizable bioreactors are much too expensive, contamination by, in particular, methane gas producing bacteria, is a potential problem. This is particularly true for the conversion of the slow to degrade lignocellulosic materials. Thus, conversion of more readily decomposable wastes, such as food processing wastes, would be more likely. Indeed, in Japan a continuous, stable (>2 months), fermentation of sugar mill wastes to hydrogen was demonstrated at the bench-scale, with yields of about 20% H_2 (from what was expected if all fermentable material was dissimilated) at a partial pressure of about 0.5 atmospheres (Morimoto, 1994). In Europe there also has been recent interest in hydrogen fermentations (Solomon et al., 1995).

Due to the above difficulties, both actual and perceived, relatively few studies have been published on hydrogen production by bacterial fermentations, at least when compared to hydrogen production by photosynthetic bacteria and microalgae, discussed next. However, this neglect is perhaps not wholly justified and more research in this area is warranted.

PHOTOFERMENTATIONS

One method for overcoming the limitations of dark fermentations is by adding an exogenous energy source, which can drive the H_2 evolution reaction to completion. The simplest such energy source is light. Almost 50 years ago it was discovered that photosynthetic bacteria can evolve H_2 (Gest and Kamen, 1949). These bacteria grow in the light under anaerobic conditions on a variety of organic substrates. When nitrogen is limiting, they can exhibit relatively high rates of H_2 evolution, completely breaking down a variety of organic substrates to H_2 (and CO_2), at high partial pressures of H_2 (even above 1 atmosphere).

These almost ideal properties suggested H_2 production from organic wastes by photosynthetic bacteria, "photofermentations", as a better choice than the dark fermentation processes discussed above. Indeed, over the past two decades considerable work by over a score of laboratories around the world has been carried out to develop H_2 production by these bacteria (Sasikala et al., 1993).

However, there are several limitations to this concept. The hydrogen production reaction in photosynthetic bacteria is due to a side reaction of the nitrogenase enzyme, and only takes place in the absence of N_2 gas. It is, essentially, an artifact of the laboratory, although that is no detriment per se. The problem is that the nitrogenase reaction requires large amounts of metabolic energy to drive the hydrogen evolution reaction. This metabolic energy must be supplied by the photosynthetic processes in these bacteria.

As light energy is diffuse, relatively large areas must be covered to capture the sunlight required by the process. And to capture the H_2 gas, the photosynthetic bacteria must be contained in a transparent an H_2 impermeable photobioreactor. Such a reactor could only be economically justified if the conversion efficiency of light energy into H_2 is very high. However, the highest reported efficiencies for H_2 evolution by photosynthetic bacteria are only about 5% of light energy converted into H_2 energy. At full solar intensities conversion efficiencies are much lower. And this efficiency calculation does not consider the energy content embodied in the organic substrates, which is similar to that of the H_2 produced.

However, even assuming that the problems of low efficiency could be overcome, the requirement for a cheap (preferably waste), fermentable substrate would be difficult to meet in most situations where small-scale hydrogen production would be desired. Indeed, the use of photofermentative hydrogen production as a method of waste treatment, which has been argued to justify such a process, must be considered speculative at present.

In conclusion, it would appear that the limitations of dark fermentations would be more easily overcome than those of photofermentations, and appear to be a better focus for future research in this area.

BIOPHOTOLYSIS

If H_2 is to be produced by photosynthetic microbes, water, not organics, would be a better substrate. This concept of a biological decomposition of water into H_2 and O_2 by sunlight, also termed biophotolysis, has attracted considerable attention for the past 20 years. Although initially cell-free systems were used (Benemann et al., 1973), such systems are primarily useful as models and for fundamental research, rather than practical approaches to hydrogen production. Using microalgae as the converters of solar into hydrogen energy, has several advantages, primarily the stability and inherently low cost of these self-replicating solar converters.

The field of basic and applied biophotolysis R&D with microalgae has generated hundreds of publications, and consumed tens of millions of dollars over the past two decades (Benemann, 1995). However, little progress has been made in moving this technology from the conceptual to the practical. There are several reasons.

First, the biological processes for hydrogen production are not very efficient. of In the laboratory conversion efficiencies equivalent to a maximum of about 10% of total solar energy can be demonstrated, similar to the efficiencies already achieved by commercial photovoltaic systems outdoors. And such high efficiencies were demonstrated in the laboratory for an algal process that simultaneously produced H_2 and O_2 from water (Greenbaum, 1988). However, these experiments were conducted under low light intensities; under full sunlight, the best conversion solar efficiencies for photosynthesis (microalgae or plants) are only about 3 to 4% of total solar energy, and even such efficiencies have not yet been demonstrated with hydrogen production systems. Although many factors (such as respiration) limit these efficiencies, the most important limitation is the low light intensity at which photosynthesis by algae, and higher plants generally, saturates.

The problem is that microalgae, like other plants, when exposed to full sunlight can use only a fraction, of the absorbed photons, with the remainder (typically about 50 - 80%) being wasted as fluorescence, heat, etc. Fundamentally, this is due to the high levels of light absorbing pigments, which results in more photons absorbed at high sunlight than can be used at high light intensities. The solution to this problem, already recognized several decades ago, is to reduce the "antenna" pigment levels, by genetic or metabolic means. Then solar conversion efficiencies should approach 10% conversion efficiency even in full sunlight (Benemann, 1990).

A second, major, problem is that the O_2 generated during water splitting, is a strong inhibitor of hydrogen evolution. Thus, a direct splitting of water into H_2 and O_2 by microalgae can only be demonstrated for sustained periods when the O_2 tensions are kept very low, as by addition of a chemical absorber or by rapid purging of the reaction vessel with an inert carrier gas (Greenbaum, 1980). Such conditions could not be scaled-up or reproduced outside a laboratory setting. Thus there is great interest in the development of oxygen stable H_2 evolving systems.

As alternatives to oxygen stable hydrogen evolution, indirect processes can be considered: the algae first fix CO_2 into starches (carbohydrates) (while simultaneously generating O_2 from water, in a conventional photosynthetic process), and then these carbohydrates are converted to H_2 gas in a second anaerobic reaction, either temporally or spatially separated from the water splitting reaction, thus avoiding the oxygen inhibition of the reaction.

Probably the single most studied of such systems uses heterocystous cyanobacteria (blue-green algae). These filamentous algae differentiate special cells, the heterocysts, found evenly spaced along the vegetative cells in the filaments, approximately every tenth to twentieth cell. Heterocysts are the site of nitrogen fixation, and protect the oxygen labile nitrogenase reaction from photosynthetically generated O_2. Thus, heterocysts are able to evolve H_2 (in the absence of N_2 gas), and this property can be used to simultaneously produce O_2 and H_2 from water (with CO_2 serving as an intermediate) with these algae (Benemann and Weare, 1974). However, the heterocyst system suffers from significant shortcomings, including low efficiencies (again due in part to the energetic costs of nitrogenase), and the need to separate H_2 from O_2 in the gas phase. Most important, the entire culture system would must be contained in a photobioreactor that allows capture of the H_2 gas. This would appear to be prohibitive at present.

Non-heterocystous cyanobacteria have also been studied extensively for hydrogen production, in a process that as temporally separates the H_2 and O_2 evolution reactions. Such a temporal separation, possibly on a diurnal time scale, would allow pumping the cultures through several stages (bioreactors), of different design, sizes, etc. Unlike the heterocystous algae, the entire surface of the conversion system need not be covered to allow for H_2 recovery: the CO_2 fixation stage could be carried out in open ponds, similar to those already being studied for production of C-containing fuels and CO_2 mitigation (Benemann, 1995, in these Proceedings).

However, even in this case, the reliance on nitrogenase for H_2 evolution would require that a large fraction, approaching half of the total surface area, would still need to be devoted to photobioreactors and H_2 recovery. In short, nitrogenase based H_2 production systems have too low potential solar conversion efficiencies, only about half of H_2 production by reversible hydrogenases, to achieve realistic efficiency and cost goals for such a process.

H_2 production by green algae appears to be inherently the most favorable approach to developing a practical biophotolysis process. In this concept, just as in the case of the non-heterocystous blue-green algae, a temporal, or more likely spatial, separation of the H_2 and O_2 evolution reactions is the case, with these reactions coupled through CO_2 fixation and metabolism.

However, in this case the reversible hydrogenase, rather than nitrogenase, would be responsible for the hydrogen produced. As this enzyme does not require

ATP for H_2 evolution, this greatly reduces the energy requirements, and thus area, for the H_2 production stage. Indeed, it may be possible to extract at least a fraction of the hydrogen in a dark, anaerobic reaction (required, anyway, to induce the hydrogenase activity of the algae). Overall as little as 10% of the total area may be sufficient for the hydrogen production stage, greatly reducing the area (and costs) of the photobioreactors for hydrogen capture and recovery (see Benemann, 1995 for a preliminary feasibility analysis of this concept).

Recently a combined system, based on both green algae and photosynthetic bacteria, was demonstrated in Japan at a small ($< 5\ m^2$) stage (Akano et al., 1995). In this process, two (appx. $2\ m^2$) open ponds were used to cultivate the green alga Chlamydomonas, which accumulates starch. Concentrating and placing the culture under anaerobic conditions resulted in the fermentation of the accumulated starch into various products (acetate, ethanol, etc., including some H_2). After fermentation was complete the algae were recycled to the growth ponds. The fermentation products, after further concentration, were fed to appx. $0.5\ m^2$ photobioreactors containing photosynthetic bacteria, resulting in hydrogen production. Although efficiencies were low ($< 0.3\%$ of total solar), and the process complex, it does demonstrate the feasibility of moving from conceptual and laboratory processes to scale-up and process engineering. The next challenge would be to replace the photosynthetic bacterial stage by a light driven hydrogen production by the green algae themselves.

CONCLUSIONS

This brief overview suggests that photobiological hydrogen production is still in its infancy, at an early stage in development. However, there are several interesting and important research issues, whose resolution could not only significantly improve the prospects for biological hydrogen production but also have applications in other fields. One such problem is the development of dark fermentation that exhibit high yields ($> 50\%$, based on input organics) at high partial pressures ($> 20\%$) of H_2. Another is the demonstration of high solar conversion efficiencies at full solar intensities by microalgae cultures. These objectives might be achieved by genetic and metabolic manipulations.

Indeed, the recent discovery by Greenbaum et al. (1995) that mutants of Chlamydomonas missing photosystem I (one of the two complexes involved in algal and plant photosynthesis) still can evolve H_2 and O_2, and fix CO_2, demonstrates the power of the combined genetic/physiological approach. This major discovery, funded in part by PETC, could provide insights in how to significantly increase overall photosynthetic efficiency, not only in H_2 production but also in CO_2 fixation and plant productivity generally. Indeed, it suggests that despite the inherent difficulties of a simultaneous H_2 and O_2 production process, continued R&D in this area could lead to practical applications.

REFERENCES

Akano, T., et al., "Hydrogen Production by Photosynthetic Microorganisms". 17th Symp.on Biotech. Fuels and Chemicals, May 10, 1995, Vail Colorado.

Benemann, J.R., J.A. Berenson, N.O. Kaplan, and M.D. Kamen. "Hydrogen Evolution by a Chloroplast-Ferredoxin-Hydrogenase System." Proc. Nat. Acad. Sci. USA, System." Proc. Nat. Acad. Sci. USA, 70: 2317-2320 (1973).

Benemann, J.R., and N.M. Weare, "Hydrogen Evolution by Nitrogen-Fixing Anabaena cylindrica Cultures." Science 184, 1917 - 1919 (1974).

Benemann, J.R. "Biomass Energy Economics." Intl. Energy J. 1 107-131 (1980).

Benemann, J.R., "The Future of Microalgae Biotechnology", in R.C. Cresswell, et al., eds., Algal Biotechnology, pp. 317-337 (1990).

Benemann, J.R., Photobiological Hydrogen Production. Report to PETC (May 1995).

Benemann, J.R., "CO_2 Capture and Biofuels Production with Microalgae". These Proceedings (1995).

Gest, H., and M.J. Kamen. "Photoproduction of Molecular Hydrogen by Rhodospirillum rubrum". Science, 109: 558 -559 (1949).

Greenbaum, E. J.W. Lee, C.V. Tevault, S.L Blankinship, and L.J. Mets. "Carbon Dioxide Fixation and Photoevolution of Hydrogen and Oxygen in a Mutant of Chlamydomonas lacking Photosystem I". Nature, in press (1995).

Greenbaum, E., "Simultaneous Photoproduction of Hydrogen and Oxygen by Phtosynthesis" Biotech. Bioeng. Symp. 10: 1-13 (1980)

Greenbaum, E., Energetic Efficiency of Hydrogen Photoevolution by Algalg Water Splitting. Biophys. J., 54: 365 - 368 (1988).

Klasson, K.T., A. Gupta, E.C. Claussen, and J.L. Gaddy, "Evaluation of Mass-Transfer and Kinetic Parameters for Rhodospirillum rubrum in a Continuous Stirred Tank Reactor". App. Biochem. Biotech., 39/40: 549-557 (1993).

Larson, E.D., and R.E. Katofsky, "Production of Hydrogen and Methanol via Biomass Gasification", In Adv. Thermochemical Biomass Conversion (1992).

Morimoto, K. Presentation, 10th World Hydrogen Energy Conf., Cocoa Beach, FL June 23, 1994

Ogden, J.M. and J. Nitsch, "Solar Hydrogen", in T.B. Johansson et al., eds., Renewable Energy, Island Press, Washington D.C., pp. 925-1010 (1992)

Sasikala, K., Ch.V. Ramana, P. R. Rao, and K.L. Kovacs, Anoxygenic Phototrophic Bacteria: Physiology and Advances in Hydrogen Technology", Adv. Appl. Microbiology, 38: 211 295 (1993)

Solomon, B.O., et al., "Comparison of the energetic efficiencies of hydrogen and oxychemicals formation in Klebsiella pneumoniae and Clostridium butyricum during anaerobic growth on glycerol. J. Biotech., 39: 107- 117 (1995).

Uffen, R.L., Proc. Natl. Acad. Sciences, U.S. 73: 7298 (1976).

Weaver, P. "Microbial Hydrogen Production". Annual Review Meet. DOE Office of Utility Technologies Hydrogen Program, Cocoa Beach, April 18-21 (1995).

Weaver, P., P.C. Maness, A. Frank, M. Lange, and J. Blaho, "Photobiological Hydrogen Production Using Whole-Cell or Cell-Free Systems." In Proc. 1993 DOE/NREL Hydrogen Program Review, Cocoa Beach, FL May 4-6 (1993).

CATALYSTS FOR THE REDUCTION OF SO_2 TO ELEMENTAL SULFUR

Y. JIN, Q. Q. YU, and S. G. CHANG
ENERGY & ENVIRONMENT DIVISION
LAWRENCE BERKELEY LABORATORY
BERKELEY, CA 94720

Catalysts have been prepared for the reduction of SO_2 to elemental sulfur by synthesis gas. A catalyst allows to obtain more than 97% yield of elemental sulfur with a single-stage reactor at 540°C. A lifetime test has been successfully performed. The mass balance of sulfur and carbon has been checked. The effect of H_2S, COS, and H_2O has been studied.

INTRODUCTION

Combustion of coal emanates flue gas containing SO_2, a pollutant causing acid rain and visibility reduction in the atmosphere. Several regenerable SO_2 scrubbing system have been developed. In these processes, sulfur dioxide from flue gas is first absorbed into an alkaline solution or adsorbed on a solid substrate, and is subsequently desorbed to produce a stream of high concentration SO_2. It is desirable to convert SO_2 to elemental sulfur for storage, transportation, and/or conversion to valuable chemicals.

Existing technologies for SO_2 conversion to elemental sulfur require multi-stage Claus reactors to achieve desirable yield. Prior to entering the Claus reactors, a proper portion of SO_2 in the gas stream must be reduced to H_2S either catalytically or by the combustion in a hydrocarbon flame under reduced conditions. A simpler process is desirable to convert SO_2 to elemental sulfur.

Sulfur dioxide can be reduced with synthesis gas to produce elemental sulfur at elevated temperatures. The reduction can be facilitated with catalysts. In addition to elemental sulfur, these reactions may produce several undesirable byproducts. These include hydrogen sulfide, carbonyl sulfide, carbon disulfide, and elemental carbon. Numerous research efforts have been carried out to develop catalysts for selective production of elemental sulfur at low temperatures. However, the results [1-4] obtained so far show only limited successes and do not warrant a commercial application. The development of a catalyst capable of obtaining very high yield of sulfur with a high space velocity at low temperatures would be required to warrant a commercial application.

EXPERIMENTAL SECTION

Catalyst Preparation

Catalysts were composed of a combination of several metal oxides supported on Al_2O_3. Two sizes of Al_2O_3 were used: 1. 30-40 mesh particles, and 2. 3mm dia. by 5 mm height granules. By mixing appropriate amounts of metal nitrate solutions with Al_2O_3, the mixture underwent stepwise heating to form the activated catalyst. The ratio of the active catalyst to carrier was about 0.3 by weight.

Apparatus and Procedure

The experimental setup consists of three separate sections: the gas supply section, the main reactor, and the detection and analysis section. Gases are supplied from compressed gas cylinders to flow meters before entering a gas mixer. The tubular reactor is fabricated from a 1.4-cm-o.d. with a 1-mm wall thickness quartz tube. The entire reactor is mounted inside a tubular furnace. A thermocouple, reaching the center of the catalytic reactor, provide measurement of the temperature of catalytic reactions. After the last section of the reactor, the gases pass through a sulfur collector at room temperatures, and then enter into an on-line trap cooled in an ice bath to condense water before entering a six-port sampling valve which is used to inject the products of the catalytic reactions into the gas chromatograph. Finally, the exit gases pass into a scrubber containing concentrated NaOH. The inlet and exit gases are analyzed by using a gas chromatograph

RESULTS AND DISCUSSION

In order to study the kinetics of the reactions and the diffusivity of the reactants, two carrier sizes were used. The smaller size carrier is 30-40 mesh Al_2O_3 particles, which were used typically in laboratory scale experiments to obtain kinetic information. The larger size carrier has a dimension of 3 mm diameter by 5 mm height cylindrical granules, which were used in scale up tests. The parametric studies were conducted on particles and granules for comparison. The lifetime experiments were performed on particles.

Particles (30-40 mesh)

Parametric Studies. The effect of temperatures, space velocity, molar ratios of reductants to SO_2 ($R = F_{(H2 + CO)}/F_{SO2}$), and molar ratios of H_2 to CO ($r = F_{H2}/F_{CO}$) on the activity of the catalyst (Cat-S) were investigated.

Figure 1 shows the results of the temperature dependence study. The experiments were carried out at r= 0.75 and R= 2, and at a space velocity of 10,000 h^{-1} with 1 g of the Cat-S. The Y_{S2} reaches 94.4 % at 480 C.

The effect of space velocity on the activity of Cat-S is shown (Figure 2). The experiments were performed at r= 0.75 and R= 2, and at 480 C with 1 g of the Cat-S. The results indicated that there was little effect on the yield of elemental sulfur over the ranges from 5,000 h^{-1} to 15,000 h^{-1}, this yield lies between 90.0 and 95.9 %. The selectivity of elemental sulfur increases with an increase of space velocity.

The effect of R on the catalyst activity is depicted in Figure 3. The experiments were conducted at r = 0.75, space velocity = 10,000 h^{-1}, and at 480 C. The results show that the optimum operating conditions should be at R = 2, when the Y_{S2} reached 93.5 %. The Y_{S2} and the C_{SO2} decreased when R was less than 2.

Synthesis gas derived from natural gas contains a molar ratio of H_2 to CO approaching 3. Therefore, a separate set of parametric studies was carried out at r = 3. The effect of temperature, space velocity, and R on the conversion of SO_2 and the yield of products was investigated.

Lifetime Tests. The lifetime test was carried out continuously for 1080 h (45 days). The results indicate that the activity of the Cat-S is very stable and does not show any changes during the entire 1080 h of the lifetime test. Figure 4 shows that the yield of elemental sulfur ranges between 93.1 and 96.5 %, which is far superior to results so far reported in the literatures [2,3,4]. These high yields were achieved at a space velocity of 10,000 h^{-1} , compared with a reported result of obtaining 69.3 - 72.8 % yield of elemental sulfur at a space velocity of 2,000 h^{-1}, and a 82.8 % sulfur yield at a space velocity of only 500 h^{-1}.

Mass Balance. The mass balance of the reaction has been performed. The sum of carbon monoxide conversion to carbon dioxide and carbonyl sulfide is $C'_{CO} = Y_{CO2} + Y_{COS}$. The average value of C_{CO} and C'_{CO} from ten experiments are 99.1% and 97.4% respectively, which indicates that carbon monoxide is essentially converted to either carbon dioxide or carbonyl sulfide.

The conversion of sulfur dioxide to hydrogen sulfide, carbonyl sulfide and elemental sulfur was measured to determine the mass balance of sulfur: $C = Y_{H2S} + Y_{COS} + Y_{S2}$. The solid elemental sulfur was collected and weighted, and was found to be about 90% of the theoretical value. It was difficult to obtain a complete recovery of elemental sulfur from the wall of the tubings and vessels. It was likely that the remaining 10% of sulfur stayed on the wall and could not be recovered.

Granules (d. 3 mm x h. 5 mm)

Parametric Studies. The effect of temperature, space velocity, and molar ratio of reactants on the activity and selectivity of the Cat-S catalyst on granules was studied. The yield of sulfur reaches 97.8% at 560 C and a space velocity of 2100 h^{-1} with synthesis gas derived from methane (i.e. r = 3).

The effect of the space velocity on the catalyst for r = 0.4, 0.75, and 3 was studied at three temperatures, 560, 520, and 480°C. The results indicate that C_{SO2}, Y_{H2S}, and Y_{S2} decrease, while Y_{COS} increases along with the increase of the space velocity. S_{S2} remains fairly constant under the experimental conditions employed.

The effect of R on the Cat-S at r = 0.4, 0.75, and 3 was studied at 560, 520, and 480°C respectively. The results indicate that at a given r value, C, Y_{H2S}, and

Y_{COS} show a slight increase along with the increase of R until R reaches 2. Beyond that however, Y_{H2S} exhibits a drastic growth with the increase of R; Y_{COS} also shows some growth with R, but to a much lesser extent than Y_{H2S}. It is obvious that Y_{S2} is the greatest when R is 2 regardless of the ratio of r.

The Effect of Contaminants. Experiments were conducted to determine the effect of contaminants: H_2S, COS, and H_2O. The addition of H_2S and COS does not change the yield of elemental sulfur to any appreciable amount, nor does it increase the yield of the H_2S and COS byproducts. The addition of a large amount of H_2O vapor (15%) results in an increase of the Y_{COS} and thus a decrease of Y_{S2} at low temperatures. The H_2O effect decreases along with the increase of the reaction temepratures; this effect becomes negligible at a temperature of about 440 C when the Y_{S2} is identical.

High Efficiency Recovery. The operating conditions of the Cat-S (granules) to obtain a Y_{S2} of more than 96 % have been determined. Y_{S2} reaches between 96.9% and 97.1% at 520°C and a space velocity from 1,800 h^{-1} to 2,000 h^{-1}; further increase of space velocity to 3,000 h^{-1}, Y_{S2} decreases to 93%. To achieve a Y_{S2} of 96% at a space velocity of 3,000 h^{-1}, the temperature of the catalytic reactions would have to be increased to 580°C.

CONCLUSION

We have developed a catalyst for reduction of SO_2 by synthesis gas. This catalyst is composed of a mixture of inexpensive transition metal oxides supported on alumina. The inventive catalyst can achieve a high conversion efficiency of SO_2 by synthesis gas with a high selectivity to elemental sulfur. Unlike the Claus process, the reaction of SO_2 with synthesis gas to form elemental sulfur is not a reversible process. As a result, a high efficiency recovery of sulfur can be achieved in a single stage reactor.

A lifetime (1080 h) test has been successfully performed. The activity of the catalyst remains very stable during the entire period of the lifetime test. The mass balance of sulfur and carbon has been checked satisfactory.

This catalyst (in granule form) can achieve 97% yield of elemental sulfur at 540 C with a space velocity of 2,000 h^{-1} or at 640 C with a space velocity of 3,000 h^{-1}.

It has been demonstrated that the contaminants, H_2S, COS, and H_2O do not affect the performance of the catalyst to any appreciable extent.

The inventive catalyst possesses very promising properties. As such, it could be utilized as a basis to develop a new process for high efficiency conversion of SO_2 to elemental sulfur by synthesis gas at a more cost effective manner than technologies available currently.

ACKNOWLEDGEMENT

This work was supported by the Assistant Secretary for Fossil Energy, U.S. Department of Energy, under Contract DE-AC03-76SF00098 through the Pittsburgh Energy Technology Center, Pittsburgh, PA.

REFERENCES

(1). Akhmedov, M.M., Shakhtakhtinskii, G. B., Agaev., A.I., Azerb. Khim. Zh. (2) 95 (1983).

(2). Akhmedov, M.M., Gezalov, S.S., Agaev, A.I., Mamedov, R.F., Zh. Prikl. Khim., 61, (1) 16 (1988).

(3). Akhmedov, M.M., Guliev, A.I., Agaev, A.I., Gezalov, S.S., Zh. Prikl. Khim., 61, (8) 1891 (1988).

(4). Akhmedov, M.M., Guliev, A.I., Ibragimov, A.A., Khim. Prom. (1), 37 (1989).

Fig. 1 The effect of temperature on the Cat-S (particles) at H_2/CO=0.75, S.V. =10,000 h^{-1}, $(H_2+CO)/SO_2$=2.

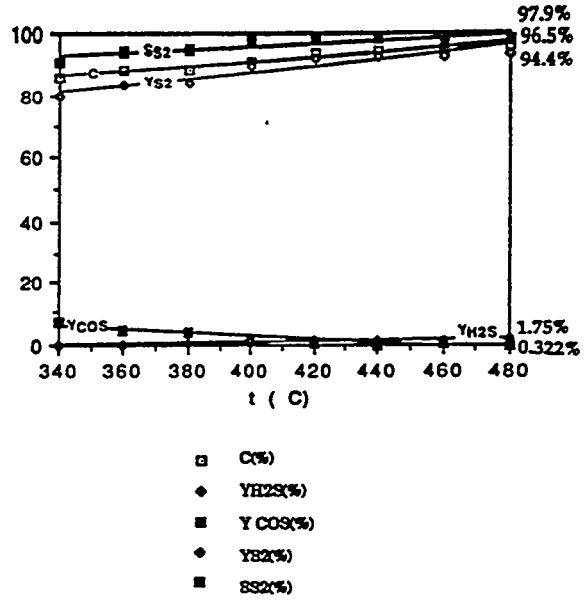

Fig. 2 The effect of space velocity on the Cat-S (particles) at H_2/CO=0.75, $(H_2+CO)/SO_2$=2, 480°C.

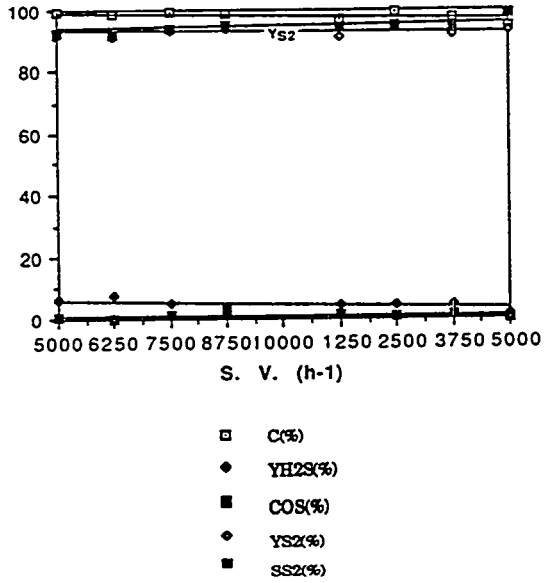

Fig. 3 The effect of molar ratio of reactants on the Cat-S (particles) at H_2/CO=0.75, S.V.=10,000 h^{-1}, 480°C.

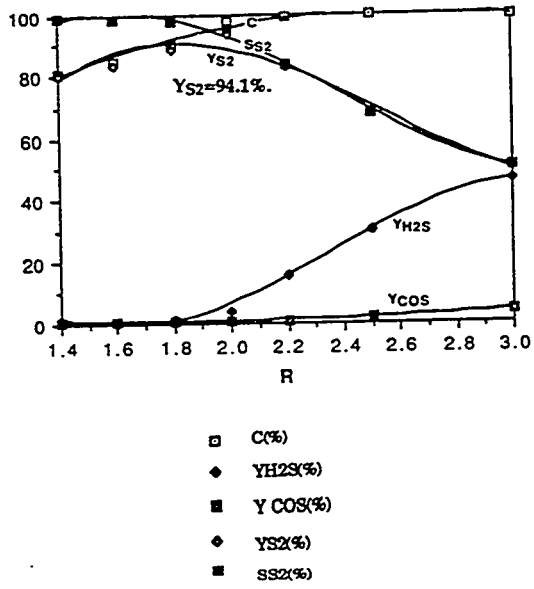

Fig. 4 The yield of sulfur as function of reaction time (H_2/CO)=3, $(H_2+CO)/SO_2$=2, S.V. =10,000 h^{-1}, 480°C.

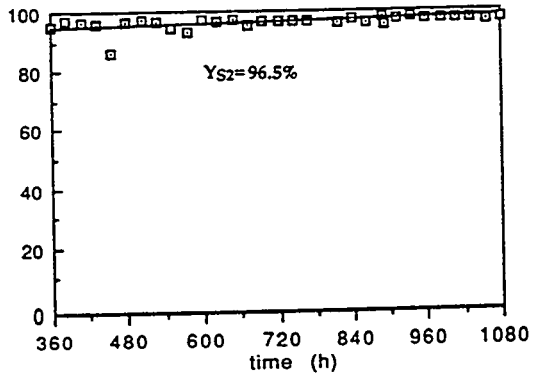

Fig. 5 The effect of 15% H_2O on the Cat-S (particles) at (H_2/CO)=0.75, S.V. =10,000 h^{-1} at varying temperatures.

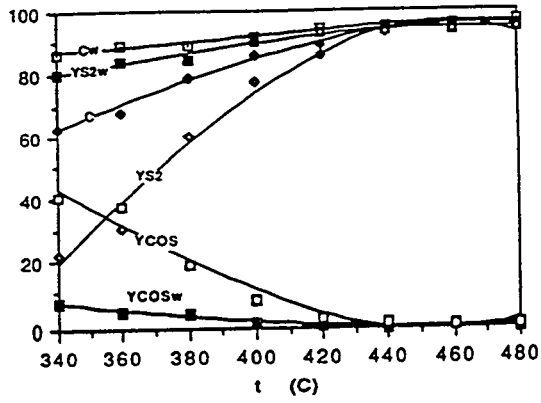

HIGH-EFFICIENCY SO_2 REMOVAL IN UTILITY FGD SYSTEMS

JAMES L. PHILLIPS, SENIOR STAFF ENGINEER
STERLING GRAY, SENIOR ENGINEER
DAVID DEKRAKER, SENIOR ENGINEER
GARY M. BLYTHE, PRINCIPAL ENGINEER
RADIAN CORPORATION, AUSTIN, TEXAS

INTRODUCTION

The U.S. Department of Energy (DOE) and the Electric Power Research Institute (EPRI) have contracted with Radian Corporation to conduct full-scale testing, process modeling, and economic evaluations of six existing utility flue gas desulfurization (FGD) systems. The project objective is to evaluate low capital cost upgrades for achieving up to 98% sulfur dioxide (SO_2) removal efficiency in a variety of FGD system types. The systems include dual-loop, packed absorbers at Tampa Electric Company's Big Bend Station; cocurrent, packed absorbers at Hoosier Energy's Merom Station; dual-loop absorbers with perforated-plate trays at Southwestern Electric Power Company's Pirkey Station; horizontal spray absorbers at PSI Energy's Gibson Station; venturi scrubbers at Duquesne Light's Elrama Station; and open spray absorbers at New York State Electric and Gas Corporation's (NYSEG's) Kintigh Station. All operate in an inhibited-oxidation mode except the system at Big Bend (forced oxidation), and all use limestone reagent except the Elrama system (Mg-lime).

The program was conducted to demonstrate that upgrades such as performance additives and/or mechanical modifications can increase system SO_2 removal at low cost. The cost effectiveness of each upgrade has been evaluated on the basis of test results and/or process model predictions for upgraded performance and utility-specific operating and maintenance costs. Results from this program may lead some utilities to use SO_2 removal upgrades as an approach for compliance with Phase 2 of Title IV of the Clean Air Act Amendments (CAAA) of 1990. This paper summarizes the results of testing, modeling, and economic evaluations that have been completed since July 1994.

EXPERIMENTAL METHODS

The test program at each FGD system has typically consisted of three phases. The first phase is baseline testing where the SO_2 removal performance of a single, representative absorber module is measured at normal operating conditions. The baseline tests also involve measuring SO_2 removal efficiencies over a range of conditions, such as varied slurry pH set points and absorber liquid-to-gas (L/G) ratios, to obtain data to calibrate EPRI's FGDPRISM (FGD Process Integration and Simulation Model) to that system. The calibrated model is then used to predict the SO_2 removal capabilities of the system, including upgrades. Next, the best performance additives and/or upgrades are selected and a parametric test series is run to evaluate the effectiveness of those upgrades for achieving increased SO_2 removal at full scale. Where the selected upgrade includes performance additives, system-wide additive consumption tests are conducted as the third phase of testing. Finally, these results are used to perform economic evaluations of the costs for each

upgrade to achieve high SO_2 removal efficiencies. The cost effectiveness of the upgrades is evaluated by comparing them with the projected market price of SO_2 allowance purchases.

Results for five of the six utility FGD systems included in the program have been presented at previous Contractors Conferences. This paper updates the results for two of these sites: PSI Energy's Gibson Station and Duquesne Light's Elrama Station. For the sixth program site, at NYSEG's Kintigh Station, all of the testing has been conducted since the July 1994 Contractors Conference. Therefore, all of the results for this site are discussed.

RECENT RESULTS FOR PSI ENERGY'S GIBSON STATION

Review of Previous Results for this Site. PSI Energy's Gibson Unit 5 is a 650-MW generating plant that fires coal with a sulfur content ranging from 2.4 to 3.5 wt.%. The unit has a wet limestone reagent FGD system that uses four Kellogg/Weir horizontal-gas-flow absorber modules. The FGD system uses a small amount of dolomitic lime for magnesium enhancement and operates in an inhibited-oxidation mode. Sodium formate and dibasic acid (DBA) additives were considered as upgrade options for this site.

Baseline tests showed that the SO_2 removal efficiency of the FGD system was about 86% at design operating conditions, while the unit was firing a lower-sulfur coal (~2.4 % S). The system operating conditions were three modules and four pumps per module in service (27 ft/sec flue gas velocity, 73 gal/macf L/G ratio), with a pH set point of 5.3.

Just prior to the parametric test series, while the unit was firing a higher-sulfur coal (~3.5 %S), a test was conducted without additive but at an elevated L/G ratio (four modules with four pumps in service) and an elevated pH set point (~5.7). This test showed that the module SO_2 removal efficiency could be increased to 96% without using additional performance additives. However, these operating conditions result in increased power and limestone consumption.

Parametric tests with sodium formate additive showed that, with the higher-sulfur coal, the SO_2 removal efficiency could be increased to 88% at design baseline conditions (three-module/four-pump operation and 5.3 pH), with a formate ion concentration of 2750 ppm. This compares to a predicted SO_2 removal of less than 75% at these same high-sulfur-coal conditions without the additive. By changing the operating conditions to an elevated L/G ratio of 95 gal/macf (four-module, four-pump operation) and 5.7 pH, an SO_2 removal efficiency of 97.5% was observed at a lower formate ion concentration of 1425 ppm.

A long-term sodium formate consumption test was conducted, with the formate ion concentration maintained at 1050 ppm in the reaction tanks. The consumption rate measured was equivalent to 10.6 lb of sodium formate per ton of SO_2 removed by the FGD system. Approximately half of the consumption was due to nonsolution losses from the system, primarily coprecipitation of the additive into the FGD system byproduct solids.

A long-term DBA consumption test was also performed, with DBA being added to the entire FGD system to maintain a concentration of 1150 ppm in the reaction tanks. The consumption rate

measured was equivalent to 9.2 lb of DBA per ton of SO_2 removed by the FGD system. Approximately three-quarters of the consumption was due to nonsolution losses, with that equally split between coprecipitation and oxidative degradation of the additive.

Sodium formate appeared to have a detrimental effect on byproduct solids dewatering properties at this site. After formate was added to the FGD system, the settling rate of the slurry solids and the filter cake solids content measured by laboratory tests each decreased. However, there was no apparent change in crystal size or shape, based on scanning electron microscope (SEM) photographs of solids samples with and without sodium formate present. In contrast, DBA appeared to have a beneficial effect on solids dewatering properties. After DBA was added, the settling rate of the slurry solids and the filter cake solids content measured by laboratory tests both increased. However, as with the sodium formate test results, there was no apparent change in crystal size or shape based on SEM photos of solids samples with and without DBA.

Economic Evaluation Results. Since the 1994 Contractors Conference, results of the baseline and parametric tests were used to calibrate EPRI's FGDPRISM model to the Gibson Station FGD system. Because the baseline and parametric test series were conducted at significantly different inlet SO_2 levels, FGDPRISM model simulations were used to perform technical and economic evaluations of the various upgrade options at a consistent coal sulfur content of 3.0 wt.%. The options evaluated with the model include operating at high L/G ratio (four-module/four-pump operation), decreasing reagent utilization (higher recycle slurry pH), using sodium formate additive, and using DBA additive.

The results for these upgrade options were compared to the design baseline operating conditions. These include three-module and four-pump operation, 85% limestone utilization, 9500 ppm dissolved magnesium concentration, and no flue gas bypass, all at a boiler load of 620 MW. For these conditions, the baseline SO_2 removal efficiency is approximately 80%.

Increasing the L/G ratio by operating with all four modules in service resulted in the largest removal increase at the lowest cost. Increasing the L/G ratio in this manner increases the SO_2 removal efficiency to 93% at an average cost of $48 per additional ton of SO_2 removed. As a result, an additional 13,200 tons of SO_2 can be captured. The other options, when considered individually, resulted in smaller increases in SO_2 removal and at higher costs. No individual upgrade option was capable of increasing the SO_2 removal to 95% or greater, so operation at a high L/G ratio was evaluated in combination with the other options. For high L/G operation, 95% SO_2 removal could be achieved either with a higher pH set point, which would decrease reagent utilization to about 80%, or by using either sodium formate or DBA additive at a concentration of about 500 ppm. The average costs for achieving 95% SO_2 removal with these options ranged from about $58 per ton (80% utilization or 500 ppm DBA) to $64 per ton of additional SO_2 removed (500 ppm formate). At 95% removal, a total of 15,000 additional tons of SO_2 can be removed relative to design baseline performance.

The net annual values of the upgrade options vary as a function of the SO_2 removal level achieved. The net annual value of achieving 93% SO_2 removal by operating at high L/G with all four modules in service is approximately $2.6 million, assuming an SO_2 allowance value of $250/ton, or $1.3

million assuming a value of $150/ton. When combined with other upgrade options, a maximum net annual value of approximately $3.0 million is achieved at 96% removal based on a $250/ton allowance value. At an allowance value of only $150/ton, a maximum net annual value of $1.4 million is achieved at a slightly lower removal of about 95%.

A sensitivity analysis was also performed to examine the impact of operation at a higher unit load (650 MW), a minimum level of flue gas bypass (5%), and a higher coal sulfur content (3.4%). At these conditions, four-module, four-pump operation is required to achieve the overall SO_2 removal efficiency of 82% necessary for compliance, although this would allow a 12.5% flue gas bypass rate. Upgrades considered involved reducing the flue gas bypass rate to the specified minimum of 5% and using either sodium formate or DBA additives, still with four-module, four-pump operation. The analysis shows that an overall SO_2 removal of 90 to 91% can be achieved with 1000 to 1500 ppm of either additive. The maximum net annual value of $1.5 million is achieved with DBA additive if allowances are valued at $250/ton. For a lower allowance value of only $150/ton, the maximum annual value achieved is $0.7 million.

RECENT RESULTS FOR DUQUESNE LIGHT'S ELRAMA STATION

Review of Previous Results for this Site. The first step in identifying low-cost upgrades for the Elrama FGD system was to conduct baseline tests to measure the performance of the magnesium-lime reagent venturi scrubbers as they normally operate. The FGDPRISM model was calibrated to the Elrama scrubber performance using these data, then used to predict how the scrubber would perform with a variety of potential upgrade options. After modeling the candidate upgrade options, a cursory economic evaluation of each option was performed. The options that appeared to be most cost effective were further evaluated in the parametric test series. Parametric test results were then used to conduct a second round of economic evaluations based on measured rather than modeled performance.

The two most promising options, which were subsequently tested during the parametric tests, involved operating at elevated thiosulfate concentrations and at increased venturi pressure drop, respectively. In the parametric tests, sodium thiosulfate concentrations were varied from the normal level of 170 ppm to as high as 2800 ppm. Tests were performed at two venturi pressure drops: the normal value of 10 inwc and a higher value of 12 inwc. Each condition was also tested at two pH values: the normal value of 7.2 and a lower value of 6.5.

The baseline SO_2 removal for the parametric series was about 89%. With elevated thiosulfate levels, improved SO_2 removal was obtained for three scenarios: pH 6.5 and 12 inwc venturi pressure drop, pH 7.2 and 10 inwc venturi pressure drop, and pH 7.2 and 12 inwc venturi pressure drop. These results are summarized in Table 1. The highest SO_2 removal efficiencies were measured at the pH 7.2 and 12 inwc venturi pressure drop conditions; a maximum of 93% removal was obtained at sodium thiosulfate concentrations of 1600 to 2700 ppm.

The results summarized above were reported in preliminary form at the July 1994 Contractors Conference. The following is a discussion of the results of the second round of upgrade economic evaluations, which were based on the full-scale parametric test results.

Economic Evaluation Results. The costs associated with operating at each test condition are also summarized in Table 1. At the highest SO_2 removal conditions of pH 7.2 and 12 inwc venturi pressure drop, the costs were estimated to range from $105 to $149/additional ton of SO_2 removed, depending on the thiosulfate concentration. Assuming an SO_2 credit value of $150/ton, the overall net value of operating at the elevated venturi pressure drop ranges from $3,000 per year to $65,000 per year, depending on the thiosulfate concentration. The costs or savings associated with improved SO_2 removal are compared to the base case parametric test, where 89.1% SO_2 removal efficiency was achieved at a pH of 7.2, a venturi pressure drop of 10 inwc, and a thiosulfate concentration of 170 ppm.

The lowest cost operating scenario was for the pH 6.5, 12 inwc venturi pressure drop conditions. The results in Table 1 show that for elevated thiosulfate concentrations, it is possible to improve the SO_2 removal efficiency while achieving an overall savings in operating costs. The savings come from improved lime utilization at the lower operating pH. At an assumed SO_2 allowance value of $150/ton, the value of operating at the pH 6.5, 12 inwc pressure drop conditions (compared to the base case) can be as much as $360,000 per year.

Laboratory settling tests indicated that the settling rate of the scrubber solids improved at the higher thiosulfate concentrations. This suggests that the thickeners would be able to better concentrate the scrubber liquor solids and lower the moisture content of the waste solids. This could result in substantial savings in waste disposal costs, a benefit that was not considered in these economics. However, because the parametric tests were performed on a single tower, it was not possible to determine what effect would occur in the full-scale thickeners if all of the towers were operated in this mode. System-wide testing at high thiosulfate concentrations would be required to determine if Elrama could realize further cost savings through reduced waste solids moisture.

RESULTS FROM NYSEG'S KINTIGH STATION

System Description. The NYSEG Kintigh Station is a 700-MW facility located near Barker, New York, that typically fires a 2.0 to 2.8 % sulfur coal. The unit is equipped with a limestone FGD system employing six open spray absorber modules. Each absorber has five recycle pumps independently feeding five spray header levels. At design conditions, only four modules and four spray headers per module are required to be in operation. The FGD system operates in an inhibited oxidation mode. Sodium formate additive was the only upgrade option tested at this site.

Summary of Test Results. Baseline tests showed that the SO_2 removal efficiency of the test module at normal full-load operating conditions (pH 5.6, flue gas velocity of 9 ft/s, four recycle pumps in service) was about 86%. Parametric tests with sodium formate additive showed that with a formate ion concentration of 3800 ppm in the recycle slurry liquor, the test module's SO_2 removal efficiency could be increased to 99.4%. The project target of 95% removal could be achieved with a formate ion concentration of only 500 ppm.

In a subsequent long-term additive consumption test, sodium formate was added to the entire FGD system to maintain an average formate ion concentration of 1080 ppm in the recycle slurry liquor. At this formate concentration, the FGD system SO_2 removal efficiency averaged about 97%. The

total sodium formate consumption rate was measured to be equivalent to 16.6 lb/ton of SO_2 removed. Of the total consumed, 12% was solution loss with the moist filter cake, 32% was lost by precipitation into the filter cake solids, 6% was lost by vaporization into the flue gas, and the remaining 50% was attributed (by difference) to degradation. The sodium formate additive had no measurable effect on the process chemistry or on the dewatering properties of the calcium sulfite byproduct solids.

Results of Economic Analyses. The economics of sodium formate addition were evaluated based on a capital cost of $300,000 for a 100 lb/hr additive storage and delivery system, using operating cost data provided by NYSEG. These results show that by using sodium formate additive at 1000 ppm (as formate ion) in the recycle slurry to raise the module SO_2 removal efficiency to nearly 98%, the Kintigh FGD system could remove more than 10,000 additional tons per year of SO_2 at an average additional cost of only $76/ton. Depending on the assumed value of SO_2 allowances, the estimated net annual value of the additional SO_2 removal for this optimum case ranged from $800,000 (assuming a value of $150/ton) to $1.8 million (assuming $250/ton).

Further analysis based on performance predictions with the calibrated FGDPRISM model suggested that approximately 97% removal could be obtained by operating with a finer limestone grind. This was predicted to remove an additional 9800 tons of SO_2 per year (relative to baseline performance) at an average cost of only $53 per additional ton removed. This finer grinding might be done by operating the reagent preparation system at a lower throughput for two shifts per day instead of the current one shift per day. Some modifications to the ball mill classifier would also be required. Additional tests would be required to verify the results of these FGDPRISM predictions.

CONCLUSIONS

The results from this program show that upgrades to existing FGD systems can be a very cost-effective component of a utility's strategy for complying with the CAAA of 1990. Table 2 provides a summary of results for all six sites included in the program. For five sites, the goal of cost-effectively achieving 95 to 98% overall SO_2 removal has been met. Two sites have exceeded this goal, with 99% overall SO_2 removal appearing to be very cost effective. At the sixth site, the goal was nearly met, with a maximum of 93% SO_2 removal being attained.

The costs for achieving these high SO_2 removal levels appear to be very attractive. The estimated incremental costs for the five sites that achieved 95% or greater SO_2 removal range from $39/ton to $76/ton of additional SO_2 removed. For the sixth site, the most cost-effective option actually showed a predicted reduction in FGD system operating costs, although this case resulted in an increase in SO_2 removal of only 3 percentage points above the baseline level. To put these estimated costs (or savings) into perspective, in the first EPA auction for SO_2 allowances, the average successful bid price was $150/ton. EPRI estimates that at the beginning of Phase 2 for the CAAA (the years 2000 through 2005), SO_2 allowance market prices will range from $250/ton to $500/ton of SO_2 in 1992 dollars.[1] Furthermore, we estimate that the cost of generating SO_2 allowances by installing new FGD systems on units firing medium- to high-sulfur coal would be at the upper end of this range. SO_2 allowances generated at $76/ton or less in existing FGD systems should be very desirable.

The amount of SO_2 allowances that can be generated by upgrading existing FGD systems can be substantial. At the Pirkey Station, more than 21,000 tons/yr of additional allowances can be generated, which would be sufficient to completely offset the Phase 2 SO_2 emissions from a 250-MW unit with no FGD system firing a medium-sulfur coal.

These results are very encouraging. Several of the six utilities plan to implement upgrade options tested at their site. The results from these sites may be applicable to a number of other existing FGD systems. Furthermore, the methodology applied in this program can be applied to any FGD system to evaluate the potential for cost-effectively upgrading its performance.

REFERENCES

1. Torrens, I. and J. Platt. "Update on Electric Utility Response to the CAAA." ECS Update, No. 30, p.3, Fall 1993.

Table 1. Parametric Test Economics for the Duquesne Light Elrama Station

	Measured SO_2 Removal %	Net Increase in SO_2 Removal ton/hour	Thiosulfate Concen-tration ppm	Total Cost $/ton SO_2	Net Annual Value @ $150/ton $1000/yr	Net Annual Value @ $250/ton $1000/yr
Base Case	89.1		170			
Case 1 - pH 7.2, 10 inwc						
Test 3	90.1	509	454	125	13	64
Test 7	91.1	993	1021	135	15	114
Test 11	91.5	1197	1579	147	4	124
Test 15	90.9	891	2705	205	(49)	40
Case 2 - pH 7.2, 12 inwc						
Test 2	92.0	1451	170	105	65	210
Test 4	92.2	1578	454	111	61	219
Test 8	92.5	1731	1021	122	48	221
Test 12	93.0	1986	1579	130	39	238
Test 16	93.2	2062	2705	149	3	209
Case 3 - pH 6.5, 12 inwc						
Test 6	87.3	(916)	437	453	277	186
Test 10	90.7	815	1135	(272)	344	426
Test 14	92.0	1477	1667	(94)	360	508
Test 18	91.8	1375	2836	(79)	315	452

Table 2. Summary of SO_2 Removal Upgrade Project Results

Utility	Station (Unit)	Absorber Type	Reagent	Oxidation Mode	Observed Base SO_2 Removal	Upgrade Options	Optimum SO_2 Removal	Est. Incremental Cost of Add'l SO_2 Removed, $/ton	Additional SO_2 Removed, tons/yr
Tampa Electric	Big Bend (#4)	Dual-loop, Packed	Limestone	Forced	94	DBA Additive	99	65	4,400
Hoosier Energy	Merom (#1 and #2)	Co-current, Packed	Limestone	Inhibited	83[1]	DBA Additive	97	61	15,100
SWEPCo	Pirkey	Dual-loop, Tray	Limestone	Inhibited	80[2]	DBA Additive	99	39	21,200
PSI Energy	Gibson (#5)	Horizontal Spray Tower	Limestone	Inhibited	80[3]	Sodium Formate, DBA Additive	95	63	15,100
Duquesne Light	Elrama	Venturi	Mg-Lime	Inhibited	86 to 89	Increase in Thiosulfate Level, Venturi Pressure Drop	92	-94[4]	1,500
NYSEG	Kintigh	Vertical Spray Tower	Limestone	Inhibited	86[5]	Sodium Formate Additive	98[5]	76	10,600

[1] Includes the effects of flue gas bypass; SO_2 removal across the test module was measured at 86 to 90%.
[2] Includes the effects of flue gas bypass; SO_2 removal across the test module was measured at 97%.
[3] Includes the effects of flue gas bypass; SO_2 removal across the test module was measured at 86%.
[4] The most cost effective upgrade option actually resulted in a net decrease in system operating costs, with a modest increase in SO_2 removal capability.
[5] Assumes no flue gas bypass.

Portions of the data obtained at Hoosier Energy's Merom Station are the result of an effort that has been jointly sponsored by the Rural Electric Research Program of the National Rural Electric Cooperative Association and EPRI. Funding for the FGDPRISM portion of this program was provided by EPRI.

FUNDAMENTAL MECHANISMS IN FLUE GAS CONDITIONING

Todd R. Snyder
Research Environmental Engineer
Principal Investigator

P. Vann Bush
Manager, Particulate Science and Engineering Group
Program Manager

Southern Research Institute
2000 Ninth Avenue, South
Birmingham, AL 35205

Contract DE-AC22-91PC90365
June 1991 to July 1995

OBJECTIVES

The overall goal of this research project has been to formulate a model describing effects of flue gas conditioning on particulate properties. By flue gas conditioning we mean any process by which solids, gases, or liquids are added to the combustor and/or the exhaust stream to the extent that flue gas and particulate properties may be altered. Our modeling efforts, which are included in our Final Report, are based on an understanding of how ash properties, such as cohesivity and resistivity, are changed by conditioning. Flue gas conditioning involves the modification of one or more of the parameters that determine the magnitude of forces acting on the fly ash particles, and can take place through many different methods. Modification of particulate properties can alter ash resistivity or ash cohesivity and result in improved or degraded control device performance. Changes to the flue gas, addition of particulate matter such as flue gas desulfurization (FGD) sorbents, or the addition of reactive gases or liquids can modify these properties. If we can better understand how conditioning agents react with fly ash particles, application of appropriate conditioning agents or processes may result in significantly improved fine particle collection at lower capital and operating costs.

LITERATURE REVIEW

We began this project with an extensive literature search to assess current knowledge of interparticle forces, sorbent and ash interactions, and flue gas conditioning. We summarized the findings of our review in two Topical Reports published in the first year of the contract. The Topical Reports emphasize the crucial roles water plays in bulk fly ash behavior and fly ash collection. Adsorbed water is an almost universal factor in the interaction of particles, even in cases of very low relative humidities. Water can be present as adsorbed monolayers or multiple layers on particle surfaces, or as "free" mobile water on the surface of the particles. The form of the water depends on the relative humidity (RH) of the gas, the morphology of the particles, the geometry of the contact points, and the surface chemistry of the particles. Agents can be applied to particles to alter the affinity of their surfaces to water, and thereby affect the adhesion.

Adsorbed water will form liquid bridges between particles when relative humidity exceeds some critical level for condensation to occur at contact points. A meniscus forms around the point of contact between particles, and the surface tension of the liquid exerts a capillary force between particles. If the particle surfaces dry after liquid bridges have been formed, residual solid bridges between particles can be formed. Any water-soluble salt can act as an adhesive in this way. Solid bridges are the strongest

of interparticle bonds. ESPs and fabric filters typically operate in such a way as to systematically, or occasionally, create liquid and consequential solid bridges between collected particles.

Effects of Particle Bonding Strength on ESP Operation

In electrostatic precipitation, cohesivity and electrical resistivity are two major properties of the particulate matter that affect performance. (Particle size is a third major property but unlike cohesivity and resistivity it can not be modified by flue gas conditioning.) Electrical resistivity of the collected material dictates the allowable current density that can be imposed on the material without causing electrical breakdown. Electrical breakdown in the collected particulate layer is the source of back corona (ionization within and from the collected layer) that can degrade particle charging and collection by spewing neutralizing ions into the interelectrode region and by forcing operation at reduced voltages and corona currents. If the electrical resistivity of a layer of particles is high enough ($\gg 10^{11}$ Ω-cm), the imposition that it makes on operating voltages and currents can dramatically lower ESP collection efficiency. If electrical resistivity is too low ($\ll 10^{8}$ Ω-cm), the charge on the particles and the applied electric field are insufficient to hold the particles on the collecting electrodes. The resulting phenomenon is called non-rapping, or electrostatic, reentrainment and can also dramatically lower ESP collection efficiency. Below about 400 °F the electrical resistivity of particulate matter can be decreased by lowering the temperature, or by adding some agent to the surface of the particles that enhances conduction of charge (water and SO_3 vapor are the most common additives that are used). Flue gas desulfurization systems that lower the gas temperature through cooling by evaporation of water, either as a constituent of a sorbent slurry or water spray, can produce conditions in ESPs at which the resistivity of the particulate matter is very low. Southern Research Institute (SRI) and others have documented cases of substantial non-rapping reentrainment in ESPs downstream of FGD systems.

Ash dislodged from the collection electrodes by rapping must fall off as large agglomerates in order to reach the hopper. If ash cohesivity is too low, a substantial portion of this ash may be redispersed into individual particles (or very small agglomerates). These ash particles and small agglomerates are consequently reentrained in the flue gas stream, placing an increased load on the ESP. When particles collected in the last ESP field are reentrained, outlet mass concentrations can increase significantly.

Liquid Bridges and Fabric Filtration

Ash characteristics affect three main facets of fabric filtration: filtering pressure drop, the removal of collected ash during cleaning cycles, and, in some cases, the overall collection efficiency of the fabric filter. Once stable operation (with constantly increasing filtering pressure drop) has been reached during a filtration cycle, the rate of increase of the pressure drop is entirely dependent on the concentration and characteristics of the particles being collected and the strength of the bonds between them. Darcy's Law, which describes the resistance to gas flow through a porous medium, indicates that particle morphology, specifically surface area, has a strong effect on pressure drop. (Resistance increases as the size of the particles decreases, or as the particles become rougher.) In general, flue gas conditioning has not been shown to significantly alter these aspects of particle morphology.

Conditioning has been shown to be quite effective in altering filter cake porosity, the other main characteristic of the cake that controls flow resistance. Porosity of a filter cake can be increased by the deposition of a liquid layer on the surfaces of the ash particles prior to their collection on the cake. The liquid layer increases the bonding strength between ash particles, and causes the particles to form an agglomerate with an increased porosity. Filtering pressure drop can be substantially reduced if filter cake porosity can be increased.

After each filtration cycle, cleaning energy is used to dislodge the recently collected ash so it can fall into the hopper for ultimate disposal. If the particle-to-particle bonds in the filter cake are too strong, the cleaning energy may not be sufficient to dislodge the cake. During cleaning the ash dislodged from the filter cake must fall off as large agglomerates if it can be expected to reach the hopper. If the

bonding forces between particles are too low, a substantial portion of ash dislodged during cleaning may be redispersed into individual particles (or very small agglomerates). This ash does not fall quickly enough into the hopper, and it is consequently recaptured during the next filtration cycle. This recollection of ash places an excessively high load on the baghouse.

PARAMETRIC TESTS OF FLY ASHES AND POWDERS

Following our literature review, we investigated fly ash conditioning and interparticle bonding forces in the laboratory. Because of the importance of liquid bridges in ash particle bonding, and because many of the various types of conditioning currently in use rely on liquid bridges to provide increased bonding strength, we concentrated on understanding and measuring liquid bridges on fly ashes and other powders. Since the material most commonly responsible for these adsorbed layers and liquid bridges is water, relative humidity was a key experimental parameter. The strength of interparticle attraction and bonding is controlled by such factors as particle morphology, total contact area, and other surface characteristics of the particles (chemical compounds, adsorbed water, etc.) By varying these factors and performing selected analyses of bulk samples of fly ashes and fine powders, we related relative humidity to surface chemistry, particle morphology, and consequently, bulk ash cohesivity and resistivity. As suggested by our literature review, increased amounts of adsorbed water increased the cohesivity of the ash. We also verified adsorbed water reduces bulk ash resistivity. As the amount of water adsorbed onto ash samples increased, the tensile strengths of the samples also increased. This trend was noted for relative humidities above about 20 to 40 % for most samples. At very low humidities the tensile strengths of many of the samples we tested were also relatively high. (Detailed summaries of our laboratory analyses and results are included in the various Quarterly Technical Progress Reports issued under this contract.)

PILOT-SCALE TESTS TO VERIFY THE ROLES OF ADSORBED LIQUID

In order to verify the relationships we identified in our literature review and laboratory analyses, we conducted three pilot-scale tests on a slipstream taken from SRI's 6 million Btu/hr Coal Combustion Facility (CCF). We designed these tests to determine the effects that adsorbed water (induced by flue gas humidification) had on the permeability of filter cakes, and to determine the conditions and factors that control electrostatic reentrainment of previously collected ash layers in an ESP. The first and second pilot-scale tests have been discussed in earlier papers and reports prepared under this project. In this paper, we compare the results of this earlier testing with the results from our third and final test. In each test we withdrew and conditioned a slipstream of flue gas and entrained fly ash particles from the CCF process stream. For our third test, the CCF burned Powder River Basin (PRB) coal. Since we evaluated PRB coal fly ash in our laboratory studies, CCF tests of this coal provided an excellent opportunity for the comparison of the results of our pilot-scale tests to our laboratory results.

Flue gas temperature and water content were the primary independent variables in our test matrix. The normal relative humidity in the CCF flue gas was around 1.7 % (at 300 °F). Our laboratory data and our review of field experiences indicated that the most likely conditions for electrostatic reentrainment would be high relative humidity and relatively cool flue gas. We also expected that the strongest liquid bridges that we could form in the dust cake in our Fabric Filter Sampling System (FFSS) would result from relatively moist conditions.

In our third test, water and/or steam were injected directly into various points in the CCF, upstream of our slipstream system which consisted of a small ESP and our FFSS. This injection scheme allowed us, within certain constraints, to control both duct moisture and temperature in our slipstream system. The heat exchangers in the CCF ductwork were used to vary the temperature of the flue gas without modifying its water content. Because of its configuration in the slipstream system, the temperature of the FFSS was controlled independently of the rest of the system. Our FFSS withdrew about 2.5 acfm of flue gas from this conditioned stream. The remainder of the slipstream flow passed through the ESP and a venturi, and into the CCF pulse-jet baghouse. The CCF was operated so the pressure drop

between points where we accessed the CCF process stream induced the desired flow of 280 acfm through the ESP.

Our slipstream ESP was a relatively small, single field, single flow passage unit with a specific collection area of 62 ft^2/kacfm, and was < 90 % efficient. These factors aided in our characterizations of reentrainment. We installed continuous monitors upstream and downstream of the ESP to measure total mass concentrations in the flue gas and monitored temperature at critical points throughout the system. We installed a wet-bulb thermocouple at the outlet of the ESP to use with dry thermocouple readings from the same location to derive moisture contents of the flue gas from a standard psychrometric chart. We used two different means for identifying the onset of electrostatic reentrainment. Because the ESP we used had windows at both ends that allowed illumination and viewing of the wires and plates, we were able to visually inspect the collected ash layer on the plates as the conditions in the ESP were varied. We also observed the outlet mass monitor output as we attempted to induce reentrainment.

In order to analyze the effects that duct humidification had on the filtration characteristics of the ash collected in the FFSS, we observed two main parameters: the rate of pressure drop increase across the filtering fabric, and the amount of ash entering the FFSS. We measured the mass concentration entering the FFSS by periodically placing an absolute filter upstream of the FFSS. This allowed us to normalize the rate of filtering pressure drop increase by the mass concentration entering the FFSS. (The mass of ash reaching the filter cake cannot be directly measured because of the near-continuous operation of the FFSS, and the influence that the geometry of the FFSS transform has on selective particle settling.)

Several attempts were made to induce electrostatic reentrainment in the ESP. Our general approach was to establish a stable condition (moisture and temperature) in the ESP and then to build an ash layer (without rapping the plates) at these conditions. The ESP was typically operated at an applied voltage of 38 - 41 kV and current densities ranging between 0.8 and 3 nA/cm^2. (Higher voltage and current settings were avoided due to the possibility of high-voltage sparks and corresponding damage to the data acquisition system and/or optical mass monitors.) Once the layer was formed, we would alter the flue gas moisture and/or temperature while we observed the ash layer. During our second pilot-scale test our visual observations of the ash layers deposited on the ESP plates indicated that the appearance of the layer depended on the relative humidity in the ESP during deposition. When ash layers were deposited at around 275 °F (1.2 % RH) the ash layer looked smooth, with many large craters in its surface. In contrast, the ash layers deposited under high humidity conditions (22 % RH at about 165 °F) appeared fluffy, and the surface of the layer seemed to be composed of small (1/32 inch diameter) agglomerates of ash particles. Since the major reentrainment phenomena we observed (at about 193 °F and 17 to 20 % RH) were from these fluffy ash layers, the characteristics (porosity and tensile strength) of the layer may be key factors in inducing reentrainment.

In our third test, our initial attempt at inducing reentrainment in the ESP was with an ash layer we formed at around 200 °F and with flue gas having about 22 % H_2O by volume (27 % RH). We used water and steam injection into the CCF duct to create and hold these conditions. The ash layer on the ESP plates was formed into plateaus up to 0.25 inch thick. We began a gradual increase in ESP temperature by adjusting the CCF's heat exchangers while attempting to hold the water content constant at about 22 % by volume. During this ramp up in temperature, the steam generator malfunctioned and over the two hours we ramped the ESP temperature up to about 220 °F, the water content of the flue gas dropped to about 15 % H_2O by volume. During this period we did not observe any significant non-rapping reentrainment.

For our next attempt at inducing electrostatic reentrainment, we built an ash layer at about 200 °F and about 30 % H_2O by volume (37 % RH). We then observed the layer as we decreased the water content of the flue gas while holding gas temperature constant. We continued this trial until the water content had been reduced to 15 % H_2O by volume (18 % RH). As before, we observed no

electrostatic reentrainment of the ash layer. We continued to observe the layer as we increased the flue gas temperature in the ESP up to about 265 °F and gradually decreased the water content to about 8 % by volume (3 % RH). This trial also failed to induce reentrainment. We then rapped the plates and built a new ash layer at 210 °F and 24.5 H_2O by volume (24 % RH). Once the ash layer had matured, we discontinued all water and steam injection and observed the ash layer as it dried out gradually while the CCF used its heat exchangers to hold the temperature constant. As before, no electrostatic reentrainment was observed during this transition period. Our final attempt to induce reentrainment began with the formation of a new ash layer at about 200 °F and 10.5 % H_2O by volume (13 % RH). No water or steam were injected into the CCF duct during this period. After the ash layer had been collected at these conditions, we ramped the ESP temperature up to 270 °F. By the end of this period of rising temperatures, the relative humidity in the flue gas was 3.5 %. No reentrainment was generated during this procedure.

The data we obtained with the FFSS during our second and third pilot-scale tests are summarized in Table 1. The final column in this table normalizes the rate of pressure drop increase by the mass we collected in the mass train thimble filters we periodically placed upstream of the FFSS. This normalized value should provide a fair indication of relative changes in K_2 at different flue gas conditions. The relative humidity values presented in Table 1 are based on the moisture measured in the ESP inlet duct during the FFSS filtration test periods.

Table 1
Summary of FFSS Operation

test/run	FFSS fabric temperature, °F	$\delta\Delta P/\delta t$, in. H_2O/ hr (a)	inlet mass load rate, g/hr	approximate RH in FFSS, %	$\delta\Delta P/M$, in. H_2O/g
2/1	300	0.23	7.6	1.3	0.030
2/2	300	0.22	7.6	1.3	0.029
2/3	300	0.40	11	1.2	0.037
2/4	260	0.30	6.8	2.5	0.044
2/5	220	0.11	4.9	6.1	0.022
2/6	190	0.00	--	--	--
2/7	165	0.01	2.5	22	0.0040
2/8	165	0.01	3.0	23	0.0034
3/1	225	0.375	1.720	5.2	0.218
3/2	220	0.394	--	9.1	--
3/3	217	0.449	--	15.1	--
3/4	231	0.325	--	16.3	--
3/5	231	0.259	0.834	7.7	0.310
3/6	229	0.293	1.501	7.3	0.195
3/7	281	0.218	0.672	3.0	0.324
3/8	343	0.442	1.180	1.2	0.375

(a) ΔP is the pressure drop across the dust cake and fabric, δt is the time interval.

With two exceptions, the values in Table 1 indicate that the normalized rate of pressure drop increase falls as humidity increases. (The data obtained for tests/runs 2/4 and 3/5 vary from this trend.) As discussed above, we attribute this reduction in the accumulation of pressure drop at higher relative humidities to increased porosity induced by liquid bridging between particles. Like the filtration results we obtained with an eastern, bituminous low-sulfur coal ash (test 2), the results of the third test seem to indicate that the PRB ash can also be conditioned with water to improve filtration characteristics by increasing dust cake porosity. For liquid bridges to be able to increase dust cake porosity above the characteristic value associated with an ash, free, mobile water must exist on the

surfaces of the particles which comprise the dust cake. Once the cake is formed at an elevated porosity, that porosity should remain intact even if the adsorbed surface water is subsequently immobilized. In our laboratory studies, we related the high calcium content of PRB ash to the immobilization of adsorbed water. We believe that the calcium and the silica present in the ash undergo a pozzalonic reaction with water that adsorbs on the surface of the ash particles to form hydrocalcium silicates. In the dust cake, additional water is continuously adsorbed on the particle surfaces in the dust cake because fresh flue gas is continuously passing through the cake and over the surfaces of the collected particles. Therefore, we postulate that free water is always available for the formation of liquid bridges between the particles on the surface of the dust cake and the newly arriving particles as they are captured by the cake.

For adsorbed water to affect tensile strength and cohesivity, it must exist and remain as free water on the surfaces of the ash particles. If the water originally adsorbed on the particle surfaces becomes strongly bound up as hydrocalcium silicates (or possibly other compounds), it is no longer available to form or maintain liquid bridges. With respect to ash resistivity, the inclusion of hydrated water in the chemical matrix of the ash particles does affect volume conduction through the ash layer collected in an ESP; however, continuously present free surface water is needed for improved surface conduction.

Two factors tend to hold previously collected ash on the ESP plate. In most cases, the electrical clamping force derived from the applied electric field across the ash layer and the resistance to current flow through the layer is sufficient to hold the collected ash on the plate. However, this clamping force will diminish and possibly even become a repelling force as the resistivity of the ash decreases due to a decrease in ash temperature and/or the adsorption of water onto the surfaces of the particles. The magnitude of the effects of temperature and adsorbed water on ash resistivity and clamping force depend on the particular characteristics of the ash and the structure of the ash layer.

Over the wide range of conditions we created in the ESP, we could not modify resistivity, cohesivity, and/or tensile strength sufficiently to induce electrostatic reentrainment of the PRB ash. To help understand this behavior, we measured the tensile strength of this ash as a function of relative humidity. As with other ashes we have characterized in this way, the PRB coal ash exhibited a relative minimum in tensile strength. For this ash, this minimum tensile strength exists between 22 and 50 % RH. Figure 1 compares the tensile strength of this ash with measured values for the eastern, bituminous low-sulfur coal ash that did reentrain during our second pilot-scale test.

Figure 2 shows the dependence of resistivity on temperature for the two ashes described above. This figure includes data showing the effects that water vapor conditioning has on the laboratory-measured resistivity of the PRB coal ash. (Similar behavior has been noted for the other ashes we have characterized.) Because in many of our pilot-scale trials we increased the relative humidity and lowered the ash temperature concurrently (as would occur with simple water injection), the reduction in clamping force can be linked to an increase in relative humidity. The overall tensile strength of the ash layer provides the second factor that holds the collected ash layer on the ESP plate. Although we observed that the magnitude of this tensile strength varies as a function of the amount of adsorbed water on the ash particles (Figure 1), its overall contribution to holding the ash on the plate is always positive.

Because of the dependence of the electrical clamping force and the tensile strength on ash temperature and adsorbed water, the overall force adhering the ash to the plate can change significantly as temperature and humidity change. Figure 3 demonstrates how relative humidity affects the way these two factors combine with the characteristics of the collected ash to either hold the ash on the plate or cause electrostatic reentrainment. Figure 3(a) shows for two ashes how the electrical clamping force becomes negative after enough water is adsorbed on the surfaces of the ash particles. (As mentioned above, this increase in adsorbed water is usually accompanied by decreases in ash temperature and subsequent reductions in the resistivity of ash.) Figure 3(b) presents a generalized relationship between tensile strength and relative humidity for these same two hypothetical ashes. In Figure 3(c),

the electrical clamping force has been added to the adhering force due to the tensile strengths of the ashes to demonstrate that for an ash with the proper characteristics, electrostatic reentrainment can occur over a finite range of conditions.

ACKNOWLEDGMENTS

This work was sponsored by the U.S. Department of Energy, Pittsburgh Energy Technology Center under Contract No. DE-AC22-91PC90365. Mr. Tom Brown is the Project Manager.

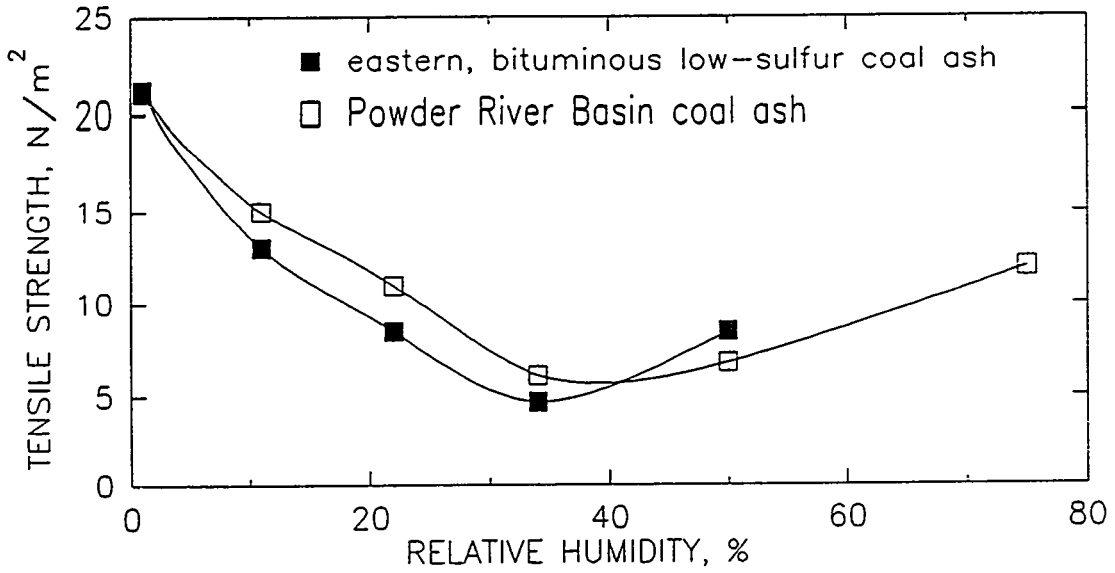

Figure 1. Tensile strength as a function of relative humidity for PRB coal ash and eastern, bituminous low-sulfur coal ash.

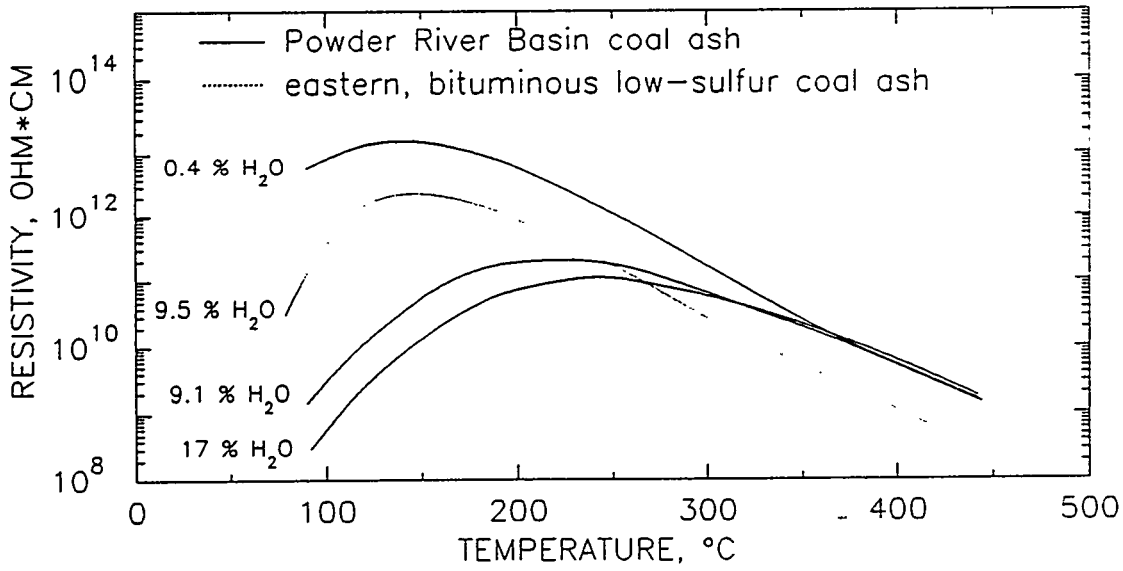

Figure 2. Resistivity as a function of temperature for PRB coal ash measured for ash samples conditioned at three different moisture contents, and eastern, bituminous low-sulfur coal ash measured for an ash sample conditioned at 9.5 % water by volume.

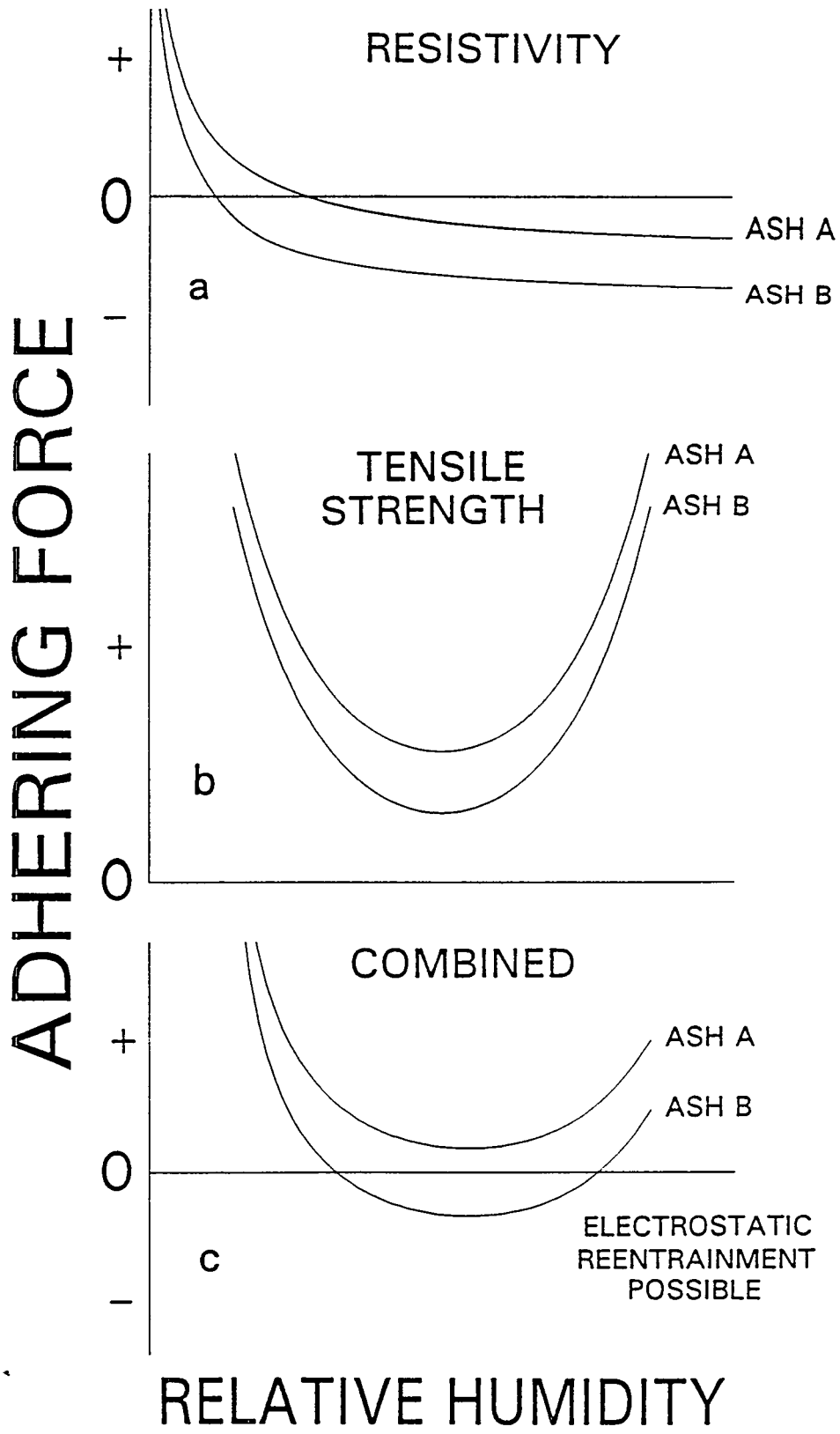

Figure 3. This figure demonstrates how relative humidity affects the way the electrical clamping force and tensile strength combine to yield conditions that can be conducive to electrostatic reentrainment.

ENHANCED PERFORMANCE OF ELECTROSTATIC PRECIPITATORS THROUGH CHEMICAL MODIFICATION OF PARTICLE RESISTIVITY AND COHESION

Michael D. Durham, Ph.D., Kenneth E. Baldrey, C. Jean Bustard, Timothy G. Ebner, Sharon M. Sjostrom, and Richard H. Slye

ADA Technologies, Inc.
304 Inverness Way So.
Englewood, CO 80112
(303) 792-5615

Introduction

Control of fine particles, including particulate air toxics, from utility boilers is required near-term by state and federal air regulations. Electrostatic precipitators (ESP) serve as the primary air pollution control device for the majority of coal-fired utility boilers in the Eastern and Midwestern United States. Cost-effective retrofit technologies for fine particle control, including flue gas conditioning, are needed for the large base of existing ESPs. Flue gas conditioning is an attractive option because it requires minimal structural changes and lower capital costs. For flue gas conditioning to be effective for fine particle control, cohesive and particle agglomerating agents are needed to reduce reentrainment losses, since a large percentage of particulate emissions from well-performing ESPs are due to erosion, rapping, and non-rapping reentrainment.

A related and somewhat ironic development is that emissions reductions of SO_2 from utility boilers, as required by the Title IV acid rain program of the 1990 Clean Air Act amendments, has the potential to substantially increase particulate air toxics from existing ESPs. The switch to low-sulfur coals as an SO_2 control strategy by many utilities has exacerbated ESP performance problems associated with high resistivity flyash. The use of flue gas conditioning has increased in the past several years to maintain adequate performance in ESPs which were not designed for high resistivity ash. However, commercially available flue gas conditioning systems, including NH_3/SO_3 dual gas conditioning systems, have problems and inherent drawbacks which create a need for alternative conditioning agents. In particular, NH_3/SO_3 systems can create odor and ash disposal problems due to ammonia outgassing. In addition, there are concerns over chemical handling safety and the potential for accidental releases.

Program Objectives

The purpose of this program funded by the Department of Energy Pittsburgh Energy Technology Center (PETC) is to identify, evaluate, and develop cost-effective ESP conditioning agents to improve removal of fine particle air toxics from coal-fired combustion flue gas streams. This goal can be met by reduction of reentrainment losses of collected ash and by control of ash resistivity.

The project has focused on the development of cohesive agents to overcome reentrainment problems associated with low particle holding force. This effort has encompassed an extensive laboratory screening, followed by bench-scale and pilot-scale tests. Discovery of a promising cohesivity agent and resistivity modifier in August, 1994, led to a further round of laboratory and pilot-scale field testing in late 1994. Because of the commercial potential for this additive, its chemical composition is being kept confidential; it has been designated ADA-23 in the following discussion of test results. It meets cost and toxicity selection criteria for the overall project in that it is a common food additive.

Laboratory Evaluation of ADA-23

ADA-23 was first tested in the laboratory as an additive for ADA's fabric filter flue gas conditioning project. On this project, screening tests with many conditioning agents were conducted using a laboratory flue gas generator and a portable filter test device. ADA-23 was one of several agents which were found to modify filter dust cake properties for flyash from a Texas lignite coal, resulting in reduced particle emissions and lower filter pressure drop. This finding led to an evaluation of the performance of ADA-23 as an ESP conditioning agent, beginning with the investigation of its effect on flyash resistivity as measured in the ADA resistivity apparatus.

The additive was injected into the ADA laboratory test fixture, where a simulated flue gas stream is passed through an additives injection chamber and then through the resistivity measurement chamber. In this system, both flyash and gas constituents are added dynamically to create specific gas composition and ash content. Moisture of the flue gas is controlled with a temperature-controlled humidifier upstream of the additives chamber. In the chamber the additive under test is sprayed into the flow with a fine mist atomizer. Additive volume to the injection nozzle is controlled with a precision peristaltic pump.

The simulated flue gas stream contains flyash that is added to the flow by a screw feeder; the injection rate is controlled by a variable speed motor. Entrained flyash is collected downstream of the additive injection chamber in the ADA resistivity apparatus, a modified point-plane electrostatic precipitator. In the resistivity cell, a dust layer is collected by either electrical precipitation or by filtering across an electrically isolated metal frit. Following precipitation, the thickness of the collected flyash layer is measured, and then the resistivity of the dust layer is determined from the measured voltage and current across the dust layer at a uniform field strength of 4 kV/cm.

Tests at Cold-Side ESP Conditions

Redispersed flyash was obtained from a generating station that fires a Texas lignite coal. Sulfur content of the lignite coal is approximately 0.6% and the flyash is low in alkali metals, sodium and potassium. The combination of low sodium and low sulfur content is associated with high-resistivity ash at cold-side ESP temperatures for a variety of coals. This ash resistivity was more than 10^{13} ohm-cm at 300 °F. It should be noted that the simulated flue gas mixture did

not contain free SO_3 vapor, which also contributed to the high resistivity of the unconditioned ash.

Two parameters were varied to determine the impact of additive ADA-23 on flyash resistivity. Tests were run over an extended flue gas temperature range of 200 to 450 °F. The concentration of additive was tested over a range comparable to that for SO_3 conditioning systems. The additive, ADA-23, demonstrated dramatic reductions in resistivity of the lignite flyash over the entire temperature range tested, as shown in Figure 1. At all temperatures tested, the resistivity could be decreased to the optimal 10^{10} ohm-cm range. Increasing the concentration of the additive at a constant temperature of 310 °F caused a reduction in flyash resistivity from about two to over four orders of magnitude. It should be noted that the liquid injection rate was identical for all test cases. The concentration of additive in the injected solution was varied to meet the target additive-to-flyash mass ratio. For tests without additive, water was injected at the same liquid feed rate.

For both baseline and conditioned samples, the ash layer was collected via point-plane electrostatic precipitation. Figure 2 plots the rate of ash layer precipitation in the resistivity apparatus; it is seen to increase with increasing additive concentration. This result is in part due to resistivity improvement, but it is also indicative of ash layer cohesivity. When collecting an unconditioned high-resistivity ash, the resistivity measurement cell typically exhibits increased blow-off for dust layers more than 1 mm thick. Conditioning with ADA-23 produced dust layers up to 4.1 mm thick without significant reentrainment.

Based on results to date using aqueous spray injection, the new additive has definite commercial potential as a conditioning agent for cold-side ESPs. The most important driver affecting the commercialization of the additive will likely be the chemical amounts required to achieve optimal conditioning. Tests have indicated that at the injection rates which work successfully in a spray chamber, conditioning with the additive in a liquid spray delivery system will certainly be cost-competitive with commercial systems. Further testing is needed at full-scale to optimize additive injection in a full size duct and to demonstrate the technology for cold-side applications.

Tests at Hot-Side ESP Conditions

All of the test data for ADA-23 has indicated that flue gas conditioning for resistivity modification is applicable to a wider temperature range than for conventional SO_3 conditioning. Based on our experimental results and on knowledge of the additive's chemistry and physical properties, it appeared that conditioning could extend the ash surface conduction mode to temperatures normally dominated by volume (bulk) conduction. If so, conditioning with ADA-23 could alleviate ESP performance problems associated with sodium ion depletion in ash layers of hot-side ESPs.

To test whether ADA-23 could be used to condition hot-side ESPs, laboratory resistivity tests were recently conducted using ADA's flue gas simulator and additive injection chamber. Tests were first run at 700 °F with an ash sample from a hot-side ESP at a plant firing a western

subbituminous coal. This ESP has historically exhibited severe performance problems associated with a low sodium content in the coal. Resistivity of fresh ash at hot-side operating temperatures has typically been measured in the 10^{10} - 10^{11} ohm-cm range; it is expected that the resistivity increases significantly for an aged ash layer. For this test, the additive and ash were injected at 700 °F in a 10% moisture, air environment. As seen in Figure 3, the additive reduced resistivity at 700 °F by up to two orders of magnitude. The amount of the resistivity reduction can be controlled by the concentration of the additive. This demonstrates that conditioning can be effective at hot-side temperatures.

Further laboratory resistivity tests were conducted using a mixture of 75% SiO_2 and 25% Al_2O_3 powder. This synthetic "flyash" mix was created to entirely eliminate alkali ion charge carriers from the dust layer and thereby present a worst-case ash to condition. The mixture of refractory powders was redispersed on the resistivity measurement frit and was heated to 700 °F in a 10% moisture gas stream. The powder layer was conditioned by injecting liquid additive as an aqueous spray in the spray additive chamber upstream of the resistivity measurement cell at 700 °F. Additive was brought into contact with the powder layer by drawing sample gas through the powder layer and the porous sample frit. Baseline tests were also conducted with no flue gas conditioning by injecting a water spray rather than an additive solution. Resistivity of the baseline powder sample was 4 x 10^9 ohm-cm; conditioning with the additive successfully lowered resistivity by an order to magnitude to 4 x 10^8 ohm-cm. While the unconditioned powder layer at this temperature exhibited only moderate resistivity, the test demonstrated that the additive can effectively reduce resistivity independent of sodium or lithium ion charge carriers at hot-side conditions.

SRI Coal Combustion Facility Test

Pilot-scale tests were conducted on a 300 acfm slipstream at the Southern Research Institute Coal Combustion Facility (SRI CCF) during a trial burn of a Powder River Basin coal (Bell Ayr). The tests reconfirmed the previous laboratory results that ADA-23 injected as an aqueous spray is effective as a conditioner for high resistivity flyash. Additionally, ESP performance of a single field, 9" wire-plate ESP was improved by conditioning with ADA-23, as measured by both increased electrical field strength and by decreased outlet particulate emissions. Importantly, the additive worked successfully in an actual flue gas environment.

The ESP was instrumented to continuously monitor voltage, current, flow rate, temperatures, and outlet particulate. In addition, at each test condition, both a "clean plate" and a "dirty plate" V/I curve was taken manually. Resistivity was measured continuously at the ESP inlet with a measurement cycle of less than 30 minutes. Resistivity samples were collected by filtering across an electrically isolated metal frit, rather than by point-plane precipitation. This modification reduced the required sample time and it improved test repeatability. Dust layers collected by this method were approximately 0.2 to 1 mm thick.

The test began with a baseline condition at an ESP inlet temperature of 300 °F, without spray conditioning. Flue gas moisture content was 9.5%. Baseline flyash resistivity was 5 x 10^{11} ohm-cm. At this condition, the pilot-scale ESP was operating poorly, with an electrical field

strength of only 0.5 nA/cm^2. Throughout the test, ESP secondary voltage was maintained at 40 kV to avoid sparking to avoid disruption of the data acquisition and computer control system.

Conditioning with ADA-23 reduced the ash resistivity to 9 x 10^9 ohm-cm. Electrical field strength improved to 2 nA/cm^2 with the baseline unconditioned layer still on the plates. The plates were rapped clean and conditioning with ADA-23 continued at the same rate. Once a layer had built up, ESP field strength increased to 8 nA/cm^2. Spray injection was then switched to water at the same flow rate. Resistivity returned to 4 x 10^{11} ohm-cm, essentially a repeat of baseline. ESP electrical conditions also began to degrade. This confirmed that the improved electrical conditions during additive injection were not a result of water spray cooling. The improved electrical conditions resulted in lower particle emissions from the ESP as measured by a real-time optical mass monitor.

Additional Pilot-Scale Tests

The performance tests with ADA-23 first in the laboratory and then at SRI's CCF were conducted with spray injected in special additives spray chambers at low gas velocity. Once the additive was shown to work predictably under these conditions, the next step was to evaluate spray conditioning at typical duct conditions. For this, a further test was conducted at a Colorado power plant firing a Powder River Basin coal.

Flue gas was extracted isokinetically from an 18 inch diameter duct that supplies a particulate control pilot plant in operation at the power plant. The slipstream is extracted from the plant duct downstream of the air heater and upstream of a reverse gas baghouse. An atomizing spray nozzle manifold was inserted into the slipstream duct approximately 40 ft. and a 90 degree bend upstream of a sample probe. Liquid feed to the nozzle manifold was controlled with a peristaltic pump. The sample probe drew flue gas isokinetically to a portable ESP at a flow rate of approximately 60 acfm. In all, sample residence time from injection to the ESP inlet was less than 2 seconds. Velocity in the duct was 50 - 60 ft/second and the gas temperature was 250 °F. The sample was reheated to a constant 300 °F at the ESP inlet.

The portable ESP was configured as a single channel wire/plate at a 9" plate spacing with standard 0.1" diameter bare wires. This configuration was intended to approximate the performance characteristics of a typical full-scale ESP. Special teflon baffles were installed around and beneath the collection plates to minimize sneakage. The flow rate was set to provide an SCA of 180 ft^2/kacfm. The high voltage power supply was spark limited with an industry-standard power controller.

ESP voltage and current were monitored continuously and V/I curves were taken to sparking for each test condition. Multiple resistivity measurements were taken at the ESP inlet for each test condition. Outlet particulate concentrations were monitored by a Triboflow monitor, which produces a response proportional to the number of charged particles contacting the probe. Conditioning reduced the ash resistivity from a baseline of mid 10^{11} ohm-cm to 10^9 ohm-cm. The ESP conditions also improved and the triboflow monitor response was also

reduced during conditioning periods. Based on these results, the following conclusions were reached:

- Aqueous additives solutions can be successfully injected into a turbulent flue gas stream at 40-60 ft/second gas velocity;
- Liquid droplet size for the nozzle array was less than 40 μm Sauter mean diameter based on manufacturer's specifications for the nozzle;
- A residence time of 1 - 2 seconds between injection and control device is adequate for conditioning;
- Flue gas spray cooling is 5 - 10 °F for the conditioning rates required with ADA-23;
- Effective spray distribution will be critical to the success of conditioning. This must be tested at full-scale.

Ash Characteristics

Based on tests that ADA has conducted to date, additive conditioning with ADA-23 at effective concentrations does not alter fly ash chemical and handling characteristics. During this test, samples of ash from a pilot particulate control device were taken during a baseline period with no conditioning and during additive injection. The samples were submitted to an independent testing laboratory for elemental analysis and for TCLP analysis for leachable metals. The TCLP analysis indicates that the conditioned flyash is not enriched in any of the leachable metals, including the volatile metals, mercury and selenium. Conditioning with ADA-23 should produce a non-hazardous waste suitable for commercial sale or conventional landfilling.

Conclusions

Following are the conclusions reached from the laboratory and field performance tests with ADA-23:

- Cohesivity effects due to ADA-23 are evident from observations of high tensile strength ash layers developed in the resistivity device;
- ADA-23 is an effective resistivity modifier for low-sulfur high-resistivity western coals;
- Surface conduction mode through ash layers is extended to a higher temperature range of cold-side ESP operation (>350 °F).ADA 23 is effective at hot-side ESP temperatures;
- ESP electrical characteristics and particulate collection can be significantly improved by conditioning;
- Conditioned ash should be suitable for commercial use (TCLP tests indicate no enrichment in volatile metals);
- Ash handling is not impaired at conditioning levels required for resistivity control.

Further testing is needed at full-scale at both cold-side and hot-side ESP conditions with a high-resistivity, subbituminous coal. This is necessary to develop additive delivery systems, optimize and define the additive concentration, and to demonstrate the technology. Tests at the pilot-scale provide ample evidence of performance to justify this step.

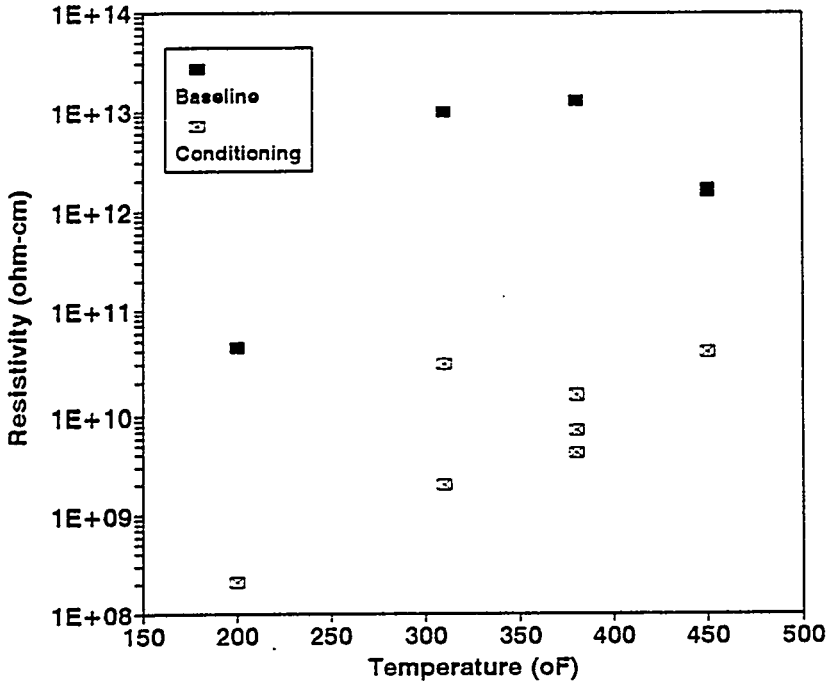

Figure 1. Additive ADA-23 Effect on Flyash Resistivity as a Function of Temperature.

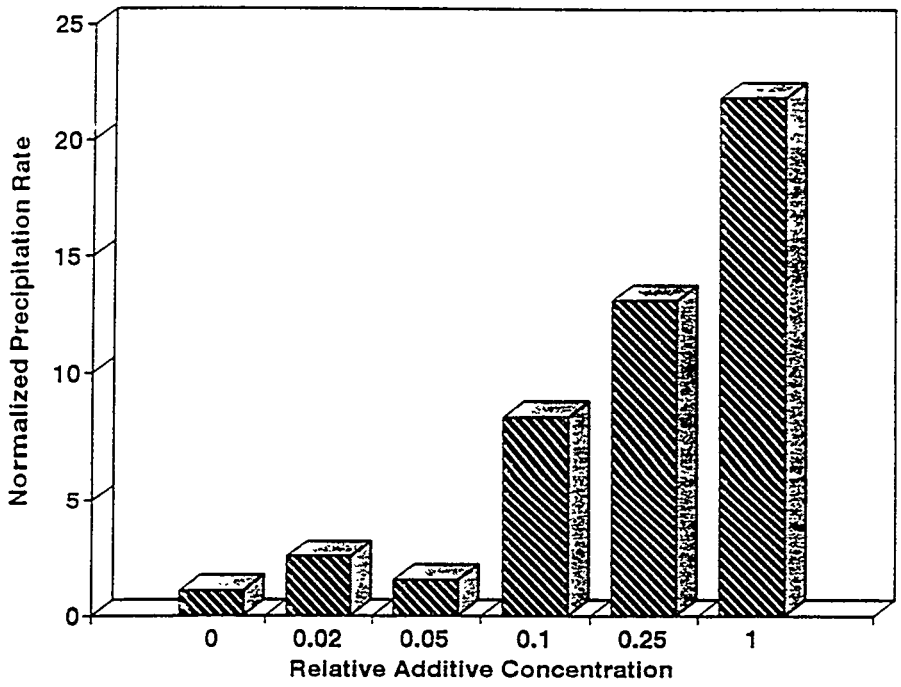

Figure 2. Flyash Precipitation Rate as a Function of Relative Additive Concentration.

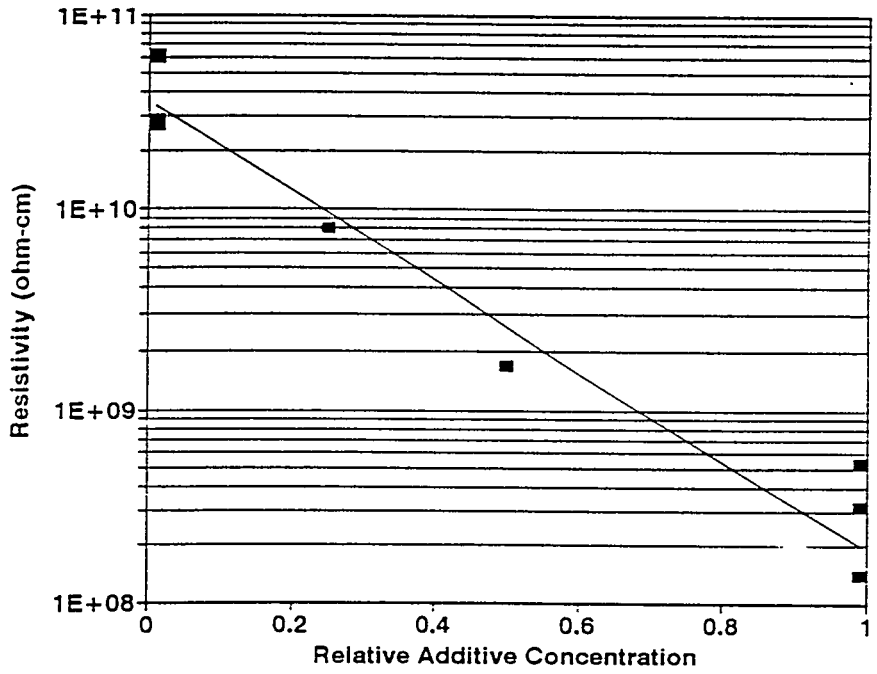

Figure 3. Resistivity versus Additive Concentration for a Hot-Side ESP Flyash at 700 °F.

NON TOXIC ADDITIVES FOR IMPROVED FABRIC FILTER PERFORMANCE

C. JEAN BUSTARD
Scientist

KENNETH E. BALDREY
Senior Research Engineer

TIMOTHY G. EBNER, SHARON M. SJOSTROM
Research Engineers

RICHARD H. SLYE
Senior Research Technician

ADA Technologies, Inc.
304 Inverness Way South, Suite 110
Englewood, CO 80112
(303) 792-5615

Introduction

The overall objective of this three-phase Small Business Innovative Research (SBIR) program funded by the Department of Energy Pittsburgh Energy Technology Center (PETC) is to commercialize a technology based upon the use of non-toxic, novel flue gas conditioning agents to improve particulate air toxic control and overall fabric filter performance. The ultimate objective of the Phase II program currently in progress is to demonstrate that the candidate additives are successful at full-scale on flue gas from a coal-fired utility boiler. This paper covers bench-scale field tests conducted during the period February through May, 1995.

The bench-scale additives testing was conducted on a flue gas slipstream taken upstream of the existing particulate control device at a utility power plant firing a Texas lignite coal. These tests were preceded by extensive testing with additives in the laboratory using a simulated flue gas stream and re-dispersed flyash from the same power plant. The bench-scale field testing was undertaken to demonstrate the performance with actual flue gas of the best candidate additives previously identified in the laboratory. Results from the bench-scale tests will be used to establish operating parameters for a larger-scale demonstration on either a single baghouse compartment or a full baghouse at the same site.

The bench-scale field test matrix included four separate phases that were scheduled over a three month period. The phases included 1) set-up, mechanical checkout and baseline testing, 2) screening tests, 3) optimization tests, and 4) long-term operation. Nine additives were screened

during the bench-scale field tests. Of these, six decreased outlet emissions; one of these also reduced the number of bag cleans per hour. The additive that reduced both the number of bag cleans per hour and the outlet emissions was further optimized and tested for a one-week longer-term test. This additive reduced the outlet emissions by an order of magnitude and reduced the number of cleans required by a factor of 2 to 8.

Experimental Apparatus

The test equipment consisted of an isokinetic sample probe, an additive contact chamber, an additive injection assembly, and the ADA Filter Test Device (FTD), as shown in Figure 1. In the additives contact chamber, a small, dual-fluid nozzle atomizes and injects an aqueous solution of diluted additive into the flue gas stream. Additive liquid flowrate is metered and controlled with a precision peristaltic pump. The liquid injection rates were set to minimize flue gas spray cooling due to water evaporation to less than 45°F below duct temperatures for the initial bench-scale screening, and to a maximum of 15°F below duct temperature during the later optimization tests.

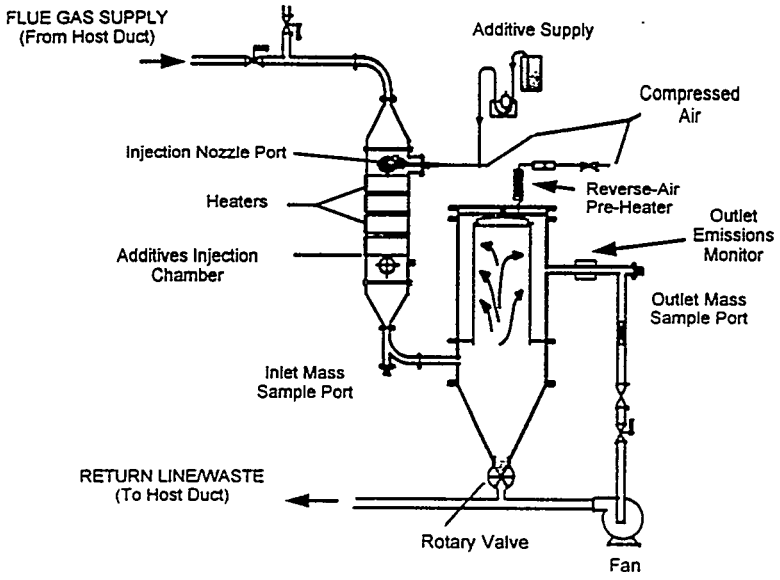

Figure 1. Sketch of the ADA bench-scale Filter Test Device (FTD), configured for reverse-gas cleaning, and the upstream additives injection chamber.

For the bench-scale additives tests, the FTD was configured for reverse-gas cleaning with an 8-inch diameter fiberglass bag of a weight and weave to match the bags currently in use in the shake/deflate baghouse of the host power plant. Relative outlet particulate emissions were measured using a Triboflow™ monitor installed downstream of the FTD filter chamber. The Triboflow™ instrument measures particle concentration via detection of the electric charge on

particles which impact a sensor in the gas stream. Outlet emissions measured by the Triboflow™ monitor were confirmed periodically by particulate mass measurements via EPA Method-17.

A primary parameter of interest for fabric filter performance is the cleaning frequency required to maintain a baghouse at a given average pressure drop. Cleaning frequency and pressure drop are interdependent; some baghouses are operated on a fixed cleaning schedule and the average pressure drop is monitored to gauge performance. Other baghouses are operated by initiating the cleaning sequence at a maximum pressure drop with the cleaning frequency as the dependent variable. The latter approach was used during the bench-scale testing; the FTD control logic was configured such that the bag was cleaned when the pressure drop across the filter bag reached 5-inches H_2O. A pressure initiate of 5-inches H_2O across the tubesheet was chosen based on previous experience with the FTD and with pilot-scale and full-scale baghouse operation. This value represents a pressure drop within an acceptable range for baghouse fans and it provides meaningful data for comparison to other baghouses when using new filter bags.

At an operating power plant, flue gas temperatures, flyash concentration, and gas composition change with normal variations in plant operations (load, coal composition, and combustion conditions). These data were collected during the bench-scale tests for two reasons: 1) the performance of the FTD is affected by variations in flue gas conditions and 2) a full-scale additive injection system may need to control with respect to either a specific process parameter or a combination of parameters.

Site Description

The particulate control equipment at the host plant includes an electrostatic precipitator operating in parallel with a shake/deflate baghouse. Flue gas conditioning with ammonia is used to maintain performance of the particulate control equipment. The ammonia injection location for the host system is located downstream of the sample ports where the FTD was installed. The operating air-to-cloth ratio for the baghouse was nominally 2.5 ft/min; this was chosen as the target air-to-cloth ratio for the FTD for the screening tests. The bag fabric for the FTD testing was also chosen to match the weight and weave of the fiberglass bags currently used in the host plant baghouses. Thus, the FTD test conditions matched those in the full-scale shake/deflate baghouses as closely as possible.

Set-up, Mechanical Checkout and Baseline Testing

During this phase of the testing, the FTD was installed on the host duct in a reverse gas configuration (Figure 1). Following mechanical checkout to verify proper operation, the FTD was operated unattended for eight days to establish a stable baseline. This baseline test was performed without any additive or water injection. Baseline particulate mass tests were conducted at the FTD inlet scoop location to determine mass loading, flue gas moisture content, and stack velocity. Mass concentration measurements in the FTD inlet line during the baseline tests indicated a loading of 11 gr/acf entering the FTD. This loading is at the upper limit of what

can be considered representative at this site, however, it is unusually high for power plants in general. The host duct temperature at the inlet extraction location ranged from 360 to 400°F. The FTD chamber temperature and the additives contact chamber were maintained at nominally 400°F for all tests. At the end of baseline testing, the cleaning frequency was 3 cleans per hour with a clean initiate set-point at a tubesheet pressure drop of 5 inches H_2O. The Triboflow™ monitor registered an average signal of 35% at the FTD outlet.

Additive Screening

A re-evaluation of laboratory results in an actual flue gas environment was identified as an essential first step in the bench-scale field tests. It is difficult to accurately simulate particle size distribution in the laboratory due to inherent limitations in collecting and re-dispersing a representative ash sample. The laboratory ash sample was probably biased to larger particles (as compared to the size distribution in the flue gas). The ash was valuable in comparing the effectiveness of the additives, however, small particles (less than 3 μm), which are present in disproportionately low levels in laboratory testing, are more challenging for a baghouse to filter. A further potential bias, in this instance, was the effect of residual ammonia in the laboratory ash sample. Also, fluctuations in actual flue gas conditions could not be duplicated in the laboratory.

Screening tests were conducted for the best-performing additives identified in previous laboratory tests. The same bag used during initial baseline tests was left in place for the screening tests. Water was injected following the initial baseline to determine the effect, if any, of water alone. Once the operation stabilized with water injection, short additive injection runs were conducted (3-5 cleaning cycles) to document short-term changes in performance. The system was then returned to baseline with water injection. After re-establishing water-only baseline conditions, the next additive was injected and the procedure repeated. Additives were injected at the rates previously determined in the laboratory trials.

Screening tests were completed for nine candidate additives. Of these nine candidates, two were identified for optimization and long-term testing at the bench-scale. The results for the screening tests as compared to baseline are shown in Table 1. Data is presented in terms of percent reduction in outlet emissions and percent change in cleaning frequency. ADA-6 and ADA-14 were initially selected for optimization and longer-term testing because they significantly reduced outlet emissions and reduced the number of cleans required to maintain the tubesheet pressure drop at a given level. ADA-9 and ADA-10 were considered secondary options because they significantly reduced outlet emissions without increasing the number of cleans required to maintain the tubesheet pressure drop.

A screening test was repeated for ADA-14 using plant make-up water to prepare the additive solution. This test was conducted to identify potential problems with additive delivery components (spray nozzle, pump) or with solution chemistry when plant water is used to mix additives (it would be an advantage at this site if plant water could be used as the carrier liquid). The performance results were similar to those presented in Table 1 for ADA-14. There was also no indication of nozzle pluggage. If further tests with plant make-up water are conducted, it will

be important to monitor total suspended solids and if necessary, make modifications to prevent possible nozzle plugging.

Table 1. Bench-Scale Screening Test Results

Additive	Cleaning Frequency change to baseline	Reduction in Emissions % change to baseline
ADA-7	33% increase	78
ADA-6	78% decrease	98
ADA-9	0	70
ADA-10	0	96
ADA-14	20% decrease	90
ADA-18	0	0
ADA-19	112% increase	90
ADA-20	0	0
ADA-21	0	0

A final screening test was conducted to better simulate flue gas conditions which will likely be present during a full-scale test. Since ammonia will probably be injected during compartment or full-scale testing, but was not present in the FTD flue gas slipstream, it was necessary to document the effect of ammonia on the additives performance. Ammonia was injected into the inlet of the FTD at a rate of 25 ppm. After 8 hours of ammonia-only injection there was no noticeable effect on outlet emissions or cleaning frequency. Previous testing with ammonia showed that the beneficial effect of ammonia is very sensitive to SO_3 levels in the flue gas. Because no effect was seen, it was assumed that the SO_3 level was probably very low (SO_3 measurements were not made). ADA-14 was then injected at the previous screening test concentration simultaneously with the ammonia. Again performance results were similar to those presented in Table 1 and it was therefore concluded that ammonia did not negatively impact the effect of ADA-14.

Optimization Tests

Based on the results from the screening tests, additive optimization was scheduled to be performed on ADA-6 and ADA-14. Initial optimization of ADA-6 revealed that this additive did not perform as indicated in the screening tests. Boiler load had decreased significantly during screening of ADA-6. It was initially believed that this contributed only partially to the ADA-6 success during screening. Apparently, the grain loading to the inlet of the FTD plummeted with boiler load and, subsequently, the caused time between cleans to increase. It was concluded based on the additional optimization test data that ADA-6 was not a viable candidate.

As an alternative to ADA-6, ADA-10 was tested. ADA-10 decreased outlet emissions; however, the time between cleans also decreased significantly, even at very low concentrations.

This behavior indicated that this additive was forming an overly cohesive ash and was not acceptable for further testing.

A full series of optimization tests was performed on ADA-14. These results are presented in Table 2. The additive-to-ash concentration is presented as normalized to a value identified as the optimized concentration. Concentration rate was increased incrementally, while the effect on performance was noted for at least 4 hours. At very low concentrations a 60% decrease in outlet particle loading was measured. As the concentration was increased, the cleaning frequency decreased and further reductions in outlet emissions occurred. At two times the screening test concentration, the time between cleans was 5 times greater and the outlet emissions were 99% less that baseline conditions. These tests were very encouraging for several reasons: 1) performance improvement was directly proportional to additive concentration, 2) beneficial performance occurred at very low injected concentrations, and 3) response times to additive concentration changes were nearly immediate. After observing the effect on performance from the additives, it is believed that relatively low concentrations can be used and that the effect will improve over time.

Table 2. ADA-14 Bench-Scale Optimization Test Results

Normalized Concentrations	Cleaning Frequency decrease to baseline	Reduction in Emissions % change to baseline
0.25	No Change	No Change
0.5	No Change	60%
0.75	50-75%	60-99%
1.0	100%	60-99%
1.5	200%	80-90%
2.0	400%	99%

A new bag was used for step two in the optimization process. Additive injection was begun immediately at startup to document if improved performance could be realized on new bags. The injection rate was the normalized concentration of 1. The additive did not appear to have a detrimental effect on start-up performance, and this was considered the beginning of the long-term test. If additive injection at startup had appeared to cause problems, the bag would have been changed out and a baseline established before beginning the long-term tests.

Long Term Tests

Longer-term (one week) tests were run at the optimized conditions identified from the optimization tests. The objective of these tests were to observe the impact of continuous operation and flue gas fluctuations on additive performance. During the long-term tests, inlet and outlet mass tests were completed to quantify particulate collection efficiency. One additive was evaluated during the long-term test.

Long-term tests were performed using ADA-14 at a normalized additive-to-ash ratio of 1. The beginning of optimization step two marked the beginning of the long-term test. Additive injection was started within the first hour of exposure of the bag to flue gas. Figure 2 graphically compares the results from the long-term test to a baseline test in terms of time between cleans, post-clean pressure drop, Triboflow™ signal, and duct temperature. A total of 140 hours operation were obtained. An interpretation of these results follows:

- In general, the time between cleans was at least 2 times longer with additive injection. This value fluctuated with host boiler load conditions and when the injection nozzle plugged. For example, around 120 hours the load decreased significantly. This can be seen as a decrease in temperature. The time between cleans increased to nearly 8 times the baseline values. There are two phenomena occurring. First, the ash loading decreased (as documented earlier) thus reducing time between cleans. In addition, when the ash loading decreased the additive-to-ash ratio increased because the injection concentration was not changed. As shown in the optimization tests, improvement in baghouse performance is directly proportional to additive concentration.
- Outlet emissions, as measured by the Triboflow™ meter, were significantly lower when ADA-14 was injected. In general, the signal was 70% lower compared to baseline. Comparing Method 17 mass tests conducted during baseline testing and ADA-14 injection to the Triboflow™ signal resulted in a correlation factor of 0.92. Therefore, ADA-14 reduced outlet emissions by nearly an order of magnitude.
- During additive injection, the post-clean pressure drop quickly increased to 3.0 inches H_2O and appeared to stabilize below 4.0 inches H_2O. In comparison, the baseline data show that without additive injection the post-clean pressure drop increased more gradually at first, but continued to increase to a level nearly an inch greater than that with additives. This shows that the additive is forming a dustcake that has better cleaning properties. This lower post-clean pressure drop contributes to the increase in time between cleans with additive injection.
- Host duct temperature is presented because it was the only continuously monitored parameter that followed boiler load. This plot shows that boiler load was fairly similar between the baseline and long-term tests. This is important, because it would be difficult, if not impossible, to compare the two test periods if boiler load had been significantly different.

Conclusions

Bench-scale tests were performed on actual flue gas from an operating power plant with nine additives. The results from these tests showed that one additive, ADA-14, significantly improved baghouse performance by reducing both outlet emissions and cleaning frequency. Repeatable results were obtained through screening, optimization, and long-term tests. Testing also showed that plant make-up water (pond water) could be used as the carrier fluid and that ammonia injection did not interfere with ADA-14's beneficial properties.

Based on the excellent results with ADA-14, arrangements for a larger scale test, nominally 10 MW(e), are being pursued.

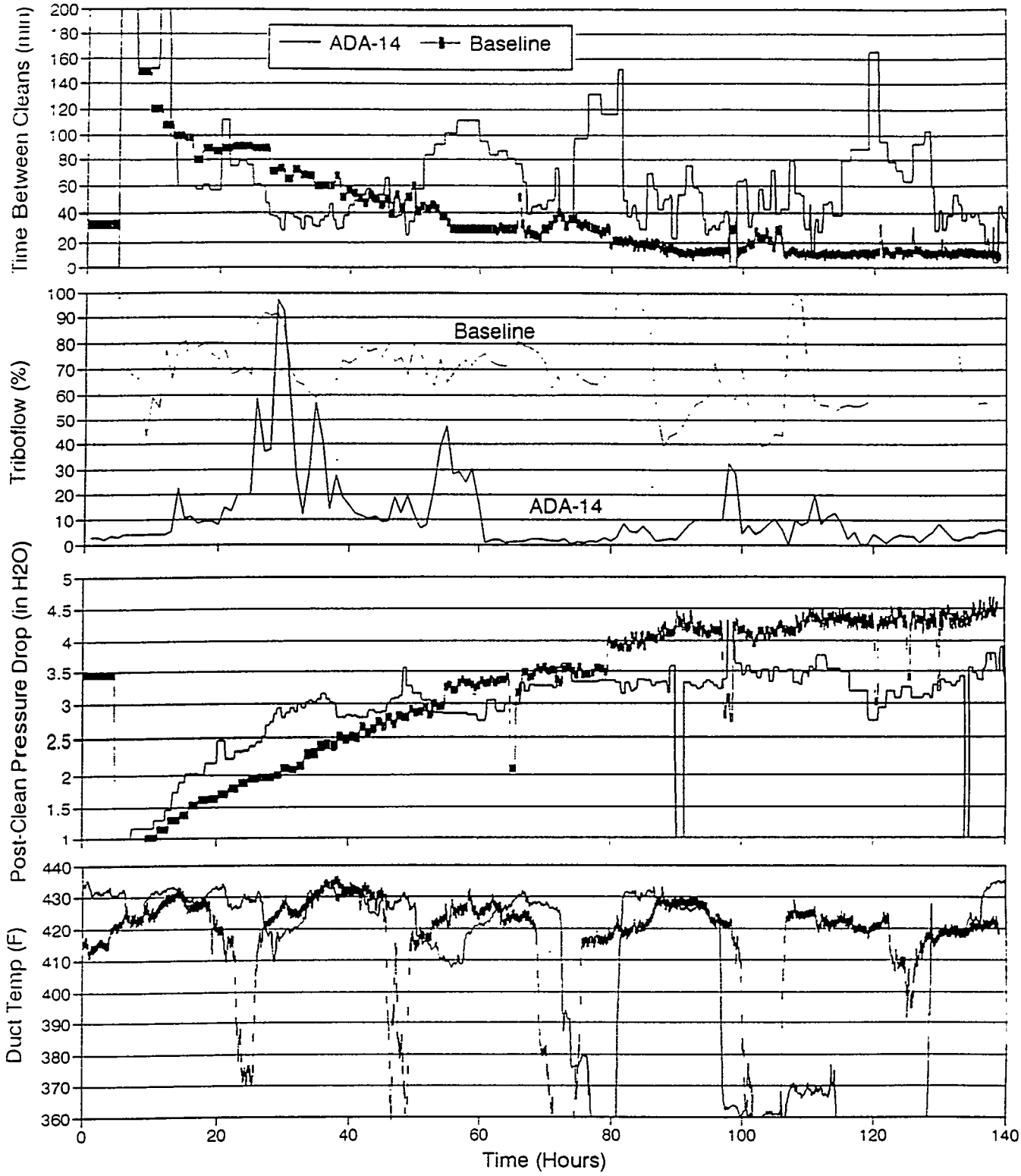

Figure 2. History of FTD performance during baseline and ADA-14 injection. All plots are trends of 5 minute averages except Triboflow™, which is a trend of 1 hour averages.

The following manuscript was unavailable at time of publication.

A GENERIC NO$_x$ CONTROL INTELLIGENT SYSTEM (GNOCIS) FOR COAL-FIRED POWER PLANTS

John N. Sorge
Southern Company Services
P.O. Box 2625
Birmingham, AL 35202-2625

Please contact author(s) for a copy of this paper.

The Integrated Environmental Control Model

Edward S. Rubin, Michael B. Berkenpas and Jayant R. Kalagnanam
Center for Energy and Environmental Studies
Carnegie Mellon University
Pittsburgh, PA 15213

Introduction

The capability to estimate the performance and cost of emission control systems is critical to a variety of planning and analysis requirements faced by utilities, regulators, researchers and analysts in the public and private sectors. The computer model described in this paper has been developed for DOE to provide an up-to-date capability for analyzing a variety of pre-combustion, combustion, and post-combustion options in an integrated framework. A unique capability allows performance and costs to be modeled probabilistically, which allows explicit characterization of uncertainties and risks.

Modeling Framework

Previous reports have described earlier development and applications of the Integrated Environmental Control Model (IECM).[1,2] The IECM provides a systematic and integrated treatment of emission control options employing pre-combustion, combustion and post-combustion control methods. The model was developed to provide preliminary performance and cost estimates for new coal-fired power plants. Of particular interest were a number of advanced environmental control technologies being supported by DOE. For comparative purposes, however, a set of "baseline" technologies representing current commercial systems also is part of the IECM framework. Table 1 lists the technologies currently included. For each technology, a process performance model was developed to account for all energy and mass flows (including air pollutants and solid wastes) associated with that process. Coupled to each performance model, an economic model was developed to estimate the capital cost, annual operating and maintenance (O&M) costs, and total levelized cost of each technology. The technology models developed for the IECM in the mid-to-late 1980s now are being updated and enhanced to reflect more recent design criteria and associated performance and costs. The status of major IECM components is briefly reviewed in the paragraphs below.

Coal Cleaning Processes. The IECM includes models of both conventional and advanced coal cleaning processes. The conventional processes include four plant designs of increasing complexity, which provide increasing capability for sulfur as well as ash removal. Each of these plant designs (referred to as cleaning levels 2, 3, 4 and 5) can be optimized to achieve a target sulfur or ash reduction while maximizing overall yield (thus, minimizing costs). Data requirements for these models includes coal-specific washability data plus cleaning circuit design parameters such as top size and bottom size for different coal fractions.

Models of several advanced physical coal cleaning processes also have been developed based on limited data for several U.S. coals. While these processes are capable of achieving higher levels of sulfur and ash reduction than conventional processes, their costs also are higher. Several of these processes have been developed to provide "super-clean" coal for use in coal-liquid mixture fuels, which compete with other premium fuels such as oil or gas.

Table 1. Emissions control technology options for the IECM

Plant Area	Baseline Processes	Advanced Processes
Physical Coal Cleaning	• Level 2 Plant • Level 3 Plant • Level 4 Plant • Froth Flotation	• Selective Agglomeration • Heavy Liquid Cyclones • Coal-Pyrite Flotation • Magnetic Separation
Combustion Controls	• Low NO_x Burners	• Reburning (gas)[a] • Slagging Combustors[a]
Post-Combustion Controls	• Selective Catalytic Reduction (Hot-side and Cold-Side)	• NOXSO • Copper Oxide • Electron Beam • Advanced SO_2/NO_x Removal[a]
	• Wet Limestone FGD • Wet Limestone with Additives • Wet Lime FGD • Lime Spray Dryer	
	• Electrostatic Precipitator (Cold-side) • Reverse Gas Fabric Filter • Pulse Jet Fabric Filter	
Waste Disposal & By-Product Recovery	• Landfill • Ponding	• Sulfur Recovery • Sulfuric Acid Recovery • Gypsum

[a] To be completed in project Phase II.

Base Power Plant. Performance and cost models of a base power plant are needed to accurately characterize the cost of integrated emission control systems, particularly when coal cleaning is employed. The IECM base plant performance model includes detailed mass and energy balances, fuel combustion equations, and thermodynamic relationships to calculate flue gas flow rates, plant efficiency, and net power generation. The environmental performance of the furnace also is determined from mass and energy balances where possible, or from empirical relationships where necessary, as in the case of NO_x emissions. A detailed model of the air preheater also has been developed to properly account for energy credits when advanced environmental control processes are used.

Revised cost models for the base power plant have been developed based on recent data from EPRI for three furnace designs related to coal rank (bituminous, subbituminous and lignites). The new cost algorithms estimate capital costs and annual O&M costs as a function of key design parameters.

NO_x Controls. The IECM includes both in-furnace and post-combustion NO_x control options. Currently, the in-furnace combustion controls include low NO_x burners for a new power plant meeting or exceeding federal New Source Performance Standards. Additional combustion options suitable for NO_x retrofits currently are being developed and will be implemented in the IECM during 1995.

Post-combustion control methods include both "hot-side" and "cold-side" selective catalytic reduction (SCR) systems. New SCR performance and cost models incorporate recent data

and experience from SCR units worldwide. The revised models contain a larger number of system design parameters, a more detailed characterization of catalyst activity, and additional details related to capital cost and O&M cost parameters.[4] While SCR systems on coal-fired plants are only now emerging commercially in the United States, their widespread use in Europe and Japan, often in combination with FGD, represents the benchmark design for comparisons with advanced emissions control systems being developed by DOE.

Particulate Emission Controls. The IECM includes performance and cost models of cold-side electrostatic precipitators and fabric filters. Performance and cost models for both technologies recently have been updated to reflect current applications.[4] The revised ESP performance model calculates total particulate removal as a function of ash composition and flue gas properties, while fabric filter performance is related primarily to the air-to-cloth ratio. The latter models also have been expanded to include both reverse gas and pulse jet fabric filter designs. Recent EPRI studies have been used to update the economic models for all particulate collectors in the IECM.

Flue Gas Desulfurization Systems. Substantial improvements in FGD system design, accompanied by reductions in cost, have been seen over the past decade, and recent enhancements to the IECM modules now reflect these changes.[5] New FGD performance and cost models have been developed for the IECM for four common types of FGD systems: (1) wet limestone with forced oxidation; (2) wet limestone with dibasic acid additive; (3) magnesium-enhanced wet lime system; and (4) a lime spray dryer system. The new cost models reflect the results of recent studies for EPRI, while the new performance models represent the capabilities of modern commercial systems.

Combined SO_2/NO_x Removal Processes. A key element of DOE's Clean Coal Technology program focuses on advanced processes for combined SO_2 and NO_x removal to achieve high performance goals at lower cost than the conventional combination of SCR plus FGD. Models of three SO_2/NO_x control systems have been developed for the IECM: the fluidized-bed copper oxide process, the NOXSO process, and the electron beam process. The copper oxide and NOXSO processes are of continuing interest to DOE, and earlier versions of the performance and cost models for these two processes are being refined and updated at the present time.

Waste Disposal and By-Product Recovery Systems. IECM revisions treat solid waste disposal as a variable cost item associated with a particular control technology, consistent with the costing method used by EPRI and others. Thus, boiler bottom ash disposal is included in the base plant model, fly ash disposal costs are incorporated in the ESP or fabric filter models, and FGD wastes or by-product credits are treated in the FGD cost models.

Advanced processes employing combined SO_2/NO_x removal produce by-product sulfur or sulfuric acid rather than a solid waste. Because the sulfur or sulfuric acid plant is a significant part of the overall plant cost, separate engineering models have been developed for these two components. These models are sensitive to input gas composition and other parameters affecting overall process economics.

Probabilistic Capability

A unique feature of the IECM is its ability to characterize input parameters and output results probabilistically, in contrast to conventional deterministic (point estimate) form. This method of analysis offers a number of important advantages over the traditional approach of examining uncertainties via sensitivity analysis. Probabilistic analysis allows the interactive effects of variations in many different parameters to be considered simultaneously, in contrast to sensitivity analysis where only one or two parameters at a time are varied, with all others held constant. In addition, probabilistic analysis provides quantitative insights about the *likelihood* of certain outcomes, and the probability that one result may be more significant than another. This type of information is generally of greater use than simple bounding or "worst case" analyses obtained from sensitivity studies, which contain no information on the likelihood of worst case occurrences.

The ability to perform probabilistic analysis comes from the use of a new software system which uses a non-procedural modeling environment designed to facilitate model building and probabilistic analysis. In addition to a number of standard probability distributions (e.g., normal, lognormal, uniform, chance), the IECM can accommodate any arbitrarily specified distribution for input parameters. Given a specified set of input uncertainties, the resulting uncertainties induced in model outputs are calculated using median Latin Hypercube sampling, an efficient variant of Monte Carlo simulation. Results typically are displayed in the form of a cumulative probability distribution showing the likelihood of reaching or exceeding various levels of a particular parameter of interest (e.g., emissions or cost).

Model Applications

The IECM is intended to support a variety of applications related to technology assessment, process design, and research management. Examples of questions that can be addressed with the IECM include the following:

- What uncertainties most affect the overall costs of a particular technology?
- What are the key design trade-offs for a particular process ?
- What are the potential payoffs and risks of advanced processes vis-a-vis conventional technology?
- Which technologies appear most promising for further process development?
- What conditions or markets favor the selection of one system design (or technology) over another?
- How can technical and/or economic uncertainties be reduced most effectively through further research and development?

The IECM also has been modified to allow estimation of retrofit costs as well as new plant costs. A series of user specified "retrofit factors" may be applied at the process area level for a particular system to estimate the higher costs of retrofit facilities. To operate the IECM, a new graphical interface has been developed which provides an extremely user-friendly mode of operation. As currently configured, the IECM runs on a Macintosh computer.

Illustrative Results

Here we present results illustrating the probabilistic capabilities of the IECM as applied to a single power plant as shown in Figure 1. This case corresponds to an Appalachian medium sulfur (2.1%S) coal for a power plant with a net capacity of 300 MW. Table 2 shows the input parameter values and uncertainty distributions assumed for this example. The plant is

assumed to achieve 95% SO_2 removal employing a wet limestone FGD system with forced oxidation.

Cost results are shown in Figure 2. These figures show the cumulative effect of uncertainties in different model parameters. For example, for capital cost (Figure 2a),

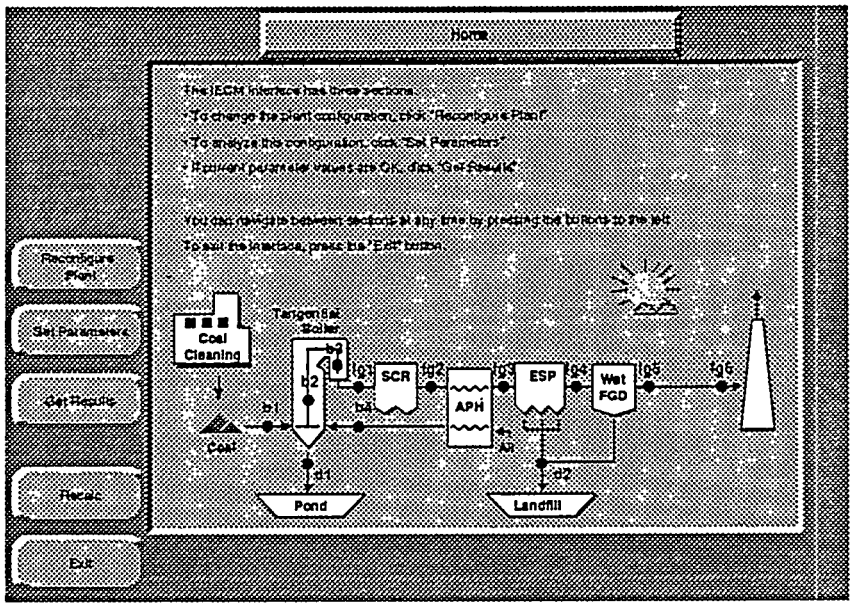

Figure 1. User interface screen showing the case study plant configuration.

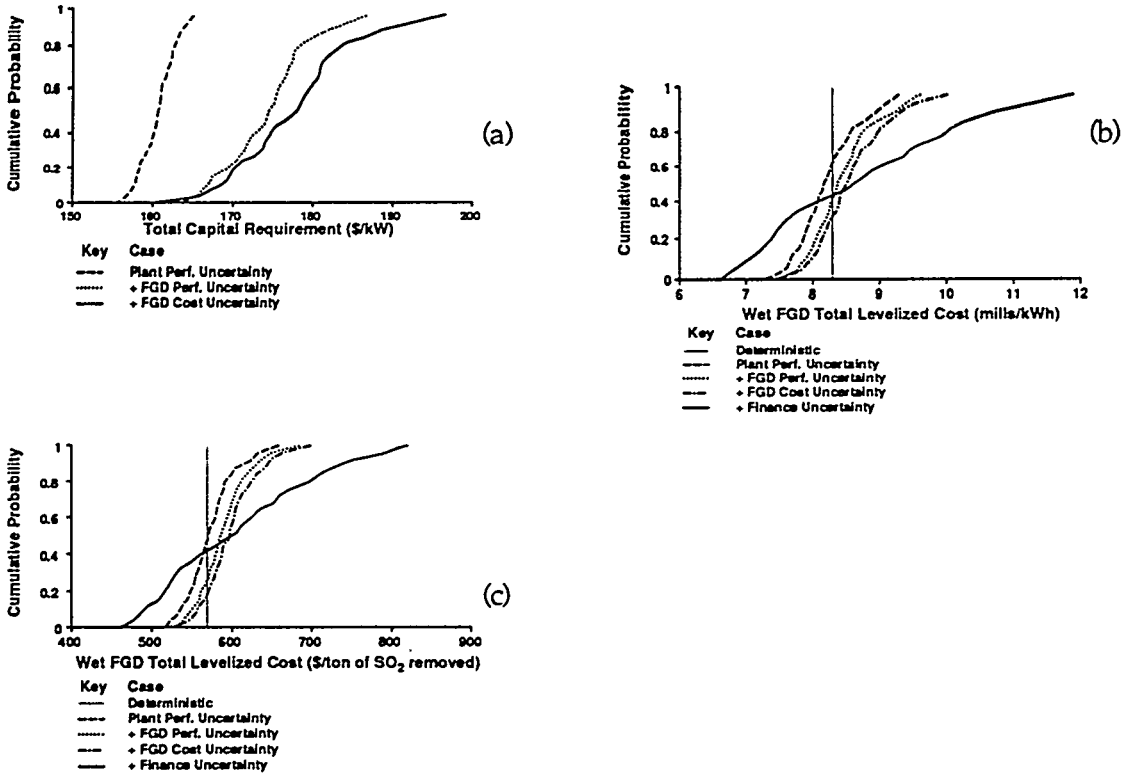

Figure 2. Probabilistic results for case study: (a) FGD capital cost; (b) total levelized cost; (c) cost per ton of SO_2 removed. All costs are in constant 1993 dollars.

Table 2. Performance and cost parameter uncertainties for case study

Model Parameter	Nominal Value	Probability Distribution[a]	Parameter Range[b]
Gross Capacity	330 MW (300 MW net)	None	
Coal Sulfur Content[c]	2.13 wt%	None	
Steam Cycle Heat Rate	7880 Btu/kWh	Neg. Half Normal (1,0.018)	(7599, 7871)
Capacity Factor	65%	Normal (1,0.07)	(58, 72)
Excess Air (boiler)	20%	Uniform (0.75,1.25)	(15,25)
Air Preheater Leakage	19%	Triangle (0.4,1,1.25)	(9, 23)
Economizer Outlet Temp.	700 °F	Normal (1,0.03)	(666, 734)
Air Preheater Outlet Temp.	300 °F	Normal (1,0.03)	(285, 315)
Energy for Coal Pulverizers	0.6% MW_g	Normal (1, 0.03)	(0.57, 0.63)
Energy for Steam pumps	0.65% MW_g	Normal (1, 0.03)	(0.61, 0.68)
Energy for Fans	1.5% MW_g	Normal (1,0.03)	(1.4, 1.6)
Energy for Cooling Towers	1.8% MW_g	Normal (1,0.03)	(1.7, 1.9)
Energy for Misc. Equip.	1.3% MW_g	Normal (1,0.03)	(1.2, 1.4)
SO_2 Removal Efficiency	95 %	None	
Particulate Removal Efficiency	50 %	None	
Reagent Stoichiometry	1.03	Triangular (0.99,1,1.05)	(1.02,1.03,1.08)
Capacity of each Absorber	50%	Uniform(1,1.2)	(50, 60)
Gas Temp. Exiting Reheater	152 °F	None	
Total Pressure Drop	10 in H_2O	Normal (1,0.03)	(9.5, 10.5)
Chloride Removal Efficiency	90 %	None	
Gen. Facilities Capital	10% PFC	Lognormal(1,1.3)	(6.3, 15.9)
Eng. & Home Off. Fees	10% PFC	Half Normal (1,0.17)	(10.1, 13.3)
Project Contingency	15% PFC	Normal (1,0.11)	(12.3, 17.9)
Process Contingency	2% PFC	Half Normal (1,0.5)	(2.0, 4.0)
Limestone Cost	$15/ton	Uniform(0.7,1.3)	(10.5, 19.5)
Disposal Cost	$8.15/ton	Normal(1,0.1)	(6.8, 9.5)
Operating Labor Rate	$20/hr	Uniform(0.75,1.25)	(15,25)
Inflation Rate	0%	None	
Plant Book Life (years)	30 yrs	None	
Real Return on Bonds	4.6%	None	
Real Return on Com. Stock	8.7%	None	
Real Return on Pref. Stock	5.2%	None	
Real Cost Escalation Rate	0%/yr	None	
Federal Tax Rate	36.7 %	None	
State Tax Rate	2 %	None	
Property Tax Rate	2 %	None	
Investment Tax Credit	0%	None	
Fixed Charge Factor	0.0877	Uniform(0.7,1.3)	(0.06, 0.11)
O&M Levelization Factor	1.00	Normal (1,0.03)	(0.95, 1.05)

[a] For normal distributions the values in parenthesis are the mean and the standard deviation normalized on the nominal value. Uniform distributions show the range, and triangular distributions the range and mode also normalized on the nominal value.

[b] The parameter range for the normal distribution encloses two standard deviations or about 95% of the values.

uncertainties in only the base power plant parameters introduces some skewness to the curve, reflecting primarily the input distribution for steam cycle heat rate. That heat rate distribution (see Table 2) reflects a potential for improved plant efficiency relative to the nominal (deterministic) case. Additional uncertainties in the FGD system performance parameters introduce a larger variation in plant capital costs, and this is expanded further when uncertainties in model cost parameters also are added. In this case, the shift to the right toward higher costs reflects the parameter input distributions used for this example, in particular the assumptions of possible vessel oversizing, higher contingency costs, and higher reagent stoichiometry relative to the nominal design values. As a result of these more conservative design assumptions, Figure 2a shows a 95 percent confidence interval ranging from $163 to $196/kW, compared to the nominal (deterministic) value of $165/kW.

Similar results are seen in Figures 2b and 2c for the total levelized cost and cost per ton of SO_2 removal. Here, the cumulative probability distributions also show the effect of additional uncertainties in plant operation and financial parameters which affect annual revenue requirements. Again, the input assumptions in this example reflect a greater potential for higher rather than lower costs relative to the nominal parameter values. Thus, in Figure 2c the cost per ton of SO_2 removed varies from $470 to $805/ton for the 95 percent confidence interval, compared to a nominal value of $570/ton with no uncertainties. Figure 2c shows about a 60 percent chance that the uncertainties assumed in this example will lead to a higher cost per ton than the deterministic value.

While one can see graphically in Figures 2 that certain sets of parameters have a more pronounced effect on overall uncertainty than others, more formal mathematical methods can be used to identify the key parameters whose uncertainty most affects the outcome. The importance of an input variable is derived by assessing its influence on the output variable of interest. For linear relationships this can be accomplished by the use of partial correlation coefficients. For nonlinear relations, such as those involved here, it becomes more difficult to assess the importance of individual variables. However, if the model output is a monotonic function of the input then it is possible to linearize the relationship by using rank transformations on the input and output values. The transformation involves replacing each value of a variable by its rank. Now the partial correlation coefficient on the rank transformed variables (PRCC) can be used to assess the importance of each input variable.

The results of such an analysis are shown in Table 3 for the plant in this example. In general, plant size and coal sulfur content are the variables that most affect plant costs. However, other parameters also strongly affect either capital cost, O&M costs, or total levelized cost in this example. For instance, the design absorber capacity — which varies from 50 to 60 percent of the flue gas flow rate in this analysis — is the second most important parameter affecting FGD capital cost for this plant. Note that the rank order of different variables may vary from case to case, depending on the magnitude and uncertainty in each parameter. Because a large number of technical and economic factors affect the performance and cost of environmental control systems, PRCC analysis can be especially useful for identifying key process variables whose uncertainty might be reduced through targeted research and development, especially for advanced environmental control technologies.

Table 3. Results of partial rank correlation coefficient (PRCC) analysis showing the five most important model parameters affecting FGD cost for the illustrative example

Model Parameter	Capital Cost (M$)	O&M Cost (M$)	Total Levelized Cost (mills/kWh)	SO_2 Removal Cost ($/ton)
Gross Capacity	1	1	1	2
Coal Sulfur Content	3	2	3	1
Capacity Factor		4	4	5
Fixed Charge Factor			2	3
Absorber Capacity	2			
Reagent Stoichiometry	4			
Electricity Cost		3	5	4
Limestone Cost		5		
General Facilities Cost	5			

Conclusion

This paper has described an integrated modeling framework for evaluating the cost and performance of power plant emission control systems. While the illustrative examples in this paper focus on modern FGD systems, a key purpose of these models is to facilitate comparisons between alternative systems, particularly advanced technologies that may offer improved performance and/or cost characteristics. In such cases, the probabilistic capability of the models described here can be especially helpful in quantifying the risks as well as potential payoffs of advanced technologies, investment strategies, and R&D priorities.

Acknowledgments

The model described in this paper were developed under Contract No. DE-AC22-92PC91346 from the U.S. Department of Energy, Pittsburgh Energy Technology Center (DOE/PETC).

References

1. Rubin, E.S., et al., Final Report to DOE/PETC, Pittsburgh, PA, Contract No. DE-AC22-87PC79864, 214p, April 1991.

2. Rubin, E.S., et al., "Development of the Integrated Environmental Control Model: Update on Project Status," *Proceedings of the Tenth Annual Coal Preparation, Utilization, and Environmental Control Contractor's Conference*, DOE/PETC, Pittsburgh, PA, July 1994.

3. Frey, H. C. and E.S. Rubin, Quarterly Progress Report to DOE/PETC, Contract No. DE-AC22-92PC91346, January 1994.

4. Kalagnanam, J.R. and E.S. Rubin, Quarterly Progress Report to DOE/PETC, Contract No. DE-AC22-92PC91346, July 1994.

5. Kalagnanam, J.R., and Rubin, E.S., Quarterly Progress Report to DOE/PETC, Contract No. DE-AC22-92PC91346, September 1994 (Revised March 1995).

Hollow Fiber Contactors for Simultaneous SO_x/NO_x Removal

ABHOYJIT S. BHOWN
NEERAJ R. PAKALA
TRACY RIGGS
TROY TAGG
SRI INTERNATIONAL
333 RAVENSWOOD AVENUE
MENLO PARK, CA 94025

KAMALESH K. SIRKAR
SUDIPTO MAJUMDAR
DEBABRATA BHAUMIK
NEW JERSEY INSTITUTE OF TECHNOLOGY
UNIVERSITY HEIGHTS
NEWARK, NJ 07102

INTRODUCTION

Control of SO_x and NO_x emissions from coal-fired utility and industrial boilers is a topic of growing national and international importance. Whereas a host of commercial and semi-commercial processes exist (Drummond and Gyorke, 1986), increasingly stringent emission standards mandate that processes be low cost, highly efficient, and, ideally, produce marketable byproducts. Although a wide range of site-specific economic factors dictate the best choice of SO_x and NO_x control, removal of SO_2 by wet limestone scrubbing and removal of NO_x by selective catalytic reduction (SCR) are regarded as the best commercialized technologies for this application. A typical wet limestone plant requires approximately $100 to $120 of capital investment per kilowatt of electric power generating capacity and has power and miscellaneous operating costs in the range of 5 to 6 mils per kilowatt hour (kWh). The SCR process requires approximately $70 to $100 of capital investment per kilowatt of electric power generating capacity. Its operating costs, including ammonia consumption, is in the range of 1.8 to 2.2 mils per kWh. These costs can add approximately 20% to the final cost of generated electricity, a significant burden on rate payers.

Our proposed research is aimed at developing (to a subscale prototype size) a new process for removal of SO_x and NO_x that is more than 20% less costly than limestone scrubbing of SO_2 and selective catalytic reduction of NO_x, removes at least 95% of the SO_x and 75% of the NO_x, and produces salable byproducts with no waste material. To accomplish this objective, we intend to develop a regenerable wet scrubbing process for SO_x and NO_x that exploits the advantages of a class of novel contacting devices, known as hollow fiber contactors (HFC), and that uses novel SO_x and NO_x absorption chemistry. The HFC devices will bring substantial capital cost savings to our process. The novel use of the contactors for regenerating the SO_2 scrubbing liquor and the novel NO_x absorption chemistry will help reduce the energy consumption.

This development program will include three phases conducted over 60 months. The initial phase, encompassing the first 24 months of the project, will emphasize demonstrating the technical feasibility of each component of the flue gas control process—including process chemistry, mass transfer rates, and the ability of the HFC modules to function in the presence of particulate matter. At the end of this phase, we expect to have demonstrated 99% SO_2 removal efficiency and 85% NO_x removal efficiency in the laboratory. These efficiency targets are greater than the final goals of this project. The second phase of the work is designed to develop scale-up rules for the HFC modules and to test the longevity of the NO_x scrubbing chemistry. In the 15 months of this second phase, we expect to demonstrate 97% SO_2 removal efficiency and 80% NO_x removal efficiency with scalable modules and to show that our NO_x chemistry is

industrially robust. The third phase of the project will take place in the final 21 months wherein we will concentrate on building and operating a sub-scale proto-type system with a capacity of handling about 100 cubic feet per minute of flue gas. We expect to be able to demonstrate 95% SO_2 removal efficiency with 75% NO_x removal efficiency with the sub-scale prototype.

PROCESS DESCRIPTION

Our concept involves SO_2 scrubbing followed by NO_x scrubbing with regeneration of the individual scrubbing liquors (Figures 1 and 2). The desorbed, concentrated SO_2 and NO_x streams are fed to conventional sulfuric acid and NO_x reduction devices that are not part of the proposed research but which we include for costing estimates as part of the overall process. Both absorption and desorption vessels are based on HFC technology. The basic features of an HFC are that it allows phases to contact without mixing and that there is a large amount of interfacial contact area per unit volume of vessel (Qi and Cussler, 1985). The fiber material (e.g., polypropylene) is hydrophobic, and the fiber walls have small pores (e.g., 0.05 μm) so that gas/liquid contact surface area is created on the liquid side of the pores. Because the walls of the fibers are thin (e.g., 25 μm), there is minimal mass transfer resistance added by the wall of the fiber (diffusion time through the stagnant pore gas is about 0.1 milliseconds). So long as the aqueous phase pressure exceeds that of the gas phase, the interface is stable. The aqueous phase pressure must, however, be kept less than the breakthrough pressure of about 150 psi. Commercially available hollow fibers have sufficiently high mechanical strength to withstand more than 100 psig external pressure and 60 psig internal pressure (Bhave and Sirkar, 197; Majumdar et al., 1988). The fiber wall eliminates entrainment of liquid in the gas and allows independent control of the liquid and gas flow rates. However, the key element of this technology is that the surface area per unit vessel volume is 7 to 30 times higher than that of a traditional packed tower contactor. Consequently, the vessel volume for a given amount of mass transfer is substantially decreased, leading to reduced cost of the scrubber vessel.

Scrubbing SO_2 from flue gases with HFC devices is not new (e.g., Ogundiran et al., 1989; Sengupta et al., 1990). Variants of the HFC technology can, however, be used very efficiently for regenerating these scrubber liquors, and it is this aspect that constitutes part of the novelty of our approach.[1] For regenerating the SO_2 liquor, we intend to contact the liquor with an organic solvent in a hollow fiber contacting device. The organic solvent must have high affinity for SO_2 and very little solubility in water (e.g., dimethyl-aniline). The rationale for using organic extractants is that these have approximately half the heat capacity of water so that the SO_2 can be heat stripped at lower costs (Tung and Kuhr, 1989). These organic liquids cannot be used for direct scrubbing of flue gases because of unacceptably large contamination of the flue gas by the organic solvents.

HFC devices are used so the organic extraction can be done without mixing—so there are no emulsions formed and no phase separation steps required. Further, the high specific contact area results in an extraction vessel much smaller than conventional ones. There are two options for conducting this extraction. In Option A, the SO_2-rich scrubber liquor is passed in the lumen of the HFC, and organic solvent flows on the shell. Sulfur dioxide is preferentially extracted by the organic liquid. The organic liquid is taken to a separate vessel and heated to desorb the SO_2. In Option B, the hollow fibers are divided into two bundles. The SO_2-rich liquor passes down the lumen of one of the bundles, and organic solvent occupies the shell space around the hollow fibers. In the other bundle of hollow fibers, a low pressure is maintained with a small flow of water vapor to draw and sweep the SO_2 through the organic liquid (Figure 3). In this option, no further vessel is required for desorbing the SO_2 from the organic solvent. This particular form of a hollow fiber contactor is known as a hollow fiber contained liquid membrane, (HFCLM; Majumdar, et al., 1988; Sengupta, et al., 1988).

---

[1] For the NO_x stripper, however, there is little incentive to use anything other than a conventional stream stripping device. Consequently, we will use conventional technology to regenerate the NO_x liquor.

PROCESS CHEMISTRY

SO_2 Scrubbing. Substantial information exists on the advantages and disadvantages of various chemistries for both SO_x and NO_x absorption (Harkness et al., 1986; Jethani et al., 1990; Oliver and Greenaway, 1989; Roberts and Friedlander, 1980; Oliver, 1989). For wet regenerable SO_2 scrubbing processes, all of the chemistries are essentially different means of providing alkalinity to the solution to induce a high solubility for SO_2 (in the form of HSO_3^- and/or $SO_3^=$. Typical absorbent solutions consist of water with dissolved sodium sulfite (Wellman-Lord process), magnesia, ammonia, sodium sulfide, sodium citrate, soda ash, potassium carbonate, or potassium citrate (Pfizer Sultrol process). We intend to study several of these chemistries and pure water for SO_2 scrubbing.

Whereas these chemistries are well understood, two novel features of the HFC absorber can be exploited to make these chemistries more cost effective than they can be in traditional contactors. First, there are no losses by entrainment of liquor in the flue gas in an HFC device. Second, the liquid/gas flow rate ratio can be much higher in an HFC absorber than in a conventional absorber because the gas and liquid flow rates are independent of each other. Consequently, the concentration of total dissolved alkalinity can be kept lower and still remove the required fraction of SO_2 from the flue gas. Reduced dissolved alkalinity will result in increased lifetime of the SO_2 scrubbing compounds.

NO_x Scrubbing. For NO_x scrubbing, selection of suitable chemistry has been historically one of the most difficult problems. Many unsuccessful attempts have been made to design an ideal scrubbing chemistry. Based on developments in the 1970s, a number of commercial processes have used ferrous chelates based on ethylene-diaminetetraacetic acid (EDTA). Nitric oxide forms a coordination complex with Fe^{2+}-EDTA, and the reaction rates are very fast. Unfortunately, however, as a regenerable process, EDTA chemistry has been proven to be quite expensive because the Fe^{2+} species is oxidized easily to the ineffective Fe^{3+} species. Also a large number of unwanted chemical reactions take place in the scrubber liquor, creating the need for very costly and capital-intensive treatment steps of the scrubbing liquor.

We intend to focus instead on novel water soluble phthalocyanine compounds, developed by SRI, and novel water soluble polymeric derivatives of EDTA, similar to those described by Bedell et al. (1988), both of which we will synthesize in our laboratories. We have already shown under limited flue gas conditions that these compounds bind NO and NO_2 reversibly with no interference from O_2, CO_2, or SO_2.

Finally, one of the potentially greatest advantages of our process (as it relates to process chemistry) is separate SO_2/NO_x scrubbing liquors. This separation will reduce substantially the wide variety of complex side reactions that lead to the need for convoluted regeneration schemes or expensive blowdown in other processes (e.g., Liu et al., 1988).

Extraction of SO_2 from Spent Scrubbing Liquor. The third aspect of the process chemistry is an organic solvent for extracting SO_2 from spent scrubbing liquor. Several suitable solvents are available with a high SO_2 affinity and no propensity to form solid adducts with SO_2: dimethylaniline (DMA), quinoline, and various ethers such as diethylene glycol dimethyl ether (diglyme), triethylene glycol dimethyl ether (triglyme), and tetraethylene glycol dimethyl ether (tetraglyme; Demyanovich and Lynn, 1987). Indeed, DMA and the glymes have been used for commercial absorption processes for SO_2 and H_2S (Kohl and Riesenfeld, 1985). To limit our effort on this topic, we will restrict ourselves to DMA. To overcome small losses of DMA by volatilization, we will synthesize DMA oligomers.

RESULTS

To date we have worked on nine elements of the program: SO_2 scrubbing tests, synthesis of SO_2 and NO_x extraction compounds, their capacity and reversibility tests, spent SO_2 liquor regeneration tests, NO scrubbing tests, integrated NO life tests, particle deposition, economic evaluation, and performance of scalable modules. Previous results on some of these elements are

presented elsewhere (Gottschlich et. al., 1993 and Bhown et al., 1994). More recent results are discussed next.

SO_2 Scrubbing. In our previous reports (Gottschlich et al., 1993 and Bhown, et al., 1994), we indicated that SO_2 removal rates more than 95% were obtained using 200 fiber, 23 cm long HFC with 0.2 M aqueous Na_2SO_3 solution. Therefore, we shall not discuss these results here.

SO_2 Absorbing Compounds. Bhown, et al., 1994, presented several compounds synthesized by SRI and their performance toward SO_2 liquor generation. Amongst these compounds d-DMA was reported to be the leading candidate. Figure 4 manifests the performance of d-DMA under repeated exposure to SO_2 at different temperatures. At 50°C, excepting Runs 5 and 6, the results given in the figure show that d-DMA sustains and performs well over repeated exposures to SO_2. Therefore, we use d-DMA in all our further studies.

SO_2 Spent-Liquor Regeneration. We reported earlier that spent 0.2 M Na_2SO_3 solution was successfully (>98%) regenerated using DMA in a separate 1000 fiber HFC. Therefore, we shall not discuss these results here.

NO Absorbing Compounds. Earlier we reported several phthalocyanine compounds synthesized by SRI and their ability to absorb NO. Amongst these compounds, 3-ph exhibited superior performance and also showed no oxidation in the presence of O_2. The life tests on this compound are presented below under separate task.

NO Scrubbing. NO removal rates more than 85% were obtained using 3-ph solution in a 300 fiber HFC. From the results obtained it was shown that mass transfer is a strong function of gas flowrate and also depends on reaction kinetics at low temperatures. Thus our absorption tests are conducted at temperatures close to 50°C.

Particle Deposition. We generated 0.2 μm silica particles (typical of fly ash material) into gas streams using pneumatic nebulizers. The particles were shown (Figure 5) to agglomerate when dispersed into gas streams from liquid. The lumens of a 1155 fiber HFC were exposed to a gas stream (11.67 L/min) containing 30 mg/m^3 of particles for a period of 80 hours. The pressure drop across the length of the fibers was observed to increase gradually at the beginning of deposition and rapidly afterwards reaching about 100" water in 30 hours (Figure 6). Figure 7 shows the effect of the particle deposition on the mass transfer coefficient (MTC) during the entire operation. We speculate that the overall drop of about 20% in MTC is due to accelerated condition used in the tests as well as difficult nature of experiments.

Integrated NO Life Tests. In our previous report (Bhown et al., 1994), we demonstrated that one of the phthalocyanine compounds (3-ph) exhibited superior mass transfer characteristics for absorbing NO. Therefore, in order to further demonstrate the absorption/desorption behavior of 3-ph, we have carried-out 30 hours worth of integrated absorption and desorption experiments. Figure 8 gives the absorption and desorption results. In these tests, simulated flue gas contained 500 ppm NO, 4.5% O_2, and balance N_2. The approximate flat nature of both absorption and desorption curves indicate that 3-ph does not undergo any deactivation or deterioration under repeated exposure to NO. Longer exposure tests are currently being conducted.

Economic Evaluation. Based on our laboratory (Phase I of the program) test results, we estimated the costs of major battery limit equipment and associated utility costs. The design basis for the calculations are given in Table 1 and the comparison of the costs of the proposed process with that of the traditional processes are presented in Table 2. The capital costs are low by a factor of two compared to that of widely employed wet limestone and SCR technology. In addition, the processing costs of the present process is also less compared to that of existing technologies.

Performance of Scalable Modules. In this Phase II of the project, in order to readily scaleup the process to commercial level, we intend to use rectangular HFCs as shown in Figure 9. Our preliminary design estimates indicate that the modules can effectively treat gas flowrates up to 200 SLM. We will present the mass transfer results in the meeting.

REFERENCES

Bedell, S. A., S. S. Tsai, and R. R. Grinstead, "Polymeric Iron Chelates for Nitric Oxide Removal from Flue Gas Streams," *Ind. Eng. Chem. Res.*, **27**, 2092 (1988).

Bhave, R. R. and K. K. Sirkar, "Gas Permeation and Separation with Aqueous Membranes Immobilized in Microporous Hydrophobic Hollow Fibers," ACS Symposium Series No. 347, in *Liquid Membranes Theory and Applications*, R. D. Noble and J. D. Way, Eds., (American Chemical Society, Washington, DC, 1987) p. 138.

Bhown, A. S., D. B. Alvarado, N. R. Pakala, K. K. Sirkar, S. Majumdar, and D. Bhaumik, "Hollow Fiber Contactors for Simultaneous SO_x/NO_x Removal," Proceedings of the Ninth Annual Coal Preparation, Utilization, & Environmental Control Contactors Conference, Pittsburgh, PA (July 1994).

Demyanovich, R. J., and S. Lynn, "Vapor-Liquid Equilibria of Sulfur Dioxide in Polar Organic Solvents," *Ind. Eng. Chem. Res.*, **26**, 548 (1987).

Drummond, C. J., and D. F. Gyorke, "Research Strategy for the Development of Flue Gas Treatment Technology," ACS Symposium Series No. 319, in *Fossil Fuels Utilization: Environmental Concerns*, R. Markuszewski and B. D. Blaustein, Eds., (American Chemical Society, Washington, DC, 1986), p. 146.

Harkness, J.B.L., R. D. Doctor, and R. J. Wingender, "Flue Gas Desulfurization/ Denitrification Using Metal-Chelate Additives," U. S. Patent No. 4,612,175, Sept. 16, 1986.

Gottschlich, D. G., A. S. Bhown, S. Ventura, K. K. Sirkar, S. Majumdar, and D. Bhaumik, "Hollow Fiber Contactors for Simultaneous SO_x/NO_x Removal," Proceedings of the Ninth Annual Coal Preparation, Utilization, & Environmental Control Contactors Conference, Pittsburgh, PA (July 1993).

Jethani, K. R., N. J. Suchak, and J. B. Joshi, "Selection of Reactive Solvent for Pollution Abatement of NO_x," *Gas Separation & Purification*, **4**, 8 (1990).

Kohl, A. and F. Riesenfeld, *Gas Purification*, 4th ed., (Gulf Publishing Company, Houston, 1985).

Liu, D. K., L. P. Frick, and S. G. Chang, "A Ferrous Cysteine Based Recyclable Process for the Combined Removal of NO_x and SO_2 from Flue Gas," *Env. Sci. and Technol.*, **22**, 219 (1988).

Majumdar, S., A. K. Guha, and K. K. Sirkar, "A New Liquid Membrane Technique for Gas Separation," *AIChE J.*, **34**, 1135 (1988).

Ogundiran, O. S., S. E. Le Blanc, and S. Varanasi, "Membrane Contactors for SO_2 Removal from Flue Gases," Pittsburgh Coal Conference, September 1989.

Oliver, E. D., "NO_x Removal," SRI International Process Economics Program Report No. 200 (May 1989).

Oliver, E. D. and D. Greenaway, "SO_2 Removal from Flue Gas," SRI International Process Economics Program Report No. 63C (December 1989).

Qi, Z. and E. L. Cussler, "Microporous Hollow Fibers for Gas Absorption," *J. Membr. Sci.*, **23**, 321 (1985).

Roberts, D. L. and S. K. Friedlander, "Sulfur Dioxide Transport Through Aqueous Solutions," *AIChE J.*, **26**, 593-610 (1980).

Sengupta, A., R. Basu, and K. K. Sirkar, "Separation of Solutes from Aqueous Solution by Contained Liquid Membranes," *AIChE J.*, **34**, 1698 (1988).

Sengupta, A., B. Raghuraman, and K. K. Sirkar, "Liquid Membranes for Flue Gas Desulfurization," *J. Membr. Sci.*, **51**, 105 (1990).

Tung, S. E. and R. W. Kuhr, "Flue Gas Desulfurization Test Facility," presented at the Fifth Annual Coal Preparation, Utilization, and Environmental Control Contractors' Conference, Pittsburgh, PA, July 31-August 3, 1989.

Table 1. BASIS FOR EXAMPLE DESIGN OF 500 MW (e) SO_X/NO_X PLANT

Flue gas flowrate	1 million actual ft^3/min 2.25×10^{10} sccm
Flue gas temperature	160°F
Flue gas pressure	760 mm Hg
Flue gas composition	
SO_X	3000 ppm(v)
NO_X	450 ppm
CO_2	14%
H_2O	8%
O_2	3.3%
N_2	74.4%
Fraction of SOx/NO_X removed in absorbers	
SO_X	98%
NO_X	85%
Pressure drop	
SO_X scrubber (flange to flange)	10" H_2O
NO_X scrubber (flange to flange)	10" H_2O

Table 2. COMPARISON OF HF PROCESS WITH TRADITIONAL PROCESSES

		Capital Cost ($/kW)	Operating Costs[1] (mils/kWH)	Processing Cost[2] (mils/kWH)
(A)	Proposed Option A			
	SO_2/NO_X scrubbing/regenerating	$60.50	7.76	9.16
	Small scale H_2SO_4 plant[3]	10.40	0.49	0.75
	Small scale SCR NO_X reduction plant	7.90	0.55	0.73
	Total Option A	$78.80	8.8	10.64
(B)	Traditional Process			
	(1) Wet Limestone plus SCR[4]	$185.50	7.33	12.14
	(2) Wellman Lord plus SCR	$333.00	10.45	16.18
	(3) Citrate plus SCR	$303.00	8.99	14.26

1 Operating costs include utilities, raw materials and labor and other administrative overhead.

2 Includes amortized capital costs at 20% year plus operating costs.

3 Source: Elkin, 1985.

4 Selective catalytic reduction capital cost is $70.80/kw and operating cost is 2.02 mils/kwh in each traditional process.

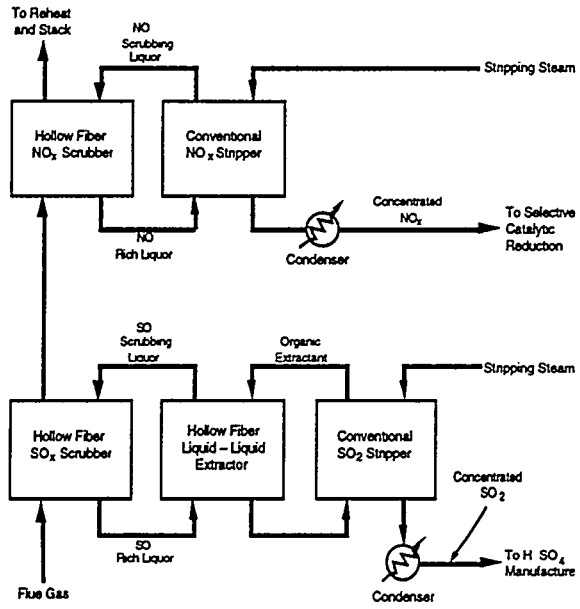

Figure 1. Proposed SO_x /NO_x wet scrubbing with hollow fiber contacting devices. (Option A for SO_2 liquor regeneration)

SO_2 liquor regeneration occurs in hollow fiber liquid – liquid extraction (LLE) device.

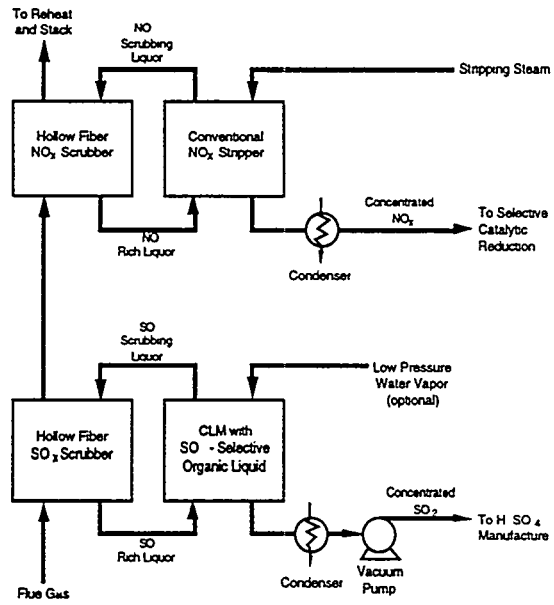

Figure 2. Proposed SO /NO, wet scrubbing with hollow fiber contacting devices. (Option B for SO_2 liquor regeneration)

SO_2 liquor regeneration occurs in hollow fiber contained liquid membrane (CLM) device. Condenser/vacuum pump system combine to give driving force for operation of CLM.

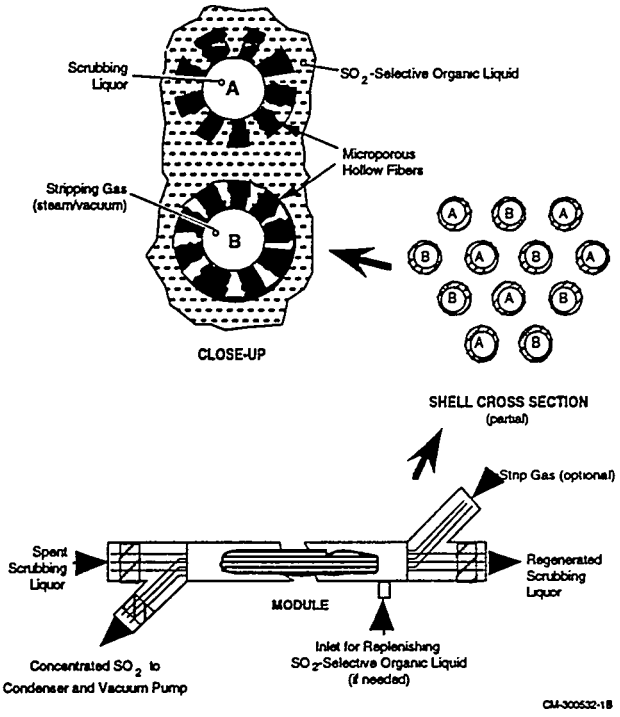

Figure 3. Hollow fiber contained liquid membrane for regenerating SO_2 scrubber liquor.

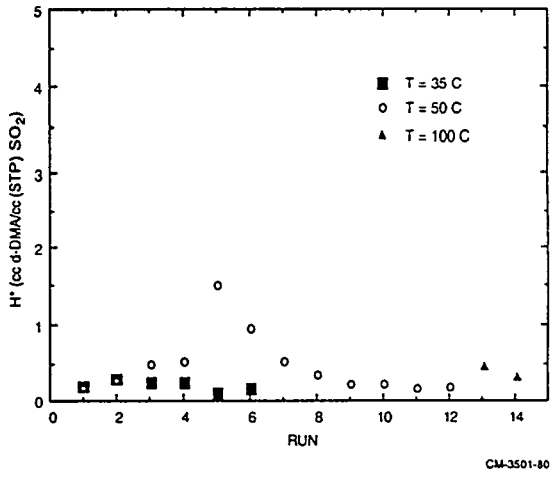

Figure 4. Lifetime tests on d-DMA for SO_2 absorption/desorption.

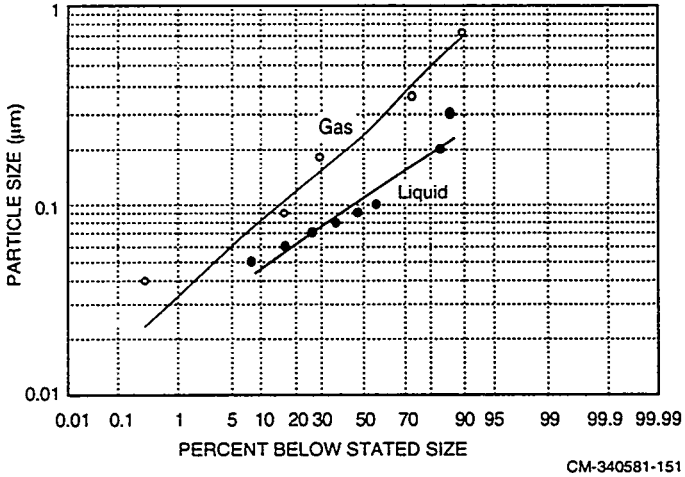

Figure 5. Particle size distribution in gas and liquid phases.

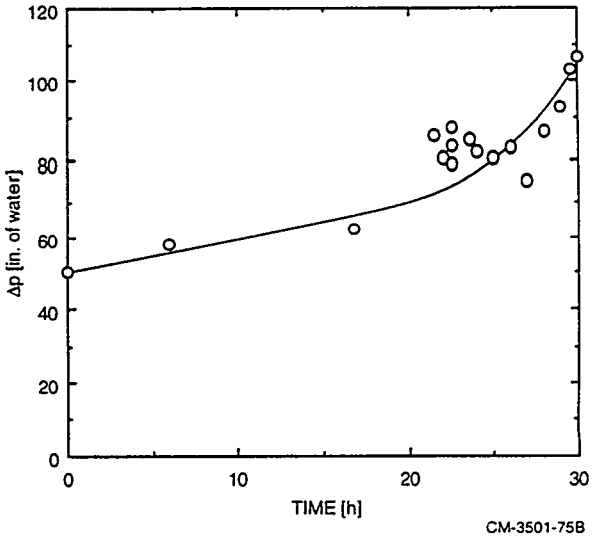

Figure 6. Pressure drop across HFC as a function of deposition time.

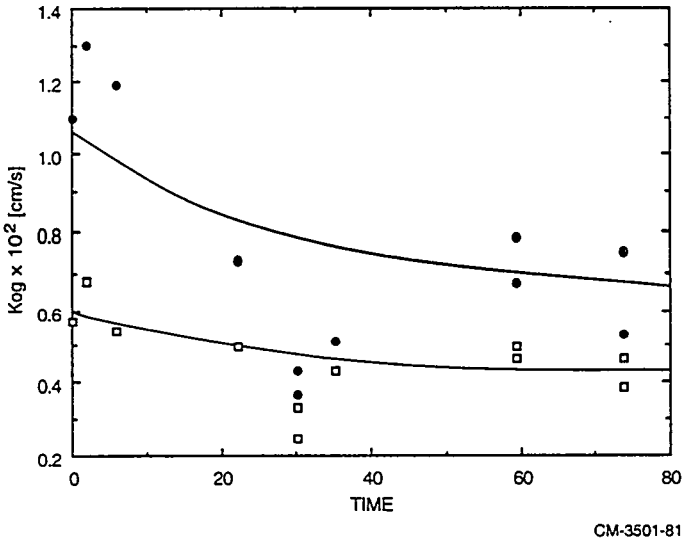

Figure 7. 1155-fiber HFC mass transfer coefficient with particle deposition.

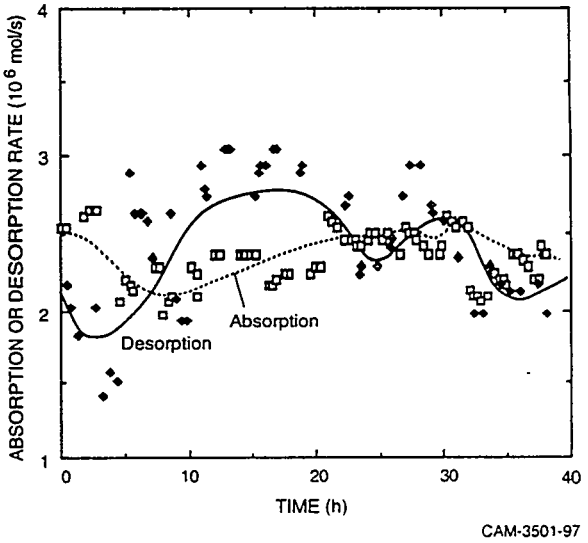

Figure 8. Simultaneous NOx absorption and desorption tests using 3-pH solution.

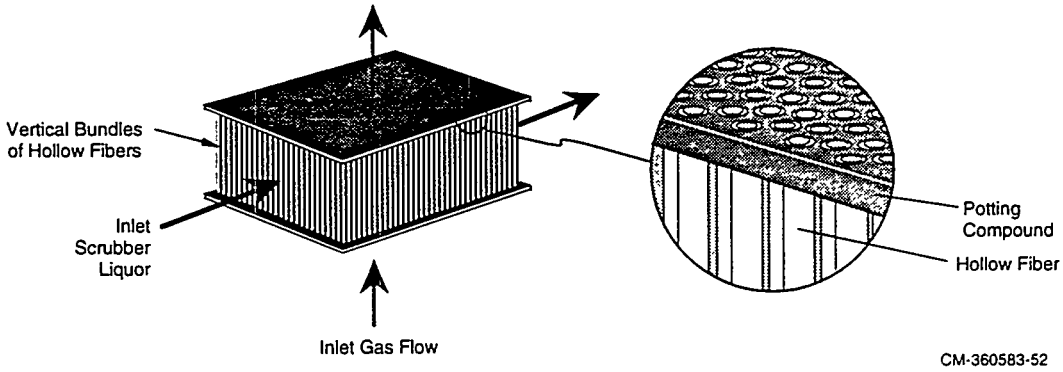

Figure 9. Cross-flow pattern of gas and liquid flow in a rectangular hollow fiber cassette (module).

DEVELOPMENT OF THE ADVANCED COOLSIDE SORBENT INJECTION PROCESS FOR SO_2 CONTROL

J. A. WITHUM, J. T. MASKEW, W. A. ROSENHOOVER,
M. R. STOUFFER, AND M. M. WU
CONSOL Inc.
RESEARCH & DEVELOPMENT
4000 BROWNSVILLE ROAD
LIBRARY, PA 15129

ABSTRACT

The goal of this work was to develop a low-capital-cost process capable of over 90% SO_2 removal as an economically attractive option for compliance with the Clean Air Act. The Advanced Coolside Process uses a contactor to simultaneously remove fly ash and saturate the flue gas with water, followed by sorbent injection into the highly humid flue gas and collection of the sorbent by the existing particulate collector. High sorbent utilization is achieved by sorbent recycle. The original performance targets of 90% SO_2 removal and 60% sorbent utilization were exceeded in 1000 acfm pilot plant operations using commercial hydrated lime as the only sorbent. Process optimization simplified the process equipment, resulting in significant cost reduction. Recent accomplishments include completion of equipment testing and sorbent optimization, a waste management study, and a long-term performance test. An economic evaluation for the optimized process projects capital costs 55% to 60% less than those of limestone forced oxidation wet FGD. The projected levelized control cost is 15% to 35% lower than wet FGD (25% lower for a 260 MWe plant burning a 2.5% sulfur coal), depending on plant size and coal sulfur content.

BACKGROUND AND INTRODUCTION

In-duct dry sorbent injection technology has been actively developed in the U.S. since the early 1980s. The performance of these processes was established through the development of the Coolside process[1-3] and the HALT process[4] and through the DOE duct injection technology development program.[5] These development efforts included pilot-scale tests, proof-of-concept tests, and a full-scale utility demonstration. Demonstrated performance was in the range of 40-50% SO_2 removal at 2.0 Ca/S molar ratio. Additionally, the 105 MWe demonstration of the Coolside process at the Ohio Edison Edgewater Station[3] showed that an SO_2 removal of 70% can be attained by improving calcium hydroxide sorbent activity with sodium-based additive injection at a 0.2 Na/Ca molar ratio (~32% sorbent utilization).

Process performance data and economic analyses support the attractiveness of duct sorbent injection for a range of retrofit applications.[6] However, the applicability as a compliance option for the Clean Air Act or other regulations can be expanded by increasing SO_2 removals and sorbent utilizations. Higher SO_2 removals became more important for retrofit technologies with the passage of the 1990 Clean Air Act Amendments. Higher sorbent utilization reduces operating cost.

The objectives of the work reported here were to improve the applicability of in-duct sorbent injection technology as a compliance option for the 1990 Clean Air

Act Amendments and to reduce total SO_2 control costs. Specific desulfurization performance targets were to achieve 90% SO_2 removal and 60% sorbent utilization, while retaining the low capital cost and retrofit advantages inherent to in-duct sorbent injection technology. These targets represent a substantial improvement over existing sorbent injection technologies.

Initial pilot plant tests indicated that a process concept, referred to as the Advanced Coolside process, had the potential to achieve the process performance targets stated above.[7] This process is described in the next section. Pilot plant development of the Advanced Coolside process focused on the following areas:

- Optimization of sorbent recycle to improve sorbent utilization efficiency and SO_2 removal capability.
- Optimization of process equipment to reduce capital and operating costs.
- Optimization of sorbent systems for improved performance and reduced cost.
- Evaluation of process operability issues.
- Evaluation of solid waste disposal as well as possible solid by-product utilization.

Process conceptual design and economic evaluation was an ongoing consideration during the development program. This allowed research and development to focus on approaches with the most potential for improving the process design and the process economics.

DESCRIPTION OF ADVANCED COOLSIDE PROCESS

Figure 1 shows a schematic of the Advanced Coolside process. The process achieves greater SO_2 removal and sorbent utilization than previous duct sorbent injection processes because it is operated at a higher flue gas humidity, and more fully exploits the potential of sorbent recycle. The key to the process is a gas/liquid contacting device downstream of the air preheater. The contactor serves two purposes: to nearly saturate the flue gas with water and to remove most of the coal fly ash from the flue gas. The sorbent is injected downstream of the contactor into the highly humid flue gas. Hydrated lime is very active for SO_2 capture near the saturation point, even in the absence of liquid water droplets. Because the flue gas is already humidified prior to sorbent injection, there is no strict residence time requirement for droplet evaporation, although residence time affects SO_2 removal as discussed below. SO_2 is removed by the sorbent in the duct and by that collected in the existing electrostatic precipitator (ESP) or baghouse. The heat of reaction between SO_2 and hydrated lime raises the temperature of the flue gas by roughly 8-10 °F for each 1000 ppm of SO_2 removed. Therefore, the particulate collector can be operated at an increased approach to saturation. However, because hydrated lime activity is highly sensitive to the approach to saturation, this reaction heat effect also acts as a limiting mechanism for SO_2 capture.

The spent sorbent is captured by the existing particulate collector as a dry powder. Sorbent recycle is an integral component of the Advanced Coolside process, allowing the sorbent utilization target of 60% to be exceeded. The potential for recycle is increased because fly ash is removed separately before sorbent injection. Furthermore, process performance can be improved by adding small amounts of water to the recycle sorbent prior to re-injection. The water

acts to maintain a close approach to saturation by evaporating, counteracting the heat of reaction. The moisture addition step is a key to maintaining sorbent activity and, thus, to exceeding the SO_2 removal target of 90%.

Equipment design optimization was focused on the flue gas/water contactor. For the initial pilot plant tests the contactor was a relatively complex device.[7] In the process design optimization program, second and third generation contactors were designed, tested, and optimized. The improved contactor designs significantly reduce capital and operating costs. The third generation design consists of a low-pressure-drop, in-duct venturi followed by a cyclonic separator.

EXPERIMENTAL

This process development program was carried out in a 1000 acfm (ca. 0.3 MWe equivalent) pilot plant. Figure 2 is a schematic of the Advanced Coolside desulfurization pilot plant. It was designed to simulate integrated Advanced Coolside operation, including combined flue gas saturation and fly ash removal by a contactor, sorbent injection downstream of the contactor into the saturated flue gas, and steady-state continuous sorbent recycle with wetting of the recycle sorbent. The pilot plant, operating procedures, and analytical procedures are described in detail elsewhere.[7-9]

Test sorbents were analyzed using a Micromeritics Digisorb 2600 nitrogen adsorption apparatus (for surface area and pore size distributions), a Malvern Instruments 2600C EASY Particle Sizer M5.4, a LECO CHN-1000 analyzer, and a Perkin Elmer 7-Series Thermogravimetric Analyzer.

The equipment for the waste/by-product characterization study includes a laboratory mixer, a mechanical soil compactor and a unconfined compression tester. TCLP and ASTM leaching tests were conducted as specified in the standard methods. The moisture-density relationships and unconfined compressive strengths of Advanced Coolside wastes were determined with laboratory equipment complying with ASTM Standards. Waste samples were pelletized using a Littleford Brothers LM-130 batch mixer, a 36" I.D. rotary disc pelletizer and a 55-gal curing drum. Pellet properties were determined using a sieve shaker and an LA abrasion machine according to ASTM Standards.

DISCUSSION

Recycle Optimization

Process Performance Goals Exceeded. The recycle optimization tests showed that the process performance targets of 90% SO_2 removal and 60% sorbent utilization could be exceeded. The 90% SO_2 removal target was achieved at sorbent utilizations over 70%. At conditions simulating the use of a baghouse for particulate collection, very high SO_2 removal (>99%) was achieved while maintaining at least 60% sorbent utilization. Sorbent recycle was a key to achieving these levels of performance.

The tests conducted to simulate SO_2 removal in a utility boiler unit equipped with an ESP achieved 90% SO_2 removal at sorbent utilizations of up to about 75% (Table 1). These tests were conducted with frequent baghouse pulse cleaning and

with hot air reheat to partially quench the SO_2 removal reaction in the baghouse. Based on mass transfer calculations, ESP removal may be limited to about 30% of the SO_2 in the flue gas at the ESP inlet.

The tests conducted without reheat and less frequent baghouse pulsing to simulate SO_2 removal in a plant with a baghouse showed very high efficiency SO_2 removal (90 to >99%) while maintaining the target of 60% sorbent utilization (Table 2).

Effect Of Fresh Ca/S Ratio and Recycle Ratio. Increasing the fresh Ca/S ratio and/or the recycle ratio (lb recycle sorbent/lb fresh hydrated lime) increases the amount of calcium available for reaction with SO_2. By maintaining a sufficiently high concentration of available calcium in the sorbent, the process target of 90% SO_2 removal can be achieved or exceeded. For example, at a 10 °F approach to saturation in the baghouse and with water addition to the recycle at a ratio of 0.15 lb H_2O/lb recycle, increasing the total available Ca/S ratio from 1.8 to 2.2 increased the in-duct SO_2 removal from 60% to 70% and the system SO_2 removal from 84% to 90% (Table 2). In both cases of this example, 70% of the available calcium came from the fresh hydrated lime; the remainder came from the recycle sorbent.

Effect of In-duct Residence Time. High SO_2 removals and sorbent utilizations were achieved with 1.7 to 2.7 sec in-duct residence time. Below 1.7 sec residence time, SO_2 removals were significantly lower. Between 1.7 and 2.7 sec there was little effect of additional residence time on in-duct SO_2 removal.

Moisture Addition to Recycle. Moisture acts primarily to maintain a close approach to saturation by counteracting the reaction heat effect. Moisture also provides surface water to the sorbent particle which can enhance gas/solid reactions. The addition of moisture to the recycle sorbent had a strong positive effect on desulfurization performance of the sorbent. For example, at a 1.2 fresh Ca/S mol ratio, 5.0 lb/lb recycle ratio and a 10 °F approach in the baghouse, the addition of 0.15 lb H_2O/lb of recycle sorbent increased the in-duct SO_2 removal from 59% to 81% and the system removal from 73% to 88%. The sorbent utilization increased from 61% with no moisture addition to 71% with moisture addition.

The optimum moisture addition level in the pilot plant tests was between 0.10 and 0.15 lb water/lb recycle sorbent. Increasing moisture addition level to 0.20 lb/lb resulted in a decrease in performance because of sorbent agglomeration. However, the optimum water addition level determined in pilot tests does not apply directly to large-scale operation because the ratio of transport air to sorbent is about an order of magnitude greater in the pilot plant than a typical large-scale transport system. Consequently, in the pilot plant more water is required on the sorbent to allow for the evaporation into the dry transport air. Based on heat and mass balance calculations the moisture addition level would be about 0.05 lb H_2O/lb solid for a 250 MW plant burning a 2.5% sulfur coal, which is less than half that used in the pilot plant tests.

Equipment Design Optimization

Equipment design optimization was a key to reducing the cost of the Advanced Coolside process. One focus of design optimization was the contactor. A third generation contactor was designed that is mechanically simpler than the original[7]

and second generation[8-9] designs. Design optimization also was focused on the sorbent recycle equipment.

Contactor Design Improvements. The third generation contactor (Figure 3) was designed to reduce capital cost and a reduced plant footprint. It consists of a low-pressure-drop, in-duct venturi followed by cyclonic separator; the total design Δp was 5" W.C. Water is sprayed by hydraulic nozzles in the throat of the venturi, which reduces water droplet size and provides turbulent contact between droplets and flue gas for efficient particle capture and humidification. The water/fly ash mix is separated from the flue gas by the downstream separator.

The pilot plant venturi contactor was an off-the-shelf design with minor modifications. The contact time between the venturi throat and the cyclonic separator was about 0.1 sec. This contactor allowed reasonably close approaches (ca. 0 to 4 °F) to be achieved.

The fly ash collection efficiency of the venturi contactor was greater than 90% in pilot plant tests conducted with EPA Method 17 sampling. Fly ash collection efficiency was independent of gas flow over a range of 380 to 1025 acfm. The results indicate that a single venturi contactor can handle the range of turndown required for a commercial application to follow changing boiler load.

Operability of the third generation contactor was good throughout the performance tests. There were no problems with fly ash accumulation in the venturi, on the spray nozzles or in the cyclonic separator.

Optimization Of Recycle Sorbent Treatment Equipment. A test was conducted in which the recycle sorbent was wetted using a pilot-scale, continuous pugmill. Performance of the pugmill was compared to the high intensity mixer used in previous pilot plant tests. The results indicate that a pugmill can produce a satisfactory product, from both materials handling and reactivity standpoints. These results are encouraging because a pugmill has substantially lower capital and operating costs than the high intensity mixer.

Other Design Optimization. In addition to the pilot plant optimization testing discussed above, engineering studies were conducted to explore process improvements in all major process subsystems. Key areas identified for process improvement/cost reduction include:

- Use of hydrocyclones instead of a thickener to concentrate the fly ash slurry before mixing with spent sorbent.
- Use of on-site lime hydration of quicklime for larger plants.
- Simplification of the flue gas reheat system.
- Improvements in the recycle handling system design.
- Simplification of the ductwork conceptual design.

Sorbent Optimization

The Sorbent Optimization program included pilot plant evaluation of different sorbents including several commercial hydrated limes and specially prepared high surface area limes, an evaluation of hydration variable effects in a pilot hydrator, and testing of additive promotion. The results showed that process performance is relatively insensitive to hydrated lime source, unlike the

conventional Coolside process. Small amounts of additives incorporated during the recycle wetting step incrementally improved desulfurization in the baghouse, but were not necessary to exceed the performance targets.

Pilot plant tests were conducted on five different commercial hydrated limes. The limes tested were from different geographic areas and were selected from among the largest hydration plants in the country. The BET surface areas of the commercial hydrates tested ranged from 14 to 24 m^2/g. Three specially-prepared, high surface area hydrated limes were tested in the pilot plant; surface areas ranged from 35 m^2/g to 41 m^2/g. The desulfurization results showed only a small variation among the limes tested. Thus, a variety of commercial hydrated limes can be used to achieve the process performance goals of 90% SO_2 removal and 60% sorbent utilization. The relative insensitivity of the process to hydrated lime source is advantageous, allowing the use of the lowest cost available hydrated lime.

A statistically designed test program was conducted to determine the effect of hydration variables on hydrated lime properties and the effects of these properties on desulfurization performance. This program was conducted by Dravo Lime Company using a 100 lb/hr pilot hydration test facility. Data analysis indicates that there was no significant correlation of desulfurization activity with sorbent physical properties or with quicklime source.

Recycle tests were conducted with small amounts of additives incorporated in the combined recycle and fresh sorbent during the moisture addition step. A moderate enhancing effect of small amounts (ca. 0.03 mol/mol fresh Ca) of inorganic chloride compounds (NaCl, $CaCl_2$) on sorbent performance was observed in the baghouse but not in the duct. Therefore, use of small amounts of these additives may be an attractive means of achieving high SO_2 removal efficiencies (90 to >99%) in a plant with a baghouse. Additive incorporation in the recycle pretreatment step is attractive because it uses existing equipment and commercially available hydrated lime.

Once-through tests were conducted with a finely pulverized limestone. Although limestone is not a sufficiently active sorbent for commercial use in the Advanced Coolside process, the results indicated that $CaCO_3$ does have significant desulfurization activity (23% removal in duct and 31% system removal at 2.0 Ca/S mol ratio). This may be a significant observation, since some $Ca(OH)_2$ is converted to $CaCO_3$ in the Advanced Coolside process. The activity difference may be largely a result of the lower surface area of limestone (1.6 m^2/g) compared to that of hydrated lime.

Process Performance Tests

The objective of the performance testing was to generate performance and operability data for design and scale-up of the process. The performance test consisted of about one week of operation with two shifts per day followed by three separate weeks of 24 hour/day operation. The total on-stream time was 295 hours. The purpose of the initial week of testing was to establish near steady-state operating conditions and sorbent composition. The purpose of the around-the-clock operation was to evaluate performance and operability issues during longer periods of continuous operation. Although the test was divided into three periods of 24 hour/day operation, the same sorbent material was used; that is,

the baghouse material collected at the end of one period was used as the recycle material at the beginning of the subsequent test period.

The test conditions for the performance test were selected based on the results of the process optimization tests. The Ca/S ratio was in the range of 1.2 to 1.3 for the test. The recycle ratio was 7 lb/lb fresh lime and the recycle water addition level was about 0.12 lb/lb recycle. The third generation contactor (venturi + centrifugal separator) was employed for all the testing; it was operated to achieve near saturation conditions. The SO_2 removal averaged about 90% during the performance test.

Although the scale of the 1000 acfm pilot plant is not sufficient to completely resolve process operability issues, the performance test provided a positive indication of the operability of the Advanced Coolside process. The key operability issues evaluated were operation of the flue gas duct with sorbent injection at high humidity and operation of the recycle sorbent wetting, handling and transport systems. These and other issues should be further evaluated in larger scale, longer term tests.

There were no major operating problems in the flue gas duct with injection of wetted recycle sorbent at high humidity. The pilot plant had a duct configuration with numerous changes in flue gas direction, presenting more potential for operating problems than typical commercial systems. Because soot blowers are included in the conceptual process design, the duct was periodically air lanced with 50 to 80 psig air to simulate soot blowing. The soot blowing was effective in preventing accumulation of solids in the pilot plant duct. The material which adhered to the duct walls was generally soft and easily removed and carried to the baghouse by the soot blowing. The soot blowing was used primarily at elbows and near the sorbent injection point. The amount of accumulation in straight duct runs was small and tended to level off with time even without soot blowing.

For most of the performance test, the recycle sorbent was effectively wetted, fed, and transported to the flue gas stream. Recycle handling did, however, require frequent operator attention, although much of this attention was specific to the small scale and the specific equipment employed in the pilot plant. There were instances of eductor plugging, a fairly common problem in small-scale systems, because the orifice in the eductor venturi is quite small. It is anticipated that this would not be a significant problem with properly designed commercial scale pneumatic transport equipment.

After longer periods of continuous operation with high sorbent utilization, the wetted recycle material tended to agglomerate more. This increased the difficulty of feeding the material and somewhat reduced desulfurization performance. Agglomeration occurs when more water is added to the recycle sorbent than can be incorporated into the available sorbent pore volume. The pore volume of sorbent decreases at higher utilization levels. Although less sorbent agglomeration would be expected in a full-scale process (because less added water is needed, as discussed earlier), this is an important phenomenon to be addressed for process scale-up.

During the process performance tests, observed levels of CO_2 pickup were higher than observed during short term tests; this may have contributed to sorbent

agglomeration because $CaCO_3$ formation reduces pore volume and, thus, moisture-carrying capacity.

Waste Management Evaluation

The initial objective of the waste management study was to develop the data needed for designing the waste handling and disposal systems for the process. The test program was expanded to include exploratory tests of by-product utilization options. This involved pelletization tests and preliminary evaluation for production of synthetic aggregate materials.

The Advanced Coolside process generates two waste streams: the dry spent sorbent from the particulate collector and the fly ash/water slurry collected in the contactor that is subsequently concentrated. The proposed concept for disposal or utilization is to mix the two streams, controlling the overall moisture content by proper design of the fly ash slurry concentration system.

Three Advanced Coolside waste samples were prepared for use in the waste management study to simulate waste produced from a boiler using feed coals with 7.5% ash and 3.5%, 2.5% and 1.5% sulfur. Advanced Coolside waste samples were characterized to ensure that adequate information is available on the physical and chemical nature of the waste for the design and construction of safe and stable landfills.

The maximum dry bulk density of Advanced Coolside waste ranged from 75 to 80 lb/ft^3 with increasing fly ash component in the waste. The moisture content which gave the maximum density (optimum moisture) was about 32% (dry basis). At optimum moisture and compacted to 95% of Proctor density, Advanced Coolside waste had unconfined compressive strength that is suitable for landfill disposal. The strength increased from 20 psi (uncured) to 100 psi or higher after 28 days of curing. As a point of reference for unconfined compressive strength values, bulldozers used in landfills exert pressures ranging from about 12 psi to about 19 psi.

Advanced Coolside waste leachates were prepared using both the TCLP and ASTM leaching procedures. The trace element (As, Ba, Cd, Cr, Pb, Hg, Se and Ag) concentrations were well below (by at least a factor of 50) RCRA allowable limits. Thus, the waste can be classified as non-hazardous for landfill disposal. In addition, the concentrations of Fe, Mn, Ca, Na, Al, sulfate, K and total dissolved solids (TDS) in the leachates were similar to those from other dry flue gas desulfurization (FGD) wastes.

Pelletization takes advantage of the cementitious properties of the Advanced Coolside waste to make products that may be applicable for use as synthetic aggregates. Pellets produced from Advanced Coolside waste were lightweight, had low bulk specific gravity, and had a desirably low LA abrasion index, low water absorption, and a coarse size distribution; however, they also had a high soundness index (i.e, low durability). These data indicate that pellets made from Advanced Coolside wastes may have potential for use as lightweight coarse aggregates in concrete masonry units. For this use, there is no soundness index specification. Since waste disposal can be a significant portion of the operating cost, a more thorough evaluation of other pellet characteristics for this application, along with an evaluation of potential economic impacts, is recommended.

Conceptual Process Design and Economic Evaluation

The primary objectives of this task were to develop a conceptual design for a utility-scale application of the Advanced Coolside Process and to assess the economic attractiveness of the process. An additional objective was to identify process areas for potential cost reductions to guide research efforts in areas that would most impact the economics.

Based on the results of an interim economic study, economic targets were established for the process midway through the project. These were to achieve a 20% levelized cost advantage and a 50% capital cost advantage over limestone wet scrubbing for a range of plant sizes and coal sulfur levels. Based on conversations with utilities, these levels of cost advantage would make it attractive to consider a less developed technology.

A final conceptual process design and economic study for the Advanced Coolside Process was performed. It describes a complete conceptual process design for full-scale, coal-fired applications of the process. Advanced Coolside process costs are compared to those of limestone forced oxidation (LSFO) wet FGD technology. The process economics were investigated for coal sulfur levels ranging from 1.0% to 3.5% (as-received) and plant sizes ranging from 160 to 512 gross MW. The final economic study incorporates the results of pilot plant process optimization work which has resulted in a significant reduction in process costs.

The Advanced Coolside process enjoys a capital and levelized cost advantage relative to LSFO in all coals and plant sizes examined in this study. Figures 4 and 5 show capital and levelized cost comparisons for a 2-5% S coal. The figures further indicate that the economic targets established in the first interim evaluation have been achieved for a wide range of coal sulfur contents and plant sizes. The projected capital cost of Advanced Coolside is 55% to 60% lower than limestone forced oxidation wet FGD. Total levelized SO_2 control cost in \$/ton SO_2 removed ranged from 15% to 35% lower than LSFO, over the range of plant sizes and coal sulfur contents investigated. For a mid-range plant size (260 MW) and a mid-range coal sulfur content (2.5%), the levelized cost advantage is 25%. The levelized cost is sensitive to sorbent transportation charges and as a result is highly site-specific.

EPRI Technical Assessment Guidelines were followed. To make a fair comparative evaluation, similar design philosophies, equipment cost algorithms, and financial assumptions (Table 3) were used for the evaluation of both Advanced Coolside and limestone forced oxidation technologies. Both processes were evaluated for 90% SO_2 reduction. The process design for the limestone forced oxidation wet FGD process was recently updated based on current commercial trends to reflect the state of the art. This includes the use of a single absorber module with no spares.

CONCLUSIONS

1. The Advanced Coolside process achieved the process SO_2 removal target of 90% at sorbent utilization efficiencies of over 70%. The keys to achieving this performance were achieving near saturation in the contactor and optimizing sorbent recycle, including the moisture addition step.

2. The Advanced Coolside process has the potential for very high SO_2 removal efficiency (90% to greater than 99%).

3. The contactor was redesigned for significantly reduced capital and operating costs and smaller plant footprint compared to the initial design. Other process design improvements were realized, including improvements in the recycle wetting and handling systems, the sorbent preparation and handling system, the waste handling system, and the flue gas duct design.

4. The Advanced Coolside process is relatively insensitive to the lime source. This is an economic advantage, allowing the use of the lowest cost sorbent available.

5. The addition of small amounts of additives to the recycle sorbent during the water addition step can improve desulfurization performance in a baghouse, but this is not required to achieve performance targets.

6. Pilot plant operation provided a positive indication of the operability and retrofit potential of the Advanced Coolside process. Recycle test duration ranged up to 150 hours. A long-term (300 hr) performance test with 24 hr/day operation was conducted under optimized process conditions.

7. The waste management evaluation indicated that the combined spent sorbent/fly ash waste is suitable for landfill disposal.

8. A final process conceptual design and economic evaluation projects capital costs less than one half of those for limestone forced oxidation wet FGD. The projected total SO_2 control cost on a levelized basis is 25% lower than wet FGD for a 260 MWe plant burning a 2.5% sulfur coal. The levelized cost is sensitive to sorbent cost and, thus, is highly site-specific. This cost advantage meets previously established economic goals for increasing the attractiveness of the technology for electric utilities.

RECOMMENDATIONS FOR FUTURE DEVELOPMENT OF THE ADVANCED COOLSIDE PROCESS

- Demonstration of the process on at least the 5-10 MWe scale to confirm the scale up of process performance and operability.
- Further process development of by-product utilization could give the process unique advantages over conventional FGD technology.
- The capability of the process to control air toxics should be investigated. A literature analysis suggests that the Advanced Coolside process has important features for the control of mercury and HCl. Both the gas/liquid contactor and the sorbent entrainment zone provide low temperature and efficient mass transport conditions important for capture of these species. Furthermore, the relatively high recycle ratios employed could increase the feasibility of using a more expensive co-sorbent such as activated carbon.

ACKNOWLEDGMENT

This work was conducted under partial sponsorship of the U.S. Department of Energy Contract DE-AC22-91-PC90360. The authors are grateful to C. J. Drummond, T. D. Brown, R. E. Tischer, and others at DOE Pittsburgh Energy Technology Center for their support and encouragement of this project.

REFERENCES

1. Yoon, H., M. R. Stouffer, W. A. Rosenhoover, J. A. Withum, and F. P. Burke. "Pilot Process Variable Study of Coolside Desulfurization." *Environ. Progress*. 1988, 7(*2*), 104-11.
2. Stouffer, M. R., H. Yoon, and F. P. Burke. "An Investigation of the Mechanisms of Flue Gas Desulfurization by In-Duct Dry Sorbent Injection." *I&EC Research*. 1989, 28(*1*), 20.
3. Withum, J. A., H. Yoon, F. P. Burke, and R. M. Statnick. "Coolside Desulfurization Demonstration at Ohio Edison Edgewater Power Station." *ACS Div. Fuel Chem. Prepr*. 1990, 35(*4*), 1463-72.
4. Babu, M., R. C. Forsythe, C. F. Runyon, D. A. Kanary, H. W. Pennline, T. Sarkus, and J. L. Thompson. "Results of 1.0 MMBtu/Hour Testing and Plans for a 5 MW Pilot HALT Program for SO_2 Control." Proceedings of the Third Annual Pittsburgh Coal Conference, Pittsburgh, PA (September 1986).
5. O'Dowd, W. "Duct Injection Experiments at DOE-PETC," Technical Update No. 18, Duct Injection Technology Development Program. (January 1991).
6. Nolan, P. S., D. C. McCoy, R. M. Statnick, M. R. Stouffer, and H. Yoon. "Economic Comparison of Coolside Sorbent Injection and Wet Limestone FGD Processes," 1991 SO_2 Control Symposium, Washington, DC (December 1991).
7. Stouffer, M. R.; Rosenhoover, W. A.; Withum, J. A. "Advanced Coolside Desulfurization Process," *Environ. Progress* 1993, 12(2), 133-139.
8. Withum, J. A.; Rosenhoover, W. A.; Stouffer, M. R.; DeIuliis, N. J.; McCoy, D. C. "Advanced In-Duct Sorbent Injection Process for SO_2 Control," *ACS Div. Fuel Chem. Prepr*. 1994, 39(*1*), 261-6.
9. Stouffer, M. R.; Maskew, J. T.; Rosenhoover, W. A.; Withum, J. A. "Development Status of Advanced Sorbent Injection Process for SO_2 Control," *Proc. Tenth Annual Coal Preparation, Utilization, and Environmental Control Contractors Conference*, July 18-21, 1994.

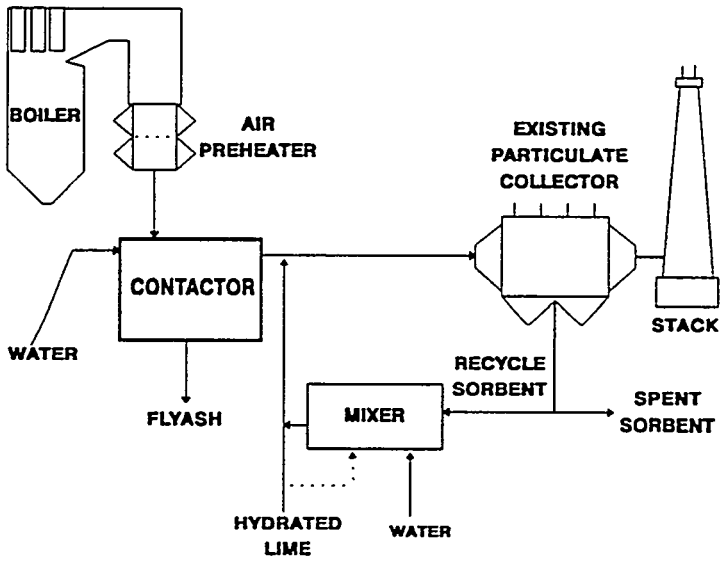

Figure 1. Schematic of the Advanced Coolside Process.

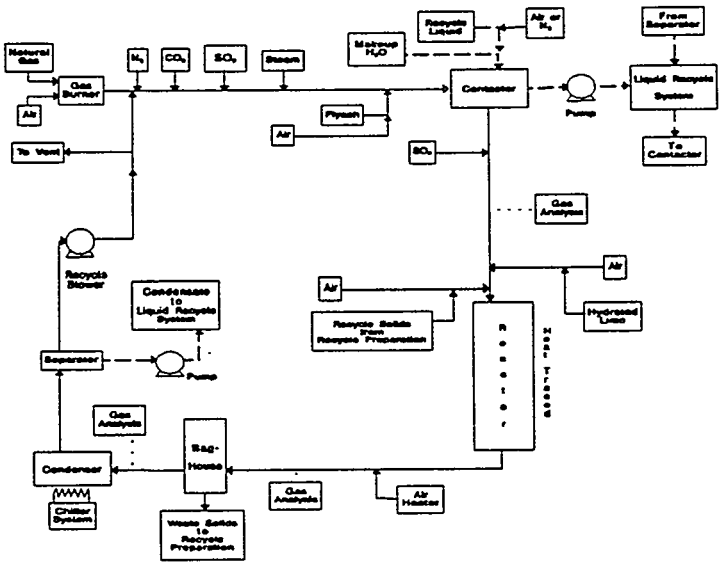

Figure 2. Schematic of the 1000 ACFM Advanced Coolside Pilot Plant.

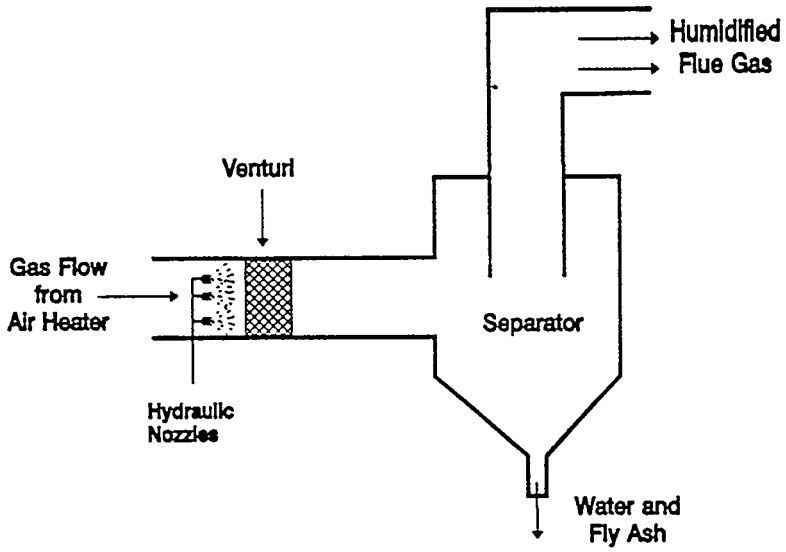

Figure 3. Schematic of the Third Generation Contactor.

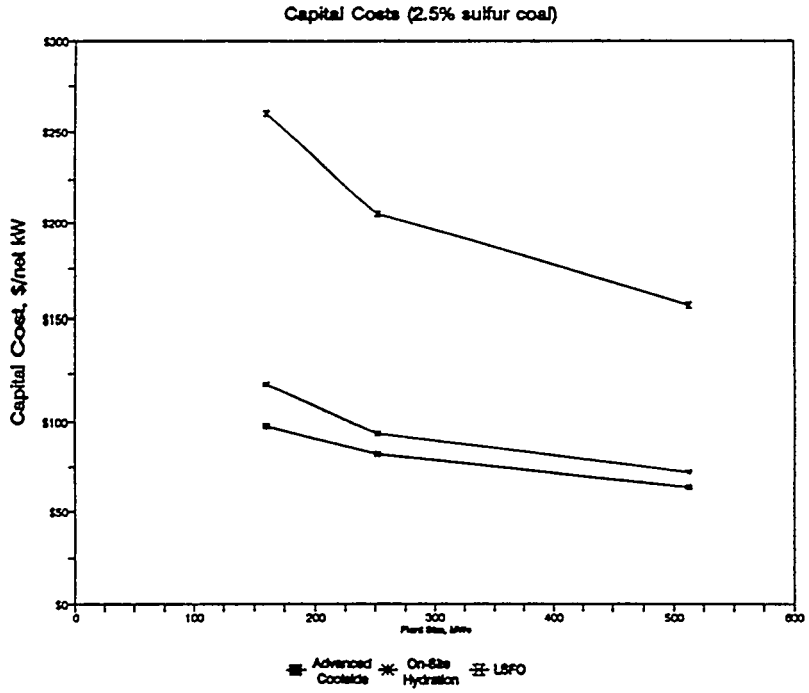

Figure 4. Comparison of Capital Costs for the Advanced Coolside Process and Limestone Forced Oxidation Wet FGD (LSFO) for a Range of Plant Sizes Burning A 2.5% S Coal. (For Advanced Coolside, on-site hydration is compared to buying hydrated lime.)

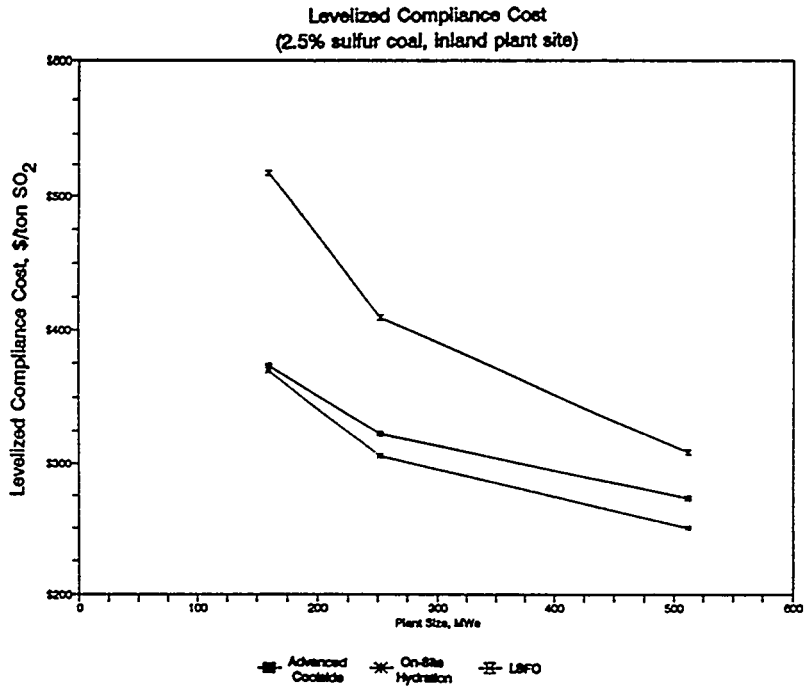

Figure 5. Comparison of Levelized SO_2 Control Costs for the Advanced Coolside Process and Limestone Forced Oxidation Wet FGD (LSFO) for a Range of Plant Sizes Burning A 2.5% S Coal and Assuming an Inland Plant Site. (For Advanced Coolside, on-site hydration is compared to buying hydrated lime.)

TABLE 1

SUMMARY OF RECYCLE TEST RESULTS: TESTS SIMULATING SO_2 REMOVAL WITH AN ESP

Test	Fresh Ca/S, mol	Recycle Ratio (a)	Water Addt'n lb/lb Recycle Sorbent	Total $Ca(OH)_2$/S mol Ratio	Approach Temp., Baghouse Inlet Approach, °F	SO_2 Removal, %		Sorbent Util., %	
						Duct	System (b)	Steady State (c)	Solids Analyses
12	1.4	4.5	0.15	2.2	23	83	90	63	62
13	1.2	6.9	0.12	2.1	23	87	90	75	70
12A	1.5	4.3	0.15	2.5	24	84	90	60	59

Common Conditions: SO_2 Inlet Concentration = 1500 ppm (dry); Flue Gas Flow = 340 SCFM

(a) lb dry recycle/lb fresh lime
(b) duct + baghouse
(c) calculated steady-state sorbent utilization

TABLE 2

SUMMARY OF RECYCLE TEST RESULTS: TESTS SIMULATING SO_2 REMOVAL WITH A BAGHOUSE

Test	Fresh Ca/S, mol	Recycle Ratio (a)	Water Addt'n lb/lb Recycle Sorbent	Total $Ca(OH)_2$/S mol Ratio	Approach Temp., Baghouse Inlet, °F	SO_2 Removal, %		Sorbent Util., %	
						Duct	System (b)	Steady State (c)	Solids Analyses
6A	1.2	5.0	0.00	2.2	10	59	73	61	58
7A	1.3	3.3	0.15	1.8	9	60	84	67	68
8A	1.2	3.4	0.10	1.8	11	64	81	65	66
9	1.5	3.5	0.15	2.2	12	70	90	61	63
10	1.2	4.9	0.15	1.7	9	81	88	71	68
11	1.6	3.9	0.15	2.4	11	91	97	60	58
11A	1.6	3.8	0.15	2.4	12	88	100	61	61
17B	1.2	6.9	0.12	1.4	10	84	92	76	72

Common Conditions: SO_2 Inlet Concentration = 1500 ppm (dry)

(a) lb dry recycle/lb fresh lime
(b) duct + baghouse
(c) calculated steady-state sorbent utilization

TABLE 3

KEY ASSUMPTIONS OF PROCESS ECONOMIC STUDY

	Advanced Coolside	Forced Oxidation Wet FGD
Delivered Sorbent Cost	$65/ton, 7% inerts (hydrated lime) $57/ton (quicklime)	$15/ton (limestone)
Waste Disposal Cost	$6.50/ton	$6.50/ton
SO_2 Removal	90%	90%
Capacity Factor	65%	65%
Capital Life	30 years	30 years
Retrofit Factor	Medium (1.22-1.34)	Medium
Location Factor	1.06	1.06
Design Philosophy	"nth" plant, 18% Capital Contingency	"nth" plant, 18% Capital Contingency
Sparing	Auxillary equip. only, no major equip.	Auxillary equip. only, no major equip.

The following manuscript was unavailable at time of publication.

EPRI's ENVIRONMENTAL CONTROL TECHNOLOGY CENTER

Robert Moser
Electric Power Research Institute
P.O. Box 10412
3412 Hillview Avenue
Palo Alto, CA 94303

Please contact author(s) for a copy of this paper.

The following manuscript was unavailable at time of publication.

INVESTIGATION OF COMBINED SO_2/NO_x REMOVAL BY CERIA SORBENTS

Dr. Ates Akyurtlu
Hampton University
Tyler Street
Hampton, VA 23668

Please contact author(s) for a copy of this paper.

PUSHING THE PULVERIZED COAL ENVELOPE WITH LEBS

JOHN W. REGAN, PROJECT DIRECTOR
RICHARD W. BORIO
MARK PALKES
ABB POWER PLANT LABORATORIES
MARK D. MIROLLI
ABB CE SYSTEMS
COMBUSTION ENGINEERING, INC.

JAMES D. WESNOR
ABB ENVIRONMENTAL SYSTEMS

DAVID J. BENDER
RAYTHEON ENGINEERS & CONSTRUCTORS, INC.

Contract No.: DE-AC22-92PC92159

ABSTRACT

In response to challenges from technologies such as IGCC and PFBC, the ABB LEBS Team has proposed removing the barriers to very large advances in environmental and thermal performance of pulverized coal plants. Pulverized coal will continue to be the source of more than half of our eiectric generation well into the next century and we must develop low-risk low-cost advances that will compete with the claimed performance of other technologies. This paper describes near-term PC technologies for new and retrofit applications which will accomplish this.

INTRODUCTION

Since the inception of the "Engineering Development of Advanced Coal-Fired Low-Emission Boiler Systems" contract (LEBS) the aggressive emissions targets have been gradually tightened and the efficiency target gradually raised in response to pressure from several directions. The contract targets for emissions are now approximately one-half of the original values for NO_X, SO_X and particulates and the efficiency target has been raised substantially - 38% to 42% (HHV, net). The ABB Team believes it would not be difficult to reduce the emissions by one-half again and to raise the efficiency target another 3-4 percentage points, and it proposes to do so.

LEBS is restricted to pulverized coal firing (PC) which is viewed by many as less glamorous than other coal-fired technologies such as IGCC and PFBC, most likely because of the misconception that PC with the Rankine steam cycle has neared its limits of efficiency and emissions performance. In truth, there is considerable room for cost-effective improvements. The path to these improvements is defined and is short. The required development effort is not great and the result will be low-risk low-cost familiar-looking systems which will be readily accepted by the very conservative, risk-averse utility industry. The technologies described below are fuel-flexible and suited to retrofit, repowering and new applications.

SUBSYSTEM TECHNOLOGIES TO ACHIEVE PERFORMANCE GOALS

In-furnace NO_X Control

General Description: The most cost effective way to reduce nitrogen oxides when burning a fossil fuel, coal in this case, is through an in-furnace NO_X reduction process. The foundation for ABB's in-furnace NO_X reduction process is TFS 2000™, a proven technology which is currently being employed on a commercial basis. The TFS 2000™ has been described in detail elsewhere [1]. Briefly, it involves substoichiometric fuel/air operation in the firing zone, the use of concentrically arranged air injection in the windbox whereby the air jets are aimed at a larger imaginary circle than the fuel jets, the use of multiple levels of separated over fire air and the use of a pulverizer with a dynamic classifier. As with all in-furnace NO_X reduction systems, the key is to be able to operate in a mode which produces low NO_X without exacerbating the combustible losses, notably the carbon content in the fly ash. Much of the work in this part of the LEBS program is aimed toward characterizing the performance of firing system configurations that build on the TFS 2000™ concept and which have been formulated by ABB to achieve even greater NO_X reduction without increasing combustible losses.

The objective of ABB's in-furnace NO_X reduction process is to reduce nitrogen oxides leaving the primary furnace to 0.1 lb NO_X/MM Btu (75 ppm @ 3% O_2) or lower while maintaining an acceptable level of carbon in the fly ash. (Further NO_X reduction can be achieved with the downstream SNO_X™ process which is discussed below.)

The process for evaluating the various firing system concepts/configurations which ABB has formulated involves the use of computational modeling, small scale experimental testing and larger scale experimental testing. Additionally, it has involved concurrent characterization of coal pulverization in an ABB-developed pulverizer with a dynamic classifier. As NO_X levels are pushed ever lower it is imperative that the fuel particle size distribution also be more tightly specified as a primary means of controlling combustible losses. Figure 1 is a flowchart showing the interaction of the various activities described above, the primary deliverable being input into the revised system design. The FSBF referred to in Figure 1 is a Fundamental Scale Burner Facility and the BSF is an 80 million Btu/hr Boiler Simulation Facility.

The two primary activities which will be addressed in this paper are preliminary results from testing in the Fundamental Scale Burner Facility (FSBF) and characterization of one of the LEBS coals in ABB's Pulverizer Development Facility. Computational modeling is underway and will be addressed briefly.

Computational Modeling: Two models are being employed to help analyze the various firing systems concepts that have been formulated. A kinetics reaction model, CHEMKIN, is being used to provide a preliminary evaluation of the potential for various concepts to achieve the desired results. It is recognized that results from this evaluation are qualitative at best and can only be used to provide trends; nevertheless its use can be an important screening tool to help prioritize the most promising concepts for further evaluation. A computational fluid dynamics model, FLUENT, is being used to further evaluate concepts under conditions which better simulate actual boiler operation. Unlike CHEMKIN which assumes either well-stirred reactor conditions or perfect plug flow conditions, FLUENT is able to simulate real-world mixing conditions. ABB's large combustion facility, the Boiler Simulation Facility (BSF) has been modeled with FLUENT. Experimental measurements from the BSF compare quite well with those predicted by FLUENT, namely parameters such as gas temperatures and gaseous concentrations like O_2 and CO. Having validated FLUENT with BSF data, the intent is to use it as well as the CHEMKIN model in ways that capitalize on their respective strengths to evaluate and screen various firing system concepts.

Fundamental Scale Burner Facility (FSBF): The LEBS plan calls for evaluation of advanced coal reburning as a supplemental NO_X reduction technology. Reburning is classically thought of as a separate, downstream (from the primary combustor) zone into which "reburn fuel" is injected followed by a "burnout zone" where air is injected

---

[1] "Development of ABB CE's Tangential Firing System 2000" presented at the '93 EPA/EPRI NO_X Conference.

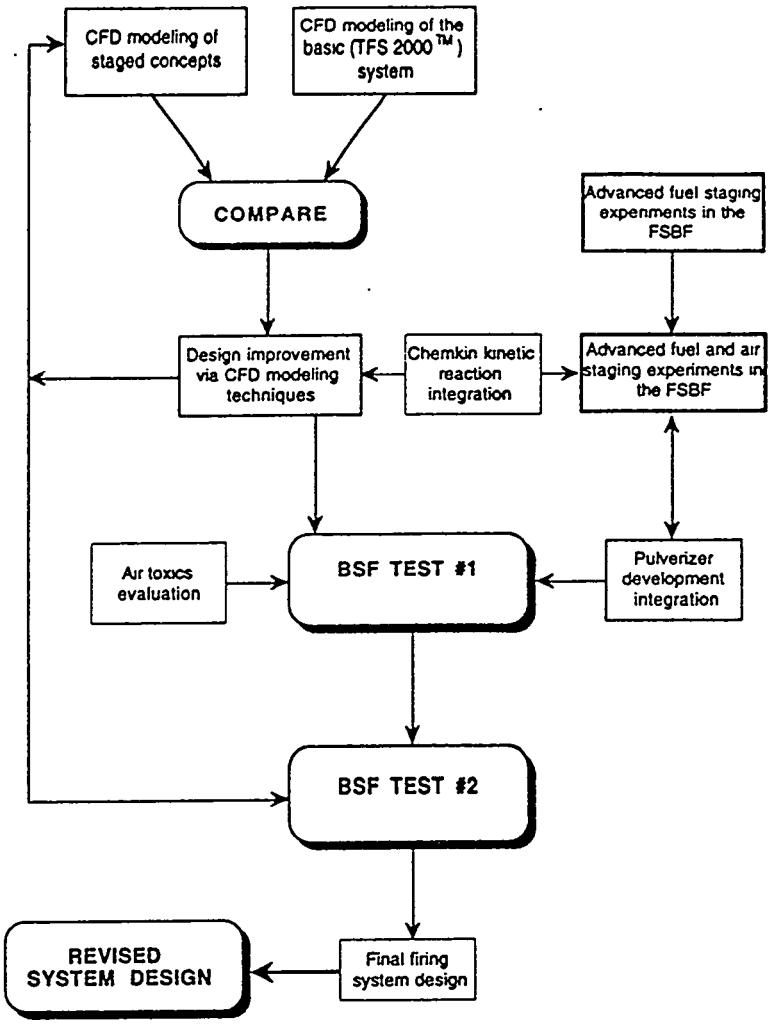

Figure 1 - LEBS Work Flow Chart

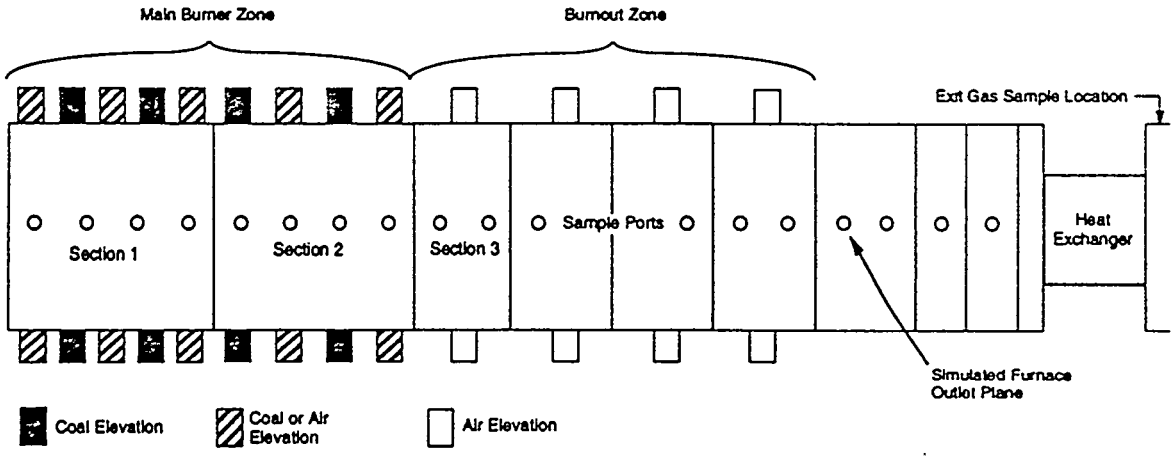

Figure 2 - Schematic of Fundamental Scale Burner Facility

to burn out the remaining combustibles from the reburn zone, which typically operates at substoichiometric conditions. Reburning in the classical sense has been shown to be an effective technology for reducing NO_X; however, when used in the traditional fashion greater residence time is needed in the separate reburn and burnout zones. However, NO_X reduction through the reburning process can and does occur within the primary combustor. The objective of testing in the FSBF has been to characterize the NO_X and combustion performance from firing system concepts which do not have the classical, separate reburn and burnout zones, but rather which employ integrated strategies within the main windbox zone that take advantage of NO_X reduction through reburn process chemistry. The advantages are less residence time, a smaller furnace and a favorable cost impact. It is believed that tangential firing, specifically building upon the already-established TFS 2000™ system, is well suited for adaptation to the integrated firing system concept.

The Fundamental Scale Burner Facility (FSBF) is a horizontally fired experimental combustor which has a capacity of 5 million Btu/hr. See Figure 2. It has been configured to simulate tangential firing; air and fuel are injected from four nozzles for each plane, or elevation, the term used to describe a plane in a tangential firing system. As noted in Figure 2 there are a number of planes from which fuel or air can be injected to simulate and evaluate a particular firing arrangement. Additionally there are air-only injectors downstream of the main windbox to simulate over fire air injection.

Low NO_X firing generally requires that the main windbox or burner zone be fired under substoichiometric conditions. Table 1 shows the relative NO_X values as a function of bulk stoichiometry in the main windbox zone as simulated in the FSBF. Configuration 1 represents a base case where all of the combustion air is injected through the main windbox; the NO_X level is arbitrarily shown as 100%. Configurations 2 and 3 show relative NO_X values for substoichiometric firing in the main windbox and with different amounts of Separated Over Fire Air (SOFA) in SOFA levels 1 and 2. As expected, substoichiometric operation results in lower NO_X and the strategy for staging the SOFA also makes a difference in the final NO_X levels.

Table 1. Relative NO_X Levels vs. Main Burner Zone Stoichiometry (MBZ) and Separated Over Fire Air (SOFA)

Configuration	NO_X%*	MBZ Stoich	SOFA 1 Stoich	SOFA 2 Stoich
1	100	1.15	1.15	1.15
2	66	0.8	1.0	1.15
3	54	0.8	0.8	1.15

*Normalized, with Case 1 assigned 100%

Initial testing in the FSBF was designed to evaluate a number of variables within the main firing zone, including firing system configuration and operating conditions, for their effect on NO_X. Table 2 shows some initial results from a number of firing system configurations, some of which employ integrated firing system strategy. Relative to the base case, configurations 4 and 5 are run to produce lower NO_X without the use of SOFA, while configurations 6 and 7 show relative NO_X levels with the use of SOFA.

Table 2. Relative NO_X Levels for Integrated Firing Configurations vs. Basecase (Configuration 1)

Configuration	NO_X%*	MBZ Stoich	SOFA 1 Stoich	SOFA 2 Stoich
1	100	1.15	1.15	1.15
4	64	1.15	1.15	1.15
5	59	1.15	1.15	1.15
6	54	0.8	0.8	1.15
7	49	0.8	0.8	1.15

*Normalized, with Case 1 assigned 100%

Testing in the FSBF is continuing; plans under our LEBS Program call for continued evaluation of firing system concepts that are hypothesized to produce ever lower NO_X levels while meeting our goal of maintaining combustible losses at minimum levels.

Coal Pulverization : As noted above, specification and control of coal particle size distribution is an important prerequisite for successful operation of a low NO_X firing system. Conditions for achieving low NO_X tend to run counter to those that are favorable for good coal combustion; therein lies the challenge. Paying attention to the proper coal particle size distribution has the obvious effect of facilitating better carbon burnout and the perhaps not-so-obvious effect of enhancing NO_X reduction through earlier release of nitrogen species in the near-burner zone where the opportunity for conversion to molecular nitrogen is increased.

ABB has constructed a Pulverizer Development Facility (PDF) for the study and characterization of coal pulverization and classification. The PDF includes a coal storage and feed system and a fine coal collection system as necessary support equipment for the pulverizer itself. The mill represents a commercial design, based on a size 323 bowl mill, but with the flexibility to change out important components within the mill, such as grinding elements and classifiers. The capacity of the PDF is about 3.5 tons/hr.

The early focus of the LEBS-related work which utilizes the PDF has been to characterize the coal particle size distribution and mill power requirements. Ideally it is desired that the top size of the coal particles be closely controlled and that classification is more efficiently carried out so that sufficiently fine particles are not recirculated needlessly back to the grinding zone of the mill. The use of a dynamic classifier is one way of accomplishing this.

Table 3 shows results from recent testing with various dynamic classifier designs as compared with a base case static classifier design. It is apparent that the goals of greater coal fineness, less coarse material and lower power requirements have all been achieved with at least two of the dynamic classifier designs. Results have been demonstrated with conventional air:coal ratios, namely 1.5 lb air/lb coal.

Future testing in the FSBF will employ the use of coals having various particle size distributions to ascertain and quantify the benefits of using finer coal.

Table 3. Dynamic Classifier Characterization

	Static Classifier	Dynamic Classifier Designation			
		HP1	HP2	RB1	RB2
Product Size (wt%)					
+50 mesh	0.1	0.2	0.0	0.0	0.0
+100 mesh	2.4	1.2	0.6	0.5	0.6
-200 mesh	84.3	85.7	92.7	93.1	90.7
Relative Power Requirements (%)	100	81	98	97	107

Stack NO_X, SO_2, Particulates and Title III Pollutants

General Description of Control Technology: Boiler outlet emissions will be controlled by a modified SNO_X™ process, referred to as the SNO_X™ Hot Scheme. The SNO_X™ process which simultaneously removes nitrogen oxides and sulfur oxides from flue gases, is a licensed technology developed by Haldor/Topsøe A/S, Denmark. The SNO_X™ technology has been demonstrated in several forms, one as a Clean Coal Technology at Ohio Edison's Niles Station, and has been constructed and operated on a commercial scale in Denmark. The SNO_X™ technology consists of five key process areas: particulate collection, NO_X reduction, SO_2 oxidation, sulfuric acid condensation, and acid conditioning. For the LEBS process, the particulate collection and NO_X reduction process are integrated into a single process step.

Particulate/NOx Control: The first step, particulate collection, will have a direct effect on the performance of the downstream SO_2 converter, particularly the frequency of cleaning the SO_2 catalyst. This is due to the inherent ability of the catalyst to retain greater than 90% of all particulate matter which enters the converter. The collection of this particulate matter, over time, will cause the gas draft loss to increase. The virgin draft loss can, however, be restored through catalyst cleaning, called screening. Higher dust loads at the SO_2 convertor inlet therefore require more frequent cleaning, and higher catalyst attrition loses. A target dust level of 0.0008-0.0016 lb/MMBtu (1-2 mg/Nm3) leaving the collector is desired. Consequently, dust emissions from the SO_2 convertor are often an order of magnitude lower.[2]

To achieve the required particulate loadings at the SO_2 converter inlet, a high efficiency collection device must be employed. For the LEBS process, a ceramic filter manufactured by CeraMem will be employed.

The construction of the ceramic filter is based on the use of porous honeycomb ceramic monoliths. These high surface area, low cost materials were developed for, and are widely used as, catalyst supports. The monoliths have many cells or passageways which extend from an inlet face to an opposing outlet face. Cell structure is usually square and cell density can vary from 25 to 1400 cells per square inch (cpi) of face area. Mean pore size can range from 4 to 50 microns.

The superior properties of commercially available monoliths make them ideally suited for applications requiring high thermal stability, mechanical strength, and corrosion resistance. These rigid ceramics have been used for years as NO_X SCR catalyst supports in combustion flue gas applications. The monolith structure used for catalyst support material is readily adapted to function as a particulate filter. The monolith structure is modified by plugging every other cell at the upstream face with a high-temperature inorganic cement. Cells which are open at the upstream face of the monolith are plugged at the downstream face. Flue gas is thereby constrained to flow through porous cell walls, and at appropriate intervals, the filter is cleaned by backpulse air.

CeraMem has developed the technology for applying thin ceramic membrane coatings to the monoliths and controlling the pore size. The thin (approximately 50 microns) membrane coating has a pore size approximately 100-fold finer than that of the monolith support. Thus the filter retention efficiency is determined by the membrane pore size, not the monolith pore size. The ceramic filter will operate as an absolute filter; that is all particulate over a certain diameter will be removed from the gas stream. The split diameter is determined and controlled by the ceramic application.

In the LEBS process, commercially-tested SCR catalyst is applied to the clean side of the particulate filter. As with other low dust SCR applications, concerns about flyash poisoning of the catalyst are eliminated, and catalyst loadings may be reduced as the catalyst will have a "higher" activity. Also, in this application, the reaction kinetics will not be controlled by mass diffusion as in other monolith applications. Instead, the kinetics will be much faster, taking advantage of "forced diffusion", where the flue gas will come into forced contact with the catalyst as it passes through the monolith wall. A third benefit of this technology in relation to SCR performance will come about from elevated conversion temperature. Typical SCR applications operate at about 675°F, whereas the LEBS application will operate at a slightly higher temperature of 750-775°F. Increased temperature should not affect catalyst life, but should improve the efficiency of the reducing reagent, in this case ammonia. The increase in temperature should result in a lower ammonia concentrations at the SCR outlet, often called slip.

Particulate and NOx Emissions Levels: Taking advantage of the clean-side catalyst application, forced diffusion kinetics, and higher reduction temperature should allow for much higher reduction efficiencies and efficient reducing reagent consumption. Early data indicate that at NO_X inlet concentrations of 200 ppm, NO_X reduction should exceed 90% without any measurable ammonia slip.

---

[2] These levels are below normal detection limits of EPA Method 5 sampling. The method collection time would have to be extended to be able to detect these emissions.

In particulate collection tests conducted at ABB's Corporate Research Facility, collection efficiency was found to be almost absolute, in most cases greater than 99.99996% with an inlet flyash loading of 4-5 lb/MMBtu (5-6 g/Nm^3). Outlet emissions could not be detected by standard EPA Method 5 techniques, and were determined to be less than 0.0000016 lb/MMBtu (0.0020 mg/Nm^3) by laser-light scattering instrumentation.

SO_2 Control: SO_2 emissions are controlled by the SO_2 oxidation catalyst, sulfuric acid condensers, and acid conditioning system. An oxidation catalyst, which is widely used in the sulfuric acid industry, converts the SO_2 to SO_3 at greater than 97% efficiency. The efficiency of the catalyst is not affected by presence of water vapor or chlorides in concentrations up to 50% and several hundred ppm, respectively. An additional benefit of the sulfuric acid catalyst is its ability to oxidize carbon monoxide and hydrocarbons present in the flue gas stream to innocuous compounds.

The SO_3 in the gas leaving the SO_2 converter is hydrated and condensed in two steps. First, the bulk of the SO_3 is hydrated to sulfuric acid vapor as the flue gas passes through the Ljungstrom air heater and the temperature drops to approximately 500°F. At this point, the flue gas is still well above the acid dewpoint, thus avoiding acid condensation and corrosion of the ductwork. The flue gas then enters the WSA Condenser, a unique tube and shell falling film condenser with the boiler combustion air used as a cooling medium on the shell side. Borosilicate glass tubes are used to convey and cool the flue gas. In both steps, the hydration and condensation reactions are exothermic, thereby adding heat to the flue gas and subsequently to the boiler thermal system. The design and operation of the WSA Condenser make possible virtually complete condensation and capture of the sulfuric acid at concentrations of 92 to 95 wt %.

SO_2, SO_3 Emissions Levels: To this point, SNO_X™ systems have not been built with SO_2 removal efficiencies of greater than 95%, and therefore, data other than that obtained at laboratory scale would not support the ability to achieve higher removal efficiencies. However, ultra-high removal efficiencies (typically greater than 98%) have been studied by Haldor/Topsoe, with the information being used to design, build, and operate high-efficiency systems. As this is a catalytic system, SO_2 removal efficiency is fixed and somewhat inflexible. If a system is designed for a specific removal efficiency, it will maintain that degree of control over a wide operating range without any drop-off, unlike chemical reagent systems which tend to become gas-side limited and lose removal capibility as inlet SO_2 levels decrease. Increasing removal efficiency would require minor modification of the convertor vessel with catalyst addition.

SO_3 emissions will be controlled by the efficient condensation system, in excess of 99.9% condensation. However, some SO_3 will pass through the system and will exit the stack, and it is expected that this amount would not be in excess of 20 ppm - a level similar to emissions from present-day wet or dry desulfurization systems.

Title III Pollutants: The Niles demonstration facility was sampled as part of the DOE/EPA Field Chemical Emissions Monitoring. It was found that the SNO_X™ technology was able to reduce Title III metal emissions by greater than 98% and Title III organic compounds were not detected at significant levels. The commercial scale facility in Denmark was also sampled by an independent team, with the results reported confirming those obtained from the Niles sampling.

Improved Thermal Efficiency: Heat addition, transfer, and recovery are of significant importance in the SNO_X™ process. The process generates recoverable heat in several ways. All of the reactions which take place with respect to NO_X and SO_2 removal are exothermic and increase the temperature of the flue gas. This heat is recovered in the air heater and WSA Condenser for use in the furnace as combustion air. Because the WSA condenser lowers the temperature of the flue gas to about 210°F, compared to the 300°F range for wet and dry scrubbers[3], additional sensible heat is recovered along with that from the heats of reaction. In comparison to an NSPS-compliant plant, 38% more heat is recovered from the flue gas stream after the boiler, itself accounting for a 1.9 percentage point increase in the net plant thermal efficiency.

[3] Although stack temperatures for wet and dry FGD systems range from 125-250°F, heat recovery - that done by the air heater - usually is limited to a minimum temperature of 300°F. After that, the flue gas is quenched, accounting for the temperature difference.

Waste and Byproducts

As shown in Table 4, unlike many other processes, the SNO_X™ process does not generate a waste product or intermediate. Also, the SNO_X™ process does not produce a "commercial grade" product which does not meet the specifications of its intended market, as has been the case with Wet FGD gypsum. The sulfuric acid produced by the SNO_X™ process, a typical analysis of which is presented in Table 5, meets or exceeds U.S. Federal Specification O-S-801E Class 1 and is commercially tradable without limitation.

The ABB project team includes, as an advisor, Peridot Chemicals. Peridot Chemicals operates two sulfuric acid production facilities and distributes acid from several international involuntary acid producers. Peridot Chemicals has provided very useful insight into the domestic sulfuric acid market.

Installation of a SNO_X™ facility, or any large acid production facility, will force a reshaping of the local acid market, and alliances could be made with local brokers, suppliers, and consumers for distribution and consumption of the acid. It is believed by sulfuric acid market experts that domestic involuntary acid production could displace international involuntary acid production.

It is expected that the flyash from the LEBS system could be sold commercially, similar to present day ash disposal. Carbon content in the flyash is expected to be less than 5%, and there is not expected to be any noticeable presence of ammonia.

Table 4. End product and disposition by technology.

Technological Advancement	Product and Disposition, Cost Comparison
1st Generation Technology - consumable reagent processes, usually sodium- or calcium-based, such as lime/limestone Wet FGD, lime Dry FGD, limestone furnace injection, and duct injection.	Landfill of sulfite/sulfate compounds with little commercial or industrial value. Calcium sulfate from wet FGD can be upgraded to commercial-grade gypsum, but at significant cost. Low capital cost, offset by high O&M cost.
2nd Generation Technology - regenerable reagent processes, such as CuO and MgO systems.	Produces chemical intermediate, usually metallic sulfide or sulfite, which must be landfilled or further processed to produce sulfuric acid or elemental sulfur. High capital cost and O&M cost.
3rd Generation Technology - catalytic (no reagent) technologies, such as SNO_X™ process.	Direct production of elemental sulfur or sulfuric acid. High capital cost, offset by low O&M cost.

On whole, it is expected that the amount of landfill material from an NSPS-compliant plant (ESP/limestone WFGD) will be reduced by approximately 85%, expressed on a heat input basis. This figure accounts for the FGD by-product, a wet mixture of calcium sulfite and calcium sulfate, being landfilled as opposed to the SNO_X™ product, commercial grade sulfuric acid, being sold. For every ton of sulfur in coal, 7.7 tons of landfill waste has been converted to 3.3 tons of sulfuric acid. With evaluations of $15 per ton landfill and $30 per ton commercial grade acid, a net swing of $214 is created, from an outlay of $115 for landfill costs to an income of $99 from acid sales (expressed on per ton S in coal basis). Comparing disposal for the LEBS SNO_X™ design to a dry FGD/fabric filter system would yield a differential of $164 in favor of the SNO_X™ plant, primarily in the reduction of landfill costs associated with a dry waste. At a acid price of $20 per ton, it is expected that the air pollution control system would operate at a financial break-even position.

Table 5. Federal Specification For Commercial Grade Sulfuric Acid and Actual Acid Analysis from Operating Unit

Criteria	Federal Specification Maximum Values	Typical Values from Operating Unit
Concentration, wt %	93.2	94.76
Color	Water Clarity, None	ND
Iron, ppm	50	3.4
Copper, ppm	50	0.025
Zinc, ppm	40	0.12
Arsenic, ppm	1	0.012
Antimony, ppm	1	<0.002
Selenium, ppm	20	26
Nickel, ppm	1	0.04
Manganese, ppm	0.2	0.065
Ammonium, ppm	10	2.9
Chloride, ppm	10	ND

HIGH EFFICIENCY POWER CYCLES

Steam Cycle: The most widely used power plant in the United States has been a subcritical single reheat cycle. It features a drum boiler operated to produce 2400psig/1000°F at the turbine throttle. In the late fifties, the industry introduced supercritical steam cycles which enabled higher plant efficiencies and improved operating costs. As the initial problems were resolved and supercritical technology matured, these plants demonstrated availabilities comparable to their subcritical counterparts. However, for a variety of reasons but mainly due to low cost of fuel, there have been no supercritical plants constructed in the United States since the late seventies.

The original incentives for supercritical cycle development in the 1950's are even more critical today. The time has come to take a hard look at cycle options and improvements in heat rate through higher steam conditions. Heat rate improvement means reduced emissions of SO_2, NO_x, CO_2, particulate, etc., per unit of electricity produced.

Figures 3 illustrates heat rate improvements with the increase in pressure and temperature for a single and double reheat plant as compared to a conventional subcritical unit. For example, a steam cycle designed with steam conditions of 3625psig (250 bar) and 1000°/1000°F offers plant heat rate improvement of over 1.4%.

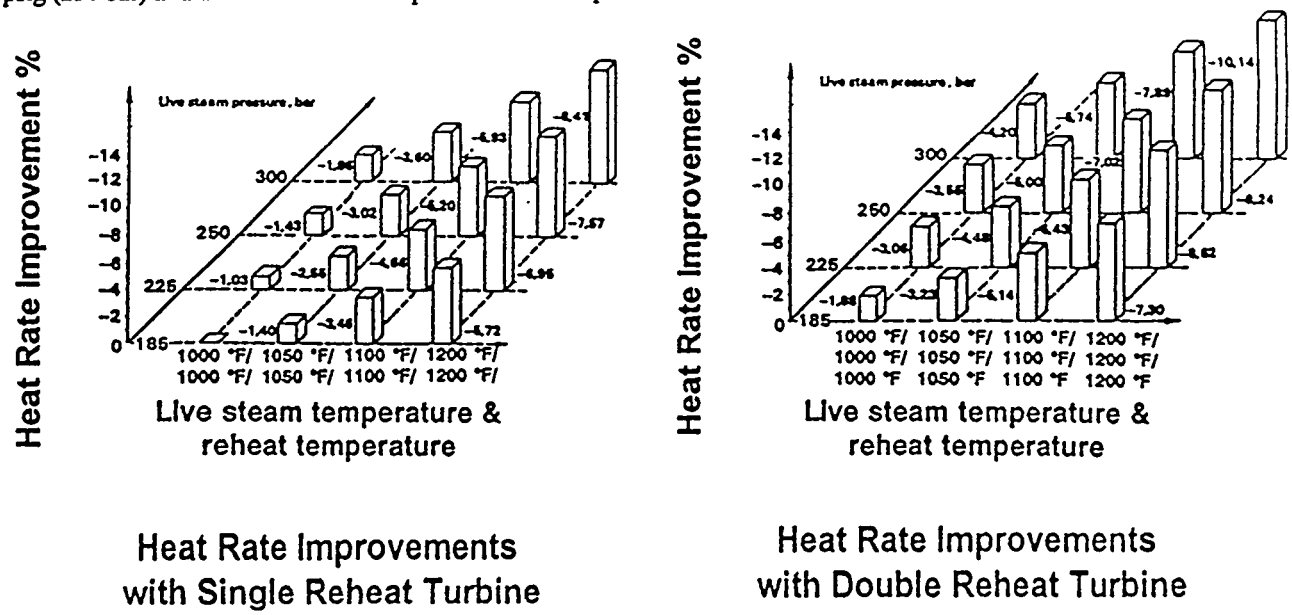

Figure 3 - Heat Rate Improvement vs Pressure and Temperature

For over a decade, ABB CE with the support from DOE and EPRI has been participating in the development of an advanced steam cycle with throttle conditions of 4500psig/1100°/1100°/1100°F. This plant is commercially available and includes state-of-the-art technical advances made in materials, manufacturing processes, design analyses, and control systems. Plants with very similar steam conditions are in successful commercial service in Japan and Denmark (where high efficiency has greater value.) Depending on the condenser pressure, plant capacity, and type of coal-fired, the net plant HHV efficiency is approximately 41% (8324 Btu/kwhr) to 43% (7937 Btu/kwhr). Although the steam conditions may appear to be advanced, they do not constitute a significant departure from the current experience. One may only need to recall the Eddystone unit of the Philadelphia Electric Company which was commissioned in 1959. With initial steam conditions of 5000 psig, 1200°F and two reheats of 1050°F, Eddystone I had the highest steam conditions and efficiency of any electric plant in the world. Due to some initial problems, very few of which were related to high temperature and pressure, the steam turbine throttle conditions were reduced to 4700 psig and 1130°F. It remains an important unit in Philadelphia Electric's future generation plan as evidenced by life extension beyond the year of 2010. However, in contrast to the Eddystone unit which was designed for base load capacity needs, the state-of-the-art plant would be capable of sliding pressure mode of operation and cycling duty with fast start-up and fast load change rates. These desired plant characteristics are accommodated by introducing a steam generator with spirally wound furnace walls, an integrated start-up system, and a split back pass for steam temperature control. The past experiences are factored into the design of critical components. Major design improvements include improved materials such as advanced ferritic alloys as T91 (9Cr) and modified 12 Cr for piping, headers, and steam turbine rotors. Better analysis techniques combined with advanced monitoring and control systems ensure that the state-of-the-art plant would be able to operate without any loss of component life over and above that expected from current units.

Higher steam conditions, such as 5000psig/1200°/1200°/1200° F, offer the prospect of an additional plant efficiency improvement of approximately 3%. The estimated net plant efficiency is in the range of approximately 42% (8126 Btu/kwhr) to 44% (7757 Btu/kwhr). Design of the high temperature components is not expected to change significantly from the state-of-the-art plant except for some material upgrade in the critical areas. For base load capacity, technology is probably available to build this plant today, particularly, if the reheat temperatures are reduced to 1150° or 1100° F. For cycling duty, the key to success lies in the application of advanced high strength ferritic and austenitic alloys developed in the past decade for such critical components as furnace wall tubing, headers, piping, and steam turbine rotors. It is believed that with some additional R&D effort the 5000 psig steam cycle can be offered commercially in the 2000 to 2002 time frame.

Significant additional thermodynamic gain can be achieved by adopting even higher steam conditions such as 6000psig/1300°/1300°/1100°F. The expected net plant efficiency should be in the range of 43.5% (7846 Btu/kwhr) to 45.5% (7501 Btu/kwhr). Since these steam conditions fall outside the realm of the current experience, there is little doubt that formidable technical problems will need to be solved. To meet the future needs for high efficiency, the industry is beginning to experiment with high steam temperature applications. Conceptual designs and preliminary test results at steam conditions of 1500psig/1500° F have been reported in the literature. To facilitate implementation of the new technology consistent with the needs of the early 21st century, perhaps the time has come for comprehensive assessment of the ultra high steam conditions.

Kalina Cycle: An alternative approach to the use of higher temperatures and pressures to gain Rankine cycle plant efficiency is to change the cycle working fluid. The use of mixtures as the working fluid provides the ability to vary the composition throughout the cycle. This realizes a structural advantage in designing a power plant cycle by providing a degree of freedom to minimize thermodynamic losses throughout the process. The Kalina cycle, currently under demonstration, is one such cycle.

In the Kalina cycle a mixture of ammonia and water is used as the working fluid. In contrast to a single component, the temperature of the ammonia/water working fluid continually changes during the boiling process. The light component (ammonia) boils off first, leaving behind a mixture with a greater concentration of the heavier component (water). As this occurs, the boiling temperature of the remaining liquid increases. This fundamental degree of freedom facilitates the minimization of thermodynamic losses.

For direct fired Kalina cycle applications (those where the source of thermal energy input to the cycle comes from fuel combustion) net plant efficiencies in the range of 45% to 50% (HHV) are possible today. This range can be achieved at vapor conditions of 2400 psig/1050°F/1050°F/1050°F. Similar to the steam Rankine cycle, increasing vapor temperatures will augment the efficiency advantage of Kalina cycles.

Kalina cycle plants can take advantage of all LEBS technological advances in combustion and emissions control. The plant cycle may be structured to accommodate the application of the SNO_X™ Hot Process, offering substantial efficiency improvement versus the conventional Rankine cycle. Finally, because the efficiency gains are a result of structural improvements in the plant cycle, the capital cost of the plant may be less than a conventional Rankine subcritical single reheat plant.

PROOF-OF-CONCEPT TEST FACILITY

If the ABB Team is selected to execute Phase IV of the LEBS Project, a 435 million Btu/hr system (coal and flue gas flow equivalent to 50 MWe net @ 42% efficiency) will be constructed as a repowering of Richmond (Indiana) Power & Light - Whitewater Valley Unit 1. Since the existing turbine/generator and most of the boiler and infrastructure may be retained, it may not be possible to demonstrate an advanced cycle. However, the system will be in commercial service during the six months of testing which will permit conclusive demonstration of: all emission control technologies, operability and reliability of a complete generating system in full commercial service, the integration (air, gas and water) of the SNO_X™ hot process with the boiler system and turbine/generator,the quality of the byproduct sulfuric acid, etc.

The major items of equipment that will be installed are:

- Complete Firing System (feeders, pulverizers, burners, air supply, burner management system) and required boiler modifications.
- Complete SNO_X™ Hot Process including ammonia/urea injection, catalytic filter, SO_2 reactor, acid condenser, acid and ash storage and handling.
- Gas bypass to maintain desired gas temperature to the SNO_X™ Hot Process.
- Air-to-Condensate Heat Exchanger to augment existing feedwater heater.
- Gas-to-Air heat exchanger.
- Clean gas ductwork to the existing stack.
- Boiler Forced Draft Fan and Drive.
- Induced Draft Fan and Drive.
- Hot air ductwork to the boiler.
- Distributed Control Systems.
- Diagnostic Devices.
- Required BOP, demolition, civil and structural work to provide a complete operating plant.

The existing boiler's air heater and associated ductwork will be removed.

The true value of the LEBS Project lies in the testing and commercial operation of a POCTF of sufficient capacity to convince the markets that LEBS represents low-risk technologies. This is the only sure path to the overall objective of expedited commercialization.

A COMMERCIAL GENERATING UNIT DESIGN

In Phase I of the Project each contractor produced the preliminary design of a commercial generating unit (CGU). The ABB Team's 400 MWe CGU illustrated in Figure 4 is an adaptation of a conventional pulverized coal-fired steam-electric plant. It will be compared to a Kalina design under a separate work effort. For each design

selected technologies have been introduced to achieve reduced levels of emissions, increased thermal efficiency, reduced waste and improved costs. These technologies involve primarily three areas:

- An advanced low-NO_X combustion system.
- The SNO_X^{TM} Hot Process.
- Advanced supercritical boiler and turbine cycle.

This combination of emission control processes meets or betters all of the target emission levels for the LEBS Project, while producing either benign or saleable by-products from the gas treatment. The advanced cycle and the SNO_X^{TM} Hot Process enable the design to meet the efficiency objective and, indirectly, the cost of electricity objective.

Expected performance of the CGU compared to an NSPS-compliant plant is listed in Table 6. The NSPS plant assumes a 2400 psi/1000°/1000° cycle with wet limestone FGD and an electrostatic precipitator.

Table 6. Emissions Reduction Performance

		NSPS PLANT	LEBS CGU
SO_2,	lb/mm Btu*	0.60	0.10
NO_X,	lb/mm Btu	0.60	0.02
Particulate,	lb/mm Btu*	0.030	0.002
Total Waste,	LB/kWh	0.352	0.117
Net Efficiency (HHV),	%	35.4	45

* 3 lb S and 15.4 Lb ash per million Btu in the coal.

Volatile organic emissions, CO and ammonia slip will be oxidized in the SO_2 oxidizer and there will be no visible stack plume. The CGU produces significantly less waste than the NSPS plant. Part of this is due to the lower amount of ash produced per kWh because of the higher efficiency cycle and the SNO_X^{TM} Hot Process. The major portion of this reduction results from the production of sulfuric acid as a commercially saleable by-product rather than the sludge normally generated by an FGD system. The plant uses a 5500 psig, 1300°F supercritical thermodynamic cycle with two reheat streams. The gross output of the generator is 468 MWe and the net plant output is 445 MWe.

The CGU has a total plant cost that is less than the cost of a current NSPS plant. The total capital requirements estimate includes the time related portions of the project estimate such as allowance for funds used during construction. The improvements come from the adoption of an aggressive commercialization plan that utilizes the concept of a "Consortium" formed to produce a number of these units on a replicated and modularized basis. These factors, coupled with ABB's commitment to a significantly reduced "cycle time" for the boiler and other key equipment results in significantly reduced schedule from award to start-up. This aggressive construction schedule improves the time-related costs.

The CGU will satisfy the objective of having a cost of electricity equal to or less than that for the NSPS plant. The calculated cost of electricity is reduced by the by-product credit received from the sale of the sulfuric acid (using a figure confirmed by an outside market study) and by an aggressive but achievable capacity factor. An independent reliability, availability and maintainability analysis was completed for the CGU. The study was based on performance data obtained from the NERC data base and utilized the industry accepted "Delphi" process to adapt the data for the CGU. One reason enhanced reliability and equivalent availability are achieved is that the SNO_X^{TM} Hot Process is "passive", i.e., it has far less mechanical equipment than is typically found in flue gas desulfurization processes that utilize lime or limestone. The simpler process, absence of mechanical equipment, and the passive character of the process results in higher reliability and availability.

The design also incorporates advanced diagnostics concepts which provide early warning of impending failures in the plant equipment. This advanced knowledge has several benefits that result in improved reliability and availability. Advanced diagnostics should enable maintenance outages to be both more effective by providing maintenance information in areas which might not be readily amenable to inspection, and shorter because preparation will be better due to a reduced number of "surprise" repairs.

Finally, the CGU will have good access and ease of maintenance because it was designed for good access and ease of construction. The plant is laid out with the "ranch" concept. This means that the stacking of equipment is minimized. Rather, it is spread out in the horizontal plane. In addition, the plant design incorporates a "backbone" utility rack for piping, cable, conduit and electrical wiring. The ground level portion of this rack is used as a maintenance access corridor that runs throughout the plant. Also, organizing piping and conduit on overhead racks provides more ground level access to equipment for maintenance. Incorporating these features in the design of the plant, and coupling them with the implementation of a "design for maintainability" approach during the detailed design stage, will result in a plant with superior availability and higher capacity factor which helps reduce the cost of electricity.

CONCLUSIONS AND FUTURE WORK

All of the foregoing are responsive to the technical, regulatory and economic needs of the power generation industry. The advanced performance of ABB's LEBS technologies coupled with efforts to minimize investor risk should make it extremely attractive to the utilities and IPPs. The near term character of the LEBS technologies chosen, coupled with the attractive performance and cost features of the ABB CGU, support a confidence in the Project Team that the proposed CGU design will be acceptable and marketable.

Testing at laboratory and pilot scale will be completed in Phase II. Phase III will consist of updating the CGU and POCTF designs based on the results of the work completed in Phase II. In addition, the licensing of the POCTF will be completed and a detailed test plan will be written.

* * * * * *

Acknowledgment: A large number of people representing the US Department of Energy - Pittsburgh Energy Technology Center, the authors' companies and advisors to the project have contributed to the work described in the paper. Any attempt to list all of their names risks omitting one or more. However, their contributions are deeply appreciated and they are hereby acknowledged and thanked sincerely.

LEGEND	
No.	DESCRIPTION
1	BOILER BUILDING
2	CATALYTIC FILTER HOUSE
3	SO_2 REACTOR
4	FIRST STAGE ECONOMIZER
5	AIR HEATER
6	CONDENSATE HEAT EXCHANGER
7	ACID CONDENSERS
8	ID FANS
9	FD FAN

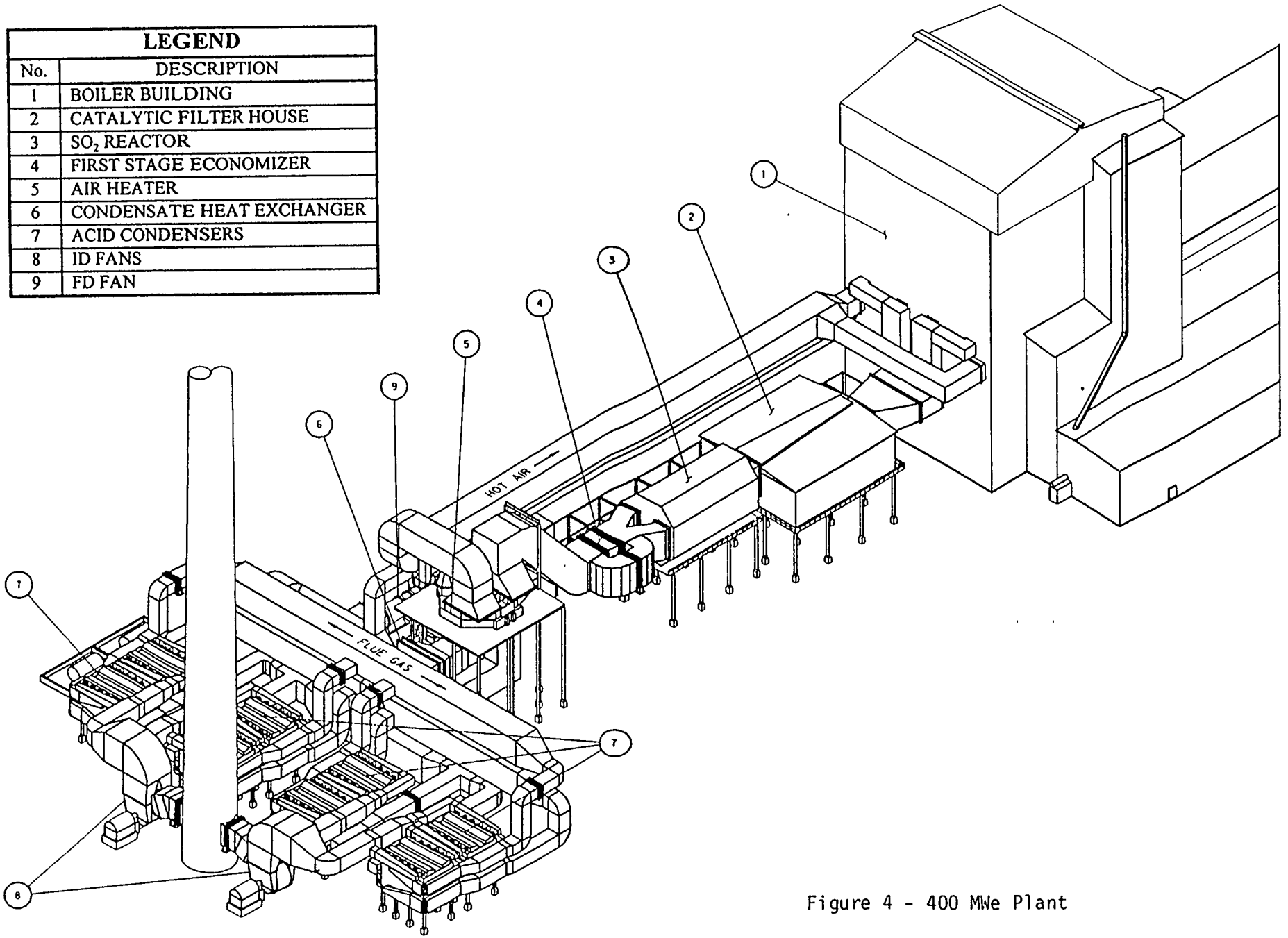

Figure 4 - 400 MWe Plant

UPDATE OF PROGRESS FOR PHASE II OF B&W'S ADVANCED

COAL-FIRED LOW-EMISSION BOILER SYSTEM

D. K. MCDONALD
BABCOCK & WILCOX
FOSSIL POWER DIVISION
BARBERTON, OHIO

D. A. MADDEN, L.W. RODGERS, AND J.L. SIVY
BABCOCK & WILCOX
RESEARCH AND DEVELOPMENT DIVISION
ALLIANCE, OHIO

Importance of LEBS - Over the past five years, advances in emission control techniques at reduced costs and auxiliary power requirements coupled with significant improvements in steam turbine and cycle design have significantly altered the governing criteria by which advanced technologies have been compared. With these advances, it is clear that pulverized coal technology will continue to be competitive in both cost and performance with other advanced technologies such as Integrated Gasification Combined Cycle (IGCC) or first generation Pressurized Fluidized Bed Combustion (PFBC) technologies for at least the next decade.

In the early 1990's it appeared that if IGCC and PFBC could achieve costs comparable to conventional PC plants, their significantly reduced NO_x and SO_2 emissions would make them more attractive. A comparison of current emission control capabilities shows that all three technologies can already achieve similarly low emissions levels (see Figure 1).

Figure 2 shows that by developing technologies that permit utilization of advanced steam conditions in a PC plant, cycle efficiency differences can also be mitigated. In fact, advanced pulverized coal fired plants are already being built in Japan and Europe with ultra-supercritical steam conditions which will achieve net plant efficiencies exceeding 40% (HHV) with very low emissions.

Driven by high fuel costs and low emissions requirements, development has progressed in Japan and Europe ahead of the United States. Present emissions limits (NSPS), fuel costs to the generating company and legislation, such as fuel adjustment clauses, do not currently justify high efficiency or extremely low emissions technologies domestically. However, this is likely to change. In recognition of the increasingly global nature of the power industry and the current lack of market support for advancement of PC technology in markets serviced by domestic suppliers, programs such as DOE's Combustion 2000 LEBS are necessary to prevent domestic technology development from falling too far behind. European and Japanese suppliers who are advancing PC technology driven by the need in their own markets will become domestic competitors with mature advanced PC designs and an experience base unavailable to U.S. suppliers.

In order to maintain relevance, B&W's goals for the LEBS program have been continually refined since the initial work began in 1993. Design performance goals began as no more than 0.2 lb NO_x/MBtu, 0.2 lb SO_2/MBtu and 0.015 lb particulate/MBtu with at least a 38% net plant efficiency (HHV) without increasing cost relative to a conventional NSPS plant. They have evolved over time to the present goals of no more than 0.1 lb NO_x/MBtu, 0.1 lb SO_2/MBtu and 0.005 lb particulate/MBtu with a net plant efficiency of 42% (HHV) while reducing solid wastes and complying with anticipated air toxics regulations at or below the cost of a conventional NSPS plant.

Program Structure - The LEBS program is structured in four Phases to be executed over a seven year period.

Phase I, which is completed, involved system analysis, R&D planning and component definition resulting in a preliminary commercial generating unit design. Phase II provides for pilot and subsystem scale testing to confirm and improve the conceptual designs developed in Phase I. In Phase III designs will be developed for the construction of a Proof-of-Concept (POC) Demonstration Facility. In Phase IV the POC facility will be constructed and operated in order to prove the readiness of the technology for commercial application.

In Phase I B&W organized four teams to focus on design of the major subsystems; NO_x Control, SO_2/Particulate Control, Boiler and Balance of Plant (BOP). As a result of those efforts the importance of controls and sensors to achieving the integration necessary to meet the performance goals was recognized and a fifth subsystem team has been formed for that purpose. Several design options were identified and evaluated by the subsystem teams during Phase I to determine the most economical approach to meet the program goals. The resulting B&W design consists of a boiler which integrates advanced low NO_x combustion and limestone injection dry scrubbing (LIDS) technologies. Figure 3 shows B&W's LEBS Commercial Generating Unit design.

This paper summarizes the status of the work in progress for Phase II of B&W's LEBS program. To better communicate progress, it is presented by subsystems.

NO_x Subsystem - Investigations in Phase I through pilot-scale testing and modeling and at the Combustion Research Facility at the Massachusetts Institute of Technology (MIT) were used to test a promising low-NO_x burner developed by MIT and benchmark it against the state-of-the-art B&W DRB-XCL® burner. While the NO_x emissions from the MIT burner were below the original DOE program goal of 0.2 lb NO_x/MBtu, it was deemed too difficult to develop it to commercial practicality within the time frame of the LEBS program.[1]

In formulating the research, development and testing (RD&T) plan for Phase II, it was decided to pursue development of a new experimental B&W advanced low-NO_x burner which had previously shown improved performance compared to the B&W DRB-XCL® and had been designed with commercialization in mind. A pilot-scale testing campaign for the B&W Advanced Low-NO_x burner was initiated in Phase II to further develop the B&W burner design. Two series of tests have been completed in the Small Boiler Simulator (SBS) Test Facility at B&W's Alliance Research Center and another is scheduled for mid-summer 1995.

The SBS provides a realistic furnace for burner development in which the DRB-XCL® and Advanced Low-NO_x burners had been extensively tested previously. Figure 4 shows a schematic of the SBS configured for PC firing. The water-cooled 5 MBtu/hr furnace has a calculated residence time from the PC burner centerline to the furnace exit of 2 seconds when operating at design capacity. The inside surface of the furnace is insulated to yield a furnace exit gas temperature of 2100 to 2300°F.

The SBS is equipped with an indirect pulverized coal feed system which allows adjustment of the primary air-to-coal ratio. During testing, stack gases were sampled continuously from a location above the convection pass section outlet through a heated sample line, furnace exit gas temperatures were measured by a K-type, high-velocity-thermocouple (HVT) probe and CO, CO_2, O_2, SO_2, and NO_x concentrations were measured in the stack gas, after filtering and drying, and plotted on a Chessell strip chart recorder.

An optical pyrometry system from Diamond Power Specialty Company called FLAMEVIEW™ was used to non-intrusively map the flame temperature two dimensionally via a patented process utilizing two-color pyrometry. Stack fly ash was sampled isokinetically according to an EPA recommended method, using an Anderson Universal Stack Sampler. Cumulative batch samples were obtained by radial traverses and analyzed for carbon utilization.

Initial testing utilized a pilot-scale B&W DRB-XCL® burner, which had previously been tested in the SBS with different coals[2], firing Illinois #6 coal for a benchmark comparison. In addition, extensive field data on the commercial scale DRB-XCL® PC burner[3] was available for comparison. A full complement of data was taken at various loads and excess air levels.

The original overfire air ports on the SBS were tested while firing with the pilot-scale DRB-XCL® burner. Two sets of ports were evaluated and the results were compared to typical field performance. Initial results showed that the lower front wall ports, located at typical residence times, gave good results, however, modifications were needed to improve the air flow direction and velocity. These modifications were incorporated with the third series of testing on the SBS with the Advanced Low-NO_x burner.

The NO_x emissions and unburned carbon (UBC) measurements during benchmark testing were similar to results obtained in the Phase I testing at MIT and previously obtained results firing other coals with the pilot-scale DRB-XCL® burner. Overall, the burner performed as expected based on commercial operation. Stoichiometries of 1.20 to 0.7 were tested with no effect in the stability of the flame and in all cases, the unburned carbon remained below 5%.

Subsequent to benchmark testing with the DRB-XCL® burner, testing of the Advanced Low-NO_x burner began with the burner in a previously tested configuration[4] to establish repeatability and to characterize the burner with Illinois #6 coal. Emission values similar to those previously obtained resulted. Air distribution, excess air, and coal delivery were varied while in this original configuration. All variations produced trends similar to those obtained previously.

Several hardware changes, including various flame stabilizer rings (FSR) and air separation vanes (ASV), were also tested. Again, key parameters were varied and operating data was recorded for each test series. All variations were compared to determine the optimum hardware and settings.

After the optimum hardware (ASV, FSR) and operating settings for the Advanced Low-NO_x burner were determined, further hardware modifications to the air flow distribution and coal delivery system were made. These changes proved to be very promising. NO_x emissions of the Advanced Low-NO_x burner were 10-15% lower than the DRB-XCL® burner benchmark values. UBC and CO emissions were found to be similar with both burners, while the burner pressure increased only slightly with the Advanced Low-NO_x burner.

Since the Advanced Low-NO_x burner was not staged during the second series of pilot-scale testing, field experience was extrapolated. These extrapolations indicate that the NO_x emissions with staging to a burner stoichiometry of 0.85 would fall below the original DOE NO_x emission goal of 0.2 lb NO_x/MBtu approaching 0.15 lb NO_x/MBtu with combustion only, progressing toward the overall process goal of 0.1 lb NO_x/MBtu.

Based on the first two series of pilot-scale testing and the results obtained from numerical modeling of various hardware and operating configurations, further improvements will be made to the Advanced Low-NO_x burner for the third test series. Staged and unstaged versions of the Advanced Low-NO_x burner will be demonstrated in the SBS in preparation for scale-up to 100 MBtu/hr for Subsystem testing scheduled to begin in January 1996. Figure 5 shows the comparison between NO_x emissions and burner configurations tested in the SBS.

SO_2/Particulate Control - Figure 3 shows the B&W LIDS system which is a limestone-based furnace injection/dry scrubbing SO_2 removal process which cost-effectively integrates three commercially-proven flue gas cleanup technologies: furnace limestone injection, dry scrubbing, and fabric filtration. Sulfur dioxide removal occurs in the boiler, in the dry scrubber, and in the fabric filter.

LIDS reduces cost using a dry scrubber for downstream SO_2 removal by permitting the use of limestone as the sorbent (as opposed to the more expensive lime used in most dry scrubbing processes), and reducing the inlet SO_2 concentration to the dry scrubber through in-furnace SO_2 removal. This latter fact permits the LIDS process to be applied to units firing high-sulfur coals.

In order to prove the predicted performance of this unique system, pilot-scale testing was conducted in B&W's SBS during Phase I. The furnace, dry scrubber, and fabric filter processes were fully-integrated to achieve the SO_2 removal goal. During those tests the furnace stoichiometric molar ratio (Ca/S) was 1.4, approach to adiabatic saturation temperature was 10°F, and slurry solids concentration was 40-45%. These conditions were

held relatively constant to obtain data over an extended period of time.

The fully-integrated LIDS system removed 98% of the SO_2 (0.10 lb SO_2/MBtu) based on an average of the data measured during the test series. Achieving the SO_2 emissions goal using the B&W LIDS process required optimal SO_2 removal performance of the entire integrated system. Average values from the individual unit operations included 23% removal in the furnace, 58% in the dry scrubber, and 95% removal in the fabric filter. These values are based on the inlet and outlet SO_2 concentrations of each operation. Figure 6 shows the total SO_2 removal accomplished at the outlet of each piece of the LIDS process.

In addition to sulfur removal, the LIDS system has also proven to be very effective in removing air toxics such as heavy metals, acid gases, and organics. The calcium-based sorbent injected into the furnace which provides numerous reaction temperature windows with high particulate availability for condensation of air toxic species and the low operating temperatures in the dry scrubber and fabric filter are believed to be the primary factors.

Since mercury is a likely target for regulation due to its potential to bioaccumulate in the food chain, screening tests of mercury emissions from the LIDS system were performed by Frontier Geosciences, Inc. to characterize the mercury capture capabilities of the process. Phase I LIDS overall mercury removal results are presented in Table 1. Total mercury removal across both the dry scrubber and fabric filter during Phase I testing consistently averaged 97% across the LIDS system.

LIDS development and demonstration in the SBS continues to further define the process. Where the Phase I LIDS demonstration showed the feasibility of achieving ultra-high SO_2 removal, potential limitations inherent to the basic LIDS system were identified. This led to further pilot-scale testing and enhancement in Phase II. The resulting enhanced LIDS process achieved 98% SO_2 removal (0.10 lb SO_2/MBtu) while eliminating the issues associated with the original LIDS system. Figure 7 shows the total SO_2 removal accomplished at the outlet of each piece of the Phase II LIDS process.

Mercury measurements were repeated to verify the high mercury removal achieved in Phase I. The measurements were once again made in triplicate at the system inlet, dry scrubber outlet, and fabric filter outlet by Frontier Geosciences, Inc. Phase II LIDS overall mercury removal results are presented in Table 2. Total mercury removal averaged 92% across the LIDS system.

Boiler - Investigation of the corrosive conditions that the furnace and superheater metals must endure and identification of potential advanced materials continues in Phase II. Data and ash samples taken from SBS testing are being used in laboratory retort tests to assess the corrosion resistance of several potential advanced materials

Three major areas impacting the boiler design are also being pursued to improve both boiler and cycle efficiencies without increasing cost; the limestone injection system, the airheater and the reheater control method.

In the preliminary design, warm, compressed air taken from the combustion air system was used to convey and inject the limestone into the upper boiler furnace. The conveying system is being re-evaluated utilizing the cool, clean flue gas leaving the fabric filter rather than the combustion air. The new system compresses and preheats the gas and limestone to a significantly higher temperature prior to injecting it into the furnace. Heat and mass balances have been made and are being evaluated. This system is expected to reduce auxiliary power, compressor cost and airheater requirements and permit an increase in economizer feedwater temperature which has been shown to improve steam cycle efficiency.

The regenerative airheater utilized in the preliminary design introduces leakage losses to the cycle and requires power to operate. To improve cycle efficiency, a heat pipe airheater is being evaluated. Initial expectations are reduction in cost, elimination of leakage losses and elimination of the auxiliary power.

Temperature control of the reheaters is critical to achieving cycle performance. A method which can

independently control the heat absorption in each reheater throughout the load range rather than using spray attemperation will result in the highest cycle efficiency. Convection pass and gas path arrangements are being considered which have potential to achieve this result.

Balance of Plant - The net cycle efficiency (HHV) produced in Phase I effort did not approach the present goal of 42%. In addition to improving boiler efficiency, several improvements in the steam cycle and reduction of auxiliary power requirements for balance of plant equipment planned for investigation.

Controls and Sensors - In order to achieve low NO_x production, precise control of the combustion conditions is necessary. Sensors are being developed to provide the ability to measure and control the air to fuel ratio for each burner in a multi-burner system. Coupled with advanced burner design and air staging, on-line control of the individual burner stoichiometry is expected to achieve the minimum possible NO_x levels from the combustion process without adversely affecting UBC. In addition, the control philosophies are being developed to operate the combustion controls required for the advanced low NO_x equipment and LIDS in an integrated manner with the boiler to achieve minimum emissions over the load range.

Future Work - B&W's CEDF will be utilized for the LEBS Phase II Subsystem testing scheduled to commence in October 1995. Preliminary characterization testing was conducted in the winter of 1994-1995 under the LEBS program using the state-of-the-art DRB-XCL® low-NO_x burner.

The CEDF is designed for a heat input of 100 MBtu/hr, and integrates combustion and post-combustion testing capabilities to facilitate the development of the next generation of power generation equipment. The furnace (Figure 8) is designed for testing a single 100 MBtu/hr burner, or multiple wall-fired burner configurations. It has been carefully designed to yield combustion zone temperatures, flow patterns, and residence time representative of commercial boilers. Boiler convection pass and air heater simulators maintain representative conditions through the entire boiler system to facilitate studies of air toxics capture in back-end flue gas clean-up devices. Representative gas phase time-temperature profiles and surface metal temperatures are maintained throughout the convection pass. Convection pass metal temperatures are maintained in the 600-1100°F range by way of a novel double-walled tube design. Following the air heater, the flue gas enters a vertical dry scrubber unit to control sulfur dioxide emissions. The resulting dry by-products are then filtered from the gas by a multi-chamber pulse-jet fabric filter.

Modifications will be made to the existing CEDF during the summer of 1995 to incorporate a LIDS system. Furnace limestone injection, solids recycle, and further instrumentation will be added. The existing dry scrubber, fabric filter and slurry slaking system will be utilized.

Preliminary POC Demonstration Facility Design- In order to satisfy the intent of Proof-of-Concept (POC) testing in a cost-effective manner, B&W has elected to further modify the 100 MBtu/hr CEDF to create the POC Demonstration Facility for Phase IV. A preliminary POC design and RD&T plan have been completed and reported to the DOE. The POC facility, which builds on the modifications made to B&W's CEDF in Phase II for Subsystem testing, will cost drastically less than the original estimates based on using a Utility plant site.

The majority of the modifications to the CEDF will be associated with the NO_x and Controls & Sensors subsystems since most of the equipment for the SO_2/Particulate subsystem will be installed for the Phase II Subsystem testing. The major modifications will include; "hardening" of the systems to permit extended periods of operation, incorporation of advanced controls and sensors integrating control of both the NO_x and SO_2/Particulate subsystems, installation of multiple opposed wall-fired advanced low-NO_x burners and an over-fire air system, and incorporation of two coal feeders to simulate multiple pulverizers.

Conclusion - With the exception of one more series of SBS testing of the Advanced Low-NO_x burner, pilot testing is completed and the design of the Subsystem Test and POC Demonstration Facilities are progress. With the completion of the Subsystem testing schedule to begin in October 1995, B&W expects to further confirm and refine our LEBS design and costs in preparation for proof-of-concept demonstration in Phase IV. With the help

of the LEBS program, B&W intends to develop a commercial PC plant design which is competitive with the other emerging advanced coal-fired technologies in both performance and cost.

Acknowledgements- The authors wish to express thanks to the U.S. Department of Energy's Pittsburgh Energy Technology Center for supporting the B&W LEBS Team's efforts.

References

1. Rodgers, L., et al., "NO_x Control Update for Low Emission Boiler System", presented at the Eleventh Annual International Pittsburgh Coal Conference, Pittsburgh, PA, September 12-16, 1994.

2. Sarv, H., "Advanced Low-NO_x PC Burner Development Program: Pilot-Scale DRB-XCL® PC Burner Characterization Report," Babcock & Wilcox Report, RDD:93:23090-005-405:01, March 1993.

3. Piepho, J., et al., "Seven Different Low-NO_x Strategies Move From Demonstration to Commercial Status," presented at Power-Gen '92, Orlando, FL, November 1992.

4. Sarv, H., "Advanced Low-NO_x PC Burner Development Program: Hollow Plug PC Burner Characterization Report," Babcock & Wilcox Report, RDD:94:25090-005-540:01, April 1994.

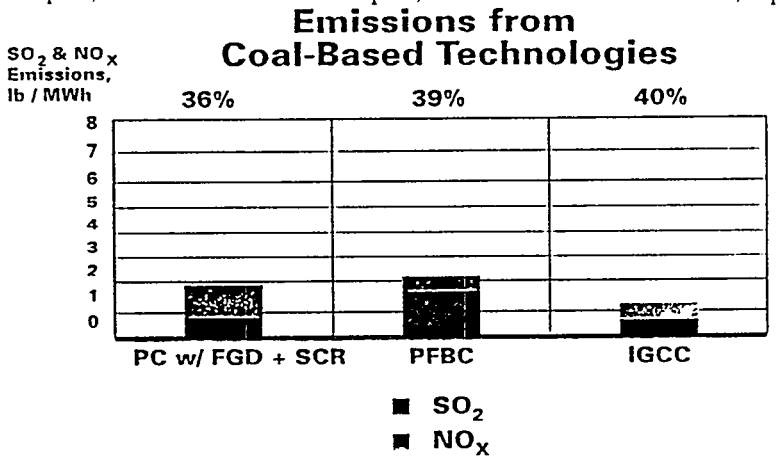

Figure 1 - Current Emissions from Coal Based Technologies.

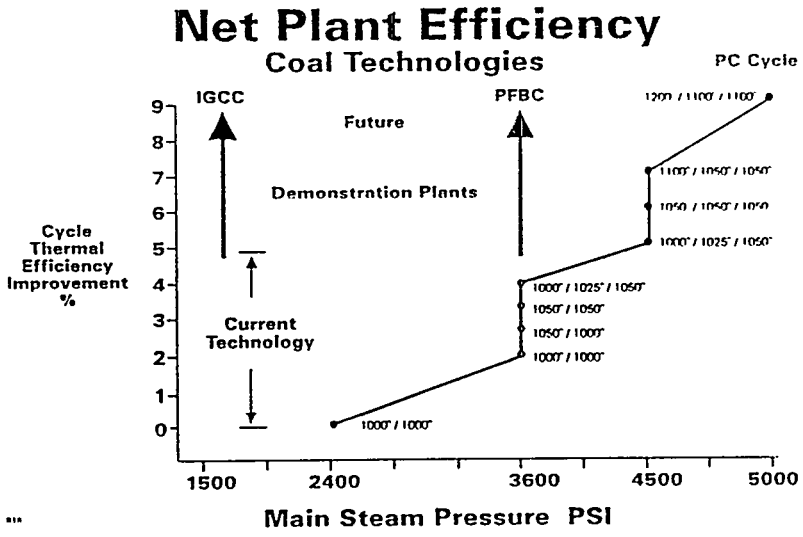

Figure 2 - Net Plant Efficiency

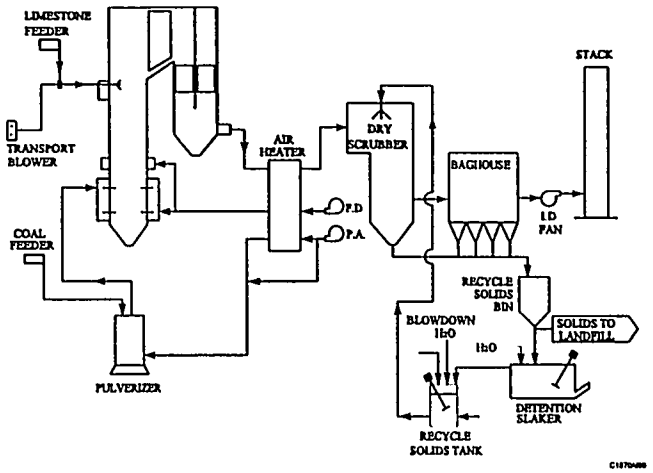

Figure 3 - LEBS Commercial Generating Unit

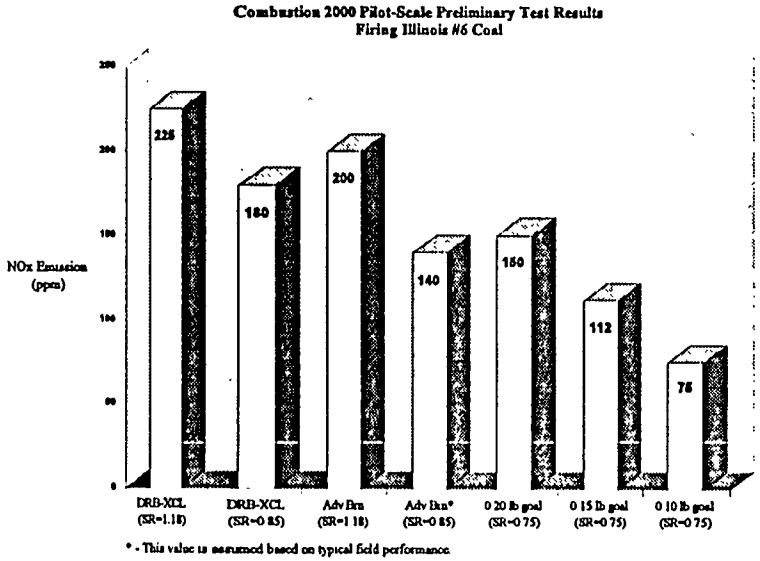

Figure 5 - NO_x Emission versus Burner Configurations Tested in the SBS

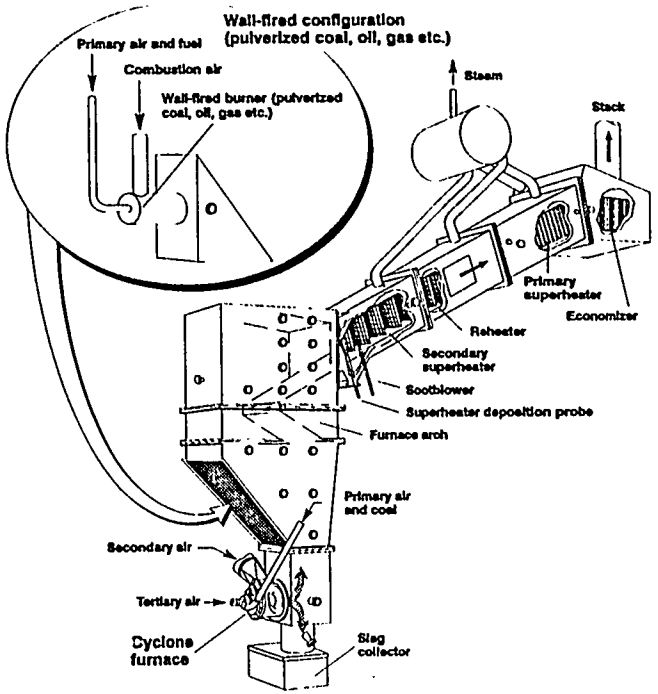

Figure 4 - B&W Small Boiler Simulator

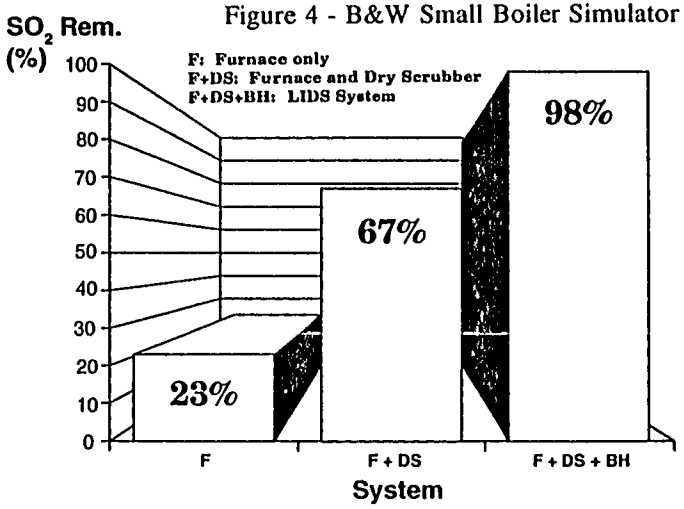

Figure 6 - Phase I LIDS Feasibility Demonstration SO_2 Removal

Stream	Total Hg, Ug / Nm3	Hg Removed Across System
Inlet Scrubber	5.0	99.06%
Inlet Baghouse	2.49	
Outlet Baghouse	0.047	
Inlet Scrubber	4.91	98.64%
Inlet Baghouse	2.33	
Outlet Baghouse	0.067	
Inlet Scrubber	6.19	93.41%
Inlet Baghouse	2.17	
Outlet Baghouse	0.408	

Table 1 - Phase I LIDS Total Mercury Removal

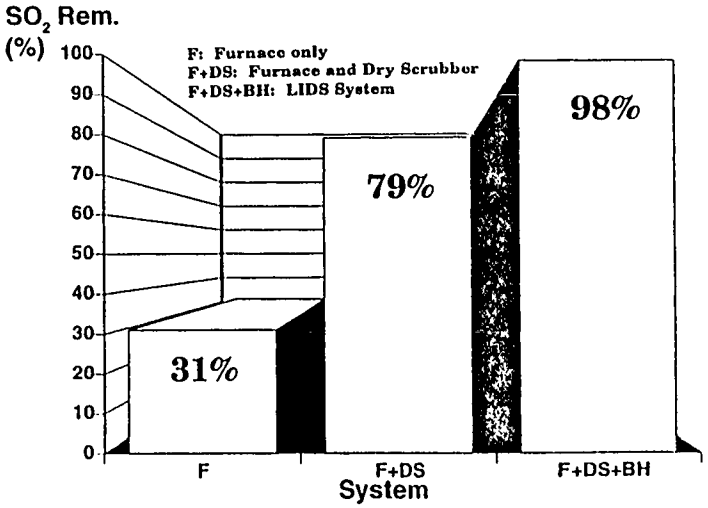

Figure 7 - Phase II LIDS Process Definition SO_2 Removal

Stream	Total Hg, Ug / Nm3	Hg Removed Across System
System Inlet	19.85	86.25%
Inlet Baghouse	4.90	
Outlet Baghouse	2.73	
System Inlet	16.49	92.97%
Inlet Baghouse	3.49	
Outlet Baghouse	1.16	
System Inlet	17.85	95.52%
Inlet Baghouse	3.58	
Outlet Baghouse	0.80	

Table 2 - Phase II LIDS Total Mercury Removal

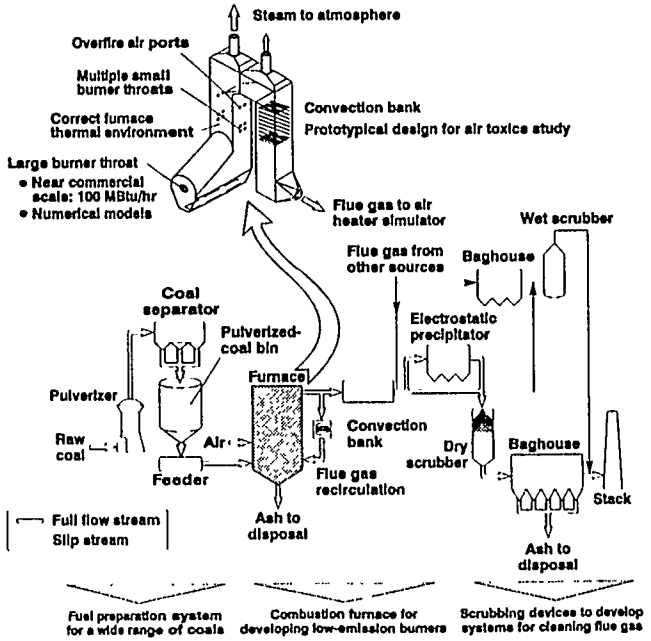

Figure 8 - B&W Clean Environment Development Facility

The following manuscript was unavailable at time of publication.

ENGINEERING DEVELOPMENT OF A LOW-EMISSION BOILER SYSTEM

Roderick Beittel
Riley Stoker Corporation
Riley Research Center
45 McKeon Road
Worcester, MA 01610

Please contact author(s) for a copy of this paper.

The following manuscript was unavailable at time of publication.

ENGINEERING DEVELOPMENT OF A HIGH-PERFORMANCE POWER GENERATING SYSTEM

Dr. Daniel J. Seery
United Technologies Research Center
411 Silver Lane
E. Hartford, CT 06118

Please contact author(s) for a copy of this paper.

DEVELOPMENT OF A HIGH-PERFORMANCE, COAL-FIRED POWER GENERATING SYSTEM WITH A PYROLYSIS GAS AND CHAR-FIRED HIGH-TEMPERATURE FURNACE

Jack Shenker
Project Manager
Foster Wheeler Development Corporation
Contract Number: DE-AC22-91PC91154
Period of Performance: March 1992 through April 1995

INTRODUCTION

A high-performance power system (HIPPS) is being developed. This system is a coal-fired, combined-cycle plant that will have an efficiency of at least 47 percent, based on the higher heating value of the fuel. The original emissions goal of the project was for NOx and SOx to each be below 0.15 lb/MMBtu. In the Phase 2 RFP this emissions goal was reduced to 0.06 lb/MMBtu. The ultimate goal of HIPPS is to have an all-coal-fueled system, but initial versions of the system are allowed up to 35 percent heat input from natural gas. Foster Wheeler Development Corporation is currently leading a team effort with AlliedSignal, Bechtel, Foster Wheeler Energy Corporation, Research-Cottrell, TRW and Westinghouse. Previous work on the project was also done by General Electric.

The HIPPS plant will use a High-Temperature Advanced Furnace (HITAF) to achieve combined-cycle operation with coal as the primary fuel. The HITAF is an atmospheric-pressure, pulverized-fuel-fired boiler/air heater. The HITAF is used to heat air for the gas turbine and also to transfer heat to the steam cycle. Its design and functions are very similar to conventional PC boilers. Some important differences, however, arise from the requirements of the combined cycle operation.

Materials considerations limit the air temperature that can be reached in the HITAF. When the effects of temperature and flow imbalances are considered, the upper limit to air temperature is around 1400°F for steel alloy tubes, and 1800°F for ceramic tubes. These limitations require that some fuel be fired in the gas turbine to achieve gas turbine inlet temperatures that are currently over 2300°F. To obtain the most benefits from the HIPPS approach, the Foster Wheeler HIPPS concept uses a pyrolysis process to convert coal into fuel gas and char. Having these two fuels available allows us to push the limits of HIPPS by using the relatively clean fuel gas in critical areas.

HIPPS CYCLES

Two arrangements for greenfields HIPPS plants have been developed. One arrangement uses a ceramic air heater in the HITAF and natural-gas-firing in the gas turbine. This is referred to as the 35 Percent Natural as HIPPS. The other option uses coal-derived fuel gas from the pyrolyzation process as the fuel for the gas turbine. This arrangement requires no natural gas and is referred to as the All Coal HIPPS. A process flow schematic of the 35 Percent Natural Gas HIPPS is shown in Figure 1. In this arrangement the HITAF has two furnaces: one for firing fuel gas, and one for firing char. The fuel gas is fired upstream from a ceramic air heater that is used for the final heating of gas turbine air in the HITAF. This air heater is an AlliedSignal design, and it raises the air temperature from

1400 to 1800°F. The fuel gas is cleaned of alkalies and particulates before it is burned, thereby protecting the ceramic air heater from the effects of alkali corrosion and tube bank fouling.

The char is fired in a separate furnace, and these combustion products transfer heat to the lower-temperature air (1030 to 1400°F) and to steam cycle tube surface. The design of these portions of the HITAF are very much like conventional PC boilers. All of the tubes that are exposed to the char flue gas are steel. A TRW slagging combustor is used for the combustion of char. It will remove 70 to 90 percent of the ash in the form of slag. This type of operation more than compensates for the increased ash content of the char relative to parent coal.

Natural gas is fired in the gas turbine to raise the air temperature to 2350°F entering the gas turbine, and some of the gas turbine exhaust is used as combustion air in the HITAF. The remaining gas turbine exhaust goes through a heat recovery steam generator before going to the stack. Back-end emissions systems will be used in the HITAF exhaust stream as required to meet specific plant requirements.

A process flow diagram for the All Coal HIPPS is shown in Figure 2. In this type of HIPPS plant, the fuel gas from the pyrolyzer is used as fuel for the gas turbine instead of natural gas. This arrangement requires that the pyrolyzer subsystem be run at higher pressure, but it simplifies the HITAF and lowers fuel costs.

In the 35 Percent Natural Gas HIPPS, it is necessary to heat the gas turbine air to 1800°F in the HITAF to limit the natural gas heat input to 35 percent of the plant heat input. This limit on natural gas consumption is a project requirement, and it forced the use of a ceramic air heater. If coal-derived fuel gas is used as the gas turbine topping combustion fuel, it is no longer necessary to push the HITAF air outlet temperature that high. The air temperature leaving the HITAF can be 1400°F which eliminates one furnace and the ceramic air heater. The entire HITAF can then be fabricated with standard, proven materials of construction.

The remaining systems of the All Coal HIPPS are similar to the 35 Percent Natural Gas HIPPS. A TRW slagging combustor is also used for char combustion, and backend emissions systems will be used as necessary to meet specific plant emissions requirements.

SYSTEM DEVELOPMENT

As part of the Phase 1 effort, engineering analysis and small-scale research have been done on HIPPS plant designs. Pilot plant testing would be part of a Phase 2 project. Some areas that have been investigated in Phase 1 follow:

Char Combustion - Char generated under conditions that would be typical of HIPPS operation was obtained and characterized. This characterization included standard laboratory tests and flat flame burner tests that were run at Brigham Young University (BYU). The results of these tests were used by TRW in the computer modeling of the slagging combustors.

The char test results were encouraging, both from the aspect of its suitability as a fuel and from the ability to adapt current combustor models for use with char. Thermogravimetric tests (TGA) showed that the weight loss for char started around the same temperature as for typical anthracite coals. This is a higher temperature than the parent Pittsburgh No. 8 coal. However, the rate of weight loss at this point was similar to that of the parent coal and much greater than anthracite coals.

In the flat flame burner tests, paticles of coal and char were passed through a flame of controlled temperature and composition. These particles were collected after different residence times to check carbon burnout, sulfur release and nitrogen release. A summary of some of the results is shown in Table 1. It can be seen that the characteristics of the char combustion are very similar to those of the parent coal combustion after the volatiles are consumed. Apparently the pyrolyzation process has an effect on the coal that is similar to the initial stages of combustion. This situation is beneficial because it will minimize the model modifications and allow the use of existing data on various coals.

Fuel Gas Combustion - Fuel gas combustion will be somewhat different in the 35 Percent Natural Gas HIPPS and the All Coal HIPPS. In the All Coal HIPPS, the fuel gas will be burned in the gas turbine topping combustor. Westinghouse has done considerable testing firing this fuel with there multi-annular swirl burner (MASB) arrangement. This combustor has been specifically designed for this fuel, and test results have shown that less than 30 percent of the ammonia in the fuel gas will become NOx [1]. The All Coal HIPPS has conditions very similar to the MASB test conditions, so we are confident that it can be applied.

In the 35 Percent Natural Gas HIPPS, the fuel gas is fired in an atmospheric pressure furnace. Tests were run to determine the characteristics of this type of combustion with a typical industrial burner. T-Thermal Corporation conducted tests with a 3MM Btu/h vortex burner. Fuel gas and the vitiated combustion air were syntesized and heated to the anticipated burner inlet temperatures. The ammonia content of the fuel gas was varied to determine the effect of ammonia on NOx generation. The burner was fired into a refractory lined furnace, and flue gas temperatures and composition were measured.

Combustion under the HIPPS conditions was stable and complete. The low-Btu fuel and relatively low oxygen content of the combustion air (19 wt%) did not present any combustion problems. Thermal NOx generation was also low (0.04 lb/MM Btu), as evidenced by runs with no ammonia in the fuel gas. There was concern that the elevated temperatures of the fuel and combustion air might increase thermal NOx. This did not turn out to be the case. The situation with the conversion of ammonia to NOx was not as good. At the anticipated ammonia content of 0.16 wt%, about 75 percent of the ammonia was converted to NOx.

This situation will require either some burner development or the use of Selective Catalytic Reduction (SCR). Although there are commercially available low-NOx burners, these burners are designed for low thermal NOx. A burner similar to the MASB could probably be developed for furnaces, but at this point we do not feel that this is necessary. Even with the ammonia conversions measured, the HIPPS NOx goals can be met with the application of proven SCR technology.

Gas Turbine - Both of our HIPPS arrangements and those of competing concepts require that gas turbine compressor discharge air be taken off the machine, heated and then brought back for topping combustion. As part of this project, General Electric has developed a preliminary design to achieve this type of operation with their Model 7FA gas turbine. The design is based on the 35 Percent Natural Gas HIPPS conditions, which include an air return temperature of 1800°F.

The basic GE design is shown in Figure 3. There are two torus-shaped headers. The inner header collects the compressor discharge air after it is used as cooling air for the combustors. This air then goes to the HITAF, where it is heated to 1800°F. The air then returns to the outer torus from which it is distributed to the 14 combustors.

As previously mentioned, Westinghouse has also developed a system that incorporates the necessary HIPPS functions. Their system was based on fuel gas combustion and the lower air return temperatures that are more typical of our All Coal HIPPS. The Westinghouse 501F gas turbine is being used as the base-case turbine for the All Coal HIPPS conceptual plat design. It is also likely that the GE design could be adapted for the application, but the necessary analyses have not yet been done.

HITAF Design - The design of the HITAF for the 35 Percent Natural-Gas HIPPS has been previously reported [2]. The HITAF for the All Coal HIPPS is shown in Figure 4. The HITAF is designed to be very similar to a conventional PC boiler. In this manner we can take advantage of existing design, fabrication and operating experience.

There are a few areas where the HITAF design deviates a little from standard boiler designs. Three walls of the furnace will be refractory-coated, primary superheater tubes. This is done to improve the thermodynamic efficiency of the system. Refractory lining of furnace evaporator tubes has been done in the past, and on a few occasions superheater technology, and the use of the TRW slagging combustor will improve the situation by lowering furnace heat fluxes and ash loadings.

With an air outlet temperature of 1400°F, the tube metal temperature will be around 1550°F. Several alloys have established allowable stresses for this temperature range. Tests would be run in a Phase 2 effort to determine which alloys have the best corrosion properties for the air heater.

Summary - The FWDC team HIPPS concept can be applied in two basic arrangements. One arrangement uses a ceramic air heater to get the maximum indirect heating of air for the gas turbine. Natural gas is then fired to achieve the required inlet gas temperature. Our ceramic air heater arrangement has benefit of operation with a relatively clean fuel, because the coal is converted to fuel gas and char. The cleaned fuel gas is used as fuel for the ceramic air heater, thereby reducing the effects of corrosion ad ash deposition.

The second arrangement of our HIPPS concept limits the indirect heating of the air to temperatures that can be achieved with steel alloy tubes. With this concept, the coal is also converted to fuel gas and char, but only the char is fired in the HITAF. The fuel gas is used as fuel for the gas turbine topping combustor. This arrangement of HIPPS will allow achievement of the ultimate program goal of a totally coal-fueled HIPPS within the scheduled time frame of the program.

REFERENCES

1 Domeracki, W. F., et al. "Topping Combustor Development for Second-Generation Pressurized Fluidized Bed Combined Cycles," ASME 94-GT-176, June 1994.

2. Strumpf, H., et al. "High Performance Power System (HIPPS) Ceramic Air Heater Development," ASME 94-JPGC-PWR-2, October 1994.

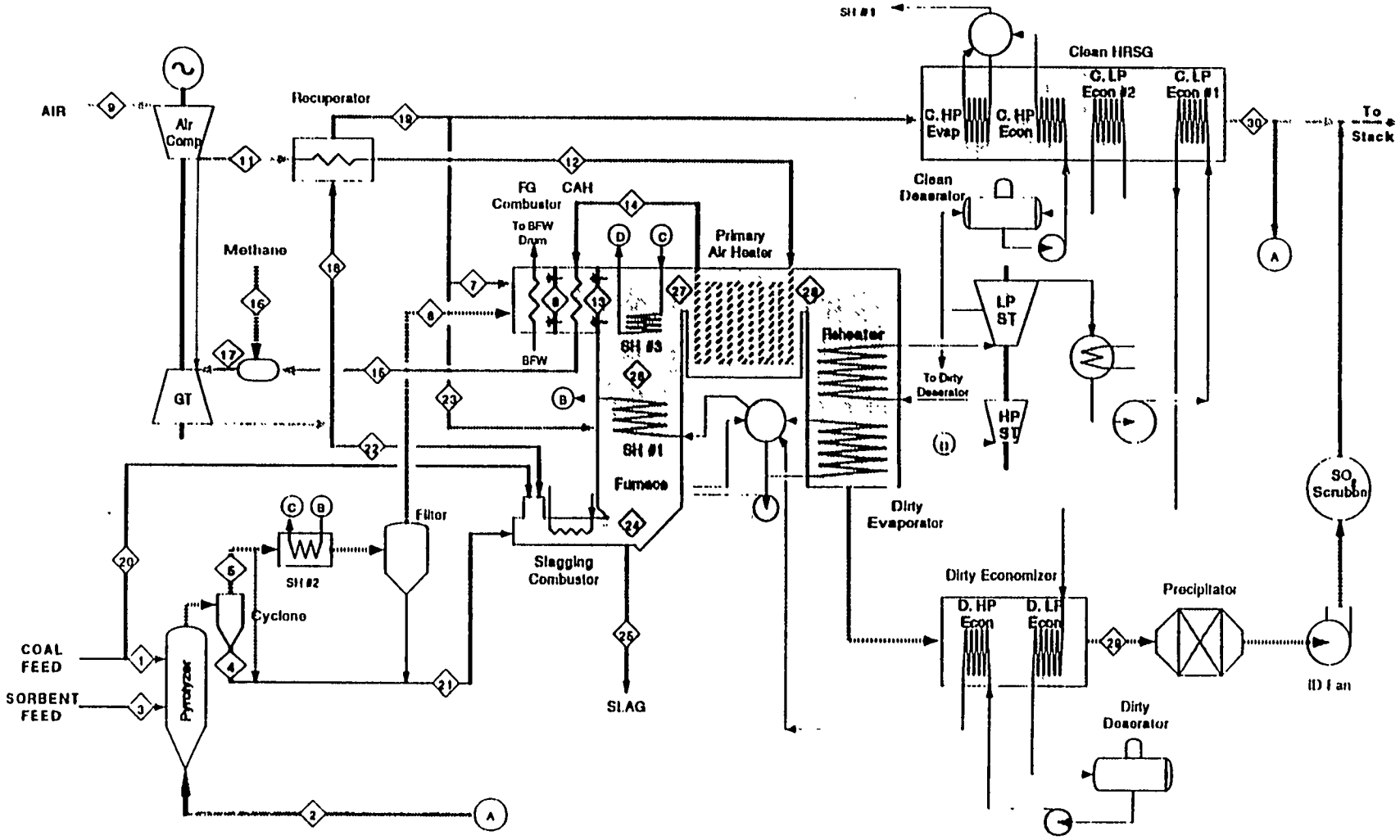

Figure 1 - 35 Percent Natural Gas HIPPS Process Flow Diagram

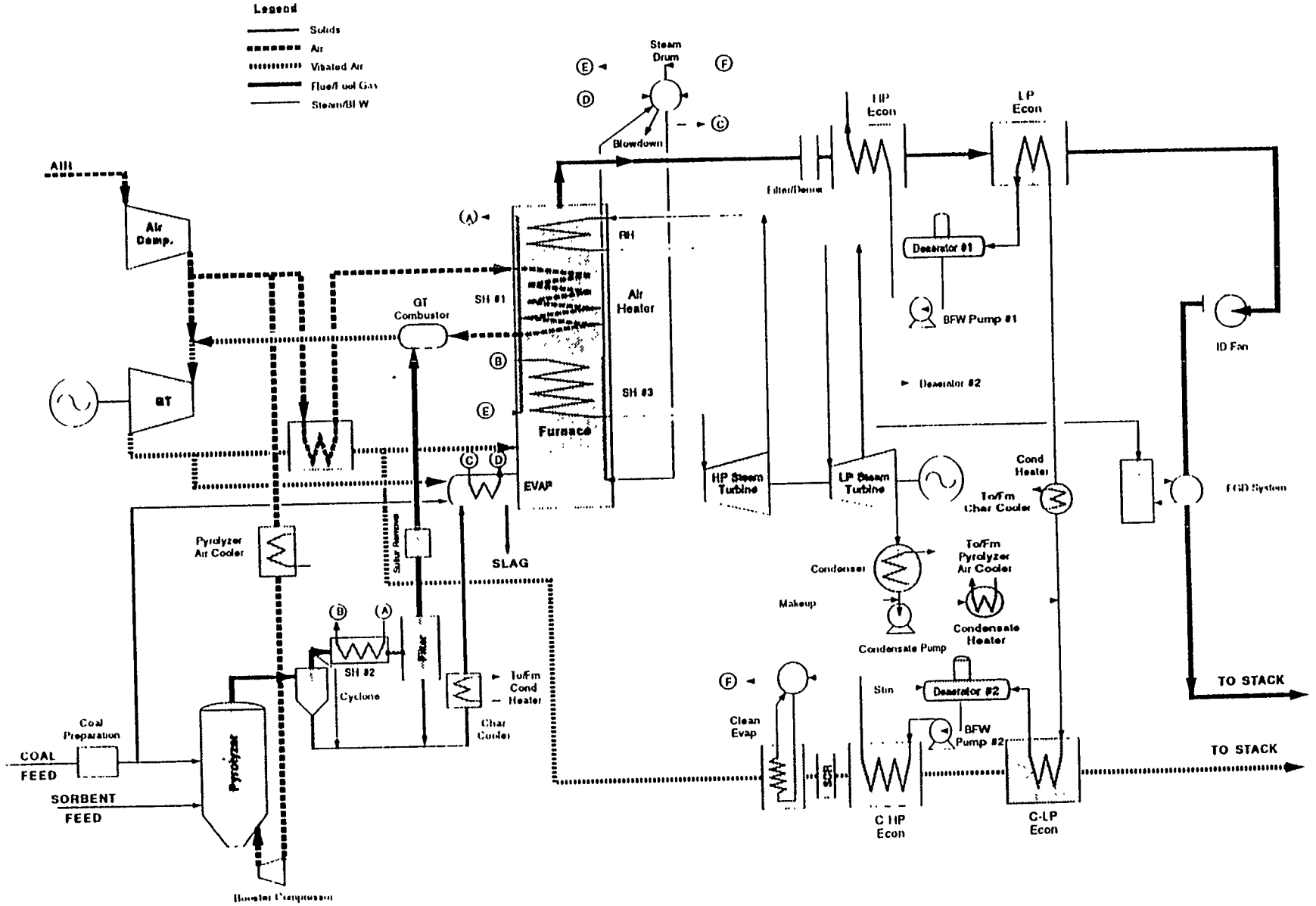

Figure 2 - All Coal HIPPS Process Flow Diagram

Table 1 - Char Burnout Results (1800 K/5% O_2)

Pittsburgh No. 8	Sampling Distance, in.	Average Burnout (% DAF)		Average Apparent Density, g/cc	Surface Area	
		Volatiles Included	Char Only		N_2, m^2/g	CO_2, m^2/g
Coal	2	50.4	0	0.38	77	241
Coal	4	58.6	14.1	0.37	44	241
Coal	6	60.5	29.6	0.42	37	188
Coal	8	63.5	30.3	0.42	33	134
Char	2	N/A	10.6	0.70	31	146
Char	4	N/A	20.4	0.65	28	149
Char	6	N/A	29.2	0.67	33	135
Char	8	N/A	34.7	0.68	31	101

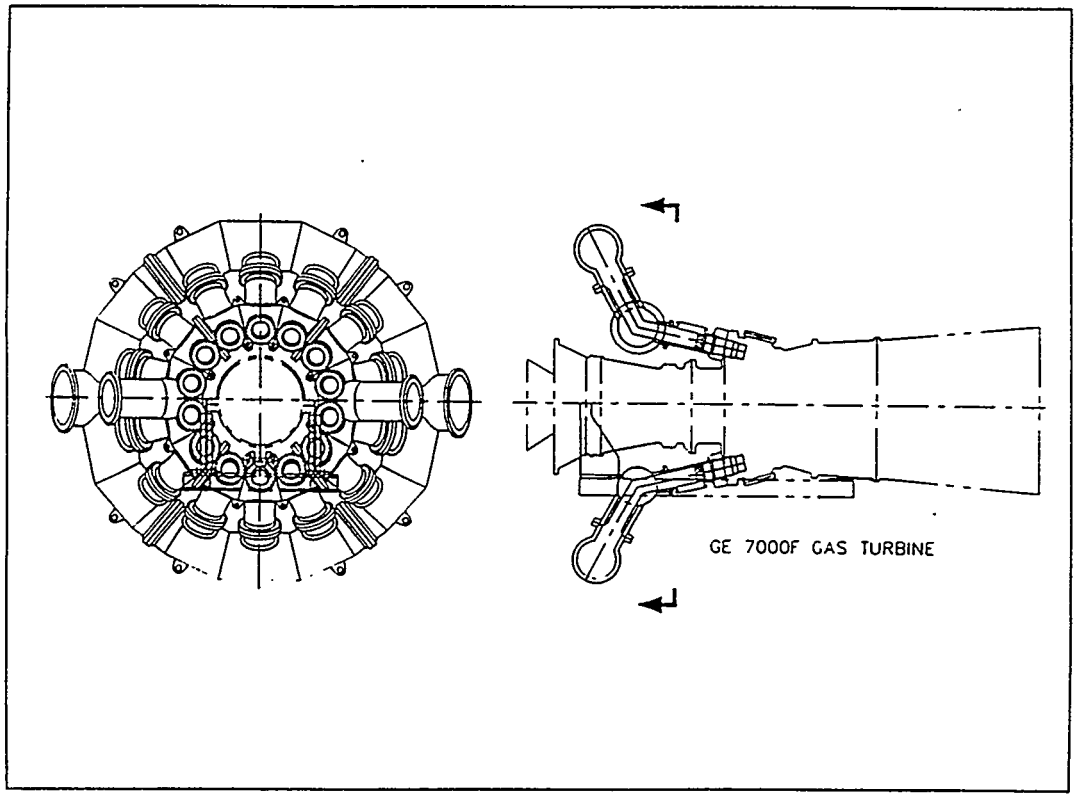

Figure 3 - GE HIPPS Gas Turbine Piping

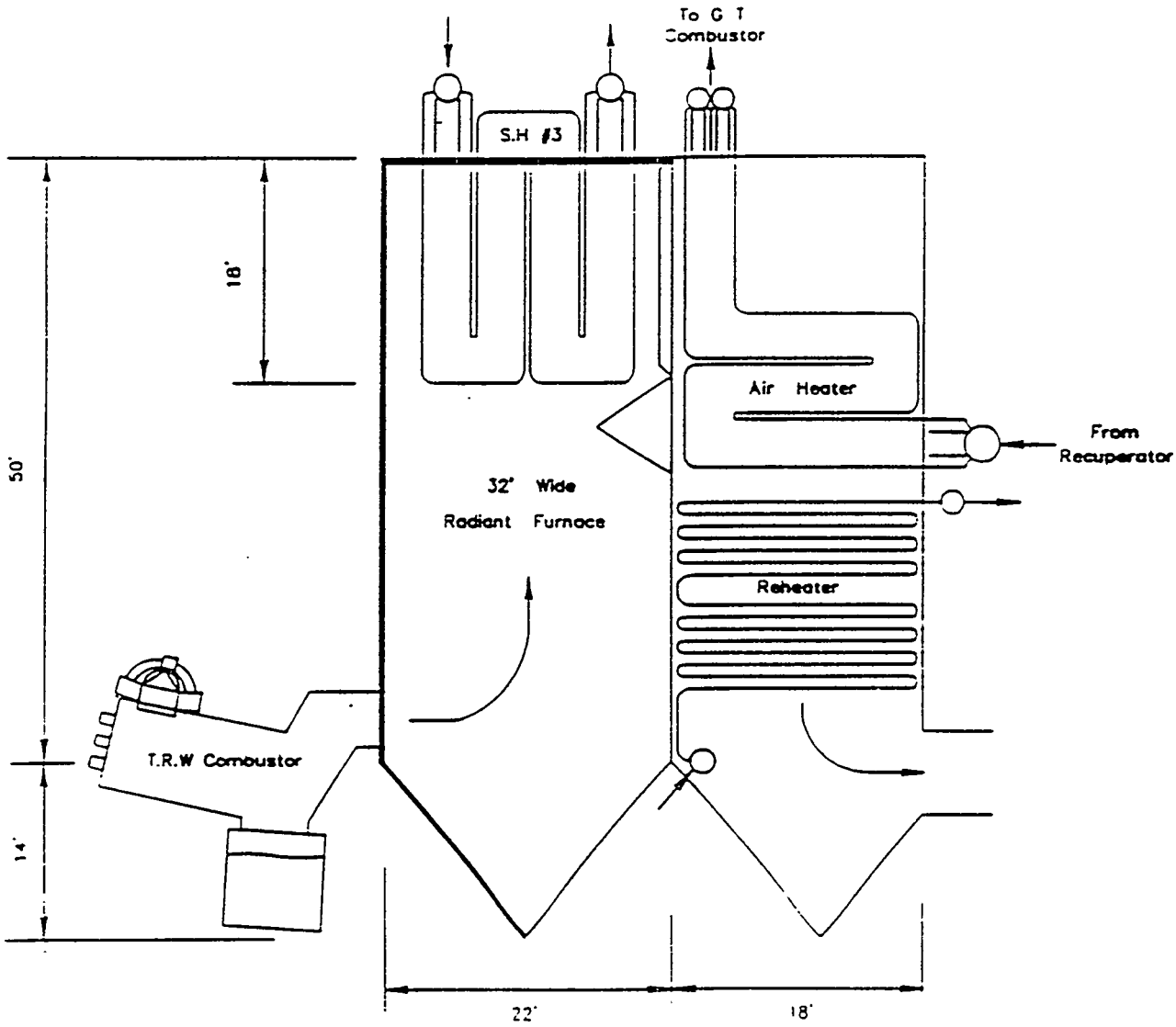

Figure 4 - HITAF for All Coal HIPPS

The following manuscript was unavailable at time of publication.

THE PHYSICS OF COAL LIQUID SLURRY ATOMIZATION

Professor Norman Chigier
Carnegie Mellon University
Pittsburgh, PA 15213-3890

Please contact author(s) for a copy of this paper.

FUNDAMENTAL STUDY OF ASH FORMATION AND DEPOSITION: EFFECT OF REDUCING STOICHIOMETRY

DR. J.J. HELBLE, DR. L.E. BOOL, DR. S.G. KANG
PSI TECHNOLOGIES

PROF. A.F. SAROFIM AND MR. T. ZENG
MASSACHUSETTS INSTITUTE OF TECHNOLOGY

PROF. G.P. HUFFMAN AND PROF. N. SHAH
UNIVERSITY OF KENTUCKY

PROF. T.W. PETERSON
UNIVERSITY OF ARIZONA

1. Objectives and Approach

This project is designed to examine the effects of combustion stoichiometry on the fundamental aspects of ash formation and ash deposit initiation. Emphasis is being placed on reducing stoichiometries associated with low-NOx combustion, although a range of oxidant/fuel ratios are being considered. Previous work has demonstrated that ash formation depends strongly upon coal mineralogy, including mineral type, size, amount, and the presence of organically associated inorganic species. Combustion temperature and the oxidation state of iron also play a significant role. As these latter items will vary with changes in stoichiometry, research to determine the net effect on deposition is required.

To achieve these goals, a research program with the following technical objectives is being pursued: 1) identify the partitioning of inorganic coal constituents among vapor, submicron fume, and fly ash products generated from the combustion of pulverized coal under a variety of combustion stoichiometries, 2) identify and quantify the fundamental processes by which the transformation of minerals and organically-associated inorganic species occurs. Identify any differences from standard excess air pulverized coal combustion conditions, 3) modify, to incorporate the effects of combustion stoichiometry, an Engineering Model for Ash Formation. The model is capable of predicting the size and chemical composition distributions of the final ash products under standard pulverized coal combustion conditions of 20% excess air. These modifications will extend the model to include phenomena that may be dominant under a broad range of stoichiometries.

Experiments, sample analyses, and modeling are being conducted at several facilities as part of this program. Detailed coal and ash sample analysis using Mössbauer spectroscopy, X-ray absorption fine structure spectroscopy (XAFS), and computer controlled scanning electron microscopy are being carried out at the University of Kentucky (UKy). Small-scale drop tube combustion tests using size and density classified coal samples are being carried out at the

Massachusetts Institute of Technology (MIT) to determine the extent of mineral coalescence and inorganic vaporization as a function of combustion stoichiometry. Combustion experiments utilizing utility grind coals are being conducted at Physical Sciences Inc. (PSI) to examine the effects of stoichiometry on mineral interactions. Deposition experiments using ash generated from combustion experiments and using pure minerals are also being conducted to investigate deposit initiation as a function of combustion conditions. PSI's Engineering Model for Ash Formation (EMAF) is being modified to include effects of combustion stoichiometry as part of this effort. Self-sustained combustion experiments are being conducted in the University of Arizona (UA) 100,000 Btu/h facility to address issues of scaling in combustion processes. The interaction of iron with aluminosilicates as a function of changing combustion conditions will be the focus of this effort. Modeling of iron-aluminosilicate interactions is being conducted as part of several tasks.

2. Coal Selection and Characterization

Four U.S. coals and one U.K. coal have been studied during this program: 1) Black Thunder sub-bituminous coal from the Powder River Basin, 2) a run-of-mine Pittsburgh #8 bituminous coal from the Appalachian Basin, 3) a washed commercial version of a Pittsburgh #8 coal obtained from DOE/PETC, and 4) a physically beneficiated product produced from Pittsburgh #8 coal, 5) Silverdale bituminous coal from the U.K., obtained as part of a collaborative effort with a program led by the utility Powergen. Coal and mineral analyses have been provided in previous reports.

3. Effect of Combustion Stoichiometric Ratio on Ash Formation

As a major element of this research program, the effect of combustion stoichiometric ratio on ash particle composition and size distributions is being examined. To date, work in laminar flow drop tube furnaces has been completed; work in the 100,000 Btu/h self-sustained combustor at the University of Arizona is ongoing. In the drop tube experiments conducted at PSI and MIT, the formation of chemically complex ash particles was found to be dependent upon combustion conditions. Less extensive formation of chemically complex phases was observed under oxygen lean conditions. Relative to the coal, however, significant amounts of chemically complex mixtures were observed under all combustion conditions. Differences may therefore simply be related to differences in stage of combustion. This trend is most clearly seen in ash generated from combustion of beneficiated Pittsburgh #8 coal. In the coal, iron-free aluminosilicate minerals were abundant, with no evidence for iron-aluminosilicate particles (Figure 1a). Considering particles that are rich in iron, aluminum, and silicon (particles that are comprised of greater than 80 mole percent Fe+Al+Si on an oxygen free basis), formation of iron aluminosilicates was observed at stoichiometric ratios of 0.6, suggesting that iron interacted with aluminosilicate minerals early in the combustion process when the residual carbon content was high. More extensive iron aluminosilicate formation, as evidenced by the broader mixture of compositions present in a ternary diagram (Figure 1), was observed at a stoichiometric ratio of 0.9. Ash generated during combustion of the coal at SR = 1.2 showed the broadest mixture of Fe-aluminosilicate compositions and in turn the highest concentration of Fe-Al-Si particles, as determined by CCSEM analysis at the University of Kentucky (Table 1). For comparison,

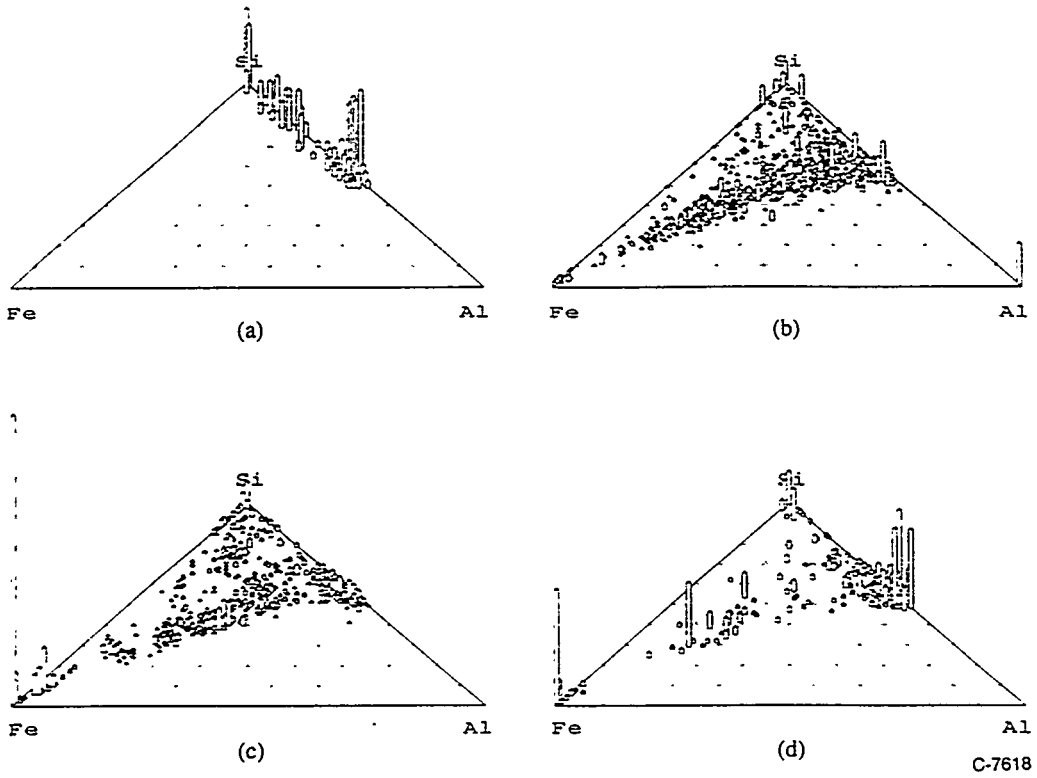

Figure 1. Fe-Al-Si ternary diagram for ash generated from combustion of a beneficiated Pittsburgh #8 coal in the PSIT drop tube reactor. Wall temperature = 1500°C, residence time = 2.6 s. Each point represents an ash composition detected by CCSEM; the height of each peak represents the normalized column of ash particles with the indicated composition. (a) coal minerals (b) ash generated at SR=1.2 (c) ash generated at SR = 0.9 (d) ash generated at SR = 0.6.

Table 1. CCSEM analysis of laboratory-generated combustion ash (volume percent) beneficiated Pittsburgh #8 coal; T_{wall} = 1500°C, t_{res} = 2.6 s.

Ash composition	SR = 0.6	SR = 0.9	SR = 1.2
Si	7.3	9.1	5.3
Si + Al	6.8	5.5	12.5
Si + Al + Fe	30.2	52.2	59.6
Fe + S	3.8	0.7	0.0
Fe + Si + S	5.9	4.3	1.2
Fe	0.6	1.2	0.7

Table 2. CCSEM analysis of laboratory-generated combustion ash (volume percent) Silverdale coal; $T_{wall} = 1500^{oC}$, $t_{res} = 2.6$ s.

Ash composition	SR = 0.6	SR = 0.9	SR = 1.2
Si	6.6	8.0	10.7
Si + Al	8.3	4.9	7.1
Si + Al + Fe	25.7	32.2	34.5
Fe + S	6.1	2.8	0.6
Fe + Si + S	4.2	1.4	1.8
Fe	0.0	4.2	3.8

results for Silverdale bituminous coal are presented in Table 2. Althcugh the percentage of ash that is Fe+Al+Si rich increased with increasing SR, the changes were small relative to those observed for the beneficiated Pittsburgh #8. Very little change with SR was observed for Silverdale coal.

The effect of carbon in the ash on the "stickiness" or adhesion efficiency of inertially impacting ash particles has also been examined. At the exit of the PSIT drop tube furnace, a ceramic converging section is inserted. This section contains uncooled ceramic tubes that are placed orthogonal to the flow direction and act as inertial impaction and collection devices. In experiments with the three Pittsburgh #8 bituminous coals, the collection efficiency (fraction collected / fraction passing through projected tube cross section) increased with increasing

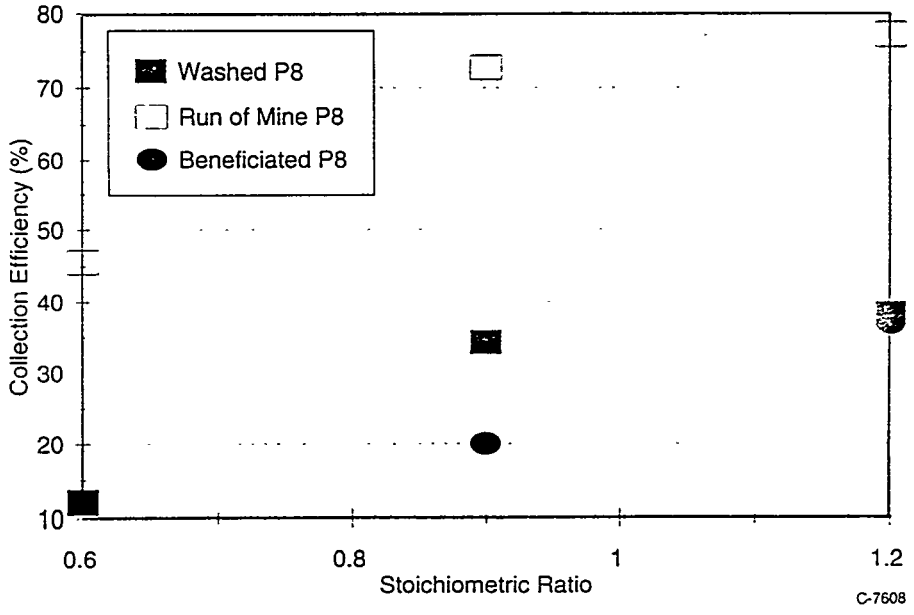

Figure 2. Ash collection efficiency for three Pittsburgh #8 bituminous coals as a function of combustion stoichiometric ratio. PSIT reactor, 2.6 s residence time, reactor wall temperature of 1500°C.

combustion stoichiometric ratio (Figure 2). This is a result of the decreasing carbon content in the ash as oxygen concentration is increased, as shown in Figure 3. In this figure, the curves represent calculated values assuming that collection efficiency under conditions of residual carbon present in the ash can be expressed as the product of X_c, 1-fraction carbon remaining, times $\eta_{\text{"pure" ash}}$, the collection efficiency under conditions of minimum carbon present in the ash,

$$\eta_{\text{effective}} = \eta_{\text{"pure" ash}} X_c.$$

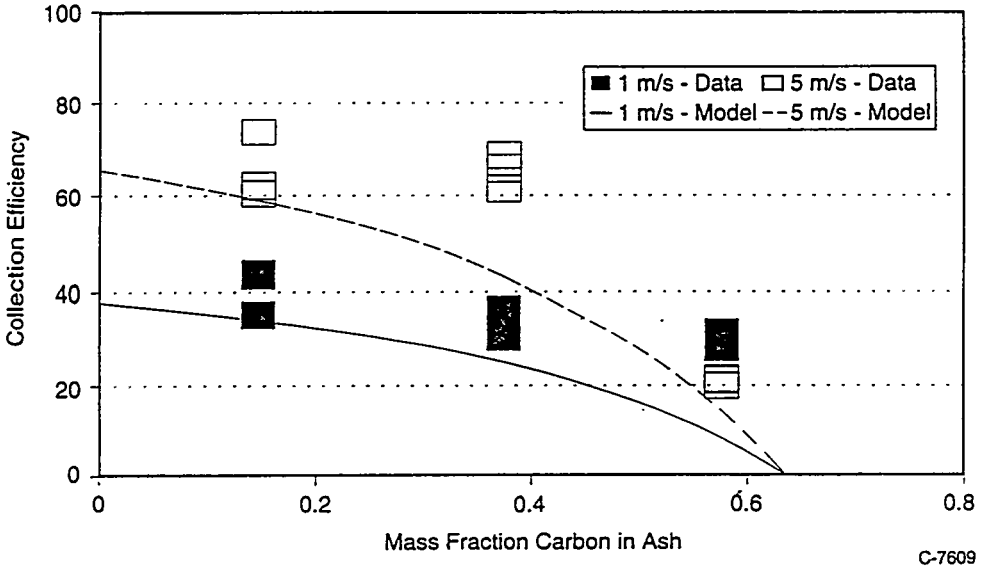

Figure 3. Ash collection efficiency for ash derived from combustion of Silverdale bituminous coal. Note that data are plotted v. the mass fraction of carbon present in the ash.

4. Effect of Oxygen Partial Pressure on Formation of Iron-containing Ash Particles

At MIT, a series of combustion experiments under varying oxygen partial pressure have been conducted with a sieved 63/75 μm sample of the washed Pittsburgh #8 coal. Ash samples collected under p_{O2} equal to 0, 0.10, 0.30, 0.60, and 1.00 (wall temperature = 1477°C in all cases) were then analyzed by Mössbauer spectroscopy at the University of Kentucky for forms-of-iron. Results are compared with the iron phase distribution in the sieved parent coal and in the bulk ash (so-called ASTM ash) in Figure 4. As oxygen partial pressure is increased, the percentage of iron in glassy phases first increases (0 to 30% oxygen) and then remains relatively constant (30 to 100% oxygen). The ratio (Fe^3/Fe^{+2}) in glass, important as a measure of ash particle stickiness, continues to increase with increasing SR, however. This suggests the existence of a threshold temperature below which iron-glass interactions will be less than the theoretically achievable level, based upon mineral distributions in the parent coal.

Mössbauer analysis of ash samples generated during combustion of the program coals in the PSIT drop tube furnace showed similar trends. As seen in Table 3, the ratio (Fe^{+3}/Fe^{+2}) for iron in glassy phases increased with increasing stoichiometric ratio for all coals. For these experiments, note that the total fraction of iron present in the glassy phases remained relatively unchanged with changing stoichiometric ratio. The lower values of (Fe^{+3}/Fe^{+2}) in glass relative

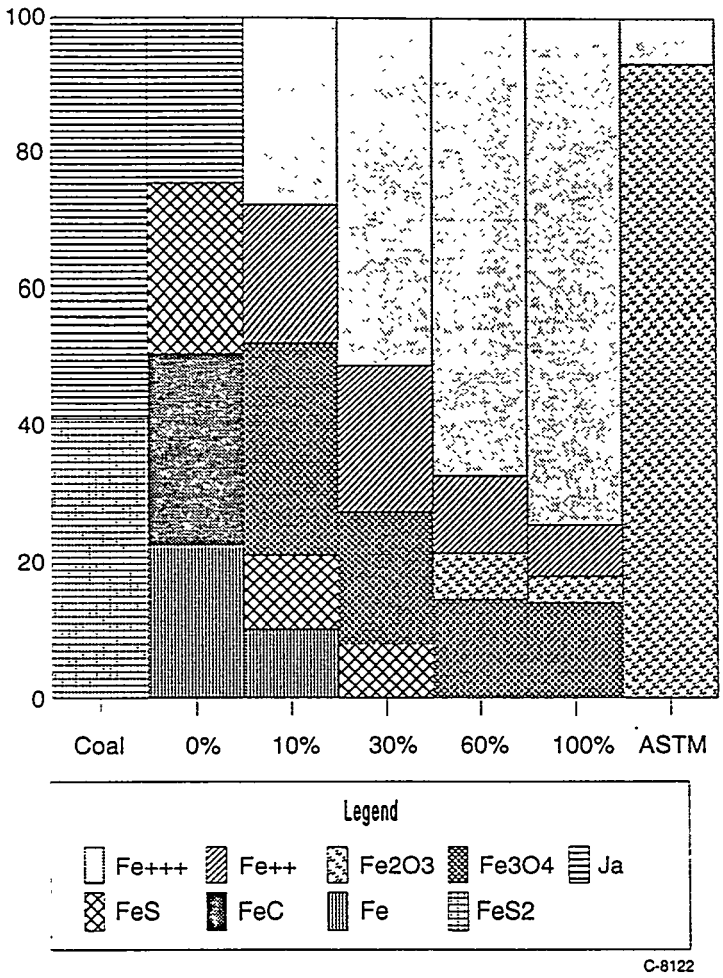

Figure 4. Iron speciation (percentage of iron in each phase) for ash samples generated from combustion of 63/75 μm washed Pittsburgh #8 bituminous coal at different oxygen partial pressures in the MIT drop tube furnace. Wall temperature equal to 1477°C for all experiments.

to the MIT data (Figure 4) are believed due to the lower particle temperatures and more dilute oxygen levels encountered in the PSIT reactor.

5. Engineering Model for Ash Formation

The Engineering Model for Ash Formation (EMAF) is designed to predict the ash composition and size distribution of a given coal based on its coal particle size and mineralogy. This model was originally designed to make these predictions based on complete combustion (e.g. super-stoichiometric conditions). To model the ash size distribution and composition for combustion under reducing conditions it was necessary to modify the model to account for the presence of unburned char. This modification was accomplished by developing a kinetic submodel, based on information in the literature, to predict the fraction of unburned char in each size range. This submodel has been discussed in program Quarterly Reports.

The output of the kinetic sub-model is used to define the fraction of minerals in each simulated coal particle that is **not** exposed during the combustion process. These minerals will generally maintain the same size and composition, as they cannot interact with other minerals. The remaining minerals are assumed to coalesce and interact with other minerals - similar to the original model. Based on these mechanisms, the model predicts the size and composition distributions of the ash that would be measured by CCSEM. Figures 5 and 6 illustrate the predicted changes in ash size and composition as a function of stoichiometric ratio for the ROM Pittsburgh No. 8. On one extreme is the one ash per mineral case, which would match those conditions where very little char burnout has taken place, such as low residence times or stoichiometric ratios. The other extreme is the completely burned out case (SR=1.2). The model predicts a smooth transition of ash mass to the larger sizes with increasing stoichiometric ratio - indicating an increase in ash coalescence with stoichiometric ratio. This increase in coalescence is also evident in the composition predictions (Figure 6). The major ash particle categories (reported on an oxygen

Table 3.
Iron distribution in ash generated from combustion of program coals at PSIT.
T_{wall} = 1500°C, t_{res} = 2.6 seconds

	SR	Fe_xS	Fe^{+2}	magnetite	Fe^{+2} glass	Fe^{+3} glass
run-of-mine Pittsburgh #8	0.6	19	0	0	81	0
	0.9	8	0	23	51	19
	1.2	0	0	22	58	20
washed Pittsburgh #8	0.6	30	25	13	32	0
	0.9	10	25	29	36	0
	1.2	6	24	36	25	9
beneficiated Pittsburgh #8	0.6	18	0	0	82	0
	0.9	4	0	11	64	21
	1.2	0	0	15	41	44
Silverdale	0.6	37	0	0	63	0
	0.9	13	0	16	71	0
	1.2	0	0	44	39	17
Black Thunder	0.6	0	22	0	24	54
	0.9	4	17	0	11	68
	1.2	0	13	0	7	80

and hydrogen-free basis) are initially Si Al K, Si, Si Al, and lesser amount of Si Al Fe and Si Al Ca. As these ash particles coalesce, the amount of Si (quartz) and Si Al K (illite) decreases, while the amount of Si Al increases. This is due to the product of Si and Si Al K mixing having a lower K content and therefore being binned in the Si Al category. There is also evidence of increased Fe - silicate coalescence as a function of increasing stoichiometric ratio (burnout).

6. Plans

In the remaining months of the program, two major tasks are to be completed. These are (1) conclusion of experiments in the UA self-sustained combustor, and (2) completion of the analysis of XAFS data collected by UKy during examination of Silverdale ash and deposit samples.

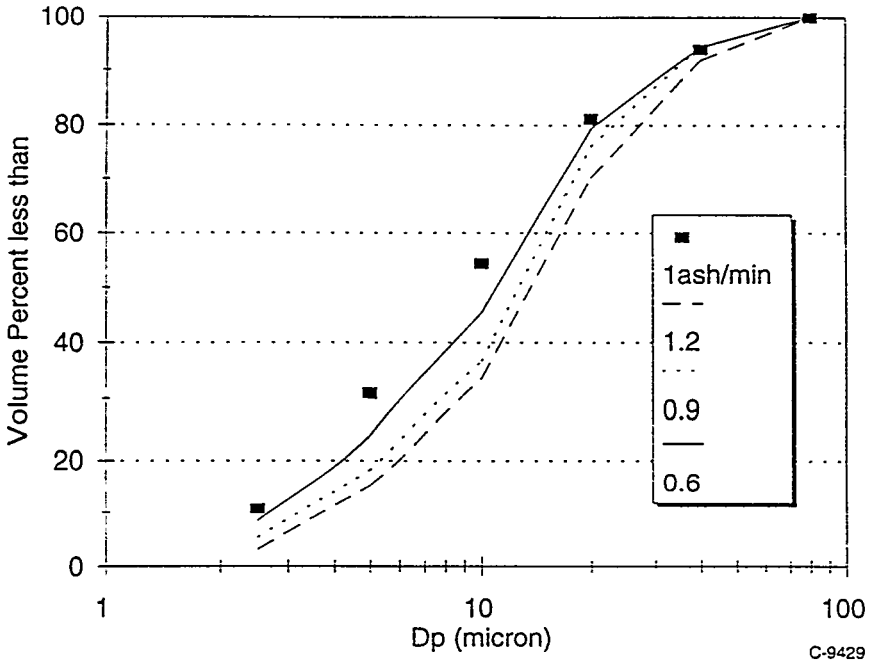

Figure 5. Predicted ash PSD as a function of stoichiometric ratio. Mineral size distribution (1 ash/min) shown for comparison. Coal: ROM Pittsburgh No. 8.

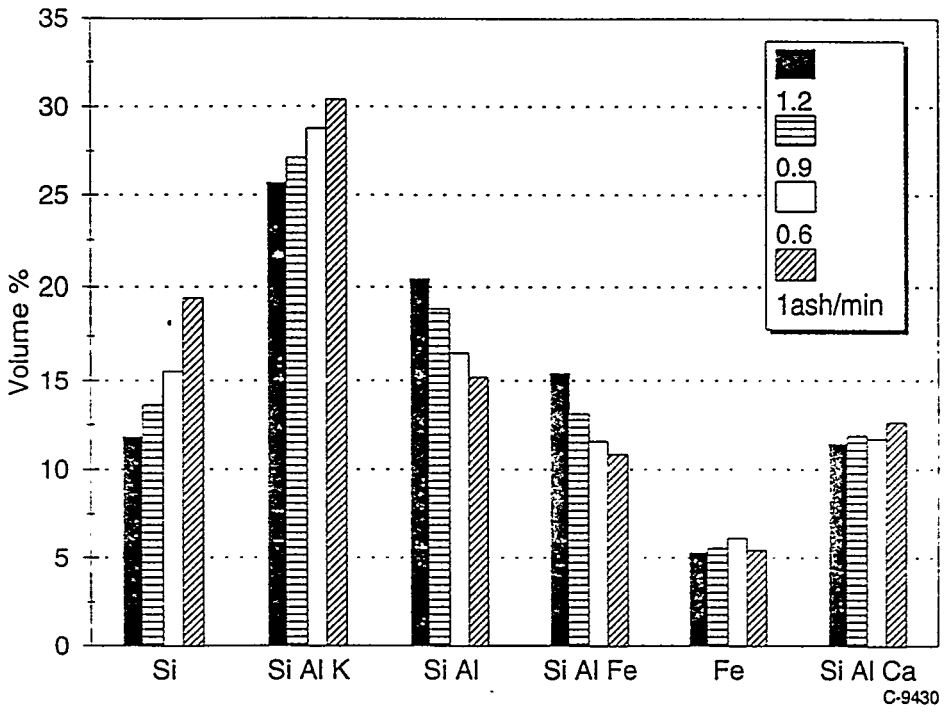

Figure 6. Model prediction for ash compostion - ROM Pittsburgh No. 8.

DEPOSIT GROWTH AND PROPERTY DEVELOPMENT IN COAL-FIRED FURNACES

LARRY BAXTER
SR. MEM. OF TECHNICAL STAFF
COMBUSTION RESEARCH FACILITY
SANDIA NATIONAL LABORATORIES
LIVERMORE, CA 94550

PROJECT OBJECTIVES AND DESCRIPTION

The objectives of this research project are: (1) to provide a self-consistent database of simultaneously measured, time-resolved ash deposit properties in well-controlled and well-defined environments and (2) to provide analytical expressions that relate deposit composition and structure to deposit properties of immediate relevance to PETC's Combustion 2000 program. This project is distinguished from related work being done elsewhere by: (1) the development and deployment of *in situ* diagnostics to monitor deposit properties, including heat transfer coefficients, porosity, emissivity, tenacity, strength, density, and viscosity; (2) the time resolution of such properties during deposit growth; (3) simultaneous measurement of structural and composition properties; (4) development of algorithms from a self-consistent, simultaneously measured database that includes the interdependence of properties; and (5) application of the results to technologically relevant environments such as those being planned under the Combustion 2000 program.

Work completed during FY94 emphasized diagnostic development. During FY95, this development work will be completed and we will emphasize application of the diagnostics to meet the other project objectives. Included in this work are the development and application of two *in situ*, real-time diagnostic systems for monitoring the properties of inorganic materials on Heat transfer surfaces and in the gas-phase during controlled combustion of selected coal samples in Sandia's Multifuel Combustor (MFC). Also, several diagnostics are being incorporated into the MFC that will eventually be used to characterize ash deposit properties.

The project comprises six subtasks, as follows:

Subtask 2.1 Diagnostics for Coal Combustion Environments

The objective of this subtask is to develop and demonstrate diagnostics capable of *in situ* measurement of: (1) condensed-phase species on surfaces in combustion environments, and (2) inorganic vapors in turbulent, particle-laden, combustion gases.

Subtask 2.2 Experimental Determination of Transport, Thermal, and Structural Properties of Ash Deposits

The objective of this subtask is to provide self-consistent, simultaneous measurement of ash deposit properties under combustion conditions that simulate commercial-scale environments such as those expected to occur in Combustion 2000 technologies. Properties to be measured simultaneously and in real time include thermal conductivity, emissivity, porosity, mass and

volume rate of growth, surface composition, and tenacity. Additional properties to be measured, but not in real time or *in situ*, include bulk elemental composition, bulk species composition, shear strength, true density, and detailed morphology.

Subtask 2.3 Analysis of Deposit Properties

The objective of this subtask is to provide an analytical capability for describing the development of deposit properties in combustion systems. Deposit properties to be predicted by this analytical method are similar to those discussed in Subtask 2.2 and include: (1) thermal conductivity, (2) emissivity, (3) porosity, (4) mass and volume rate of growth, (5) surface composition, (6) tenacity, (7) bulk elemental composition, and (8) major species composition.

Subtask 2.4 Chemical Reactions in Deposits

The objective of this subtask is to determine rates and mechanisms that describe chemical reactions in coal ash deposits that alter their properties or their morphology. This subtask is more limited in scope than the previous subtasks. We do not intend to conduct a comprehensive study of inorganic chemistry as it relates to ash deposits. We do intend to review available literature and perform calculations that allow us to capture the first-order terms that describe changes in deposit chemistry with time. This work will result in usable results, but is limited to global kinetics and simplified chemical mechanisms that outline the nature of the reactions and their dependence on operating parameters. The details of the kinetics will not be determined.

Subtask 2.5 Application to Combustion 2000 Program

The objective of this subtask is to exchange technology developed under other subtasks with ongoing Combustion 2000 efforts by other PETC contractors.

Subtask 2.6 Documentation

The objective of this subtask is to provide timely and accurate documentation of project progress, major milestones, and publishable results.

BACKGROUND

Mineral matter in coal is cited as "the nemesis of coal-burning industries" and as playing "the dominant role in fuel selection, in setting the design and size of the furnace, and in establishing how that boiler furnace will be operated" (Raask, 1985). However, the fate of mineral matter during pulverized coal combustion is relatively poorly understood, despite this importance to coal conversion systems. Significant progress in past years has been made through large measure because of PETC-sponsored research describing transformations of inorganic material during combustion. This new research project focuses on ash deposit formation and the development of deposit properties.

This research project supports the overall DOE mission of nurturing the effective and efficient use of national energy resources. It also supports the specific objective of the PETC mineral matter program to develop qualitative and quantitative understandings of mineral matter

transformations in environments typical of pulverized-coal combustors and to incorporate these into tractable, mechanistic models. Major aspects of the project are designed to support DOE's Combustion 2000 program.

RECENT PROGRESS

The focus of this discussion is on the development of a diagnostic for detecting alkali vapors in combustion diagnostics being performed as part of Subtask 2.1.

Tunable Diode Laser Spectroscopy

During this year, a diagnostic based on a tunable diode laser (TDL) was developed to detect alkali vapor in combustion environments. NaCl is one of the species of prime interest to alkali transport in coal combustion systems and is also the most difficult of the major alkali-containing species to monitor spectroscopically. While NaCl is the focus of discussion below, the same technique can be used for sulfates and other alkali-containing vapors of interest.

System Description

A tunable diode laser probes the vibrational spectrum of alkali-containing vapors such as chlorides, hydroxides, and sulfates of sodium and potassium. The vibrational bands for the hydroxides and chlorides are in the region from 330 to 400 cm^{-1} (30 to 25 μm), a region requiring more specialized equipment than is common for most molecular spectroscopy. Figure 1 illustrates the major components of this system. The following description describes the optical and essential electronic components of the system.

A tunable diode laser (TDL) provides the probe beam for analyzing the vapors. This lead-salt diode operates at low temperature (7-35 K), and is less well behaved than traditional TDLs. A Laser Photonics cryogenic (helium) compressor and cold finger maintains the laser temperature at a set value. The cold finger can accommodate up to four diode lasers simultaneously. Three are currently installed, but all of the data reported below were collected with a single diode.

The laser is tuned over a range of about 0.5 cm^{-1} by varying the diode current between its lower threshold value (typically ≈ 100 mA) and its upper limit (typically 500 mA to 1 A). The lower limit is dictated by the current required to induce lasing in the diode. The upper limit is dictated by the safe current carrying capacity of the laser. The specific frequency of the laser light is determined by a combination of temperature and current. In practice, these diodes emit approximately twelve frequencies simultaneously, depending on current and temperature. The beams from the laser are more divergent than is common in most lasers. The beams are collimated with an off-axis paraboloidal mirror, but they still diverge somewhat. The beam is chopped either by chopping the current to the diode or by passing the beam through a mechanical chopper. Beam chopping has a practical upper limit of around 5 kHz. The current controller installed with the TDL has a maximum current modulation rate of 1 kHz, but more rapid modulation can be controlled by interfacing the controller with external signal generators.

The beam then passes through a furnace used to generate reference, test, and calibration spectra. This furnace operates at temperatures up to about 1600 °C and is open at both ends. A version with windows is being developed to allow lower pressure (20 Torr), more controlled calibration

data to be obtained. The material of choice for these windows is thallium bromoiodide, generally referred to as KRS-5. Its advantages include its transparency at these wavelengths and reasonable transparency at visible wavelengths. Traditional infrared materials such as potassium bromide and sodium chloride are opaque at the wavelengths we are interested in (25-30 μm). Means of placing KRS-5 windows on either end of the furnace are still being pursued. The windows must be maintained at relatively cool temperatures, well under 100 °C for both physical and safety reasons. Thallium bromoiodide softens at low temperature and is toxic. There are known ways to protect the windows from heat or condensing inorganic vapors while providing an gas-tight seal for the furnace, but they require both composition and temperature gradients in the test cell. The furnace walls are removable and are composed of available ceramic materials, generally either mullite or silicon carbide.

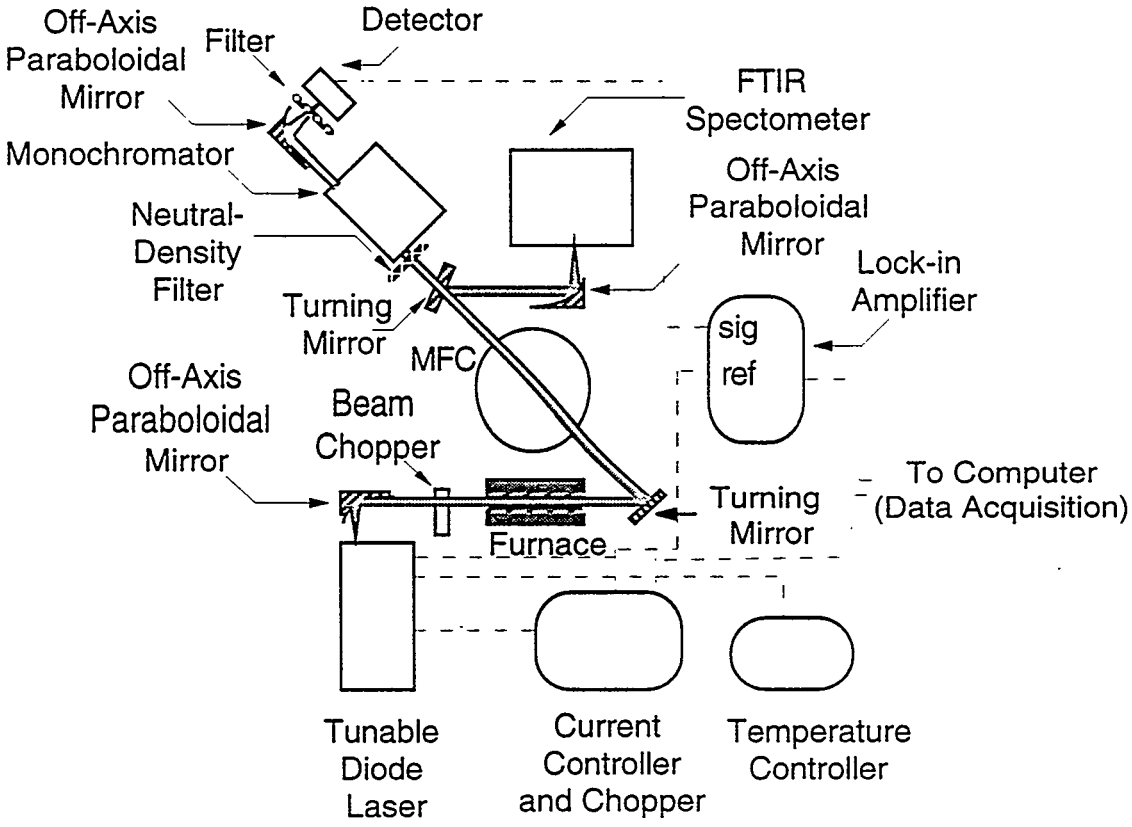

Figure 1 Schematic diagram of the TDL system used to monitor alkali-containing vapors. Optical components are illustrated as rectangles. Electronic components are illustrated with rounded corners.

After exiting the furnace, the beam is directed through the test section of the Multifuel Combustor (MFC). Significant beam steering is induced by index of refraction gradients in both the furnace and the MFC test section. The MFC has added complexities of particle interference and turbulent fluctuations in gas temperature and composition. Measures have been taken to minimize the impacts of these issues by using modulated signals and lock-in amplifier detection, averaging scans both in real time and by repeated experiments, and shielding the detector from

stray radiation.

The laser beam terminates on a copper-doped germanium detector. This detector operates at liquid helium temperature and is contained in a dewar system. Its low operating temperature (≈4 K) is not trivial to maintain, and its sensitivity to temperature variation is strong. Cold, broad bandpass filters in front of the detector are used to further reduce contributions from stray radiation sources.

The laser beam to help discriminate against stray sources of radiation and to accommodate the AC-coupled detector. The detector signal is filtered with a lock-in amplifier. The laser is scanned at a rate of about 0.01 Hz over a range of approximately 200 mA (current, rather than temperature is used to tune the laser). The current can be increased, decreased, or alternately increased and decreased from its set point.

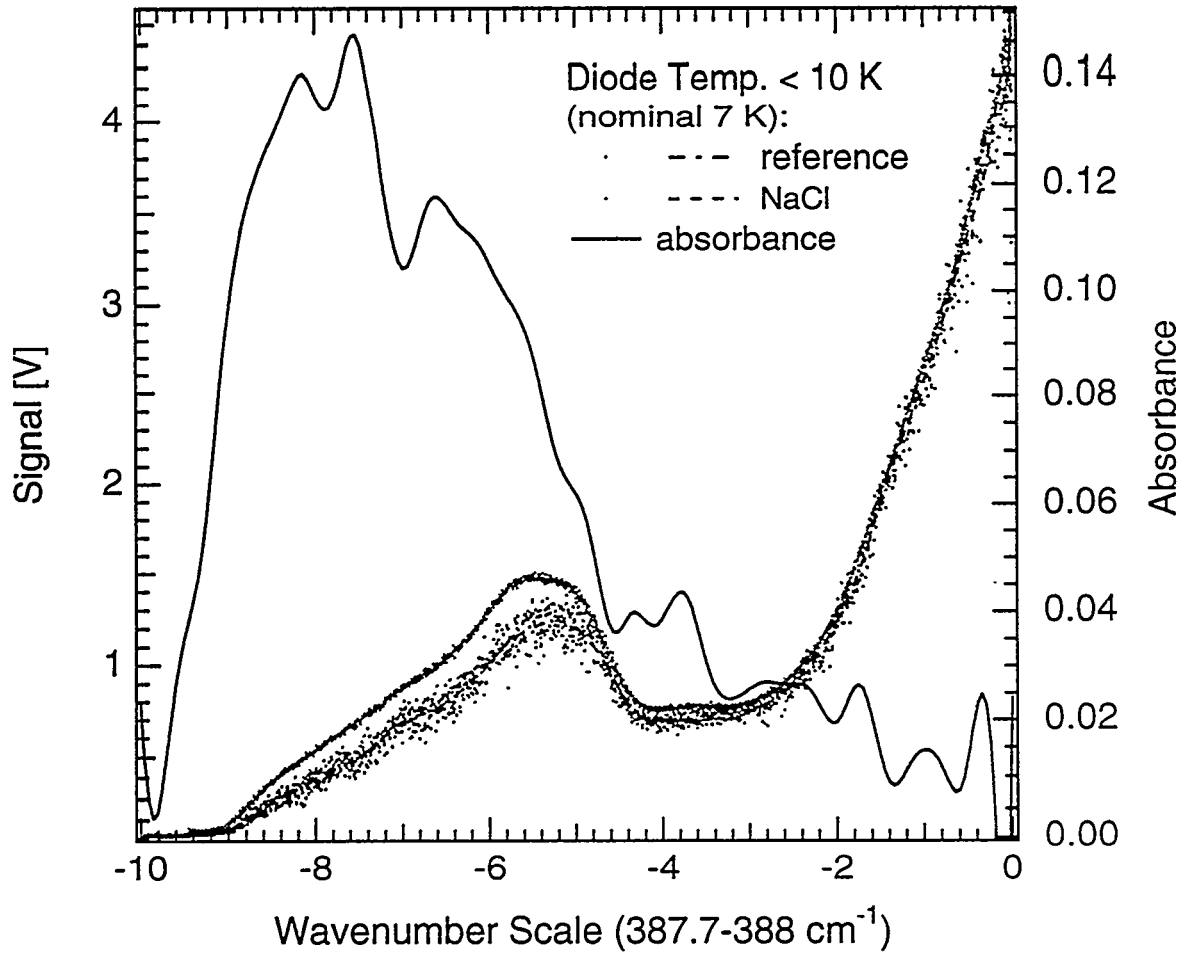

Figure 2 Reference and probe signals, together with absorbance spectrum, for a portion of the NaCl spectrum between approximately 387.7 and 388 wavenumbers. The rise in absorbance is an indicator of the NaCl R-branch bandhead located at 387.8 cm^{-1}.

Figure 2 illustrates the spectra collected recently near the bandhead of the R-branch of NaCl (NaCl spectrum illustrated in Fig. 3). The abscissa is approximately linearly proportional to wavenumbers over the approximate range from 387.7 to 388 cm^{-1}, but the wavenumber calibration has not yet been performed. The solid line, referenced to the right, represents the absorbance spectrum of sodium chloride. The intensity of the laser varies in complex ways with wavenumber, as represented by the reference beam. The wavenumber-resolved laser intensity when passing through NaCl vapor is also indicated. The data are reasonably dense and tend to obscure the lines designating the reference beam and the NaCl absorption beam. In both figures, the reference beam intensities are generally higher and less scattered than the NaCl absorption data. The absorbance spectrum is calculated from the logarithm of the ratio of reference to NaCl results.

The laser is being forced to its low-temperature limit to collect these data because the laser mode we are using barely overlaps the bandhead we are trying to measure. A more ideally located mode would allow us to perform the experiment without pushing the equipment quite as close to its performance limit. Diode lasers that operate in this region are rare – we know of only one supplier. Even for this supplier (Laser Photonics), these diodes are difficult to produce. We are working with them to obtain additional lasers with more convenient modes.

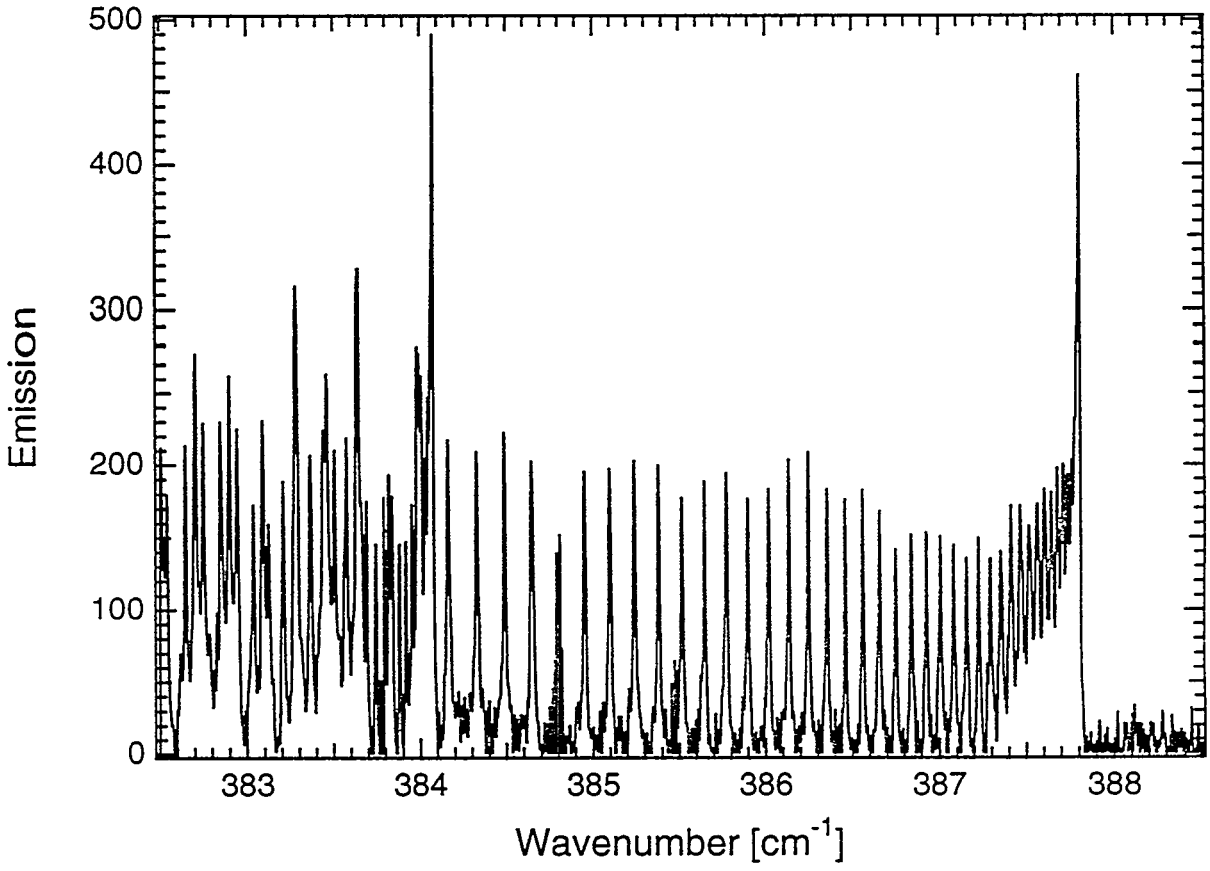

Figure 3 Emission spectra of NaCl at 20 Torr collected by collaborator Peter Bernath using high resolution FTIR spectroscopy and a heated test chamber. The data in Fig. 2 indicate an attempt to resolve the bandhead located at ≈ 388 cm^{-1} at 1 atm.

The data are encouraging. The absorbance indicates the expected dependence on wavenumber and has nearly identical peak values over this wavenumber range even if the peak laser power increases by 50%. The fine structure in the absorbance data is indistinguishable from noise, primarily because of beam steering observed during collection of the NaCl data through a hot cell. The decline of absorbance at the lowest wavenumbers (left side of the abscissa) is attributable to a loss of laser power, not a loss of absorption. The decline in absorbance at high wavenumbers is indicative of the bandhead (compare with Fig. 3).

While the data are encouraging, they are not definitive. The potential for thermal feedback from the hot furnace to the cryogenically cooled laser and detector could cause biases in laser or detector performance that, in turn, could be misinterpreted as absorption. The impact on the detector should be slight since the beams that arrive there must first pass through optical filters and a monochromator. The additional energy within the resolution of the monochromator (about 0.7 cm^{-1} in this region) is likely insufficient to change the detector temperature or otherwise bias its performance. The laser, on the other hand, is closer to the furnace. The only optical components between the laser and the furnace are choppers, baffles, mirrors, and apertures. The principal problem is that we are at the extreme limit of the laser operating window (low temperature and low current) for this laser mode to collect these data. There are other modes that operate at still lower frequency ranges, but the bandhead is the most definitive and forgiving feature of the NaCl spectrum to work with. While we continue to optimize this technique with this laser, we are also pursuing a different laser with a more conveniently available (say 387-388 cm^{-1}) tunable mode.

PRESENTATIONS AND PUBLICATIONS

The following publications were submitted in the last year based in part or in whole on PETC-sponsored work.

Baxter, L. L., Mitchell, R. E., and Fletcher, T. H. (1995 (to appear)). "Release of Inorganic Material During Coal Devolatilization." ***Combustion and Flame, to appear.***

Richards, G. H., Harb, J. N., Baxter, L. L., Bhattacharya, S., Bupta, R. P., and Wall, T. F. (1994). "Radiative Heat Transfer in PC-Fired Boilers — Development of the Absorptive/Reflective Character of Initial Ash Deposits on Walls". In *Twenty-Fifth Symposium (International) on Combustion*, . Irvine, CA: The Combustion Institute.

Wall, T. F., and Baxter, L. L. (1993). "Ash Deposits, Coal Blends, and the Thermal Performance of Furnaces". In *Engineering Foundation Conference on Coal Blending and Switching of Western Low-Sulfur Coals*, . Snowbird, Utah

Baxter, L.L., "The Effect of Low-NO_x Firing on Formation of Ash Deposits," to be presented at the 1995 Engineering Foundation Conference on the Economic Aspects of Coal Utilization, Santa Barbara, CA, January 30 - February 3, 1995

Baxter, L.L., "The effect of Low-NOx Firing on Fireside Performance," proceedings of the 1994 International Joint Power Generation Conference, Phoenix, AZ, October 3-5, 1995

Baxter, L.L., R.E. Mitchell, T.H. Fletcher, and R.H. Hurt, "Nitrogen Release During Coal Combustion," submitted to ***Energy & Fuels***

Baxter, L.L., Ash, to appear in the **Wiley Encyclopedia of Energy Technology**, 1995

The following manuscript was unavailable at time of publication.

CHARACTERIZING THE STRUCTURE OF ASH DEPOSITS FROM COAL COMBUSTORS

Everett Ramer
U.S Department of Energy
Pittsburgh Energy Technology Center
P.O. Box 10940, M.S. 84-340
Pittsburgh, PA 15236

or

Donald V. Martello
U.S. Department of Energy
Pittsburgh Energy Technology Center
P.O. Box 10940, M.S. 94-212
Pittsburgh, Pa 15236

Please contact author(s) for a copy of this paper.

The following manuscript was unavailable at time of publication.

DEVELOPMENT/TESTING OF AN INDUSTRIAL-SCALE COAL-FIRED COMBUSTION SYSTEM

Dr. Bert Zauderer
Coal Tech Corporation
P.O. Box 154
Merion, PA 19066-0154

Please contact author(s) for a copy of this paper.

MICROFINE COAL FIRING RESULTS FROM A RETROFIT GAS/OIL-DESIGNED INDUSTRIAL BOILER

Ramesh Patel, Richard W. Borio, Greg Liljedahl
ABB Power Plant Laboratories
Combustion Engineering, Inc., Windsor CT 06095

Bruce G. Miller, Alan W. Scaroni
Energy and Fuels Research Center
The Pennsylvania State University, University Park PA 16802

Jon G. McGowan
University of Massachusetts, Amherst MA 01002

INTRODUCTION/ BACKGROUND

Under U.S. Department of Energy, Pittsburgh Energy Technology Center (PETC) support, the development of a High Efficiency Advanced Coal Combustor (HEACC) has been in progress since 1987 at the ABB Power Plant Laboratories (Rini, et al., 1987, 1988). The initial work on this concept produced an advanced coal firing system that was capable of firing both water-based and dry pulverized coal in an industrial boiler environment (Rini, et al., 1990).

Economics may one day dictate that it makes sense to replace oil or natural gas with coal in boilers that were originally designed to burn these fuels. In recognition of this future possibility, the U.S. Department of Energy, Pittsburgh Energy Technology Center (PETC) has continued to support this program led by ABB Power Plant Laboratories and the Fuels Research Center of Penn State University to develop the HEACC concept. The objective of the current program is to demonstrate the technical and economic feasibility of retrofitting a gas/oil designed boiler to burn micronized coal. In support of this overall objective, the following specific areas were targeted:

- A coal handling/preparation system that can meet the technical requirements for retrofitting microfine coal on a boiler designed for burning oil or natural gas.
- Maintaining boiler thermal performance in accordance with specifications when burning oil or natural gas.
- Maintaining NOx emissions at or below 0.6 lb/MBtu (~450 ppm)
- Achieving combustion efficiencies of 98% or higher
- Calculating economic payback periods as a function of key variables

The overall program has consisted of five major tasks:

1.0 A review of current state-of-the-art coal firing system components.
2.0 Design and experimental testing of a prototype HEACC burner.
3.0 Installation and testing of a HEACC system in a commercial retrofit application.
4.0 Economic evaluation of the HEACC concept for retrofit applications.
5.0 Long term demonstration under commercial user demand conditions

This paper will summarize the latest key experimental results (Task 3) and the economic evaluation (Task 4) of the HEACC concept for retrofit applications.

BURNER INSTALLATION AND TESTING IN AN INDUSTRIAL BOILER

The overall objective of this program has been to assess the technical and economic viability of displacing premium fuels with micro-fine coal by retrofitting the previously developed High Efficiency Advanced Coal Combustor (HEACC) to a gas/oil designed industrial boiler. This paper summarizes the work involving the retrofit of a complete micro-fine pulverized coal milling and firing system to an existing 15,000 lb/hr package boiler located in the East Steam Plant of Penn State University. Combustion performance-related objectives included steady state operation on 100% coal while achieving a carbon conversion efficiency of 98%, without increasing NOx emissions above 0.6 lb/MBtu (~450 ppm). The testing was also designed to show that consistent, reliable operation of entire coal storage/handling and pulverization system could be achieved. Reliable operation of the coal preparation system in concert with satisfactory burner performance would serve as a prerequisite to the demonstration phase of the project.

The HEACC burner was previously tested (Task 2) in the Industrial Scale Burner Facility (ISBF) located at Combustion Engineering's ABB Power Plant Laboratories (PPL) in Windsor, Connecticut. A key objective of the 100 hour burner validation tests at PPL was to fine-tune the burner operating characteristics and demonstrate operation over the range of conditions expected for the field boiler tests. All performance goals were successfully achieved during these ISBF tests. The testing at PPL demonstrated the technical validity of the design improvements incorporated into the second generation HEACC. This burner was then installed as part of a complete coal handling and firing system in Penn State's commercial boiler for a 400 hour proof-of-concept test program (Task 3).

A schematic of the micronized coal preparation/firing system at Penn State is shown in Figure 1. As can be seen, the cleaned coal comes on site and is stored in a large hopper. The coal is crushed and sent via a screw feeder to a micronized coal mill (TCS system). The coal is then micronized to ~80% through 325 mesh (~18 microns MMD) in the TCS mill and pneumatically conveyed to the HEACC burner where it is then burned in the boiler. This boiler is an oil/gas designed Tampella Keeler Model DS-15; a package D-type watertube boiler capable of producing 15,000 lb/hr of saturated steam at 300 psig. It represents a typical gas/oil - designed system with a furnace volumetric heat release of 50,000 Btu/hr ft^3, standard for this class of boiler. Furthermore, its design is similar to that of many other manufacturers' (including Combustion Engineering) models.

EXPERIMENTAL TESTING RESULTS

A) OVERVIEW

During the long term test period, the boiler system was operated over a range of operating conditions. Specifically, the boiler was tested over a variety of load ranges, excess air, combustion air damper settings and burner swirl levels. Two coals Brookville Seam and Kentucky were used. Their analyses are summarized in Table 1. During the test period, boiler performance data, emissions data, electric parasitic power and house compressed air consumption data, as well as other data required for the technical and economical analysis of the system were obtained.

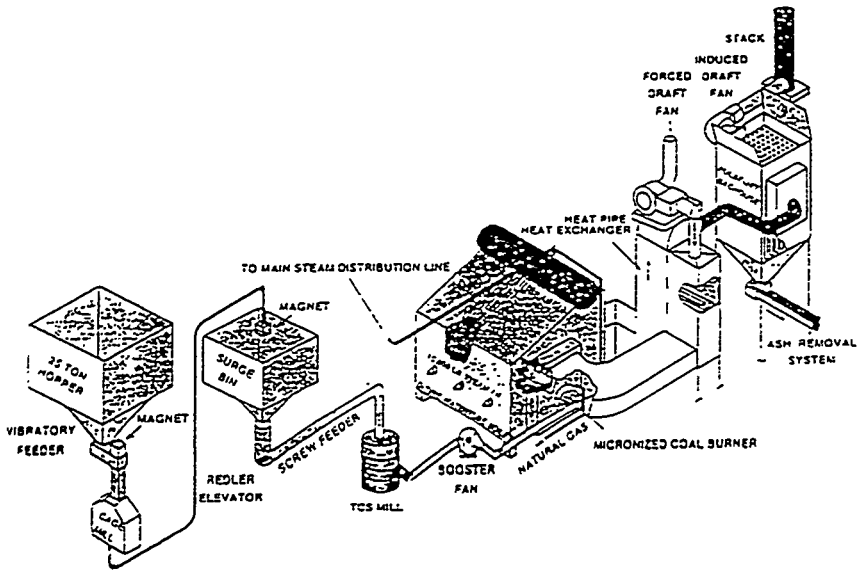

Figure 1 Micronized Coal Combustion System at Penn State

The initial burner tests included a shakedown series of runs using natural gas firing (Jennings, et al., 1994a, 1994b). At the conclusion of baseline natural gas firing, the boiler operation was directed towards hardware optimization (e.g., coal handling/preparation, burner settings) and testing with 100% coal firing. During this phase of the work, a major objective was to obtain consistent, repeatable 100% coal fired runs. This goal, along with minor modifications to the system (discussed in the next section) to increase boiler and carbon conversion efficiency resulted in several short term tests. Subsequently, the chosen hardware configuration was then used during the long term (~400 hr) test program (Task 3).

Table 1 Selected Analyses of the Brookville and Kentucky Coals

	Brookville Seam	Kentucky
Proximate, wt%		
Moisture	8.2	6.8
Volatile Matter	33.1	33.3
Fixed Carbon	55.8	55.4
Ash	2.9	4.5
HHV, Btu/lb	13,260	13,010
Ash Fusion Temp, °F		
IDT	2,820	2,803
ST	+3,000	+3,000
FT	+3,000	+3,000

B) SYSTEM CHARACTERIZATION/MODIFICATIONS

A key objective of the proof of concept testing was to determine the operating characteristics of the complete, integrated system in contrast to the operation of the individual components. Although all of the system components installed at the demonstration boiler host site were proven in either commercial operation or prior testing, the complete system from micro-fine coal production to steam production at this scale had not been previously demonstrated/proven.

The testing at Penn State indicated areas that should be carefully engineered in a commercial design. Furthermore, it was anticipated that if any problems occurred, they would likely be related to the burner (the least developed system component). However, the coal handling/feeding sub-system as it related to boiler system operability proved to be a critical component during initial testing. Some of the key system modifications and operational problems relating to the Penn State boiler are discussed below.

TCS Mill

The TCS mill and booster fan operated well without constant supervision. Initial system testing, however, revealed a coal settling problem in the mill outlet duct. This problem was corrected by a specially designed diffuser/transition section fitted to the mill exit. In addition, a detailed experimental study was carried out to characterize the effect of mill air flow rate and mill speed, on coal particle size distribution (PSD) and top size for the two coals tested. This was done as part of an effort to determine the milling conditions necessary to reduce the coal PSD and top size in order to achieve maximum coal combustion efficiency. In addition, the results were used to evaluate the feasibility for external classification to reduce the coal top size. The mill speed was a most important parameter to obtain the desired coal PSD. The results from these tests were used to optimize the mill settings for coal fineness during the experimental test program. Table 2 presents typical optimized mill operating conditions.

Table 2 Mill Performance Summary

- Typical mill air flow rate: 370-400 acfm
- Typical coal feed rate: 16.5- 18.5 lb/min

Particle Size (microns)	Brookville Seam Coal	Kentucky Coal
Top Size	190-300	250-275
D_{80}	50-70	50-70
D_{50}	25-30	25-30

Furnace Modifications

The furnace geometry was slightly altered during the test program by installing a ceramic wall at the exit of the radiant section of the boiler. The basic idea was to improve carbon burnout by making better use of the entire boiler volume through changing the gas patterns and temperature profile in the boiler. This was done because analytical (CFD) modeling showed that the flame was skewed from the burner to the furnace outlet and that the entire furnace volume was not being effectively used (Model results were subsequently verified by suction pyrometry).

Boiler System Operability

During the initial testing period, a number of operational problems involving the coal handling and boiler system were encountered. They were primarily related to the weather (cold, snow), the coal (particle size, moisture content), the burner/boiler system (unstable/ low u.v. flame scanner signal), or mechanical difficulties (feedwater pump, steam valves). With the exception of the coal handling problems caused by high moisture, these problems were all addressed and solved during the shakedown test series. The coal moisture problems will be fully addressed prior to beginning the 1000 hour demonstration test (Task 5).

C) SUMMARY OF EXPERIMENTAL RESULTS

Under the 400 hour test program, Brookville Seam and Kentucky coals were evaluated, the furnace geometry was modified by installing a ceramic wall, two coal guns (the RO-II with and without a coal deflector/accelerator and the I -Jet) were tested, and the operating conditions

and without a coal deflector/accelerator and the I -Jet) were tested, and the operating conditions (excess air and firing rate) were varied. During the course of the long term coal only tests, no support fuel was required and the burner operated with excellent ignition stability. A typical summary of the microfine coal firing (both coals) is given in Table 3.

Table 3 Microfine Coal Firing Results

Boiler Operation:	
Steam Flow Rate (lb/hr)	13,240
Boiler Efficiency (%)	84.1 (3% O_2)
Combustion Performance	
Carbon Conversion Efficiency (%)	95.3
NOx at 3% O_2 (ppm)	413 (0.56 lb/MBtu)
Burner Pressure Drop (in H_2O)	8

During this test program, key performance variables were monitored in detail: boiler efficiency, combustion efficiency, and NOx emissions. A summary of the results involving these parameters follows.

Boiler Thermal Performance

Boiler thermal performance when firing micro-fine coal was essentially comparable to that achieved when firing natural gas. In fact, because of the greater latent heat loss when burning natural gas (greater formation of water due to higher hydrogen content), firing micro-fine coal actually gave slightly higher boiler efficiencies despite the need to run at higher excess air levels.

During the relatively short operating periods, usually less than 16 hours, ash deposits did not cause significant changes to the boiler thermal performance. It is recognized, however, that longer term operation could result in greater build-up of ash deposits which could impact heat transfer. Because of the relatively short duration of the tests, any build-up of ash deposits would slough off when the boiler was shut down. A better test of the possible impact of ash deposits will occur during the long term demonstration phase of the work (Task 5.0).

NOx Emissions

The NOx emissions target was 0.6 lb NOx per million Btu fired; this translates to about 450 ppm at 3% O_2. Testing with 100% microfine coal showed that this target was achieved (in general a NOx emissions value of 0.56 lb NOx per million Btu was routinely met) while meeting nearly all other required conditions. It is acknowledged that the optimum conditions for low NOx will generally exacerbate carbon conversion efficiencies. Indeed, this was the case with the HEACC burner and the challenge was to find a reasonable balance between meeting the NOx target while not aggravating the carbon conversion efficiency.

Combustion Efficiency

The target for combustion efficiency was 98%. The highest combustion efficiency obtained during the test program was slightly over 96%. However, this value was not compatible with meeting the NOx target, and was not able to be routinely repeated. A value of 95% combustion efficiency was able to be routinely achieved, and was compatible with meeting the NOx target.

Considerable effort was spent in trying to determine how combustion efficiency might be improved to meet the target. The challenge to meet the combustion efficiency targert of 98% is, indeed a very difficult one. The bulk boiler residence time is about 0.7 seconds. Further complicating the task is the aspect ratio of the boiler, i.e. the length of the boiler is not very much greater than its height or width (approximatelt 8 ft long x 8 ft high x 6 ft wide). It is

aggravates the situation. Burner modifications are being looked at which might increase the particle residence time.

Coal particle size distribution was also evaluated, the premise being that carbon content must be directly proportional to particle size. While the larger particle size fraction of the collected particulate (fly ash) did contain higher carbon contents than the smaller size fractions, the differences were not as great as expected. For example, it would not be possible to dramatically reduce the carbon content of fly ash by eliminating coal particles larger than 150 microns.

SYSTEM ECONOMICS

This phase of the work involved an economic evaluation of coal firing for existing small industrial boiler installations. In addition to a base case evaluation (the 15,000 lbm/hr natural gas fired Penn State boiler), various economic sensitivity studies which provide insight into the economics for other unit sizes, fuel price scenarios, capacity factors and other variables were carried out. The primary objective of this analysis was to determine how the coal option compares with natural gas firing on an annual basis. With coal firing the capital costs for the retrofit modifications as well as some additional operating and maintenance costs must be justified by the savings in fuel costs. The evaluation summarized here defines the incremental costs and savings on an annual basis as a result of the use of coal as a substitute for natural gas firing. The first year incremental operation and maintenance cost savings and the total retrofit capital requirement were then used to determine a simplified payback period. The details of the data and results have been summarized in a recent publication (Patel, et al., 1995).

KEY RESULTS FROM THE ECONOMIC EVALUATION

A series of economic comparisons were carried out for the base case and other systems involving different economic input parameters. For these studies a range of differential fuel costs were used, and other sensitivity studies were carried out to determine the effect of unit size, annual operating time, and carbon heat loss on simplified pay back time. Figures 3 to 5 show the results of these sensitivity studies. In addition to differential fuel costs (see Fig. 3), other sensitivity variables studied were shown to have significant effects on payback period. As shown in Fig. 4, increasing unit size is shown to quickly improve the economics. Also, as shown in Fig. 5, changes in the annual operating time from 4000 to 8000 hrs/yr showed significant effects on payback period. Typically industrial boilers have very high capacity factors (the base case for this study used 7000 Hrs/yr (equivalent to an 80 percent capacity factor)). Fig. 8 is of most interest as it shows that variations in carbon heat loss (combustion efficiency) have no significant effect on payback period for the range studied (2 to 6%).

Although this analysis was done relative to natural gas as the base fuel, the results can also be generally applied to oil firing as well. By knowing the differential fuel cost the payback period can be approximated from the attached curves. Although boiler efficiency with oil firing is typically about 5 percent better than with natural gas, the effect on payback period is relatively insignificant as was shown by the results of the carbon heat loss sensitivity study.

CONCLUSIONS/ RECOMMENDATIONS

The following specific conclusions are based on the results of the coal fired testing at Penn State and the initial economic evaluation of the HEACC system:

- A coal handling/ preparation system can be designed to meet technical requirements for retrofitting micro-fine pulverized coal.

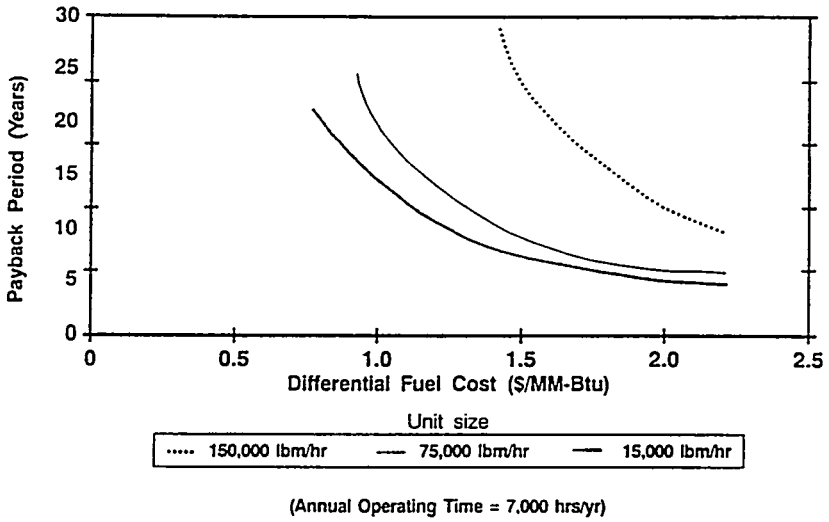

Figure 3 Payback Period as a function of Differential Fuel Cost and Unit Size

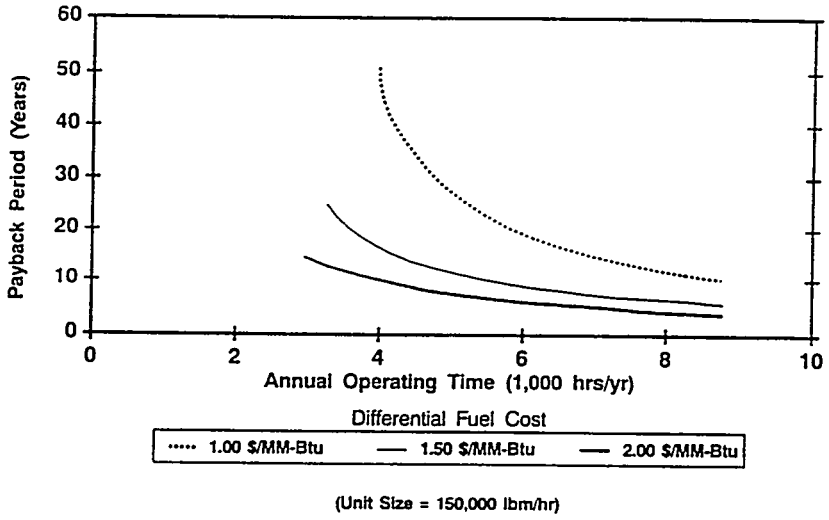

Figure 4 Payback Period as a function of Annual Operating Time

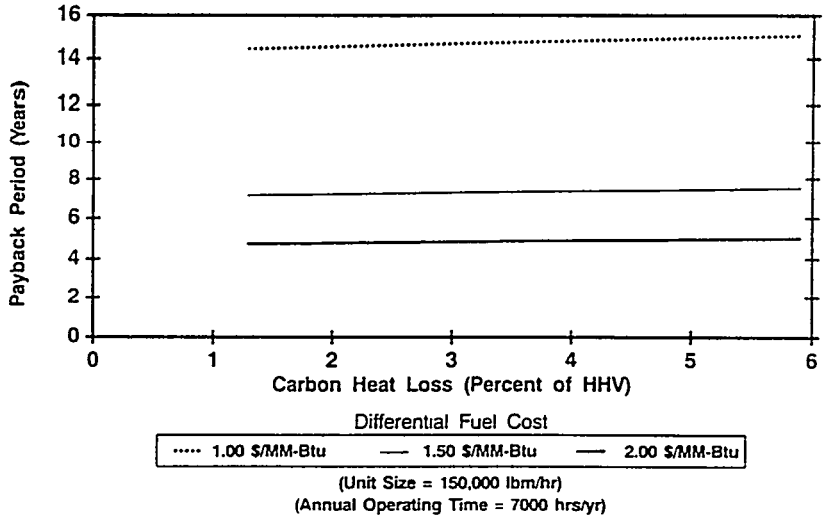

Figure 5 Payback Period as a function of Carbon Heat Loss

- The boiler thermal performance met requirements
- Combustion efficiencies of 95% could be met on a daily average basis, somewhat below the target of 98%
- NOx emissions can meet the target of 0.6 lb/million Btu
- The economic payback was very sensitive to fuel differential cost, unit size, and annual operating hours

As a result of recent long term tests using micronized coal (in another program), Penn State has experienced some convective pass ash deposition problems. To alleviate this problem they are planning to install additional soot blowers. Also, as a result of problems encountered during the 400 hour testing, the following modifications are planned for the Penn State system:

Coal feeding improvements
a) Improved raw coal/ storage and transport
b) Redesign/installation of a surge bin bottom
c) Installation of a gravimetric feeder
Monitoring of ash deposit effects
a) Air sparge/soot blower systems
b) Monitoring effects on heat transfer in the furnace and the convective pass
c) The use of ash deposition probes

In addition, ABB CE plans to modify the burner for more precise aerodynamic control of the fuel and air streams to improve the combustion efficiency and NOx emissions. Based on the results summarized in this paper the ABB/Penn State team and DOE/PETC have decided to conduct a 1000 hr demonstration (Task 5) of this program; it is currently scheduled to begin in July 1995.

REFERENCES

Patel, R. L., (1995), "Experimental Testing of a Retrofit Industrial Sized Burner Using Microfine Coal, "Proc. 20th International Conference on Coal Utilization & Fuel Systems".

Jennings, P. J., et al. (1994a), "Installation and Initial Testing of Micronized Coal in a Gas/Oil - Designed Package Boiler," Proc. 19th International Conference on Coal and Slurry Technology.

Jennings, P. J., et al. (1994b), "Development and Testing of a High Efficiency Advanced Coal Combustor: Industrial Boiler Retrofit," Proc. 11th International Pittsburgh Coal Conference, University of Pittsburgh.

Jennings, P. J., Rini, M. J., and McGowan, J. G. (1993), "Conversion of a Gas/Oil Designed Package Boiler to Micronized Coal Firing," Proc. Tenth International Pittsburgh Coal Conference, University of Pittsburgh.

Rini, M. J., Jennings, P. J., and McGowan, J. G. (1993), "Demonstration of a High Efficiency Advanced Coal Combustor for an Industrial Boiler," Proc. 18th International Conference on Coal and Slurry Technology.

Rini, M. J., LaFlesh, R. C., and McGowan, J. G. (1990), "Large Scale Combustion Applications of Beneficiated Coal Fuels," Proc. 15th International Conference on Coal and Slurry Technology.

Rini, M. J.. et al. (1988) "Progress in the Development of a High Efficiency Advanced Combustor for Boiler Retrofit," Proc. 13th International Conference on Slurry Technology.

Rini, M. J., et al. (1987) "Development of a High Efficiency Advanced Coal Combustor for Boiler Retrofit," Proc. 12th International Conference on Slurry Technology.

The following manuscript was unavailable at time of publication.

DEVELOPMENT/TESTING OF A COMMERCIAL-SCALE COAL-FIRED COMBUSTION SYSTEM

Ravi R. Chandran
Manufacturing and Technology Conversion Int'l.
6001 Chemical Road
Baltimore, MD 21226

Please contact author(s) for a copy of this paper.

The following manuscript was unavailable at time of publication.

DEVELOPING COAL-BASED FUEL TECHNOLOGIES FOR DOD FACILITIES

Dr. Alan W. Scaroni
Pennyslvania State University
Energy & Fuels Research Center
C211 Coal Utilization Lab
University Park, PA 16802

Please contact author(s) for a copy of this paper.

COMBUSTION CHARACTERIZATION OF BENEFICIATED COAL-BASED FUELS

O. K. Chow and A. A. Levasseur
ABB POWER PLANT LABORATORIES
Research and Technology
COMBUSTION ENGINEERING, INC.

Contract No. DE-AC 2289 PC 88654

INTRODUCTION

The Pittsburgh Energy Technology Center (PETC) of the U.S. Department of Energy is sponsoring the development of advanced coal-cleaning technologies aimed at expanding the use of the nation's vast coal reserves in an environmentally and economically acceptable manner. Because of the lack of practical experience with deeply beneficiated coal-based fuels, PETC has contracted Combustion Engineering, Inc. to perform a multi-year project on "Combustion Characterization of Beneficiated Coal-Based Fuels."

The objectives of this project include: 1) the development of an engineering data base which will provide detailed information on the properties of Beneficiated Coal-Based Fuels (BCFs) influencing combustion, ash deposition, ash erosion, particulate collection, and emissions; and 2) the application of this technical data base to predict the performance and economic impacts of firing the BCFs in various commercial boiler designs.

The technical approach used to develop the data base includes: bench-scale fuel property, combustion, and ash deposition tests; pilot-scale combustion tests, and full-scale combustion tests. Subcontractors to CE to perform parts of the test work are the Massachusetts Institute of Technology (MIT), Physical Science Inc. Technology Company (PSIT), and the University of North Dakota Energy and Environmental Research Center (UNDEERC).

To date, twelve beneficiated coal-based fuels have been acquired through PETC and tested at ABB Power Plant Laboratories Fireside Performance Test Facility (FPTF). These fuels included products from the micro-bubble flotation (Feeley, et al, 1987), spherical oil-agglomeration (Schaal, et al, 1990) selective micro-agglomeration (Corser, et al, 1992) and advanced froth flotation (Harrison, et al, 1992) processes. The results from these fuels indicate that firing the BCFs improved furnace heat transfer and fly ash erosion compared to their respective feed coals (Chow, et al, 1992). The predicted boiler performance and economic impacts when firing similar fuels in a 560 MW coal-designed and a 600 MW oil-designed unit showed good results (Hargrove, et al, 1994). However, there are still various technical aspects that need to be addressed for the effective utilization of BCFs. The beneficiated products are usually in wet filter cake form, they must be prepared in a fuel form that can be handled and re-dispersed prior to firing. The preparation process can change the original fuel particle size and association of inorganic particles, and hence can affect fly ash formation and deposition behaviors. Also, it is not clear how much of the improved performance is associated with grinding alone and how much of the benefit is attributed to the advanced coal cleaning process.

This paper will discuss the results from a series of combustion test runs recently conducted in the FPTF to address the effect of fuel fineness on performance. A conventionally cleaned at the mine Pittsburgh No. 8 was acquired and prepared at standard pulverized-coal fuel grind (70% through 200 mesh), fine grind (90% through 200 mesh) and ultra-fine grind (three fuel fineness. The three fuels were tested at firing rates ranged from 3.0 x 10^6 Btu/h to 4.0 x 10^6 Btu/h, under no staging and staged low NOx firing conditions.

RESULTS

Test Fuel

The ASTM analyses of the Pittsburgh No. 8 test coal is shown in Table 1. In general, the fuel and ash properties of this coal are consistent to those of typical Pittsburgh No. 8 feed coals previously evaluated in this program. It has approximately 2 % total sulfur. The ash fusion temperatures were relatively low to moderate, and moderate to high iron content in the ash.

Table 1

ASTM ANALYSES OF PITTSBURGH No. 8 COAL

Quantity	Pittsburgh No.
Proximate, wt. %	
Moisture	3.4
Volatile Matter	33.3
Fixed Carbon	56.5
Ash	6.8
Ultimate, wt. %	
Hydrogen	5.0
Carbon	73.5
Sulfur	1.8
Nitrogen	1.5
Oxygen	8.0
Ash Loading, lb/10^6 Btu	4.97
HHV, Btu/lb	13,673

Quantity	Pittsburgh No.
Ash Fusion Temp., °F	
I. T.	2310
S. T.	2420
H. T.	2480
F. T.	2530
Ash Composition, wt%	
SiO_2	47.8
Al_2O_3	25.8
Fe_2O_3	16.8
CaO	2.8
MgO	0.7
Na_2O	0.4
K_2O	1.3
TiO_2	1.1
P_2O_5	0.2
SO_3	2.5

The test coal was prepared in three grinds to provide a wide range of fuel fineness for evaluation. The standard (70% through 200 mesh) and fine (90% through 200 mesh) grinds were prepared in a ABB-CE size 271 bowl mill, and the ultra-fine (100% through 200 mesh) grind coal was prepared in a roller mill equipped with a turbine classifier. The resulting particle size distributions and mass mean diameter for each fuel fineness are shown in Figure 1.

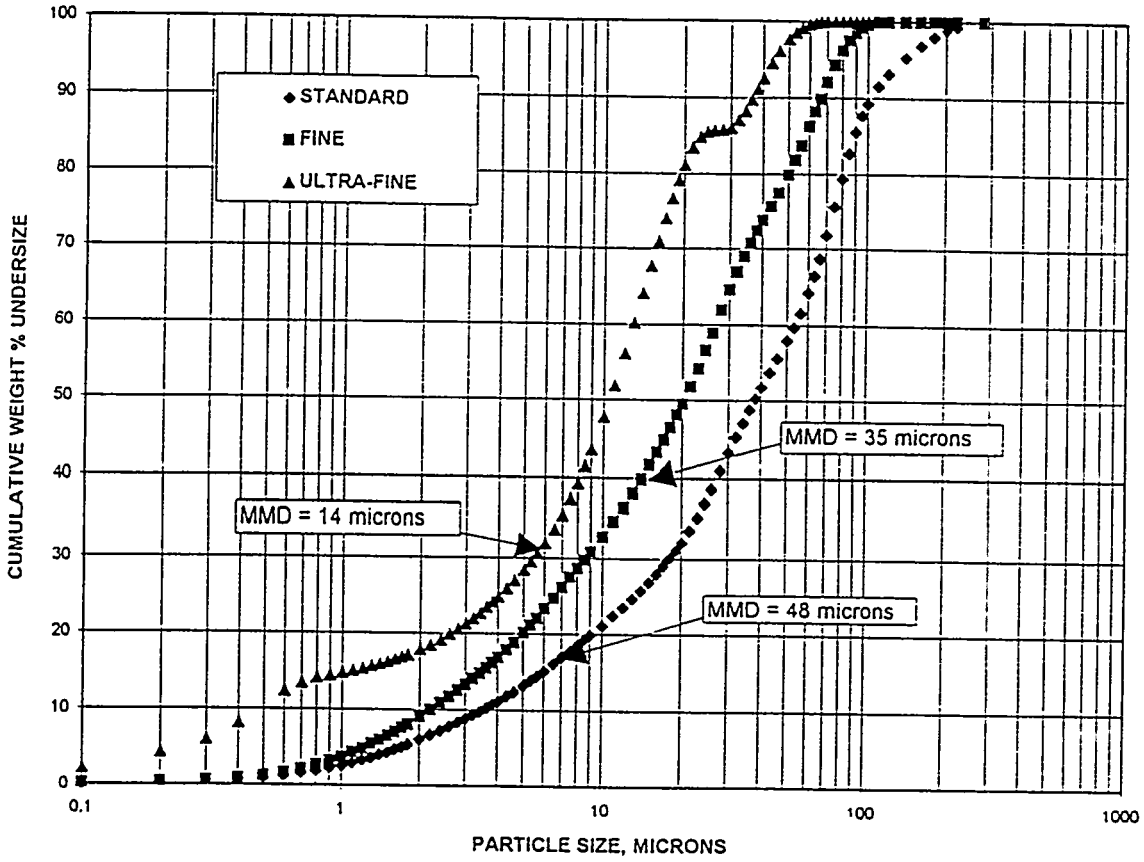

Figure 1. Particle size distributions of the standard, fine and ultra-fine grind Pittsburgh No. 8 fuels

Combustion Characteristics

In general, good, stable flames were obtained firing the Pittsburgh No. 8 at the three fuel fineness under standard and staged firing conditions. In all cases, carbon conversions improved with finer grind fuels.

A summary of the carbon conversions at the lower furnace of the FPTF is shown in Table 2. In all test runs, carbon conversions were greater than 99% at the FPTF stack exit. Carbon conversions at the lower furnace were significantly higher firing the finer grind fuels than the standard grind at either unstaged or staged firing conditions. However, the ultra-fine did not show significant improvement over the fine grind. During ultra-fine firing, the fine particles tended to agglomerate together and to form a scale on the feed system walls, resulting in occasional pulsing flame.

Table 2

Carbon Conversions of Pittsburgh No. 8 in The FPTF Lower Furnace

Fuel Fineness	Firing Rate, 10^6 Btu/h	Burner Stoichiometry	Carbon Conversion, %
Standard	4.0	1.2	95.6
	3.7	0.85	89.2
	3.0	0.6	88.1
Fine	4.0	1.2	99.3
	3.7	0.85	96.5
	3.0	0.6	89.5
Ultra-fine	4.0	1.2	99.2
	3.7	0.85	97.6
	3.0	0.6	96.8

Furnace Slagging

The furnace slagging characteristics of the Pittsburgh No. 8 coal significantly improved with finer grind fuels. A summary of the waterwall heat flux test results is shown in Table 3. The firing rate for the two staged conditions was reduced in anticipation of worsened furnace slagging performance. Previous test results from the FPTF firing a similar Pittsburgh No. 8 coal have shown furnace deposits developed under staged firing conditions were more tenaciously bonded to the waterwall panels (Chow, et. al., 1994).

Table 2

Heat Flux Summary of Beneficiated Micro-Agglomerate Fuels

Fuel Fineness	Firing Rate 10^6 Btu/h	Burner Stoichiometry	Furnace Temp., °F	Avg. Heat Flux, Btu/h/ft^2	Heat Flux Recovery, %
Standard	4.0	1.2	2990	64,104	37
	3.7	0.85	2900	65,348	41
	3.0	3.0	2740	44,217	67
Fine	4.0	1.2	2970	69,152	74
	3.7	0.85	2920	75,558	83
	3.0	0.6	2720	55,946	89
Ultra-fine	4.0	1.2	2960	83,271	77
	3.7	0.85	2920	96,687	100
	3.0	0.6	2720	51,579	92

Firing the two finer grind fuels resulted in higher average heat fluxes than with the standard grind. These results are most likely caused by the more rapid heat release rate from burning smaller coal particles. There was no noticeable difference in deposit coverage or deposit thickness developed from firing either fuel grinds. Thin, molten deposits were developed at all firing conditions with each fuel. However, deposit removal by soot blowing significantly improved firing the two finer grind fuels. Waterwall heat flux recoveries after soot blowing were significantly higher with the two finer grinds than the standard grind under similar firing and flame temperature conditions (Figure 2).

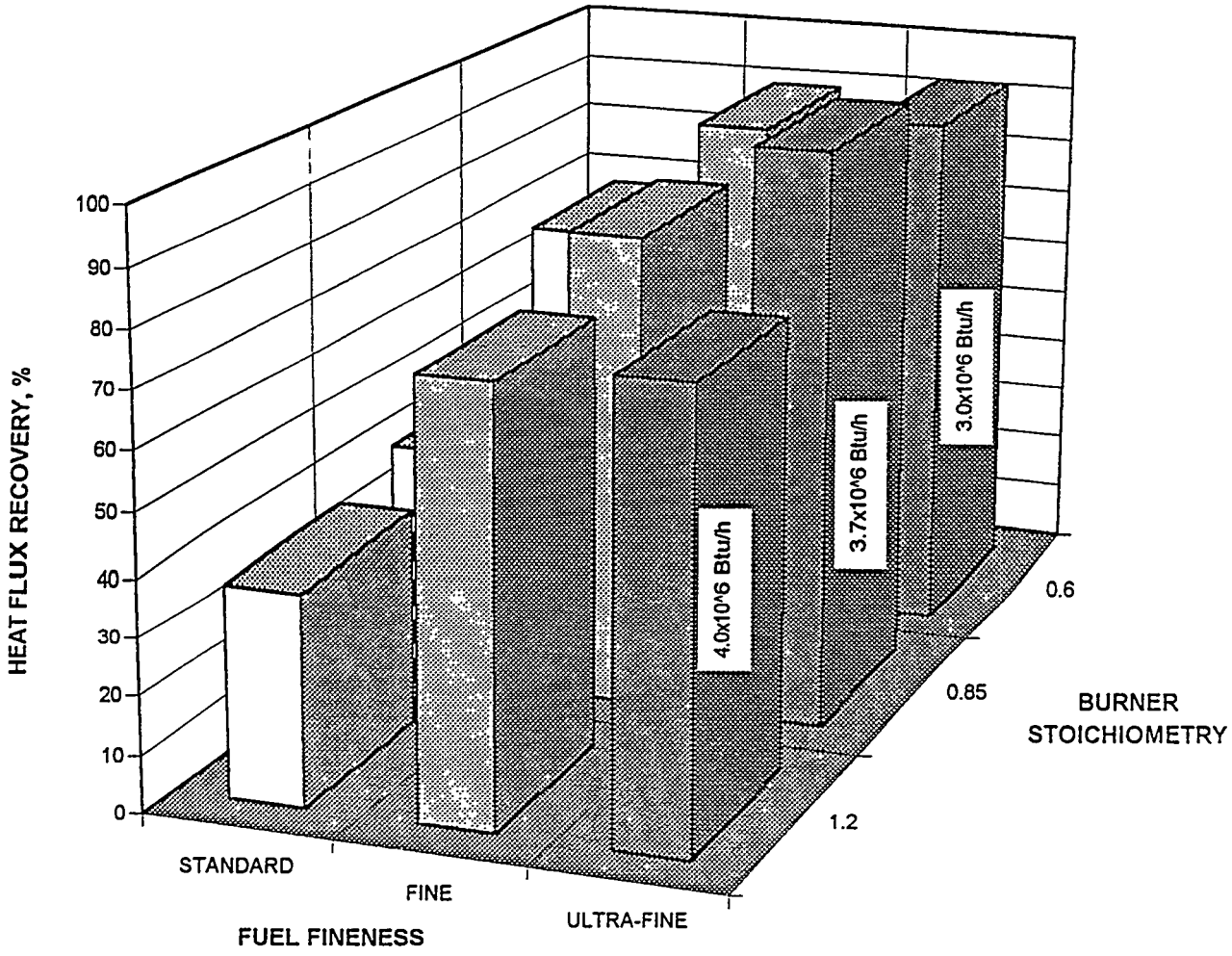

Figure 2 Effect of Fuel Fineness on Waterwall Deposit Cleanability

Convection Pass Fouling

The fouling characteristics of the Pittsburgh No. 8 coal was not affected by the fuel fineness. The FPTF results showed all three grinds had low fouling potentials at the gas temperature range tested (2100°F to 2350°F). The deposit buildup rates in the convective pass were low. Soot blowing was not required over a 12-hour period. Deposits developed were sintered, and could be easily removed from the tube surfaces. There was little difference in fouling characteristics between firing the fuels under standard or staged low NOx firing conditions.

Fly Ash Erosion

Fly ash erosion rate decreased with finer grinds. However, the reduction was relatively small compared to the BCF test results. As illustrated in Figure 3, the normalized erosion rate was reduced only by 6% and 15%, fine grind and ultra-fine grind, compared to standard grind.

The above results would indicate that the significant improvements observed firing the BCFs (over 60%) are mostly due to beneficiation. The cleaning process was effective in removing the larger inorganic particles and more erosive constituents such as quartz in the fuels.

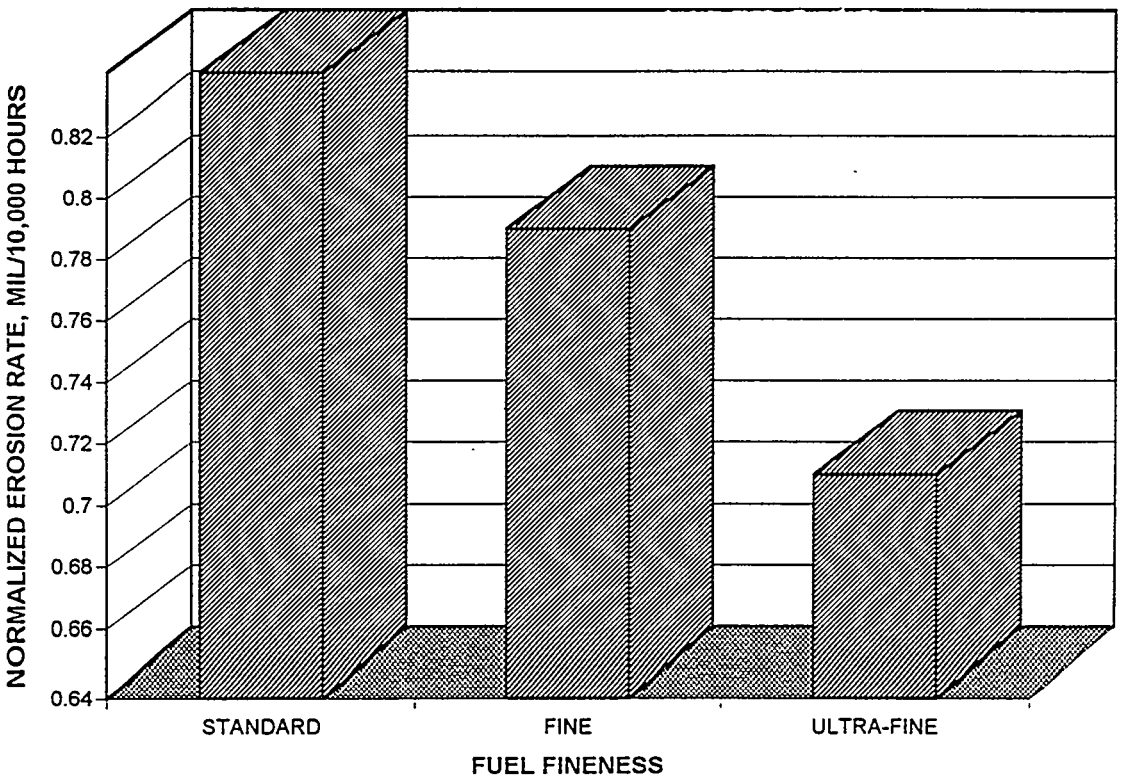

Figure 3 Effect of Fuel Fineness on Fly Ash Erosion Rates

CONCLUSIONS

Many of the beneficial effects associated with firing BCFs were observed with firing finer grind fuels. The combustion and carbon conversions of Pittsburgh No. 8 coal improved with finer fuel grinds at either unstaged or staged firing conditions. Furnace slagging also show significant improvement. Although similar waterwall deposits were generated between the three fuel grinds, deposit cleanability by soot blowing was significantly improved. Firing the finer grind fuels also resulted in higher average heat flux in the lower furnace. Improvement in ash fouling was not detected due to the low fouling characteristics of the test coal. Fly ash erosion was also reduced firing the finer grind fuels. However, the improvement was not as significant as with the BCFs.

A technical and economic evaluation of firing finer grind fuels in commercial units should be undertaken to compare with the BCF results.

REFERENCES

Chow, O. K., Griffith, B. F., Levasseur, A. A. and Hargrove, M. J., "Evaluation of Beneficiated Coal Micro-agglomerates in Various Fuel Forms," The Nineteenth International Conference on Coal Utilization & Fuel Systems, March 21-24, 1994.

Chow, O.K., Nsakala, N, Levasseur, A. A., Hargrove, M. J. "Fireside Combustion Performance Evaluation of Beneficiated Coal-Based Fuels," 92-JPGC-FACT-1, October, 1992.

Corser, M., Henshaw, W. and Logan, C., "Engineering Development of Selective Agglomeration Technology," Eighth Annual Conference on Coal Utilization & Environmental Control Contractors Conference, July 27-30, 1992.

Harrison, K., "Engineering Development of An Advanced Froth Flotation Technology," Eighth Annual Conference on Coal Utilization & Environmental Control Contractors Conference, July 27-30, 1992.

Hargrove, M. J., Gurvich, B., Kwasnik, A., Liljedahl, G., Miemiec, L. "Predictions of Boiler Performance When Firing Beneficiated Coal-Based Fuels," Proceedings of the 19th International Technical Conference on Coal Utilization and Fuel Systems, March, 1994

Schaal, A. M. and Lippsmeyer, B. C., "Proof-of-Concept Results Using the Arcanum/Bechtel Spherical Agglomeration Approach to Clean Ultra-fine Coals," EPRI's 15th Annual Fuel Science Conference, Palo Alto, California, June 19-21, 1990.

Feeley III, T. J. and Hervol, J. D., "Testing of Advanced Physical Coal Cleaning Processes," Fourth Annual Pittsburgh Coal Conference, Pittsburgh, Pennsylvania, September 28 - October 2, 1987.

DEVELOPMENT OF A PHENOMENOLOGICAL MODEL

FOR COAL SLURRY ATOMIZATION

JOHN P. DOOHER
ADELPHI UNIVERSITY
GARDEN CITY, NY

BACKGROUND AND INTRODUCTION

Highly concentrated suspensions of coal particles in water or alternate fluids appear to have a wide range of applications for energy production. For enhanced implementation of coal slurry fuel technology, an understanding of coal slurry atomization as a function coal and slurry properties for specific mechanical configurations of nozzle atomizers should be developed.

GOALS AND OBJECTIVES OF PROPOSED PROGRAM

As has been demonstrated, the complexity of coal slurries has prohibited obtaining a reasonable understanding of coal slurry atomization. The complex rheological behavior of many types of coal slurries requires an extensive characterization for each type of coal, each type of coal particle size distribution, chemical additive composition, and coal concentration. The relationship of these properties to the atomization process is therefore unclear and the ability to make a prediction as to whether a specific slurry will atomize well or whether a specific coal is suitable for combustion applications does not exist unless extensive testing is performed for each slurry. The overall objective of this program is to develop a phenomenological model for coal slurry atomization which has the capability of distinguishing atomization properties for different coal slurries. In order to avoid complications due to mechanical factors, the model will be developed for one type of air blast atomizer configuration.

Subsidiary technical objectives include:

- Ascertain the effect of physio-chemical properties of coal slurries on atomization.
- Ascertain the statistical influence on coal slurry atomization.
- Predict the atomized drop size of a coal slurry from a few basic coal and slurry properties.

ATOMIZATION MODELING (PHENOMENOLOGICAL APPROACH)

In order to model spray atomization of coal slurry fuels it is important to extract those elements of liquid fuel atomization which are most important. These are listed as follows:

* Particle Size Distribution of spray droplets

* Mechanical Parameters

  Atomization air or steam
  Orifice size
  Nozzle velocity of air
  Exit velocity of liquid
  Nozzle pressure

* Physical Characteristics of Liquid Fuel

  Viscosity
  Density
  Gas-liquid interfacial tension

The next step is to examine the theoretical basis for jet breakup and atomization. The first step is to analyze the basic hydrodynamics of liquid jets.

General Theory of the Break Up of Liquid Masses

For small amplitude perturbations, the Navier Stokes Equation can be replaced by

$$\delta V / \delta t = - \nabla p/\rho + \upsilon \nabla^2 V \qquad (1)$$

where υ is the kinematic viscosity, i.e. $\eta = \rho \upsilon$

With low velocities and the low viscosity

$$\delta V/ \delta t \sim V / \tau \sim a/\tau^2$$

$$\nabla p/\rho \sim p/a\rho$$

where τ is a characteristic time and a the characteristic dimension, i.e. jet radius. Noting that $P\sigma = \sigma /a$ is the pressure due to surface tension.

$$\delta V / \delta t \sim a/\tau^2 \sim P\sigma/ \rho a \sim \sigma/ \rho a^2$$

which gives a break up time τ of

$$\tau \sim \sqrt{\rho a^3/\sigma} \qquad (2)$$

The intact length of the jet with velocity U_0 is given by

$$L \sim \eta_0 \tau$$

With low velocities and large viscosity,

$$\delta V / \delta t \sim 0$$

$$\upsilon \nabla^2 V \sim \upsilon V / a^2 \sim \upsilon / a\tau$$

$$\upsilon V / a^2 \sim \upsilon / a\tau \sim P\sigma / \rho a \sim \sigma / \rho a^2$$

yielding a break up time τ

$$\tau \sim \rho\upsilon a / \sigma \sim \eta a / \sigma$$

The analysis presented here is based on techniques described in Levich.[1]

Intact length is $L \sim U_0 \tau$

For high air velocities, V_A the pressure due to the air P_A is important, i.e.

$$P_A \sim \rho_A V_A^2 >> P\sigma .$$

If the viscosity, υ is small

$$\delta V / \delta t \sim a/\tau^2 \sim P_A / \rho a \sim \rho_A V_A^2 / \rho a \qquad (3)$$

$$\tau \sim a/V_A \sqrt{\rho/\rho_A}$$

where ρ_A is the air density.

Intact length is $L \sim \tau V_A \sim \sqrt{\rho/\rho_A}\ a$

For large viscosity,

$$\upsilon / a\tau \sim \rho_A V_A^2 / \rho a$$

$$\tau \sim \upsilon\rho/\rho_A V_A^2 \sim \eta/\rho_A V_A^2 \qquad (4)$$

Intact length of jet $\sim \tau V_A = \mu/\rho_A V_A$

These phenomenological estimates provide the necessary relationship to develop a phenomenological model since the underlying breakup mechanisms are delineated under varying conditions that can occur in spray atomization. The next step in the analysis considers the break up of drops formed from jet disintegration.

Drop Break Up

The case Non-Turbulent Flow is considered first. As the drop impinges on the air stream, it is flattened as shown in Figure 1.

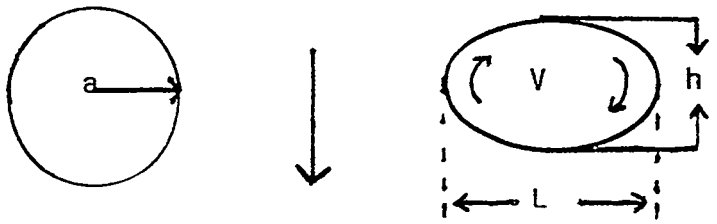

Figure 1.

The flattened drop will develop a minimum surface tension pressure on the flattened end

$$(P_\sigma)\,\text{min} \sim \sigma\ h/l^2\ .$$

If the internal pressure generated by the fluid in the drop circulating with a velocity V exceeds (P_σ) min then the drop will rupture. The force exerted by the external air on the

drop is given by $\rho_A V_A^2$ and that exerted by the circulating fluid on the drop surface is ρV^2. These must balance and equal the minimum surface tension.

$$\rho V^2 \sim \rho_A V_A^2 \sim \sigma h/l^2$$

If v is the volume of the drop then

$$l^2 h = v$$

$$l^2 = v/h$$

$\Delta p \sim \sigma /h \sim \rho_A V_A^2$ is the work done by compressing the drop which is equal to the increase in surface energy.

Therefore,

$$h = \sigma /\rho_A V_A^2$$

It follows that

$$\rho_A V_A^2 \sim \sigma /v h^2 \sim \sigma^3/v\rho_A^2 V_A^4 = \sigma^3/(4/3\pi)a_{cr}^3 \rho_A^2 v_A^4$$

or

$$(4/3\pi)a_{cr}^3 \sim \sigma^3/\rho_A^3 U_A^6$$

$$a_{cr}/a \sim \sigma /\rho_A V_A^2 a \sim W_e^{-1} \qquad (5)$$

What this means is that drops greater than a_{cr} in size will break up until the drop size is less than a_{cr} .

For turbulent flow, the results are modified as follows:

$$a_{cr}/a \sim = (W_e)^{-3/5} (\rho_A /\rho)^{2/5} \qquad (6)$$

In the next section, progress in determining the extensional viscosity of fluid are discussed.

EXTENSIONAL VISCOSITY MEASUREMENTS

The definition of extensional viscosity can be visualized in the simple case of the uniform extension of a cylinder of an incompressible Newtonian fluid along its axis. In a cylindrical coordinate system where z is oriented along the cylinder axis and the radial dimension is r, we may write the following for the case of symmetry about the ϕ direction:

$$\sigma_{rr} = -p + 2\mu \frac{\delta v_r}{\delta r} \tag{7}$$

$$\sigma_{\phi\phi} = -p + 2\mu \frac{v_r}{r} \tag{8}$$

$$\sigma_{zz} = -p + 2\mu \frac{\delta v_z}{\delta z} \tag{9}$$

For the stress equation where p is the hydrostatic pressure, and σ_{rr}, $\sigma_{\phi\phi}$, and σ_{zz} are the extra stresses normal to planes perpendicular to the r, ϕ, and z axis, respectively. The equation of continuity for an incompressible fluid is given by

$$\frac{v_r}{r} + \frac{\delta v_r}{\delta r} + \frac{\delta v_z}{\delta z} = 0 \tag{10}$$

We now note that

$$\sigma_{rr} + \sigma_{\phi\phi} = -2p + 2\mu \left(\frac{v_r}{r} + \frac{\delta v_r}{\delta r}\right) = -2p - 2\mu \frac{\delta v_z}{\delta z} \tag{11}$$

but since for equilibrium, $\sigma_{rr} = \sigma_{\phi\phi} = 0$, we obtain

$$p = -\mu \frac{\delta v_z}{\delta z} \tag{12}$$

Combining equations to eliminate p yields

$$\sigma_{zz} = 3\mu \frac{\delta v_z}{\delta z} = n_e \frac{\delta v_z}{\delta z} \tag{13}$$

where n_e is defined as the extensional viscosity, which is 3μ for a Newtonian fluid. There is evidence that the extensional viscosity can have an effect on atomization.[2,3]

Adelphi Extensional Viscometer

The Adelphi extrusion rheometer was modified to provide extensional flow. The viscometer is comprised of a testing chamber approximately 2 feet in length and 2 inches in diameter, followed by a 15" tube of diameter 0.19 inches. The diameter ratio of 10:1 provides adequate convergence for extensional effects. The sample is placed in the testing chamber. The testing chamber cover is fastened to the chamber wall and extrusion pressure is adjusted to an initial pressure. Samples are extruded and weighed and flow rates determined. The pressure is increased as determined by sample viscosity. Characteristic pressure versus shear rate curves are drawn and evaluated. From the resultant curve, the power law index, n, and the viscosity are determined. The extensional viscosity is determined using Binding's [4] analysis which subtracts the pressure losses in the extrusion tube which is viscometric in nature, leaving data on the entry pressure to the contraction which is directly related to the extensional viscosity.

In order to determine the effectiveness of the extensional viscometer, a verification was made using Binding's analysis to determine power law behavior of extensional viscosity. Figure 2 shows a log plot of the entry pressure vs. flow rate. Analysis indicates a slope of 1.2 consistent with the Newtonian calibration fluid.

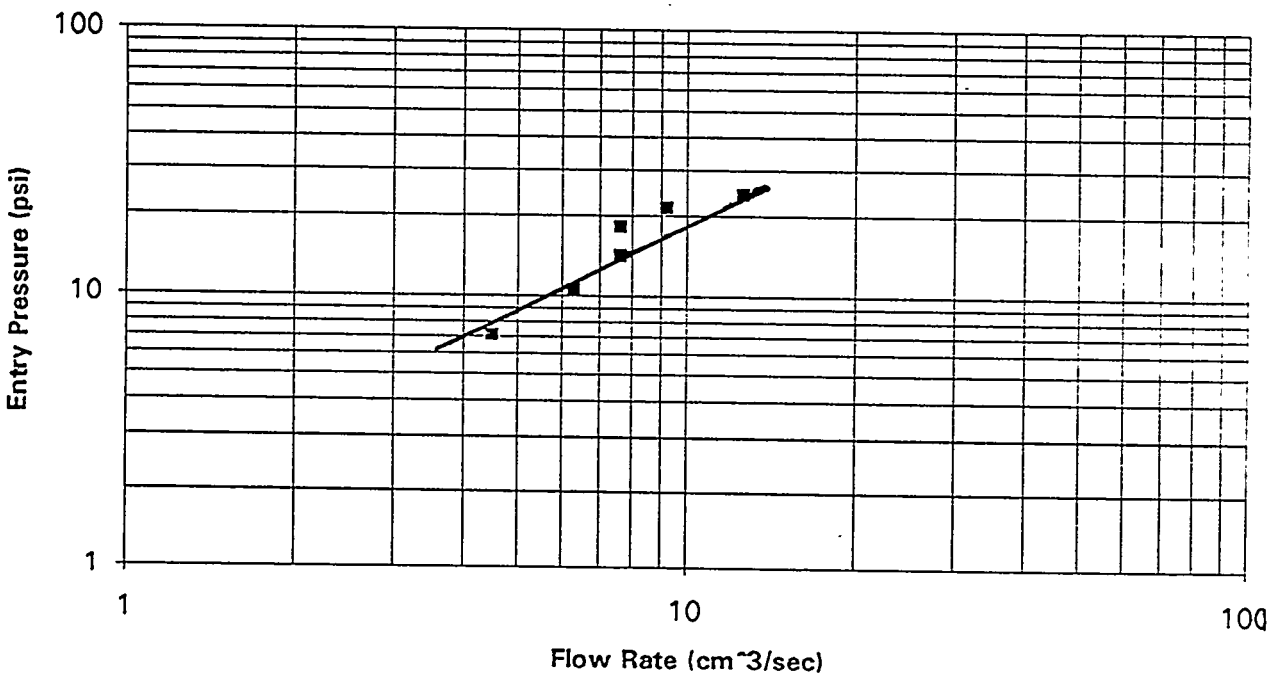

Figure 2. Log Plot of Entry Pressure vs. Flow Rate - Calibration Curve

1 V. G. Levich, Physicochemical Hydrodynamics, Prentice Hall 1962.

2 W. Rakitsky, "Rheological Properties of Coal Water Fuels Significant for Fine Spray Production During Combustion," Third Annual Pittsburgh Coal Conference Pittsburgh, PA, September 1986.

3 J. Dooher, D. Wildman, "A Comparison of Rheological and Atomization Data For Coal Water Mixtures and Liquid Mixtures," Fourteenth International Conference on Coal and Slurry Technology, April 1989, Clearwater, FL.

4 D.M. Binding, J. Non-Newtonian Fluid Mech., 27 (1988) 173-189.

KRAKÓW CLEAN FOSSIL FUELS AND ENERGY EFFICIENCY PROJECT

THOMAS A. BUTCHER AND BARBARA L. PIERCE
DEPARTMENT OF APPLIED SCIENCE
BROOKHAVEN NATIONAL LABORATORY
UPTON, NEW YORK 11973

The Support for Eastern European Democracy (SEED) Act of 1989 directed the U.S. Department of Energy (DOE) to undertake an equipment assessment project aimed at developing the capability within Poland to manufacture or modify industrial-scale combustion equipment to utilize fossil fuels cleanly. This project is being implemented in the city of Kraków as the "Kraków Clean Fossil Fuels and Energy Efficiency Project." Funding is provided through the U.S. Agency for International Development (AID) . The project is being conducted in a manner that can be generalized to all of Poland and to the rest of Eastern Europe [1].

The historic city of Kraków has a population of 750,000. Almost half of the heating energy used in Kraków is supplied by low-efficiency boilerhouses and home coal stoves. Within the town, there are more than 1,300 local boilerhouses and 100,000 home stoves. These are collectively referred to as the "low emission sources" and they are the primary sources of particulates and hydrocarbon emissions in the city and major contributors of sulfur dioxide and carbon monoxide.

PROJECT DESCRIPTION

The project plan includes three phases which have been developed through extensive working contacts between DOE and Polish representatives. Phase I was planned to gather information about the characteristics of the existing sources, the costs and performance expectations for some selected pollution reduction options, options for municipal actions promoting pollution reduction, and relative cost-effectiveness of options. In the second phase, a series of public meetings was conducted to inform U.S. and Polish companies about the program. Phase III is the largest part of the program. In this phase, 50% cost-share funding is provided to develop U.S./Polish joint ventures producing goods or services addressing the low emission sources. At present eight U.S. companies are active in Kraków as part of this program.

Brookhaven National Laboratory has been involved with Phase I of this program which involves efforts both on the Polish and the U.S. side. A part of the Phase I work has addressed building energy demands and the impacts which conservation measures may have on fuel use and emissions. DOE's Office of Conservation and Renewable Energy is the lead DOE office for this part of the work and results from this effort are not included here. All other aspects of the program are being managed by DOE's Office of Fossil Energy through the Pittsburgh Energy Technology Center (PETC). Brookhaven National Laboratory (BNL) as well as Burns and Roe Services Corp. have been supporting PETC. Work being done in Kraków is being managed by the Biuro Rozwoju Krakowa (BRK or Kraków Development Office) and BRK is working under subcontract to BNL.

The Phase I work started in 1991 and parts of it have been presented in papers and a series of reports. A report summarizing all of the Phase I work, including the building energy conservation activities, has recently been completed. Major components of Phase I are as follows:

TESTING

Heating stoves in Kraków are very large masonry furnaces with ornate tile exteriors. It has been estimated that there are about 7 million of these stoves throughout Poland. During the heating season, these stoves are fired once or twice each day. The fire burns actively for about an hour. During this time the masonry is heated and this stored heat keeps the apartment warm for the next 12 hours. During Phase I a testing program on these stoves was completed. One of the objectives of the test program was to provide baseline thermal efficiency and emissions data as input to evaluations of costs and benefits of alternative options for heating these flats as discussed below. The second primary objective was to provide an assessment of the possibility of reducing emissions by using improved fuels in these stoves. A facility for studying the emissions and efficiency of home stoves was build the Academy of Mining and Metallurgy in Kraków with guidance and test equipment provided by U.S. participants. The system uses a dilution tunnel method to determine gaseous pollutant emission rates and flue gas sensible heat loss rate on a continuous basis. Particulates are sampled in the dilution tunnel and are averaged over the firing cycle. One of the U.S. companies currently active in Kraków is continuing to use this facility in their work on improved briquettes.

A second aspect of the Phase I testing work included hand-fired and stoker-fired boilers. Tests were conducted at two of the larger stoker-fired boiler houses and included investigations of the benefits of using improved fuels. Hand-fired boilers in Kraków include steel and cast iron units and coke, coal/coke mixtures, and coal are used as fuels. Tests were done at two sites with each of these fuels and also some locally made briquettes.

Details of the testing program and results have been presented earlier [2,3]. Using these results as well as results of an inventory done of the boiler and stove population in the city the contribution of the most important source categories to the total emissions inventory in the city can be estimated. This is presented in Table 1.

Table 1. Comparison of Contribution of Boilers and Home Stoves to Kraków Emissions

		Annual Emissions (metric tons per year)				
	Fuel Use (MT/yr.)	Particulates	CO	Volatile Organics	NOx	SO2
Stokers without cyclones	20473	173	415	0	73	600
Stokers with cyclones	217193	911	2717	0	685	6350
Hand-fired boilers-coke	51748	77	3622	28	74	918
Hand-fired boilers - coal/coke mixtures	51953	256	3866	325	60	1033
Hand-fired boilers - coal	32276	339	1688	132	71	585
Home stoves - coal fired	85000	1530	3620	221	470	782
Totals:	458642	3286	15928	706	1433	10270

ENGINEERING STUDIES

The Phase I engineering studies examined specific options for reducing emissions which were selected by the program's Bilateral Steering Committee as the most promising for the future. The purpose of

this analysis was to determine the costs of implementing the options. In some cases these costs are very specific to the part of the city and here site specific analyses were done. These studies included:

- Extension of the district heating system to allow local, hand-fired boilers to be shut down.
- Replacement of existing hand-fired boilers with new gas-fired units.
- Conversion of home stoves to electric heating
- Modernization of boiler houses (new boilers and pollution controls)
- Supply of improved fuels for the home stoves.

AIR QUALITY ANALYSIS

For each specific option dispersion modelling studies were done to provide estimates of the impacts that implementation would have on local air quality. These results have been very important in showing city groups specific benefits which they will realize from options which may have economic burdens. Also analyses were done to evaluate the impact of completing the most promising measures throughout the entire city, effectively eliminating pollution from these small sources. The results show that success in eliminating the low source pollution would greatly improve the city's air quality. It is not enough, however, to bring the city fully into compliance with targeted ambient air quality standards.

INCENTIVES ANALYSIS

The primary objective of incentives analysis is to define and evaluate incentives that the city could offer to encourage implementation of options under investigation in this project. Based on an economic analysis of each of these options, possible incentives are identified. The incentives are then evaluated in terms of their technical and legal feasibility, cost, and effectiveness. Some results of the incentives analysis are discussed in more detail below.

PUBLIC RELATIONS

A public opinion survey was administered to the residents of Kraków. Results show that most residents consider air pollution to be an important issue and that most residents consider industry and traffic to be the main sources of air pollution. A significantly higher portion of Old Town residents feel that the low-stack sources are the most important sources, however. While residents state that they are willing to pay to reduce pollution, the amount that they are willing or able to pay is probably not sufficient. Residents also feel that city authorities should take responsibility for cleaning the air.

Based on the survey results, a public relations campaign has been defined to inform Kraków's residents about the low-stack sources and about this project. This is being done through press releases and briefings for journalists, seminars, and production of brochures and educational films.

COMPARISON OF OPTIONS

At the present time the studies described above have largely been completed and a comprehensive Phase I report has been prepared and is being reviewed by various groups within the city. With all of this information in-hand it becomes appropriate to make comparisons of the relative costs and benefits of the various options. Generally, reducing pollution from these sources will present a cost burden which can be met in a variety of ways including direct capital subsidies, higher energy costs, increased rents, directed tax reliefs, low interest loans from environmental funds etc. Regardless of how the costs are absorbed it is clearly in the best interest of the city to promote the most cost-

effective options. There are many different ways in which options can be compared. One approach being used in this program is based on a spreadsheet program written under DOE sponsorship specifically for making simple comparisons between such options [4].

The spreadsheet program was written as a screening tool, providing a rapid method of analysis of many options primarily to aid policy decisions on a city-wide scale. Two important simplifying assumptions are used in the model including: 1) constant fuel and electric energy prices over the project life, and 2) the use of averaged capital costs for conversions between options and other costs averaged for large categories of emission sources. This spreadsheet was never intended and should not be used for project investment analysis which must be done on a case-specific basis with energy price escalation scenarios based on actual expected project start dates. This second point is especially important in Poland and other Central European countries where energy prices have been changing rapidly. Even with these limitations the spreadsheet program is a very effective and efficient tool for the kind of rapid comparisons for which it is intended.

In the spreadsheet program all of the low emission sources in the city are placed into categories based on physical characteristics and type of fuel used. This spreadsheet has been developed as a general tool and has been applied to several Central European cities. In the application to Kraków the low emission sources have been divided into 25 categories. For each of these categories information is entered on total current (baseline) fuel use, efficiency, fuel type and cost, air pollutant emission factors, operating costs, and maintenance costs. In Kraków this information was derived from surveys made of the boiler and stove populations and also from the engineering cost studies and the source testing program conduced as part of this work. For some categories the baseline fuel use is input as zero, but all other parameters are fully defined. These categories which have zero current fuel use are considered possible future options as replacements for some portion of the current capacity. For example one category is coal-fired tile stoves with a very substantial current fuel use and another is the same stoves firing smokeless briquettes which are not yet available in Kraków. In a spreadsheet run the impacts of using such a candidate alternative fuel in some or all of the home stoves can be evaluated.

In evaluating options using the spreadsheet there are several choices:

1. heating capacity can be changed from one category to another (for example from hand-fired boilers to gas-fired boilers);
2. the efficiency of boilers or stoves in a category can be increased (by adding economizers to boilers for example);
3. heat demand and fuel use in a specific category can be reduced through building energy conservation measures;
4. pollution controls can be added or upgraded in a specific source category.

For each of these choices capital costs of the modifications must be input as well as operating, fuel, and maintenance costs. Output from a spreadsheet run includes total emissions for each pollutant before and after the option is implemented, and total annual "user" costs before and after. The user costs include energy costs, operating costs, and maintenance costs.

Capital costs include direct costs which the end users must pay for implementation of the project but generally do not include all infrastructure costs such as upgrading electrical or gas distribution networks to meet increased demand following conversions. It is assumed that such costs are met by the utilities and are reflected in current energy prices.

The spreadsheet program provides details of costs and emissions of specific pollutants before and after conversion in tabular and graphical form. It is useful, also, to have a single number which indicates the cost effectiveness of each case being evaluated. To do this emissions of specific pollutants are first combined into a single "Equivalent Emission" defined as:

$$Ee = 2.9\ (Ep+ENO_X) + 0.5\ ECO + ESO_2$$

where: Ee = Equivalent Emissions, metric tons per year
Ep = particulate emissions, metric tons per year
ENO_X = nitrogen oxide emissions, metric tons per year
ECO = carbon monoxide emissions, metric tons per year
ESO_2 = sulfur dioxide emissions, metric tons per year

Conversion or upgrade capital costs are then annualized assuming a project life of 20 years and an interest rate of 15%. This annualized capital cost is then added to the annual user cost and the result is termed the "user combined cost". Finally, for any specific option implemented the change in user combined cost is calculated per-ton of reduction of equivalent emissions. This user combined cost-per-ton of Ee reduction is then taken as a primary basis for comparing options. In addition to this relative measure of option cost-effectiveness it is also necessary to consider the impact of options on total emissions. Options which are highly cost effective but which do not have substantial impacts on total emissions obviously should not be given high priority.

Table 2 shows a comparison of a selected group of options. The comparison is based on the combined cost-per-ton of Equivalent Emission reduced as discussed above and also the capital investment required per ton on Equivalent Emission reduction. Options 1 to 5 address the home stoves. In options 1,2, and 3 the stoves would simply change to the use of smokeless briquettes. In the Phase I test work fuels of this type were tested and produced very dramatic reductions in emissions, most notably particulates which decreased by a factor of 10. This fuel is not currently on the market however, and there is some uncertainty about its actual price. Also during the Phase I test program a new procedure for operating the stove was developed which led to reduced emissions with the briquettes and increased efficiency. Options 1-3 in Table 1 include different assumptions about price and efficiency for the briquettes. Option 1 is very optimistic and assumes that the briquettes can be sold for about the same price as current coal and that the new operating procedure will be promoted with the new fuel. In this case the residents will have reduced annual operating costs leading to a negative value for the combined cost per ton figure. Option 2 represents the same price assumptions but does not take credit for increased efficiency with briquettes. Again the option looks very attractive. In Option 3 the briquettes are assumed to cost much more than coal - $115/ ton compared to $80/ton - and there is no credit taken for efficiency improvement. This option is certainly less attractive but it is still very competitive with some of the others.

Under Option 4 home stoves in the Łobzow part of Kraków are converted to electric heating. This part of the city has spare electric power capacity and is considered to be very suitable for such electric conversions. In making these conversions the stove is not removed but electric resistance heating elements are simply inserted into the firebox. It is assumed that the owner of the converted stove will have installed a dual rate electric meter and only use the heating inserts during the low-rate daily time periods. In Option 5 the stoves are removed, and a small gas-fired boiler and hydronic heating system are installed in each flat. This option has been receiving considerable attention in the city and is being implemented in some areas. It is clearly, however, an expensive approach.

Table 2. Comparison of Selected Options for Reducing Emissions From Low Sources in Kraków

Option		Combined Cost per Metric Ton of Equivalent Emission Reduction	Capital Cost per Metric Ton of Equivalent Emission Reduction
1	Use of smokeless briquettes in home stoves assuming current efficiency is 52% and efficiency with briquettes is 72%. Same price for both fuels.	-$ 507.	$ 0.
2	Use of smokeless briquettes in home stoves assuming efficiency is 52% both with current fuel and briquettes. Similar price for both fuels.	- $237.	$ 0.
3	Use of smokeless briquettes in home stoves assuming efficiency is 52% both fuels. Current coal price is $80/metric ton and briquette price is $115/metric ton.	$ 390.	$ 0.
4	Conversion of home stoves to electric heating in Łobow part of Kraków.	$ 473.	$ 5,181.
5	Replacement of home stoves with small, gas-fired heating boilers.	$1,267.	$ 8,500.
6	Conversion of hand-fired boilers which use coal to gas	$1,070.	$3,160.
7	Conversion of hand-fired boilers which use coke to gas.	$1,730.	$9,035.
8	Conversion of hand-fired boilers which use coal to coal/coke mixtures.	$1,245.	$ 0.
9	Elimination of hand-fired boilers which use coke by connection to the district heating system	-$177.	$6,100.
10	Elimination of hand-fired boilers which use coal by connection to the district heat system	-$114.	$2,190.
11	Stoker-fired boilers - use of graded coal, addition of controls and improved operations	$ 84.	$ 946.
12	Stoker-fired boilers - boiler house modernization including new boilers and pollution controls	$3,280.	$10,900.

Options 6 to 10 address the small hand-fired boilers. In options 6 and 7 boilers currently firing coal and coke are converted to gas firing (boiler replacement). This option is clearly an expensive one but it is being promoted very strongly within some parts of the city for which no other option is available. Conversion of coal-fired boilers to gas is more attractive than coke-fired boilers simply because of the higher emission factors with coal-firing. In option 8 boilers which currently fire coal are converted to coal/coke mixtures which yield considerable reductions in particulate emissions. It is interesting to note that this approach is less attractive than direct conversion to gas. With conversion to the mixed fuel the emissions reductions are not as great as with conversion to gas and there is still the need for operators to be present. In Options 9 and 10 the hand-fired boilers are eliminated by connecting their load to the district heating system. This involves the replacement of the boilers by heat exchanger stations. The figures in Table 1 show this to be a very attractive option. It should be noted, however, that capital costs for connection to the district heat system are very site specific. For the areas evaluated during the Phase I engineering studies these costs ranged from $22 to $598 per kW of capacity. An average value of around $90/kW was used for the figures listed in Table 2.

Options 11 and 12 address the larger, stoker-fired boilers. In Option 11 it is assumed that the performance of the existing boilers is improved through the addition of automatic controls which will allow the boilers to operate at lower excess air levels and higher efficiency. In addition it is assumed that the current fine coal used in these boilers is replaced by graded coal, properly sized. With this approach it is assumed that the boiler efficiency is improved by about 10% and the capital cost of the controls is $17/kW. The graded coal is assumed to cost $42/ton compared to $31/ton for the baseline coal. Option 12 represents a drastic modernization of the boiler houses including the installation of Polish made fluid bed boilers burning very low grade fuel with a sorbent added, and a baghouse dust collector. The capital cost for this option is $244/kW. This option was developed during the Phase I studies as part of a general modernization study conducted jointly by Polish and American firms. Work in the U.S. was done by Burns and Roe Services Co. and Burns and Roe Engineering Co. Of the options considered this was the lowest cost approach.

Another approach towards comparing options involves examining the amount of emission reduction per dollar required from the city . During the Phase I work recommendations were developed for incentives programs to promote specific options [5]. These options in every case involve some cost to the city. The level of incentive was developed to make the option economically attractive to the owner,investor, or resident involved. The economic evaluations done as part of these were more site specific and detailed than those included in the spreadsheet discussed above. Several scenarios were used for energy price trajectories. Table 3 shows the results of this comparison using one energy price scenario.

Table 3 includes two cases for the use of briquettes in home stoves. Both assume that initially subsidies will be applied to effectively make this fuel less expensive than coal. The difference in the two scenarios is the rate at which those subsidies would later be withdrawn.

Generally the results in Table 3 show a relationship between options which is similar to the results of the simpler spreadsheet analysis. The use of the briquettes and connection to the district heating system are more attractive than the other options.

Table 3. Incentives and Equivalent Emission Reductions

Option	Incentives Required (Present Value over 20 Years)	Equivalent Emissions Reduction per $1,000 (tons)
Connect hand-fired boilers to the district system	$198,005.	17.43
Convert hand-fired boilers in Old Town to gas	$759,858.	5.19
Convert tile stoves to electric inserts	$975,571.	5.04
Briquettes (gradual withdrawal of subsidies)	$1,360,000.	24.63
Briquettes (rapid withdrawal of subsidies)	$600,743.	55.77

PLANS

Currently, eight U.S. companies are working to develop joint venture projects in Kraków as part of Phase III program. These projects are focused in the option areas which now appear most attractive for the city including: briquettes, modernization of the stoker-fired boiler houses, and expansion of the district heating system. BNL in cooperation with BRK in Kraków are now beginning some new activities which have been designed to help both these joint venture projects as well as the city of Kraków more directly. This work includes: seminars for other Polish cities on the work in Kraków, a conference to be held in Kraków in October, 1995, the development of a master plan for the reducing pollution from the low emission sources , the development of a Geographical Information System within Kraków to allow rapid evaluation of low emission source projects, site-specific feasibility studies in support of the Phase III projects, and direct assistance to the U.S. companies currently working in Kraków.

REFERENCES

1. Gyorke, D.E. Pittsburgh Energy Technology Center's overview of the Kraków projects. Proc. Conf. on Alternatives for Pollution Control from Coal-Fired Low Emission Sources, Plzeň, Czech Republic, April 1994. pp. 7-18. (DOE Report CONF-9404166).
2. Jaszczur, T., Lewandowski, M., Szewczyk, W., Zaczkowski, A., and Butcher, T., Coal-fired tile stoves-efficiency and emissions. ASHRAE Transactions 1995, V. 101, Pt.1
3. Cyklis,P., Kowalski, J., Króll, J., Włodkowski, A., Zaczkowski, A., Boron,J. and Butcher,T.,Heating boilers in Kraków, Poland: options for improving efficiency and reducing emissions. ASHRAE Transactions 1995, V. 101, Pt.1
4. Hershey, R., Barta, E. Progress in emission reduction and heating system modernization in Cesky Krumlov. Proc. Conf. on Alternatives for Pollution Control from Coal-Fired Low Emission Sources, Plzeň, Czech Republic, April 1994. pp. 51-60. (DOE Report CONF-9404166).
5. Uberman, R., Łazęcki, A., Pierce, B. Incentives for reducing emissions in Kraków. Proc. Conf. on Alternatives for Pollution Control from Coal-Fired Low Emission Sources, Plzeň, Czech Republic, April 1994. pp. 19-28. (DOE Report CONF-9404166).

STUDIES OF THE COMBUSTION OF COAL/REFUSE DERIVED FUELS USING THERMOGRAVIMETRIC- FOURIER TRANSFORM INFRARED-MASS SPECTROMETRY

HUAGANG LU, JIGUI LI, WILLIAM G. LLOYD, JOHN T. RILEY, AND WEI-PING PAN
CENTER FOR COAL SCIENCE
DEPARTMENT OF CHEMISTRY
WESTERN KENTUCKY UNIVERSITY

INTRODUCTION

According to a report of the Environmental Protection Agency (EPA), "Characterization of Municipal Solid Waste (MSW) in the United States", the total MSW produced in the U.S. increased from 179 million tons in 1988 to 195 million tons in 1990.[1] The EPA predicted that the country would produce about 216 million tons of garbage in the year 2000.[2] The amount of waste generated and the rapidly declining availability of sanitary landfills has forced most municipalities to evaluate alternative waste management technologies for reducing the volume of waste sent to landfills. The fraction of MSW that is processed by such technologies as separation and recycling, composting, and waste-to-energy was forecast to increase from a few percent today to 30-40% by the year 2000.[3]

Waste-to-energy conversion of MSW can appear to be attractive because of the energy recovered, the economic value of recycled materials, and the cost savings derived from reduced landfill usage. However, extra care needs to be taken in burning MSW or refuse-derived fuel (RDF) to optimize the operating conditions of a combustor so that the combustion takes place in an environmentally acceptable manner. For instance, polychlorinated dibenzodioxins (PCDDs) and polychlorinated dibenzofurans (PCDFs) have been found in the precipitator fly ash and flue gas of some incinerator facilities in the United States and Europe. The amount of PCDDs and PCDFs occurs only in the parts-per-billion to parts-per-trillion range, but these chlorinated organics exhibit very high toxicity (LD_{50} < 10 μg/Kg). The compound 2,3,7,8-tetrachlorodibenzodioxin has been found to be acnegenic, carcinogenic, and teratogenic. This has slowed or even stopped the construction and operation of waste-to-energy plants.[4-7]

Some important studies have been conducted to reduce the release of chlorinated organics. Recently, Lindbauer[8] reported that co-firing an MSW combustor with 60% coal drastically reduced the PCDD/PCDF levels. Sulfur in coal was also found to reduce PCDD/PCDF formation, even at S/Cl ratios as low as 0.64.[9] It was indicated that sulfur can suppress the production of Cl_2 so that the formation of chlorinated aromatics is inhibited by the Deacon reaction:

$$SO_2 + Cl_2 + H_2O \text{ -----> } SO_3 + 2HCl \qquad (1)$$

However, it is important to note that, depending on the coal type, the coal combustion environment can contain organic precursors and Cl_2 that can actually facilitate PCDD/PCDF formation. Additional research is needed to develop optimum co-firing conditions and parameters. Investigations are also needed to determine why and how the co-firing of high sulfur coals with MSW reduces the polychlorinated organic residue emissions from the MSW.

In this paper we report the thermal analytical behavior of two coals, polyvinyl chloride (PVC), cellulose, and newspaper. The PVC, cellulose, and newspaper can be used to formulate a "representative" synthetic MSW.

EXPERIMENTAL

The materials used in this project included two bituminous coals, a medium molecular weight PVC resin from the OxyChem Corporation, cellulose from the Whatman Co., and shredded newspaper. Analytical data for the samples are given in Table 1.

A TA Instruments Model 951 Thermogravimetric Analyzer (TG) interfaced to a Perkin Elmer 1650 Fourier Transform Infrared Spectrometer (FTIR) was used in this study. The horizontal quartz furnace of the TG was connected to the 10 cm gas cell of the FTIR using an insulated teflon tube heated to a temperature of 150°C. The TG was also interfaced to a VG Thermolab Mass Spectrometer (MS) using a fused silica capillary sampling tube heated to approximately 170°C. A teflon splitter divides the gases from the TG into two parts, one to the FTIR (~95%), and the other to the MS (~5%). Figure 1 is a schematic of the TG-FTIR-MS system.

In the TG experiments all samples (~300 mg each) were heated in air (50 mL/min) at a rate of 10°C/min to 700°C. The spectra and profiles of gaseous species evolving from the TG system were recorded and analyzed by the TGA-FTIR-MS analytical system.

RESULTS AND DISCUSSION

TG-DTG Results

A comparison of the TG curves for the five raw materials (cellulose-001, newspaper-002, PVC-003, coal 90003-005, and coal 92073-006) are shown in Figure 2. The TG thermograms reveal some distinguishing characteristics of the five raw materials:

- There is no moisture in the PVC.
- The PVC, newspaper, and cellulose decompose at much lower temperatures and more rapidly than the coals.
- Ignition peaks are obvious for the newspaper (388°C) and cellulose (372°C) samples.
- Residues decrease in the order of coal 92073 (24.8%), coal 90003(8.75%), newspaper (6.58%), cellulose (0.57%), and PVC (0%).
- Newspaper continues to decompose until nearly 700°C

For PVC, the initial weight loss is clearly due to the loss of HCl. This can be inferred from the percentage (47.5%) of HCl in PVC and is confirmed by FTIR data. The second and third weight loss are contributed by different molecular weight PVC chains. The newspaper is not decomposed completely, possibly owing to the presence of mineral fillers.

FTIR Results

Figures 3 and 4, as examples, are three-dimensional FTIR graphs of Coal 92073 and PVC. The relative axes are absorbance (vertical), wavenumber (horizontal) and time (perspective). However, there are some differences between the two spectra. There are more water peaks in 90003 than in 92073 (1300-1700 cm-1 and 3500-4000 cm-1). This can be attributed to more volatile matter

and hydrogen in 90003. The COS (2073 cm-1) and SO_2 (1374 cm-1) peaks are stronger for coal 92073 than for 90003 due to the higher sulfur content. In coal 92073 spectra, the peaks at 1771 and 1171 cm-1 can be attributed to acetic acid by comparing their shapes and wavenumber with standard spectra. Since the absorption of acetic acid from 3300 to 2500 cm-1 may overlap the HCl peaks around 2800 cm^{-1}, the HCl peaks cannot be seen even though there is chlorine (289 ppm) in 92073.

Another way to present results from the FTIR spectra is to construct evolved gas profiles at a specific wavenumber. Much more CO_2 than any other gas is released during combustion and as a consequence must be plotted on a scale different from the other gases. In the PVC evolved gas profile, HCl is released first at 230-400°C with some CO_2 from the low molecular weight PVC groups. This is in accordance with the TG/DTG results. CH_4 peaks are obvious, while they cannot be found in the spectra of newspaper and cellulose. In the spectra of newspaper and cellulose, there are a lot of water peaks between 250-450°C that correspond to the release of CO_2 and CO. This is because of a large oxygen content and OH functional groups in these materials. Also, compared with PVC many more organic acids (mainly as formic and acetic acids) are produced during the combustion of newspaper and cellulose. These can be identified in the three dimensional spectra by groups of peaks at 2500-3400 (OH), 1700-1800 (C=O), 1033 for methanol, 1106 for formic acid and 1175 cm-1 for acetic acid. The appearance of these materials can be attributed to the poly-hydroxyl structures of newspaper and cellulose.

The evolved gas profile curves for PVC are quite characteristic. The HCl gas is released first and the absorbance reaches its maximum at approximate 320°C. However, the combustion of PVC occurs at 570°C, which is shown by the profiles for carbon dioxide and monoxide from PVC. This corresponds to the third weight loss in its TG-DTG curve. These results imply that the PVC is not readily flammable due to its chlorine content. In the profiles of newspaper and cellulose, the absorbance curves of carbonyl (C=O) and C-O have the same shape and reach their maxima at about 370°C. This indicates that these two peaks belong to the same compound, formic acid.

As a comparison of methane profiles for the two coals and PVC, it shows that methane forms at about 500°C. As previously mentioned, because of the high oxygen content in newspaper and cellulose, no methane forms during the combustion of these materials. It is notable that there is some methane released from the coals between 230°C and 380°C, but not from PVC. This is probably due to initial pyrolysis of the coals. The methane around 500°C is produced from the combustion of the coal matrix and the PVC carbon chain.

In summary, the identified characteristic peaks (not including water peaks which appear in every sample) in the FTIR spectra of the five raw materials are listed in Table 2.

VG Thermolab Gas Analyzer Results

The Thermolab Gas Analyzer, is a low-range, low-sensitivity quadrupole mass spectrometer, operating currently to a maximum of 200 amu. As it analyzes unchromatographed mixtures of gaseous molecules, its output requires great care in interpretation. Nevertheless, some useful information can be obtained, especially in conjunction with other sources of structural information, such as from FTIR spectra.

For Coal 92073 the profiles of peaks M/Z 18, 32, 44, 60 and 64 can be attributed to the ions of H_2O, O_2, CO_2, COS, and SO_2, respectively. The water profile shows three peaks. The first peak around 100°C is the moisture in coal. The second and third peaks are produced by the combustion and decomposition of coal. The oxygen profile remains stable until about 350°C after which the

oxygen decreases due to its consumption through combustion of the coal matrix. The inverse peak indicates a maximum consumption of oxygen. In addition, sulfur dioxide shows three peaks. This result is the same as that obtained in the FTIR spectra. In 92073, carbonyl sulfide is very obvious and SO_2 shows three decomposition phases (See Figure 5).

Figure 6 shows some mass peak profiles for PVC. The M/Z 36 and 38 are formed at the same time over a range of 200 to 450°C and strongly suggest the isotopes HCl^{35} and HCl^{37}. Also, the M/Z 70, 72 and 74 suggest the isotopes $^{35}Cl_2$, ^{35}Cl-^{37}Cl and ^{37}Cl-^{37}Cl. This conclusion can be demonstrated by the ratio of their integration areas. The ratio of M/Z 36 to 38 is 0.333, which is close to the chlorine isotope fraction 0.325. Furthermore, M/Z 70 to 72 to 74 appear at exactly the same point, with mass ratio 0.26 : 0.663 : 1.00, as compared with the predicted mass ratio of 0.11 : 0.65 : 1.00. The major aromatic volatile components, toluene, indane, biphenyl, anthracene, styrene and indene form at the second decomposition step 420-460°C.

CONCLUSIONS

The TG-FTIR-MS system was used to identify molecular chlorine, along with HCl, CO, CO_2, H_2O, and various hydrocarbons in the gaseous products of the combustion of PVC resin in air. This is a significant finding that will lead us to examine this combustion step further to look for the formation of chlorinated organic compounds.

The combination of TG-FTIR and TG-MS offers complementary techniques for the detection and identification of combustion products.

The TG-MS technique allows one to study reaction pathways for the formation of gaseous products during combustion.

ACKNOWLEDGEMENTS

The authors gratefully acknowledge the financial support of the U.S. Department of Energy through the University Coal Research Program and the National Science Foundation through the Research at Undergraduate Institutions Program.

REFERENCES

1. Steuteville, R., Biorecycle, 1992, 33(10), 10.
2. Dichristina, M., Popular Science, 1990, 237(10), 57.
3. McGowin, C.R.; Petrill, E.M.; Perna, M.A.; Rowley, D.R., "Fluidized Bed Combustion Testing of Coal/Refuse-Derived Fuel Mixtures", Babcock and Wilcox, Report from EPRI Project RP718-2, 1989.
4. Kasasek, F.K.; Clement, R.G.; Viau, A.C., J. Chromatography, 1982, 239, 173.
5. Tiernan, T.O.; Taylor, M.L.; Garrett, J.H.; Van Ness, G.F.; Solch, J.C.; Dies, D.A.; Wagel, D.J., Chemosphere, 1983, 12, 595.
6. Olie, K.; Berg, M.; Hutzinger, O., Chemosphere, 1983, 12, 627.
7. Liberti, A.; Goretti, G.; and Russo, M.V., Chemosphere, 1983, 12, 661.
8. Lindbaurer, R.; Wurst, F.; Prey, T., Chemosphere, 1992, 25, 1409.
9. Gullett, B.K.; Raghunathan, K., "The Effect of Coal Sulfur on Dioxin Formation", Final Technical Report for Illinois Clean Coal Institute, Carterville, IL, 1993.

Table 1. Analytical Data for Raw Materials

Parameter	Coal 93003 IL # 6	Coal 92073 KY # 9	PVC Resin	Cellulose	Newspaper
% moisture[A]	8.76	9.88	0	3.12	4.21
% ash	8.12	26.34	0.36	0	4.30
% vol. matter	34.3	32.6	99.6	100	84.8
% carbon	75.07	59.53	38.79	44.84	47.68
% hydrogen	5.21	3.50	4.21	6.66	6.48
% nitrogen	1.64	1.17	0	0	0.07
% sulfur	1.26	4.44	0.22	0.02	0.05
% oxygen	8.32	4.99	8.97	48.5	41.4
% chlorine	0.38	0.029	47.46	0.010	0.016
Btu/lb	13,428	10,335	8,556	6,940	8,081

[A] Moisture is as-determined. All other analyses are reported a dry basis.

Table 2. Identification of Peaks (wavenumber, cm^{-1}) in FTIR Spectra

	90003	92073	PVC	Newspaper	Cellulose
CH_4	3016	3016	3016	-----	-----
HCl	2798	2798	2798	-----	-----
CO_2	2356	2356	2356	2356	2356
CO	2178	2178	2178	2178	2178
Carbonyl Sulfide (COS)	2073	2073	-----	------	-----
C=O	-----	-----	1798	1790	1790
			1788	1773	1777
			1776	1747	1746
			1734	1734	1734
			1717	1717	1724
SO_2	1374	1374	-----	-----	-----
Acetic acid	-----	-----	1175	1175	1175
Formic acid	-----	-----	1106	1107	1107
Methanol	-----	-----	1036	1033	-----
Ethylene	950	950	950	950	950
1,3-Butdiene	910	-----	910	-----	-----
Furan	-----	-----	-----	745	744
Xylene	740	741	741	-----	-----
HCN	712	712	-----	-----	-----

TGA-FTIR-MS ANALYTICAL SYSTEM

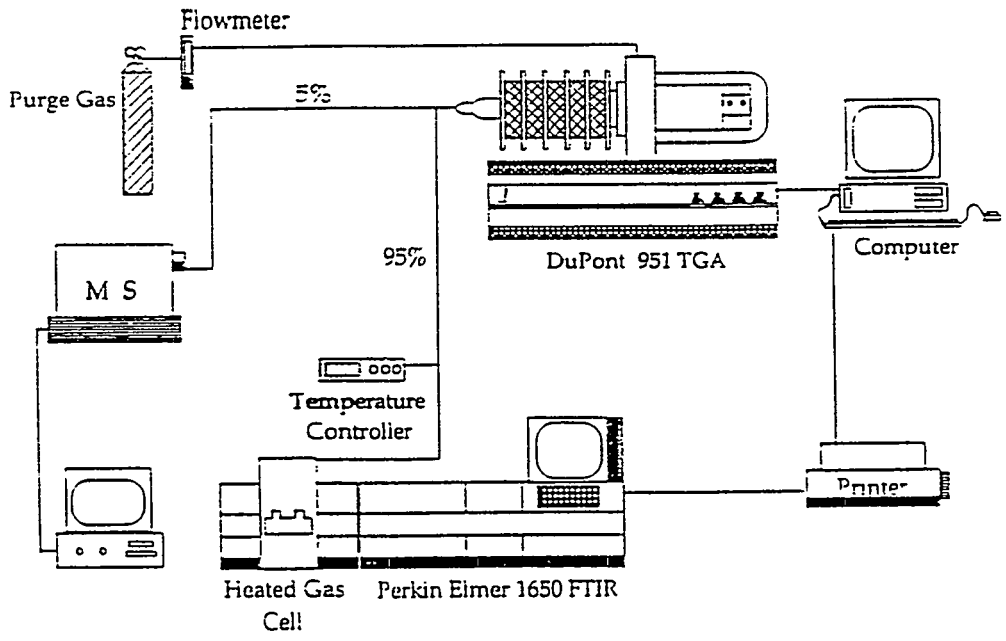

Figure 1

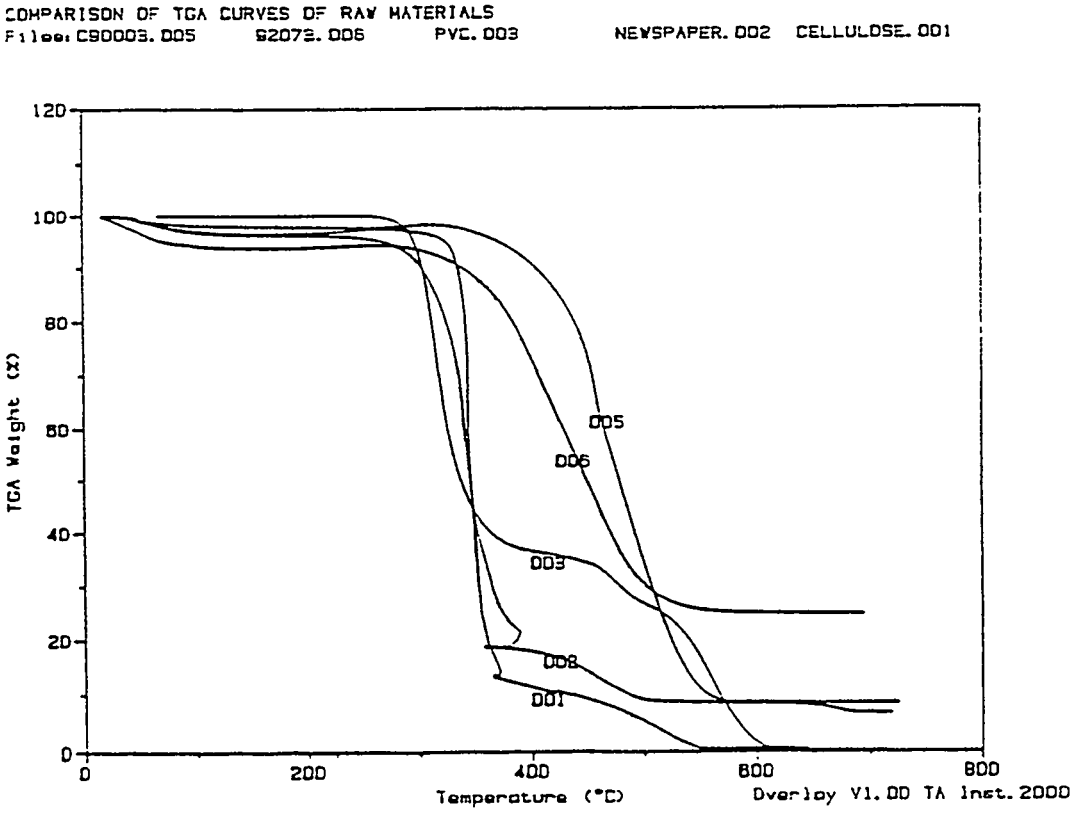

Figure 2

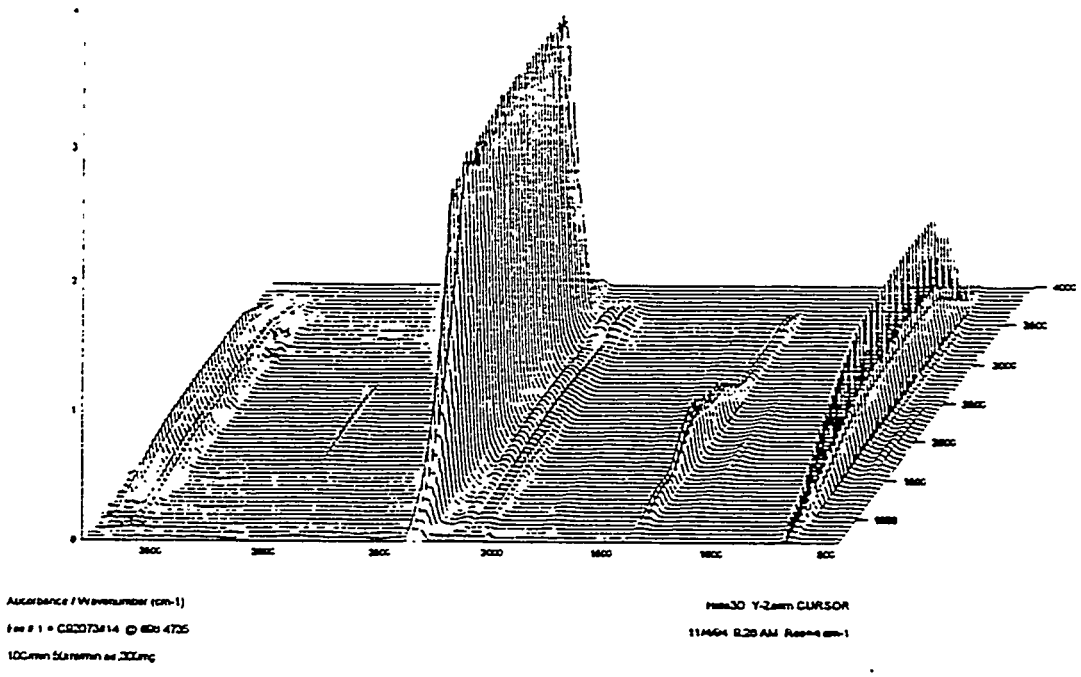

Figure 3

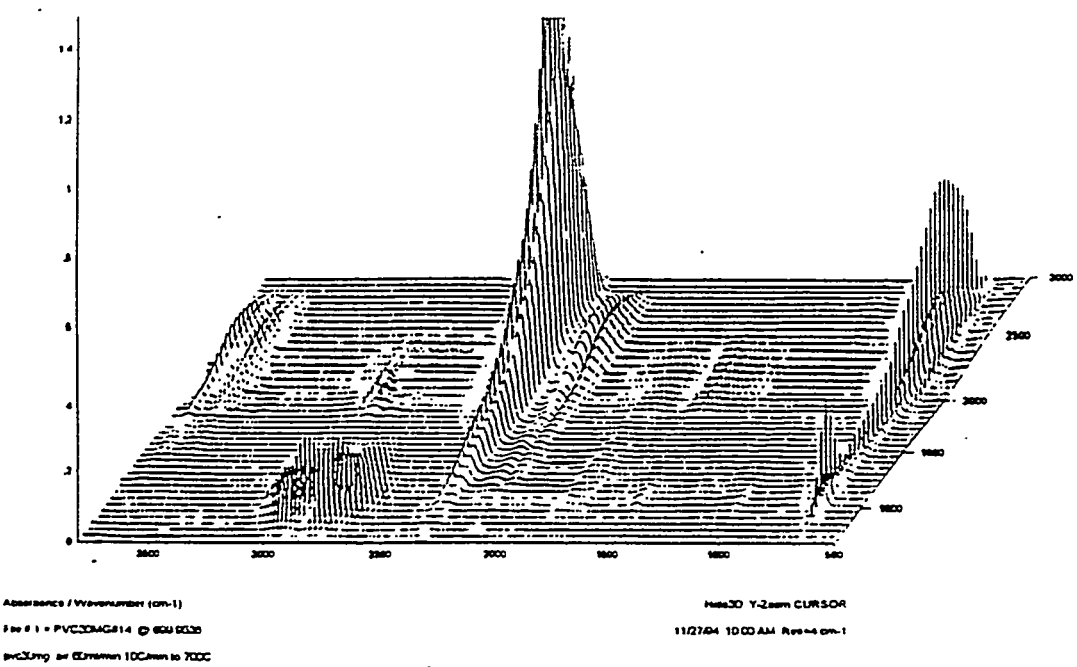

Figure 4

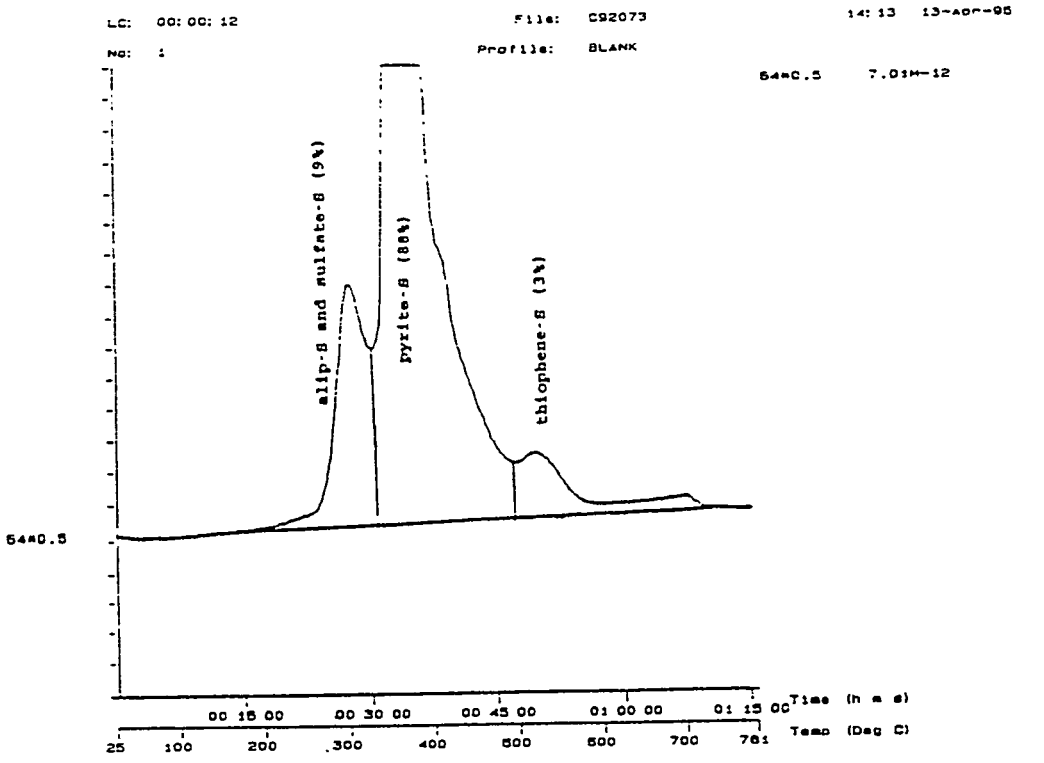

Figure 5

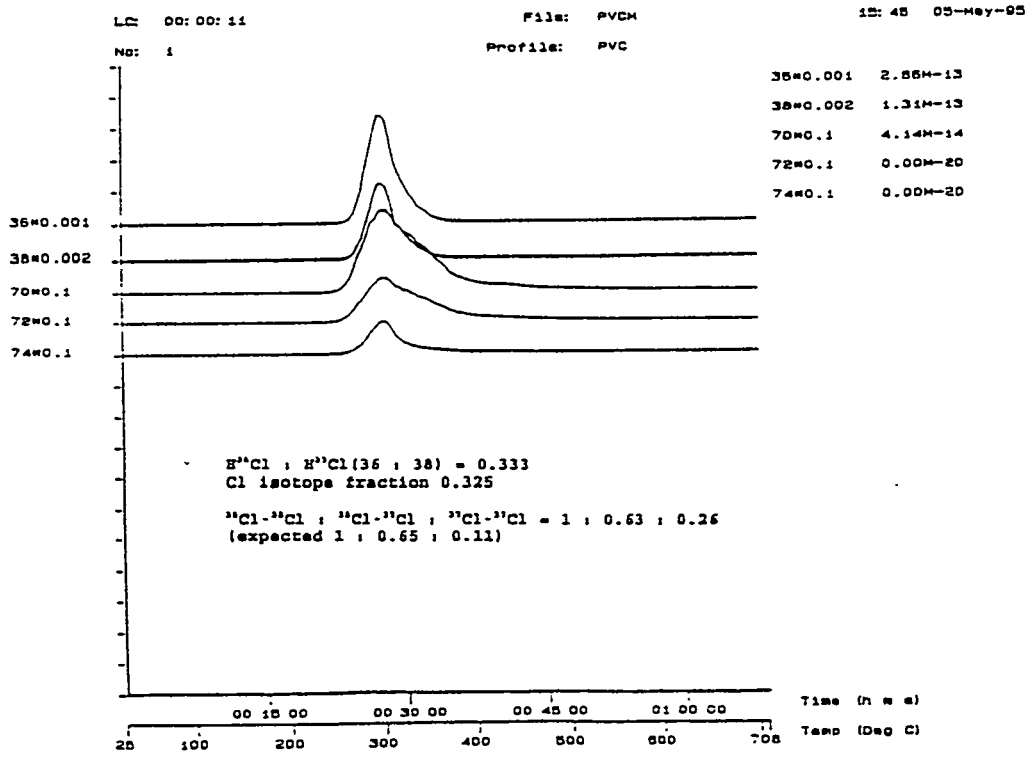

Figure 6

The following manuscript was unavailable at time of publication.

COMBUSTION CHARACTERIZATION OF COAL FINES

Dr. Houshang Masudi
Prairie View A&M University
Prairie View, TX 77446

Please contact author(s) for a copy of this paper.

The following manuscript was unavailable at time of publication.

THE EFFECT OF COAL BENEFICIATION ON THE RHEOLOGY/ATOMIZATION OF COAL-WATER SLURRIES

Dr. Frank Ohene
Grambling State University
Department of Chemistry
Box 4218
Grambling, LA 71245

Please contact author(s) for a copy of this paper.

CONTROLLING MERCURY AND SELENIUM EMISSIONS FROM COAL-FIRED COMBUSTORS USING A NOVEL REGENERABLE NATURAL PRODUCT

RICHARD J. SCHLAGER, SCIENTIST
ROGER W. MARMARO, RESEARCH ENGINEER
DARYL L. ROBERTS, PRINCIPAL SCIENTIST

ADA TECHNOLOGIES, INC.
304 INVERNESS WAY SOUTH, SUITE 110
ENGLEWOOD, CO 80112
(303) 792-5615

ABSTRACT

This program successfully demonstrated the key components that are needed for a practical, regenerable sorption process for removing and recovering mercury from flue gas streams: 1) a proprietary natural product removed mercuric chloride from synthetic flue gas, 2) several new noble metal sorbents were shown to capture elemental gas-phase mercury from synthetic coal combustion flue gas, and 3) both the natural product and the noble metal sorbents could be regenerated in the laboratory (chemical method for the natural product, thermal method for noble metal sorbents).

Several sorbents were tested for their ability to collect selenium oxide during the program. These tests, however were not definitive due to inconclusive analytical results. If follow-on testing is funded, the ability of the proposed sorbents to collect selenium and other metals will be evaluated during the field testing phase of the program.

A preliminary economic analysis indicates that the cost of the process appears to be substantially less than the cost of the state-of-the-art method, namely injection of activated carbon, and it also appears to cost less than using noble metal sorbents alone.

INTRODUCTION

Mercury is emitted from industrial sources in a variety of chemical forms depending on the specific process and flue gas conditions. For example, mercury is known to exist as elemental mercury [Hg^0] and as mercuric chloride [$HgCl_2$] in coal combustion flue gas (Schmidt and Brown, 1994). The fate and subsequent environmental and health impact of mercury in coal combustion flue gas is determined by the chemical speciation of the mercury and by the nature of the air pollution control devices in operating coal-fired power plants. A knowledge of the relative concentrations of mercury between its different forms will be required for air pollution control devices to operate effectively. An example of this principle is given in Table I for coal-fired power plants. In attacking the problem of mercury and selenium emissions from coal

combustion facilities, it is logical to take separate (but not unrelated) approaches for systems with scrubbers and for systems without scrubbers.

The purpose of this research program was to investigate sorbents that are capable of removing elemental mercury, mercuric chloride, and selenium from a synthetic flue gas.

Table I. Mercury Removal Under Different Process Conditions

Plant	Ash Loading to Spray Dryer	Coal Cl	% Mercury Removed
A	High	Low	**14**
B	High	Low	**23**
C	High	Low	**6**
G	High	Low	**16**
E	Low	High	**55**
H	Low	High	**44**
F	Medium	High	**89**
D	High	High	**96**

TEST APPARATUS

Phase I testing consisted of the following: 1) evaluating the mercury uptake capability (using elemental mercury) of a number of candidate sorbents having the potential of being regenerated, 2) evaluating the uptake capability of selected sorbents to mercuric chloride and selenium, and 3) evaluating the regenerability of selected sorbents.

In the natural product test, the sorbent was held in a Teflon tube with an inside diameter of 3/8". We used two grams of the material, one gram of 1/16"-diameter beads and one gram of 1/8"-diameter beads. The gas flow rate through the bed was 100 standard cubic centimeters per minute (sccm). The sorbent bed was held at 130°F and at ambient pressure (12 psia); at these conditions the 100 sccm flow rate calculates to a superficial velocity of 3.4 cm/sec and an approximate bed residence time of four seconds.

The noble metal sorbents were tested in a separate apparatus wherein the sorbent was held in a 0.5"-I.D. quartz tube that was placed inside an oven. This oven was held at 300°F during the sorption tests and was heated to 700°F to thermally regenerate the sorbents. The gas flow rate through the bed during these tests was 600 sccm, and the mass concentration of elemental mercury was 2,843 $\mu g/m^3$. The mass of sorbent in each test was approximately 5 grams, and the sorbents occupied approximately 10 cm^3 of volume. The pressure in the quartz tube was 12.5 psia. Under these conditions, the superficial velocity of the gas through the sorbent bed was 15 cm/sec, and the bed residence time was approximately 0.5 sec. The concentration of mercury was well above that of actual coal combustion flue gas but gave us the ability to load the sorbents with mercury in a reasonable amount of time. In a typical run of four

hours duration between regeneration steps, 0.41 milligrams of mercury was delivered to the sorbent bed.

TEST RESULTS

Natural Product Sorbents

The natural product was found to take up mercuric chloride from the gas phase but it did not to take up elemental mercury. This result is in keeping with the current understanding of the mechanism by which this material sorbs metals, specifically, formation of a charge complex of a metallic ion with the electron pair on the nitrogen atom in the structure of the sorbent molecule. The mercuric chloride was removed from the synthetic gas stream with an efficiency of 58% in the single test that was done.

Although we were successful in making a constant source of selenium oxide (permeation tube with gravimetric calibration), we were unable to find the selenium in our acid impinger bottles when a carrier gas flowed over the permeation tube and straight through three impinger bottles in series. Follow-up testing will be performed during Phase II to ascertain the fate of selenium within the proposed sorbent system.

Early Phase I testing was directed at using the natural product exposed to synthetic flue gas at temperatures of 300°F. The material was not stable at this condition due to its high surface area. To address the thermal resistance of the sorbent, a small sample was made with low surface area (10 m^2/g). This form was much more resistant to higher temperatures based on thermal gravimetric analysis. The low surface area sorbent was just as stable as the native material (no weight loss until the temperature exceeds 450°F) whereas the high surface area material began to lose weight at about 290°F. This test shows that the natural product can be fabricated in a form to be stable at higher temperatures if this property is desired. It is believed that surface area is a less important factor when using the material to capture mercuric chloride than the thermal stability.

Noble Metal Sorbents

Four sorbents containing noble metals were evaluated during Phase I. All of the sorbents were capable of collecting elemental mercury. In addition, all sorbents were capable of releasing the mercury by subjecting them to a thermal cycle. A real-time elemental mercury analyzer was used in the testing to measure mercury concentrations entering and exiting sorbent test beds. All tests were conducted at 280°F.

Figure 1 shows the results of a test of one of the sorbents. The sorbent was collecting virtually 100% of the mercury between the time periods of 6,000 and 22,000 seconds. Occasionally (at 13,000 sec., 16,000 sec., and 22,000 sec.) the inlet mercury concentrations were checked by bypassing the gas flow directly to the analyzer. Figure 2 shows the results of regenerating this sorbent. The temperature of the sorbent was raised to 600°F, where a substantial amount of mercury was driven from the sorbent. The temperature was increased in

several steps to a maximum of 950°F. Little additional mercury was released above a temperature of 750°F.

Although all the noble metal sorbents exhibited a capacity to collect elemental mercury, an optimization of the sorbents was not attempted during Phase I.

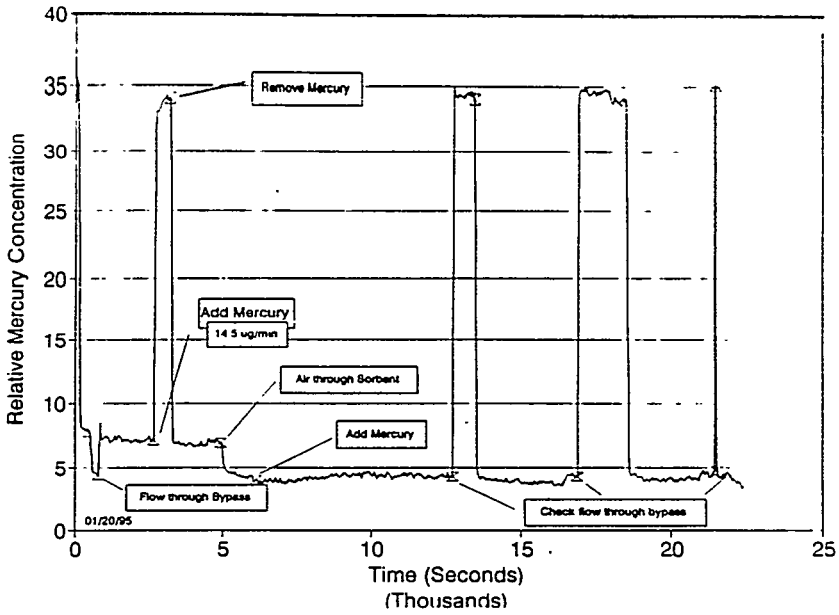

Figure 1. Sorption test of a noble-metal sorbent.

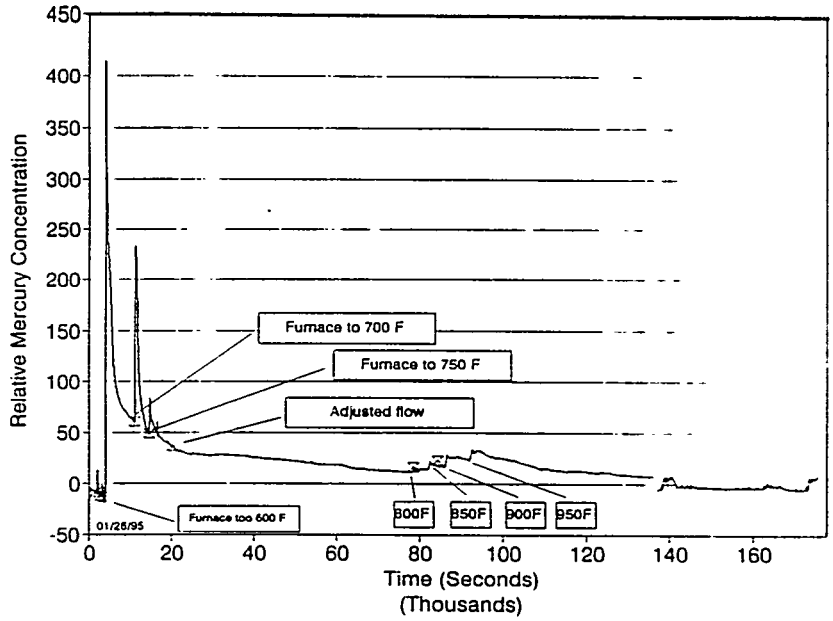

Figure 2. Regeneration of noble metal sorbent.

CONCLUSIONS

Following are conclusions based on the results of the Phase I program:

- Natural product beads, when appropriately wetted in a gel form, will effectively sorb mercuric chloride from synthetic flue gas.
- Noble metal sorbents collect elemental mercury and are regenerable by thermal treatment.
- Taken together, the gelled natural product beads and the new noble metal sorbents are the only set of sorbents that can solve vapor phase mercury contamination problems generated by mercury in the flue gas of coal combustors.
- A combination of noble metal sorbents with gelled natural product beads would potentially have substantial cost savings over the use of solely noble metal sorbents.
- Natural product beads with surface areas near 10 m^2/g are as thermally stable as the native natural product (no decomposition at 450°F).

REFERENCES

Schmidt, C.E. and T.D. Brown (1994). "Comprehensive Assessment of Air Toxics Emissions from Coal-Fired Power Plants," paper number 94-WA68A.03, 87th Annual Meeting of the Air and Waste Management Association, June 19-24.

The following manuscript was unavailable at time of publication.

INTERACTIONS BETWEEN TRACE METALS, SODIUM, AND SORBENTS IN COMBUSTION

Professor Jost O.L. Wendt
University of Arizona
Chemical Engineering Department
J.W. Harshbarger Building
Tucson, AZ 85721

Please contact author(s) for a copy of this paper.

The following manuscript was unavailable at time of publication.

LOW COST SYNTHESIS OF NANOCRYSTALLINE SiC WITH FULLERENE PRECURSORS

Dr. S. Anha
Materials & Electrochemical Research Corporation
7960 S. Kolb Road
Tucson, AZ 85706

Please contact author(s) for a copy of this paper.

The following manuscript was unavailable at time of publication.

MATERIALS SUPPORT FOR THE DEVELOPMENT OF A HIGH-TEMPERATURE ADVANCED FURNACE

Kristin Breder
Oak Ridge National Laboratory
P.O. Box 2008
Oak Ridge, TN 37831

Please contact author(s) for a copy of this paper.

INVESTIGATION OF THE EFFECT OF THE COAL PARTICLE SIZES ON THE INTERFACIAL AND RHEOLOGICAL PROPERTIES OF COAL-WATER SLURRY FUELS

KEN D. KIHM, ASSOCIATE PROFESSOR
PAUL DEIGNAN, RESEARCH ASSISTANT
DEPARTMENT OF MECHANICAL ENGINEERING
TEXAS A&M UNIVERSITY
COLLEGE STATION, TX 77843-3123

ABSTRACT

Experiments were conducted to investigate the effect of particle size on coal-water slurry (CWS) surface tension properties. Two different coal powder samples of different size ranges were obtained through sieving of coal from the Upper Elkhorn Seam. The surfactant (anionic DDBS-soft, dodecylbenzene sulfonic acid) concentration varied from 0 to 1.0% in weight while the coal loading remained at 40% in weight for all the cases. A du Nouy ring tensiometer and a maximum bubble pressure tensiometer measured the static and dynamic surface tensions, respectively. The results show that both static and dynamic surface tensions tend to increase with decreasing coal particle sizes suspended in CWS fuels. Examination of the peak pressure, minimum pressure, surfactant diffusion time, and dead time were also made to correlate these microscopic pressure behavior with the macroscopic dynamic surface tension and to examine the accuracy of the experiment.

INTRODUCTION

Coal-water slurry atomization involves interactions between three different phases: solid (coal particles), liquid (water and additives), and gas (air or steam). Surface or interfacial tension is one of the significant properties in determining atomization characteristics of liquid or slurry fuels. Under the quasi-equilibrium conditions of low shear-rates of excessively slow atomization, the static surface tension of the fluid is an appropriate measure of the fluid's ability to form small radius droplets. However, the surfactants, additives or wetting agents presented in the CWS formulation do not reach an equilibrium concentration throughout the solid-liquid or liquid-vapor interfaces at higher shear rates. Therefore, dynamic surface tension should be a more appropriate measure in assessing the atomization that usually occurs at high shear rates.

The dynamic surface tension of a fluid is simply a measurement of the surface tension at a particular rate of surface formation or shear rate. The static and dynamic surface tension values are the same for pure fluids, such as water. The values of dynamic surface tension for slurry mixtures containing solid particles and various additives may be much higher than the corresponding static surface tension because insufficient time exists for the migration of surfactant additives to the atomized interface from the bulk mixture. The difference between the two surface tension values increases at higher shear rates that allows less time for the surfactant migration.

It is the intention of the present work to examine the effect of coal particle sizes on CWS static and dynamic surface tension properties. Rheology shows that the slurry viscosity generally increases with decreasing mean particle size [1]. When particles are suspended in the solution dispersed with additives and/or solvents, adsorption or solvation layers are formed on the particle surface which increases the effective volume (f) of the particle. This effective volume increase is particularly significant for small particles which can explain the increase of the slurry viscosity with

decreasing mean particle size. To the extent of our literature survey, no such correlation for surface tension, whether static or dynamic, has been published. Examination of particle size effect on interfacial properties of CWS fuels is attempted using specially prepared coal particle samples.

EXPERIMENTAL PROCEDURES

Maximum Bubble Pressure Technique

Figure 1 illustrates the operating principle of the maximum bubble pressure tensiometer technique for dynamic surface tension measurement [2]. The CWS sample was contained in a vessel into which is inserted a specially designed capillary tube with a small outlet diameter of one millimeter. As bubbles were formed, grew, and detached from the capillary tube orifice, variations of the bubble pressure occurred because of the change in bubble radius. For each bubble, maximum pressure was recorded when the bubble radius reached its minimum at the orifice radius. For different bubble generation frequencies, the dynamic surface tension was calculated from the measured maximum bubble pressure substituted into a simple relation

$$\sigma = (p_{max} - \rho g h)\, r_c/2 \qquad (1)$$

where ρ is the sample fluid (CWS) density, g is the gravitational acceleration, h is the height above the capillary outlet, and r_c is the radius of the capillary outlet. The maximum bubble pressure, p_{max}, corresponds to the inside air pressure when the radius of the growing bubble is equal to the capillary radius, r_c. The KRUSS Model BP1 tensiometer was adopted to measure dynamic surface tension of CWS fuels. The accuracy of the tensiometer was tested by measuring surface tension for distilled and deionized water. The result ensured a satisfactory measurement accuracy showing less than 2% deviations from the surface tension values listed in the CRC Handbook [3].

Modification of the Existing Kruss Tensiometer

Analog signal output from the diaphragm type pressure transducer of the Kruss tensiometer is interfaced with an A-to-D board installed in an 386 PC. ATLAB data acquisition software from Data Translation Co. samples the analog signal at a rate of 0.2 kHz and digitizes them into the computer hard disk memory. One batch of data scanning over the specified bubble frequency range from one to ten per second requires approximately 1 MB hard disk memory capacity. A simple FORTRAN program identifies the peak voltage, minimum voltage, bubble life time, and dead time.

Figure 2 shows a temporal history of voltage readings for a typical case of 1% DDBS-soft aqueous solution. One cycle period of the curve is equivalent to the bubble life time, or the reciprocal of the bubble frequency. The bubble pressure increases as the nitrogen gas inflow makes the bubble grow and the bubble diameter decreases from the infinitely large curvature of the initially flat interface at the orifice exit. The bubble pressure increase as the bubble diameter decreases with time. The bubble pressure increases at a faster rate when a surfactant acts to reduce the surface "holding" tension. While the bubble pressure increases, the surfactant migrates to the newly created bubble surfaces. The surface is 'aged' with surfactant diffusion during the period of ascending curve, which is now called 'Diffusion time'. The bubble pressure reaches its maximum value (peak voltage) when the bubble grows to the orifice diameter.

Further growth of the bubble beyond the peak voltage increases the bubble diameter and the bubble pressure decreases first smoothly, and then the descending pressure curve becomes irregular most probably because of the geometrical distortion of the enlarged bubble. The enlarged and distorted bubble detaches from the orifice and the cycle completes at the time of the minimum voltage reading. The duration from the peak till the cycle completion does not directly influence the measurement of the maximum bubble pressure, and this time period is now called 'Dead time'.

Preparation of CWS Fuel Samples of Different Coal Particle Size Ranges

Coarsely ground Upper Elkhorn Seam coal provided by DOE-PETC was classified into several different size ranges using a sieve shaker. To minimize the coal oxidation during the sieving, the sieve array was sealed with tape and the duration of sieve shaking was kept at a minimal necessary level. In most cases, the sieving was completed within thirty minutes. Two samples containing the largest and the finest particles were selected for testing so the effect of particle size on surface tension values could be distinctively observed. The coarse sample contains coal particles in the range of 180 to 250 μm, and the fine sample contains coal particles less than 63 μm. The present report presents results for only DDBS-soft surfactant which shows the best performance among the tested five surfactants [4]

The coal and water was completely mixed by a rotating mixer running for twelve to twenty-four hours. The specified amount of surfactant was then added and mixed by a magnetic stirrer for 5 minutes. All the present experiment used 40% weight CWS fuels. The slurry viscosity increases with increasing ratio of the packing density which is defined as the ratio of the solid volume fraction to the maximum attainable solid volume fraction, i.e., f/f_m [1]. The relatively uniform size distribution of the sieved coal particles tends to reduce the maximum attainable solid volume fraction and increases the packing density compared with coal powder of a wide size distribution. 50% or higher weight CWS fuel samples were too viscous and the tensiometers were not able to function with acceptable accuracy.

RESULTS AND DISCUSSION

Static Surface Tension

A du Nouy ring tensiometer measured static surface tension for the coarse and fine CWS samples mixed with DDBS-soft surfactant in Fig. 3. The static surface tension decreases with increasing surfactant concentration and approaches a saturated value beyond a certain surfactant concentration. Before reaching this certain concentration, which is called a critical micelle concentration (CMC), the fine CWS sample shows larger surface tension values than the coarse sample and the CMC of the fine CWS is higher than the coarse CWS.

The dashed arrows indicate the CMC of the fine sample, the solid arrows represent the CMC of the coarse sample, and the empty arrows are for the CMC of an aqueous solution of the specified surfactant. The CMC values for CWS fuels are higher than their aqueous counterparts. The primary reason for this is believed to be the surfactant adsorption on the coal particle surfaces which requires more amount of surfactant than the aqueous solution (Fig. 4). The higher CMC of the fine CWS compared with the coarse CWS can also be explained by the surface adsorption. Smaller coal particles create more total surface area than larger particles for the same coal loading, which causes the overall surface adsorption of surfactant to increase. This needs higher surfactant concentration for the saturated surface tension level and higher CMC.

Dynamic Surface Tension

Figure 5 shows dynamic surface tension versus bubble frequency for the two selected CWS samples of 40% coal weight containing DDBS-soft surfactant. The family of curves in each plot, from the top to the bottom, correspond to 0, 0.1%, 0.5% and 1.0% concentrations. At each surfactant concentration, the fine CWS fuel shows consistently higher dynamic surface tension values than the coarse CWS under the same bubble frequency. Two reasons can be listed for the distinction: (1) smaller coal particles of higher number density contained in the fine CWS sample

enhance the physical blockings against the surfactant migration to the bubble-created surface and reduce the surfactant diffusion into the bubble surface (Fig. 4), and (2) the increased total particle surface areas of the fine CWS sample increase the surfactant adsorption.

For the case with no surfactant mixed, the top curve in each plot, the higher surface tension for the fine CWS is attributed to the different bubble surface characteristics depending on the particle size. When the surfactant concentrations are zero or close to the static CMC level of 0.1%, the dynamic surface tension is nearly independent of the bubble frequency, which shows that the dynamic effect on surface tension is not pronounced for low surfactant concentrations. With increasing surfactant concentration, however, the dynamic surface tension shows a gradual increase with increasing bubble frequency, as the increased bubble frequency does not allow sufficient migration time for the surfactant.

Peak Voltage and Minimum Voltage

Figures 6-a and b show the temporal history of peak and minimum voltage readings for the fine and coarse CWS samples, respectively. The peak voltage data directly convert to evaluate the dynamic surface tension values. The peak voltage data obtained for the fine sample (Fig. 6-a) and the coarse sample (Fig. 6-b) show close similarity to the dynamic surface tension curves presented in Figs. 4-a and b, respectively. The higher dynamic surface tension of the fine CWS sample, which has been discussed in depth in the previous section, explains the higher peak voltage and the relatively lower dynamic surface tension of the coarse CWS results in the lower peak voltage. this finding is consistent regardless whether the surfactant is presented (1.0%) or not.

The nearly constant minimum voltage over the range of bubble frequencies at a given surfactant concentration shows that the system recovers to an identical initial condition before beginning of the next cycle. This also ensures the accuracy of the dynamic surface tension measurement that assumes an identical initial condition regardless of the bubble frequency. The minimum voltage for the coarse sample gradually varies with the bubble frequency range, but not showing any particular temporal correlation. This variation is attributed to the bubble pressure detection uncertainties associated with the presence and movement of relatively large coal particles at the gas-liquid interface.

The minimum voltage represents the hydrostatic pressure at the depth of the interface at the time of cycle completion or of new cycle initiation. The minimum voltage can decrease when the gas-liquid interface recedes from the orifice exit and stays inside the orifice at the time of cycle completion. The receding of the gas-liquid interface is likely to occur at higher surfactant concentration that enhances the solution wetting and increases the interface penetration inside the orifice. Results for both fine and coarse samples (Figs. 6-a and b) show that the minimum voltage level decreases with increasing surfactant concentration.

Increase in the minimum voltage could occur when the hydrostatic pressure is higher than that at the orifice exit. This may occur as a result of an incomplete bubble detachment at the end of the cycle. The remaining undetached portion of the bubble can result in a deeper initial depth than the orifice exit and the pressure transducer will detect a higher hydrostatic pressure than it should be. This type of bias may occur at extremely high bubble frequencies where the dead time is insufficient for full recovery of the cycle with a complete bubble detachment. A high-speed synchronized cinematograph could be employed to carefully visualize the bubble growth and detachment as a future investigation.

Dead Time

Figures 7-a and b show the percent dead time over the bubble life time as a function of the bubble frequency for the fine and coarse CWS samples with or without surfactant. This ratio increases linearly with increasing bubble frequency and also increases with increasing surfactant concentration. Reduced surface tension at higher surfactant concentrations expedites the bubble growth rate and shorten the diffusion time. The dead time, which occupies the remainder of the bubble life time, increases and the percent dead time goes up with increasing surfactant concentration for a given bubble life time.

For a fixed surfactant concentration the dead time ratio increases with the bubble frequency. This implies that the percent diffusion time decreases with increasing bubble frequencies and the surface aging by the surfactant migration is insufficiently achieved. This relatively short diffusion time at higher bubble frequencies retards a full benefit of surfactant. Larger dynamic surface tension values measured at higher bubble frequencies (see Figs. 4-a and b, for example) are attributed to the shortened diffusion time with increasing bubble frequency.

CONCLUSION

The effects of coal particle size on the CWS interfacial properties by measuring the dynamic surface tension using a Kruss tensiometer and by examining the detailed bubble pressure variation with time. Fundamental conclusions reached are:

1) Examination of interfacial properties of CWS fuel samples of different coal particle size ranges shows that the CWS static and dynamic surface tensions tend to increase with decreasing coal particle sizes. This finding consists with the measured peak voltages, which converts into the dynamic surface tension.
2) For the case of coarse CWS sample, the relatively larger coal particles cause the minimum voltage to slightly fluctuating, but remaining nearly constant through the range of bubble frequencies considered. The minimum voltage remains constant for the fine CWS sample.
3) The dead time ratio over the bubble life time increases with the bubble frequency and also increases with the surfactant concentration. This is attributed to the expedited bubble pressure rise rate due to the increased surfactant dispersion.

ACKNOWLEDGMENT

This work was supported by the US Department of Energy, Pittsburgh Energy Technology Center (PETC), Contract No. DE-FG22-94PC94120 under the supervision of Dr. Soung S. Kim, Technical Project Monitor at DOE-PETC. The tested coal powder was provided by Mr. David Wildman of DOE-PETC. The tested surfactants and partial financial support were provided from Dr. Paul Berger of Witco Inc. of Houston.

REFERENCES

1. G. D. Botsaris, and Y. M. Glazman, 1989, Interfacial Phenomena in Coal Technology, Marcel Dekker, New York, Chap. 3.
2. B. W. Brian, and J. C. Chen, 1987, "Surface Tension of Solid-Liquid Slurries," AICHE Journal, Vol. 33, No. 2, pp. 316-318.
3. R. C. Weast (ed.), 1988, CRC Handbook of Chemistry and Physics, CRC Press, Boca Raton, F-34.
4. K. D. Kihm, 1994, "Development and Use of an Apparatus to Measure the Dynamic Surface Properties of Coal-Water Slurry Fuels for Applications to Atomization Characteristics," DOE Report, Contract No. DE-FG-22-92PC92156.

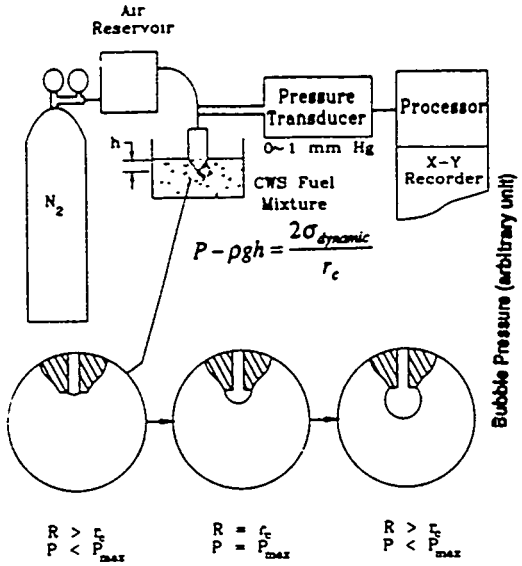

Fig. 1 Schematic illustration of maximum bubble pressure technique.

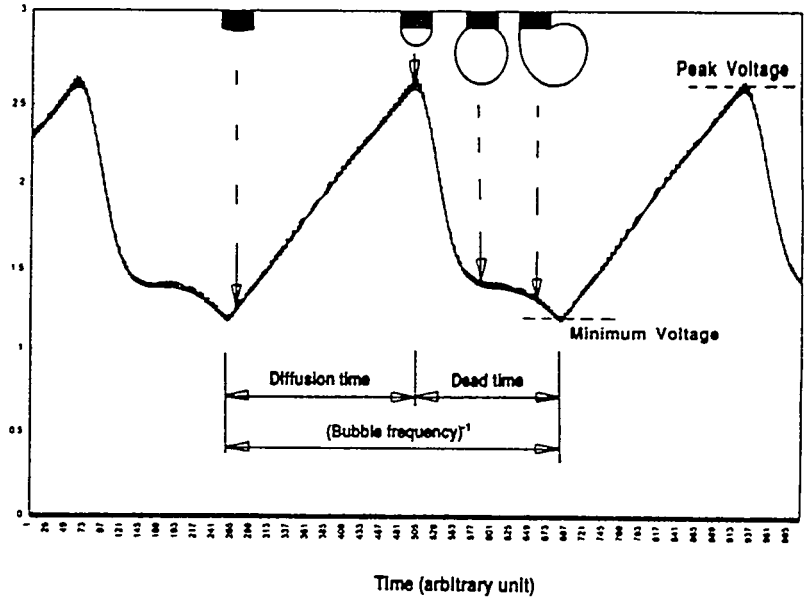

Fig. 2 Temporal history of the bubble pressure.

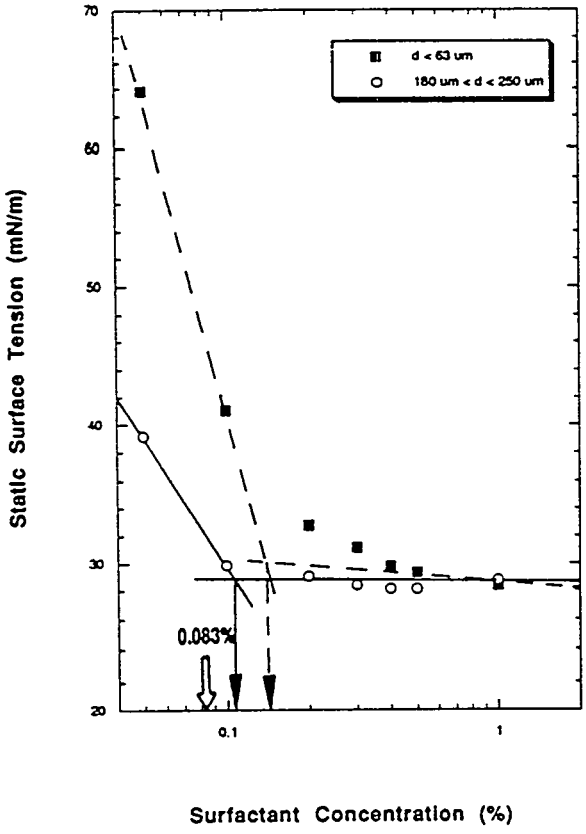

Fig. 3 Static surface tension versus concentration of DDBS-soft surfactant for 40% weight CWS fuels containing different particle sizes.

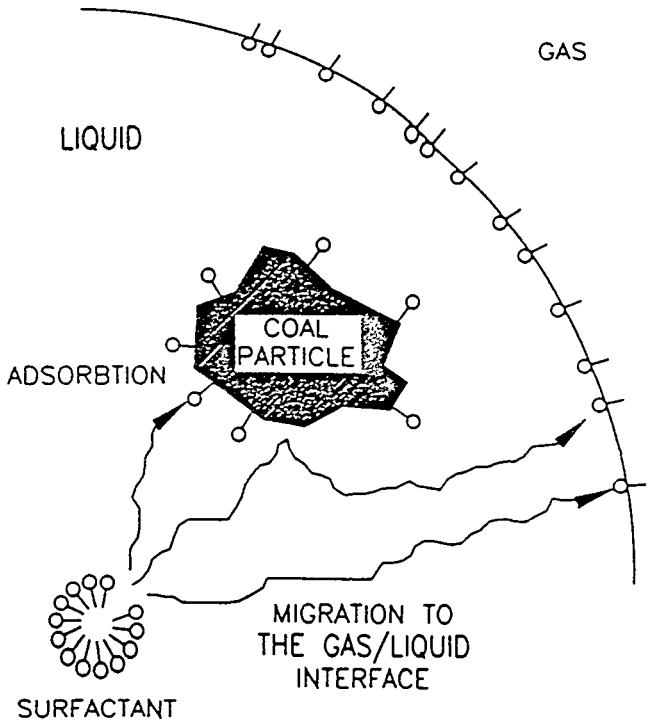

Fig. 4 Schematic illustration of adsorption of surfactant at coal surfaces and physical blocking of surfactant migration by coal particle.

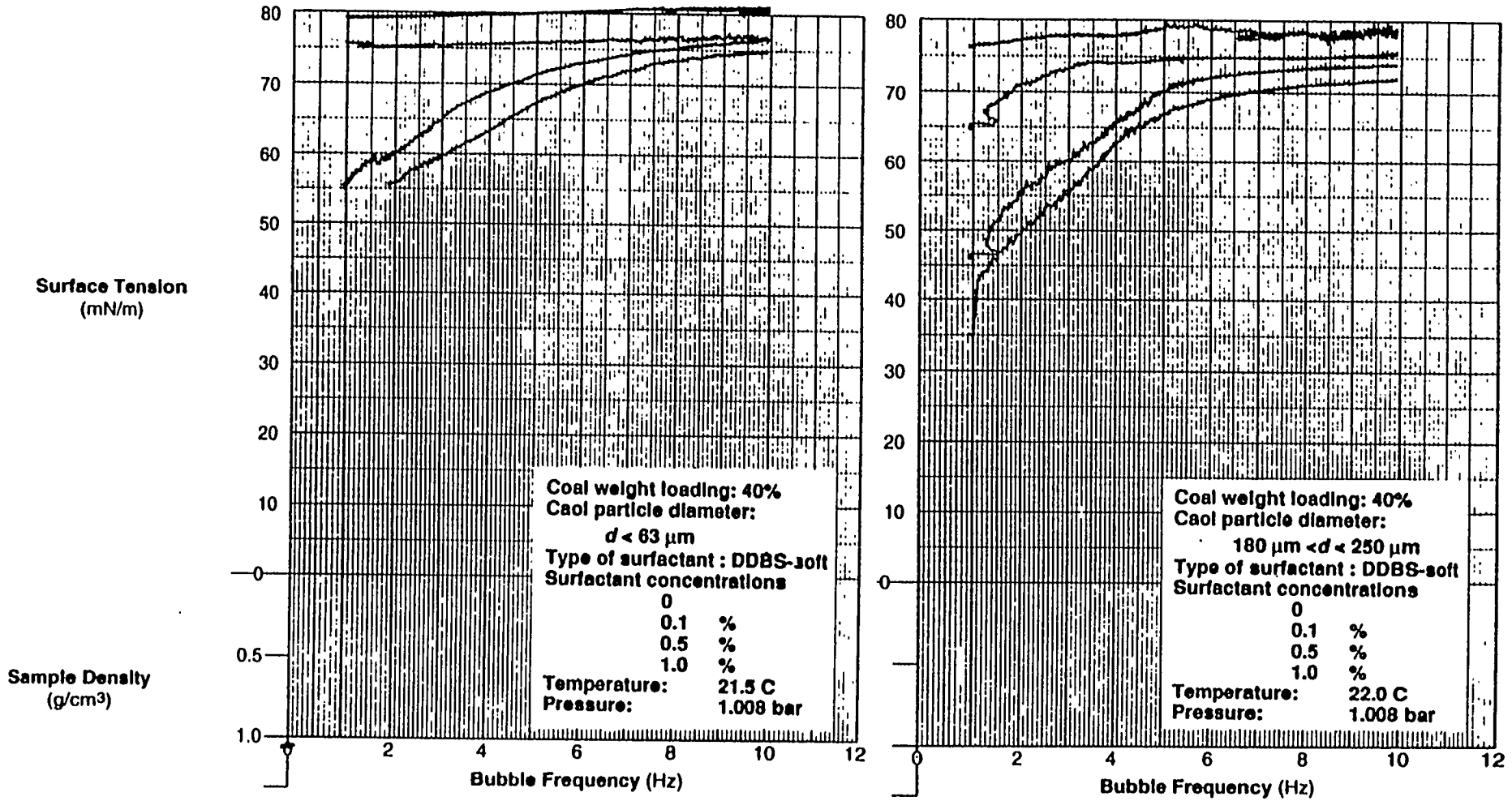

Fig. 5 Dyanmic surface tension versus bubble frequency for different surfactant concentrations.

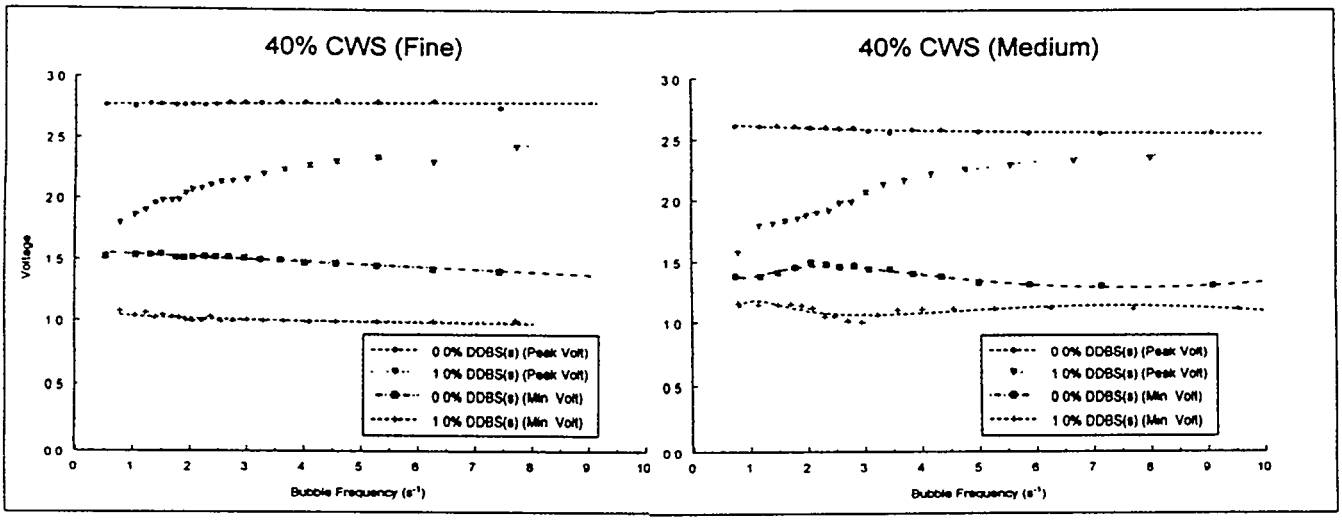

Fig. 6 Peak and minimum voltages versus bubble frequency for (a) fine CWS sample, and (b) coarse CWS sample.

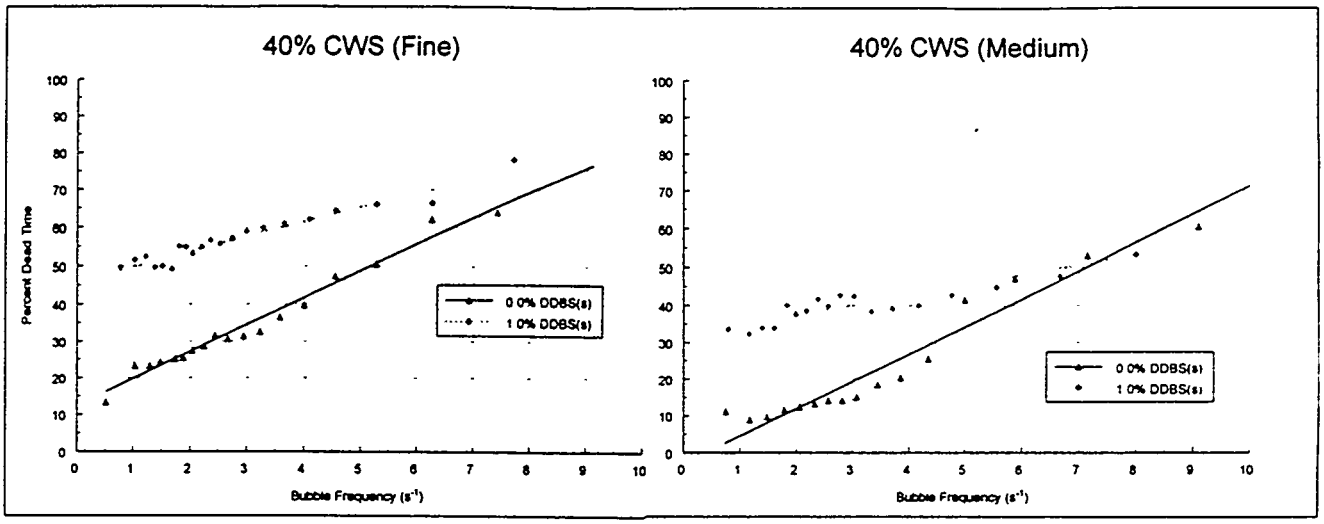

Fig. 7 Percent dead time over the bubble life time versus bubble frequency for (a) fine CWS sample, and (b) coarse CWS sample.

RECENT ADVANCES IN THE USE OF SYNCHROTRON RADIATION FOR THE ANALYSIS OF COAL COMBUSTION PRODUCTS

BERNARD MANOWITZ
BROOKHAVEN NATIONAL LABORATORY
UPTON, NEW YORK 11973

CONTRACT NUMBER: AS-227-APD

Two major coal combustion problems are the formation and build-up of slag deposits on heat transfer surfaces and the production and control of toxic species in coal combustion emissions. The use of synchrotron radiation for the analysis of coal combustion products can play a role in the better understanding of both these phenomena.

An understanding of the chemical composition of such slags under boiler operating conditions and as a function of the mineral composition of various coals is one ultimate goal of this program.

The principal constituents in the ash of many coals are the oxides of Si, Al, Fe, Ca, K, S, and Na. The analytical method required must be able to determine the functional forms of all these elements both in coal and in coal ash at elevated temperatures. One unique way of conducting these analyses is by x-ray spectroscopy.

The Extended X-Ray Absorption Fine Structure (EXAFS) and X-Ray Absorption Near Edge Structure (XANES) spectroscopic techniques and other applications to the chemical speciation of coal combustion products have been described previously.[1] Therefore only a short summary will be included here. The experiment involves scanning through the K- or L-shell absorption edge of the element in question. The structure of the absorption edge, consisting of transitions to unoccupied molecular levels, can be compared to those of model compounds for identification. The relative position of the absorption edge can yield information regarding the oxidation state of the element. This portion is the XANES portion of the spectrum. The EXAFS region, extending from about 60 eV above the absorption edge, represents scattering from neighboring constituents and can be used to determine the coordination number and coordination distance of a specific element from its neighboring atoms.

The best source of excitation energy for these experiments is an electron storage ring emitting synchrotron radiation (SR).[2] The National Synchrotron Light Source (NSLS) at Brookhaven National Laboratory is a 2.5-GeV storage ring and emits a continuous spectrum of x-rays to an energy of about 30 keV. Beam line X-19A is dedicated to XANES and EXAFS and is being adapted to the performance of this investigation.

The program involves a combined effort between the staff of the University of Kentucky, PSI Technology, Inc. and Brookhaven National Laboratory. The principal responsibility of the staff at Brookhaven National Laboratory is to upgrade the X-19 beam

line facility to permit the entire series of light element analyses and to permit high temperature *in-situ* analysis.

Speciation analysis of S, K, Ca, and Fe compounds have been accomplished with the Si(111) crystals and Si(220) crystals. As can be seen from Figure 1, the soft x-ray capability of this beam line can be extended by using large D-spacing crystals such as InSb, YB_{66}, and mica. An InSb crystal and a mica crystal have been obtained and will be tested.. In both cases it is anticipated that the heat loading of the first crystal in the white beam will change the latice constant of the crystals due to thermal expansion. Even if the mica crystals can only be used for a few experiments, they are inexpensive enough to be replaced.

For the analysis of compounds of elements present in low concentrations and particularly for the analysis of compounds of toxic trace elements it is important that the sensitivity of the system be high. The originally designed X-19A beam line system could speciate compounds of light elements present in the 100 ppm concentration range.

Recent advances have permitted a marked improvement in the systems sensitivity. We have recently replaced the original 10-mil Be window with an 8 μmBe window. As can be seen in Figure 2, the thin window will permit us to study elements as light as sodium and will increase the flux of sulfur edge radiation at the target by a factor of 3-4.

In addition, we have installed a strong focussing mirror which provides, at least, a 25-1 horizontal beam focus (i.e., 25.4 mm of horizontal beam squeezed into ~1 mm.) The results are better beam uniformity and 2-3 times more flux on the sample.

The combination of these two improvements now permit us to speciate compounds of light elements present in the 20-30 ppm range.

A 100-element detector is under development which should provide much higher sensitivities. The data collection path is straightforward with 100 detecting elements in a single Si wafer feeding charge proportional to the energy of the detected photon into 100 fast/slow shaping amplifiers which provide further gain and condition the slow signals for energy discrimination via pulse height analysis with 100 single channel analyzers. Diagnostics and calibration components make it possible to view, in close to real time, the energy spectrum of the photons being emitted from the sample. The technical advantage of such a detector is provided by the ability to use energy discrimination to separate the desired fluorescence signal from scattering and to alleviate the dead time associated with individual detectors at high count ranges.

Two examples of the application of x-ray near edge spectroscopy to coal combustion problems are the analysis of iron compounds in an *in-situ* combustion cell and the analysis of chromium compounds in a utility boiler ash.

During combustion, iron may become incorporated into glassy aluminosilicate-derived as particles. Because glassy particles are often sticky, these particles may also deposit on and adhere to available surfaces. In prior research conducted at PSI, particle stickiness has been

shown to be a function of particle viscosity. Thus, knowledge of the precise composition of iron-containing glass particles is an important parameter in determining their viscosity and stickiness. In addition to composition, the oxidation state of iron-containing glasses must also be known. For iron dissolved in glass, the (+2) oxidation state results in a significantly lower viscosity that does the (+3) oxidation state.

To understand and eventually predict the deposition of iron-containing ash particles, it is therefore critical that the precise chemical state of iron at the point of encounter with an impaction surface be known. XANES spectroscopy is one technique useful for determining the chemical speciation of iron. Typically XANES spectroscopic analysis is conducted on a sample that has been quenched and removed from the combustion process. While this provides valuable insight into the possible state of iron, the possibility of quench-induced phase formation cannot be avoided.

In this program, an *in-situ* combustion furnace and measurement cell have been constructed by PSI, U. Kentucky, and Brookhaven National Laboratory personnel to permit measurement of the forms of iron and other elements without the need for quenching and sample removal. This permits the state of iron to be measured in deposit samples.

Figure 3 illustrates the spectra from Fe K edge spectroscopy of an *in-situ* deposit of K energy #9 coal tailings at 1500°C under oxidizing and reducing conditions. The spectra indicate principally Fe_2O_3 at 20% oxygen and $Fe_{1-x}S$(pyrrhotite)-Fe_2O_3 at 5% oxygen. Further *in-situ* combustion runs are planned to improve our knowledge of Fe combustion chemistry.

In previous work at PSI and the University of Kentucky it was shown that chromium in coal and fly ash may be present in the more benign (+3) oxidation state. In these samples of fly ash and coal analyzed, no evidence for the highly carcinogenic (+6) form was obtained. While encouraging, these results were obtained for only a few coals that were burned in the laboratory. Further, measurements of only 'bulk ash' were made; no effort at analyzing form or concentration as a function of particle size was attempted. The possibility that the small amount of chromium associated with fine respirable particles may be in the (+6) oxidation state cannot be ruled out from the bulk ash measurements, because the (+6) signal would be overwhelmed by the (+3) signal from the bulk of the ash mass.

Because the air emissions of any trace element are dependent upon the element's association with the finest fly ash particles, it is desirable to determine the form of elements such as chromium *as a function of particle size*. Previous work with the "major" coal ash elements has indicated that combustor size does not significantly affect the ash formation process, so we do not expect a large difference for chromium (or any other trace element). Nevertheless, the statement that combustor size does not affect chromium transformations cannot be made the certainty until comparative measurements have been made.

Two samples of fly ash were obtained from a field TVA unit. The samples contain only particles <2.5 μm in size and were collected under conditions of "high load" and "low load." Elemental analysis of the ash by ICP-MS indicate a chromium concentration of 1304 ppm in the high load sample and 1670 ppm in the low load sample.

We plan to analyze these samples by near edge spectroscopy for Cr(+3) and Cr(+6). It is further planned to address remaining uncertainties in the combustion behavior of chromium by a series of laboratory experiments with TVA coal to generate size fractionated fly ash samples. Subsequent measurements will provide data on the dependence of chromium oxidation state on particle size and comparative data on chromium evolution in small and full scale systems.

Acknowledgments

Research is supported by the Pittsburgh Energy Technology Center, U.S. Department of Energy, Under Contract No. DE-AC02-76CH00016.

References

1. A. Bianconi, "XANES spectroscopy," in X-Ray Absorption, D.C. Koningsberger and R. Prins, eds., Wiley and Sons, New York, 1988, pp. 573-661.

2. A. Winick, "Properties of synchrotron radiation," in Synchrotron Radiation Research, H. Winick and S. Doniach, eds., Plenum Press, New York, 1980, pp. 11-25.

SOFT X-RAY MONOCHROMATOR CRYSTALS

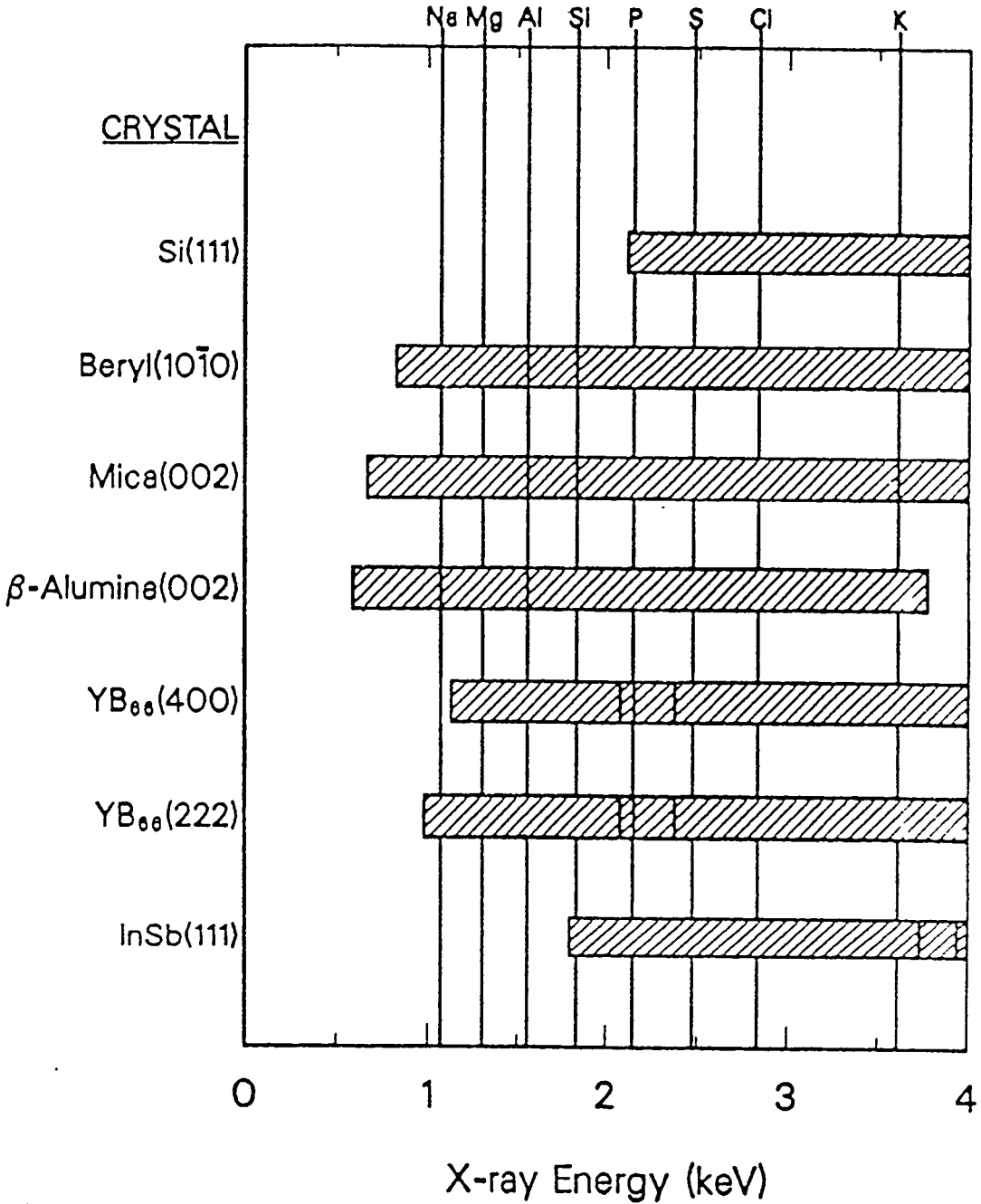

Figure 1. **Ranges of energy accessible using listed monochromator crystals. Elemental absorption edge energies are shown on abscissa at top.**

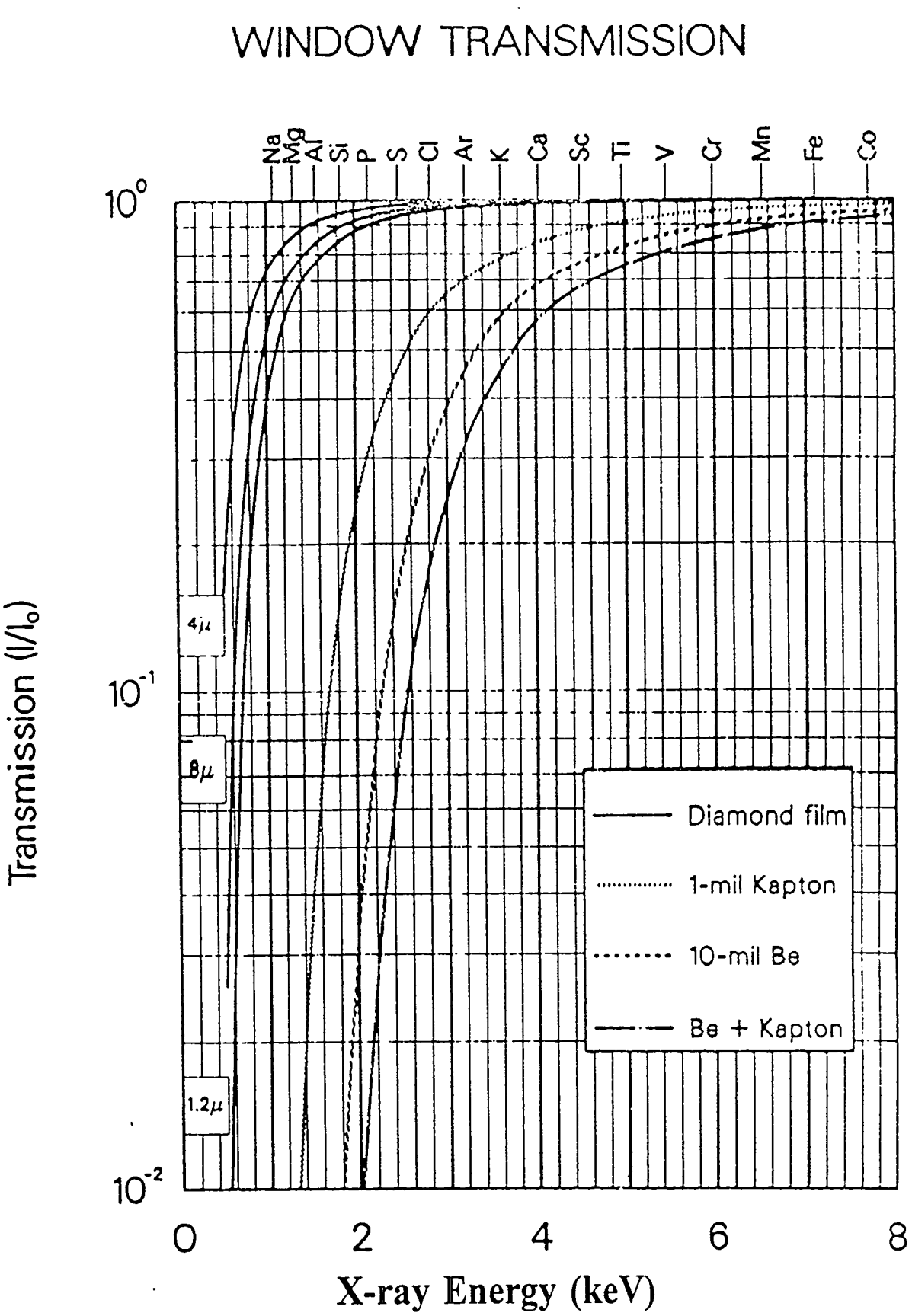

Figure 2. **Transmission for beam line windows in the soft x-ray range. The new film window is 0.8 μm thick.**

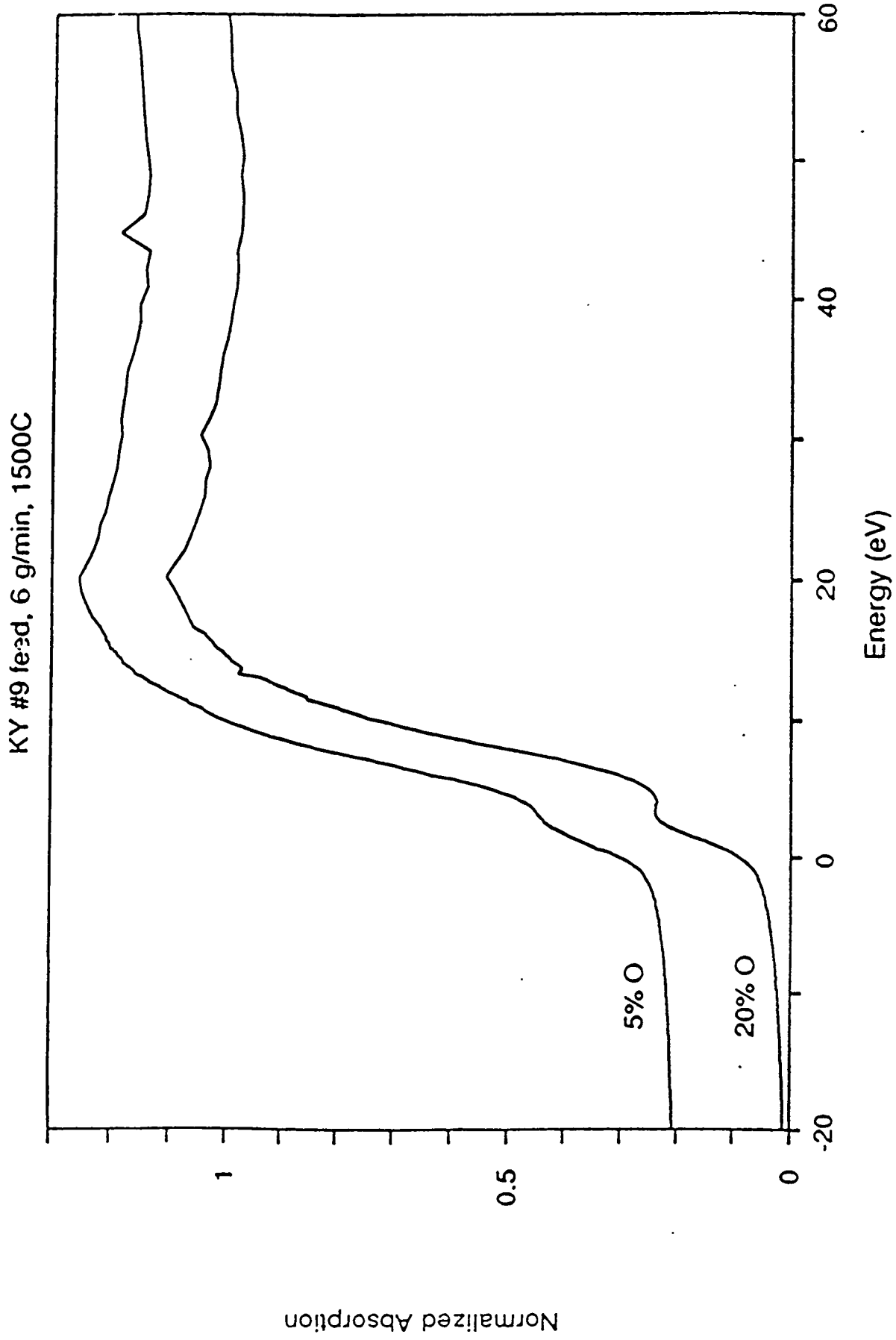

Figure 3. Fe K-edge XANES of *in-situ* deposit of Kentucky #9 coal at 1500°C under oxidizing and reducing conditions.

The following manuscript was unavailable at time of publication.

DEVELOPMENT OF A ROTARY COMBUSTOR FOR REFIRING PULVERIZED COAL BOILERS

Michael J. Virr
Spinheat, Ltd.
428 Old Stratfield Road
Fairfield, CT 06430

Please contact author(s) for a copy of this paper.

The following manuscript was unavailable at time of publication.

FLUID DYNAMICS OF ASH DEPOSITION

Frank Shaffer
U.S. Department of Energy
Pittsburgh Energy Technology Center
P.O. Box 10940, M.S. 84-340
Pittsburgh, PA 15236

Please contact author(s) for a copy of this paper.

PARTICULATE EMISSION ABATEMENT FOR KRAKOW BOILER HOUSES

S. Ronald Wysk
LSR Technologies, Inc.
Acton, MA U.S.A.

Jan Surówka
Polish Foundation for Energy Efficiency
Katowice, Poland

Miroslaw Litke
Eco Instal
Poznan, Poland

Introduction

Environmental clean-up and pollution control are considered top priorities in Poland. The magnitude of environmental problems and public awareness of it has forced the Polish government to implement more aggressive regulatory controls. The extent of this condition has in fact prompted the government to designate pollution control as a top priority for foreign investment.

During the past five years, Poland has also made significant progress in reorienting its central-planned economy to one based on open market principals. Efforts to decentralize has led to the privatization of many government-owned businesses with a concomitant shift in buying decisions to privately-owned enterprises. This movement toward privatizing the economy along with cleaning and protecting the environment has created numerous business opportunities for both Polish and foreign companies. As a result, there's been a drastic downsizing of large formerly state-owned companies. And, new startups and small businesses have become the main hope in reviving the Polish economy.

The Krakow Clean Fuels and Energy Efficiency Program was promulgated by the U.S. AID and Department of Energy to assist Poland in its effort to restructure. The City of Krakow has experienced severe environmental damage during the past two or three decades due to its heavy dependency and inefficient use of low grade coals, lack of pollution controls, and because of its climate and weather patterns. Airborne pollutants, especially particulate matter, are discharged from low stacks burning coal, mainly unwashed. As a result, levels of suspended particulate matter can reach dangerous levels during the winter heating seasons.

This paper discusses one of the eight projects for environmental cleanup in Krakow initiated by the Department of Energy. The project uses a newly developed technology for particulate control, called a *Core Separator* developed by LSR Technologies, Inc. in the U.S.A. The Polish Foundation for Energy Efficiency has assisted LSR in identifying appropriate markets for the *Core Separator* and in implementing the new technology. Eco Instal, a leading manufacturer of environmental equipment in central Poland, has also participated in this project and has already produced a number of units for commercial applications.

Technology Description

The *Core Separator* is a new technology developed through research sponsored by the Department of Energy and Environmental Protection Agency. Some *Core Separator* units have been placed in commercial operation in the U.S. All of the units now in service are performing difficult separations, i.e., those involving dust particles with small aerodynamic diameters. Historically, mechanical separators have been ineffective in removing dust particles with diameters below 10 microns. In comparison, the *Core Separator* is able to remove a high percentage of particles even at 2-3 microns in diameter. This is roughly equivalent to the performance of a medium-efficiency electrostatic precipitator (ESP).

Some of the features and benefits of the *Core Separator* relative to other devices for particulate control are as follows:

- Operation based entirely on centrifugal principals
- A three component system utilizing gas recirculation
- Roughly 4-8 times lower dust penetration than from cyclones
- High efficiency in removing respirable (PM10) particles
- Very high turndown performance
- High temperature capability
- Ease of operation and maintenance

A simplified schematic of the *Core Separator* system is shown in Figure 1. The system includes two conventional components, a cyclone collector for extracting solids and a fan for flow recirculation. The *Core Separator* is actually a multitude of cylindrical units. Each unit has a single inlet for the stream to be treated and two outlets, one for the cleaned gas stream and the other containing a highly concentrated recirculation stream. The dust-laden recirculation stream is fed to the cyclone and then returns again by means of the fan. The processes of separation and collection are accomplished separately in different components. The *Core Separator* cleans the inlet stream and detains dust particles in the system. Since its efficiency is quite high, the dust particles cannot leave the system. They recirculate again and again until collected in the cyclone.

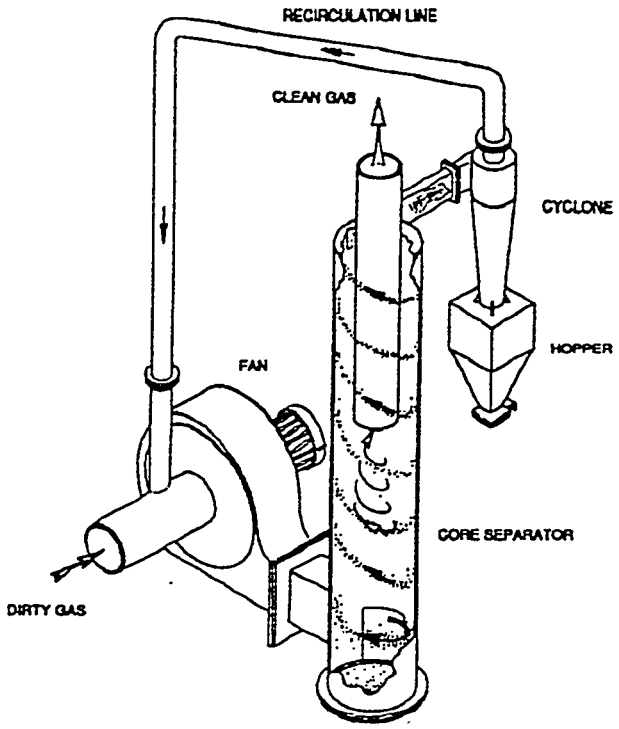

Figure 1

Two factors govern the performance of *Core Separator* systems: (1) a high separation efficiency of the *Core Separator*, and (2) an interaction between individual components. To achieve high separation efficiency, a proper recirculation flow is required. By varying recirculation flow in the *Core Separator*, the tangential and radial velocities can be controlled independently to maintain them in the proper ratio.

The *Core Separator* System can be arranged in a variety of configurations depending on process conditions, required performance, inlet dust concentration, abrasiveness of solids, etc. The *Core Separator* component actually predetermines the efficiency of the system even if the collector efficiency is low. The following formula can be used to calculate partial collection efficiency when the collector is situated downstream of the *Core Separator*,

$$E_{sys} = \frac{E_{cs} \times E_{cyc}}{1 - E_{cs}\left(1 - E_{cyc}\right)}$$

When the collector is situated upstream of the *Core Separator*,

$$E_{sys} = \frac{E_{cyc}}{1 - E_{cs}\left(1 - E_{cyc}\right)}$$

Here E_{CS}, E_{cyc} and E_{sys} relate to the *Core Separator*, collector and *Core Separator* system partial separation efficiencies, respectively.

During the past year, a series/parallel modular design has been developed to facilitate scaleup in capacity. It has been tested under a wide range of conditions and with numerous dust compositions, primarily coal flyash. The efficiency of the *Core Separator* has been generalized and compared against other dust collector types. As shown in Table 1, the penetration of dust emissions from it are several times lower than from cyclonic collectors, which are commonly used in Krakow boilers. For this reason, the *Core Separator* can make a significant contribution to emissions reduction in Krakow.

Table 1. Normalized Emissions from Various Dust Collectors

Dust Collectors	Collection Efficiency, %	Penetration (Emission), %	Normalized Penetration (Emission)
Cyclone	50.6	49.4	14.5
Multiple Cyclone /Medium Efficiency/	78.0	22.0	6.47
Multiple Cyclone /High Efficiency/	86.3	13.7	4.03
Wet Scrubber	88.7	11.3	3.32
Venturi	96.6	3.4	1.0
ESP /Medium Efficiency/	98.2	1.8	0.53
Fabric Filter /Medium Efficiency/	96.6	3.4	1.0
ESP /High Efficiency/	99.58	0.42	0.12
Fabric Filter /High Efficiency/	99.77	0.23	0.07
Core Separator	99.92	0.08	0.02

Environmental Regulations in Krakow

Krakow with its 750,000 population relies heavily on hard coal as a heating fuel. In 1992, it was estimated that 35% of the heating needs were provided by more than 2,900 local boilers consuming about 370,000 tons of coal annually. A major portion of heating needs was also provided by two local power plants, Łeg and Skowina. By 1995, the district heating system was extended to several new parts of the city. Also, many old boilers were retired and others were converted to natural gas. As a result, it is estimated that in mid-1995 the boiler population in Krakow had been reduced approximately in half.

All of the regional counties of Poland (called voivoids) including Krakow have developed medium and long range plans for emission abatement that are more in line with western Europe. The intent of the medium range plan (five years in length and complete by the year 2000) is to bring Poland closer to European environmental standards and enabling it to join the European Union (EU) in due course. The Polish government has shown a commitment to enact legislation which is in line with its international obligations and EU recommendations concerning emissions. In July 1994, Poland signed in Oslo the Sulfur Protocol for interborder contamination of air. Its obligations from this protocol are substantial, including a 90% reduction in SO_2 from new plants and specific targeted reductions.

However, while Polish standards for SO_2 and other gaseous pollutants are in line with its European neighbors, the limits for dust emissions are not. This can be seen in Table 2, which provides a summary of the relevant permitted emissions related to fuels combustion. To obtain limits expressed as mg/M^3, the following conversion factors can be used:

- Coal Fuels — 420 M^3 Flue Gas/GJ
- Liquid Fuels — 370 M^3 Flue Gas/GJ
- Gaseous Fuels — 300 M^3 Flue Gas/GJ

The relevant permitted emissions related to combustion processes presented in Table 2 are from the Ministry of Environmental Protection Natural Resources and Forestry.

In comparison with standards used in other nations, the particulate standard in Poland is not very stringent. Unlike the limits proposed for SO_2, NO_x, and other gaseous pollutants, the proposed limits for dust emissions are many times higher than those of other countries as shown in Table 3. In order to meet the ambient air quality standards set for protected areas such as Krakow, these standards may have to be tightened significantly.

Table 2. Permitted Emission Limits (Poland)

Fuel	Furnace	Permitted Emissions for Combustion Processes (g/GJ)								
		Group A [1]			Group B [2]			Group C [3]		
		SO_2	NO_2 [4]	Dust	SO_2	NO_2 [4]	Dust	SO_2	NO_2 [4]	Dust
Hard Coal	Fixed Grate	990	35	1850	720	35	1370	650	35	1370
	Mechanical Grate	990	160	800	640	95	600	200	95	600
	Pulverized Coal 1	1240	495	170	870	170	90	200	170	90
	Pulverized Coal 2	1240	330	260	870	170	130	200	170	130
Brown Coal	Pulverized Coal 1	1540	225	140	1070	150	70	200	150	70
	Pulverized Coal 2	1540	225	140	1070	150	95	200	150	95
Coke	Fixed Grate	410	45	720	410	45	235	410	45	235
	Mechanical Grate	500	145	310	250	145	235	250	110	235
Oil	Boilers < 50 MW	1720	120	—	1250	120	—	125	90	—
	Boilers > 50 MW	1720	120	—	1250	160	—	170	120	—
Nat. Gas	Boilers < 50 MW	—	60	—	—	35	—	—	35	—
	Boilers < 50 MW	—	145	—	—	85	—	—	85	—
Wood	Grate	—	50	—	—	50	—	—	50	—

1) Group A relates to existing installations during the day of the Ordinance (1990) until Dec. 31, 1997.
2) Group B relates to existing installations during the day of the Ordinance (1990) and after Dec. 31, 1997.
3) Group C relates to new installations placed in operation after Dec. 31, 1994.
4) Signifies the sum of NO and NO_2 converted to NO_2.

Table 3. Particulate Emission Standard, Various Countries

Country	Size	Particulate Standard	Dust Emission (mg/M^3)
U.S. (after 1978)	> 73 MW_T	13 g/GJ	40
U.S. (after 1984)	> 29 MW_T	22 g/GJ	67
U.S. (after 1971)	> 73 MW_T	43 g/GJ	133
Germany	< 5 MW_T	65 g/GJ	185
Germany	> 5 MW_T	20 g/GJ	57
Netherlands	> 10 MW_T	10 g/GJ	28
Czech Republic	< 25 MW_T	52 g/GJ	150
Czech Republic	> 25 MW_T	20 g/GJ	56
European Union	> 50 MW_T	20 g/GJ	56
China	< 5 MW_T	52 g/GJ	150
Australia	< 5 MW_T	70 g/GJ	200
Chile	> 5 MW_T	20 g/GJ	56
Poland	Traveling Grate/Coal	**600 g/GJ**	**1,715**
Poland	Pulverized Coal	**90 g/GJ**	**257**

Summary and Conclusions

There is a sizeable stoker-fired boiler population in Krakow and throughout Poland. Emissions from these boilers, especially dust emissions, have caused a significant deterioration in ambient air quality in Krakow. The combination of extensive coal combustion and the city's location in a valley having a thermal inversion often results in a heavy smog containing suspended particulate matter.

Several approaches have been suggested to improve air quality including coal cleaning, fuel switching, extension of the district heating system, and the use of more efficient control technology. The *Core Separator* fits into this last category as a more efficient dust collector. Dust emissions from the *Core Separator* are typically 4 to 8 times lower than from conventional cyclonic collectors. The implementation of this device can therefore have a significant impact on air quality in Krakow.

However, the widespread use of improved technology can only result if appropriate emission regulations are in place and those regulations are enforced. In this regard, the particulate standard in Poland is conspicuously less ambitious than those of its neighbors. For example, the Czech Republic which uses coal from adjacent coal basins has a particulate standard that is many times lower than Poland's. Since Poland is both an importer and exporter of air pollution, its emission standards should be compatible with those of its neighbors.

Three *Core Separator* units have been sold in early 1995 and are scheduled for commercial operation this year. These units will be for use on both stoker-fired and fluidized bed boilers. While this represents some success for this project, it is generally believed that many more units could be sold if tougher regulations for dust emission were in place. Such a measure has been recommended to the U.S./Polish Bilateral Steering Committee.

References

1. Master Plan for Low Level Air Pollution/Emissions Abatement, Republic of Poland, Interim Report, Nov. 1994.

2. Ordinance of the Ministry of Environmental Protection Natural Resources and Forestry of 12th February 1990 on Protection of Air Against Pollution. Poland.

3. Smolensky, L.A., Easom, B.H. and Wysk S.R., "A *Core Separator* System for Fine Particulate Removal," Eighth Annual Coal Preparation, Utilization, and Environmental Control Contractors Conference, U.S. Dept. of Energy, July 27-30, 1992.

4. Cyklis, P., et al, "Characteristics of Krakow's Boiler Population," Proceedings of Conference on Alternatives for Pollution Control from Coal-Fired Emission Sources, Plzen, Czech Republic 1994.

AUTHORS INDEX

A

B

C

D

E

F

G

H

I

J

K

L

M

N

O

P

Q

R

S

T

U

V

W

X

Y

Z

*U.S. Government Printing Office 1995 609-453